EMERGING
INFECTIOUS DISEASES ®

Tickborne Diseases

EMERGING INFECTIOUS DISEASES®

EDITOR-IN-CHIEF
D. Peter Drotman

EMERGING INFECTIOUS DISEASES®

Tickborne Diseases

November 2018

On the Cover

Ernst Liebenauer (1884–1970), *In Entrenchment, World War I* (c. 1915). Watercolor, pencil, and gouache on paper, 5.6 in x 4 in/14.2 cm x 10.1 cm. Digital image from private collection, Atlanta, Georgia, USA.

About the Cover p. 2136

2006

2017

Letters

2069

Books and Media

About the Cover

Etymologia

2129

DPDx

Diagnostic Assistance and Training in Laboratory Identification of Parasites

A free service of CDC available to laboratorians, pathologists, and other health professionals in the United States and abroad

Diagnosis from photographs of worms, histological sections, fecal, blood, and other specimen types

Expert diagnostic review

Formal diagnostic laboratory report

Submission of samples via secure file share

Visit the DPDx website for information on laboratory diagnosis, geographic distribution, clinical features, parasite life cycles, and training via Monthly Case Studies of parasitic diseases.

Leishmaniasis in Northern Syria during Civil War

**Khalid Rehman, Julia Walochnik, Johannes Mischlinger,
Bodour Alassil, Richard Allan, Michael Ramharter**

Since the onset of the ongoing civil war in Syria, the governmental surveillance system for leishmaniasis has lost access to provinces of northern Syria. The MENTOR Initiative, an international not-for-profit organization, was commissioned to implement an integrated leishmaniasis control program, providing an opportunity to reassess the epidemiology of leishmaniasis in northern Syria. Epidemiologic data and biologic samples for molecular species diagnostics were collected from collaborating local health centers. Incidence peaked in March 2015 at 7,743 estimated monthly cases. High levels of transmission were observed in traditional endemic regions but extended to previously hypoendemic regions, such as Al-Raqqa and Al-Hasakah. Incidence decreased to 3,209 in July 2015. Data indicate that the prewar trend of increasing incidence of cutaneous leishmaniasis accelerated during the beginning of armed conflict but declined after implementation of the comprehensive control program by the MENTOR Initiative. Molecular analysis revealed a spectrum of *Leishmania* species and sporadic cases of visceral leishmaniasis.

Leishmaniasis is caused by different *Leishmania* species. The infection may be cutaneous, mucocutaneous, or visceral, depending on the species involved and the immune status of the patient. The common term Aleppo boil indicates the historic importance of cutaneous leishmaniasis (CL) in Syria. Before the ongoing civil war began, the national leishmaniasis control program in Syria delegated general treatment responsibilities to primary healthcare centers (HCCs) and other health services of the governmental health system. Official World Health Organization (WHO) statistics indicate that ≈14,000 new CL cases occurred per year during 1994–2000. Incidence increased after that, to 27,825 in 2010. In addition to the main burden of CL, sporadic cases of visceral leishmaniasis (VL) (25–55 cases/y) were reported to governmental authorities (*1*).

Author affiliations: Medical University of Vienna, Vienna, Austria
(K. Rehman, J. Walochnik, J. Mischlinger, M. Ramharter);
Bernhard Nocht Institute for Tropical Medicine, Hamburg,
Germany (J. Mischlinger, M. Ramharter); University Medical Center
Hamburg-Eppendorf, Hamburg (J. Mischlinger, M. Ramharter);
The MENTOR Initiative, West Sussex, UK (B. Alassil, R. Allan)

After the onset of civil war, reports emerged about a dramatic increase in CL cases in Syria and neighboring Jordan (*2–4*). These reports were based largely on anecdotal observations of clinical cases in refugees from Syria. However, because of a loss of access of governmental authorities to leishmaniasis-endemic regions within Syria, no reliable epidemiologic data have been recorded and published since the onset of the civil war. In addition, international organizations initially providing treatment structures for CL within Syria operated with conflicting case definitions and reporting systems for leishmaniasis, thus bringing forth unreliable epidemiologic data.

The MENTOR Initiative (http://thementorinitiative.org), an international humanitarian organization, was commissioned by the US Agency for International Development and UK Department for International Development to plan and implement a comprehensive leishmaniasis control program in northern Syria. The organization's principal aim is to relieve tropical diseases in humans, with a focus on vectorborne diseases in the context of complex emergencies. Activities in Syria were launched in September 2013, and a comprehensive control program was set up with both a preventive and a curative component. To provide firm evidence for the magnitude of the leishmaniasis epidemic and to accompany and evaluate the rollout of the leishmaniasis control program, an epidemiologic surveillance system was established. The principal aims of this system were to collect reliable data for the epidemiology of leishmaniasis, to investigate the comparative distribution of *Leishmania* species in clinical samples, and to evaluate diagnostic and therapeutic activities of affected populations in northern Syria.

Materials and Methods

The leishmaniasis control program was based on current WHO recommendations for integrated vector control management (*5*) aimed at reducing both the vector density and parasite reservoirs. Sand fly populations were targeted by large-scale implementation of indoor residual spraying, provision of long-lasting insecticide-treated nets, long-lasting insecticide-treated curtains, and waste management. The leishmanial parasite reservoir was targeted by providing curative services for local populations.

Organizational Setup, Study Area, and Health Infrastructure

Because of the precarious, ever-changing security situation in northern Syria, the MENTOR Initiative opted to not deploy external, international personnel into the conflict zone. A headquarters for coordination of activities was set up in the border region between Syria and Turkey. Implementation of the control program was based on voluntary collaboration of local Syrian HCCs, which had been detached from governmental administration and supply since the onset of the civil war. Healthcare workers in Syria were invited to travel to the mission's headquarters, where they were offered logistical support and training in the diagnosis and treatment of CL and VL. Pentavalent antimonial therapy was provided to healthcare workers for treating patients at their HCCs.

Collection of Epidemiologic Data for Northern Syria Provinces

Epidemiologic, clinical, and demographic data were collected from all collaborating HCCs in the target regions. Healthcare workers cleaned lesions with antiseptic solutions and then scraped the margins of ulcerated wounds with sterile lancets. The scraped material was transferred to a glass slide, then fixed with methanol and stained with Giemsa stain. Diagnosis of CL was established by trained healthcare workers at each HCC. Where appropriate laboratory facilities were available, healthcare workers used light microscopy to detect amastigote forms of *Leishmania* spp. (6,7). Rapid tests (IT-LEISH Individual Rapid Test; Bio-Rad Laboratories, Hercules, CA, USA) were used for diagnosis of VL (8).

Molecular–Epidemiologic Survey of Cutaneous Leishmaniasis at Sentinel Sites

For confirmation of the accuracy of the HCC diagnostic services and to obtain molecular–epidemiologic evidence, skin samples were collected at sentinel sites and transported to headquarters for further analysis. Two representative sentinel sites were selected for this molecular epidemiologic substudy in the provinces of Idlib (Heish HCC) and Aleppo (Batranah HCC).

Heish HCC was located in rural Idlib in a district called Al Ma'ra. During the survey period in 2015, the catchment population of this HCC was 5,933, and the population of internally displaced persons (IDPs) was 1,367. Most of the IDPs had come from Hama and southern Aleppo, because Heish was relatively secure in comparison with those areas. Batranah HCC was located in the Jebel Saman district in southeastern Aleppo. The catchment area of this HCC had a population of ≈3,500, with <500 IDPs. All patients who arrived at these sites during the period of molecular data collection were invited to participate.

Sampling involved first the cleaning of the affected skin with moistened gauze. Then, sterile filter paper was pressed against the moist base and the margins of the ulcer to allow for absorbing wound secretions (9,10).

Molecular Analysis of Skin Samples

Biologic samples were shipped to the Medical University of Vienna (Vienna, Austria) for further analysis. We extracted DNA using the QIAmp DNA Mini Kit (QIAGEN, Vienna) according to the manufacturer's instructions for dried blood spots.

We tested all samples by a universal *Leishmania* PCR protocol using the LITSR/L5.8S primer pair (11) and following the protocol of Schönian et al. (12). To further discriminate species within the *L. donovani/infantum* complex, we ran 3 more PCR protocols for species differentiation: K26-PCR (13), cpbE/F-PCR (14,15), and HSP70-PCR (16) (online Technical Appendix, https://wwwnc.cdc.gov/EID/article/24/11/17-2146-Techapp1.pdf).

Ethics Considerations, Data Collection, and Data Analysis

Because there was no operational, accredited ethics committee for the northern provinces of Syria, we submitted the study protocol to the ethics committee of the Medical University of Vienna. Oral consent was obtained from all patients before study-related procedures. Because of the extraordinary security situation and fear of causing a potential risk for the life of participants if there were a written record of personal information, in the light of activities by the rebel groups, investigators decided not to obtain written informed consent or any identifiable personal information in study-related documentation. The ethics committee approved this approach.

Data Analysis

We performed descriptive data analysis using JMP (https://www.jmp.com) and STATA/SE15.0 (https://www.stata.com). We used Microsoft Office (Microsoft, Redmond, WA, USA) to perform data visualization.

Results

The MENTOR Initiative's Leishmaniasis Control Program in Northern Syria

The MENTOR Initiative's first target regions were the provinces of Aleppo and Idlib; the group subsequently expanded its activities to Al-Raqqa, Al-Hasakah, and Hama. It was a challenge to reliably estimate the total population residing in the target regions because of the frequent and unpredictable movements of persons after military and political actions and the lack of a stable administrative control over the region.

The MENTOR Initiative supported a network of ≈200 HCCs, of which 161 HCCs provided reliable data over an extended follow-up period. These health facilities included HCCs and mobile clinics in each province (43 and 21 in Aleppo, 40 and 18 in Idlib, 7 and 12 in Hama, 7 and 5 in al-Raqqa, 8 and 0 in Al-Hasakah, respectively). The approximate geographic and population coverage in the target regions is provided in Table 1.

Epidemiology of CL in Northern Syria

The number of HCCs varied over the study period, mostly because of the changing security situation, which, in turn, led to movement of persons and, in some cases, loss of access to these health facilities. New cases of CL were recorded in HCCs in the provinces of Aleppo, Idlib, Hama, Al-Raqqa, and Al-Hasakah over varying periods, ranging from 2.5 months to 16 months (Table 1; Figures 1, 2). The total number of new cases per year has been estimated based on the observation period and the estimated coverage of HCCs participating in the reporting system of the MENTOR Initiative. Data indicate a yearly incidence of 4,683–20,110 cases/year in these provinces. The total number of new CL patients was estimated at 64,498 cases in 2015 (Table 1).

Data indicate that the estimated incidence of CL was 5,883 cases/month at the onset of the study in the target region. This incidence further increased to ≈7,599 cases/month at its peak in February 2015. After the effective rollout of the leishmaniasis control program, the monthly incidence of CL was reduced to 2,476 cases/month in February 2016 (Figure 1).

Treatment outcome was assessed in 45,302 patients during the study period. Among those, 18% (8,312) were lost to follow-up, and therefore no outcome could be attributed. Among the remaining 36,990 patients, a favorable outcome was recorded by the treating healthcare workers in 35,931 (97.14%, 95% CI 96.96%–97.30%).

Molecular–Epidemiologic Survey of CL at 2 Sentinel Sites

Of the 249 patients who agreed to participate in this substudy, 104 (42%) were female and 145 (58%) were male, and 139 (56%) had skin lesions suggestive for CL. The median age of participants was 11 years (interquartile range [IQR] 6–17 years), and the median body mass index was 19 (IQR 16–25) (Table 2). In Aleppo, only patients with CL participated in this study. However, the survey had to be prematurely discontinued in Aleppo after the recruitment of 55 participants because of the worsening security situation in the area at the time of the study.

Samples were taken from skin ulcers in 139 patients; 99 specimens were successfully shipped to Vienna (40 samples were lost as a result of security problems at the border crossing between Syria and Turkey). We confirmed *Leishmania* spp. infection in 93 (94%) of the 99 samples using PCR. Most *Leishmania* infections were caused by strains of *L. tropica* (n = 73, 78% [95% CI 69%–86%]). We detected *L. major* in 12 samples (13% [95% CI 7%–21%]). Seven infections were caused by *L. infantum* and 1 strain was identified as *L. donovani* (combined proportion of *L. donovani/infantum* complex 9% [95% CI 4%–16%]). The relative proportion of *L. infantum* cases was higher in Idlib province (n = 6, 86% [95% CI 42%–100%]) than in Aleppo province (n = 1, 14% [95% CI 0%–58%]) (Table 3).

We performed the K26 PCR successfully in 5 of 8 samples identified as belonging to the *L. infantum/donovani* complex. Retrieved bands were ≈280 bp in 1 case (*L. infantum*, strain 268) and ≈370 bp in 1 case (*L. donovani*, strain 275) (Figure 3, panel A); the other samples produced double bands at ≈800/900 bp (Figure 3, panel B). We also used cpbEF-PCR on the *L. donovani* strain, producing bands of ≈400 bp, and on 1 *L. infantum* strain, producing bands of ≈360 bp (Figure 4). We performed HSP70 PCR with the *L. donovani* strain and 1 *L. infantum* strain (Figure 5). To further confirm and investigate the identity of the *L. donovani* strain, we obtained DNA sequences for the ≈370-bp band of the K26 PCR and the 2 fragments of the HSP70 PCR (together ≈1280 bp). The 368-bp K26 sequence showed highest sequence similarity (358/371 bp) to a *L. donovani* strain isolated from a patient in Israel (GenBank accession no. HQ170543), and the 1,286-bp HSP70 fragment showed 100% similarity (562/562 bp) to the 562-bp fragments available from 4 *L. donovani* strains isolated from CL patients in Turkey close to the Syria border and 1 strain

Table 1. New cases of cutaneous leishmaniasis diagnosed at collaborating health centers, northern Syria

Province	New cases observed during study period	Health centers	Mobile clinics	% Program coverage of area	New cases estimated*	New cases reported in 2008 (*1,17*)	Incidence ratio
Aleppo†	12,296	43	21	70	13,174	18,603	0.7
Idlib†	21,451	40	18	80	20,110	3,883	5.2
Hama†	10,103	7	12	50	15,155	2,219	6.8
Al-Raqqa‡	5,546	7	5	65	11,376	290	39.2
Al-Hasakah§	439	8	0	45	4,683	290	16.1
Total	49,835	105	56		64,498	25,285	2.6

*Standardized cases for 1 year per province.
†16-month observation period.
‡9-month observation period.
§2.5-month observation period.
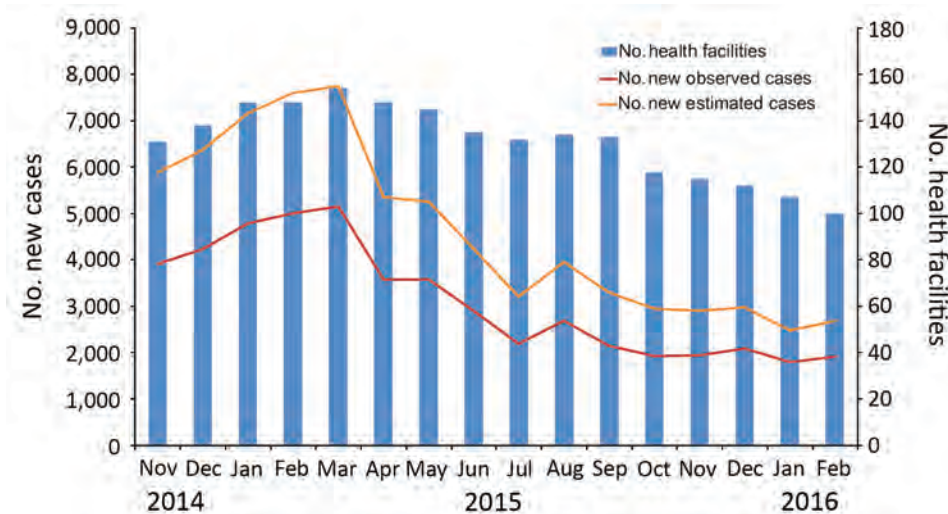
Figure 1. Number of observed and estimated cases of cutaneous leishmaniasis diagnosed in healthcare centers in target regions for leishmaniasis control programs, northern Syria, November 2014–February 2016.

isolated from a CL patient in Cyprus (GenBank accession nos. KU949373–77) and >99% similarity (1,283/1,286 bp) to the *L. donovani* strain pasteur (GenBank accession no. CP022643) and several other *L. donovani* strains. We submitted sequence data obtained in this study to GenBank (accession numbers pending).

Cases of VL at Collaborating HCCs

During the study period, 11 cases of VL were reported. Seven patients were male, and 7 were children <5 years of age (range 3 months–39 years). Seven patients were reported from Aleppo province and 4 from Idlib. Seven patients had ongoing fever and 1 patient high-grade fever. Anemia was reported for 6 patients and hepatosplenomegaly for 3 patients. Five patients additionally underwent bone marrow aspiration and showed positive PCR results for *L. infantum* infection. All patients with diagnoses of VL were treated systemically with pentavalent antimonials for 30 days, following current WHO guidelines (*18*).
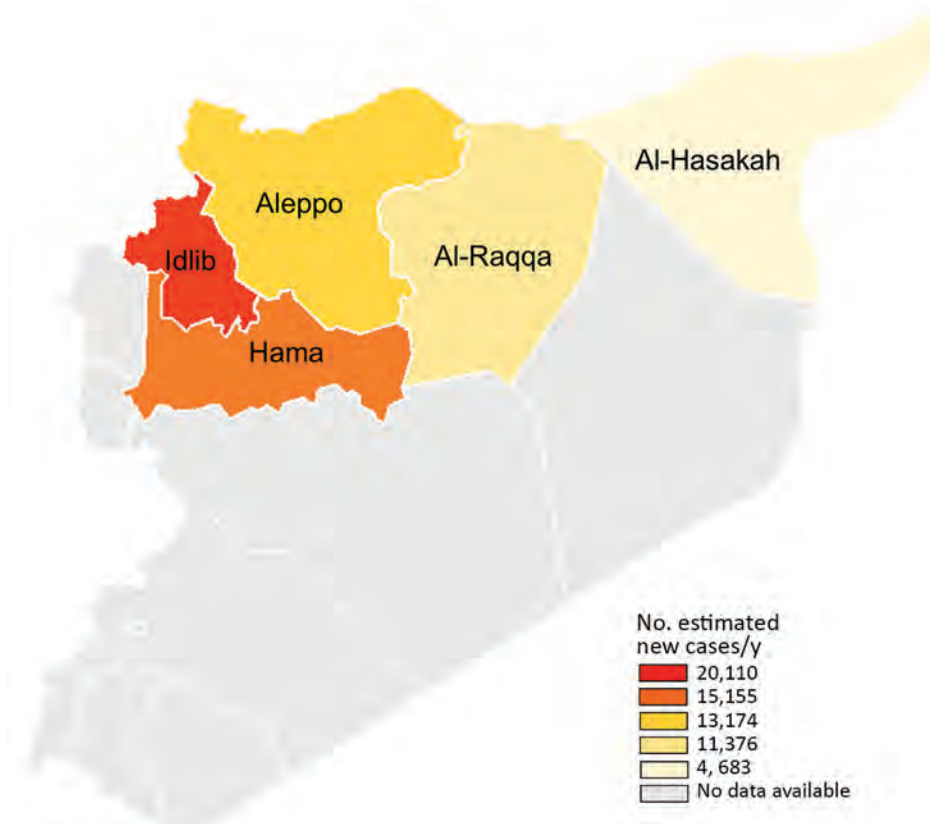
Figure 2. Target region for leishmaniasis control programs in northern Syria (color shading) and the number of estimated new cases of cutaneous leishmaniasis per year by province in this region.

No. estimated new cases/y
- 20,110
- 15,155
- 13,174
- 11,376
- 4,683
- No data available

Table 2. Description of participants in the molecular epidemiologic substudy, northern Syria*

Characteristic	Total participants, N = 249
Age, y	
Median (IQR)	11 (6–17)
≤10	107 (43)
11–20	86 (34.5)
21–30	22 (8.8)
31–40	11 (4.4)
41–50	7 (2.8)
51–60	7 (2.8)
≥61	9 (3.6)
Sex	
M	145 (58.2)
F	104 (41.8)
Body mass index, kg/m^2	
Median (IQR)	19 (16–25)
Presence of skin lesions, n = 139	
Idlib	84 (60.4)
Aleppo	55 (39.6)
Absence of skin lesions, n = 110	
Idlib	110 (100)
Aleppo	NA

*Values are no. (%) except as indicated. IQR, interquartile range; NA, not available.

Discussion

Syria has been a hotspot of leishmaniasis transmission for centuries. After a continuous decrease of leishmanial transmission in the past century, which was driven at least in part by vector control activities of the national malaria elimination campaign, WHO country data show a gradual but steady increase in annual case incidence from ≈14,000 per year to an average of 27,825 reported CL cases/year before the onset of the civil war (*1,17*) (Figure 6).

The governmental health system in Syria disintegrated in most parts of the northern provinces after the onset of the civil war; at the same time, reports from neighboring regions indicated a surge in leishmaniasis cases in refugee populations from Syria. The MENTOR Initiative set out to collaborate with most local leishmaniasis treatment centers in the target provinces, becoming, in practice, the only external collaborating institution for leishmaniasis control in the target regions. It is assumed that the number of HCCs did not greatly affect the overall measure of incidence, because patients seeking ongoing treatment courses went to other operational centers within the program when needed. Based on this information and the comprehensive reporting system, the

MENTOR Initiative was in a position to reliably assess and monitor the incidence of CL in northern Syria.

Thus, this survey provides epidemiologic data about the incidence of CL and VL in the war-affected regions of northern Syria since the onset of the civil war. Based on these data, a yearly incidence of 64,498 cases of CL was estimated, constituting a 2.6-fold increase in leishmaniasis transmission in the northern provinces over the ≈25,000 cases of CL reported by the national authorities before the civil war, in 2008 (Table 1). This increase is in line with several anecdotal reports about an observed surge of leishmaniasis cases in refugees from Syria (*2–4*).

These data indicate a noteworthy change in the epidemiology of leishmaniasis transmission on a regional level. The provinces of Aleppo, Hama, and Idlib were the traditional hotspots of CL endemicity, whereas the provinces of Al-Raqqa and Al-Hasakah reported relatively few cases before the civil war (*1*). The survey results we report demonstrate, in contrast to prewar data, that the most dramatic increase in leishmaniasis transmission occurred in regions of previously low transmission intensity, including a nearly 40-fold increase in incidence of cases in Al-Raqqa province. This change in the local epidemiology of leishmaniasis is most likely the result of a combination of factors, including large-scale population movement within the war-affected provinces and an increase in vector abundance as a result of an exponential increase in suitable sites for vector breeding caused by the barrel bombing of urban buildings, creating cracked walls and a buildup of domestic waste across cities and towns, conditions in which sand flies thrive and reproduce.

After the full implementation of this integrated leishmaniasis control program, estimated monthly case counts decreased progressively from March 2015 (n = 7,743) to February 2016 (n = 2,679). This change indicates a reduction of leishmaniasis transmission by >2-fold after the implementation of the control activities. Despite seasonal variations in incidence of leishmaniasis, most recent data indicate that control activities were able to reduce CL incidence to levels comparable to prewar conditions.

VL occurred sporadically during the study period; a total of 11 cases were reported by the participating HCCs. In contrast to the increases in CL, there was no notable increase in the reported incidence of VL in northern Syria at

Table 3. Molecular epidemiology of *Leishmania* spp. in samples collected at sentinel sites, Northern Syria*

Category	*L. tropica*	*L. major*	*L. infantum*	*L. donovani*
Province				
Idlib	50 (83, 71–92)	3 (5, 1–14)	6 (10, 4–21)	1 (2, 0–9)
Aleppo	23 (70, 51–84)	9 (27, 13–46)	1 (3, 0–16)	0 (0, 0–11)
Sex				
M	43 (80, 66–89)	5 (9, 3–20)	5 (9, 3–20)	1 (2, 0–10)
F	30 (77, 61–89)	7 (18, 8–34)	2 (5, 1–17)	0 (0, 0–9)
Age, median (IQR)	13 (7–24)	7.5 (4.5–19)	10 (6–25)	7 (7–7)

*Values are no. (%, 95% CI) except as indicated. IQR, interquartile range.

Figure 3. A) Results of K26 PCR assay (*13*) on patient samples identified as belonging to the *Leishmania infantum/donovani* complex in study of leishmaniasis control programs in northern Syria. Lane 1, step marker; lanes 2 and 3, *L. infantum* strain 268 with 3 and 6 μL of DNA, respectively; lane 4, *L. donovani* strain 275 with 3 μL of DNA. B) Results of K26 PCR assay (*13*) on patient samples identified as belonging to the *Leishmania infantum/donovani* complex in study of leishmaniasis control programs in northern Syria. Lane 1, step marker; lanes 2 and 3, *L. infantum* strain 278 with 3 and 6 μL of DNA, respectively.
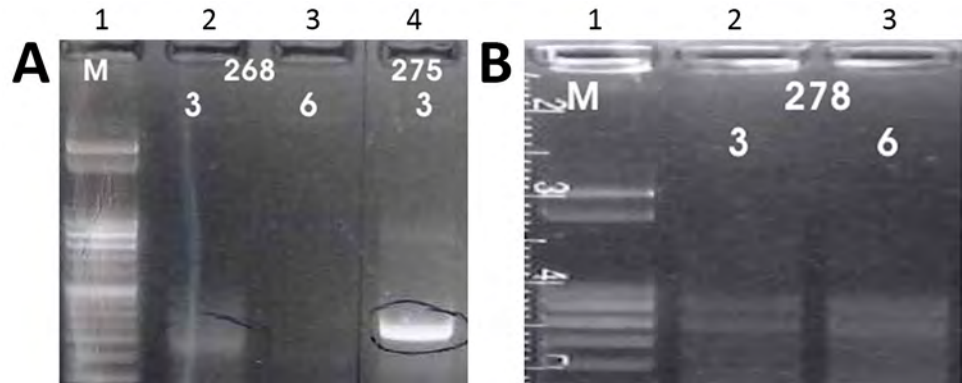
the time of this study, compared with prewar data. However, asymptomatic cases may have occurred but were unreported within the communities, and in some HCCs, related

illnesses and deaths may have been misreported along with other unidentified causes of death.

Molecular analysis of leishmaniasis is recommended in high-resource settings to guide appropriate treatment. Previous data reported *L. tropica* as the main leishmanial species causing CL in northern Syria and *L. major* as the main species causing CL in southern Syria (*19–22*). This survey confirmed *L. tropica* as the predominant species in northern Syria, causing nearly 80% of cutaneous lesions. *L. major* was the second most prevalent species, accounting for 13% of all *Leishmania* species. *L. infantum* and *L. donovani*, which are considered classical pathogens for VL, were repeatedly confirmed in skin lesions of patients participating in this survey. In Syria, *L. infantum* has been reported previously as a causative agent of CL in humans (*21*); however, *L. donovani* had previously been isolated only from sand flies (*23*). Further, *L. donovani* has repeatedly been found in the neighboring countries Cyprus, Turkey, Iraq, and Israel (*24–28*). Recently, several cases of most likely autochthonous *L. donovani* infections have been reported from southeastern Anatolia in the direct vicinity of the border with Syria, and these were also cases of CL (*29*). In that study, *L. tropica* and *L. infantum* were described as the main causative agents of CL in Turkey, which fits well with our results for Syria. CL caused by *L. donovani* has also been documented from Cyprus (*26*). Moreover, numerous cases of CL caused by *L. donovani* have been documented from Sri Lanka (*30*). In summary, these molecular data demonstrate a surprising diversity of locally endemic *Leishmania* species causing cutaneous disease.

The challenging security situation led to several limitations in the conduct of the reported research activities. No accurate estimates of the actual population residing in the northern provinces were available because of the massive population movement within Syria, migration in neighboring countries, and casualties of the civil war. To address
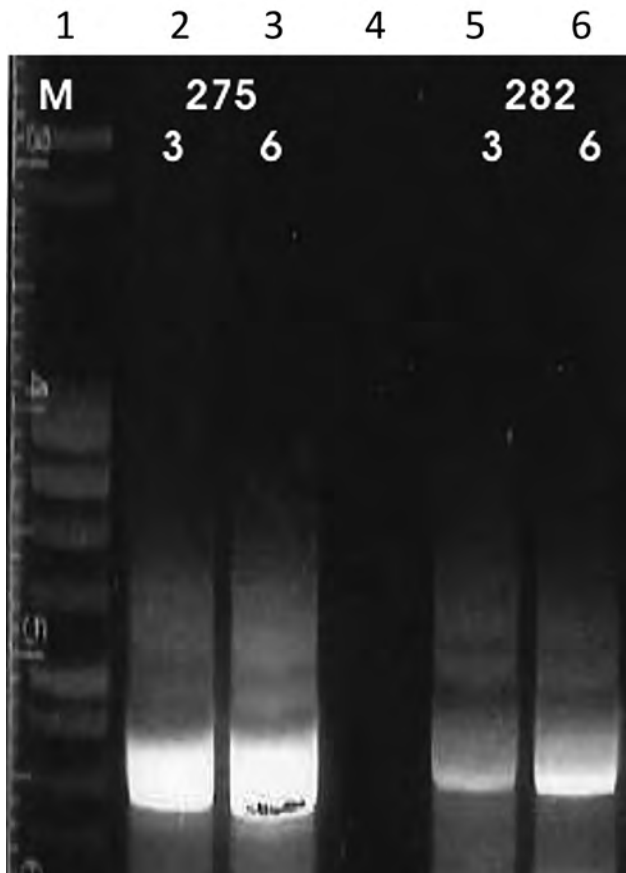
Figure 4. Results of cpb-EF PCR (*14*,*15*) on patient samples identified as belonging to the *Leishmania infantum/donovani* complex in study of leishmaniasis control programs in northern Syria. Lane 1, step marker; lanes 2 and 3, *L. donovani* strain 275 with 3 and 6 μL of DNA, respectively; lane 4, negative control; lanes 5 and 6, *L. infantum* strain 282 with 3 and 6 μL of DNA, respectively.

Figure 5. Results of HSP-70 PCR (*16*) on patient samples identified as belonging to the *Leishmania infantum/donovani* complex in study of leishmaniasis control programs in northern Syria. Lane 1, step marker; lanes 2–4, N fragment of *L. donovani* strain 275 and *L. infantum* strains 282 and 268; lanes 5–7, blank; lanes 8–10, T fragment of *L. donovani* strain 275 and *L. infantum* strains 282 and 268.

these limitations, we relied on approximations used by international institutions for this analysis. The safety situation made direct access to the participating HCCs in Syria impossible for external MENTOR personnel. Therefore, the control program and the epidemiologic assessments had to rely on collaborating local staff. Local healthcare workers traveled often under precarious safety situations to the border region with Turkey to receive training and supplies for the control activities within Syria. Because of these constraints, a more detailed investigation was not feasible, and the investigation had to be limited to aspects deemed of

highest importance for the implementation and evaluation of the ongoing leishmaniasis control program.

It was within this challenging safety situation that the MENTOR Initiative developed and deployed this large leishmaniasis control program. Epidemiologic data indicate that the control program started in a period of rapidly rising leishmaniasis transmission in northern Syria during the civil war. A further increase in leishmaniasis transmission was avoided. However, political stability and a stable security situation are required, above all, to further stabilize and successfully control leishmaniasis in northern Syria.
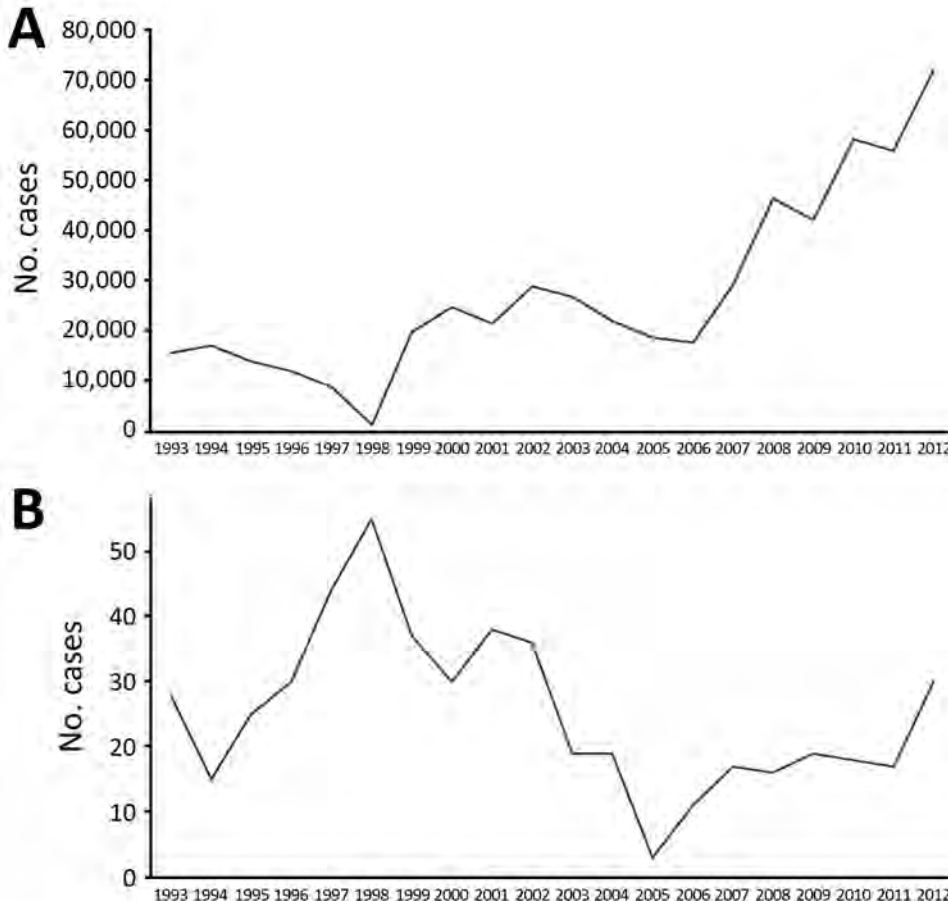
Figure 6. Cases of (A) cutaneous and (B) visceral leishmaniasis in northern Syria during 1993–2012, before the onset of the civil war (*1,17*).

Acknowledgments

About the Author

Dr. Rehman is a public health professional who is currently working with the Indus Hospital in Pakistan on a malaria control program. He has extensive experience in vectorborne disease control in Africa, Asia, and the Middle East. His research interests revolve around vectorborne diseases, especially malaria, leishmaniasis, and others.

References

1. World Health Organization. Global Health Observatory country views: Syrian Arab Republic, 1994–2010 [cited 2014 Aug 28]. http://www.who.int/leishmaniasis/resources/SYRIAN_ARAB_REPUBLIC.pdf
2. Salam N, Al-Shaqha WM, Azzi A. Leishmaniasis in the Middle East: incidence and epidemiology. PLoS Negl Trop Dis. 2014;8:e3208. http://dx.doi.org/10.1371/journal.pntd.0003208
3. Hayani K, Dandashli A, Weisshaar E. Cutaneous leishmaniasis in Syria: clinical features, current status and the effects of war. Acta Derm Venereol. 2015;95:62–6. http://dx.doi.org/10.2340/00015555-1988
4. Alasaad S. War diseases revealed by the social media: massive leishmaniasis outbreak in the Syrian spring. Parasit Vectors. 2013;6:94. http://dx.doi.org/10.1186/1756-3305-6-94
5. World Health Organization. Global strategic framework for integrated vector management; 2004 [cited 2017 Jan 2]. http://apps.who.int/iris/bitstream/handle/10665/68624/WHO_CDS_CPE_PVC_2004_10.pdf?sequence=1
6. Boggild AK, Miranda-Verastegui C, Espinosa D, Arevalo J, Adaui V, Tulliano G, et al. Evaluation of a microculture method for isolation of Leishmania parasites from cutaneous lesions of patients in Peru. J Clin Microbiol. 2007;45:3680–4. http://dx.doi.org/10.1128/JCM.01286-07
7. Boggild AK, Miranda-Verastegui C, Espinosa D, Arevalo J, Martinez-Medina D, Llanos-Cuentas A, et al. Optimization of microculture and evaluation of miniculture for the isolation of Leishmania parasites from cutaneous lesions in Peru. Am J Trop Med Hyg. 2008;79:847–52.
8. Peruhype-Magalhães V, Machado-de-Assis TS, Rabello A. Use of the Kala-Azar Detect® and IT-LEISH® rapid tests for the diagnosis of visceral leishmaniasis in Brazil. Mem Inst Oswaldo Cruz. 2012;107:951–2. http://dx.doi.org/10.1590/S0074-02762012000700019
9. Valencia BM, Veland N, Alba M, Adaui V, Arevalo J, Low DE, et al. Non-invasive cytology brush PCR for the diagnosis and causative species identification of American cutaneous leishmaniasis in Peru. PLoS One. 2012;7:e49738. http://dx.doi.org/10.1371/journal.pone.0049738
10. Boggild AK, Valencia BM, Espinosa D, Veland N, Ramos AP, Arevalo J, et al. Detection and species identification of Leishmania DNA from filter paper lesion impressions for patients with American cutaneous leishmaniasis. Clin Infect Dis. 2010;50:e1–6. http://dx.doi.org/10.1086/648730
11. El Tai NO, Osman OF, El Fari M, Presber W, Schönian G. Genetic heterogeneity of ribosomal internal transcribed spacer in clinical samples of Leishmania donovani spotted on filter paper as revealed by single-strand conformation polymorphisms and sequencing. Trans R Soc Trop Med Hyg. 2000;94:575–9. http://dx.doi.org/10.1016/S0035-9203(00)90093-2
12. Schönian G, Nasereddin A, Dinse N, Schweynoch C, Schallig HD, Presber W, et al. PCR diagnosis and characterization of Leishmania in local and imported clinical samples. Diagn Microbiol Infect Dis. 2003;47:349–58. http://dx.doi.org/10.1016/S0732-8893(03)00093-2
13. Haralambous C, Antoniou M, Pratlong F, Dedet JP, Soteriadou K. Development of a molecular assay specific for the Leishmania donovani complex that discriminates L. donovani/Leishmania infantum zymodemes: a useful tool for typing MON-1. Diagn Microbiol Infect Dis. 2008;60:33–42. http://dx.doi.org/10.1016/j.diagmicrobio.2007.07.019
14. Hide M, Bañuls AL. Species-specific PCR assay for L. infantum/L. donovani discrimination. Acta Trop. 2006;100:241–5. http://dx.doi.org/10.1016/j.actatropica.2006.10.012
15. Zackay A, Nasereddin A, Takele Y, Tadesse D, Hailu W, Hurissa Z, et al. Polymorphism in the HASPB repeat region of east African Leishmania donovani strains. PLoS Negl Trop Dis. 2013;7:e2031. http://dx.doi.org/10.1371/journal.pntd.0002031
16. Van der Auwera G, Maes I, De Doncker S, Ravel C, Cnops L, Van Esbroeck M, et al. Heat-shock protein 70 gene sequencing for Leishmania species typing in European tropical infectious disease clinics. Euro Surveill. 2013;18:20543. http://dx.doi.org/10.2807/1560-7917.ES2013.18.30.20543
17. World Health Organization. Number of cases of cutaneous leishmaniasis reported; data by country, 2005–2016 [cited 2018 June 22]. http://apps.who.int/gho/data/view.main.NTDLEISHCNUMv
18. World Health Organization. Control of the leishmaniases. World Health Organ Tech Rep Ser. 2010;(949):xii–xiii, 1–186, back cover.
19. Belazzoug S, Pratlong F, Rioux JA. [A new zymodeme of Leishmania tropica, agent of Aleppo boil (Syria)]. Arch Inst Pasteur Alger. 1988;56:95–9.
20. Al-Nahhas SA, Kaldas RM. Characterization of Leishmania species isolated from cutaneous human samples from central region of Syria by RFLP analysis. ISRN Parasitol. 2013;2013:308726. http://dx.doi.org/10.5402/2013/308726
21. Haddad N, Saliba H, Altawil A, Villinsky J, Al-Nahhas S. Cutaneous leishmaniasis in the central provinces of Hama and Edlib in Syria: Vector identification and parasite typing. Parasit Vectors. 2015;8:524. http://dx.doi.org/10.1186/s13071-015-1147-0
22. Khiami A, Dereure J, Pratlong F, Martini A, Rioux JA. La leishmaniose cutane humaine à Leishmania major MON-26 aux environs de Damas (Syrie). Bull Soc Pathol Exot. 1991;84:340–4.
23. Rioux J, Leger N, Haddad N, Desjeux P. Natural infestation of Phlebotomus tobbi (Diptera, Psychodidae) by Leishmania donovani s. st. (Kinetoplastida, Trypanosomatidae) in Syria. Parassitologia. 1998;40(Suppl1):148.
24. Zackay A, Nasereddin A, Schnur L, Jaffe C. Molecular characterization of Leishmania donovani in Israel, GenBank accession no. HQ170543; 2016 [cited 2018 Jun 22]. https://www.ncbi.nlm.nih.gov/nuccore/315454626/
25. Alam MZ, Haralambous C, Kuhls K, Gouzelou E, Sgouras D, Soteriadou K, et al. The paraphyletic composition of Leishmania donovani zymodeme MON-37 revealed by multilocus microsatellite typing. Microbes Infect. 2009;11:707–15. http://dx.doi.org/10.1016/j.micinf.2009.04.009
26. Antoniou M, Haralambous C, Mazeris A, Pratlong F, Dedet JP, Soteriadou K. Leishmania donovani leishmaniasis in Cyprus. Lancet Infect Dis. 2008;8:6–7. http://dx.doi.org/10.1016/S1473-3099(07)70297-9

27. Bhattacharyya T, Boelaert M, Miles MA. Comparison of visceral leishmaniasis diagnostic antigens in African and Asian *Leishmania donovani* reveals extensive diversity and region-specific polymorphisms. PLoS Negl Trop Dis. 2013; 7:e2057. http://dx.doi.org/10.1371/journal.pntd.0002057

28. Gouzelou E, Haralambous C, Amro A, Mentis A, Pratlong F, Dedet JP, et al. Multilocus microsatellite typing (MLMT) of strains from Turkey and Cyprus reveals a novel monophyletic *L. donovani* sensu lato group. PLoS Negl Trop Dis. 2012;6:e1507. http://dx.doi.org/10.1371/journal.pntd.0001507

29. Özbilgin A, Harman M, Karakuş M, Bart A, Töz S, Kurt Ö, et al. Leishmaniasis in Turkey: visceral and cutaneous leishmaniasis caused by *Leishmania donovani* in Turkey.

Acta Trop. 2017;173:90–6. http://dx.doi.org/10.1016/j.actatropica. 2017.05.032

30. Kariyawasam UL, Selvapandiyan A, Rai K, Wani TH, Ahuja K, Beg MA, et al. Genetic diversity of *Leishmania donovani* that causes cutaneous leishmaniasis in Sri Lanka: a cross sectional study with regional comparisons. BMC Infect Dis. 2017; 17:791. http://dx.doi.org/10.1186/s12879-017-2883-x

Address for correspondence: Michael Ramharter, University Medical Center Hamburg-Eppendorf, Department of Tropical Medicine, Bernhard Nocht Institute for Tropical Medicine and I. Department of Medicine, Bernhard-Nocht Straße 74, 20359 Hamburg, Germany; email: ramharter@bnitm.de

August 2017: **Vectorborne Infections**

- Added Value of Next-Generation Sequencing for Multilocus Sequence Typing Analysis of a *Pneumocystis jirovecii* Pneumonia Outbreak

- *Bartonella quintana*, an Unrecognized Cause of Infective Endocarditis in Children in Ethiopia

- Characteristics of Dysphagia in Infants with Microcephaly Caused by Congenital Zika Virus Infection, Brazil, 2015

- Zika Virus Infection in Patient with No Known Risk Factors, Utah, USA, 2016

- Acute Febrile Illness and Complications Due to Murine Typhus, Texas, USA

- High Infection Rates for Adult Macaques after Intravaginal or Intrarectal Inoculation with Zika Virus

- Lyme Borreliosis in Finland, 1995–2014

- Characterization of Fitzroy River Virus and Serologic Evidence of Human and Animal Infection

- Genomic Characterization of Recrudescent *Plasmodium malariae* after Treatment with Artemether/ Lumefantrine

- Molecular Characterization of *Corynebacterium diphtheriae* Outbreak Isolates, South Africa, March–June 2015

- Clinical Laboratory Values as Early Indicators of Ebola Virus Infection in Nonhuman Primates

- Global Spread of Norovirus GII.17 Kawasaki 308, 2014–2016
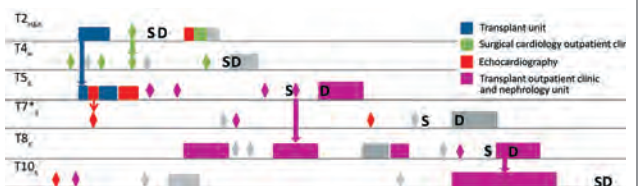
- Maguari Virus Associated with Human Disease

- Human Infection with Highly Pathogenic Avian Influenza A(H7N9) Virus, China

- Human Metapneumovirus and Other Respiratory Viral Infections during Pregnancy and Birth, Nepal

- Preliminary Epidemiology of Human Infections with Highly Pathogenic Avian Influenza A(H7N9) Virus, China, 2017

- Real-Time Evolution of Zika Virus Disease Outbreak, Roatán, Honduras

- Clonal Expansion of New Penicillin-Resistant Clade of *Neisseria meningitidis* Serogroup W Clonal Complex 11, Australia

- Genesis of Influenza A(H5N8) Viruses

- Density-Dependent Prevalence of *Francisella tularensis* in Fluctuating Vole Populations, Northwestern Spain

- Occupational Exposures to Ebola Virus in Ebola Treatment Center, Conakry, Guinea

- West Nile Virus Outbreak in Houston and Harris County, Texas, USA, 2014

- Serologic Evidence of Scrub Typhus in the Peruvian Amazon

EMERGING INFECTIOUS DISEASES

https://wwwnc.cdc.gov/eid/articles/issue/23/8/table-of-contents

Rickettsia typhi as Cause of Fatal Encephalitic Typhus in Hospitalized Patients, Hamburg, Germany, 1940–1944

Jessica Rauch, Birgit Muntau, Petra Eggert, Dennis Tappe

We evaluated formalin-fixed paraffin-embedded tissue specimens from 7 patients who died with encephalitic typhus in Hamburg, Germany, during World War II. The archived specimens included only central nervous system tissues >70 years old that had been stored at room temperature. We demonstrated successful detection of *Rickettsia typhi* DNA by a nested qPCR specific to *prsA* in 2 patients. These results indicate that *R. typhi* infections contributed to typhus outbreaks during World War II. Immunohistochemical

analyses of brain tissue specimens of *R. typhi* DNA–positive and –negative specimens showed perivascular B-cell accumulation. Around blood vessels, nodular cell accumulations consisted of CD4-positive and CD8-positive T cells and CD68-positive microglia and macrophages; neutrophils were found rarely. These findings are similar to those of previously reported *R. prowazekii* tissue specimen testing. Because *R. typhi* and *R. prowazekii* infections can be clinically and histopathologically similar, molecular analyses should be performed to distinguish the 2 pathogens.

*R*ickettsia typhi* infection, also known as murine or endemic typhus, is, except for its often milder course, clinically indistinguishable from epidemic typhus caused by *R. prowazekii*. Infection with *R. typhi* or *R. prowazekii* causes a clinical syndrome of high fever, headache, and rash. The central nervous system (CNS), cardiac, and pulmonary complications that occur are responsible for fatality rates of 4% for untreated endemic typhus and 30% for epidemic typhus (*1–3*). Whereas *R. typhi* is transmitted by fleas (oriental rat flea *Xenopsylla cheopis* and cat flea *Ctenocephalides felis*), *R. prowazekii* is transmitted by the human body louse *Pediculus humanus corporis*. Both of these pathogens are obligate intracellular zoonotic bacteria and Biosafety Level 3 pathogens (*1–3*); *R. prowazekii* is classified as a Centers for Disease Control and Prevention category B bioweapon agent.

Human infection with these bacteria occurs after inoculation of flea or louse feces in the skin lesion caused by the arthropod bite or by inhalation of dust containing dried vector feces. The appearance of epidemic louseborne typhus is often attributed to overcrowding and unhygienic conditions, such as those seen in prisons and refugee, labor, and concentration camps, and is associated with poverty and war worldwide. In contrast, the occurrence of murine fleaborne typhus is sporadic and linked to the presence of rats, often in coastal subtropical regions. Large epidemics of louseborne typhus occurred during World War I and II, leading to high fatalities in civilian populations, forced laborers, imprisoned persons, and military personnel.

We examined brain tissue samples from persons who had died from typhus in an infectious disease hospital in Hamburg, Germany, during World War II. We characterized *R. typhi* and *R. prowazekii* infections by using histologic, immunohistochemical, and molecular techniques.

Materials and Methods

Typhus Cases

We identified typhus cases by screening the books of arrivals from the Bernhard Nocht Institute Department of Pathology (Hamburg) for clinical and histopathologic descriptions of typhus. The Bernhard Nocht Institute Department of Pathology served as a center for infectious disease pathology diagnosis and received typhus specimens from multiple hospitals in Hamburg. We retrieved from the archives formalin-fixed, paraffin-embedded (FFPE) tissue blocks, which had been stored at room temperature. Clearance by the local ethics committee was obtained (no. WF-034/17) for our analyses.

Histology and Immunohistochemical Analyses

For each FFPE tissue block, we analyzed a standard hematoxylin and eosin stained section microscopically for typhus nodules and documented the presence and numbers of lesions semiquantitatively. We screened sections for intracellular rickettsiae using Giemsa stains.

We performed immunohistochemical studies with antibodies against CD3 (1:400 dilution; EpitMics, Burlingame, CA, USA), CD20 (1:150 dilution; Agilent, Santa Clara, CA, USA), CD4 (1:30 dilution; Cell Marque, Rocklin, CA, USA), CD8 (1:20 dilution; Cell Marque), CD68 (1:100 dilution; Agilent), CD177 (1:33 dilution; Zytomed, Berlin, Germany), and inducible nitric oxide synthase (iNOS, 1:100 dilution; Zytomed). After pretreatment of FFPE tissue sections with buffers containing Trilogy (medac diagnostika, Tornesch, Germany; at 95°C for CD177), EDTA (pH 8 for CD4), or citrate (pH 6 for CD3, CD20, CD8, CD68, and iNOS) and endogenous peroxidase blocking, we incubated the sections with the respective antibodies in Antibody Diluent Solution (Zytomed) at 4°C overnight. Then, we incubated with either AEC 2-Component Detection Kit and 3-amino-9-ethylcarbazole substrate (DCS, Hamburg, Germany) for immunoperoxidase staining or AP Detection Kit and Fast Blue substrate (DCS) for immunophosphatase staining. Brain tissue from 5 patients without encephalitis served as negative controls, and lymphatic tissue served as a positive control for immunologic staining of immune cells.

Molecular Assays

We ran samples through 3 rounds of processing: FFPE tissue block sectioning, DNA extraction, and quantitative PCR (qPCR). For each round, FFPE tissue blocks from typhus patients and negative control patients (patients with unrelated conditions, e.g., liver amebiasis) were placed in alternating order (i.e., 2 typhus patient samples, 1 negative control, 2 typhus patient samples, 1 negative control, and so on), cut into 5-µm slices, and deparaffinized. Before and after each round of sectioning and between sectioning different samples, we cleaned the microtome and microtome blades with DNA-ExitusPlus (AppliChem, Darmstadt, Germany). We performed DNA extractions with tissue sections in the same order as previously mentioned using the QIAamp DNA FFPE Tissue Kit (QIAGEN, Hilden, Germany). We included 2 additional negative controls (water) per round of extraction.

We performed panrickettsial real-time qPCRs targeting the *ompB* and *gltA* genes (*4,5*). In addition, we used a typhus group rickettsiae–specific qPCR targeting the *rpr331* gene (*6*) and nested species-specific qPCRs detecting the *prsA* genes (*7,8*) of the *R. typhi* and *R. prowazekii* genomes (online Technical Appendix Table, https://wwwnc.cdc.gov/EID/article/24/11/17-1373-Techapp1.pdf). We ran a β-actin gene qPCR (*9*) in parallel to check DNA quality.

Tissue sectioning, DNA extraction, and qPCR were performed in different levels of the building and by different personnel. No positive control was used in the qPCR.

Results

Seven patients (1 in 1940 and 6 in 1944) had a clinical diagnosis of typhus and a histopathologic diagnosis of typhus on the basis of FFPE tissue blocks. All samples were of CNS tissues (cerebral cortex, pons, medulla oblongata, and cerebellum); 1–3 different CNS regions were available per patient (Table). All but the case from 1940 (patient 6) originated from Langenhorn hospital in the northern part of Hamburg.

Typical typhus nodules (Figure 1) were found in all cases. Lesions varied in size and location; most were seen in the pons or medulla oblongata (Table). No intracellular rickettsiae were found in Giemsa-stained sections. Immunohistochemical stains with CD20 antibody indicated B cells were only rarely present in perivascular regions and were not found in nodules. In contrast, T cells (CD3-positive cells) contributed prominently to nodule cell composition, consisting of ≈60% CD8+ T cells and ≈40% CD4+ T cells (Figure 2, panels A–C). CD177+ neutrophils were found in nodules rarely, and when present, these neutrophils were scattered mostly throughout the brain parenchyma (D. Tappe, unpub. data). In contrast, a strong signal was seen for CD68+ microglia and macrophages in and around the nodules (Figure 2, panel D). No iNOS+ cells were found (D. Tappe, unpub. data).

The panrickettsial qPCR, typhus group rickettsiae–specific *rpr331* qPCR, and *R. prowazekii*–specific nested qPCR results indicated all samples were negative for rickettsial genomic material. However, the nested *prsA* qPCR indicated tissue sections of the pons of 2 patients (patient 3 and patient 5; Table) were positive for *R. typhi* DNA. Positive qPCR results were obtained again with the pons of these patients when the extractions and qPCRs were repeated. All negative controls (FFPE blocks from patients with unrelated conditions and water) were negative. We sequenced the 2 amplicons (201 bp in length, including sequences of the outer primers; patient 3, GenBank accession no. MH553441), and BLAST analyses (http://www.blast.ncbi.nlm.nih.gov) showed sequence identity with *R. typhi* strains B9991CWPP (GenBank accession no. CP003398), TH1527 (GenBank accession no. CP003397), and Wilmington (GenBank accession no. AE017197) (online Technical Appendix Figure).

Discussion

Cases of typhus resulting from war, population displacement, poverty, and overcrowding are usually attributed to epidemic louseborne *R. prowazekii* (*1*). We show successful amplification of *R. typhi* DNA for 2 out of 7 patients with fatal typhus and encephalitis during World War II by a specific nested qPCR with FFPE CNS tissue samples stored for >70 years. Because of this finding, the diagnosis of murine typhus was made retrospectively for these 2 patients. For the remaining 5 patients, no rickettsial DNA could be amplified in the limited tissue materials available, possibly because of poor DNA quality. Nested PCRs are more sensitive than conventional PCRs, which could explain why the panrickettsial qPCRs and typhus group–specific qPCRs did not amply genomic DNA, whereas the nested PCR did

Table. Characteristics and results of microscopic and molecular analyses of patients with typhus during World War II, Hamburg, Germany, 1940–1944*

Patient no.	Age, y/sex	Brain region	Frequency of typhus nodules	β-actin qPCR, C_t, round 1/2/3†	*Rickettsia typhi*-specific nested *prsA* qPCR, C_t
1	U/U	Medulla	+	37.2/–/44.5	–
		Pons	+++	–/–/35.7	–
2	U/U	Cerebellum	+	39.1/37.3/39.6	–
		Pons	++	37.1/34.7/37.2	–
		Cortex	++	35.3/33.3/38.1	–
3	U/U	Pons	++	37.3/–/**38.1**	23.8
		Cortex	+	35.1/–/37.7	–
4	U/U	Medulla	+++	–/–/42.5	–
		Pons	+	37.8/–/35.4	–
5	U/M	Pons	++	–/35.9/–	–
		Pons	+	**31.0**/–/–	32.4
6	U/U	Medulla	+	36.9/–/–	–
7	29/F	Cerebellum	+	40.0/35.1/–	–

*C_t, cycle threshold; qPCR, quantitative PCR; U, unknown; +, ++, +++, semiquantitative microscopic measurements (+, low; ++, medium; +++, high); –, negative result.
†From each brain region block, three 5-μm tissue sections were used for each round (n = 3) of extraction and amplification. The β-actin qPCR C_t of the respective round from which successful *R. typhi* DNA amplification was achieved is bolded.
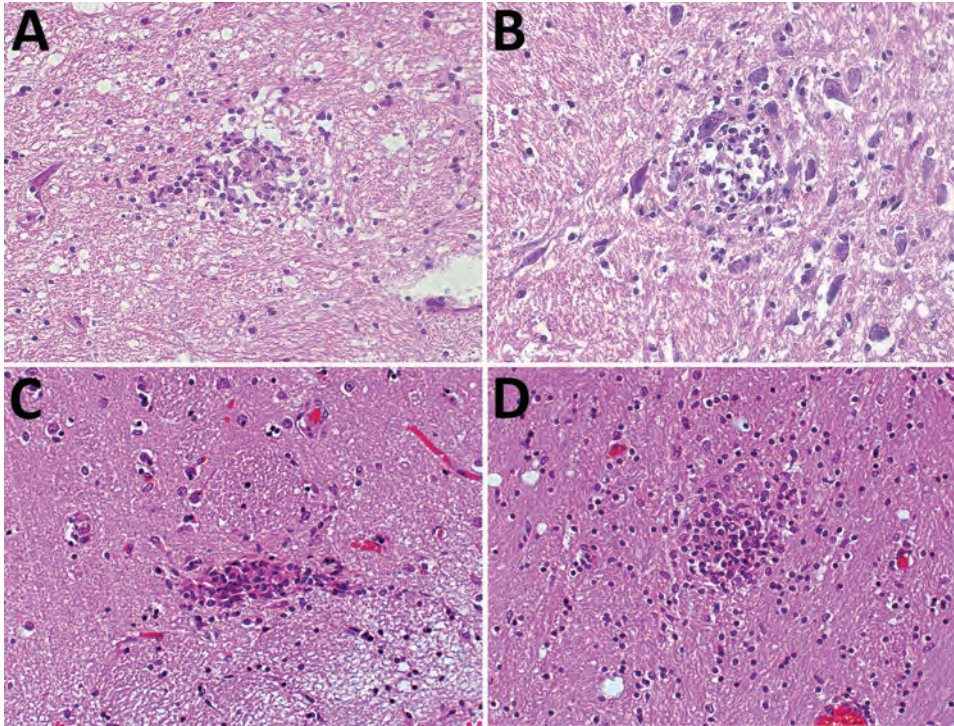
Figure 1. Hematoxylin and eosin staining of typical typhus nodules in brain of typhus patients during World War II, Hamburg, Germany, 1940–1944. Most nodules were found in the pons and medulla oblongata. A) Loose nodule. B) Spongy nodule amid large neuronal cells. C) Compact typhus nodule along longitudinal blood vessel. Note hyperemia of other blood vessels nearby. D) Another compact nodule with hyperemic blood vessels nearby. Original magnifications ×40.

with samples from 2 patients. Because nested PCRs are prone to contamination, we took several precautions: we included several negative controls (which remained negative throughout the study), omitted the positive control, and ran the nested PCR as a qPCR.

No intracellular bacteria were found by conventional light microscopy in Giemsa-stained brain sections. We could only assess CNS tissues because other tissue types had not been archived; the reason for the absence of these tissues is unclear. Microscopy results negative for rickettsial bacteria in brain tissue sections of typhus patients are in line with old reports; the doubtless detection of rickettsiae on microscopic examination of epidemic typhus patient samples was notoriously difficult (*10,11*). We did not attempt immunofluorescence testing of tissue sections. The postmortem detection of tissue nodules in brain sections during microscopic examination has been regarded as specific for epidemic typhus. Such typhus nodules were first described in the skin of patients with rash during epidemic typhus (typhus exanthematicus) in 1913. Shortly thereafter, during World War I, these nodules were found postmortem in the brains of epidemic typhus patients. The nodules were shown to be most prominent in the medulla and pons, also as seen in our study, followed by the basal ganglia, cortex, hippocampus, and cerebellum (*11–13*). In the 1910s, typhus was correctly described as a discontinuous vasculitis that could also occur in the brain involving lesions that form in endothelial cells of the intima of capillaries and small arteries. Inflammatory nodules

always arranged around a blood vessel and were composed of lymphocytes, plasma cells, neutrophil granulocytes, and glia cells (*12,13*). In contrast with autopsy data of epidemic typhus, only rare reports of histopathologic findings of murine typhus exist. Typical rickettsial vascular injury and perivasculitis with lymphocytes, monocytes, and macrophages had been described in the CNS of murine typhus cases (*14,15*). In our study, immunohistochemistry confirmed the histopathologic findings of all these old reports. We also differentiated the T-cell subsets, showing that most T cells are CD8 positive. Using histopathology and immunohistochemistry, we found no obvious cell composition differences between nodules positive and those negative for *R. typhi* DNA. Thus, a similar histologic architecture and composition of typhus nodules in murine and epidemic typhus can be assumed.

The 7 cases examined in our study represent a minor fraction of the typhus cases seen in Langenhorn Hospital. The hospital had opened a ward specifically for typhus patients in May 1942, and 320 cases were seen during the following 2 years (*16*). Forced laborers from Russia who had typhus had also been admitted to this hospital (*17*).

Murine typhus is often a mild illness but can become more severe in refugee camps (*18*), and fatal and severe CNS cases of murine typhus have been described (*14,19,20*). Murine and epidemic typhus can be discerned neither histopathologically nor clinically (except perhaps by their expected respective severities and associated mortality rates, the presence of vectors, or flea or louse
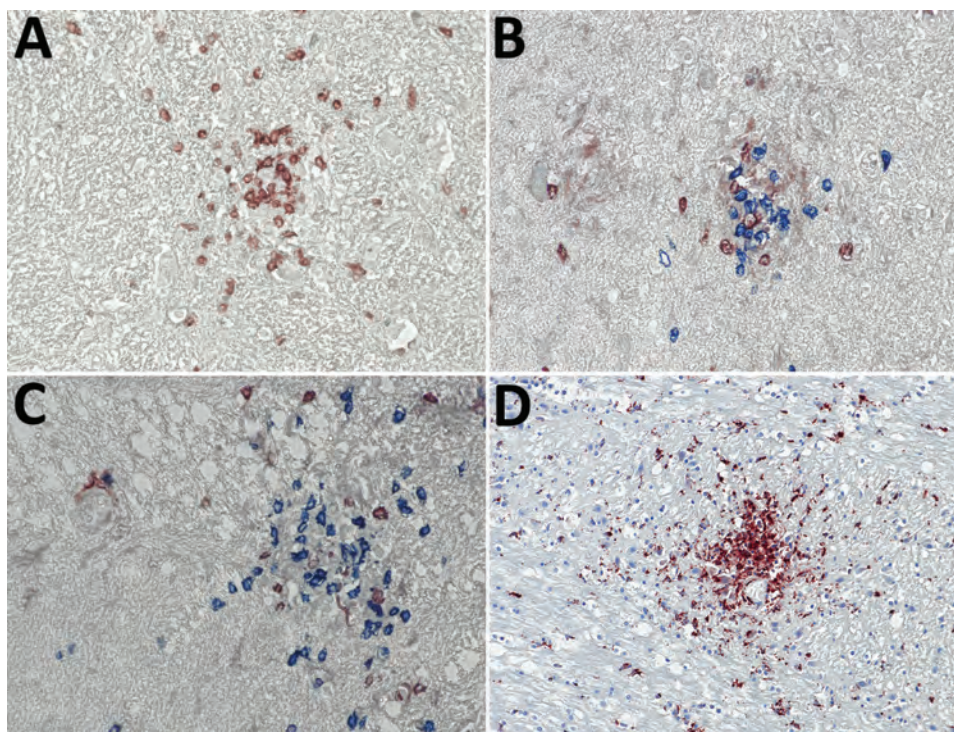
Figure 2. Immunohistochemical analyses of nodule cell compositions from typhus patients during World War II, Hamburg, Germany, 1940–1944. Tissue sections were incubated with specific antibodies and visualized with immunoperoxidase (brown) or immunophosphatase (blue) stains and lightly counterstained with hematoxylin. A) CD3 stain (brown) for T cells and CD20 stain (blue) for B cells. Only T cells are visible within the nodule. Original magnification ×40. B, C) CD4 stain (brown) and CD8 stain (blue) for T cell subsets. The nodules consist of a mixture of both cell types, with a predominance of CD8-positive cytotoxic T cells. Original magnifications ×40. D) CD68 stain (brown) for macrophages and microglia. A strong positivity is seen in the nodules and staining is also scattered in the surrounding brain parenchyma. Original magnification ×20.

bite reactions on the skin). Eschars are usually absent in both forms of typhus. Serologic discrimination of the 2 species by cross-absorption and Western blotting (*21*) and molecular differentiation are confined to reference laboratories and only became available half a century after the cases were investigated.

The natural reservoir for *R. typhi* is rats, and unhygienic conditions that occur during times of civil disturbance promote the expansion of rat populations and their fleas and, thus, also the likelihood of persons acquiring murine typhus. Fleas remain infected for life, and their lifespan and feeding behavior are not altered by *R. typhi* infection (*22*). However, the *R. typhi* bacterium has also been shown experimentally to replicate in the body louse (*22*). Similar to infection with *R. prowazekii*, lice infected with *R. typhi* become red due to the rupture of their epithelial gut linings caused by the multiplication of rickettsiae, which reduces their lifespan. Thus, we speculate that *R. typhi* might also be transmitted by body lice under conditions of civil disturbance previously shown to favor the spread of *R. prowazekii*.

In conclusion, we show evidence that *R. typhi* played a role during local outbreaks or epidemics of typhus that were classically attributed to *R. prowazekii*. Therefore, more cases of typhus should be investigated molecularly to determine the type of rickettsial pathogen involved. Whether *R. typhi* was transmitted during World War II by lice remains to be elucidated.

About the Author

Dr. Rauch is a biochemist at the National Reference Center for Tropical Diseases, Bernhard Nocht Institute, Hamburg, Germany. Her research interests focus on diagnostic methods and the immune response to rickettsial diseases.

References

1. Bechah Y, Capo C, Mege JL, Raoult D. Epidemic typhus. Lancet Infect Dis. 2008;8:417–26. http://dx.doi.org/10.1016/S1473-3099(08)70150-6
2. Civen R, Ngo V. Murine typhus: an unrecognized suburban vectorborne disease. Clin Infect Dis. 2008;46:913–8. http://dx.doi.org/10.1086/527443
3. Tsioutis C, Zafeiri M, Avramopoulos A, Prousali E, Miligkos M, Karageorgos SA. Clinical and laboratory characteristics, epidemiology, and outcomes of murine typhus: a systematic review. Acta Trop. 2017;166:16–24. http://dx.doi.org/10.1016/j.actatropica.2016.10.018
4. Keller C, Krüger A, Schwarz NG, Rakotozandrindrainy R, Rakotondrainiarivelo JP, Razafindrabe T, et al. High detection rate of *Rickettsia africae* in *Amblyomma variegatum* but low prevalence of anti-rickettsial antibodies in healthy pregnant women in Madagascar. Ticks Tick Borne Dis. 2016;7:60–5. http://dx.doi.org/10.1016/j.ttbdis.2015.08.005
5. Mourembou G, Lekana-Douki JB, Mediannikov O, Nzondo SM, Kouna LC, Essone JC, et al. Possible role of *Rickettsia felis* in acute febrile illness among children in Gabon. Emerg Infect Dis. 2015;21:1808–15. http://dx.doi.org/10.3201/eid2110.141825
6. Leulmi H, Socolovschi C, Laudisoit A, Houemenou G, Davoust B, Bitam I, et al. Detection of *Rickettsia felis*, *Rickettsia typhi*, *Bartonella* species, and *Yersinia pestis* in fleas (Siphonaptera)

from Africa. PLoS Negl Trop Dis. 2014;8:e3152. http://dx.doi.org/10.1371/journal.pntd.0003152

7. Papp S, Rauch J, Kuehl S, Richardt U, Keller C, Osterloh A. Comparative evaluation of two *Rickettsia typhi*-specific quantitative real-time PCRs for research and diagnostic purposes. Med Microbiol Immunol (Berl). 2017;206:41–51. http://dx.doi.org/10.1007/s00430-016-0480-z

8. Rauch J, Eisermann P, Noack B, Mehlhoop U, Muntau B, Schäfer J, et al. Typhus group rickettsiosis, Germany, 2010–2017. Emerg Infect Dis. 2018;24:1213–20. http://dx.doi.org/10.3201/eid2407.180093

9. Socolovschi C, Mediannikov O, Sokhna C, Tall A, Diatta G, Bassene H, et al. *Rickettsia felis*-associated uneruptive fever, Senegal. Emerg Infect Dis. 2010;16:1140–2. http://dx.doi.org/10.3201/eid1607.100070

10. da Rocha-Lima H. Zum nachweis der *Rickettsia prowazeki* bei fleckfieberkranken. Munch Med Wochenschr. 1917;1:33–5.

11. Wolbach SB, Todd JL, Palfrey FW. The etiology and pathology of typhus. Being the main report of the Typhus Research Commission of the League of Red Cross Societies to Poland. Cambridge (MA, USA): The League of Red Cross Societies at the Harvard University Press; 1922.

12. Ceelen W. Histologische befunde bei fleckfieber. Klin Wochenschr (Berlin). 1916;21:530–2.

13. Spielmeyer W. Die zentralen veränderungen beim fleckfieber und ihre bedeutung für die histopathologie der hirnrinde. Z Gesamte Neurol Psychiatr. 1919;47:1–54. http://dx.doi.org/10.1007/BF02896244

14. Walker DH, Parks FM, Betz TG, Taylor JP, Muehlberger JW. Histopathology and immunohistologic demonstration of the distribution of *Rickettsia typhi* in fatal murine typhus. Am J Clin Pathol. 1989;91:720–4. http://dx.doi.org/10.1093/ajcp/91.6.720

15. Binford CH, Ecker HD. Endemic (murine) typhus; report of autopsy findings in three cases. Am J Clin Pathol. 1947;17:797–806. http://dx.doi.org/10.1093/ajcp/17.10.797

16. Mannweiler E. Geschichte des Instituts für Schiffs-und Tropenkrankheiten in Hamburg, 1900–1945. In: Kraus O, editor. Abhandlungen des Naturwissenschaftlichen Vereins in Hamburg. Keltern-Weiler (Germany): Goecke & Evers; 1998.

17. Wulf S. Das Hamburger Tropeninstitut 1919 bis 1945. 1st ed. Berlin: Dietrich Reimer Verlag; 1994.

18. Cowan G. Rickettsial diseases: the typhus group of fevers—a review. Postgrad Med J. 2000;76:269–72. http://dx.doi.org/10.1136/pmj.76.895.269

19. Pether JV, Jones W, Lloyd G, Rutter DA, Barry M. Fatal murine typhus from Spain. Lancet. 1994;344:897–8. http://dx.doi.org/10.1016/S0140-6736(94)92875-4

20. Xu Z, Zhu X, Lu Q, Li X, Hu Y. Misdiagnosed murine typhus in a patient with multiple cerebral infarctions and hemorrhage: a case report. BMC Neurol. 2015;15:121. http://dx.doi.org/10.1186/s12883-015-0383-4

21. La Scola B, Rydkina L, Ndihokubwayo JB, Vene S, Raoult D. Serological differentiation of murine typhus and epidemic typhus using cross-adsorption and Western blotting. Clin Diagn Lab Immunol. 2000;7:612–6.

22. Houhamdi L, Fournier PE, Fang R, Raoult D. An experimental model of human body louse infection with *Rickettsia typhi*. Ann N Y Acad Sci. 2003;990:617–27. http://dx.doi.org/10.1111/j.1749-6632.2003.tb07436.x

Address for correspondence: Dennis Tappe, Bernhard Nocht Institute for Tropical Medicine, Bernhard-Nocht-Str 74, 20359 Hamburg, Germany; email: tappe@bnitm.de

May 2016: Vectorborne Diseases

https://wwwnc.cdc.gov/eid/articles/issue/22/5/table-of-contents

EMERGING INFECTIOUS DISEASES

Epidemiology of Buruli Ulcer Infections, Victoria, Australia, 2011–2016

Michael J. Loftus, Ee Laine Tay, Maria Globan, Caroline J. Lavender,
Simon R. Crouch, Paul D.R. Johnson,[1] Janet A.M. Fyfe[1]

Buruli ulcer (BU) is a destructive soft-tissue infection caused by the environmental pathogen *Mycobacterium ulcerans*. In response to rising BU notifications in the state of Victoria, Australia, we reviewed all cases that occurred during 2011–2016 to precisely map the time and likely place of *M. ulcerans* acquisition. We found that 600 cases of BU had been notified; just over half were in residents and the remainder in visitors to defined BU-endemic areas. During the study period, notifications increased almost 3-fold, from 66 in 2013 to 182 in 2016. We identified 4 BU-endemic areas: Bellarine Peninsula, Mornington Peninsula, Frankston region, and the southeastern Bayside suburbs of Melbourne. We observed a decline in cases on the Bellarine Peninsula but a progressive increase elsewhere. Acquisitions peaked in late summer. The appearance of new BU-endemic areas and the decline in established areas probably correlate with changes in the level of local environmental contamination with *M. ulcerans*.

Buruli ulcer (BU) is a destructive skin and soft tissue infection caused by *Mycobacterium ulcerans*. Although the infection is most prevalent in sub-Saharan Africa, cases have been reported in 33 countries (*1*). The primary risk factor for acquisition of BU is residence in or visitation to a BU-endemic area; however, the environmental reservoirs and modes of transmission within these areas are not completely understood. Recently, researchers have proposed that in Victoria, Australia, possums (arboreal marsupials) are environmental reservoirs and amplifiers (*2,3*) and biting insects are mechanical vectors (*4–6*).

At least 3 areas in Australia are considered BU endemic: a small far northern region of Queensland near the Daintree Rainforest, the Capricorn Coast of Queensland, and select coastal regions of Victoria (*7–10*). We describe the recent epidemiology of all known cases of BU in Victoria that occurred during 2011–2016. We aimed to accurately map current and new BU-endemic areas and compare and contrast the changing incidence in these locations, to document disease severity and associate this with diagnostic delay, and to identify times of increased transmission risk.

Methods

Study Population

The study population comprised all case-patients with BU notified to the Victorian Department of Health and Human Services (DHHS) from January 1, 2011, through December 31, 2016. In Victoria, almost all cases of BU are diagnosed or confirmed by PCR performed at 1 reference center (*11,12*). A positive PCR is sufficient for notification of a case of BU. All PCR-positive samples were subsequently cultured for reference purposes according to World Health Organization (WHO) guidelines (*13*).

Enhanced surveillance data collection forms have been in use by DHHS since January 1, 2011 (*14*); where required, public health officers obtain additional information through telephone interviews with clinicians or patients. Information obtained includes patient sex, date of birth, residential address, occupation, residence in or travel to BU-endemic areas within the preceding 12 months, date of symptom onset, date of first visit to a healthcare worker, date when BU was first suspected, form(s) of disease (ulcer, papule, nodule, plaque, cellulitis, edema), location of lesion(s), size of affected area including palpable induration (graded by WHO categories I, II, III [*15*]), laboratory results, and treatment details. If enhanced surveillance forms were incomplete or ambiguous with respect to travel to BU-endemic areas, date of symptom onset, or first visit to a healthcare worker, 1 author (M.L.) conducted follow-up telephone interviews.

Author affiliations: Victorian Department of Health and Human Services, Melbourne, Victoria, Australia (M.J. Loftus, E.L. Tay, S.R. Crouch); Austin Health, Heidelberg, Victoria, Australia (M.J. Loftus, P.D.R. Johnson); Victorian Infectious Diseases Reference Laboratory, Melbourne (M. Globan, C.J. Lavender, J.A.M. Fyfe); The University of Melbourne, Parkville, Victoria, Australia (P.D.R. Johnson)

[1]Joint senior authors.

Definitions

We defined a case-patient as a patient with a clinical lesion and a positive *M. ulcerans* PCR or culture result (usually both). We defined BU-endemic areas as suburbs or towns (defined by nationally recognized suburb/locality boundaries [16]) where ≥2 residents had been affected by BU without recalled travel history to another known BU-endemic area in the preceding year; suburbs or towns adjacent to a known endemic area with ≥1 affected resident or visitor without recalled travel history to any other known endemic areas in the preceding year; or suburbs or towns where *M. ulcerans* had been detected in environmental samples (2,17). Severe disease was defined as WHO category II or III disease at diagnosis (14).

BU-endemic areas were further classified by grouping into the following broad geographic regions: Bellarine Peninsula, Mornington Peninsula, Frankston region, and the southeastern Bayside suburbs (Figure 1). A full list of suburbs or towns considered BU endemic and their grouping into categories is available in online Technical Appendix Table 1 (https://wwwnc.cdc.gov/EID/article/24/11/17-1593-Techapp1.pdf).

We defined residents as case-patients with a postal address in a BU-endemic area or case-patients who reported residing in a BU-endemic area more than half of the year before symptom onset. The remainder were defined as nonresidents. The exception was residents of the Frankston region and southeastern Bayside suburbs; if
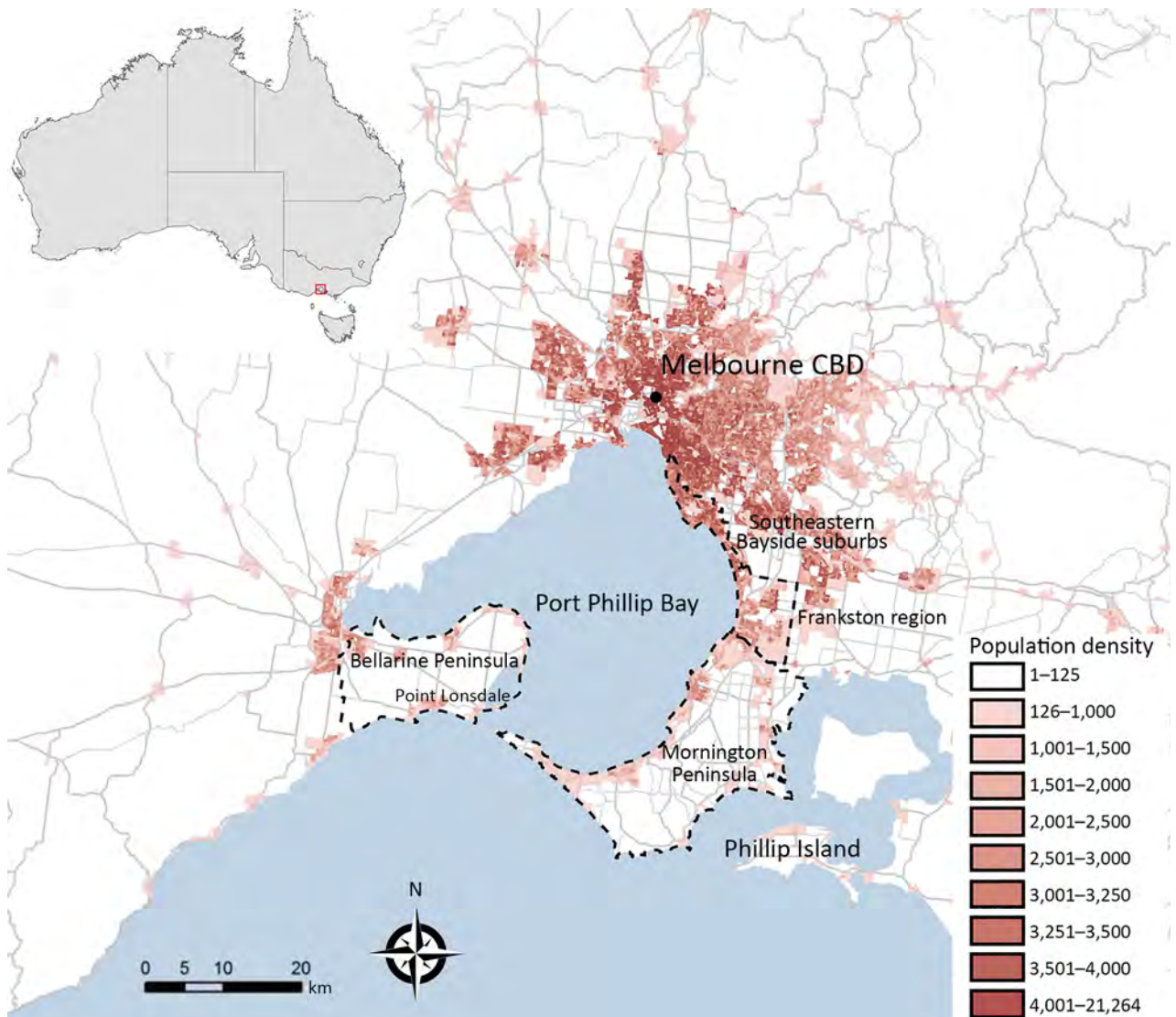
Figure 1. Melbourne, Victoria, Australia, and surrounding areas, showing population density and outlines of the 4 geographic regions used in study of the epidemiology of Buruli ulcer infections in Victoria, Australia, 2011–2016. Population density calculated as residents per square kilometer, according to the Australian Bureau of Statistics 2013 estimated resident population data at the level of Statistical Area Level 1 (*18*). Inset shows location of Melbourne in Australia. CBD, central business district.

these case-patients had a history of travel to BU-endemic areas with higher BU incidence rates, their residency status was determined at a case conference as resident, nonresident, or unclear.

We defined likely exposure location (LEL) as the most likely place of BU acquisition, recorded at the suburb and regional levels. In April 2017, four authors (M.J.L., E.L.T., D.D.R.J., J.A.M.F.) held a case conference to allocate residency status and LEL for case-patients for whom these factors were questionable. The panel considered the frequency, duration, and nature of exposures to BU-endemic areas; the timing of exposures relative to symptom onset (considering the average incubation period of 4–5 months [19,20]); and the relative rates of BU in each location in the year of their exposure. Decisions were reached by consensus.

Confidence in LEL was expressed as definite, probable, or multiple. The term definite was applied to all residents of higher risk BU-endemic areas (Bellarine or Mornington Peninsulas), residents of lower risk BU-endemic areas (Frankston region or the southeastern Bayside suburbs) without significant travel history to other BU-endemic areas, and nonresidents who had traveled to only 1 BU-endemic area. The term probable was applied to residents of the Frankston region or the southeastern Bayside suburbs or nonresidents with exposure to ≥ 2 BU-endemic areas where 1 location was clearly most likely to be responsible. The term multiple was applied to residents of the Frankston region or southeastern Bayside suburbs and to nonresidents with exposure to ≥ 2 BU-endemic areas where no location was considered more likely than another to be responsible.

Some cases could be assigned different degrees of confidence between the suburb and region of exposure. For instance, someone who traveled to many towns within the Mornington Peninsula could be classified as having had multiple exposures at the suburb level but definite exposure at the regional level. If a patient had also been exposed to interstate or overseas BU-endemic regions, where possible, we performed variable-number tandem-repeat typing on the isolate to identify the region of origin (21).

Statistical Analyses

We performed descriptive analyses of data and reported means or medians, depending on their distribution. Rates were calculated by using the Australian Bureau of Statistics midyear estimated resident population data (22). To explore significant associations between groups, we used χ^2 or Fisher exact tests for categorical variables and Mann-Whitney U or Kruskal-Wallis tests to compare the time between symptom onset and first healthcare visit and between symptom onset and BU diagnosis between groups. We used the Edwards test for seasonal trends (23) to determine the periodicity of monthly totals of date of symptom onset, first visit to a healthcare worker, and diagnosis. We investigated

the predictors of disease severity by using logistic regression. Independent variables with p<0.2 in univariate analysis were considered in multivariate analysis.

Maps were prepared by using an ESRI ArcGIS server version 10.4.1, accessed from Geocortex Essential online mapping software (http://www.geocortex.com). All data preparation and analyses were conducted by using Microsoft Excel 2010 (Redmond, WA, USA) and Stata version 13.0 (StataCorp LLC, College Station, TX, USA).

Ethics Statement

DHHS officers obtained all identifying data in this study under the legislative authority of the Public Health and Wellbeing Act 2008, Victoria. This act covers notifiable diseases; separate ethics approval was not required.

Results

Demographics and Rates of Disease

During 2011–2016, a total of 600 BU cases were notified to DHHS; annual case numbers increased from 66 cases in 2013 to 182 cases in 2016 (Figure 2). During March and April 2017, telephone interviews were required to obtain further information for 117 (19.5%) case-patients regarding their travel history and LELs; these calls were completed for 98 (83.8%) of 117 contactable case-patients.

Of the 600 case-patients, 342 (57.0%) were male; the median age was 54 years (range 1–95 years). In terms of residency, 16 case-patients were considered residents of the Frankston region or southeastern Bayside suburbs but had substantial exposures to other higher risk BU-endemic areas; 6 were considered nonresidents, and residency status for 10 was deemed unclear. Thus, the 10 case-patients with unclear status were excluded from subsequent analyses of residents versus nonresidents. Of the remaining 590 case-patients, 369 (61.5%) were classified as residents and 221 (36.8%) as nonresidents of BU-endemic areas. On average, residents were much older (median age 58 years) than nonresidents (median age 44 years) (p<0.0001) and accounted for over half of all cases each year, varying between a low of 54.4% in 2016 and a high of 72.0% in 2015 (Figure 2).

The overall rates in Victoria were 1.1–3.0 cases/100,000 population (Figure 2). However, because of the focal distribution of BU, rates for certain suburbs or towns were significantly higher. For instance, for residents of the adjoining towns Rye and Tootgarook on the Mornington Peninsula, the combined rate was 366 cases/100,000 population in 2016, which is >100-fold higher than the state average. Across the 6-year study period, the rates of BU among residents of the 4 geographic regions were 7.6 cases/100,000 population on the Bellarine Peninsula, 3.1 cases/100,000 population on the Mornington Peninsula, 1.1 cases/100,000 population in the
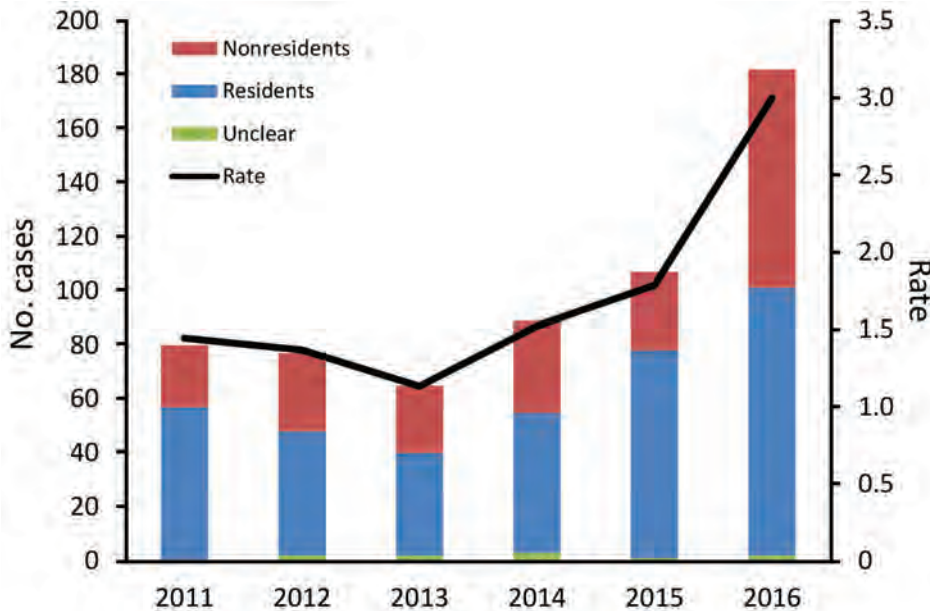
Figure 2. Number of Buruli ulcer cases and incidence rate (no. cases/100,000 persons), by year and resident status, Victoria, Australia, 2011–2016.

Frankston region, and 0.6 cases/100,000 population in the southeastern Bayside suburbs.

LELs at the Regional Level

Of the 600 case-patients, 565 (94.2%) had LELs at the regional level defined as definite, 13 (2.2%) as probable, and 18 (3.0%) as multiple. For 3 case-patients—all residents of metropolitan Melbourne—no exposure to a BU-endemic area was reported, and for 1 case-patient, no information regarding travel was available.

The most common LELs by region were the Mornington Peninsula (247/565, 43.7% of definite exposures) and the Bellarine Peninsula (235, 41.6%), followed by the Frankston region (50, 8.8%) and the southeastern Bayside suburbs (25, 4.4%) (Figure 3). Although the Mornington

and Bellarine Peninsulas were linked to a similar number of LELs over the entire study period, their patterns differed greatly (Figure 4). LELs were highest for the Bellarine Peninsula in 2011 (61 LELs) and steadily declined to only 21 in 2016. In contrast, LELs were initially very few for the Mornington Peninsula (only 31 in the first half of the study period) and increased substantially from 2015 on. More than half of all LELs linked to the Mornington Peninsula were notified in 2016 alone.

When the 31 case-patients with probable or multiple exposures were also considered, LELs linked to the southeastern Bayside suburbs and Frankston region increased disproportionately (Bayside suburbs, 48% increase, from 25 to 37 exposures; Frankston, 22% increase, from 50 to 61). Increases for the Mornington Peninsula (11%, from
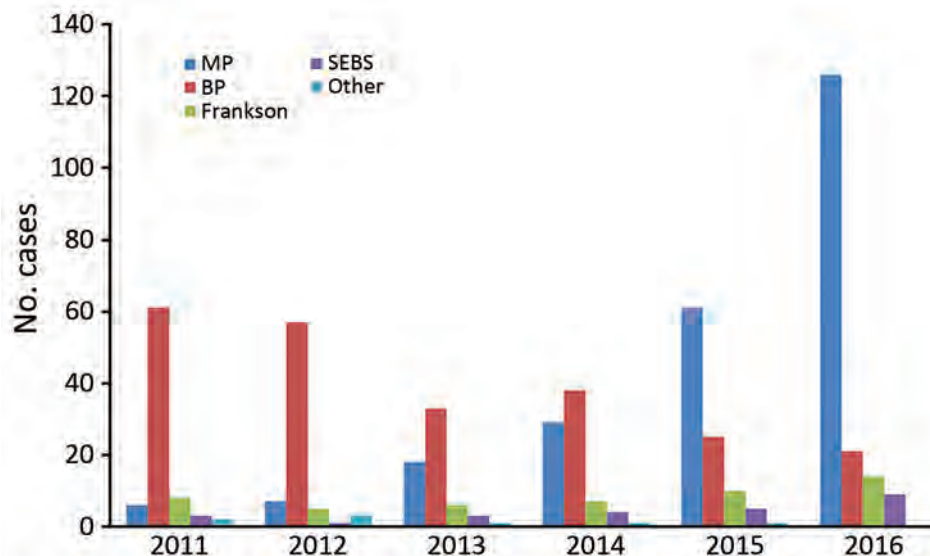
Figure 3. *Mycobacterium ulcerans* likely exposure locations, by region and year (definite cases only), Victoria, Australia, 2011–2016. BP, Bellarine Peninsula; MP, Mornington Peninsula; SEBS, southeastern Bayside suburbs.
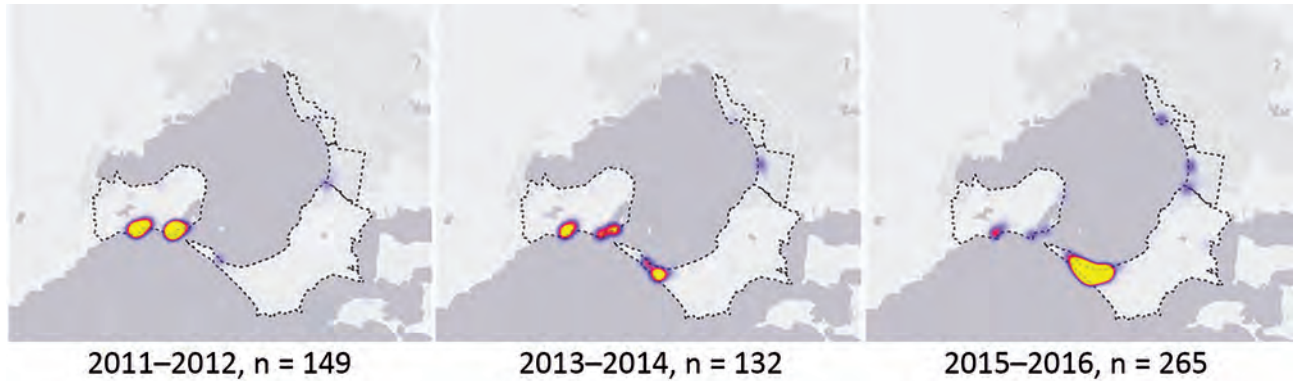
Figure 4. Heat maps of *Mycobacterium ulcerans* likely exposure locations (definite cases only), by 2-year period, Victoria, Australia, 2011–2016.

247 to 273) and the Bellarine Peninsula (6%, from 235 to 249) were smaller (online Technical Appendix Table 2).

Date of Symptom Onset

Information regarding the date of symptom onset was available for 494 (82.3%) of the 600 patients and regarding the date of first visit to a healthcare worker for 497 (82.8%) patients. With regard to date of symptom onset, the monthly variation was best described by a simple harmonic curve (p<0.0001), which showed a trough in early January (summer in the Southern Hemisphere) and a peak in early July (winter in the Southern Hemisphere). Onset of symptoms was lowest in January (summer, 6 cases) and highest in June (winter, 82 cases) (Figure 5, panel A). The same seasonal pattern was found for residents and nonresidents; peaks and troughs occurred in identical months.

The monthly variation in the dates of first visit to a healthcare worker and diagnosis of BU were also best described by simple harmonic curves (p<0.0001 for both). Peaks for visit to a healthcare worker occurred in mid-August and for BU diagnosis in mid-September (Figure 5, panels B, C).

Clinical Features

The site of BU lesion was available for 585 (97.5%) of the 600 case-patients; among these, the most common site of infection was the lower limbs (424/585, 72.4%). More than two thirds of those lesions (51.0% overall) were below the knee; the remainder were predominantly on the upper limbs (23.3%), and a small proportion were on the torso (0.7%) or head and neck (0.8%) (Tables 1, 2). Univariate analysis revealed no significant associations between site of infection and patient age or sex. Lesion location has recently been accurately mapped in a separate study of patients with BU in Victoria (*24*).

Information regarding the form of disease was available for 536 (89.3%) case-patients. Only 1 form of disease was documented for most patients, 2 forms for 12 patients, and 3 forms for 1 patient. The most common form of disease was an ulcer (455/536, 84.9%), followed by a papule (37, 6.9%), a nodule (22, 4.1%), cellulitis (20, 3.7%), plaque (8, 1.5%), or edema (7, 1.3%).

Overall, 415 (69%) patients had WHO category I disease, 71 (11.8%) category II, and 37 (6.2%) category III. For the remaining 77 (12.8%), no information regarding disease severity was available (Tables 1, 2). No relationship was found between severe disease and year of BU diagnosis (online Technical Appendix Table 3). Multivariable analysis revealed an increased likelihood of severe BU disease among older patients (>60 years) (odds ratio [OR] 2.19, 95% CI 1.38–3.47) and visitors to BU-endemic regions (OR 1.87, 95% CI 1.16–3.02) (Table 3). Although
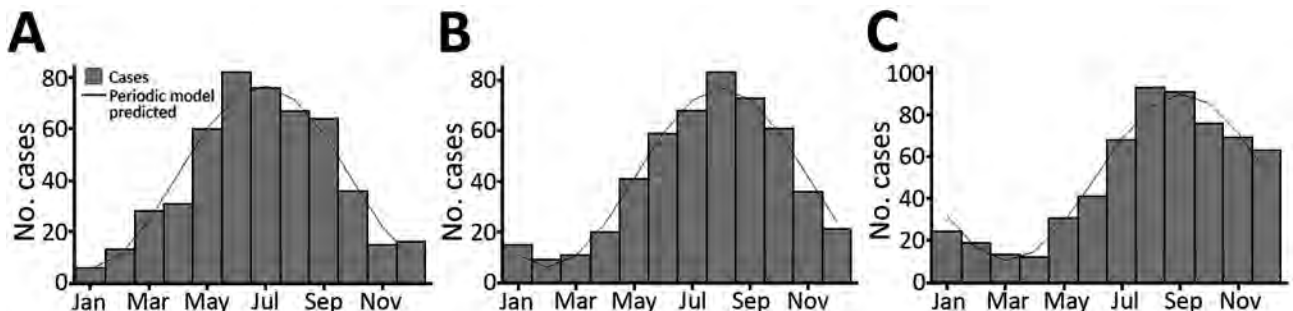
Figure 5. Timing of A) symptom onset, B) first visit to a healthcare worker, and C) diagnosis of Buruli ulcer for patients with *Mycobacterium ulcerans* infection, Victoria, Australia, 2011–2016.

Table 1. Clinical site and severity, delays to first healthcare visit and diagnosis, and management strategies for Buruli ulcer case-patients, by age and region of exposure, Victoria, Australia, 2011–2016*

Variable	Total no. (%)	Age group, y				Exposure, definite at area level, n = 565			
		<15	15–60	>60	p value†	BP	MP	Other	p value†
Total	600	72 (12.0)	285 (47.5)	243 (40.5)		235 (39.2)	247 (41.2)	83 (13.8)	
Lesion site, total no.	585	71	278	236	0.381‡	228	240	82	0.003‡
Lower limb	424 (72.5)	52 (70.3)	210 (75.5)	162 (68.6)		154 (67.5)	182 (75.8)	58 (70.7)	
Below knee	306 (52.3)	31 (41.9)	149 (53.6)	126 (53.4)		109 (47.8)	129 (53.8)	45 (54.9)	
Knee or above	86 (14.7)	16 (21.6)	48 (17.3)	22 (9.3)		33 (14.5)	39 (16.3)	10 (12.2)	
Unspecified	32 (5.5)	5 (6.8)	16 (5.8)	14 (5.9)		12 (5.3)	14 (5.8)	3 (3.7)	
Upper limb	140 (23.9)	17 (23)	61 (21.9)	62 (26.3)		71 (31.1)	45 (18.8)	19 (23.2)	
Other sites	12 (2.1)	1 (1.4)	6 (2.2)	5 (2.1)		2 (0.9)	9 (3.8)	1 (1.2)	
Head/neck	5 (0.9)	1 (1.4)	2 (0.7)	2 (0.8)		1 (0.4)	4 (1.7)	0 (0.0)	
Torso	4 (0.7)	0 (0)	2 (0.7)	2 (0.8)		1 (0.4)	2 (0.8)	1 (1.2)	
Buttock/perineum	3 (0.5)	0 (0)	2 (0.7)	1 (0.4)		0	3 (1.3)	0	
>1 site	9 (1.5)	1 (1.4)	1 (0.4)	7 (3.0)		1 (0.4)	4 (1.7)	4 (4.9)	
WHO category, total no.	523	64	244	215	0.041	198	221	69	0.219
I	415 (79.3)	53 (82.8)	204 (83.6)	158 (73.5)		166 (83.8)	171 (77.4)	52 (75.4)	
II	71 (13.6)	7 (10.9)	30 (12.3)	34 (15.8)		23 (11.6)	34 (15.4)	9 (13.0)	
III	37 (7.1)	4 (6.3)	10 (4.1)	23 (10.7)		9 (4.5)	16 (7.2)	8 (11.6)	
Time to healthcare visit					0.0146				0.2770
Median (IQR), d	28 (14–60)	21 (14–36)	30 (14–60)	21 (14–49)		28 (14–42)	30 (14–60)	30 (14–60)	
Time to diagnosis					0.1536				0.0001
Median (IQR), d	63 (35–109)	63 (39–122)	65 (37–114)	54 (31–103)		46 (27–83)	70 (37–119)	82 (21–127)	
Treatment, total no.	517	65	227	214	0.606	205	210	69	0.281
Antimicrobial drugs only	328 (63.4)	41 (63.1)	145 (63.9)	142 (66.4)		137 (66.8)	135 (64.3)	37 (53.6)	
Surgery only	27 (5.2)	2 (3.1)	16 (7)	9 (4.2)		12 (5.9)	9 (4.3)	5 (7.2)	
Antimicrobial drugs and surgery	162 (31.3)	22 (33.8)	77 (33.9)	63 (29.4)		56 (27.3)	66 (31.4)	27 (39.1)	
Surgery, total no.	165	19	81	65	0.621	59	66	26	0.671
Debridement	54 (32.7)	6 (31.6)	29 (35.8)	19 (29.2)		20 (33.9)	23 (34.8)	5 (19.2)	
Narrow excision	53 (32.1)	8 (42.1)	26 (32.1)	19 (29.2)		19 (32.2)	20 (30.3)	10 (38.5)	
Wide excision	58 (35.2)	5 (26.3)	26 (32.1)	27 (41.5)		20 (33.9)	23 (34.8)	11 (42.3)	

*Values are no. (%) patients except as indicated. BP, Bellarine Peninsula; IQR, interquartile range; MP, Mornington Peninsula; WHO, World Health Organization.
†p value provides comparisons across all categories.
‡p value provides comparison between lower limb, upper limb, all other sites, and patient age or exposure location.

exposure to BU-endemic regions other than the Bellarine and Mornington Peninsulas seemed to be associated with an increased risk for severe disease, this association did not reach statistical significance (OR 1.997, 95% CI 0.98–3.94). No association with patient sex was found.

Time to Diagnosis

All 600 cases of BU were confirmed with PCR testing. Culture results were available for 489 patients; results for 419 (85.7%) were positive for *M. ulcerans*. For some case-patients, the diagnosis of BU was first considered only after being indicated by histologic examination of surgical specimens and later confirmed by PCR.

The median time between symptom onset and first visit to a healthcare worker was 28 days. This time did not differ significantly between residents and nonresidents (p = 0.5253), and although delay to first healthcare visit was shorter for Bellarine Peninsula residents (21 days) than for Mornington Peninsula residents or all other residents, this difference was not significant (p = 0.185 and p = 0.174, respectively) (Table 4). Case-patients 15–60 years of age

sought healthcare significantly later (median 30 days) than did younger (<15 years) (21 days, p = 0.021) or older (>60 years) (21 days, p = 0.0179) case-patients (Table 1).

The overall median delay from symptom onset to BU diagnosis was 63 days. Diagnoses were made far sooner for residents (median delay 48 days) than for nonresidents (median delay 79 days) (p<0.0001). The median delay to diagnosis was even shorter for Bellarine Peninsula residents, only 34 days (p<0.0001) (Table 4). Regardless of resident status, the average diagnostic delay for case-patients with definite LELs on the Bellarine Peninsula was shorter (46 days) than for those with definite LELs on the Mornington Peninsula (70 days) or other areas (82 days) (p = 0.0001). The longer delay to diagnosis among nonresidents, and those not exposed on the Bellarine Peninsula, was primarily driven by the delay between first visit to a healthcare worker and receiving the diagnosis of BU (Tables 1, 3).

Treatment

Treatment information was available for 517 (86.1%) patients. Of these, 490 (94.8%) received antimicrobial

Table 2. Clinical site and severity, delays to first healthcare visit and diagnosis, and management strategies for Buruli ulcer case-patients, by sex, Victoria, Australia, 2011–2016*

Variable	Male	Female	p value†
Total no.	342 (57.0)	258 (43.0)	
Lesion site, total no.	333	252	0.116‡
Lower limb	231 (69.4)	193 (76.6)	
Below knee	167 (50.2)	139 (55.2)	
Knee or above	39 (11.7)	47 (18.7)	
Unspecified	25 (7.5)	7 (2.8)	
Upper limb	87 (26.1)	53 (21)	
Other sites	8 (2.4)	4 (1.6)	
Head/neck	2 (0.6)	3 (1.2)	
Torso	4 (1.2)	0 (0.0)	
Buttock/perineum	2 (0.6)	1 (0.4)	
>1 site	8 (2.4)	2 (0.8)	
WHO category, total no.	295	228	0.078
I	226 (76.6)	189 (82.9)	
II	42 (14.2)	29 (12.7)	
III	27 (9.2)	10 (4.4)	
Time to healthcare visit			0.6153
Median (IQR), d	29 (14–60)	28 (14–42)	
Time to diagnosis			0.5134
Median (IQR), d	63 (35–109)	65 (36–117)	
All treatment, total no.	296	221	0.03
Antimicrobial drugs only	189 (63.9)	139 (62.9)	
Surgery only	9 (3.0)	18 (8.1)	
Antimicrobial drugs and surgery	98 (33.1)	64 (29)	
Surgical treatment, total no.	91	74	0.331
Debridement	33 (36.3)	21 (28.4)	
Narrow excision	25 (27.5)	28 (37.8)	
Wide excision	33 (36.3)	25 (33.8)	

*Values are no. (%) patients except as indicated. IQR, interquartile range; WHO, World Health Organization.
†p value provides comparisons across all categories.
‡p value provides comparison between lower limb, upper limb, all other sites, and patient sex.

drugs; however, specific details of chosen agents and duration of regimen were inconsistently reported on enhanced surveillance forms and therefore were not analyzed. Surgery was performed for 189 (36.6%) of these 517 case-patients; 162 (85.7%) concomitantly received antimicrobial drugs, and 27 (14.3%) underwent surgery only. Women were more likely than men to undergo surgery only (p = 0.01) (Tables 1, 3).

Discussion

BU is a geographically restricted infection that occurs as local outbreaks. The environmental reservoir and mode of transmission to humans who enter BU-endemic regions is of intense scientific interest because primary prevention will not be possible until these issues have been definitively resolved.

In our epidemiologic investigation, we established that BU incidence is increasing in the temperate state of

Table 3. Logistic regression model showing adjusted and unadjusted associations between identified factors and severe Buruli ulcer disease, Victoria, Australia, 2011–2016*

	Disease severity, no. (%) patients†		Univariate model		Multivariate model	
Factor	Category I	Categories II and III	OR (95% CI)	p value	aOR (95% CI)	p value
Age, y						
≤60	257 (83.4)	51 (16.6)	1.00			
>60	158 (73.5)	57 (26.5)	1.82 (1.19–2.79)	0.006	2.19 (1.38–3.47)	0.001
Sex						
F	189 (82.9)	39 (17.1)	1.00			
M	226 (76.6)	69 (23.4)	1.48 (0.96–2.29)	0.079	1.36 (0.85–2.16)	0.199
Residence						
Resident	251 (82.3)	54 (17.7)	1.00			
Visitor	156 (75.0)	52 (25.0)	1.55 (1.01–2.38)	0.046	1.87 (1.16–3.02)	0.01
Unclear	8 (80.0)	2 (20.0)	1.16 (0.24–5.63)	0.852	NC	
Exposure						
Bellarine Peninsula	166 (83.8)	32 (16.2)	1.00			
Mornington Peninsula	171 (77.4)	50 (22.6)	1.52 (0.93–2.48)	0.097	1.35 (0.81–2.24)	0.244
Other	52 (75.4)	17 (24.6)	1.70 (0.87–3.30)	0.120	2.00 (0.87–3.94)	0.056
Time to diagnosis, d‡			1.002 (0.999–1.005)	0.254		

*aOR, adjusted odds ratio; NC, not calculable because there were no data; OR, odds ratio.
†Severe disease is defined as World Health Organization category II or III.
‡Not included in the logistic regression model because it did not meet the prespecified threshold for significance of p<0.2.

Table 4. Demographic and clinical data and management strategies for Buruli ulcer case-patients, by resident status, Victoria, Australia, 2011–2016*

Characteristic	Residents				Nonresidents		Overall
	All	BP	MP	p value†	All	p value‡	
Total no. cases	369	146	151		221		600
Age, y							
Median (IQR)	58 (38–71)	55 (33–71)	59 (40–71)	0.7081	44 (24–65)	<0.0001	54 (31–9)
<15	32 (8.7)	11 (7.5)	13 (8.6		39 (17.6)		72 (12)
15–60	168 (45.5)	72 (49.3)	65 (43)		110 (49.8)		285 (47.5)
>6	169 (45.8)	63 (43.2)	73 (48.3)	0.555	72 (32.6)	<0.0001	243 (40.5)
Sex							
M	213 (57.7)	79 (54.1)	94 (62.3)		124 (56.1)		258 (43)
F	156 (42.3)	67 (45.9)	57 (37.7)	0.155	97 (43.9)	0.701	342 (57)
Year of diagnosis, total no.	369	146	151		221		600
2011	57 (15.4)	43 (29.5)	4 (2.6)		23 (10.4)		80 (13.3)
2012	46 (12.5)	34 (23.3)	4 (2.6)		29 (13.1)		77 (12.8)
2013	38 (10.3)	16 (11)	13 (8.6)		25 (11.3)		65 (10.8)
2014	52 (14.1)	24 (16.4)	16 (10.6)		34 (15.4)		89 (14.8)
2015	77 (20.9)	18 (12.3)	46 (30.5)		29 (13.1)		107 (17.8)
2016	99 (26.8)	11 (7.5)	68 (45)	<0.0001	81 (36.7)		182 (30.3)
WHO category, total no.	305	118	127		208		523
I	251 (82.3)	102 (86.4)	103 (81.1)		156 (70.6)		415 (79.3)
II	35 (11.5)	13 (11)	15 (11.8)		35 (15.8)		71 (13.6)
III	19 (6.2)	3 (2.5)	9 (7.1)	0.338	17 (7.7)	0.129	37 (7.1)
Median time to seeking healthcare, d (IQR)	28 (14–60)	21 (14–42)	28 (14–60)	0.1853	30 (14–60)	0.5253	28 (14–60)
Median time to diagnosis, d (IQR)	48 (27–94)	34 (22–62)	51 (29–95)	0.0016	79 (48–123)	<0.0001	63 (35–109)
Treatment, total no.	301	124	129		206		517
Antimicrobial drugs only	208 (69.1)	90 (72.6)	86 (66.7)		115 (55.8)		328 (63.4)
Surgery only	17 (5.6)	7 (5.6)	5 (3.9)		10 (4.9)		27 (5.2)
Antimicrobial drugs and surgery	76 (25.2)	27 (21.8)	28 (21.7)	0.844	81 (39.3)	0.003	162 (31.3)
Surgical treatment, total no.	78	27	27		83		165
Debridement	27 (34.6)	13 (48.1)	10 (37)		26 (31.3)		54 (32.7)
Narrow excision	26 (33.3)	6 (22.2)	10 (37)		24 (28.9)		53 (32.1)
Wide excision	25 (32.1)	8 (29.6)	7 (25.9)	0.482	33 (39.8)	0.592	58 (35.2)

*Values are no. (%) patients except as indicated. BP, Bellarine Peninsula; IQR, interquartilie range; MP, Mornington Peninsula; WHO, World Health Organization.
†p value provides comparison between Bellarine Peninsula residents and Mornington Peninsula residents.
‡p value provides comparison between all residents and nonresidents.

Victoria, Australia, but that this increase is not uniform. Previously, the most BU-endemic region in Victoria has been the Bellarine Peninsula (*4,8*), where incidence is now progressively falling but has been matched by the appearance of new BU-endemic foci on the Mornington Peninsula and in the southeastern Bayside suburbs of Melbourne. Rather than describing a single epidemic of BU in Victoria, it is probably more accurate to propose that we are observing 3–4 distinct outbreaks with different dynamics.

We found a clear seasonal pattern in the timing of symptom onset —a peak in midwinter and a trough in midsummer—consistent with trends shown in previous reports from Victoria (*8,25,26*). Given the median incubation period for BU in Victoria of 4.5 months (*19,20*), most infections there are probably acquired in summer and autumn. Among nonresidents, this trend could be explained purely by increased tourism to beachside BU-endemic regions during warmer months. However, it is noteworthy that seasonality in symptom onset among residents, who were exposed to BU-endemic areas throughout the year, was identical. This finding suggests that transmission risk is specific to the warmer months, perhaps relating to a vector (e.g., higher mosquito numbers), seasonal rainfall patterns or warmer temperatures, or human behavior (e.g., wearing less clothing, spending more time outside) (*24*).

Delays to diagnosis were significantly shorter among residents of BU-endemic areas than among nonresidents and among Bellarine Peninsula residents than among Mornington Peninsula residents. This finding is broadly consistent with previously reported delays of 28 days among Bellarine Peninsula residents and 72 days among nonresidents (*25*) or 42 days among a cohort consisting predominantly of Bellarine Peninsula residents (*8*). Diagnostic delays may be driven by delays in seeking healthcare, delays in healthcare professionals making the correct diagnosis, or both. In our cohort, large discrepancies in overall diagnostic delay between patient groups seemed to be driven primarily by delays in making the correct diagnosis after patients visited a doctor. Our findings probably reflect patients and general practitioners in non–BU-endemic or recently BU-endemic areas being relatively unfamiliar with BU compared with those in more established

BU-endemic areas and subsequently delaying the initiation of BU-specific diagnostic testing (such as PCR). Several public health campaigns have been introduced to increase awareness of BU on the Bellarine Peninsula, and further research is under way to clarify other specific factors associated with diagnostic delays in Victoria (27).

When calculated across the entire cohort, diagnostic delay was not associated with more severe disease. This finding is somewhat counterintuitive because in the absence of appropriate therapy, most lesions will enlarge and progress over time. However, this cohortwide analysis may be confounded by unaccounted differences among case-patients in the aggressiveness of their disease, their healthcare-seeking behavior, and our inability to control for other factors such as concurrent conditions or immunosuppression. For instance, someone with a rapidly progressive lesion may seek healthcare sooner, be tested more proactively, and receive an early diagnosis of severe disease, whereas another patient with a slowly progressive lesion may seek healthcare later, undergo fewer investigations, and receive a diagnosis after many months with milder disease. Although we found no signal at the population level that diagnostic delay was associated with worse outcomes, public health awareness programs to encourage patients and local doctors to consider BU early remain reasonable.

A recent article, published after our manuscript was submitted, describes clinical information for 426 BU patients at a single tertiary center on the Bellarine Peninsula from 1998 through May 2017 (28). Of note, those authors report increasing severity of disease over time, a finding that was not replicated in our more epidemiologically focused analysis, albeit over a much shorter time (online Technical Appendix Table 3). Although cases overlap between these 2 articles, our analyses included all notified cases occurring in a 6-year period, which reduces potential referral bias. However, our clinical information was obtained via telephone interview, whereas Tai et al. directly assessed their patients, providing them with more detailed clinical information than we had access to (28).

We have previously shown a close association between BU in humans and outbreaks of BU in possums on the Bellarine and Mornington Peninsulas (2,17). Possums are arboreal marsupials that are common in Victoria, in BU-endemic and nonendemic areas. On the basis of our previous work, we think the changing epidemiology of BU reported here is driven primarily by new outbreaks of BU in local possum populations with spillover to humans mediated by environmentally contaminated biting insects (4,24,29). Of note, the window of human exposure may be quite short; a recent study reported 10 family clusters in which transmission to family members occurred almost simultaneously (30).

Limitations of our study include the use of retrospective surveillance data, the long incubation period of BU that introduces recall bias, the contiguous nature of BU-endemic regions, and the shifting geographic distribution of BU, all of which made it challenging to allocate LELs precisely. Although we can use census data for rates of diseases in local populations, the unquantified high levels of tourism to BU-endemic regions during summer make it impossible to accurately estimate the true population at risk or to give a quantitative estimate of risk per day of exposure for visitors.

Although BU is rarely life-threatening, the extent of illness (31) and economic costs (32) are substantial and increase among patients with larger and more advanced lesions. The findings of our study can guide public health responses. The shorter diagnostic delay among residents of the Bellarine Peninsula suggests that increased community awareness leads to earlier disease detection. Furthermore, understanding the seasonality of BU can guide the optimum timing of different public health strategies. The timing of efforts to reduce BU acquisition should vary by season. Efforts such as promoting avoidance of biting insects through appropriate clothing or use of insect repellent (6) and, potentially, efforts to control mosquito numbers should occur during summer and autumn. Efforts focusing on raising awareness and promoting earlier diagnosis of BU among general practitioners and members of the public should occur during autumn and winter.

About the Author

Dr. Loftus was an advanced trainee in infectious diseases medicine at Austin Health in Melbourne, Australia, during 2017. He led this study during a 6-month public health training placement with the Victorian DHHS.

References

1. World Health Organization. Global Health Observatory data [cited 2017 May 22]. http://www.who.int/gho/neglected_diseases/buruli_ulcer/en/
2. Fyfe JA, Lavender CJ, Handasyde KA, Legione AR, O'Brien CR, Stinear TP, et al. A major role for mammals in the ecology of *Mycobacterium ulcerans*. PLoS Negl Trop Dis. 2010;4:e791. http://dx.doi.org/10.1371/journal.pntd.0000791
3. Wallace JR, Mangas KM, Porter JL, Marcsisin R, Pidot SJ, Howden B, et al. *Mycobacterium ulcerans* low infectious dose and mechanical transmission support insect bites and puncturing injuries in the spread of Buruli ulcer. PLoS Negl Trop Dis. 2017;11:e0005553. http://dx.doi.org/10.1371/journal.pntd.0005553
4. Johnson PD, Azuolas J, Lavender CJ, Wishart E, Stinear TP, Hayman JA, et al. *Mycobacterium ulcerans* in mosquitoes captured during outbreak of Buruli ulcer, southeastern Australia. Emerg Infect Dis. 2007;13:1653–60. http://dx.doi.org/10.3201/eid1311.061369
5. Johnson PD, Lavender CJ. Correlation between Buruli ulcer and vector-borne notifiable diseases, Victoria, Australia. Emerg Infect Dis. 2009;15:614–5. http://dx.doi.org/10.3201/eid1504.081162

6. Quek TY, Athan E, Henry MJ, Pasco JA, Redden-Hoare J, Hughes A, et al. Risk factors for *Mycobacterium ulcerans* infection, southeastern Australia. Emerg Infect Dis. 2007;13:1661–6. http://dx.doi.org/10.3201/eid1311.061206

7. Steffen CM, Smith M, McBride WJ. *Mycobacterium ulcerans* infection in North Queensland: the 'Daintree ulcer'. ANZ J Surg. 2010;80:732–6. http://dx.doi.org/10.1111/j.1445-2197.2010.05338.x

8. Boyd SC, Athan E, Friedman ND, Hughes A, Walton A, Callan P, et al. Epidemiology, clinical features and diagnosis of *Mycobacterium ulcerans* in an Australian population. Med J Aust. 2012;196:341–4. http://dx.doi.org/10.5694/mja12.10087

9. Johnson PD, Veitch MG, Leslie DE, Flood PE, Hayman JA. The emergence of *Mycobacterium ulcerans* infection near Melbourne. Med J Aust. 1996;164:76–8.

10. Francis G, Whitby M, Woods M. *Mycobacterium ulcerans* infection: a rediscovered focus in the Capricorn Coast region of central Queensland. Med J Aust. 2006;185:179–80.

11. Fyfe JA, Lavender CJ, Johnson PD, Globan M, Sievers A, Azuolas J, et al. Development and application of two multiplex real-time PCR assays for the detection of *Mycobacterium ulcerans* in clinical and environmental samples. Appl Environ Microbiol. 2007;73:4733–40. http://dx.doi.org/10.1128/AEM.02971-06

12. Ross BC, Marino L, Oppedisano F, Edwards R, Robins-Browne RM, Johnson PD. Development of a PCR assay for rapid diagnosis of *Mycobacterium ulcerans* infection. J Clin Microbiol. 1997;35:1696–700.

13. World Health Organization. Laboratory diagnosis of Buruli ulcer: a manual for health care providers: Geneva: The Organization; 2014.

14. Victorian Department of Health and Human Services. Notification of *Mycobacterium ulcerans* (Buruli ulcer) [cited 2017 Apr 17]. https://www2.health.vic.gov.au/about/publications/formsandtemplates/notification-of-mycobacterium-ulcerans

15. World Health Organization. Treatment of *Mycobacterium ulcerans* disease (Buruli ulcer): Geneva: The Organization; 2012.

16. Research Data Australia, Department of the Prime Minister and Cabinet. VIC Suburb/Locality Boundaries—PSMA Administrative Boundaries [cited 2017 May 8]. https://researchdata.ands.org.au/vic-suburblocality-boundaries-administrative-boundaries/644824

17. Carson C, Lavender CJ, Handasyde KA, O'Brien CR, Hewitt N, Johnson PD, et al. Potential wildlife sentinels for monitoring the endemic spread of human Buruli ulcer in South-East Australia. PLoS Negl Trop Dis. 2014;8:e2668. http://dx.doi.org/10.1371/journal.pntd.0002668

18. Australian Bureau of Statistics. Population by age and sex, regions of Australia, 2013. Canberra (ACT, Australia). The Bureau; 2014.

19. Trubiano JA, Lavender CJ, Fyfe JA, Bittmann S, Johnson PD. The incubation period of Buruli ulcer (*Mycobacterium ulcerans* infection). PLoS Negl Trop Dis. 2013;7:e2463. http://dx.doi.org/10.1371/journal.pntd.0002463

20. Loftus MJ, Trubiano JA, Tay EL, Lavender CJ, Globan M, Fyfe JAM, et al. The incubation period of Buruli ulcer (*Mycobacterium ulcerans* infection) in Victoria, Australia—remains similar despite changing geographic distribution of disease. PLoS

21. Ablordey A, Swings J, Hubans C, Chemlal K, Locht C, Portaels F, et al. Multilocus variable-number tandem repeat typing of *Mycobacterium ulcerans*. J Clin Microbiol. 2005;43:1546–51. http://dx.doi.org/10.1128/JCM.43.4.1546-1551.2005

22. Australian Bureau of Statistics. Australian demographic statistics, December 2016. Canberra (ACT, Australia); The Bureau; 2017.

23. Edwards JH. The recognition and estimation of cyclic trends. Ann Hum Genet. 1961;25:83–7. http://dx.doi.org/10.1111/j.1469-1809.1961.tb01501.x

24. Yerramilli A, Tay EL, Stewardson AJ, Kelley PG, Bishop E, Jenkin GA, et al. The location of Australian Buruli ulcer lesions– implications for unravelling disease transmission. PLoS Negl Trop Dis. 2017;11:e0005800. http://dx.doi.org/10.1371/journal.pntd.0005800

25. Quek TY, Henry MJ, Pasco JA, O'Brien DP, Johnson PD, Hughes A, et al. *Mycobacterium ulcerans* infection: factors influencing diagnostic delay. Med J Aust. 2007;187:561–3.

26. Veitch MG, Johnson PD, Flood PE, Leslie DE, Street AC, Hayman JA. A large localized outbreak of *Mycobacterium ulcerans* infection on a temperate southern Australian island. Epidemiol Infect. 1997;119:313–8. http://dx.doi.org/10.1017/S0950268897008273

27. Coutts S, Tay EL. Factors influencing delayed presentation and diagnosis for Buruli ulcer in Victoria, 2011–2016. Presented at: Communicable Diseases Control Conference; 2017 Jun 26–28; Melbourne, Victoria, Australia.

28. Tai AYC, Athan E, Friedman ND, Hughes A, Walton A, O'Brien DP. Increased severity and spread of *Mycobacterium ulcerans*, southeastern Australia. Emerg Infect Dis. 2018;24:58–64. http://dx.doi.org/10.3201/eid2401.171070

29. Lavender CJ, Fyfe JA, Azuolas J, Brown K, Evans RN, Ray LR, et al. Risk of Buruli ulcer and detection of *Mycobacterium ulcerans* in mosquitoes in southeastern Australia. PLoS Negl Trop Dis. 2011;5:e1305. http://dx.doi.org/10.1371/journal.pntd.0001305

30. O'Brien DP, Wynne JW, Buultjens AH, Michalski WP, Stinear TP, Friedman ND, et al. Exposure risk for infection and lack of human-to-human transmission of *Mycobacterium ulcerans* disease, Australia. Emerg Infect Dis. 2017;23:837–40. http://dx.doi.org/10.3201/eid2305.160809

31. Friedman ND, Athan E, Hughes AJ, Khajehnoori M, McDonald A, Callan P, et al. *Mycobacterium ulcerans* disease: experience with primary oral medical therapy in an Australian cohort. PLoS Negl Trop Dis. 2013;7:e2315. http://dx.doi.org/10.1371/journal.pntd.0002315

32. Pak J, O'Brien DP, Quek T, Athan E. Treatment costs of *Mycobacterium ulcerans* in the antibiotic era. Int Health. 2012;4:123–7. http://dx.doi.org/10.1016/j.inhe.2011.12.005

Address for correspondence: Paul Johnson, Infectious Diseases Department, Austin Health, PO Box 5555, Heidelburg 3084, Melbourne, VIC, Australia; email: paul.johnson@austin.org.au

Cryptococcus gattii Complex Infections in HIV-Infected Patients, Southeastern United States

Kaylee T. Bruner,[1] Carlos Franco-Paredes, Andrés F. Henao-Martínez, Gregory M. Steele, Daniel B. Chastain

Medscape EDUCATION ACTIVITY

In support of improving patient care, this activity has been planned and implemented by Medscape, LLC and Emerging Infectious Diseases. Medscape, LLC is jointly accredited by the Accreditation Council for Continuing Medical Education (ACCME), the Accreditation Council for Pharmacy Education (ACPE), and the American Nurses Credentialing Center (ANCC), to provide continuing education for the healthcare team.

Medscape, LLC designates this Journal-based CME activity for a maximum of 1.00 **AMA PRA Category 1 Credit(s)™**. Physicians should claim only the credit commensurate with the extent of their participation in the activity.

All other clinicians completing this activity will be issued a certificate of participation. To participate in this journal CME activity: (1) review the learning objectives and author disclosures; (2) study the education content; (3) take the post-test with a 75% minimum passing score and complete the evaluation at http://www.medscape.org/journal/eid; and (4) view/print certificate. For CME questions, see page 2140.

Release date: October 16, 2018; Expiration date: October 16, 2019

Learning Objectives

Upon completion of this activity, participants will be able to:

- Assess the epidemiology of *Cryptococcus gattii* complex infections in HIV-infected patients, based on a case series report

- Evaluate the clinical features of *C. gattii* complex infections in HIV-infected patients, based on a case series report

- Determine the clinical implications of *C. gattii* complex infections in HIV-infected patients, based on a case series report

CME Editor

Thomas J. Gryczan, MS, Technical Writer/Editor, Emerging Infectious Diseases. *Disclosure: Thomas J. Gryczan, MS, has disclosed no relevant financial relationships.*

CME Author

Laurie Barclay, MD, freelance writer and reviewer, Medscape, LLC. *Disclosure: Laurie Barclay, MD, has disclosed the following relevant financial relationships: owns stock, stock options, or bonds from Pfizer.*

Authors

Disclosures: **Kaylee T. Bruner, PharmD; Carlos Franco-Paredes, MD, MPH; Gregory M. Steele, RN, MSN, FNP-BC;** and **Daniel B. Chastain, PharmD,** *have disclosed no relevant financial relationships.* **Andrés F. Henao-Martínez, MD,** *has disclosed the following relevant financial relationship: served as an advisor or consultant for Bayer.*

Author affiliations: Phoebe Putney Memorial Hospital, Albany, Georgia, USA (K.T. Bruner, G.M. Steele, D.B. Chastain); Hospital Infantil de Mexico, Federico Gomez, Mexico City, Mexico (C. Franco-Paredes); University of Colorado Denver Anschutz Medical Campus, Aurora, Colorado, USA (C. Franco-Paredes, A.F. Henao-Martínez); University of Georgia College of Pharmacy, Albany (D.B. Chastain)

Cryptococcus gattii traditionally infects immunocompetent hosts and causes devastating pulmonary or central nervous system disease. However, this infection rarely occurs in patients infected with HIV. We report 3 cases of HIV-associated *C. gattii* complex infections in the southeastern United States. Detection of *C. gattii* in HIV-infected patients in this region warrants increased awareness of this threat to ensure appropriate diagnosis and treatment to optimize patient outcomes.

[1]Current affiliation: Archbold Medical Center, Thomasville, Georgia, USA.

*C*ryptococcus gattii is an encapsulated fungus found primarily in tropical and subtropical regions such as Australia and South America (*1*). *C. gattii* was first documented as an emerging pathogen in the United States in 1999 when an outbreak occurred in Oregon and Washington (*1*). More recently, sporadic cases have been reported throughout the southeastern United States (*2–4*). Theories for the emergence of *C. gattii* in temperate areas have included climate change, increased travel, and anthropogenic activity; however, the exact mechanism remains unknown (*1,4*).

C. gattii was previously known as variant of *C. neoformans* but was later recognized as an independent species of *Cryptococcus* (*4*). Recently, *C. gattii* was reclassified as a species complex comprised of 4 individual species (*5*). Similar to *C. neoformans*, *C. gattii* is acquired through inhalation; infection can progress to pneumonia and central nervous system disease by dissemination into the bloodstream. *C. gattii* has been associated with increased virulence and more severe neurologic manifestations than *C. neoformans*, resulting in major illness and death (*3*). Although treatment is currently the same as for *C. neoformans*, it has previously been suggested that more aggressive management of neurologic complications, including decreasing elevated intracranial pressure and possibly early use of dexamethasone, might be warranted for *C. gattii* cases (*2, 3*). In addition, longer duration of induction therapy, averaging approximately 6 weeks, has been required for *C. gattii* infections (*6*).

C. gattii infection has traditionally been reported more often in immunocompetent persons, in contrast to *C. neoformans,* which is more prominent in severely immunocompromised hosts, particularly among those with HIV/AIDS (*3,7*). However, more recent evidence has identified some potential risk factors for *C. gattii* meningoencephalitis. These factors include antibodies against granulocyte–macrophage colony-stimulating factor, which leads to macrophage dysfunction, and chronic medical conditions, including diabetes mellitus and other illnesses, such as end-stage liver or renal disease (*8–10*).

Cases of *C. gattii* meningoencephalitis in HIV-infected patients have been reported rarely in areas with high HIV prevalence, such as Botswana and sub-Saharan Africa (*11*). It appears that the only cases reported of *C. gattii* in HIV/AIDS patients in the United States have been limited to a small number in southern California (*12*).

We report 3 cases of *C. gattii* complex meningitis and pneumonitis in HIV-infected patients residing in southwestern Georgia. These cases should alert clinicians for detection of HIV-associated *C. gattii* complex in the southeastern United States.

Case-Patient 1

A 34-year-old man with a history of infection with HIV and medication noncompliance was admitted to Phoebe Putney Memorial Hospital (Albany, GA, USA) because of a 5-week history of nausea, vomiting, and weight loss. He also had headaches, photophobia, and subjective syncope. The patient had a CD4+ T-cell count of 6 cells/mm^3 and an HIV-1 RNA level of 71,265 copies/mL. He reported no recent travel history or exposure to animals. At admission, initial workup included a barium swallow procedure and kidney, ureter, and bladder radiography. These procedures showed no unusual findings.

After we observed an additional syncopal episode, we ordered a test for serum cryptococcal antigen (CrAg) and magnetic resonance imaging (MRI) of the brain because of the HIV status of the patient and concern for an intracranial infectious process. After detection of a serum CrAg titer >1:2,560, a lumbar puncture (LP) was performed on day 4 of hospitalization. The LP showed an opening pressure of 24 cm of water, 5 leukocytes/mm^3 (6% polymorphonuclear cells and 94% mononuclear cells), 0 erythrocytes/mm^3, a protein level of 29 mg/dL, and a glucose level of 49 mg/dL. A positive result (titer >1:2,560) was observed for CrAg in cerebrospinal fluid (CSF).

The patient was given intravenous (IV) amphotericin B lipid complex (5 mg/kg/d) and oral flucytosine (25 mg/kg 4×/d). On day 5, a repeat LP was performed to evaluate intracranial pressure and showed identical opening and closing pressures of 5 cm of water. After 5 days of treatment with amphotericin B lipid complex and flucytosine, renal dysfunction and thrombocytopenia developed on hospital day 9. The patient was then given oral fluconazole (800 mg 1×/d). Blood and CSF cultures grew *Cryptococcus* sp., which we further identified as *C. gattii* complex by using matrix-assisted laser desorption/ionization-time of flight mass spectrometry.

MRI of the brain showed enhancement of right frontal lobe adjacent to the lateral ventricle with subtle nodular enhancement within the right caudate head. Nonenhancing T2 and fluid-attenuated inversion recovery MRI showed hyperintensities within bilateral deep nuclei.

After 14 days of antifungal therapy, the patient was deemed stable. He was discharged and received oral fluconazole (800 mg 1×/d). He was scheduled for follow-up in the outpatient clinic 2 weeks later for a repeat LP and initiation of antiretroviral therapy (ART). Unfortunately, the patient did not return for continued care.

Case-Patient 2

A 47-year-old man with a medical history of hypertension and infection with HIV was admitted to Phoebe Putney Memorial Hospital because of a 2-week history of fever, nausea, headaches, and unsteady gait. Outpatient records showed a CD4+ T-cell count of <20 cells/mm^3 and an HIV-1 RNA level of 1,653 copies/mL, for which he was recently given ART. This therapy consisted of emtricitabine (200

mg 1×/d), tenofovir disoproxil fumarate (300 mg 1×/d), raltegravir (400 mg 2×/d), and etravirine (200 mg 2×/d).

MRI of the brain performed at admission was unremarkable, with no definitive evidence of acute ischemic, intracranial hematoma, or enhancing intracranial lesion. Initially, the patient was given levofloxacin for treatment of possible sinusitis, but he continued to experience intermittent episodes of fever and persistent headaches. On day 2 after admission, an LP was performed and showed increased opening pressure, 85 leukocytes/mm³ (1% polymorphonuclear cells and 99% mononuclear cells), 11 erythrocytes/mm³, a protein level of 96 mg/dL, and glucose level of 42 mg/dL. A positive result (titer >1:256) was observed for CrAg in CSF.

The positive finding for CrAg prompted initiation of induction therapy for cryptococcal meningitis, which consisted of IV liposomal amphotericin B (5 mg/kg/d) and oral flucytosine (25 mg/kg 4×/d). CSF cultures grew yeast, which we eventually identified as *C. gattii* complex by using l-canavanine, glycine, bromothymol blue (CGB) agar. Blood cultures remained sterile throughout hospitalization. The patient was given IV dexamethasone (4 mg every 6 h) because of recurrent headaches. Before completion of 14 days of induction therapy, a repeat LP was performed and showed an opening pressure of 43 cm of water, a closing pressure of 30 cm of water, 97 leukocytes/mm³ (100% mononuclear cells), 4 erythrocytes/mm³, a protein level of 89 mg/dL, and a glucose level of 58 mg/dL. CSF remained positive for CrAg, but the titer decreased to 1:16, and the CSF culture remained sterile.

The patient was discharged and received voriconazole and a dexamethasone taper over a 6-week period. Voriconazole was continued for 6 months and was chosen for the consolidation phase of treatment because there is some evidence that the MIC of voriconazole is lower than the MIC of fluconazole for most *C. gattii* complex isolates (13,14). During the subsequent 5 years of follow-up, his ART was changed to abacavir (300 mg 2×/d), lamivudine (150 mg 2×/d), and raltegravir (400 mg 2×/d). The patient continued secondary prophylaxis with oral voriconazole until CD4+

T-cell counts were ≥100 cells/mm³ for at least 3 months. Recent laboratory results showed undetectable HIV-1 RNA and a CD4+ T-cell count of 256 cells/mm³.

Case-Patient 3

A 47-year-old man with a history of depression and infection with HIV for ≈20 years was admitted to Phoebe Putney Memorial Hospital because of suicidal ideation caused by persistent pain. He also reported body aches, fatigue, and weakness for a 1-month duration, but denied pulmonary symptoms or fevers. He was previously receiving ART, but had been noncompliant for the previous 2 years because of homelessness.

At admission, initial examination showed a CD4+ T-cell count of 26 cells/mm³, an HIV-1 RNA level of 272,152 copies/mL, positive result for serum CrAg (titer 1:160), and a right hilar mass by chest radiograph. The patient was given IV amphotericin B lipid complex (5 mg/kg/d) and oral flucytosine (25 mg/kg 4×/d). An LP showed 3 leukocytes/mm³ (100% mononuclear cells), 4 erythrocytes/mm³, a protein level of 42 mg/dL, and a glucose level of 62 mg/dL. The patient had a negative result for CrAg in CSF.

Because of these findings, we performed computed tomography (CT) of the chest and identified a mass (4.0 cm × 2.5 cm) with central cavitation in the right lower lobe abutting the pleural surface (Figure). The patient underwent a CT-guided lung biopsy to evaluate the right lower lobe mass. Pathologic examination demonstrated fibrous tissue and numerous cystic spaces containing macrophages and variably sized organisms with a thick capsule that were strongly positive when stained with Grocott's methanamine silver special stain. The morphologic features were consistent with those of a *Cryptococcus* sp. We observed many budding yeasts by using Gram stain.

The patient continued to receive oral flucytosine (25 mg/kg 4×/d), but because of an acute kidney injury after 3 days, amphotericin B lipid complex was replaced with IV fluconazole (800 mg in a single dose), followed by oral fluconazole (400 mg 1×/d). He remained hospitalized for an

Figure. Computed tomography images of the chest of an HIV-infected 47-year-old man (case-patient 3) with *Cryptococcus gattii* complex infection, southeastern United States. Transverse (A) and frontal (B) views without intravenous contrast showed a mass (arrows) (4.0 cm × 2.5 cm) that had central cavitation posteriorly in the right lower lobe abutting the pleural surface. The central cavitary portion of this lesion had a maximum length of ≈1.3 cm and no evidence of fluid level or internal soft tissues.
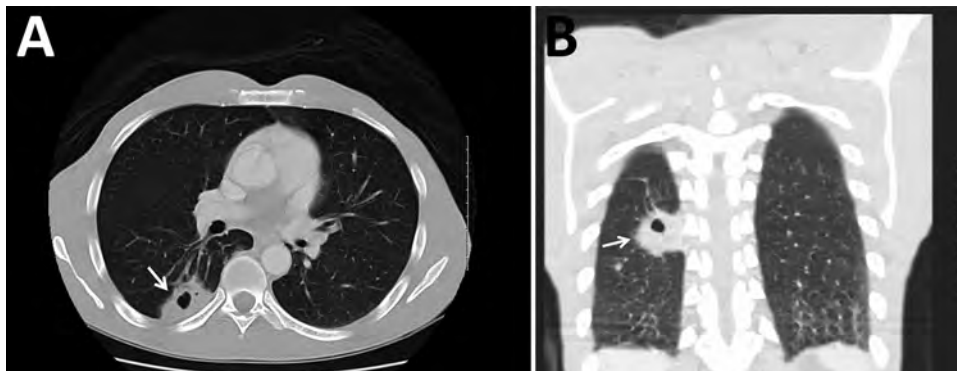
additional 3 days until growth on CGB agar was identified as *C. gattii* complex. At that time, the patient had improved considerably and was discharged.

During outpatient treatment, the patient received emtricitabine (200 mg/d), dolutegravir (50 mg/d), darunavir (800 mg/d), and cobicistat (150 mg/d). A CT of his abdomen and pelvis to evaluate lower abdominal pain was performed ≈6 months later and showed resolution of the initial mass. We detected a new 20-mm lesion within the right lower lobe, which was not observed in previous studies. The patient continued to receive fluconazole (400 mg 1×/d) for an additional 12 months without subsequent radiographic monitoring. His most recent laboratory results showed a CD4+ T-cell count of 250 cells/mm^3 and an HIV-1 RNA level <40 copies/mL while receiving the aforementioned ART.

Discussion

We report 3 cases of *C. gattii* complex infections in HIV-infected patients in the southeastern United States (southwestern Georgia). Given the increasing recognition of *C. gattii* complex in southwestern Georgia, it is routine practice at our institution to plate cryptococcal isolates on CGB agar to distinguish between *C. neoformans* and *C. gattii* complex (*4,15*). Since implementation of this practice in 2012, of 30 clinical isolates of *Cryptococcus* sp., 3 (10%) have been identified as the *C. gattii* complex. Although the environmental source of these infections in southwestern Georgia remains unknown because the 3 patients in this case series had no previous travel, we believe that their immunocompromised state characterized by low CD4+ T-cell counts is a contributing factor for acquiring infection with *C. gattii* complex.

Historically, most cases of infection with *C. gattii* were identified in patients who were immunocompetent or otherwise healthy and lived in the Pacific Northwest region of the United States because of endemicity of this fungi to this region (*3*). However, recent data suggest a longer duration of endemicity in the southeastern United States than in the Pacific Northwest, specifically because of the *C. gattii* VGI-SE clade (*16,17*).

Data from the 1960s and 1980s indicated detection of *C. neoformans* serotypes B and C, now recognized as *C. gattii*, from clinical and environmental isolates. However, the first cases of *C. gattii* infections from regions outside of the Pacific Northwest were reported in 2009. In a retrospective database review by the Centers for Disease Control and Prevention for 2004–2011, a total of 96 case-patients infected with *C. gattii* were identified; 81 resided in the Pacific Northwest (Washington and Oregon) and most were infected with the VGII outbreak strain, which was acquired from the outbreak on Vancouver Island in Canada (*10*). Nonoutbreak strains VGI and VGIII were confined

to HIV-negative persons residing in states outside the Pacific Northwest in comparison with outbreak case-patients, of whom 3 were infected with HIV. Similar to the findings for case-patient 3 in our case report, 59% of patients in the Pacific Northwest outbreak had *C. gattii* pneumonia; however, 75% had respiratory symptoms, but case-patient 3 had no respiratory symptoms (*10*).

In 2010, 276 isolates of *Cryptococcus* sp. in HIV-infected patients were reported in southern California, of which 34 isolates were identified as *C. gattii*, demonstrating that *C. gattii* had been present previously in immunocompromised patients (*12*). More recently, 25 case-patients outside the Pacific Northwest have been reported; 5 had *C. gattii* pulmonary disease, 12 had central nervous system disease, and 8 had a combination of the 2 *C. gattii* diseases (*2*). Of the 25 case-patients reported, 7 resided in the southeastern states: 1 in Florida, 5 in Georgia, and 1 in Alabama. The HIV status of these case-patients was not reported; however, the case-patient in Florida was an otherwise healthy native of Florida who had no known travel to areas to which *C. gattii* is endemic (*18*). Similar to case-patients 1 and 2, two previous case-patients with *C. gattii* meningitis were reported in southwestern Georgia (*3,15*). The surprising difference was that these patients were HIV negative and otherwise healthy.

Speciation of cryptococcal isolates is essential because *C. gattii* complex meningoencephalitis might have more severe clinical manifestations requiring aggressive management of intracranial hypertension with early evacuation of CSF and treatment with steroids (*3*). Use of dexamethasone for treatment of *C. gattii* complex meningitis has been associated with positive outcomes by potentially decreasing cerebral edema and tissue damage (*19,20*). In a small retrospective study of 16 patients in Papua New Guinea infected with *C. gattii*, most patients who received corticosteroids had reduced rates of vision loss and blindness (*21*). In addition, case-patients infected with the *C. gattii* complex might require prolonged courses of amphotericin B–based therapy compared with case-patients infected with *C. neoformans* (*6*). Finally, there appears to be different antifungal susceptibility to azoles that might suggest the use of voriconazole instead of fluconazole for the consolidation phase of antifungal therapy (*13,14*).

Early identification of the *C. gattii* complex can be challenging because of limited accessibility of tests that differentiate *Cryptococcus* spp., including use of CGB agar (*22*). Because of lack of availability of testing in local microbiology laboratories, it is likely that infection with *C. gattii* complex is underreported.

On the basis of the cases presented in this report and continued detection of *C. gattii* in the southeastern United States, we believe routine testing to differentiate *C. neoformans* from *C. gattii* is warranted and further investigation is

required to determine appropriate treatment in comparison with treatment for *C. neoformans*. In addition, healthcare providers should be aware of this pathogen and its potential to cause devastating disease in immunocompromised and immunocompetent patients.

About the Author

Dr. Bruner is a clinical pharmacist in the Emergency Department, Archbold Medical Center, Thomasville, GA. Her research interests are targeted temperature management, infectious diseases, and emergency medicine.

References

1. Datta K, Bartlett KH, Baer R, Byrnes E, Galanis E, Heitman J, et al.; *Cryptococcus gattii* Working Group of the Pacific Northwest. Spread of *Cryptococcus gattii* into Pacific Northwest region of the United States. Emerg Infect Dis. 2009;15:1185–91. http://dx.doi.org/10.3201/eid1508.081384
2. Harris JR, Lockhart SR, Sondermeyer G, Vugia DJ, Crist MB, D'Angelo MT, et al. *Cryptococcus gattii* infections in multiple states outside the US Pacific Northwest. Emerg Infect Dis. 2013;19:1620–6. http://dx.doi.org/10.3201/eid1910.130441
3. Franco-Paredes C, Womack T, Bohlmeyer T, Sellers B, Hays A, Patel K, et al. Management of *Cryptococcus gattii* meningo-encephalitis. Lancet Infect Dis. 2015;15:348–55. http://dx.doi.org/10.1016/S1473-3099(14)70945-4
4. Harris J, Lockhart S, Chiller T. *Cryptococcus gattii*: where do we go from here? Med Mycol. 2012;50:113–29. http://dx.doi.org/10.3109/13693786.2011.607854
5. Hagen F, Khayhan K, Theelen B, Kolecka A, Polacheck I, Sionov E, et al. Recognition of seven species in the *Cryptococcus gattii*/*Cryptococcus neoformans* species complex. Fungal Genet Biol. 2015;78:16–48. http://dx.doi.org/10.1016/j.fgb.2015.02.009
6. Chen SC, Korman TM, Slavin MA, Marriott D, Byth K, Bak N, et al.; Australia and New Zealand Mycoses Interest Group (ANZMIG) Cryptococcus Study. Antifungal therapy and management of complications of cryptococcosis due to *Cryptococcus gattii*. Clin Infect Dis. 2013;57:543–51. http://dx.doi.org/10.1093/cid/cit341
7. Mitchell DH, Sorrell TC, Allworth AM, Heath CH, McGregor AR, Papanaoum K, et al. Cryptococcal disease of the CNS in immunocompetent hosts: influence of cryptococcal variety on clinical manifestations and outcome. Clin Infect Dis. 1995;20:611–6. http://dx.doi.org/10.1093/clinids/20.3.611
8. Brouwer AE, Siddiqui AA, Kester MI, Sigaloff KC, Rajanuwong A, Wannapasni S, et al. Immune dysfunction in HIV-seronegative, *Cryptococcus gattii* meningitis. J Infect. 2007;54:e165–8. http://dx.doi.org/10.1016/j.jinf.2006.10.002
9. Cheng PY, Sham A, Kronstad JW. *Cryptococcus gattii* isolates from the British Columbia cryptococcosis outbreak induce less protective inflammation in a murine model of infection than *Cryptococcus neoformans*. Infect Immun. 2009;77:4284–94. http://dx.doi.org/10.1128/IAI.00628-09
10. Harris JR, Lockhart SR, Debess E, Marsden-Haug N, Goldoft M, Wohrle R, et al. *Cryptococcus gattii* in the United States: clinical aspects of infection with an emerging pathogen. Clin Infect Dis. 2011;53:1188–95. http://dx.doi.org/10.1093/cid/cir723
11. Steele KT, Thakur R, Nthobatsang R, Steenhoff AP, Bisson GP. In-hospital mortality of HIV-infected cryptococcal meningitis patients with *C. gattii* and *C. neoformans* infection in Gaborone, Botswana. Med Mycol. 2010;48:1112–5. http://dx.doi.org/10.3109/13693781003774689
12. Chaturvedi S, Dyavaiah M, Larsen RA, Chaturvedi V. *Cryptococcus gattii* in AIDS patients, southern California. Emerg Infect Dis. 2005;11:1686–92. http://dx.doi.org/10.3201/eid1111.040875
13. Lockhart SR, Iqbal N, Bolden CB, DeBess EE, Marsden-Haug N, Worhle R, et al.; *Cryptococcus gattii* PNW Public Health Working Group. Epidemiologic cutoff values for triazole drugs in *Cryptococcus gattii*: correlation of molecular type and in vitro susceptibility. Diagn Microbiol Infect Dis. 2012;73:144–8. http://dx.doi.org/10.1016/j.diagmicrobio.2012.02.018
14. Espinel-Ingroff A, Aller AI, Canton E, Castañón-Olivares LR, Chowdhary A, Cordoba S, et al. *Cryptococcus neoformans*–*Cryptococcus gattii* species complex: an international study of wild-type susceptibility endpoint distributions and epidemiological cutoff values for fluconazole, itraconazole, posaconazole, and voriconazole. Antimicrob Agents Chemother. 2012;56:5898–906. http://dx.doi.org/10.1128/AAC.01115-12
15. Sellers B, Hall P, Cine-Gowdie S, Hays AL, Patel K, Lockhart SR, et al. *Cryptococcus gattii*: an emerging fungal pathogen in the Southeastern United States. Am J Med Sci. 2012;343:510–1. http://dx.doi.org/10.1097/MAJ.0b013e3182464bc7
16. Lockhart SR, Iqbal N, Harris JR, Grossman NT, DeBess E, Wohrle R, et al. *Cryptococcus gattii* in the United States: genotypic diversity of human and veterinary isolates. PLoS One. 2013;8:e74737. http://dx.doi.org/10.1371/journal.pone.0074737
17. Lockhart SR, Roe CC, Engelthaler DM. Whole-genome analysis of *Cryptococcus gattii*, southeastern United States. Emerg Infect Dis. 2016;22:1098–101. http://dx.doi.org/10.3201/eid2206.151455
18. Kunadharaju R, Choe U, Harris JR, Lockhart SR, Greene JN. *Cryptococcus gattii*, Florida, USA, 2011. Emerg Infect Dis. 2013;19:519–21. http://dx.doi.org/10.3201/eid1903.121399
19. Lane M, McBride J, Archer J. Steroid responsive late deterioration in Cryptococcus neoformans variety gattii meningitis. Neurology. 2004;63:713–4. http://dx.doi.org/10.1212/01.WNL.0000134677.29120.62
20. Phillips P, Chapman K, Sharp M, Harrison P, Vortel J, Steiner T, et al. Dexamethasone in *Cryptococcus gattii* central nervous system infection. Clin Infect Dis. 2009;49:591–5. http://dx.doi.org/10.1086/603554
21. Seaton RA, Verma N, Naraqi S, Wembri JP, Warrell DA. The effect of corticosteroids on visual loss in Cryptococcus neoformans var. gattii meningitis. Trans R Soc Trop Med Hyg. 1997;91:50–2. http://dx.doi.org/10.1016/S0035-9203(97)90393-X
22. Klein KR, Hall L, Deml SM, Rysavy JM, Wohlfiel SL, Wengenack NL. Identification of *Cryptococcus gattii* by use of L-canavanine glycine bromothymol blue medium and DNA sequencing. J Clin Microbiol. 2009;47:3669–72. http://dx.doi.org/10.1128/JCM.01072-09

Address for correspondence: Daniel B. Chastain, University of Georgia College of Pharmacy, 1000 Jefferson St, Albany, GA 31701, USA; email: daniel.chastain@uga.edu

Detection of Tickborne Relapsing Fever Spirochete, Austin, Texas, USA

Jack D. Bissett, Suzanne Ledet, Aparna Krishnavajhala, Brittany A. Armstrong, Anna Klioueva, Christopher Sexton, Adam Replogle, Martin E. Schriefer, Job E. Lopez

In March 2017, a patient became febrile within 4 days after visiting a rustic conference center in Austin, Texas, USA, where Austin Public Health suspected an outbreak of tickborne relapsing fever a month earlier. Evaluation of a patient blood smear and molecular diagnostic assays identified *Borrelia turicatae* as the causative agent. We could not gain access to the property to collect ticks. Thus, we focused efforts at a nearby public park, <1 mile from the suspected exposure site. We trapped *Ornithodoros turicata* ticks from 2 locations in the park, and laboratory evaluation resulted in cultivation of 3 *B. turicatae* isolates. Multilocus sequencing of 3 chromosomal loci (*flaB*, *rrs*, and *gyrB*) indicated that the isolates were identical to those of *B. turicatae* 91E135 (a tick isolate) and BTE5EL (a human isolate). We identified the endemicity of *O. turicata* ticks and likely emergence of *B. turicatae* in this city.

Globally, spirochetes that cause tickborne relapsing fever (TBRF) are neglected pathogens, and diagnosis of this disease is challenging because of its nonspecific manifestations. Signs and symptoms of TBRF include cyclic febrile episodes, nausea, and vomiting (*1*). The bacterium *Borrelia turicatae* is the primary known causative species of TBRF in low-elevation, arid regions in the southern United States, and a unique manifestation of this disease is neurologic symptoms that further complicate an accurate diagnosis (*2*). In Texas, most cases of infection with *B. turicatae* have been associated with cave explorers, outdoor enthusiasts, undocumented migrants, and military personnel (*2,3*). Currently, it is not mandatory to report a diagnosis of TBRF in Texas.

An additional complication with defining public health effects of infection with *B. turicatae* is the dynamics between the pathogen and its tick vector (*Ornithodoros turicata*). These ticks have a life span of 10 years and can

endure starvation for ≥5 years. However, *B. turicatae* remains infectious in these ticks (*4*). Except for persons bitten in karst formations (topographies formed from dissolution of soluble rocks) that can contain swarms of *O. turicata* ticks (*2*), attached ticks are rarely seen because these ticks are rapid feeders and transmission of *B. turicatae* occurs within seconds of the tick bite (*5,6*). In addition, *B. turicatae* is maintained transovarially and tick larvae are difficult to see because of their small size (*6*). After feeding, ticks return to their cavity dwelling, which includes wood cracks, leaf litter, and small- and medium-size mammal nests and dens (*2,7,8*).

Little is known regarding the maintenance of *B. turicatae* in nature. Most laboratory isolates have resulted from feeding field-collected ticks on immunologically naive mice and culturing the spirochetes from infected murine blood (*9*). *B. turicatae* has also been cultured from the blood of sick domestic dogs (*9,10*) and a human (*11*). Furthermore, there is an absence of *B. turicatae* isolates from wild vertebrates, which further limits understanding the etiology of TBRF.

We report clinical manifestations of TBRF for a patient from Austin, Texas, USA. Using species-specific genetic and antigenic markers (*12–14*), we identified the etiologic agent as *B. turicatae*. Because access to the alleged exposure site was not available, we collected *O. turicata* ticks in a nearby public park. Collected ticks indicated the endemicity of the vector to Austin. These ticks were evaluated for infection by feeding them on immunologically naive mice. We report the transmission and isolation of TBRF spirochetes in culture medium. Partial sequencing of the flagellin B (*flaB*), 16S rRNA (*rrs*), and DNA gyrase B (*gyrB*) genes (total 2,398 bp) indicated probable emergence of *B. turicatae* in Austin, Texas.

Materials and Methods

The Patient
The patient was a 34-year-old previously healthy woman whose illness began on March 29, 2017, when she had a

headache, myalgias, arthralgias, and malaise. On March 30, 2017, she traveled to California on a previously scheduled trip and was febrile. The patient had a temperature of 104°F that increased to 105°F, at which point she sought medical treatment at an urgent care clinic. Complete blood counts, and levels of electrolytes, blood urine nitrogen, creatinine, and liver enzymes were within references ranges. She was given intravenous fluids, discharged with a diagnosis of a viral illness, and given instructions for symptomatic treatment of this illness.

Over the next 2 days, the patient still had a high fever, which prompted her to return to the urgent care clinic. Given her ongoing signs and symptoms, she was referred to a local hospital emergency department in California where she underwent computed tomographic imaging of her brain and a lumbar puncture for cerebrospinal fluid analysis. Computed tomographic imaging of the brain showed no abnormalities. Analysis of cerebrospinal fluid also failed to demonstrate abnormal findings. It was again concluded that she likely had a viral infection and was discharged from the emergency department with instructions for symptomatic treatment.

On April 2, 2017, she reported a blotchy maculopapular rash that began on her extremities and spread to her trunk. The rash was nonpruritic, persisted for several days, then gradually faded away. The patient returned home to Austin, Texas, with a temperature of 104°F and continued to have a mild headache in conjunction with intermittent fever. She did not have nausea, vomiting, or diarrhea. Given her ongoing symptoms, on April 9, 2017 she sought an evaluation at an acute care hospital emergency department. At the emergency department assessment, a hematoxylin and eosin–stained peripheral thin blood smear was prepared for evaluation of bloodborne pathogens.

Real-Time PCR Analysis

We performed a real-time PCR assay on DNA extracted from the spirochete-positive peripheral thin blood smear. We scraped 10% of the contents of the slide with a scalpel and placed the contents in a tube containing 200 μL of phosphate-buffered saline (GIBCO, Gaithersburg, MD, USA). We then extracted DNA by using a QIACube (QIAGEN, Valencia, CA, USA), a tissue protocol, and an elution of 100 μL. A total of 5 μL of the eluted DNA extract was used per 20-μL final volume reactions with primers and probes specific for the *B. turicatae* glycerophosphodiester phosphodiesterase (*glpQ*) gene (forward primer 5′-GCCTGTCAGAATGAAAAA-3′, reverse primer 5′-CACCTCTGTGAGCTATAATT-3′, and probe FAM-5′-TGAGTATGACAAACAAAAAACCACCA-3′-BHQ) and the *B. hermsii glpQ* gene (forward primer 5′-TCCTGTCAGGGCGAAAAAAT-3′, reverse primer 5′-GCTGGCACCTCTGTGAGCTAT-3′, and probe FAM-5′-AGTCAAAACCAAAAATCACCA-3′-BHQ). The PCR was performed as described (*14*). A no template (DNA) sample was used as a negative control, and DNA extracted from *B. turicatae* and *B. hermsii* cultures were used as positive controls.

Immunoblotting

We also performed immunoblotting for relapsing fever group *Borrelia* spp. and *B. turicatae*, as described (*3,13,15*). We subjected protein lysates from 1×10^7 *B. turicatae* and 1 μg of recombinant *Borrelia* immunogenic protein A (rBipA) to electrophoresis by using Mini PRO-TEAN TGX Precast Gels (Bio-Rad, Hercules, CA, USA) and transferred them onto Immobilon polyvinylidene difluoride membranes (Millipore, Billerica, MA, USA). rBipA was produced as a thioredoxin fusion protein to facilitate solubility and is ≈15 kDa larger than the native protein (*13*).

We sent a deidentified serum sample collected 50 days after infection to Baylor College of Medicine (Houston, TX, USA) for evaluation. This sample was diluted 1:200 in Tropix I-Block Protein-Based Blocking Reagent (ThermoFisher Scientific, Waltham, MA, USA), and polyvinylidene difluoride membranes were probed for 1 hour. Recombinant protein G conjugated to horseradish peroxidase (ThermoFisher Scientific) diluted 1:4,000 was used as the secondary molecule, and antibody reactivity was detected by chemiluminescence using the Amersham Enhanced Chemiluminescence ECL Western Blotting Detection Reagent (GE Healthcare, Little Chalfont, UK).

Collection of *O. turicata* Ticks

Because access to the alleged exposure site was not available, we selected a field site in a public park near the suspected exposure site. We determined that the park was in Austin by using the Jurisdictions Web Map maintained by the Enterprise Geospatial Service Program of the City of Austin (http://www.austintexas.gov/department/gis-and-maps). Collection efforts were performed in July and November 2017. We placed CO_2 tick traps with dry ice as bait in locations with promising *O. turicata* tick habitats, as described (*7*). As ticks emerged from leaf litter, we stored them in vials labeled according to collection site and date. We collected 20 nymphal ticks from the first location in July and November 2017. We identified the second location in November 2017 and collected 30 nymphs from this site.

Tick Feedings and Isolation of Spirochetes

All animal studies were approved by the Institutional Animal Care and Use Committee at Baylor College of Medicine. The laboratory animal program follows standards and guidelines established by the Association for Assessment and Accreditation of Laboratory Animal Care and the National Institutes of Health Office of Laboratory Animal Welfare. Animal husbandry was provided by trained veterinary staff and animal care technicians.

We randomly selected 10 *O. turicata* nymphs from each collection vial and allowed them to feed on ICR mice obtained from the Institute of Cancer Research (Philadelphia, PA, USA) (*16*). Animals were sedated by inhalation of isoflurane (Henry Schein, Melville, NY, USA), and ticks were placed on the shaved abdomen of mice and allowed to feed to repletion. Upon completion of the blood meal, ticks were stored in TTP TubeSpin Bioreactor Tubes (MidSci, St. Louis, MO, USA) and housed at 25°C and a relative humidity of 85%.

We examined the 3 mice for spirochete infection for 10 days by nicking the tip of the tail and expressing a drop of blood onto a microscope slide. A coverslip was placed over the blood and examined at 20× magnification by using a CX33 Trinocular Dark Field Microscope (Olympus, Center Valley, PA, USA). When spirochetes were observed, we obtained a terminal blood sample from the sedated mouse by using cardiac puncture. We centrifuged ≈500 μL of blood at 5,000 × *g* for 10 min and then inoculated 50 μL of serum into 4 mL of modified Barbour–Stoenner–Kelly (mBSK) medium (*17*). Cultures were grown at 35°C in an atmosphere of 5% CO_2 and examined for spirochetes every 4 days. When exponential growth was reached, we passaged cultures into two 50-mL culture tubes containing fresh mBSK medium for isolation of genomic DNA and generation of stocks (stored in glycerol). For DNA isolation, we produced spirochete pellets by centrifuging the 50-mL culture tubes at 8,000 × *g* for 20 min and extracted genomic DNA as described (*18*). We designated the 3 isolates from the mice as BRP1, BRP1a, and BRP2.

Plasmid Analysis and Genetic Typing of Relapsing Fever Spirochete Isolates

We performed reverse-field electrophoresis to resolve plasmid content, as described (*9*). In addition to BRP1, BRP1a, and BRP2, we compared genomic DNA plasmid profiles with the 91E135 isolate, which originated in Crockett County, Texas (*9*). Total DNA was used from the 91E135 isolate passaged 5 times and from the Austin isolates passaged 2 times after initial isolation from mice.

We subjected 500 ng of genomic DNA from each isolate to electrophoresis at 100 V for 15 min and at 80 V for ≈40 hours by using a PPI-200 Programmable Power Inverter (MJ Research, Inc., Waltham, MA, USA). Gels were stained with GelRed Nucleic Acid Stain (Phenix Research Products, Candler, NC, USA) according to the manufacturer's instructions.

We performed multilocus sequencing for relapsing fever *Borrelia flaB*, *rrs*, and *gyrB* genes. Amplicons were generated by using specific primer sets (Table). For the *rrs* gene, we used primers UniB and FD3 to generate the amplicon, and the remaining internal *rrs* gene primers were used for sequencing. PCR conditions were an initial incubation at 94°C for 2 min, followed by 35 cycles at 94°C for 30 s, annealing at 55°C for 30 s, and an extension at 72°C for 3 min. After the last cycle, an extension was performed at 72°C for 5 min. We analyzed PCR products by agarose gel electrophoresis to confirm the expected molecular size. Each amplicon was sequenced by Lone Star Laboratories (Houston, TX, USA) by using specific primers (Table). Chromatograms were analyzed, and poor sequences were trimmed by using Vector NTI software (Life Technologies, Grand Island, NY, USA). We performed a BLAST (https://blast.ncbi.nlm.nih.gov/Blast.cgi) search with assembled contiguous DNA segments (contigs) to speciate isolates.

Results

Initial Diagnosis of Relapsing Fever Borreliosis

The patient was afebrile on initial presentation to the emergency department, but a fever quickly developed (temperature

Table. PCR primers used in multilocus sequence analysis of tickborne relapsing fever spirochete, Austin, Texas, USA*

Gene locus and primer	Primer sequence, 5′ → 3′
rrs	
UniB†	TACAAGGAGGTGATCCAGC
FD3†	AGAGTTTGATCCTGGCTTAG
16s (−)‡	TAGAAGTTCGCCTTCGCCTCTG
16s (+)‡	TACAGGTGCTGCATGGTTGTCG
Rec 4‡	ATGCTAGAAACTGCATGA
P6 Rev	TTTACAGCGTAGACTACCAG
P8 For	AAACGATGCACACTTGGTGT
P10 Rev	ACATAAGGGCCATGATGATT
flaB	
flaLL§	ACATATTCAGATGCAGACAGAGGT
flaRL§	GCAATCATAGCCATTGCAGATTGT
gyrB	
gyrB 5′+3§	GCTGATGCTGATGTTGATGG
gyrB 3′§	GGCTCTTGAAACAATAACAGACATCGC

*flaB, flagellin B; For, forward; *gyrB*, gyrase B; Rev, reverse; *rrs*, 16S rRNA.
†Reported by Le Fleche et al. (*19*).
‡Reported by Porcella et al. (*20*).
§Reported by Barbour et al. (*21*).

103.3°F). Her health deteriorated, and she became tachycardic (heart rate 125 beats/min) and mildly hypotensive (blood pressure 92/38 mm Hg). An initial complete blood count showed a leukocyte count of 6,700 cells/mm³, a hemoglobin level of 11.1 g/dL, and a platelet count of 145,000/mm³. Levels of liver enzymes, bilirubin, blood urea nitrogen, and creatinine were within reference limits.

At the hospital visit, the patient reported a travel history to Cancun, Mexico, during February 14–20, 2017, but she had no illness during or upon return from that trip. Also, she had no extensive travel history outside Austin, during February–March 29, 2017, when her illness began. However, during March 24–26, the patient spent a weekend at a rustic conference center in Austin where attendees from throughout the United States converged. Austin Public Health had previously investigated the conference center as the exposure site for an outbreak of TBRF the previous month, but tick trapping efforts were unsuccessful.

During the conference, the patient noticed several insect bites on her legs. However, she did not report seeing ticks. Given her travel history to Cancun, the emergency department physician suspected malaria and requested a peripheral blood smear. Instead of malaria parasites, spirochetes were visualized (Figure 1) and a diagnosis of relapsing fever was made. Treatment with doxycycline was initiated on the evening of hospital admission, and her fever resolved within 24 hours. Modest leukopenia (leukocyte count 3,300 cells/mm³) and thrombocytopenia (71,000 platelets/mm³) then developed. Her other signs and symptoms rapidly resolved over the next 3 days, and she was discharged on April 12, 2017.

Diagnosis of Exposure to *B. turicatae*

Because blood was not collected during the initial hospitalization of the patient to identify the infectious agent, we retrospectively implemented 2 molecular approaches to identify the causative agent. First, we extracted DNA from a portion of a blood smear and performed a real-time PCR with primers and probe specific for *B. turicatae glpQ* gene. This assay detected *B. turicatae* but did not detect *B. hermsii*. For this real-time PCR, the amplicon was 67 bp, and given the small size, we did not evaluate the sequence or submit it to GenBank.

The average cycle threshold of the assay was 28.81, and use of primers and probe specific for *B. hermsii* showed negative results. A no template control also showed negative results.

Second, we assessed a serum sample against *B. turicatae* protein lysates and rBipA. Results also indicated that the patient was infected with *B. turicatae* (Figure 2). Immunoblotting detected reactivity to 7 protein bands in the *B. turicatae* protein lysate and to rBipA (Figure 2, panel A). A positive control serum sample was used from a
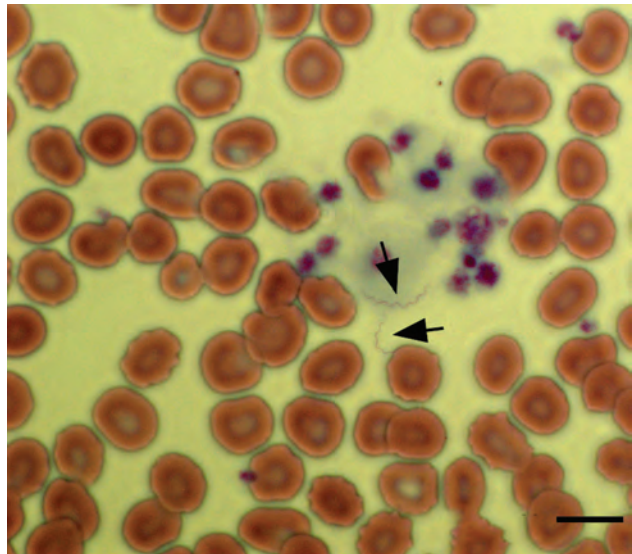
Figure 1. Giemsa-stained peripheral blood smear of a 34-year-old woman with tickborne relapsing fever, Austin, Texas, USA, showing 2 spirochetes (arrows). Scale bar indicates 20 μm.

previous case report (*15*), and the negative control human serum sample indicated no serologic cross-reactivity (Figure 2, panels B, C).

Evaluation of Infected *O. turicata* Ticks from a Public Park

We collected *O. turicata* ticks in a public park near the rustic conference center from the base of a tree that had 2 dens containing rodent waste, which suggested rodent activity in the area (Figure 3). Ticks emerged from leaf litter ≈20 min after we placed CO_2 traps, and we collected ticks ≈30 cm from a cavity opening. Within 5 days after feeding
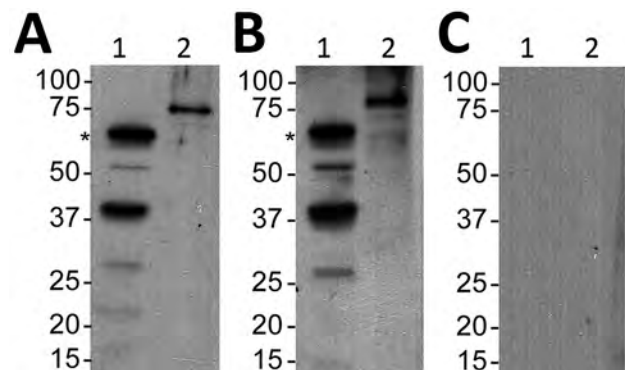
Figure 2. Serologic responses to *Borrelia turicatae* protein lysates and rBipA in 34-year-old woman with tickborne relapsing fever, detected by immunoblotting, Austin, Texas, USA. A) Serum sample from the case-patient; B) positive control serum sample from another case-patient; C) negative control sample. Lane 1, *B. turicatae*; lane 2, rBipA. Values on the left are in kilobases. Asterisks (*) indicate the size of native BipA. rBipA, recombinant *Borrelia* immunogenic protein A.

Figure 3. Location of collection sites for *Ornithodors turicata* ticks, Austin Texas, USA. Two rodent dens (insets) were located at the base of an oak tree. Carbon dioxide traps were placed at the openings until ticks emerged. *Borrelia turicatae* isolates BRP1 and BRP1a originated from ticks that were collected from the den shown at bottom left, and isolate BRP2 originated from the den shown at the bottom right.

ticks from each location on naive mice, spirochetes were visualized by microscopy in the blood. After we inoculated mBSK medium with a serum sample, spirochetes propagated. Once spirochetes entered the late logarithmic growth phase, we passaged them, which confirmed maintenance of these isolates by vitro cultivation. The 3 isolates were designated BRP1, BRP1a, and BRP2.

Sequence Analysis and Plasmid Diversity of BRP1, BRP1a, and BRP2 Isolates of *B. turicatae*

We performed multilocus sequencing to characterize the 3 spirochete isolates that originated in Austin. Sequences of 1,400, 566, and 432 bases were generated for the *flaB, rrs,* and *gyrB* genes, respectively (GenBank accession nos. MH503949–51, MH507599–601, and MH507602–04, respectively). Assessment of DNA sequences by BLAST analysis indicated 100% nucleotide identity to the 91E135

and BTE5EL isolates of *B. turicatae.* Isolates 91E135 and BTE5EL originated from field-collected ticks and a febrile soldier from Texas, respectively (*3,9,11*).

We performed reversed-field gel electrophoresis and identified variation in plasmid diversity between the BRP1, BRP1a, BRP2, and 91E135 isolates of *B. turicatae* (Figure 4). The 3 isolates from Austin contained an ≈40-kb linear plasmid that was absent from 91E135. In addition, BRP1 contained an ≈60-kb linear plasmid that was absent from 91E135, BRP1a, and BRP2.

Discussion

We report TBRF in a patient from Austin, Texas. The patient had limited travel history outside Austin in the days before onset of signs and symptoms. Real-time PCR amplification of the *B. turicatae glpQ* gene and seroconversion for *B. turicatae* rBipA also helped identify the causative agent. Given that the suspected exposure site was previously investigated by Austin Public Health but ticks were not found, it was useful to collect *O. turicata* ticks near the site and assess their infectious status. Tick transmission feedings resulted in propagation of 3 isolates (BRP1, BRP1a, and BRP2), and results of multilocus sequencing of these isolates were identical to those of a human isolate and a tick isolate (*3,9,11*). Assessment of total genomic DNA indicated plasmid diversity between the 3 strains and the 91E135 isolate. Ticks that transmitted BRP1 and BRP1a were collected from the same den area at separate times during the year, which suggests circulation of ≥2 *B. turicatae* variants in the tick population.

Little effort has been invested in active surveillance of TBRF in Texas over the past 70 years (*22,23*), and more work is needed to understand the burden of this disease and maintenance of the spirochete in nature. Evidence indicates the endemicity of *O. turicata* ticks in San Antonio, Dallas, and Austin (*7,22,24*), the seventh, ninth, and eleventh most populous cities, respectively, in the United States. *O. turicata* ticks are considered an arthropod reservoir of *B. turicatae* because they have a 10-year life span and might endure years of starvation while retaining the ability to transmit *B. turicatae* (*25*). *O. turicata* ticks have also been collected in a variety of habitats, including caves, dens, rodent nests, and human dwellings (*2,7,9*). However, there is a paucity of information regarding mammals involved in maintaining *B. turicatae* in nature.

The life cycle of *B. turicatae* in the vertebrate host consists of periods when the bacterium is undetectable in the blood (*5,13*). Thus, indirect approaches are needed for improved surveillance. rBipA can support these studies because of the specificity of the protein to TBRF spirochetes (*12,13*). BipA homologs have not been identified in other pathogens, and previous studies indicated that serologic responses to the protein can discriminate between
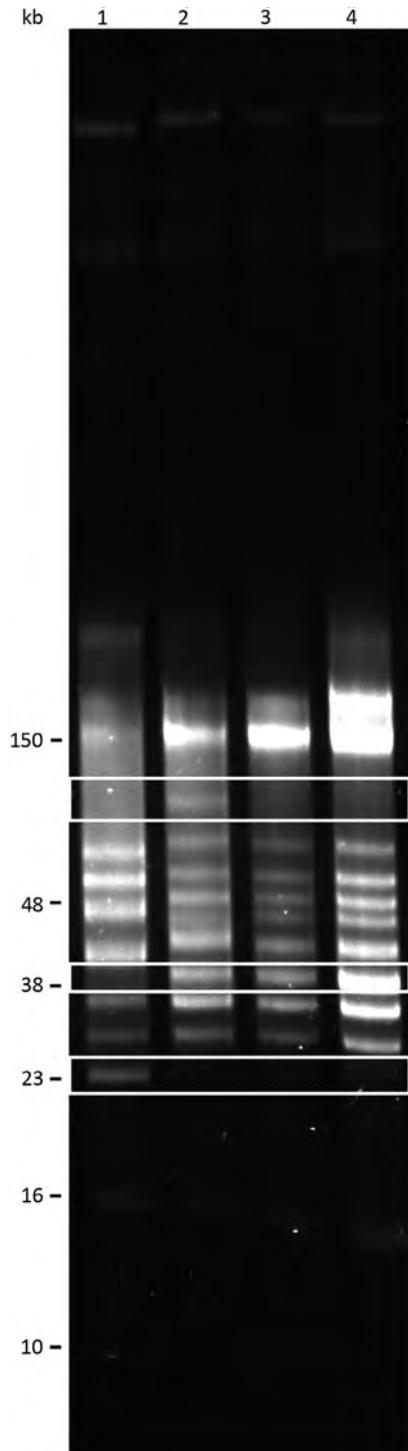
Figure 4. Reversed-field gel electrophoresis of *Borrelia turicatae* isolates collected from *Ornithodors turicata* ticks, Austin, Texas, USA (BRP1, BRP1a, and BRP2) and an isolate from previously field-collected ticks (91E135) (*9*). Lane 1, 91E135; lane 2, BRP1; lane 3, BRP1a; lane 4, BRP2. White boxes indicate a plasmid in BRP1 that is absent from the other strains (top); plasmids unique to BRP1, BRP1a, and BRP2 (middle); and a plasmid in 91E135 strain that is absent in isolates from Austin (bottom).

infections caused by Lyme disease and TBRF *Borrelia* species (*12,13*). Future efforts will focus on using rBipA as a novel diagnostic antigen for surveillance of *B. turicatae*.

TBRF is typically considered a disease of outdoor enthusiasts and impoverished persons living in primitive conditions (*1–3,11,15,26*). However, our study suggests emergence of *B. turicatae* in urban areas. The location where ticks were collected was in a densely populated region of the city. However, the maintenance of this pathogen in nature remains unclear. The elusive life cycle of *O. turicata* ticks also poses challenges in understanding the ecology of *B. turicatae*. Furthermore, given the nonspecific clinical manifestations of disease, the public health effect of *B. turicatae* remains vague. Our findings indicate that surveillance efforts should be increased in Austin, Texas, to evaluate emergence of TBRF.

About the Author

Dr. Bissett is an infectious disease physician practicing general infectious diseases in Austin, Texas. His research interests include transplant-related infections, mechanical cardiovascular support device infections, orthopedic device infections, HIV infection, viral hepatitis, and emerging infectious diseases.

References

1. Dworkin MS, Schwan TG, Anderson DE Jr, Borchardt SM. Tick-borne relapsing fever. Infect Dis Clin North Am. 2008;22:449–68, viii. http://dx.doi.org/10.1016/j.idc.2008.03.006
2. Rawlings JA. An overview of tick-borne relapsing fever with emphasis on outbreaks in Texas. Tex Med. 1995;91:56–9.
3. Christensen AM, Pietralczyk E, Lopez JE, Brooks C, Schriefer ME, Wozniak E, et al. Diagnosis and management of *Borrelia turicatae* infection in febrile soldier, Texas, USA. Emerg Infect Dis. 2017;23:883–4. http://dx.doi.org/10.3201/eid2305.162069
4. Davis GE. Relapsing fever: the tick *Ornithodoros turicata* as a spirochetal reservoir. Public Health Rep. 1943;58:839–42. http://dx.doi.org/10.2307/4584474
5. Boyle WK, Wilder HK, Lawrence AM, Lopez JE. Transmission dynamics of *Borrelia turicatae* from the arthropod vector. PLoS Negl Trop Dis. 2014;8:e2767. http://dx.doi.org/10.1371/journal.pntd.0002767
6. Davis GE. *Ornithodoros turicata:* the male; feeding and copulation habits, fertility, span of life, and the transmission of relapsing fever spirochetes. Public Health Rep. 1941;56:1799–802. http://dx.doi.org/10.2307/4583854
7. Donaldson TG, Pèrez de León AA, Li AY, Castro-Arellano I, Wozniak E, Boyle WK, et al. Assessment of the geographic distribution of *Ornithodoros turicata* (Argasidae): climate variation and host diversity. PLoS Negl Trop Dis. 2016; 10:e0004383. http://dx.doi.org/10.1371/journal.pntd.0004383

8. Adeyeye OA, Butler JF. Field evaluation of carbon dioxide baits for sampling *Ornithodoros turicata* (Acari: Argasidae) in gopher tortoise burrows. J Med Entomol. 1991;28:45–8. http://dx.doi.org/10.1093/jmedent/28.1.45

9. Schwan TG, Raffel SJ, Schrumpf ME, Policastro PF, Rawlings JA, Lane RS, et al. Phylogenetic analysis of the spirochetes *Borrelia parkeri* and *Borrelia turicatae* and the potential for tick-borne relapsing fever in Florida. J Clin Microbiol. 2005;43:3851–9. http://dx.doi.org/10.1128/JCM.43.8.3851-3859.2005

10. Piccione J, Levine GJ, Duff CA, Kuhlman GM, Scott KD, Esteve-Gassent MD. Tick-borne relapsing fever in dogs. J Vet Intern Med. 2016;30:1222–8. http://dx.doi.org/10.1111/jvim.14363

11. Kingry LC, Batra D, Replogle A, Sexton C, Rowe L, Stermole BM, et al. Chromosome and linear plasmid sequences of a 2015 human isolate of the tick-borne relapsing fever spirochete, *Borrelia turicatae*. Genome Announc. 2016;4:4. http://dx.doi.org/10.1128/genomeA.00655-16

12. Lopez JE, Schrumpf ME, Nagarajan V, Raffel SJ, McCoy BN, Schwan TG. A novel surface antigen of relapsing fever spirochetes can discriminate between relapsing fever and Lyme borreliosis. Clin Vaccine Immunol. 2010;17:564–71. http://dx.doi.org/10.1128/CVI.00518-09

13. Lopez JE, Wilder HK, Boyle W, Drumheller LB, Thornton JA, Willeford B, et al. Sequence analysis and serological responses against *Borrelia turicatae* BipA, a putative species-specific antigen. PLoS Negl Trop Dis. 2013;7:e2454. http://dx.doi.org/10.1371/journal.pntd.0002454

14. Breuner NE, Dolan MC, Replogle AJ, Sexton C, Hojgaard A, Boegler KA, et al. Transmission of *Borrelia miyamotoi* sensu lato relapsing fever group spirochetes in relation to duration of attachment by *Ixodes scapularis* nymphs. Ticks Tick Borne Dis. 2017;8:677–81. http://dx.doi.org/10.1016/j.ttbdis.2017.03.008

15. Wilder HK, Wozniak E, Huddleston E, Tata SR, Fitzkee NC, Lopez JE. Case report: a retrospective serological analysis indicating human exposure to tick-borne relapsing fever spirochetes in Texas. PLoS Negl Trop Dis. 2015;9:e0003617. http://dx.doi.org/10.1371/journal.pntd.0003617

16. Krajacich BJ, Lopez JE, Raffel SJ, Schwan TG. Vaccination with the variable tick protein of the relapsing fever spirochete *Borrelia hermsii* protects mice from infection by tick-bite. Parasit Vectors. 2015;8:546. http://dx.doi.org/10.1186/s13071-015-1170-1

17. Battisti JM, Raffel SJ, Schwan TG. A system for site-specific genetic manipulation of the relapsing fever spirochete *Borrelia hermsii*. Methods Mol Biol. 2008;431:69–84.

18. Simpson WJ, Garon CF, Schwan TG. Analysis of supercoiled circular plasmids in infectious and non-infectious *Borrelia burgdorferi*. Microb Pathog. 1990;8:109–18. http://dx.doi.org/10.1016/0882-4010(90)90075-2

19. Le Fleche A, Postic D, Girardet K, Peter O, Baranton G. Characterization of *Borrelia lusitaniae* sp. nov. by 16S ribosomal DNA sequence analysis. Int J Syst Bacteriol. 1997;47:921–5. http://dx.doi.org/10.1099/00207713-47-4-921

20. Porcella SF, Raffel SJ, Anderson DE Jr, Gilk SD, Bono JL, Schrumpf ME, et al. Variable tick protein in two genomic groups of the relapsing fever spirochete *Borrelia hermsii* in western North America. Infect Immun. 2005;73:6647–58. http://dx.doi.org/10.1128/IAI.73.10.6647-6658.2005

21. Barbour AG, Maupin GO, Teltow GJ, Carter CJ, Piesman J. Identification of an uncultivable *Borrelia* species in the hard tick *Amblyomma americanum*: possible agent of a Lyme disease-like illness. J Infect Dis. 1996;173:403–9. http://dx.doi.org/10.1093/infdis/173.2.403

22. Eads RB, Henderson HE, McGregor T, Irons JV. Relapsing fever in Texas; distribution of laboratory confirmed cases and the arthropod reservoirs. Am J Trop Med Hyg. 1950;30:73–6. http://dx.doi.org/10.4269/ajtmh.1950.s1-30.73

23. Brumpt E. Study of *Spirochaeta turicatae*, n. sp., agent of sporadic recurrent fever of the United States transmitted by *Ornithodoros turicata* [in French]. Comptes Rendus des Séances de la Société de Biologie et de ses Filiales (Paris). 1933;13:1369.

24. Whitney MS, Schwan TG, Sultemeier KB, McDonald PS, Brillhart MN. Spirochetemia caused by *Borrelia turicatae* infection in 3 dogs in Texas. Vet Clin Pathol. 2007;36:212–6. http://dx.doi.org/10.1111/j.1939-165X.2007.tb00213.x

25. Francis E. Longevity of the tick *Ornithodoros turicata* and of *Spirochaeta recurrentis* with this tick. Public Health Rep. 1938;53:2220–41. http://dx.doi.org/10.2307/4582740

26. Dworkin MS, Shoemaker PC, Fritz CL, Dowell ME, Anderson DE Jr. The epidemiology of tick-borne relapsing fever in the United States. Am J Trop Med Hyg. 2002;66:753–8. http://dx.doi.org/10.4269/ajtmh.2002.66.753

Address for correspondence: Job E. Lopez, Department of Molecular Virology and Microbiology and the National School of Tropical Medicine, Baylor College of Medicine, Houston, 1 Baylor Plaza, Houston, Texas 77030, USA; email: job.lopez@bcm.edu

Effects of Pneumococcal Conjugate Vaccine on Genotypic Penicillin Resistance and Serotype Changes, Japan, 2010–2017

Kimiko Ubukata, Misako Takata, Miyuki Morozumi, Naoko Chiba, Takeaki Wajima,
Shigeo Hanada, Michi Shouji, Megumi Sakuma, Satoshi Iwata;
the Invasive Pneumococcal Diseases Surveillance Study Group

To clarify year-to-year changes in capsular serotypes, resistance genotypes, and multilocus sequence types of *Streptococcus pneumoniae*, we compared isolates collected from patients with invasive pneumococcal disease before and after introductions of 7- and 13-valent pneumococcal conjugate vaccines (PCV7 and PVC13, respectively). From April 2010 through March 2017, we collected 2,856 isolates from children and adults throughout Japan. Proportions of PCV13 serotypes among children decreased from 89.0% in fiscal year 2010 to 12.1% in fiscal year 2016 and among adults from 74.1% to 36.2%. Although nonvaccine serotypes increased after introduction of PCV13, genotypic penicillin resistance decreased from 54.3% in 2010 to 11.2% in 2016 among children and from 32.4% to 15.5% among adults. However, genotypic penicillin resistance emerged in 9 nonvaccine serotypes, but not 15A and 35B. Multilocus sequence typing suggested that resistant strains among nonvaccine serotypes may have evolved from clonal complexes 156 and 81. A more broadly effective vaccine is needed.

Among persons in all age groups, but particularly infants and elderly persons, *Streptococcus pneumoniae* remains a major cause of invasive pneumococcal disease (IPD) (e.g., pneumonia, meningitis, and sepsis), although generally effective antimicrobial agents are available (*1*). In the United States, 7-valent pneumococcal conjugate vaccine (PCV7) has been administered to children since 2000, resulting in both individual and herd immunity, with declines in pneumococcal infection among children and elderly persons (*2–6*). Unfortunately, introduction of PCV7

Author affiliations: Keio University School of Medicine, Tokyo, Japan (K. Ubukata, M. Takata, M. Morozumi, N. Chiba, M. Sakuma, S. Iwata); Tokyo University of Pharmacy and Life Sciences, Tokyo (T. Wajima); Toranomon Hospital, Tokyo (S. Hanada); National Cancer Center Hospital, Tokyo (M. Shouji, S. Iwata)

was followed by an increase in serotype 19A showing penicillin resistance and often multidrug resistance (*5–8*). In 2010, vaccination for children was upgraded to 13-valent pneumococcal conjugate vaccine (PCV13), which covers 6 additional serotypes: 1, 3, 5, 6A, 7F, and 19A (*9*). Introduction of PCV13 contributed to decreases in IPD (*10,11*), pneumonia (including community-acquired pneumonia without bacteremia) (*12,13*), and acute otitis media (*14–16*) caused by *S. pneumoniae* belonging to vaccine serotypes, especially 6A and 19A. As an indirect effect of wide administration of PCVs to children, pneumococcal infections in adults have also decreased, representing herd immunity (*11,12,17–23*).

Despite these benefits, in countries where PCV7 or PCV13 was introduced, proportions of disease preventable by PCVs gradually decreased because vaccine-serotype pneumococci were replaced by nonvaccine serotypes (NVTs). Increases in NVTs such as 6C, 15A/B/C, 23A, and 35B have been reported in the United States (*24–28*); 15A and 23B in Norway (*18*) and Germany (*29*); and 12F, 15A, 24F, and 35B in France (*30*).

In November 2010 in Japan, PCV7 vaccination use among children <5 years of age was introduced voluntarily by the Provisional Special Fund for the Urgent Promotion of Vaccination. In April 2013, PCV7 was officially incorporated into the vaccination program as public administration; in November of that year, PCV7 was replaced by PCV13. Promotion of PCV7 vaccination for children rapidly halved the number of IPD cases caused by vaccine-serotype pneumococci among children (*31*) and also produced a herd effect benefiting elderly persons (*32*). After PCV7 introduction, however, among persons of all ages, IPD caused by non-PCV7 serotypes such as 19A, 15A, 15B, 15C, 22F, and 24F showed relative increases in 2013. In November 2014, the Japanese Ministry of Health, Labour and Welfare began promoting vaccination of adults ≥65 years of age with 23-valent pneumococcal polysaccharide vaccine

(PPSV23). In this study, we aimed to clarify year-to-year changes in capsular serotypes, genotypes of penicillin and macrolide resistance, and diversity of sequence types (STs) in all pneumococcal isolates collected throughout Japan during April 2010–March 2017.

Methods

Patients and Pneumococcal Strains

We included all specimens from patients of any age with IPD. Pneumococcal isolates from normally sterile clinical samples were collected from clinical laboratories at 341 hospitals participating in this IPD surveillance study. Each hospital had a microbiology laboratory as described previously (31), and participating hospitals were distributed nearly uniformly throughout Japan. These hospitals took part in the surveillance project after written permission was granted by the laboratory director or hospital director. This study was approved by the Keio University School of Medicine Ethics Committee (approval no. 20140432).

A total of 2,856 pneumococcal strains were collected from April 2010 through March 2017 (online Technical Appendix Figure 1, https://wwwnc.cdc.gov/EID/article/24/11/18-0326-Techapp1.pdf). The first surveillance interval, April 2010–March 2011 (designated 2010), represented the pre-PCV7 period. The second surveillance interval, April 2011–March 2014 (designated 2011–2013, the PCV7 period), showed effects of PCV7 vaccination for children <5 years of age. The third surveillance interval, April 2014–March 2017 (designated 2014–2016, the PCV13 period), reflected PCV13 vaccination for children <5 years of age.

During the pre-PCV7 period, the rate of voluntary PCV7 vaccination among children in Japan was <10%. The PCV7 period corresponded to the Urgent Promotion of PCV7, a vaccination incentive program for children. The PCV7 vaccination rate throughout Japan was estimated at 50%–60% in 2011, 80%–90% in 2012, and >95% in 2013. During the PCV13 period, corresponding to substitution of PCV13 for routine vaccination, coverage remained >95%. In elderly persons (≥65 years of age), the rate of vaccination with PPSV23, starting in 2014, has remained at ≈54% as of 2017 (Vaccine Medical Affairs of Merck Sharp and Dohme K.K., Tokyo, Japan, pers. comm., 2017 Apr 1).

Pneumococcal isolates were sent promptly from each clinical laboratory to the Department of Infectious Diseases, Keio University School of Medicine (Tokyo, Japan), accompanied by a survey form completed by the attending physician. In compliance with ethics guidelines for epidemiology in Japan, patients were not identified.

Serotype and Resistance Genotype

We determined serotypes by using the capsular quellung test with antiserum purchased from Statens Serum Institute (Copenhagen, Denmark). Alterations in 3 penicillin-binding protein genes that mediate β-lactam resistance in *S. pneumoniae* (*pbp1a*, *pbp2x*, and *pbp2b*) were identified by real-time PCR as described previously (33). The *mef*(A) and *erm*(B) genes, which mediate macrolide resistance, were also identified by real-time PCR (33). Quinolone resistance was analyzed by sequencing the quinolone resistance–determining region in the genes *gyrA*, *gyrB*, *parC*, and *parE* in strains showing MICs of levofloxacin exceeding 4 µg/mL.

Genotypes (g) based on gene analysis were represented as follows: penicillin-susceptible *S. pneumoniae* (gPSSP), possessing 3 normal *pbp* genes; penicillin-intermediate *S. pneumoniae* (gPISP), subclassified as gPISP (*pbp2x*), gPISP (*pbp2b*), gPISP (*pbp1a*+*pbp2x*), gPISP (*pbp1a*+*pbp2b*), or gPISP (*pbp2x*+*pbp2b*); and penicillin-resistant *S. pneumoniae* (gPRSP), which possessed 3 abnormal *pbp* genes (31,33). Serotype and resistance genotype results were promptly reported to laboratory staff at each referring hospital.

Susceptibility Testing

For all isolates, we redetermined the MICs of 6 antimicrobial agents by using agar-dilution methods with reference strains R6 and ATCC49619 (34). The agents tested were penicillin, ampicillin, cefotaxime, meropenem, vancomycin, and levofloxacin.

Multilocus Sequence Typing

We performed multilocus sequence typing (MLST) analysis for all 2,849 isolates that could be cultured. Primers used for MLST were based on sequences listed at https://pubmlst.org/spneumoniae/. Clusters of related STs were analyzed by using eBURST version 3 (http://eburst.mlst.net/).

Statistical Analyses

For statistical analyses, we used Ekuseru-Toukei 2015 software (Social Survey Research Information, Tokyo, Japan) and R software 3.5.0 (R Foundation of Computational Statistics, Vienna, Austria). We used the χ^2 and Fisher exact tests as appropriate. We considered $p<0.05$ to indicate statistical significance.

Results

Relationships between IPD Type and Patient Age

Relationships between IPD type and patient age are shown in Table 1. IPD types were classified into 4 categories: pneumonia with bacteremia (41.9%), including empyema and pleuritis; bacteremia with unknown focus (37.0%); meningitis (15.4%); and others (5.6%), including endocarditis, necrotizing fasciitis, cellulitis, arthritis, and spondylitis. Pneumonia with bacteremia was most common among adults, especially

Table 1. Invasive pneumococcal disease in all patients, by age group, Japan, April 2010–March 2017

Disease	Total, no. (%), n = 2,856	Age, y, no. (%)								p value
		≤2, n = 731	3–5, n = 181	6–17, n = 94	18–49, n = 201	50–64, n = 387	65–74, n = 530	75–84, n = 457	≥85, n = 275	
Pneumonia with bacteremia*	1,198 (41.9)	130 (17.8)	35 (19.3)	22 (23.4)	83 (41.3)	167 (43.2)	261 (49.2)	300 (65.6)	200 (72.7)	<0.001
Bacteremia with focus unknown	1,058 (37.0)	455 (62.2)	116 (64.1)	33 (35.1)	46 (22.9)	104 (26.9)	158 (29.8)	92 (20.1)	54 (19.6)	<0.001
Meningitis	440 (15.4)	109 (14.9)	22 (12.2)	34 (36.2)	56 (27.9)	80 (20.7)	79 (14.9)	43 (9.4)	17 (6.2)	<0.001
Other†	160 (5.6)	37 (5.1)	8 (4.4)	5 (5.3)	16 (8.0)	36 (9.3)	32 (6.0)	22 (4.8)	4 (1.5)	0.002

*Includes empyema (n = 32) and pleuritis (n = 25).
†Includes endocarditis (n = 6), necrotizing fasciitis (n = 1), arthritis (n = 34), cellulitis (n = 20), and spondylitis (n = 7).

those ≥75 years of age; however, among children <5 years of age, bacteremia with unknown focus was most common (p<0.001 for each). Meningitis and other IPDs were represented in higher proportions among persons 6–64 years of age (p<0.001) than among those in other age groups (p = 0.002).

Changes in Serotypes

Figure 1 shows yearly changes in pneumococcal capsular serotypes among children and adults. Pneumococcal capsular serotypes were classified into 4 groups: PCV7 serotypes (4, 6B, 9V, 14, 18C, 19F, and 23F) (PCV7); PCV13 serotypes not included in PCV7 (1, 3, 5, 6A, 7F, and 19A) (PCV13–nonPCV7); PPSV23 serotypes not included in PCV13 (2, 8, 9N, 10A, 11A, 12F, 15B, 17F, 20, 22F, and 33F) (PPSV23–nonPCV13); and NVTs not including serotypes in PPSV23 and not including 6A. Among children, the proportion of PCV7 serotypes that accounted for 73.3% of serotype strains isolated from IPD patients during the pre-PCV7 period decreased rapidly to 7.4% in 2013 after PCV7 introduction (Figure 1). In contrast, in 2013, PCV13–nonPCV7 serotypes increased from 15.7% to 25.9%, PPSV23–nonPCV13 serotypes increased from 3.0% to 18.5%, and NVT serotypes increased from 8.0% to 48.1%. During 2014, after PCV7 was replaced with PCV13, the proportion of PCV13–nonPCV7 serotypes decreased by approximately half to 11.1% in 2016, while PPSV23–nonPCV13 serotypes increased to 40.4%, in contrast to the PCV7 period.

Among adults, the proportions of PCV7 serotypes, which accounted for 43.6% of isolates during the pre-PCV7 period, decreased to 11.7% in 2013, when children were vaccinated with PCV7. However, proportions of the PPSV23–nonPCV13 doubled from 12.4% to 25.4% and NVTs doubled from 13.5% to 28.9%. PCV13–nonPCV7 serotypes decreased slightly after replacement by PCV13 in 2014, but PPSV23–nonPCV13 serotypes continued to increase.

Serotype Changes during the Pre-PCV7, PCV7, and PCV13 Periods

Changes in serotypes of pneumococcal isolates collected between the pre-PCV7, PCV7, and PCV13 periods are shown in Table 2 for children and in Table 3 for adults. Among children, proportions of PCV7 serotypes decreased rapidly from 73.3% to 30.3% during the PCV7 period and decreased further to 2.3% during the PCV13 period (p<0.001). Among PCV13–nonPCV7 serotypes, serotype 19A apparently increased during the PCV7 period, but later it decreased significantly during the PCV13 period. PCV13–nonPCV7 serotypes decreased from 21.8% during the PCV7 period to 14.9% during the PCV13 period (p = 0.031). Although serotypes 1 and 7F showed relative increases during the PCV13 period, most were isolated from patients ≥3 years of

Figure 1. Yearly changes in pneumococcal serotypes of isolates from A) 1,006 children and B) 1,850 adults with invasive pneumococcal disease in Japan, April 2010–March 2017. Specific percentages are indicated at points along data lines. Fiscal years extend from April 1 through March 31 of the following year. PCV13–nonPCV7 covers 6 serotypes (1, 3, 5, 6A, 7F, and 19A). PPSV23–nonPCV13 covers 11 serotypes (2, 8, 9N, 10A, 11A, 12F, 15B, 17F, 20, 22F, and 33F), but 2, 9N, and 17F were not isolated in this study. NVTs represent other serotypes not included in PPSV23 and 6A. NVT, nonvaccine serotype; PCV7, 7-valent pneumococcal conjugate vaccine; PCV13, 13-valent pneumococcal conjugate vaccine; PPSV23, 23-valent pneumococcal polysaccharide vaccine.
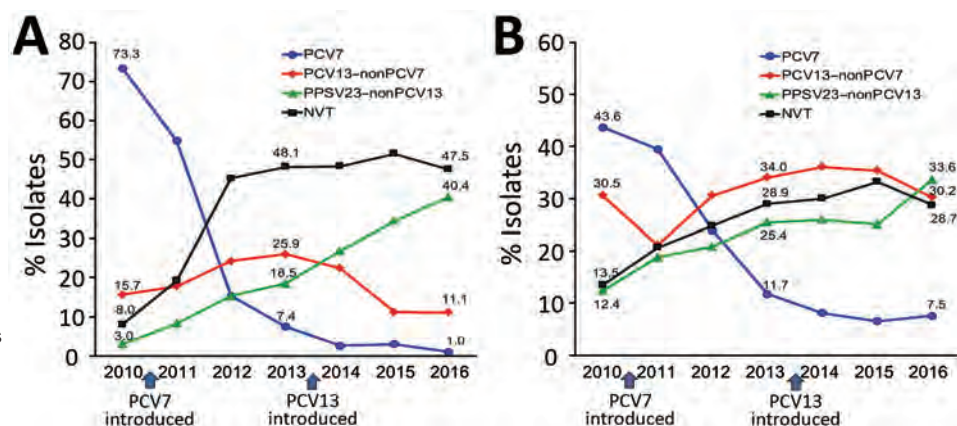
Table 2. Distribution of pneumococcal serotypes among children before PCV7 and after introduction of PCV7 and PCV13, Japan, April 2010–March 2017*

Serotype	Pre-PCV7 period, 2010, n = 300	PCV7 period 2011–2013, n = 357	PCV13 period, 2014–2016, n = 349	p value†
PCV7				
4	7 (2.3)	6 (1.7)	0	0.007
6B	83 (27.7)	49 (13.7)	2 (0.6)	<0.001
9V	9 (3.0)	2 (0.6)	1 (0.3)	0.005
14	34 (11.3)	9 (2.5)	0	<0.001
18C	4 (1.3)	4 (1.1)	1 (0.3)	0.336
19F	40 (13.3)	13 (3.6)	2 (0.6)	<0.001
23F	43 (14.3)	25 (7.0)	2 (0.6)	<0.001
Subtotal	220 (73.3)	108 (30.3)	8 (2.3)	<0.001
PCV13–nonPCV7‡				
1	0	5 (1.4)	13 (3.7)	**<0.001**
3	4 (1.3)	7 (2.0)	4 (1.1)	0.724
5	0	0	0	NA
6A	15 (5.0)	6 (1.7)	2 (0.6)	0.001
7F	1 (0.3)	2 (0.6)	6 (1.7)	0.153
19A	27 (9.0)	58 (16.2)	27 (7.7)	0.001
Subtotal	47 (15.7)	78 (21.8)	52 (14.9)	0.031
PPSV23–nonPCV13§				
8	0	0	0	NA
10A	2 (0.7)	5 (1.4)	18 (5.2)	**<0.001**
11A	2 (0.7)	1 (0.3)	4 (1.1)	0.356
12F	1 (0.3)	1 (0.3)	33 (9.5)	**<0.001**
15B	0	15 (4.2)	26 (7.4)	**<0.001**
20	0	1 (0.3)	0	NA
22F	3 (1.0)	16 (4.5)	19 (5.4)	**0.003**
33F	1 (0.3)	7 (2.0)	17 (4.9)	**0.001**
Subtotal	9 (3.0)	46 (12.9)	117 (33.5)	**<0.001**
NVT				
6C	9 (3.0)	20 (5.6)	11 (3.2)	0.159
15A	2 (0.7)	25 (7.0)	36 (10.3)	**<0.001**
15C	1 (0.3)	17 (4.8)	16 (4.6)	**<0.001**
23A	4 (1.3)	13 (3.6)	10 (2.9)	0.176
24F	1 (0.3)	20 (5.6)	52 (14.9)	**<0.001**
24B	2 (0.7)	4 (1.1)	12 (3.4)	0.197
34	1 (0.3)	6 (1.7)	7 (2.0)	0.126
35B	1 (0.3)	10 (2.8)	11 (3.2)	**0.016**
38	1 (0.3)	8 (2.2)	7 (2.0)	0.072
Other¶	2 (0.7)	2 (0.6)	9 (2.6)	**0.041**
Subtotal	24 (8.0)	125 (35.0)	171 (49.0)#	**<0.001**

*Years run from April 1 through March 31 of the following year. NA, not applicable; NVT, nonvaccine serotype; PCV7, 7-valent pneumococcal conjugate vaccine; PCV13, 13-valent pneumococcal conjugate vaccine; PPSV23, 23-valent pneumococcal polysaccharide vaccine.
†p values compare the 3 surveillance periods; boldface indicates significant increase.
‡Serotypes added to PCV7.
§Serotypes contained in PPSV23 but not PCV13.
¶Includes 7C (n = 2), 16F (n = 2), 21 (n = 2), 23B (n = 3), 28A (n = 1), 37 (n = 1), and 31 (n = 2).
#One strain identified as nontypeable was excluded from the table.

age who had received PCV7 or a single dose of PCV13. To the contrary, proportions of PPSV23–nonPCV13 serotypes and NVTs increased significantly between the pre-PCV7 period and the PCV7 period, continuing to increase up to the PCV13 period (p<0.001 for each). In particular, 9 serotypes (10A, 12F, 15A, 15B, 15C, 22F, 24F, 33F, and 35B) increased significantly after introduction of PCV7 and PCV13.

Among adults, proportions of PCV7 serotypes decreased sharply, from 43.6% during the pre-PCV7 period to 24.2% during the PCV7 period and 7.3% during the PCV13 period, particularly for serotypes 4, 6B, 9V, 14, 19F, and 23F. PCV13–nonPCV7 serotypes increased in serotypes 7F and 19A, whereas 6A showed a significant decrease because of cross-immunity with 6B (Table 3). PPSV23–nonPCV13 serotypes and NVTs increased respectively from 12.4% and 13.5% during the pre-PCV7 period to 21.9% and 24.9% during the PCV7 period and further to 27.8% and 30.9% during the PCV13 period (p<0.001 for each). In particular, significant increases were noted for serotypes 12F, 15C, 22F, 23A, 24F, and 35B. Tendencies to increase did not attain significance for serotypes 11A and 15A.

Changes in Penicillin and Other Resistance Genotypes
Figure 2 shows yearly changes of penicillin resistance genotypes among children and adults. Changes are shown from

Table 3. Distribution of pneumococcal serotypes in adults before PCV7 and after introduction of PCV7 and PCV13 administration to children, Japan, April 2010–March 2017*

Serotype	No. (%)			
	Pre-PCV7 period, 2010, n = 275	PCV7 period, 2011–2013, n = 695	PCV13 period, 2014–2016, n = 880	p value†
PCV7				
4	14 (5.1)	27 (3.9)	4 (0.5)	<0.001
6B	42 (15.3)	39 (5.6)	22 (2.5)	<0.001
9V	7 (2.5)	7 (1.0)	6 (0.7)	0.042
14	21 (7.6)	41 (5.9)	6 (0.7)	<0.001
18C	1 (0.4)	3 (0.4)	2 (0.2)	0.642
19F	14 (5.1)	23 (3.3)	15 (1.7)	0.007
23F	21 (7.6)	28 (4.0)	9 (1.0)	<0.001
Subtotal	120 (43.6)	168 (24.2)	64 (7.3)	<0.001
PCV13–nonPCV7‡				
1	1 (0.4)	4 (0.6)	13 (1.5)	0.145
3	45 (16.4)	110 (15.8)	145 (16.5)	0.939
5	0	1 (0.1)	0	NA
6A	11 (4.0)	16 (2.3)	9 (1.0)	0.006
7F	9 (3.3)	9 (1.3)	33 (3.8)	**0.006**
19A	18 (6.5)	61 (8.8)	99 (11.3)	**0.045**
Subtotal	84 (30.5)	201 (28.9)	299 (34.0)	0.093
PPSV23–nonPCV13§				
8	0	2 (0.3)	0	NA
10A	10 (3.6)	34 (4.9)	54 (6.1)	0.244
11A	3 (1.1)	23 (3.3)	34 (3.9)	0.058
12F	5 (1.8)	5 (0.7)	63 (7.2)	**<0.001**
15B	3 (1.1)	14 (2.0)	10 (1.1)	0.356
20	1 (0.4)	7 (1.0)	14 (1.6)	0.261
22F	10 (3.6)	63 (9.1)	59 (6.7)	**0.008**
33F	2 (0.7)	4 (0.6)	11 (1.3)	0.352
Subtotal	34 (12.4)	152 (21.9)	245 (27.8)	**<0.001**
NVT				
6C	13 (4.7)	49 (7.1)	52 (5.9)	0.400
15A	6 (2.2)	28 (4.0)	47 (5.3)	0.068
15C	0	12 (1.7)	7 (0.8)	**0.034**
23A	2 (0.7)	33 (4.7)	50 (5.7)	**<0.001**
24F	0	11 (1.6)	16 (1.8)	**0.049**
34	1 (0.4)	5 (0.7)	12 (1.4)	0.301
35B	7 (2.5)	22 (3.2)	55 (6.3)	**0.004**
38	3 (1.1)	7 (1.0)	11 (1.3)	0.955
Other¶	5 (1.8)	6 (0.9)	22 (2.5)	**0.042**
Subtotal	37 (13.5)	173 (24.9)#	272 (30.9)	**<0.001**

*Years run April 1– March 31 of the following year. NA, not applicable; NVT, nonvaccine serotype; PCV7, 7-valent pneumococcal conjugate vaccine; PCV13, 13-valent pneumococcal conjugate vaccine; PPSV23, 23-valent pneumococcal polysaccharide vaccine.
†p values compare the 3 surveillance periods; boldface indicates significant increase.
‡Serotypes added to PCV7.
§Serotypes contained in PPSV23 but not PCV13.
¶Includes 6D (n = 2), 7C (n = 8), 13 (n = 1), 16F (n = 6), 18B (n = 1), 23B (n = 5), 31 (n = 3), and 37 (n = 7).
#One strain identified as nontypeable was excluded from the table.

the pre-PCV7 period to the PCV7 period and further to the PCV13 period.

Among children, the proportion of gPRSP declined sharply from 54.3% in 2010 during the pre-PCV7 period to 20.4% in 2013 during the PCV7 period; gPSSP and gPISP (*pbp2x*) increased (Figure 2). In 2016 during the PCV13 period, proportions of gPRSP and gPISP (*pbp1a+2x*) further declined to 11.2% and 6.1%, respectively. However, gPISP (*pbp2b*) rapidly increased.

Among isolates from adults during the pre-PCV7 period, gPISP (*pbp2x*) was most common (34.9%), followed by gPRSP (32.4%) (Figure 2). gPSSP accounted for only 15.3%. Similar to the trend for children during the PCV7 and PCV13 periods, gPRSP among adults continually

decreased to 15.5% in 2016. However, also in 2016, gPISP (*pbp2b*) among adults increased to 8.3%, similar to the trend among children.

During the surveillance periods, macrolide-resistant isolates possessing *mef*(A) or *erm*(B) genes remained consistently high. Among children, proportions were 93.8% in 2010 and 91.8% in 2016; among adults, proportions were 87.2% in 2010 and 89.8% in 2016. Prevalence of resistance genes was 59.8% for the *erm*(B) gene mediating high macrolide resistance, 19.6% for the *mef*(A) gene mediating intermediate resistance, and 11.6% for both *erm*(B) and *mef*(A) genes (data not shown).

Isolates with mutations in both *gyrA* and *parC* genes, which are involved in resistance to quinolones, especially

Figure 2. Yearly changes in genotypic penicillin resistance in isolates from A) 1,006 children and B) 1,850 adults with invasive pneumococcal disease in Japan, April 2010–March 2017. Fiscal years extend from April 1 through March 31 of the following year. Genotypes based on abnormal *pbp1a*, *pbp2x*, and *pbp2b* genes were identified by real-time PCR and are represented as gPRSP (*1a+2x+2b*), gPISP (*1a+2x*), gPISP (*1a+2b*), gPISP (*2x+2b*), gPISP (*2x*), gPISP (*2b*), and gPSSP. g, genotype; PCV7, 7-valent pneumococcal conjugate vaccine; PCV13, 13-valent pneumococcal conjugate vaccine; PISP, penicillin-intermediate *Streptococcus pneumoniae;* PRSP, penicillin-resistant *S. pneumoniae*; PSSP, penicillin-susceptible *S. pneumoniae*.
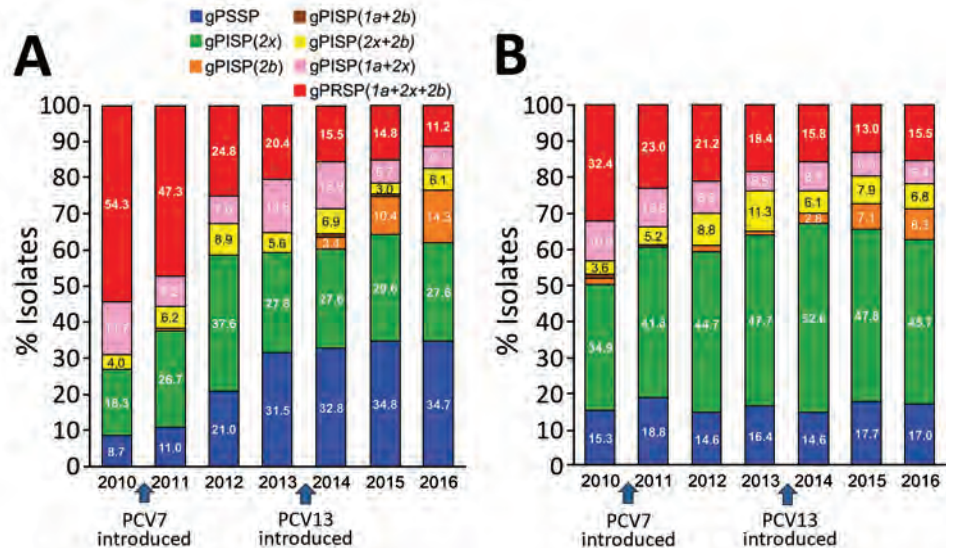
levofloxacin, accounted for <1% of all isolates. These isolates showed no tendency to increase.

Relationships between Serotypes and Resistance Genotypes

Changes of serotypes and the penicillin resistance genotypes during the 3 periods (pre-PCV7, PCV7, and PCV13) are shown in online Technical Appendix Figures 2 (for children) and 3 (for adults). Decreases in gPRSP (*pbp1a+2x+2b*) and gPISP (*pbp1a+2x*) were closely related to reduction of serotypes 6B, 14, 19F, 23F, and 6A in children and adults during the PCV7 period, and this link became stronger during the PCV13 period. Serotype 19A, including several gPRSP, decreased by half among children during the PCV13 period, but this change has not yet become evident among adults.

The proportions of PPSV23–nonPCV13 and NVT serotypes generally increased among children and adults during the PCV13 period. gPRSPs were newly identified in serotypes 15B (n = 1), 15C (n = 1), and 16F (n = 2) in isolates from children and in serotypes 6C (n = 2), 6D (n = 2), 13 (n = 1), 15B (n = 1), 15C (n = 1), 16F (n = 2), 23A (n = 1), 23B (n = 1), and 34 (n = 1) in isolates from adults.

Relationships between genotypic macrolide and penicillin resistances and serotypes are shown in online Technical Appendix Table 1. Strains possessing *mef*(A), *erm*(B), or both were identified in most of the serotypes, with the exception of serotypes 8, 18B, 28A, and 31. No relationship was observed between macrolide resistance and penicillin resistance.

Antimicrobial Susceptibility by Genotype

Susceptibilities (50% MIC, 90% MIC, and MIC range) of 6 parenteral agents (penicillin, ampicillin, cefotaxime, meropenem, vancomycin, and levofloxacin) for

S. pneumoniae strains obtained from April 2014 through March 2017, corresponding to the PCV13 period (n = 1,229), are shown in online Technical Appendix Table 2. Relationships between 6 genotypes for penicillin resistance and MICs of penicillin, ampicillin, cefotaxime, and meropenem for the strains are shown in online Technical Appendix Figure 4.

Because prevalence of gPRSP was reduced by the PCV vaccinations, the distribution of susceptibilities was shifted in favor of greater susceptibility, especially after introduction of PCV7. For penicillin and ampicillin, 90% MICs were 2 μg/mL; for cefotaxime, 1 μg/mL; and for meropenem, 0.5 μg/mL. gPRSP isolates showing high resistance for penicillin (≥8 μg/mL) were not found.

STs by Serotypes and Resistance Genotypes

STs by eBURST analyses for 2,849 pneumococcal strains are shown in Figure 3. These data are distinguished by ST and vaccine serotype (PCV7, PCV13–nonPCV7, PPSV23–nonPCV13, and NVT). Details of relationships among clonal complexes (CCs), STs, serotypes, and resistance genotypes are listed in online Technical Appendix Table 3.

By MLST analysis, 273 different STs were identified. STs of gPRSP in 11 serotypes included in PPSV23–nonPCV13 and NVTs were noteworthy: 15B (n = 2), ST242 (belonging to CC242) and ST83 (derived from CC81); 6C (n = 2), ST8352 (CC156) and ST5832 (CC5832); 6D (n = 2), ST90 (CC156) and ST282 (CC81); 13 (n = 1), ST10303 (CC156); 15A (n = 77), ST63, ST2105, ST2771, ST8354, and ST12000 (all CC63); 15C (n = 2), ST83 and ST6138 (CC81); 16F (n = 4), ST8351 (CC3117); 23A (n = 1), ST9619 (CC156); 23B (n = 1), ST2372 (CC156); 34 (n = 1), ST9395 (CC15); 35B (n = 55), ST558, ST1204, and
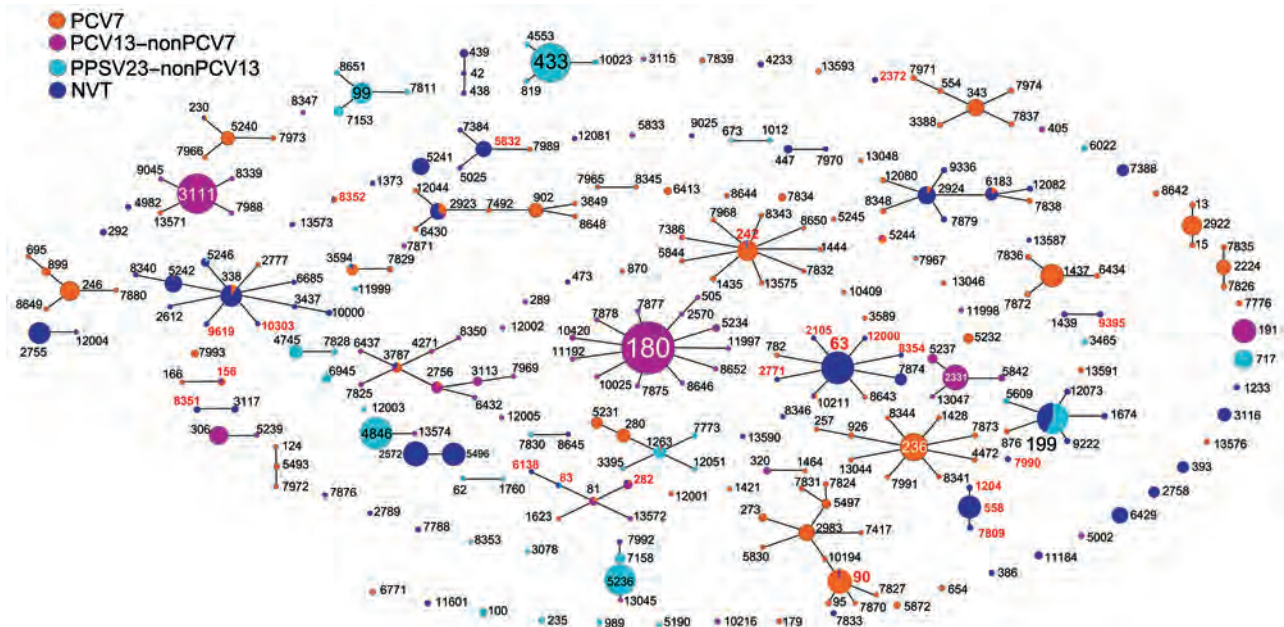
Figure 3. An eBURST (http://eburst.mlst.net/) diagram displaying pneumococcal sequence types (STs) causing invasive pneumococcal disease across patients of all age groups in Japan. All 2,849 strains are distinguished by colors to indicate PCV7, PCV13–nonPCV7, PPSV23–nonPCV13, and NVT. Size of each circle reflects the number of strains. ST numbers shown in red represent genotypes for penicillin-resistant *Streptococcus pneumoniae* confirmed among PPSV23–nonPCV13 and NVT as follows: 15B (n = 2), ST242 and ST83; 6C (n = 2), ST8352 and ST5832; 6D (n = 2), ST90 and ST282; 13 (n = 1), ST10303; 15A (n = 77), ST63 (n = 73), ST2105, ST2771, ST8354, and ST12000; 15C (n = 2), ST83 and ST6138; 16F (n = 4), ST8351; 23A (n = 1), ST9619; 23B (n = 1), ST2372; 34 (n = 1), ST9395; 35B (n = 55), ST558 (n = 49), ST1204, ST7809, ST7990, and ST156. NVT, nonvaccine serotype; PCV7, 7-valent pneumococcal conjugate vaccine; PCV13, 13-valent pneumococcal conjugate vaccine; PPSV23, 23-valent pneumococcal polysaccharide vaccine.

ST7809 (all CC558); and the remaining ST156 (CC156) and ST7990 (singleton).

A total of 6 STs identified as gPRSP belonged to the large CC156 (Figure 4). STs of 3 serotypes (13, 23A, and 23B) were derived from ST338, which includes the Colombia[23F-26] clone from the Pneumococcal Molecular Epidemiology Network (PMEN). Serotype 6C was derived from ST172, a neighbor of ST338. Of strains with serotypes 6D and 35B, each strain was distant from other gPRSPs. STs of serotypes 15B, 15C, and 6D among gPRSP belonged to CC81 (online Technical Appendix Figure 5).

In addition, STs of certain serotypes increasing in PPSV23–nonPCV13 and NVTs were noted. Serotype 12F was ST4846 (CC1527), 22F was ST433 (CC433), 23A included ST338 and ST5242 (CC156), and 24B/24F included ST2572 and ST5496 (CC2572).

Discussion

Wide use of PCVs among children in many countries has contributed to a dramatic reduction in incidence of IPD (6,10,11,35–38), pneumonia (12,13,39), and acute otitis media (14,15) caused by *S. pneumoniae*, while providing indirect herd immunity benefits for adults (11,23,40,41). Replacing PCV7 with PCV13 decidedly decreased

serotype 19A isolates among causative pathogens, but in several countries, NVTs such as 15A and 35B increased. Gradual increases of NVTs, unfortunately, have blunted the effectiveness of conjugate vaccines (42).

In Japan, introduction of PCV7 in children <5 years of age began as an official government program in November 2010, continuing until it was replaced with PCV13 in November 2013. PPSV23 vaccination for adults ≥65 years of age was implemented in October 2014. We organized nationwide surveillance beginning in April 2010, with collection of pneumococcal strains from IPD patients in all age groups throughout Japan. In this article, we describe details of changes of serotypes, penicillin resistance genotypes, and MLST analyses that have followed implementation of PCV7 and PCV13 vaccination. As in other countries where PCV13 has been introduced, proportions of PCV13 serotypes among isolates from children and adults decreased significantly during the PCV13 period. In Japan, where population density is high, the decrease suggests early effectiveness of herd immunity not only among children but also among adults. However, serotypes 7F and 19A, included in PCV13, seem to be increasing among adults; for these serotypes, no indirect effect for adults is evident. These findings indicate a need for PCV13 vaccination of elderly
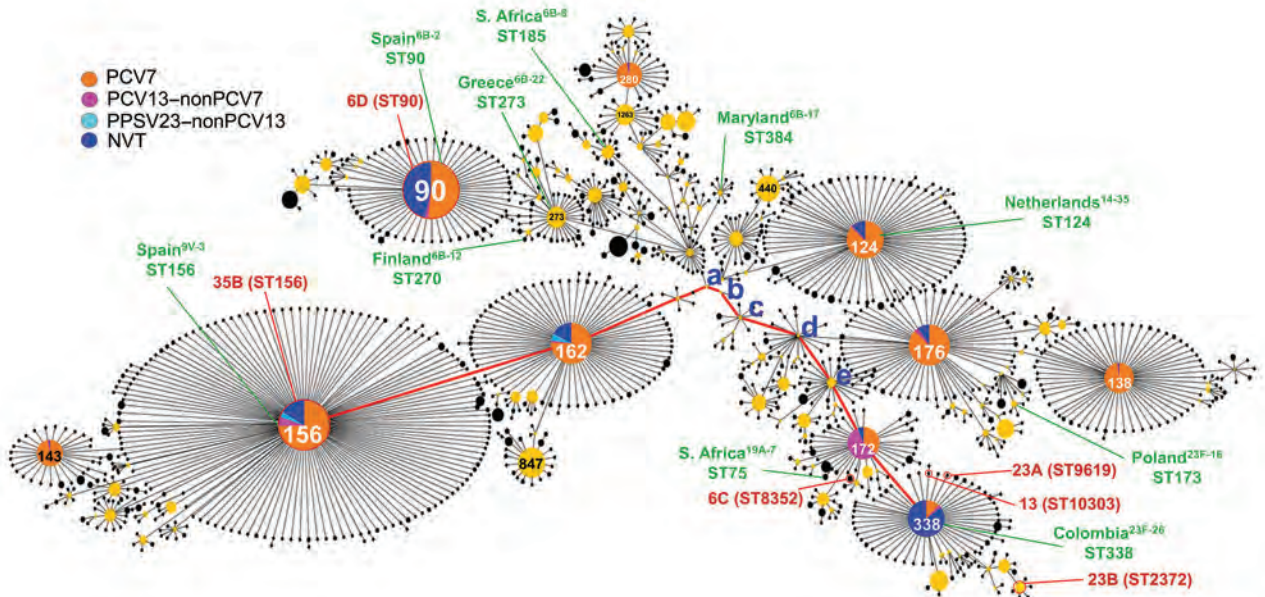
Figure 4. Details of *Streptococcus pneumoniae* clonal complex (CC) 156 (n = 4,736), including 1,308 sequence types obtained from the multilocus sequence typing website (https://pubmlst.org/spneumoniae/). Data include those from this study (n = 359). STs of 6 genotypes for penicillin-resistant *S. pneumoniae* identified in NVT serotypes belonged to CC156. STs of serotypes 6C, 13, 23A, and 23B were derived from ST338 and ST172 (shown in red). Serotypes 6D and 35B belonged to ST90 and ST156, respectively. The Pneumococcal Molecular Epidemiology Network clone identified in CC156 is also shown (in green). The red line indicates evolution from ST156 to ST338: a, ST8055; b, ST8618; c, ST4542; d, ST171; e, ST361. NVT, nonvaccine serotype; PCV7, 7-valent pneumococcal conjugate vaccine; PCV13, 13-valent pneumococcal conjugate vaccine; PPSV23, 23-valent pneumococcal polysaccharide vaccine; ST, sequence type.

and relatively immunocompromised persons, especially in Japan, where the population's average age is increasing. Of further concern is a test-negative design study conducted before introduction of PPSV23 to assess effectiveness of PPSV23 among elderly persons with community-acquired pneumonia in Japan. Effectiveness against community-acquired pneumonia caused by PPSV23 serotypes seemed low to moderate, depending on age group (*43*).

Proportions of many non-PCV13 serotypes during the PCV13 period have increased beyond proportions during the pre-PCV7 period. Nine serotypes (10A, 12F, 15A, 15B, 15C, 22F, 24F, 33F, and 35B) have increased significantly among children, and 5 serotypes (12F, 15C, 22F, 23A, and 35B) have increased significantly among adults, showing considerable overlap between age groups. Among these serotypes, 15A and 35B have increased rapidly since PCV13 introduction in Japan, as has occurred in other countries (*18,25,28–30*). The reason for increases in such serotypes is unclear; further epidemiologic surveillance may shed light on the matter.

Of note, gPRSP decreased sharply along with serotype replacements among children and adults. Highly penicillin-resistant strains with MICs ≥8 µg/mL, which sometimes were noted in serotypes 19F and 23F during the pre-PCV7 period (*33*), did not increase with introduction of PCVs.

Susceptibilities of most gPISP (*pbp2b*) in serotype 12F and of gPISP(*pbp2x+2b*) in serotypes 23A and 6C for penicillin and ampicillin ranged from 0.125 to 0.5 µg/mL. Should mutation(s) occur in the regions encoding the conserved amino acids (STMK, SSN, and KTG) in the *pbp1a* gene, antimicrobial selection pressure could easily favor development from gPISP to gPRSP.

One concern is the evolution of gPRSP among isolates from 11 NVTs according to MLST analysis. Most (all but 2) serotype 35B isolates were found to belong to the same ST558 (CC558) that was reported from the United States in 1999 (*44*). Serotype 15A was identified as ST63, which belongs to CC63, as does the PMEN clone Sweden[15A-25]. Each isolate of serotype 6D (ST282, CC81) and serotype 15B (ST83, CC81) was the same as those previously registered from South Korea (*45*) and Taiwan. These findings suggest that newly emerged resistant strains can spread rapidly between countries.

Among gPRSP identified in NVTs, STs of serotypes 6C, 13, 23A, 23B, and of both serotypes 6D and 35B, were noted to belong to CC156, which includes large numbers of isolates in ST156, ST90, ST162, ST124, ST176, and ST138; the PMEN clones Spain[9V-3], Netherlands[14-35], Spain[6B-2], Greece[6B-22], and S. Africa[6B-8] are representative among these. STs of serotypes 6C, 13, 23A, and 23B were

derived from ST172 and ST338, which diverged from ST171 (Figure 4, letter d) and evolved further. Serotypes of many isolates registered as ST172 or ST338 were either NVTs or one of the serotypes of PCV13–nonPCV7. These findings suggested that wide use of PCVs led to a decrease in STs belonging to PCV7 and PCV13 serotypes, but some STs detected among NVTs escaped from the vaccine pressure and are increasing, such as ST338. However, whether the new gPRSPs emerged in Japan or originated in another country is unknown.

Capsular switching in *S. pneumoniae* can occur as a result of homologous recombination at a site outside the *cps* locus. Of note, *pbp1a* genes are located upstream and *pbp2x* genes are located downstream of the *cps* locus (*46–48*). Recombination including these 2 *pbp* genes, driven by antimicrobial pressure, can result in concomitant exchange of the *cps* locus. Such new ST strains arising from capsular switching can exhibit penicillin resistance and increase under antimicrobial selection pressure. The diversity of serotypes, resistant genotypes, and STs we describe reflects adaptability of *S. pneumoniae* to the human environment.

In conclusion, to assess whether gPRSP in NVTs will increase in the near future, sustained surveillance for IPD is needed. Control of pneumococcal infections, particularly in elderly and immunocompromised persons, requires development of further multivalent conjugate vaccines, new vaccines targeting a different microbial component, or both. Global consensus for appropriate use of antimicrobial drugs is also valuable for limiting spread of new resistant strains within and beyond national borders.

Acknowledgments

About the Author

Dr. Ubukata is a microbiologist at Keio University School of Medicine. Her research interests include molecular epidemiology, particularly with respect to respiratory infection, as well as comprehensive rapid identification of pathogens.

References

1. O'Brien KL, Wolfson LJ, Watt JP, Henkle E, Deloria-Knoll M, McCall N, et al.; Hib and Pneumococcal Global Burden of Disease Study Team. Burden of disease caused by *Streptococcus pneumoniae* in children younger than 5 years: global estimates. Lancet. 2009;374:893–902. http://dx.doi.org/10.1016/S0140-6736(09)61204-6

2. Whitney CG, Farley MM, Hadler J, Harrison LH, Bennett NM, Lynfield R, et al.; Active Bacterial Core Surveillance of the Emerging Infections Program Network. Decline in invasive pneumococcal disease after the introduction of protein-polysaccharide conjugate vaccine. N Engl J Med. 2003;348:1737–46. http://dx.doi.org/10.1056/NEJMoa022823

3. Centers for Disease Control and Prevention. Direct and indirect effects of routine vaccination of children with 7-valent pneumococcal conjugate vaccine on incidence of invasive pneumococcal disease—United States, 1998–2003. MMWR Morb Mortal Wkly Rep. 2005;54:893–7.

4. Lexau CA, Lynfield R, Danila R, Pilishvili T, Facklam R, Farley MM, et al.; Active Bacterial Core Surveillance Team. Changing epidemiology of invasive pneumococcal disease among older adults in the era of pediatric pneumococcal conjugate vaccine. JAMA. 2005;294:2043–51. http://dx.doi.org/10.1001/jama.294.16.2043

5. Hsu HE, Shutt KA, Moore MR, Beall BW, Bennett NM, Craig AS, et al. Effect of pneumococcal conjugate vaccine on pneumococcal meningitis. N Engl J Med. 2009;360:244–56. http://dx.doi.org/10.1056/NEJMoa0800836

6. Pilishvili T, Lexau C, Farley MM, Hadler J, Harrison LH, Bennett NM, et al.; Active Bacterial Core Surveillance/Emerging Infections Program Network. Sustained reductions in invasive pneumococcal disease in the era of conjugate vaccine. J Infect Dis. 2010;201:32–41. http://dx.doi.org/10.1086/648593

7. Hicks LA, Harrison LH, Flannery B, Hadler JL, Schaffner W, Craig AS, et al. Incidence of pneumococcal disease due to non-pneumococcal conjugate vaccine (PCV7) serotypes in the United States during the era of widespread PCV7 vaccination, 1998–2004. J Infect Dis. 2007;196:1346–54. http://dx.doi.org/10.1086/521626

8. Moore MR, Gertz RE Jr, Woodbury RL, Barkocy-Gallagher GA, Schaffner W, Lexau C, et al. Population snapshot of emergent *Streptococcus pneumoniae* serotype 19A in the United States, 2005. J Infect Dis. 2008;197:1016–27. http://dx.doi.org/10.1086/528996

9. Centers for Disease Control and Prevention. Licensure of a 13-valent pneumococcal conjugate vaccine (PCV13) and recommendations for use among children—Advisory Committee on Immunization Practices (ACIP), 2010. MMWR Morb Mortal Wkly Rep. 2010;59:258–61.

10. Kaplan SL, Barson WJ, Lin PL, Romero JR, Bradley JS, Tan TQ, et al. Early trends for invasive pneumococcal infections in children after the introduction of the 13-valent pneumococcal conjugate vaccine. Pediatr Infect Dis J. 2013;32:203–7. http://dx.doi.org/10.1097/INF.0b013e318275614b

11. Moore MR, Link-Gelles R, Schaffner W, Lynfield R, Lexau C, Bennett NM, et al. Effect of use of 13-valent pneumococcal conjugate vaccine in children on invasive pneumococcal disease in children and adults in the USA: analysis of multisite, population-based surveillance. Lancet Infect Dis. 2015;15:301–9. http://dx.doi.org/10.1016/S1473-3099(14)71081-3

12. Griffin MR, Zhu Y, Moore MR, Whitney CG, Grijalva CG. U.S. hospitalizations for pneumonia after a decade of pneumococcal vaccination. N Engl J Med. 2013;369:155–63. http://dx.doi.org/10.1056/NEJMoa1209165

13. Angoulvant F, Levy C, Grimprel E, Varon E, Lorrot M, Biscardi S, et al. Early impact of 13-valent pneumococcal conjugate vaccine on community-acquired pneumonia in children. Clin Infect Dis. 2014;58:918–24. http://dx.doi.org/10.1093/cid/ciu006

14. Ben-Shimol S, Givon-Lavi N, Leibovitz E, Raiz S, Greenberg D, Dagan R. Near-elimination of otitis media caused by 13-valent pneumococcal conjugate vaccine (PCV) serotypes in southern Israel shortly after sequential introduction of 7-valent/13-valent PCV. Clin Infect Dis. 2014;59:1724–32. http://dx.doi.org/10.1093/cid/ciu683
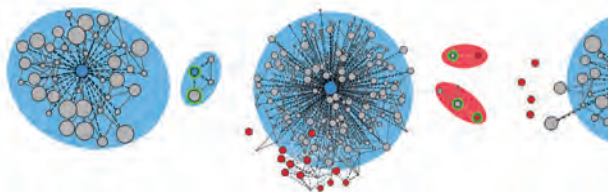
15. Kaplan SL, Center KJ, Barson WJ, Ling-Lin P, Romero JR, Bradley JS, et al. Multicenter surveillance of *Streptococcus pneumoniae* isolates from middle ear and mastoid cultures in the 13-valent pneumococcal conjugate vaccine era. Clin Infect Dis. 2015;60:1339–45.

16. Kempf M, Varon E, Lepoutre A, Gravet A, Baraduc R, Brun M, et al. Decline in antibiotic resistance and changes in the serotype distribution of *Streptococcus pneumoniae* isolates from children with acute otitis media; a 2001–2011 survey by the French Pneumococcal Network. Clin Microbiol Infect. 2015;21:35–42. http://dx.doi.org/10.1016/j.cmi.2014.08.009

17. Williams WW, Lu PJ, O'Halloran A, Kim DK, Grohskopf LA, Pilishvili T, et al. Surveillance of vaccination coverage among adult populations—United States, 2015. MMWR Surveill Summ. 2017;66:1–28. http://dx.doi.org/10.15585/mmwr.ss6611a1

18. Steens A, Bergsaker MA, Aaberge IS, Rønning K, Vestrheim DF. Prompt effect of replacing the 7-valent pneumococcal conjugate vaccine with the 13-valent vaccine on the epidemiology of invasive pneumococcal disease in Norway. Vaccine. 2013;31:6232–8. http://dx.doi.org/10.1016/j.vaccine.2013.10.032

19. Moore CE, Paul J, Foster D, Mahar SA, Griffiths D, Knox K, et al.; Oxford Invasive Pneumococcal Surveillance Group. Reduction of invasive pneumococcal disease 3 years after the introduction of the 13-valent conjugate vaccine in the Oxfordshire region of England. J Infect Dis. 2014;210:1001–11. http://dx.doi.org/10.1093/infdis/jiu213

20. Harboe ZB, Dalby T, Weinberger DM, Benfield T, Mølbak K, Slotved HC, et al. Impact of 13-valent pneumococcal conjugate vaccination in invasive pneumococcal disease incidence and mortality. Clin Infect Dis. 2014;59:1066–73. http://dx.doi.org/10.1093/cid/ciu524

21. Waight PA, Andrews NJ, Ladhani SN, Sheppard CL, Slack MP, Miller E. Effect of the 13-valent pneumococcal conjugate vaccine on invasive pneumococcal disease in England and Wales 4 years after its introduction: an observational cohort study. Lancet Infect Dis. 2015;15:535–43. http://dx.doi.org/10.1016/S1473-3099(15)70044-7

22. Alari A, Chaussade H, Domenech De Cellès M, Le Fouler L, Varon E, Opatowski L, et al. Impact of pneumococcal conjugate vaccines on pneumococcal meningitis cases in France between 2001 and 2014: a time series analysis. BMC Med. 2016;14:211. http://dx.doi.org/10.1186/s12916-016-0755-7

23. Hays C, Vermee Q, Agathine A, Dupuis A, Varon E, Poyart C, et al.; the ORP Ile de France Ouest. Demonstration of the herd effect in adults after the implementation of pneumococcal vaccination with PCV13 in children. Eur J Clin Microbiol Infect Dis. 2017;36:831–8. http://dx.doi.org/10.1007/s10096-016-2868-5

24. Gertz RE Jr, Li Z, Pimenta FC, Jackson D, Juni BA, Lynfield R, et al.; Active Bacterial Core Surveillance Team. Increased penicillin nonsusceptibility of nonvaccine-serotype invasive pneumococci other than serotypes 19A and 6A in post-7-valent conjugate vaccine era. J Infect Dis. 2010;201:770–5. http://dx.doi.org/10.1086/650496

25. Richter SS, Heilmann KP, Dohrn CL, Riahi F, Diekema DJ, Doern GV. Pneumococcal serotypes before and after introduction of conjugate vaccines, United States, 1999–2011. Emerg Infect Dis. 2013;19:1074–83. http://dx.doi.org/10.3201/eid1907.121830

26. Mendes RE, Costello AJ, Jacobs MR, Biek D, Critchley IA, Jones RN. Serotype distribution and antimicrobial susceptibility of USA *Streptococcus pneumoniae* isolates collected prior to and post introduction of 13-valent pneumococcal conjugate vaccine. Diagn Microbiol Infect Dis. 2014;80:19–25. http://dx.doi.org/10.1016/j.diagmicrobio.2014.05.020

27. Richter SS, Musher DM. The ongoing genetic adaptation of *Streptococcus pneumoniae*. J Clin Microbiol. 2017;55:681–5. http://dx.doi.org/10.1128/JCM.02283-16

28. Olarte L, Kaplan SL, Barson WJ, Romero JR, Lin PL, Tan TQ, et al. Emergence of multidrug-resistant pneumococcal serotype 35B among children in the United States. J Clin Microbiol. 2017;55:724–34. http://dx.doi.org/10.1128/JCM.01778-16

29. van der Linden M, Perniciaro S, Imöhl M. Increase of serotypes 15A and 23B in IPD in Germany in the PCV13 vaccination era. BMC Infect Dis. 2015;15:207. http://dx.doi.org/10.1186/s12879-015-0941-9

30. Janoir C, Lepoutre A, Gutmann L, Varon E. Insight into resistance phenotypes of emergent non 13-valent pneumococcal conjugate vaccine type pneumococci isolated from invasive disease after 13-valent pneumococcal conjugate vaccine implementation in France. Open Forum Infect Dis. 2016;3:ofw020. http://dx.doi.org/10.1093/ofid/ofw020

31. Chiba N, Morozumi M, Shouji M, Wajima T, Iwata S, Ubukata K; Invasive Pneumococcal Diseases Surveillance Study Group. Changes in capsule and drug resistance of pneumococci after introduction of PCV7, Japan, 2010–2013. Emerg Infect Dis. 2014;20:1132–9. http://dx.doi.org/10.3201/eid2007.131485

32. Ubukata K, Chiba N, Hanada S, Morozumi M, Wajima T, Shouji M, et al.; Invasive Pneumococcal Diseases Surveillance Study Group. Serotype changes and drug resistance in invasive pneumococcal diseases in adults after vaccinations in children, Japan, 2010–2013. Emerg Infect Dis. 2015;21:1956–65. http://dx.doi.org/10.3201/eid2111.142029

33. Chiba N, Morozumi M, Ubukata K. Application of the real-time PCR method for genotypic identification of β-lactam resistance in isolates from invasive pneumococcal diseases. Microb Drug Resist. 2012;18:149–56. http://dx.doi.org/10.1089/mdr.2011.0102

34. Clinical and Laboratory Standards Institute. Performance standards for antimicrobial susceptibility testing; 25th informational supplement (M100–S25). Wayne (PA): The Institute; 2015.

35. Miller E, Andrews NJ, Waight PA, Slack MP, George RC. Herd immunity and serotype replacement 4 years after seven-valent pneumococcal conjugate vaccination in England and Wales: an observational cohort study. Lancet Infect Dis. 2011;11:760–8. http://dx.doi.org/10.1016/S1473-3099(11)70090-1

36. Weinberger DM, Malley R, Lipsitch M. Serotype replacement in disease after pneumococcal vaccination. Lancet. 2011;378:1962–73. http://dx.doi.org/10.1016/S0140-6736(10)62225-8

37. Lepoutre A, Varon E, Georges S, Dorléans F, Janoir C, Gutmann L, et al.; Microbiologists of Epibac; ORP Networks. Impact of the pneumococcal conjugate vaccines on invasive pneumococcal disease in France, 2001–2012. Vaccine. 2015;33:359–66. http://dx.doi.org/10.1016/j.vaccine.2014.11.011

38. Gaviria-Agudelo CL, Jordan-Villegas A, Garcia C, McCracken GH Jr. The effect of 13-valent pneumococcal conjugate vaccine on the serotype distribution and antibiotic resistance profiles in children with invasive pneumococcal disease. J Pediatric Infect Dis Soc. 2017;6:253–9. http://dx.doi.org/10.1093/jpids/piw005

39. Olarte L, Barson WJ, Barson RM, Romero JR, Bradley JS, Tan TQ, et al. Pneumococcal pneumonia requiring hospitalization in US children in the 13-valent pneumococcal conjugate vaccine era. Clin Infect Dis. 2017;64:1699–704. http://dx.doi.org/10.1093/cid/cix115

40. Pilishvili T, Bennett NM. Pneumococcal disease prevention among adults: strategies for the use of pneumococcal vaccines. Vaccine. 2015;33(Suppl 4):D60–5. http://dx.doi.org/10.1016/j.vaccine.2015.05.102

41. van der Linden M, Falkenhorst G, Perniciaro S, Imöhl M. Effects of infant pneumococcal conjugate vaccination on serotype distribution in invasive pneumococcal disease among children and adults in Germany. PLoS One. 2015;10:e0131494. http://dx.doi.org/10.1371/journal.pone.0131494

42. Weinberger R, von Kries R, van der Linden M, Rieck T, Siedler A, Falkenhorst G. Invasive pneumococcal disease in children under 16 years of age: incomplete rebound in incidence

after the maximum effect of PCV13 in 2012/13 in Germany. Vaccine. 2018;36:572–7. http://dx.doi.org/10.1016/j.vaccine.2017.11.085

43. Suzuki M, Dhoubhadel BG, Ishifuji T, Yasunami M, Yaegashi M, Asoh N, et al.; Adult Pneumonia Study Group-Japan. Serotype-specific effectiveness of 23-valent pneumococcal polysaccharide vaccine against pneumococcal pneumonia in adults aged 65 years or older: a multicentre, prospective, test-negative design study. Lancet Infect Dis. 2017;17:313–21. http://dx.doi.org/10.1016/S1473-3099(17)30049-X

44. Beall B, McEllistrem MC, Gertz RE Jr, Boxrud DJ, Besser JM, Harrison LH, et al.; Active Bacterial Core Surveillance/Emerging Infections Program Network. Emergence of a novel penicillin–nonsusceptible, invasive serotype 35B clone of *Streptococcus pneumoniae* within the United States. J Infect Dis. 2002;186: 118–22. http://dx.doi.org/10.1086/341072

45. Ko KS, Baek JY, Song JH. Multidrug-resistant *Streptococcus pneumoniae* serotype 6D clones in South Korea. J Clin Microbiol. 2012;50:818–22. http://dx.doi.org/10.1128/JCM.05895-11

46. Brueggemann AB, Pai R, Crook DW, Beall B. Vaccine escape recombinants emerge after pneumococcal vaccination in the United States. PLoS Pathog. 2007;3:e168. http://dx.doi.org/10.1371/journal.ppat.0030168

47. Wyres KL, Lambertsen LM, Croucher NJ, McGee L, von Gottberg A, Liñares J, et al. Pneumococcal capsular switching: a historical perspective. J Infect Dis. 2013;207:439–49. http://dx.doi.org/10.1093/infdis/jis703

48. Chiba N, Murayama SY, Morozumi M, Iwata S, Ubukata K. Genome evolution to penicillin resistance in serotype 3 *Streptococcus pneumoniae* by capsular switching. Antimicrob Agents Chemother. 2017;61:e00478–17. http://dx.doi.org/10.1128/AAC.00478-17

Address for correspondence: Kimiko Ubukata, Keio University School of Medicine, Department of Infectious Diseases, 35 Shinanomachi Shinjyuku-ku, Tokyo 160-8582, Japan; email: ubukatak@keio.jp

Norovirus Gastroenteritis among Hospitalized Patients, Germany, 2007–2012

Frank Kowalzik, Harald Binder, Daniela Zöller, Margarita Riera-Montes,
Ralf Clemens,[1] Thomas Verstraeten, Fred Zepp

We estimated numbers of hospitalizations for norovirus gastroenteritis (NGE) and associated medical costs in Germany, where norovirus testing is high because reimbursement is affected. We extracted aggregate data for patients hospitalized with a primary or secondary code from the International Classification of Diseases, 10th Revision (ICD-10), NGE diagnosis during 2007–2012 from the German Federal Statistics Office. We assessed reliability of the coding system in patient records from a large academic hospital. Approximately 53,000–90,000 NGE hospitalizations occurred annually in Germany (21,000–33,000 with primary and 32,000–57,000 with secondary ICD-10–coded NGE diagnoses). Rates of hospitalization with NGE as primary diagnosis were highest in children <2 years of age; rates of hospitalization with NGE as secondary diagnosis were highest in adults >85 years of age. The average annual reimbursed direct medical cost of NGE hospitalizations was €31–43 million. Among patients with a NGE ICD-10 code, 87.6% had positive norovirus laboratory results.

N orovirus is a leading cause of acute gastroenteritis (AGE) in all age groups and in some industrialized countries has overtaken rotavirus as the most frequent cause of AGE cases requiring hospitalization among children since rotavirus vaccination began (*1–5*). Because of its particularly high contagiousness (*6*), norovirus-related disease is a frequent cause of community and nosocomial AGE outbreaks. Hospital outbreaks of norovirus gastroenteritis (NGE) can lead to disruption of patient care and substantial economic costs associated with containment and ward closure (*7–9*).

In Germany, rotavirus and norovirus infections are notifiable to the Robert Koch Institute (RKI) (*10*). Rotavirus vaccine has been incrementally included in immunization schedules in 5 of the 16 federal states in Germany since 2008. In 2012, vaccination coverage rates ranged from 11% to 77%, and estimated national coverage was 32% (*11*). Universal immunization for infants was recommended in 2013 (*12*). On the basis of its own analyses of notifications, RKI has identified noroviruses as the most frequent cause of AGE; estimated annual incidence of NGE is 123–130 cases/100,000 population (*13,14*). The proportion of NGE notifications associated with hospitalized case-patients ranges from 8% to 26% annually (*13,14*).

With norovirus vaccines in development (*15,16*), baseline data on the NGE burden will be useful for informing decisions on potential future vaccine introduction and impact evaluation. A unique situation exists in Germany because NGE diagnosis is directly linked to reimbursement of hospital costs, providing an incentive for testing AGE cases for their etiology. The reimbursement for an AGE case requiring hospitalization increases by ≈€400 if the cause can be shown to be norovirus, rotavirus, or adenovirus.

The German Federal Statistics Office (DESTATIS) database records statistical information throughout Germany and has been used to conduct research across healthcare disciplines (*17,18*). We retrospectively queried the DESTATIS database and conducted a medical record review to estimate the age-stratified NGE burden among hospitalized AGE patients in Germany. We further describe some epidemiologic features and costs associated with NGE cases requiring hospitalization.

Methods

The main study objective was to determine the number of NGE hospitalizations overall and stratified by age (<1, 1–17, 18–44, 45–64, 65–84 and >85 years) in Germany by using hospital discharge data obtained from DESTATIS. German inpatient data are recorded centrally and provided to DESTATIS. All hospitals are required by law to report patient information (for reimbursement purposes) on age, sex, duration of hospital stay, reason for admission, and discharge based on codes from the International

[1]Current affiliation: Global Research in Infectious Diseases, Rio de Janeiro, Brazil.

Classification of Diseases, 10th Revision (ICD-10), and the Diagnosis-Related Group (DRG). We requested information on all hospitalizations resulting from AGE (ICD-10 codes A00–A09, representing all infectious intestinal diseases) for the period 2007–2012. In addition, we specifically requested information on hospitalizations with ICD-10 code A08.1 (NGE) as the primary or secondary diagnosis and a DRG code of G67 (esophagitis, gastroenteritis, gastrointestinal bleeding, ulcers, and miscellaneous digestive system disorders). Including the base DRG code G67 enabled us to differentiate between the different DRG codes in the same base DRG group (i.e., G67 A–D), which are linked to different reimbursement amounts. For comparison, we requested similar information on rotavirus hospitalizations (ICD-10 code A08.0). We also requested data on deaths related to the same codes as the primary diagnosis.

We assessed the direct hospitalization costs associated with NGE hospitalizations in Germany (primary diagnosis), which were available for the years 2007–2009. The DRG reimbursement data from DESTATIS are independent of the duration of hospital stay and do not include surcharges based on long-stay DRG or discounts based on short-stay DRG.

To validate the reporting system for NGE cases, we reviewed the clinical files of a random selection of 1,214 patients at the University Medical Centre Mainz (Mainz, Germany) who had been tested for norovirus. Demographic, clinical, and microbiologic information was extracted by using a standardized case report form.

The study protocol was reviewed by the local ethics committee in Mainz (Landesärztekammer Rheinland-Pfalz). Because this study was noninterventional and all data were anonymized and aggregated, a waiver for ethics approval was obtained.

Statistical Analysis

We calculated incidence rates of hospitalizations with NGE by using annual population projections in Germany for the study period from DESTATIS GENESIS-Online (19). We calculated the proportions of all hospitalizations and all AGE hospitalizations that were attributable to NGE overall, by age group, and by study year.

We evaluated the total number of cases with NGE as a primary diagnosis per month of admission (available from 2009 onward) and by federal state (available for all study years) to reflect seasonal and regional distribution. To maintain confidentiality, DESTATIS applies a procedure whereby data from age groups that have <3 patients with the diagnostic condition per month are removed from the dataset. A maximum of 49 patients in any 1 year were deleted from the dataset as the result of the DESTATIS procedure, which is not expected to have affected the study findings.

The performance of the reporting system is expressed as a proportion of NGE-coded patients for whom we could identify a positive norovirus test result and the proportion of test-positive patients to whom an NGE code had been assigned; 95% CIs are provided. We performed the analyses by using SAS version 9.4 (SAS Institute Inc., Cary, NC, USA).

Results

We identified a total of 408,124 hospitalizations with an NGE diagnosis in Germany during 2007–2012, for an annual average of 68,187 hospitalizations (Table 1). The overall number of NGE hospitalizations were consistently higher than the number of rotavirus hospitalizations for all age groups except children <2 years of age. Furthermore, for each of the study years, more deaths among hospitalized patients with an NGE diagnosis occurred than among those with rotavirus AGE (Table 1).

Hospitalizations with NGE as Primary Diagnosis

The annual number of hospitalizations with NGE as the primary diagnosis ranged from 21,442 to 33,440 (average 27,910) (online Technical Appendix Table 1, https://wwwnc.cdc.gov/EID/article/24/11/17-0820-Techapp1.pdf). NGE hospitalizations represented 11.5%–15.6% of all hospitalizations with AGE as the primary diagnosis annually. The overall incidence of hospitalization with NGE as the primary diagnosis in Germany during the study period was 3.4/10,000 population (range 2.6–4.1/10,000 population) (online Technical Appendix Table 1).

Among children <1 year of age, annual incidence ranged from 34.8 to 53.1/10,000 population, and among children 1 to <2 years of age, the annual incidence ranged

Table 1. Total annual number of AGE hospitalizations and deaths in hospital (all ages), Germany 2007–2012*							
Pathogen	2007	2008	2009	2010	2011	2012	Average
Hospitalizations†							
Norovirus	53,701	67,130	63,307	91,001	67,934	66,051	68,187
Rotavirus	37,374	34,978	43,273	35,986	35,365	32,639	34,857
All causes	328,033	341,352	309,351	394,753	371,851	359,933	350,879
Deaths‡							
Norovirus	194	201	173	265	191	194	203
Rotavirus	30	55	56	53	42	40	46
All causes	2,046	2,532	2,510	2,981	3,262	3,420	2,792

*AGE, acute gastroenteritis.
†All AGE (primary and secondary diagnoses).
‡AGE as primary diagnosis only.

from 41.8 to 52.0/10,000 population (Figure 1). After the age of 2 years, NGE hospitalization incidence rates decreased rapidly with age but increased again for persons ≥65 years of age, reaching 11.8 to 20.9/10,000 population in persons ≥85 years of age (Figure 1).

In each study year, the absolute number of NGE hospitalizations was highest among adults 65–84 years of age (range 4,800–9,495/y) and children <5 years of age (range 7,438–9,729/y) (Figure 1). In each study year, the overall rate of NGE hospitalizations was higher in females than males (rate ratio 1.2 for all study years). Among hospitalized patients with NGE, 194–265 deaths (average 203) occurred annually (Table 1), most (96.3%) of which occurred among adults ≥65 years of age (data not shown). The number of deaths in children <5 years of age ranged from 0 to 5 annually.

Hospitalizations with NGE as Secondary Diagnosis

During 2007–2012, an annual average of 40,278 (range 32,259–57,561) hospitalizations occurred with an NGE ICD-10 code A08.1 listed as a secondary diagnosis (Figure 2, panel A). In any study year, the number of hospitalizations with NGE as secondary diagnosis was 1.3–1.7 times higher than for those with NGE as a primary diagnosis. In contrast to NGE as a primary diagnosis, in which the highest rates were in children, the rate of hospitalizations with NGE as a secondary diagnosis was highest in adults ≥85 years of age (range 33.6–59.1/10,000 population) (Figure 2, panel B).

Seasonal and Regional Distribution of NGE Hospitalizations (Primary Diagnosis)

NGE hospitalizations showed strong seasonality; the highest case numbers occurred during December–March for each of the study years (Figure 3). In 4 out of 5 study years, hospitalizations with a NGE diagnosis peaked before

rotavirus hospitalizations. Regional distribution of NGE hospitalizations across Germany showed marked differences: >3-fold variations in the calculated region-specific incidence rates. In 2010, the year with the most NGE hospitalizations, the incidence of NGE hospitalizations was as low as 2.2/10,000 population in Hamburg/Schleswig-Holstein and as high as 7.2/10,000 population in Saxony-Anhalt. However, we found no consistent geographic pattern (Figure 4).

Length of Stay and Cost for NGE Hospitalizations

We calculated 108,093–156,538 hospital bed days (average 131,411) each year for hospitalization with NGE as a primary diagnosis. The mean length of stay was 4.7 days (range 4.2–5.2 days); longer stays occurred among young children and older adults. Specifically, we identified hospital stays of 3.6–4.4 days in children <1 year of age, 3.0–3.7 days in children 1 to <2 years of age, 6.0–7.5 days in persons 65–84 years of age, and 7.3–8.9 days in persons ≥85 years of age. Across all age groups, the average duration of hospitalization was 3.4–4.5 times longer (17–18 days vs. 4–5 days) when NGE was a secondary diagnosis (online Technical Appendix Table 2). The data did not enable us to determine the relative contribution of the NGE to the total duration of the hospitalization.

The fixed reimbursement per hospitalization with NGE as a primary diagnosis was €1,514 in 2007, €1,639 in 2008, and €1,692 in 2009. These amounts correspond to a total reimbursed cost to the German health system ranging from €31 to €42 million annually.

Validation of the Base DRG Code G67 and ICD-10 A08.1

Among the 1,214 patients tested for norovirus for whom we reviewed the clinical files, 113 had positive and 1,101 negative results (Table 2). Of the 113 with positive results,
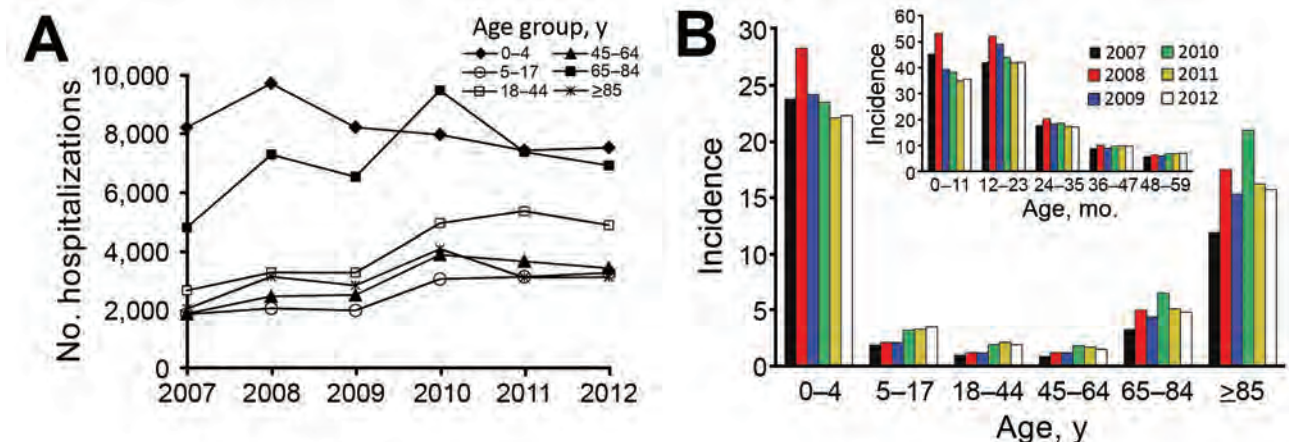
Figure 1. Annual number and incidence of hospitalizations for norovirus gastroenteritis as primary diagnosis, Germany, 2007–2012. A) Annual cases by age group; B) annual incidence (no. cases/10,000 population) by age group. Inset shows incidence by age group among children <5 years of age.
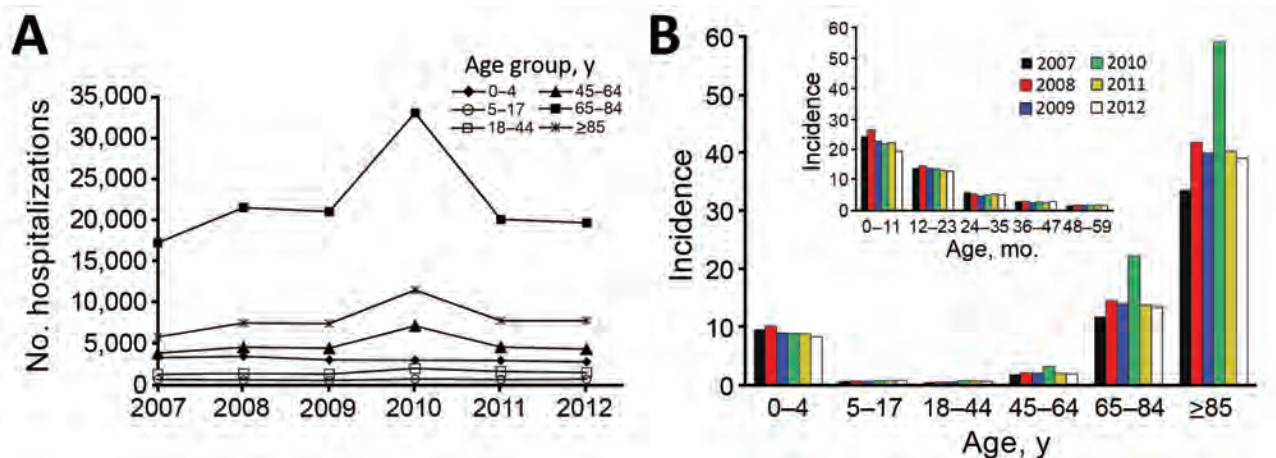
Figure 2. Annual number and incidence of hospitalizations for norovirus gastroenteritis as secondary diagnosis, Germany, 2007–2012. A) Annual cases by age group; B) annual incidence (no. cases/10,000 population) by age group. Inset shows incidence by age group among children <5 years of age.

99 had an NGE ICD-10 code assigned, suggesting that 87.6% (95% CI 81.5%–93.7%) of the positive norovirus cases are captured by the coding system. Conversely, of the 104 patients with an NGE ICD-10 code, 99 had a positive norovirus result, suggesting that 95.2% (95% CI 91.1%–99.3%) of the coded NGE cases represent laboratory-confirmed norovirus cases.

Discussion

We used national hospitalization statistics to estimate the overall burden of NGE hospitalizations in Germany. During 2007–2012, a total of 408,124 NGE-related hospitalizations occurred. On average, >60,000 hospitalizations occurred annually, including 27,910 hospitalizations with NGE as a primary diagnosis and 40,278 hospitalizations with NGE as a secondary diagnosis, as well as up to 265 NGE-related deaths at a hospital per year.

As reported in other studies of NGE epidemiology (20,21), the incidence of NGE hospitalizations by age follows a U-shaped curve, representing the highest rates in young children and the elderly. Among children <5 years of age, an annual average of >8,000 hospitalizations occurred with NGE as a primary diagnosis; among adults ≥65 years of age, the annual average was >10,000 hospitalizations.

We described hospitalizations with NGE as a primary or secondary diagnosis separately because we believe they represent different aspects of the burden caused by norovirus infections. The hospitalizations with NGE as a primary diagnosis are most likely representative of community-acquired infections, whereas the secondary NGE diagnoses are more likely to represent nosocomial infections. This assumption about secondary diagnoses might be wrong if patients entered the hospital with NGE occurring simultaneously with another disorder, where the NGE was judged to be a secondary cause of the hospitalization. This scenario might be especially true for older patients with co-occurring conditions that might have been exacerbated as a result of AGE. Also, several patients might have been hospitalized for reasons other than AGE but had onset of signs of NGE in the first 48 hours of hospitalization, which would indicate the patient acquired the infection before hospitalization.

Our estimate of the rate of hospitalization with NGE as a primary diagnosis is higher than the rate for community-acquired NGE estimated by Spackova et al. (14), based on German NGE reports made to RKI. That study estimated that 8%–19% of the 856,539 total NGE hospitalization cases over an 8-year period were community-acquired, corresponding to ≈8,500–20,000 community-acquired NGE hospitalization cases annually. The German Health Insurance Medical Service (Medizinischer Dienst der Krankenkassen [MDK]) (22) carries out a stringent quality-control program of DRG and ICD-10 codes reported by hospitals, as required by law. Because our results are based on data abstracted from this rigorously controlled reimbursement system, we believe our results are more likely to represent the actual burden of all NGE hospitalizations in Germany. Moreover, our validation of the test results in a subset of patients with AGE found a high reliability for the NGE ICD-10 code compared with actual testing, suggesting little overattribution of NGE in this setting. This finding is further supported by data provided in a study by Bernard et al. (13), which estimated norovirus cases to be underreported to RKI by a minimal underreporting factor of 1.7. Our estimates of the NGE hospitalization rate are also higher than previously reported estimates from countries such as the Netherlands (23), the United States (24), and Canada (25) but are comparable to a recent study in England (26,27); Table 3). Our estimates of annual NGE hospitalizations
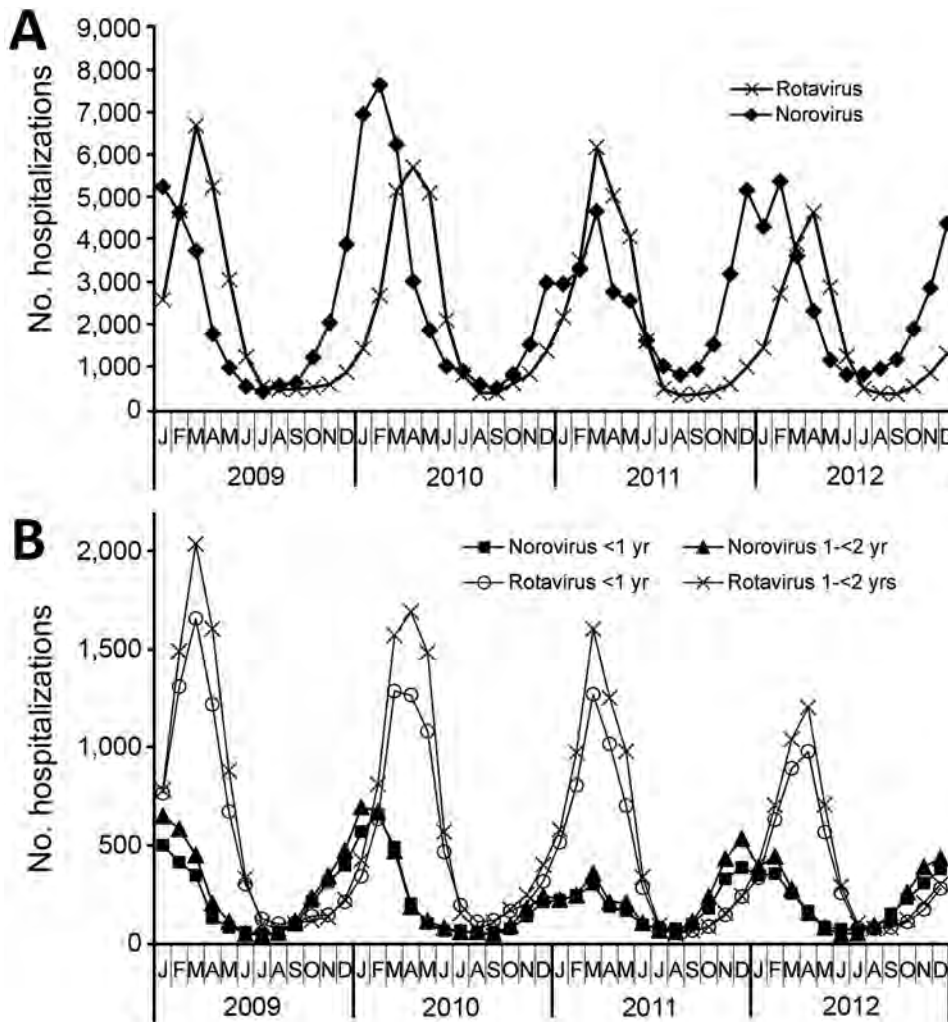
Figure 3. Monthly number of hospitalizations for rotavirus and norovirus gastroenteritis as primary diagnosis among all age groups (A) and among children 1 to <2 years of age (B), Germany, 2009–2012.

resulting in death (average 203) were in the same range as previous RKI estimates for Germany (192 annually during 2004–2008) (*14,20*).

The study years (2007–2012) preceded introduction of universal rotavirus vaccination in Germany in 2013. Considering all age groups, the number of hospitalizations caused by norovirus is markedly higher than the number caused by rotavirus. Although the highest incidence of NGE hospitalizations was in children <2 years of age, within this age group, rotavirus AGE hospitalizations continued to be more frequent.

Our study has several strengths, foremost being the data collection and recording of norovirus-related hospitalization data in Germany. We have taken advantage of the unique system in Germany, which has built-in financial incentives for norovirus testing of inpatients with AGE and mandatory reporting of laboratory-confirmed norovirus, to estimate the burden of NGE hospitalizations. This system provides a structure that, we believe, more comprehensively captures the role of norovirus in nonspecific AGE

diagnoses than is possible in many other national databases. Our study used national hospitalization data, which provided age-specific information on length of hospital stay and medical costs. We used data from a 6-year study period, which enabled us to estimate NGE burden across multiple norovirus seasons.

We could not distinguish between community-acquired and nosocomial norovirus infections. An earlier study in Germany estimated 49% of all hospitalized NGE cases to be nosocomial in origin (*14*), whereas a study in Denmark put this estimate at 63% (*28*). We found that hospitalization with NGE as a secondary diagnosis represented 59% of all hospitalizations with NGE in our study, suggesting that these cases most likely represent nosocomial infections. The higher rate of secondary diagnoses among older adults compared with younger age groups further suggests that these cases actually represent a different type of hospitalization episode. The inverse age relationship might be related to poorer underlying health and longer hospital stays resulting in potentially greater exposure to a

Figure 4. Regional distribution of norovirus hospitalizations among all age groups, by federal state, Germany, 2010. Numbers in parentheses indicate no. cases/10,000 population. Map template obtained from http://www.presentationmagazine.com/editable-maps/page/3.

We were unable to include deaths in cases coded with NGE as a secondary diagnosis because we could not ascertain that NGE was the cause of death. The number of deaths attributable to NGE might thus have been underestimated.

Although the reliance upon the reporting of NGE cases to DESTATIS is another potential limitation of our study, the finding that 95.2% of the coded cases in a sample of patients had a documented positive norovirus result suggests this reliance is unlikely to have led to a major overestimation of the actual burden of NGE hospitalizations in Germany. Our findings in a single medical center might not be generalizable to the entire country. We do not expect, however, that testing rates would differ substantially between hospitals given the financial incentive and the strict quality controls carried out by MDK (*22*). From an economic perspective, our assessment of NGE hospitalization costs only considered the reimbursable fraction and did not take into account indirect or societal costs, which would have led to substantially higher cost estimates.

On the basis of our validation assessment of ICD-10 diagnostic codes compared with norovirus laboratory results, our estimated burden of NGE hospitalizations according to ICD-10 diagnostic coding might have underestimated the actual number of NGE hospitalizations. We had, a priori, assumed that all patients with AGE caused by norovirus are tested because of financial reimbursement incentives. However, our finding that 12.4% of patients with positive norovirus results did not have a corresponding NGE ICD-10 diagnostic code in the patient's medical records suggests that underreporting of NGE hospitalization cases based on diagnostic codes has occurred. We also observed seasonality among the cases coded as unspecified AGE (ICD codes A08.3, A08.4, A08.5, and A09); peaks in winter and early spring suggest that a proportion of these cases might also be attributable to norovirus.

During the study period, most testing for norovirus in Germany was conducted by using an ELISA test. Compared with the standard reverse transcription PCR test, the sensitivity of ELISA has been estimated to be 77% and the specificity 96% (*29*). Correcting for these estimates would reduce the proportion of AGE hospitalizations caused by norovirus slightly, from an average of 13.8% to 13.2% (*30*).

In summary, by using national hospitalization discharge and cost data, we found that NGE resulted on average in 27,910 hospitalizations with NGE as a primary diagnosis and an additional 40,278 hospitalizations with NGE as secondary diagnosis annually in Germany, a number substantially

nosocomial infection. We could not exclude the possibility that some patients with NGE as a secondary diagnosis were given an unspecified AGE diagnosis as a primary diagnosis while awaiting the norovirus test results and should have had their infection counted as community-acquired instead of nosocomial. We therefore made an additional request to DESTATIS to provide us with the number of such cases and found that this combination occurred in <0.4% of patients who were given NGE as a secondary diagnosis. This finding, the consistency between our ratio of primary to secondary diagnoses to those reported by other investigators, and the age distribution support our assumption that secondary diagnoses reported by DESTATIS are most likely nosocomial NGE cases.

Table 2. Concordance between ELISA norovirus tests and the disease-specific ICD-10 code for norovirus gastroenteritis as primary diagnosis, University Medical Centre of Mainz, Germany, 2011–2012*

	ICD-10 A08.1 code, no. (%)		
Result	No	Yes	Total
Norovirus negative	1,096	5	1,101 (90.7)
Norovirus positive	14	99	113 (9.3)
Total	1,110 (91.4)	104 (8.6)	1,214 (100)

*ICD-10, International Classification of Diseases, 10th Revision.

Table 3. Published norovirus gastroenteritis hospitalization incidence rates in selected countries in Europe and North America, 1996–2013*

Country	Data source	Study years	Infection type or diagnostic position	No. cases/10,000 population
Germany (this study)	Retrospective analysis of DESTATIS hospitalization data	2007–2012	Primary diagnosis	3.4
		2007–2012	Secondary diagnosis	4.9
Germany (14)	Retrospective analysis of RKI notification data	2002–2008	Nosocomial	1.6
Germany (13)	Retrospective analysis of RKI notification data	2001–2009	Community-acquired	1.0–2.5
England (26)	Retrospective regression analysis using PHE notification data and HES emergency admissions	2000–2006	Community-acquired	1.0–4.3†
		2000–2006	Community-acquired	0.23–0.48‡
England (27)	Retrospective analysis of GP and hospital discharge databases	2007–2013	Any position	6.2–8.0
The Netherlands (23)	Retrospective analysis of national surveillance data	2009	Community-acquired	1.2
United States (24)	Retrospective regression analysis using NIS data	1996–2007	Any position	2.1
Canada (25)	Retrospective binomial generalized linear analysis using CIHI-HMDB data	2006–2011	Primary diagnosis	0.05
		2006–2011	Other diagnosis	0.17

*CIHI-HMDB, Canadian Institutes of Health Information–Hospital Morbidity Database; DESTATIS, German Federal Statistics Office; HES, Hospital Episode Statistics; NIS, Nationwide Inpatient Sample; PHE, Public Health England; RKI, Robert Koch Institute.
†Age ≥65 y.
‡Age 18–64 y.

higher than previously assumed. The associated reimbursed annual medical cost for community-acquired NGE was up to €42 million annually. These data could aid in the identification of target groups for future norovirus vaccination policies and could be used to assess the effects of vaccination on the NGE hospitalization burden after implementation.

About the Author

Dr. Kowalzik is the managing senior consultant to the Pediatric Department of the University Medical Centre of Mainz. His research focuses on the epidemiology of infectious diseases, mainly gastroenteritis caused by norovirus and rotavirus.

References

1. Lopman BA, Steele D, Kirkwood CD, Parashar UD. The vast and varied global burden of norovirus: prospects for prevention and control. PLoS Med. 2016;13:e1001999. http://dx.doi.org/10.1371/journal.pmed.1001999
2. Hemming M, Räsänen S, Huhti L, Paloniemi M, Salminen M, Vesikari T. Major reduction of rotavirus, but not norovirus, gastroenteritis in children seen in hospital after the introduction of RotaTeq vaccine into the National Immunization Programme in Finland. Eur J Pediatr. 2013;172:739–46. http://dx.doi.org/10.1007/s00431-013-1945-3
3. Bucardo F, Reyes Y, Svensson L, Nordgren J. Predominance of norovirus and sapovirus in Nicaragua after implementation of universal rotavirus vaccination. PLoS One. 2014;9:e98201. http://dx.doi.org/10.1371/journal.pone.0098201
4. Payne DC, Vinjé J, Szilagyi PG, Edwards KM, Staat MA, Weinberg GA, et al. Norovirus and medically attended gastroenteritis in U.S. children. N Engl J Med. 2013;368:1121–30. http://dx.doi.org/10.1056/NEJMsa1206589
5. Koo HL, Neill FH, Estes MK, Munoz FM, Cameron A, DuPont HL, et al. Noroviruses: the most common pediatric viral enteric pathogen at a large university hospital after introduction of rotavirus vaccination. J Pediatric Infect Dis Soc. 2013;2:57–60. http://dx.doi.org/10.1093/jpids/pis070
6. Teunis PF, Moe CL, Liu P, Miller SE, Lindesmith L, Baric RS, et al. Norwalk virus: how infectious is it? J Med Virol. 2008;80:1468–76. http://dx.doi.org/10.1002/jmv.21237
7. Johnston CP, Qiu H, Ticehurst JR, Dickson C, Rosenbaum P, Lawson P, et al. Outbreak management and implications of a nosocomial norovirus outbreak. Clin Infect Dis. 2007;45:534–40. http://dx.doi.org/10.1086/520666
8. Lopman BA, Reacher MH, Vipond IB, Hill D, Perry C, Halladay T, et al. Epidemiology and cost of nosocomial gastroenteritis, Avon, England, 2002–2003. Emerg Infect Dis. 2004;10:1827–34. http://dx.doi.org/10.3201/eid1010.030941
9. Lynn S, Toop J, Hanger C, Millar N. Norovirus outbreaks in a hospital setting: the role of infection control. N Z Med J. 2004;117:U771.
10. Revised case definitions for the submission of evidence of dengue virus and norovirus and morbidity or death from dengue fever and norovirus gastroenteritis [in German]. Bundesgesundheitsblatt Gesundheitsforschung Gesundheitsschutz. 2011;54:246–50.
11. Uhlig U, Kostev K, Schuster V, Koletzko S, Uhlig HH. Impact of rotavirus vaccination in Germany: rotavirus surveillance, hospitalization, side effects and comparison of vaccines. Pediatr Infect Dis J. 2014;33:e299–304. http://dx.doi.org/10.1097/INF.0000000000000441
12. Kowalzik F, Zepp F, Hoffmann I, Binder H, Lautz D, van Ewijk R, et al. Disease burden of rotavirus gastroenteritis in children residing

in Germany: a retrospective, hospital-based surveillance. Pediatr Infect Dis J. 2016;35:97–103.

13. Bernard H, Höhne M, Niendorf S, Altmann D, Stark K. Epidemiology of norovirus gastroenteritis in Germany 2001–2009: eight seasons of routine surveillance. Epidemiol Infect. 2014;142:63–74.

14. Spackova M, Altmann D, Eckmanns T, Koch J, Krause G. High level of gastrointestinal nosocomial infections in the German surveillance system, 2002–2008. Infect Control Hosp Epidemiol. 2010;31:1273–8. http://dx.doi.org/10.1086/657133

15. Treanor JJ, Atmar RL, Frey SE, Gormley R, Chen WH, Ferreira J, et al. A novel intramuscular bivalent norovirus virus-like particle vaccine candidate—reactogenicity, safety, and immunogenicity in a phase 1 trial in healthy adults. J Infect Dis. 2014;210:1763–71. http://dx.doi.org/10.1093/infdis/jiu337

16. Bernstein DI, Atmar RL, Lyon GM, Treanor JJ, Chen WH, Jiang X, et al. Norovirus vaccine against experimental human GII.4 virus illness: a challenge study in healthy adults. J Infect Dis. 2015;211:870–8. http://dx.doi.org/10.1093/infdis/jiu497

17. Beckmann MW, Juhasz-Böss I, Denschlag D, Gaß P, Dimpfl T, Harter P, et al. Surgical methods for the treatment of uterine fibroids—risk of uterine sarcoma and problems of morcellation: position paper of the DGGG. Geburtshilfe Frauenheilkd. 2015;75:148–64. http://dx.doi.org/10.1055/s-0035-1545684

18. Zwink N, Jenetzky E, Schmiedeke E, Schmidt D, Märzheuser S, Grasshoff-Derr S, et al. CURE-Net Consortium. Assisted reproductive techniques and the risk of anorectal malformations: a German case-control study. Orphanet J Rare Dis. 2012;7:65. http://dx.doi.org/10.1186/1750-1172-7-65

19. Statistisches Bundesamt Wiesbaden. GENESIS-Online [cited 2017 Dec 15]. https://www-genesis.destatis.de/genesis/online/logon?language=de&sequenz=statistiken&selectionname=12*&usg=ALkJrhjgxiAsKejwJNMswJxtZm3-LkALkA

20. Werber D, Hille K, Frank C, Dehnert M, Altmann D, Muller-Nordhorn J, et al. Years of potential life lost for six major enteric pathogens, Germany, 2004–2008. Epidemiol Infect. 2012;1–8.

21. Hall AJ, Lopman BA, Payne DC, Patel MM, Gastañaduy PA, Vinjé J, et al. Norovirus disease in the United States. Emerg Infect Dis. 2013;19:1198–205.http://dx.doi.org/10.3201/eid1908.130465

22. Medizinischer Dienst der Krankenversicherung [cited 2015 Nov 22]. http://www.mdk.de

23. Verhoef L, Koopmans M. W VANP, Duizer E, Haagsma J, Werber D, et al. The estimated disease burden of norovirus in the Netherlands. Epidemiol Infect. 2012;1–11.

24. Lopman BA, Hall AJ, Curns AT, Parashar UD. Increasing rates of gastroenteritis hospital discharges in US adults and the contribution of norovirus, 1996–2007. Clin Infect Dis. 2011;52:466–74. http://dx.doi.org/10.1093/cid/ciq163

25. Morton VK, Thomas MK, McEwen SA. Estimated hospitalizations attributed to norovirus and rotavirus infection in Canada, 2006–2010. Epidemiol Infect. 2015;143:3528–37. http://dx.doi.org/10.1017/S0950268815000734

26. Verstraeten T, Cattaert T, Harris J, Lopman B, Tam CC, Ferreira G. Estimating the burden of medically attended norovirus gastroenteritis: modeling linked primary care and hospitalization datasets. J Infect Dis. 2017;216:957–65.http://dx.doi.org/10.1093/infdis/jix410

27. Haustein T, Harris JP, Pebody R, Lopman BA. Hospital admissions due to norovirus in adult and elderly patients in England. Clin Infect Dis. 2009;49:1890–2. http://dx.doi.org/10.1086/648440

28. Franck KT, Nielsen RT, Holzknecht BJ, Ersbøll AK, Fischer TK, Böttiger B. Norovirus genotypes in hospital settings: differences between nosocomial and community-acquired infections. J Infect Dis. 2015;212:881–8.http://dx.doi.org/10.1093/infdis/jiv105

29. Geginat G, Kaiser D, Schrempf S. Evaluation of third-generation ELISA and a rapid immunochromatographic assay for the detection of norovirus infection in fecal samples from inpatients of a German tertiary care hospital. Eur J Clin Microbiol Infect Dis. 2012;31:733–7. http://dx.doi.org/10.1007/s10096-011-1366-z

30. Rogan WJ, Gladen B. Estimating prevalence from the results of a screening test. Am J Epidemiol. 1978;107:71–6. http://dx.doi.org/10.1093/oxfordjournals.aje.a112510

Address for correspondence: Frank Kowalzik, University Medical Centre, Pediatric Department, Mainz Langenbeckstrasse 1, D-55101 Mainz, Germany; email: frank.kowalzik@unimedizin-mainz.de

Outbreak of Tuberculosis and Multidrug-Resistant Tuberculosis, Mbuji-Mayi Central Prison, Democratic Republic of the Congo

Michel Kaswa Kayomo, Epco Hasker, Muriel Aloni, Léontine Nkuku, Marcel Kazadi,
Thierry Kabengele, Dorcas Muteteke, François Kapita, Alphonse Lufulwabo, Ya Diul Mukadi,
Jean-Jacques Muyembe-Tamfum, Margareta Ieven, Bouke C. de Jong, Marleen Boelaert

After an alert regarding ≈31 tuberculosis (TB) cases, 3 of which were rifampin-resistant TB cases, in Mbuji-Mayi Central Prison, Democratic Republic of the Congo, we conducted an outbreak investigation in January 2015. We analyzed sputum of presumptive TB patients by using the Xpert MTB/RIF assay. We also assessed the *Mycobacterium tuberculosis* isolates' drug-susceptibility patterns and risk factors for TB infection. Among a prison population of 918 inmates, 29 TB case-patients were already undergoing treatment. We found an additional 475 presumptive TB case-patients and confirmed TB in 170 of them. In March 2015, the prevalence rate of confirmed TB was 21.7% (199/918 inmates). We detected an additional 14 cases of rifampin-resistant TB and initiated treatment in all 14 of these case-patients. Overcrowded living conditions and poor nutrition appeared to be the driving factors behind the high TB incidence in this prison.

Prisons are high-risk environments for tuberculosis (TB) and multidrug-resistant TB (MDR TB) (*1*). Globally, the prevalence of TB in prisons is much higher than in the general population, both in high- and low-income countries (*2*). In sub-Saharan Africa, the spread of TB in prisons has been fueled by the HIV/AIDS epidemic (*3*). Reports from Malawi, Côte d'Ivoire, and Botswana have shown a higher prevalence of smear-positive pulmonary TB in prisons compared with the general population (*4–6*). Several factors, such as poor ventilation, HIV infection, overcrowding, malnutrition, lack of sunshine, stress, prolonged incarceration, and inadequate access to care, contribute to the rapid spread and high prevalence of MDR TB in prisons (*2*).

One of the critical barriers to TB control in prisons is limited access to high-quality TB diagnosis, which is attributable to limited screening, inaccuracy of diagnostic algorithms, and lack of laboratory facilities (*7,8*). All those factors are rampant in the Democratic Republic of the Congo (DRC) (population ≈68 million), given its protracted socioeconomic crisis and widespread poverty. Annual TB incidence in DRC is 326 cases/100,000 population (*9*). DRC is a high-burden TB country and has a high incidence of rifampicin-resistant TB (*10,11*). Preliminary data from an antimicrobial drug resistance survey in 2018 show a prevalence of rifampicin-resistant TB of 2.2% (95% CI 1.0%–3.5%) among new patients and 16.7% (95% CI 9.6%–23.7%) among previously treated case-patients (M.K. Kayomo, unpub. data).

The introduction of the Xpert MTB/RIF assay (Cepheid, Sunnyvale, CA, USA) is an important breakthrough in the fight against TB and MDR TB (*12–14*). The World Health Organization recommends this assay as a first-line diagnostic test for persons with suspected pulmonary TB who are considered to be at risk for harboring MDR TB bacilli (*15*). At the end of 2013, the DRC National Tuberculosis Program (NTP) progressively introduced the Xpert MTB/RIF technology in the provincial laboratories of DRC, mainly motivated by the lack of data on MDR TB incidence and the extremely long turnaround times associated with conventional methods. In November 2014, the NTP laboratory in Kasai Oriental Province switched from microscopy to the Xpert MTB/RIF for use in Mbuji-Mayi Central Prison because the laboratory had a large stock of cartridges that were

Author affiliations: Institute of Tropical Medicine, Antwerp, Belgium (M.K. Kayomo, E. Hasker, B.C. de Jong, M. Boelaert); National Tuberculosis Program, Kinshasa, Democratic Republic of the Congo (M.K. Kayomo, M. Aloni, M. Kazadi, T. Kabengele, D. Muteteke, F. Kapita, A. Lufulwabo); Institut National de Recherche Biomédicale, Kinshasa (M.K. Kayomo, M. Aloni, L. Nkuku, J.-J. Muyembe-Tamfum); Université de Kinshasa, Kinshasa (M.K. Kayomo, M. Aloni, J.-J. Muyembe-Tamfum); US Agency for International Development, Washington, DC, USA (Y.D. Mukadi); University of Antwerp, Antwerp (M. Ieven)

due to expire soon. By the end of 2014, the laboratory had confirmed TB in 31 of 57 sputum specimens from prisoners with presumptive TB; this number included, for the first time in the prison records, 3 patients with rifampicin-resistant TB. A total of 72 documented TB cases occurred in the prison that year, almost twice the 2013 figure.

After being alerted about the situation, the NTP head office in Kinshasa launched an outbreak investigation on January 5, 2015. Two NTP experts (M.K.K. and D.M.) were sent to review the patient histories, ascertain the emergence of TB and rifampicin-resistant TB, and implement infection control measures. We report here the outcomes of this outbreak assessment, including the incidence of TB and MDR TB, the drug-susceptibility patterns of the circulating *Mycobaterium tuberculosis* isolates, and associated risk factors for TB infection.

Methods

Ethics

The national health ethics review board of DRC (Comité National d'Ethique de la Santé) gave ethical clearance for this study (document no. 09/CNES/BN/PNMMF/2015). For this report, we only used specimens and data collected in the course of routine patient care and drug-susceptibility

surveillance. Data were delinked from any personal identifiers before data analysis and reporting. All persons who had TB or rifampicin-resistant TB diagnosed received the recommended treatment regimen (6 months for TB and 9 months for rifampicin-resistant TB). Patients with rifampicin-resistant TB were isolated at Dipumba General Hospital (Mbuji-Mayi) in a dedicated ward.

Setting

Mbuji-Mayi, the capital of Kasai Oriental Province (population ≈6.7 million), is located ≈1,000 km east of Kinshasa, the capital of DRC. In 2013, the province had an estimated annual TB incidence of 229 cases/100,000 population (M. Kazadi, unpub. data).

Mbuji-Mayi Central Prison is a medium-security correctional facility built in 1950 with a capacity of 150 inmates. It is surrounded by schools, houses, and government offices. It houses on average 900 inmates (i.e., 6 times its capacity) in 9 cells (7 cells for men, 1 for women, and 1 for juvenile inmates 15–17 years of age).

The number of prisoners per cell varies from ≈130–160 in the large (36 m²) cells to 20–30 in the small (28 m²) cells, which are also called VIP or first-class cells. On arrival, each prisoner is assigned a fixed spot, which in the regular cells is no larger than ≈0.25 m² (Figure 1). Each
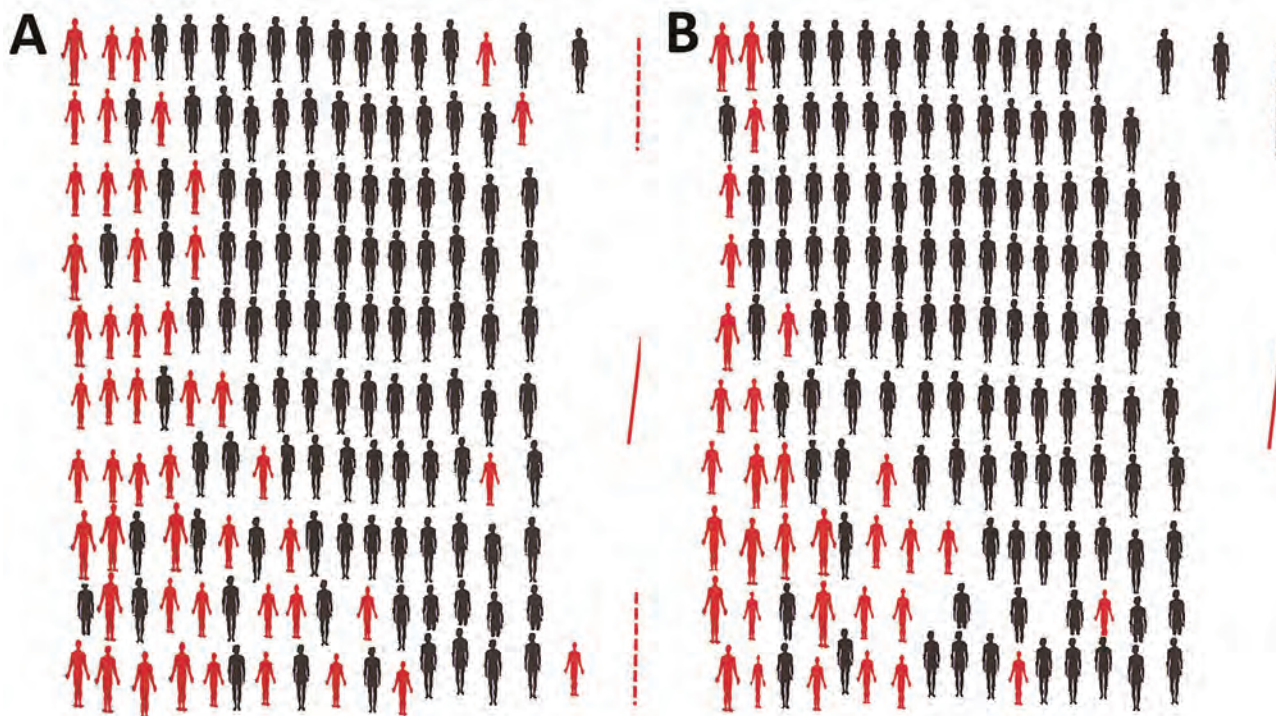
Figure 1. Location of inmates in cells 4 and 7, Mbuji-Mayi Central Prison, Democratic Republic of the Congo, February 2015. A) Cell 4 is 37 m², with 1 door (solid red line) and 2 windows (dashed red lines). B) Cell 7 is 37 m², with 1 door (solid red line) and 1 window (dashed red line). Red figures indicate TB patients. Both cells are in the designated area 2 and are extremely overcrowded, having ≥163 inmates in each. Each inmate was assigned a space of 0.22 m². Most (60%) TB patients were living in the rear of the cell, which was characterized by poor ventilation and lack of sunshine. This drawing shows the nearly exact localization of inmates during their stay inside the cell; more space is available at the entrance of the cell, which is occupied by the "chief" of the cell. TB, tuberculosis.

cell has ≥1 window, but prisoners' clothes and other possessions usually cover these. Inmates receive ≈5 hours of sunshine exposure per day in a courtyard measuring 375 m². They eat with the inmates of the same cell but meet those of other cells during morning sessions, gym, and vocational training. They also have close contact with prison staff, judges, and their own families. The duration of incarceration ranges from 1 month to >15 years. The prison has a clinic, run by 1 medical doctor and 2 healthcare workers.

Located close to the prison is an NTP clinic that conducts direct smear microscopy (no radiology) and can provide TB treatment to prisoners. Prisoners were not routinely screened for TB on entry. The NTP national policy on screening in prisons instructs chest radiograph screening upon entry, followed by smear microscopy if the radiograph results are suggestive. Further screening has to be systematically conducted every 6 months and upon release. However, prison-based TB control measures in DRC are limited in practice because of lack of resources. Until November 2014, only passive case detection for TB based on smear microscopy was implemented in Mbuji-Mayi Central Prison.

Study Procedures

The outbreak investigation team reached Mbuji-Mayi mid-January 2015 and reviewed all available NTP records as well as the prison admission register and patient files. The team also extracted from the NTP registers data on the TB notification rate in this prison for the 7 years preceding the investigation.

Assisted by provincial-level program staff and prison medical personnel, the team screened all inmates for presumptive TB. A standard form was used to collect data on previous history of TB, symptoms, duration of stay, and location in the cell. Awareness was raised among inmates about the signs and symptoms of TB, and the chief inmate of each cell as well 10 peer educators, all inmates, were trained to recognize the major symptoms of TB. Inmates with a history of TB or clinical symptoms (e.g., coughing for >2 weeks, fever, night sweats, loss of weight, and hemoptysis) were considered to be presumptive TB patients. These patients were asked to submit 1 early morning sputum sample. Samples were transported to the provincial reference laboratory located 3 km from the prison.

Laboratory Procedures

Xpert MTB/RIF

Fresh sputum samples (without any additive) were transported in standardized containers from the prison to the provincial reference laboratory to be analyzed using the Xpert MTB/RIF assay. We also recorded demographic data of patients and their TB history. A 2-mL aliquot of each sputum sample was processed in Xpert according to standard methods (12,16). From each specimen showing resistance to rifampicin, an aliquot was preserved in 70% alcohol in a Falcon tube to permit additional molecular testing in Kinshasa and at the Supranational Reference Laboratory (SRL) in Antwerp, Belgium. One aliquot without additive was transported to Kinshasa for culture.

MTBDRsl

At the Institut National de Recherche Biomédicale in Kinshasa, GenoType MTBDRsl (Hain LifeScience GmbH, Nehren, Germany) was performed on specimens showing resistance to rifampicin by Xpert MTB/RIF. Sputum samples were decontaminated with NaOH according to a modified Petroff technique (17). The sediment obtained was inoculated on Lowenstein-Jenssen and tested by using MTBDRsl according to the manufacturer's instructions (18).

Genetic Sequencing

For all available DNA extracts harboring second-line resistance patterns on MTBDRsl, sequencing of the gyrA and rrs genes was performed independently of line probe assay (LPA) results at SRL. The methodology for PCR amplification and sequencing of genes encoding gyrase A and B has been described elsewhere (19).

HIV Screening

The National HIV Program organized a mass HIV screening campaign in the prison, a few days after our arrival in Mbuji-Mayi. Skilled counselors performed pretest group counseling. Posttest counseling was carried out in a private one-on-one setting by the same counselors. Persons who tested positive were referred to the nearby NTP clinic for TB and HIV treatment.

Data Analysis

All data were double-entered into an Excel 2007 worksheet (Microsoft, Redmond, WA, USA). Both datasets were compared by using Epi Info 7.1.4 (Centers for Disease Control and Prevention, Atlanta, GA, USA); in case of discrepancies, we verified the source document. The primary outcomes of interest for this study were the prevalence rates of TB and rifampicin-resistant TB, computed as the proportion of confirmed TB or rifampicin-resistant TB patients over the total number of prisoners at the time of our visit. These data were later linked with DNA sequencing results from SRL. For this analysis, we divided the prison into 3 areas. Area 1 comprised cells 1–3 (the VIP or first-class cells, where inmates get better conditions in exchange for payment). Area 2 comprised cells 4–7 (the second-class cells). Area 3 comprised cells 8 and 9, the areas for women and juveniles. We mapped the spatial distribution of TB in the cells on a sketch showing the location of each prisoner.

We calculated the body mass index (weight in kilograms/height in meters) as a measure of adult nutritional status and used the cutoffs proposed by Bailey and Ferro-Luzzi (20) to define 3 categories of adult malnutrition (severe, moderate, and mild).

We calculated means (including SDs) and medians and ranges for continuous variables. Comparisons between groups were made by using Fisher's exact test, and 95% CIs were calculated when appropriate.

Results

Pulmonary TB

In November 2014, a total of 31 inmates had been found to be positive for TB by Xpert MTB/RIF (4 in area 1 and 25 in area 2). For 2 patients, no information on location was recorded, and they were not present any longer during our outbreak investigation. In January 2015, a total of 918 inmates were housed in Mbuji-Mayi Central Prison, 863 (94.0%) men and 26 (2.8%) women; 29 (3.1%) were juveniles. Most (716/918 [78%]) were pretrial inmates, and only 202 (22.0%) had been sentenced to imprisonment. Area 1 housed 206 inmates (22.4%), area 2 housed 657 inmates (71.6%), and area 3 housed 55 inmates (6.0%). Median age of inmates was 30 years (interquartile range 25–42 years), and 29 inmates were already undergoing TB treatment (all 29 had TB diagnosed after their entry into the prison). Out of the remaining 889 inmates, 45 were absent for various reasons or declined to be screened.

We clinically examined 844/918 inmates (91.9%) and collected sputum samples of the 475 presumptive TB patients (51.7% [475/918] of inmates). The mean age of inmates with presumptive TB was 32 years (median 31 years), and their mean duration of incarceration was 72 months (median 42 months, range 1–437 months). One Xpert MTB/RIF assay was performed per patient, and 460 valid tests were included in the final analysis, of which 170 were *M. tuberculosis*–positive and rifampin-sensitive and 14 were *M. tuberculosis*–positive and rifampin-resistant. The remaining

Table 1. HIV screening results among inmates at Mbuji-Mayi Central Prison, Democratic Republic of the Congo, March 2015

Characteristic	No. (%)
No. inmates housed in the prison	918 (100)
No. inmates who received pretest counseling	879 (95.7)
No. inmates who accepted testing	753 (85.6)
No. inmates tested	539 (71.6)
No. HIV-positive inmates	8 (1.5)
No. inmates with tuberculosis and HIV co-infection	5 (0.9)

276 tests were negative. Thus, by using the Xpert MTB/RIF assay systematically, we raised the total number of TB cases detected during November 2014–March 2015 to 201 (31 initial cases plus 170 additional cases). The overall prevalence rate of TB among the 918 prisoners housed in March 2015 was 21.7% (199/918), including 2 women and 1 juvenile.

HIV

Most (85.6% [753/879]) inmates agreed to attend a pretest counseling session for HIV (Table 1), but only 539 (71.5%) were tested for HIV because of a shortage in test kits. The overall proportion of inmates with HIV infection was 1.5% (8/539) among inmates tested, 2.6% (5/196) among inmates with bacteriologically confirmed TB, and 0.9% (3/343) inmates without TB (p = 0.12).

Trend of TB

From the beginning of 2008 through March 2015, a total of 301 TB patients were registered at Mbuji-Mayi Central Prison. Until the third quarter of 2014, the number of TB patients registered remained relatively stable, with an average of 2 new cases/quarter (range 0–9 cases/quarter). A steep increase was observed from the fourth quarter of 2014 onward (Figure 2), with 212 new TB cases registered (>70% of the caseload since 2008).

Drug Resistance

By using the Xpert MTB/RIF assay, we found 199 patients to be bacteriologically positive for TB during November 2014–March 2015. Among them, 17 (8.5%) patients (3 initial patients plus 17 additional patients) had rifampicin-

Figure 2. Number of new TB cases registered per quarter, Mbuji-Mayi Central Prison, Democratic Republic of the Congo, 2008–2015. TB cases include bacteriologically positive and clinically diagnosed TB patients. Clinical diagnosis was based on ≥1 TB-related sign or symptom, a chest radiograph abnormality consistent with TB infection, or both. During 2008–2014, bacteriologic confirmation was based on microscopic results from sputum samples collected through passive case-finding. Xpert MTB/RIF was introduced during the last quarter of 2014. Source: Democratic Republic of Congo National TB Program. Q, quarter; TB, tuberculosis.
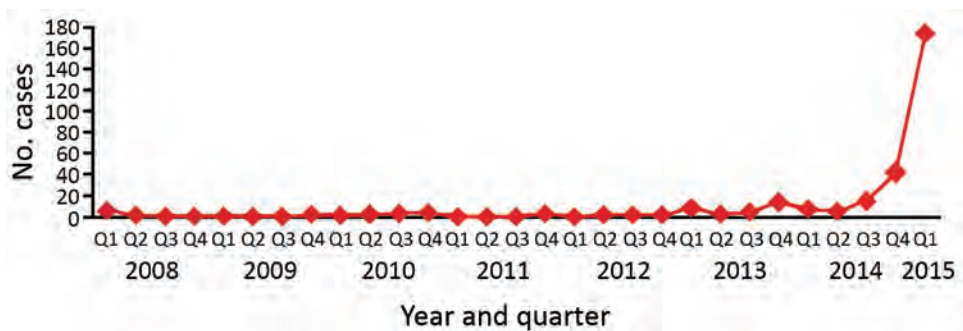
Table 2. Selected demographic and clinical characteristics of 14 inmates with diagnosed rifampin-resistant tuberculosis, Mbuji-Mayi Central Prison, Democratic Republic of the Congo, February 2015*

Area	Sex and age, y	History of treatment	Detection date	Treatment started	HIV status	Duration of incarceration, mo
1	M/31	New case	2015 Feb 10	2015 Feb 11	Neg	21
2	M/18	New case	2014 Nov 21	2014 Dec 11	Neg	18
2	M/20	Retreatment	2014 Nov 21	2014 Dec 11	Neg	28
2	M/25	New case	2015 Jan 14	2015 Jan 16	Neg	12
2	M/25	New case	2015 Jan 14	2015 Jan 16	Neg	1
2	M/55	New case	2015 Jan 14	2015 Jan 20	Neg	24
2	M/25	New case	2015 Feb 5	2015 Feb 7	Neg	19
2	M/32	New case	2015 Jan 14	2015 Jan 20	Neg	7
2	M/35	New case	2015 Jan 14	2015 Jan 20	Neg	20
2	M/27	New case	2015 Feb 16	2015 Feb 19	Neg	36
2	M/30	New case	2014 Nov 20	2014 Dec 11	Neg	3
2	M/35	New case	2015 Jan 21	2015 Jan 23	Neg	101
2	M/25	New case	2015 Jan 22	2015 Jan 24	Neg	21
2	M/24	New case	2015 Jan 22	2015 Feb 24	Neg	30

*Drug resistance testing by Xpert MTB/RIF assay. Neg, negative.

resistant TB, which is ≈3 times the expected number of TB-RR cases among new cases according to World Health Organization estimates for DRC (*10*). The overall prevalence of rifampicin-resistant TB in Mbuji Mayi Central Prison in March 2015 was equivalent to 1,852 cases/100,000 inmates. Among the 14 cases documented in March 2015 (Table 2), all but 1 were new cases. For the 3 first detected cases, documented in 2014, the delay between diagnosis to start of treatment was 21 days. This delay decreased to 48 hours for the remaining patients. No second-line drug resistance was identified among any rifampicin-resistant TB patient.

Xpert MTB/RIF results showed that all rifampicin-resistant TB was attributable to the absence of probe E. This finding supports the possibility of clonal spread of 1 strain containing a mutation in the *rpoB* 531 codon or, less likely, the 533 codon.

Risk Factors

Overcrowded Living Conditions

Most (60%) TB patients were located in the back of the cell, where ventilation is poor and sunshine is especially lacking (Figure 1). Area 2 (cells 4–7) was the most overcrowded of the 3 areas, housing 657/918 (71.5%) inmates. In cells 4 and 7, the available surface per person was no more than 0.22 m². The frequency of TB and rifampicin-resistant TB increased significantly with the number of inmates per area. Of the 199 confirmed TB patients, 19 resided in area 1, 177 in area 2,

and 3 in area 3. The prevalence of confirmed TB was 2.75 times higher in areas 2 and 3 compared with area 1 (25.3% vs. 9.2% [p<0.001]). Out of the 14 rifampicin-resistant TB case-patients identified during January–March 2015, only 1 resided in area 1 (7.1%); the others all resided in area 2.

Nutritional Status

Of the 918 inmates, 752 (82%) were screened for nutritional status; of these, 370 (49.2%) were malnourished (body mass index <18.5 kg/m²) (Table 3). In the subgroup of 170 confirmed TB patients, 142 (83.5%) were screened for nutritional status; of these, 110 (77.5%) were malnourished. Malnutrition was significantly higher among TB patients than among the other inmates (odds ratio 4.63, 95% CI 3.03–7.08).

Discussion

Our findings provide an account of the high prevalence of TB and drug-resistant TB in a large prison in DRC, where overcrowded living conditions were appalling. The prevalence of TB in this prison was 39 times higher than the estimated 549 cases/100,000 in the general population of DRC (*11*) and is 3.5 times greater than the prevalence reported from prisons in neighboring Zambia (*21*). The TB problem at Mbuji-Mayi Central Prison probably remained undetected for years because of lack of screening and the weak sensitivity of smear microscopy. Some prison studies in sub-Saharan Africa have documented higher rates of TB (*1,3,7*) in association with a higher HIV prevalence. However, in Mbuji-Mayi Central

Table 3. Nutritional status of 752 inmates at Mbuji-Mayi Central Prison, Democratic Republic of the Congo, January 2015*

Nutritional status	No. (%) inmates		
	With TB, n = 142	Without TB, n = 610	Total, N = 752
BMI >18 kg/m²	32 (22.5)	350 (57.4)	382 (50.8)
Degree of malnutrition†	110 (77.5)	260 (42.6)	370 (49.2)
Mild	53 (37.3)	95 (15.6)	148 (19.7)
Moderate	27 (19.0)	98 (16.1)	125 (16.6)
Severe	30 (21.1)	67 (11.0)	97 (12.9)

*BMI, body mass index; TB, tuberculosis.
†Malnutrition defined as BMI <18 kg/m². Severity of malnutrition: severe, BMI <16.0; moderate, BMI 16.0–16.9; mild, BMI 17.0–18.49.

Table 4. Recommended priority actions to reduce TB prevalence at Mbuji-Mayi Central Prison, Democratic Republic of the Congo*

Action
1. Ensure the screening for TB signs and symptoms of all inmates at the time of prison entry and exit. Continue active and early detection of presumptive TB patients. Raise awareness among the inmates, the prison administration, and the community of the city of Mbuji-Mayi that each cougher should be tested. Confirm presumptive diagnosis by using Xpert MTB/RIF assay. Screen for HIV by using rapid tests.
2. Initiate appropriate treatment of confirmed TB patients within 24 h under strict supervision of healthcare providers.
3. Ensure systematic screening by chest x-ray of the other inmates, the healthcare providers, and the personnel of the prison administration.
4. Feed all inmates adequate and nourishing meals, especially TB and HIV patients undergoing treatment.
5. Ventilate cells.
6. RR-TB patients may be isolated from other inmates at Dipumba General Hospital (Mbuji-Mayi), where the National TB Program was able to obtain a ward for their accommodation. However, the prison administration should find ways to ensure security.
7. Establish compulsory wearing of masks by all TB patients.
8. Establish the compulsory wearing of respirators by all staff entering the prison.
9. Ensure the decongestion of the prison by speeding up judicial proceedings, and increase space by enforcing maximal occupancy levels at the prison.

*TB, tuberculosis.

Prison, we found a relatively low HIV prevalence, although not all consenting prisoners were tested because of a shortage of HIV test kits at the time.

During our investigation, we observed the presence of several risk factors for TB spread in the prison, such as lack of TB screening upon arrival, overcrowding, lack of sunshine, very poor ventilation, and malnutrition (*3,22–26*). These factors were also documented in other prison TB outbreaks (*3,23,27–32*), but the degree of overcrowding at Mbuji-Mayi Central Prison was a staggering 6 times higher than its capacity. Some prisoners stated that they did not eat for 3 days before our investigation. Malnutrition is a known problem in the Mbuji-Mayi region; the adult malnutrition rate is 45% and >1 million persons require nutritional assistance, according to a 2014 World Food Program report (*33*). Malnutrition tends to amplify TB infection as well as the progress from TB infection to TB disease (*34–36*).

One limitation of our study is that no further investigations were conducted to check if the *M. tuberculosis* strains were related, so no hard evidence is available to attribute the high TB and rifampicin-resistant TB rates to in-prison transmission or to a high prevalence among new arrivals. Probably both factors were at work. The preliminary results of a nationwide antimicrobial resistance survey conducted in 2018 (M.K. Kayomo, unpub. data) show that the prevalence of rifampicin-resistant TB in Mbuji-Mayi was 10.4% (95% CI 0.1%–15.6%) among new patients (5 times the national average) and 36.3% (95% CI 18.9%–38.7%) among patients who were previously treated (2 times the national average). The high TB rates in Mbuji-Mayi Central Prison reflect this problem in the community, but in all probability the prison environment acted as an effective amplifier.

As an immediate response measure, the NTP team initiated TB therapy for all confirmed TB case-patients and transferred the rifampicin-resistant TB case-patients to a special isolation ward at the local hospital. We also initiated screening of prisoners upon prison entry. Our findings also led to an acceleration of pending judicial proceedings, which resulted in decongestion of the prison, and the World Food Program intervened to provide supplementary feeding.

However, sustained control of TB among incarcerated populations requires sustained efforts (Table 4). Overcrowding should be avoided, and inmates should have access to better nutrition and more sunlight exposure. Dedicated TB control with adequate diagnostic technology is needed. The active case-finding deployed in Mbuji-Mayi Central Prison using the more sensitive Xpert MTB/RIF assay increased TB case detection by 19-fold. The Xpert MTB/RIF assay offers rapid and accurate diagnostic results from biologic specimens and requires only minimal staff training (*12–14*). In prisons, use of this technology is warranted at entry point and thereafter. Passive and active case-finding should be conducted simultaneously and systematically. The high risk for TB in prison settings underscores the urgent need for dedicated TB programs to protect not only the health of prison inmates but also the health of the wider community. However, to avoid outbreaks of MDR TB in similar contexts, living conditions in prisons should be adequate. A hard-learned lesson in prison systems across the world is that safeguarding the basic human rights of these vulnerable populations (including their entitlement to space, food, and health) requires independent monitoring and subsequent action.

About the Author

Dr. Kayomo directs the National TB Program of the Democratic Republic of the Congo. His research focuses on drug-resistant TB, in collaboration with the Institute of Tropical Medicine in Antwerp, Belgium.

References

1. Balabanova Y, Nikolayevskyy V, Ignatyeva O, Kontsevaya I, Rutterford CM, Shakhmistova A, et al. Survival of civilian and prisoner drug-sensitive, multi- and extensive drug-resistant tuberculosis cohorts prospectively followed in Russia. PLoS One. 2011;6:e20531. http://dx.doi.org/10.1371/journal.pone.0020531
2. Biadglegne F, Rodloff AC, Sack U. Review of the prevalence and drug resistance of tuberculosis in prisons: a hidden epidemic. Epidemiol Infect. 2015;143:887–900. http://dx.doi.org/10.1017/S095026881400288X
3. O'Grady J, Hoelscher M, Atun R, Bates M, Mwaba P, Kapata N, et al. Tuberculosis in prisons in sub-Saharan Africa—the need for improved health services, surveillance and control. Tuberculosis (Edinb). 2011;91:173–8. http://dx.doi.org/10.1016/j.tube.2010.12.002

4. Nyangulu DS, Harries AD, Kang'ombe C, Yadidi AE, Chokani K, Cullinan T, et al. Tuberculosis in a prison population in Malawi. Lancet. 1997;350:1284–7. http://dx.doi.org/10.1016/S0140-6736(97)05023-X

5. Center for Disease Control and Prevention. Rapid assessment of tuberculosis in large prison of Botswana. MMWR Morb Mortal Wkly Rep. 2003;52:250–2.

6. Koffi N, Ngom AK, Aka-Danguy E, Séka A, Akoto A, Fadiga D. Smear positive pulmonary tuberculosis in a prison setting: experience in the penal camp of Bouaké, Ivory Coast. Int J Tuberc Lung Dis. 1997;1:250–3.

7. Dara M, Acosta CD, Melchers NV, Al-Darraji HA, Chorgoliani D, Reyes H, et al. Tuberculosis control in prisons: current situation and research gaps. Int J Infect Dis. 2015;32:111–7. http://dx.doi.org/10.1016/j.ijid.2014.12.029

8. Al-Darraji HAA, Abd Razak H, Ng KP, Altice FL, Kamarulzaman A. The diagnostic performance of a single GeneXpert MTB/RIF assay in an intensified tuberculosis case finding survey among HIV-infected prisoners in Malaysia. PLoS One. 2013;8:e73717. http://dx.doi.org/10.1371/journal.pone.0073717

9. World Health Organization. Global TB report 2017. Tuberculosis country profiles: DR of Congo [cited 2018 Apr 26]. http://www.who.int/tb/publications/global_report/gtbr2017_annex2.pdf

10. World Health Organization. Anti-tuberculosis drug resistance in the world [cited 2008 Oct 14]. http://whqlibdoc.who.int/hq/2008/who_htm_tb_2008.394_eng.pdf

11. Kaswa MK, Aloni M, Nkuku L, Bakoko B, Lebeke R, Nzita A, et al. A pseudo-outbreak of pre-XDR TB in Kinshasa: a collateral damage of false fluoroquinolone resistant detection by genotype MTBDR*sl*. J Clin Microbiol. 2014;52:2876–80. http://dx.doi.org/10.1128/JCM.00398-14

12. Boehme CC, Nabeta P, Hillemann D, Nicol MP, Shenai S, Krapp F, et al. Rapid molecular detection of tuberculosis and rifampin resistance. N Engl J Med. 2010;363:1005–15. http://dx.doi.org/10.1056/NEJMoa0907847

13. Steingart KR, Sohn H, Schiller I, Kloda LA, Boehme CC, Pai M, et al. Xpert MTB/RIF assay for pulmonary tuberculosis and rifampicin resistance in adults. Cochrane Database Syst Rev. 2013;1:CD009593.

14. Chang K, Lu W, Wang J, Zhang K, Jia S, Li F, et al. Rapid and effective diagnosis of tuberculosis and rifampicin resistance with Xpert MTB/RIF assay: a meta-analysis. J Infect. 2012;64:580–8. http://dx.doi.org/10.1016/j.jinf.2012.02.012

15. Stop TB Partnership. Global plan to stop TB 2011–2015 [cited 2010 Nov 7]. http://www.stoptb.org/assets/documents/global/plan/tb_globalplantostoptb2011-2015.pdf

16. Helb D, Jones M, Story E, Boehme C, Wallace E, Ho K, et al. Rapid detection of *Mycobacterium tuberculosis* and rifampin resistance by use of on-demand, near-patient technology. J Clin Microbiol. 2010;48:229–37. http://dx.doi.org/10.1128/JCM.01463-09

17. Petroff SA. A new and rapid method for the isolation and cultivation of tubercle bacilli directly from the sputum and feces. J Exp Med. 1915;21:38–42. http://dx.doi.org/10.1084/jem.21.1.38

18. Hain Lifescience GmbH. GenoType MTBDR*sl* version 1.0: instruction manual. Nehren (Germany): Hain Lifescience GmbH; 2008 [cited 2017 Feb 22]. https://www.hain-lifescience.de/en/products/microbiology/mycobacteria/tuberculosis/genotype-mtbdrsl.html

19. Von Groll A, Martin A, Jureen P, Hoffner S, Vandamme P, Portaels F, et al. Fluoroquinolone resistance in *Mycobacterium tuberculosis* and mutations in *gyrA* and *gyrB*. Antimicrob Agents Chemother. 2009;53:4498–500. http://dx.doi.org/10.1128/AAC.00287-09

20. Bailey KV, Ferro-Luzzi A. Use of body mass index of adults in assessing individual and community nutritional status. Bull World Health Organ. 1995;73:673–80.

21. Maggard KR, Hatwiinda S, Harris JB, Phiri W, Krüüner A, Kaunda K, et al. Screening for tuberculosis and testing for human immunodeficiency virus in Zambian prisons. Bull World Health Organ. 2015;93:93–101. http://dx.doi.org/10.2471/BLT.14.135285

22. Harries AD, Nyirenda TE, Yadidi AE, Gondwe MK, Kwanjana JH, Salaniponi FM. Tuberculosis control in Malawian prisons: from research to policy and practice. Int J Tuberc Lung Dis. 2004;8:614–7.

23. O'Grady J, Mwaba P, Bates M, Kapata N, Zumla A. Tuberculosis in prisons in sub-Saharan Africa—a potential time bomb. S Afr Med J. 2011;101:107–8. http://dx.doi.org/10.7196/SAMJ.4629

24. Human Rights Watch. Unjust and unhealthy: HIV, TB and abuse in Zambian prisons [cited 2010 Apr 27]. https://www.hrw.org/sites/default/files/reports/zambia0410webwcover.pdf

25. Jürgens R, Nowak M, Day M. HIV and incarceration: prisons and detention. J Int AIDS Soc. 2011;14:26. http://dx.doi.org/10.1186/1758-2652-14-26

26. Chaisson RE, Martinson NA. Tuberculosis in Africa—combating an HIV-driven crisis. N Engl J Med. 2008;358:1089–92. http://dx.doi.org/10.1056/NEJMp0800809

27. Ali S, Haileamlak A, Wieser A, Pritsch M, Heinrich N, Loscher T, et al. Prevalence of pulmonary tuberculosis among prison inmates in Ethiopia, a cross-sectional study. PLoS One. 2015;10:e0144040. http://dx.doi.org/10.1371/journal.pone.0144040

28. Telisinghe L, Fielding KL, Malden JL, Hanifa Y, Churchyard GJ, Grant AD, et al. High tuberculosis prevalence in a South African prison: the need for routine tuberculosis screening. PLoS One. 2014;9:e87262. http://dx.doi.org/10.1371/journal.pone.0087262

29. Moges B, Amare B, Asfaw F, Tesfaye W, Tiruneh M, Belyhun Y, et al. Prevalence of smear positive pulmonary tuberculosis among prisoners in North Gondar Zone Prison, northwest Ethiopia. BMC Infect Dis. 2012;12:352. http://dx.doi.org/10.1186/1471-2334-12-352

30. Reid SE, Topp SM, Turnbull ER, Hatwiinda S, Harris JB, Maggard KR, et al. Tuberculosis and HIV control in sub-Saharan African prisons: "thinking outside the prison cell". J Infect Dis. 2012;205(Suppl 2):S265–73. http://dx.doi.org/10.1093/infdis/jis029

31. Noeske J, Ndi N, Elo GA, Mfondih SM. Tuberculosis incidence in Cameroonian prisons: a 1-year prospective study. S Afr Med J. 2014;104:209–11. http://dx.doi.org/10.7196/SAMJ.7384

32. Ensor L. Overcrowding in South African prisons falls [cited 2006 Jul 11]. http://www.bdlive.co.za/national/2013/08/26/overcrowding-in-south-africanprisons-falls

33. World Food Program. Democratic Republic of Congo: situation report no. 5 [cited 2014 May 5]. https://reliefweb.int/sites/reliefweb.int/files/resources/WFP%20DRC%20Situation%20Report%20%235%2C%20May%202014%20%281%29.pdf

34. Chocano-Bedoya P, Ronnenberg AG. Vitamin D and tuberculosis. Nutr Rev. 2009;67:289–93. http://dx.doi.org/10.1111/j.1753-4887.2009.00195.x

35. Gibney KB, MacGregor L, Leder K, Torresi J, Marshall C, Ebeling PR, et al. Vitamin D deficiency is associated with tuberculosis and latent tuberculosis infection in immigrants from sub-Saharan Africa. Clin Infect Dis. 2008;46:443–6. http://dx.doi.org/10.1086/525268

36. Lönnroth K, Williams BG, Cegielski P, Dye C. A consistent log-linear relationship between tuberculosis incidence and body mass index. Int J Epidemiol. 2010;39:149–55. http://dx.doi.org/10.1093/ije/dyp308

Address for correspondence: Michel Kaswa Kayomo, National Tuberculosis Program, 240 Avenue Kabinda, Commune de Lingwala, Ville de Kinshasa, Democratic Republic of the Congo; email: meckkay2002@yahoo.fr

Candida auris in South Africa, 2012–2016

Nelesh P. Govender, Rindidzani E. Magobo, Ruth Mpembe, Mabatho Mhlanga, Phelly Matlapeng, Craig Corcoran, Chetna Govind, Warren Lowman, Marthinus Senekal, Juno Thomas

To determine the epidemiology of *Candida auris* in South Africa, we reviewed data from public- and private-sector diagnostic laboratories that reported confirmed and probable cases of invasive disease and colonization for October 2012–November 2016. We defined a case as a first isolation of *C. auris* from any specimen from a person of any age admitted to any healthcare facility in South Africa. We defined probable cases as cases where the diagnostic laboratory had used a nonconfirmatory biochemical identification method and *C. haemulonii* was cultured. We analyzed 1,692 cases; 93% were from private-sector healthcare facilities, and 92% of cases from known locations were from Gauteng Province. Of cases with available data, 29% were invasive infections. The number of cases increased from 18 (October 2012–November 2013) to 861 (October 2015–November 2016). Our results show a large increase in *C. auris* cases during the study period, centered on private hospitals in Gauteng Province.

The earliest reported case of infection with the yeast *Candida auris* in South Africa occurred in 2009; however, the pathogen was initially misidentified as *Candida haemulonii* (a closely related yeast), and *C. auris* was only confirmed retrospectively in 2014, when 4 other cases of *C. auris* candidemia were described in South Africa (*1*). Since descriptions in Southeast Asia in 2009, cases of *C. auris* have been reported from many countries on 6 continents (Asia, Africa, South America, Europe, North America, and most recently Oceania) (*2*).

C. auris has been associated with large healthcare-associated outbreaks because of its ability to be transmitted person-to-person by direct contact, form biofilms,

persist in the hospital environment on surfaces and on shared equipment, and resist chemical disinfection by certain products (*3–5*). Over the past 9 years, cases of *C. auris* have been detected at many hospitals in South Africa, causing large outbreaks at some facilities, and this pathogen now accounts for ≈1 of every 10 cases of candidemia (*6*). South Africa has a unique *C. auris* clade separated from Asian, Southeast Asian, and South American clades by tens of thousands of single-nucleotide polymorphisms, consistent with the hypothesis that *C. auris* emerged independently in Africa and simultaneously on several other continents (*7*). However, the prevalence and geographic extent of *C. auris* disease is likely underestimated, especially in low- and middle-income countries in Africa, because conventional laboratory methods misidentify the fungus and relatively few resource-limited countries have the capacity for identification by mass spectrometric or molecular methods (*8*). South Africa has an established national surveillance infrastructure for infectious diseases, including those caused by antimicrobial drug–resistant pathogens, that is based on a large network of well-equipped diagnostic pathology laboratories. In light of an emerging epidemic of *C. auris* infections among hospitalized patients in parts of South Africa, we sought to describe the national epidemiology of laboratory-confirmed cases during 2012–2016.

Materials and Methods

We conducted national laboratory-based surveillance for *C. auris* retrospectively over a period of >4 years, from the earliest known reports of cases in South Africa in October 2012 through November 2016 (*1*). We defined a case as a first isolation of *C. auris* from any specimen from a patient of any age admitted to any South Africa healthcare facility. We also included probable cases in which the diagnostic laboratory had used a nonconfirmatory biochemical identification method such as Vitek-2 YST (bioMérieux, Marcy l'Etoile, France) and *C. haemulonii* was cultured. The National Health Laboratory Service (NHLS) provides diagnostic pathology services to the public sector, serving ≈83% of the population of South Africa, and has ≈60 mostly hospital-based laboratories offering tests for fungal identification. We performed species-level identification for *Candida* at NHLS laboratories using several platforms during the surveillance

period, namely Vitek 2 YST, API 20C Aux, or API ID 32C (bioMérieux); Auxacolor (Bio-Rad, Hercules, CA, USA); and Microscan (Beckman Coulter, Brea, CA, USA). Some of these diagnostic platforms are known to misidentify *C. auris* as other yeasts (*9*); however, we did not include any other species in our probable case definition. Private pathology laboratory practices, which serve the remainder of the population with health insurance, have a centralized model of fungal identification; that is, central laboratories perform diagnostic tests for patient specimens referred from a large number of healthcare facilities across a region or province. These laboratories used the same yeast identification platforms; however, 1 private pathology practice introduced the Vitek MS system (bioMérieux) in 2013. In general, NHLS laboratories identified *Candida* to species level only for isolates from normally sterile sites, whereas private laboratories identified all *Candida* isolates to species level, regardless of the specimen source.

We obtained line list specimen-level data from 4 large private diagnostic pathology practices, which together serve almost the entire private health sector, for the surveillance period. We requested that these line lists included any specimens from which either *C. haemulonii* or *C. auris* was cultured. We deduplicated these laboratory data to patient level by applying the surveillance case definition and using a unique laboratory identifier. We then merged this dataset with a similar line list of cases of *C. auris* fungemia that were submitted to the National Institute for Communicable Diseases (NICD) from NHLS laboratories as part of candidemia surveillance. All these bloodstream isolates were confirmed as *C. auris* at NICD using the Bruker Biotyper system (Bruker, Bremen, Germany) or PCR amplification and sequencing of the internal transcribed spacer (ITS) domain of the ribosomal RNA gene using universal primers (*10*). Variables included in the final dataset were age or date of birth, sex, date of specimen collection, location (province and admitting hospital), specimen type, and species-level identification.

We defined a case as colonization if the isolate was cultured from central venous catheter tips (with no corresponding blood culture specimen), urine, respiratory tract specimens and skin or mucosal swabs. We defined a case as invasive disease if the source of the isolate was blood, cerebrospinal fluid, or serous fluid or tissue. Treating clinicians or hospital-based infection prevention and control (IPC) practitioners submitted the specimens that yielded these isolates; therefore, we may have detected cases of colonization because of active screening at some hospitals with outbreaks. There was no uniform practice for screening for colonization during the surveillance period, and this study preceded the interim guidance issued by NICD (*11*). To our knowledge, the number of healthcare facilities served by the laboratory network did not change over the surveillance period. We obtained approval for laboratory-based surveillance from the Human Research Ethics Committee (Medical), University of the Witwatersrand, Johannesburg.

Results

For October 2012–November 2016, we identified a total of 1,692 confirmed or probable *C. auris* cases at both public and private hospitals, although most patients (1,578/1,692, 93%) were admitted to private facilities. Of the private-sector cases, at least 647 (38%) had isolates that were identified as *C. haemulonii* and not confirmed as *C. auris*. All 114 bloodstream isolates from public-sector cases were confirmed as *C. auris* at NICD's mycology reference laboratory. Of 1,579 case-patients with a recorded specimen type, 451 (29%) had invasive disease (Table), with isolates cultured from normally sterile sites: 344 (76%) from blood, 56 (12%) from fluid, 49 (11%) from tissue, and 2 (<1%) from cerebrospinal fluid. The remaining 1,128/1,579 (71%) isolates were cultured from sites of probable colonization: 622 (55%) from urine, 288 (26%) from central venous catheter tips, 173 (15%) from respiratory tract, and 45 (4%) from skin, mucosal, or wound swabs.

Male patients accounted for 62% of cases. The median age of patients was 60 years (IQR 46–72 years); 38 patients (2%) were <18 years of age, and 9 (0.5%) were infants <1 year of age. Patients with invasive disease were younger than colonized patients: median age for invasive disease

Table. Characteristics of cases of *Candida auris* invasive disease versus colonization, South Africa, 2012–2016*

Characteristic	Cases with available data, n = 1,579	Invasive disease, n = 451	Colonization, n = 1,128
Median patient age, y (interquartile range)†	n = 1,576	55 (41–68)	63 (49–74)
Patient sex, no. (%)	n = 1,540	n = 442	n = 1,098
M	957 (62)	273 (62)	684 (62)
F	583 (38)	169 (38)	414 (38)
Health sector, no. (%)	n = 1,549	n = 439	n = 1,110
Private	1,435 (93)	325 (74)	1,110 (100)
Public	114 (7)	114 (26)	0
Province, no. (%)	n = 1,465	n = 424	n = 1,041
Gauteng	1,336 (91)	380 (90)	956 (92)
Mpumalanga	72 (5)	25 (6)	47 (5)
North West	20 (1)	7 (2)	13 (1)
Other provinces	37 (3)	12 (2)	25 (2)

*Specimen type data were unavailable for 116 cases.
†Compared using a Wilcoxon rank-sum test.

was 55 years (IQR 41–68 years) versus median 63 years (IQR 49–74 years) for colonized patients (p <0.001). All cases of colonization were detected at private-sector hospitals; at least 39% (444/1,128) of these isolates had been identified as *C. haemulonii*. In contrast, 25% (112/451) of invasive isolates had been identified as *C. haemulonii*.

Of cases with a known location, 92% (1,440/1,571) were reported from Gauteng Province, the most densely populated province and the economic and travel hub of South Africa. A median of 4 cases (interquartile range [IQR] 1–11) was reported from each of ≥94 hospitals. Of all cases with a known location, 80% (1,087/1,353) were reported from 20 private-sector hospitals, 17 of which were located in Gauteng Province (Figure 1). More than 80 cases were detected at each of 4 private hospitals in Pretoria (Gauteng Province). Large outbreaks (≥75 cases) also occurred in a private hospital in Johannesburg (Gauteng Province) and another in Rustenburg (North West Province). The number of cases increased dramatically from 18 in the baseline period (October 2012–November 2013) to 861 in a later corresponding period (October 2015—November 2016) (Figure 2).

Discussion

We have demonstrated a dramatic increase in the number of confirmed or probable cases of *C. auris* over 4 years in South Africa. Of concern, *C. auris* was detected at a large number of hospitals; most patients were admitted to private-sector hospitals in Gauteng Province. Most cases were probably caused by colonization, but *C. auris* is now also a common cause of invasive disease, accounting for 10% of all cases of candidemia in recent national surveillance (*6*). We collected minimal patient information through this surveillance but were able to document that most cases occurred among adults rather than children.

The factors that have led to the emergence and rapid spread of a unique clade of *C. auris* in hospitals in South Africa are not well established. Azole-resistant *C. parapsilosis*

is already endemic in private-sector hospitals in Gauteng Province (*12*). We have previously hypothesized that these strains of azole-resistant *C. parapsilosis* initially emerged as a consequence of indiscriminate use of fluconazole for prophylaxis and treatment and that suboptimal adherence to IPC practices caused the transmission of the pathogen within hospitals. This setting is the same one in which *C. auris* has become endemic and has caused large hospital outbreaks.

The trend we observed is consistent with increased detection of *C. auris* in other regions of the world. For instance, India has seen a large increase in the number of *C. auris* cases, from 12 in 2013 to ≥350 in 2017 (*13*). By the end of May 2018, the United States had 311 cases and 29 probable cases of *C. auris* (*14*).

Although *C. auris* has now been isolated from ≥94 hospitals across South Africa, most cases were detected at a small number of hospitals in a restricted geographic region. Focused attention on antifungal stewardship and multimodal IPC interventions at these facilities could limit further outbreaks and minimize transmission of this pathogen within South Africa and across South Africa's borders. Cross-border transmission from South Africa has already been documented (*15*). However, *C. auris* is notoriously difficult to eradicate from hospitals or units once it has become endemic, in part because of its ability to adhere to polymeric surfaces and form biofilms (*16*). Thorough decontamination has been recommended to reduce the environmental bioburden (*2*).

Early detection of *Candida* species is recommended to facilitate appropriate treatment and implement IPC measures; however, standard biochemical platforms cannot reliably identify *C. auris* in microbiology laboratories. Many diagnostic pathology laboratories in South Africa used methods that could not reliably identify *C. auris* during the surveillance period, but these methods have been largely replaced in 2018 with more accurate methods of identification, including Vitek 2 YST-ID with version 8.01 software (bioMérieux), matrix-assisted laser desorption/ionization-time
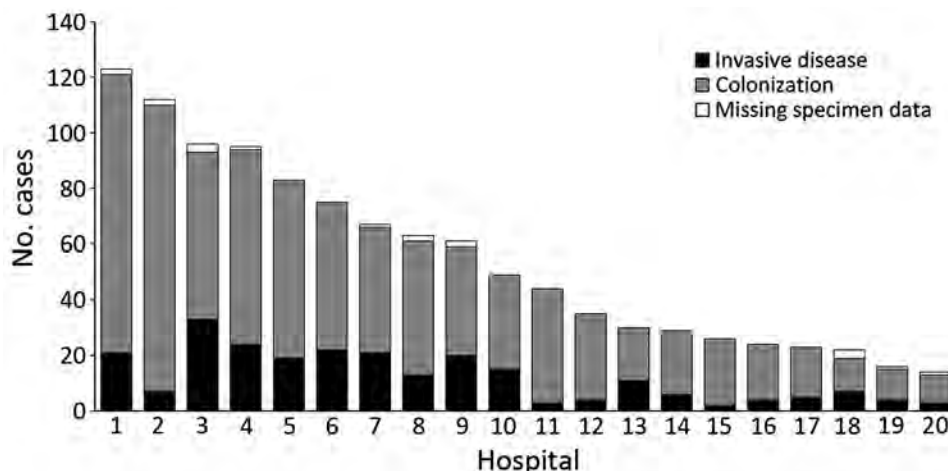

Figure 1. Distribution of cases of *Candida auris* by type of infection, South Africa, 2012–2016. Data are from the top 20 private hospitals that reported cases. n = 1,087.
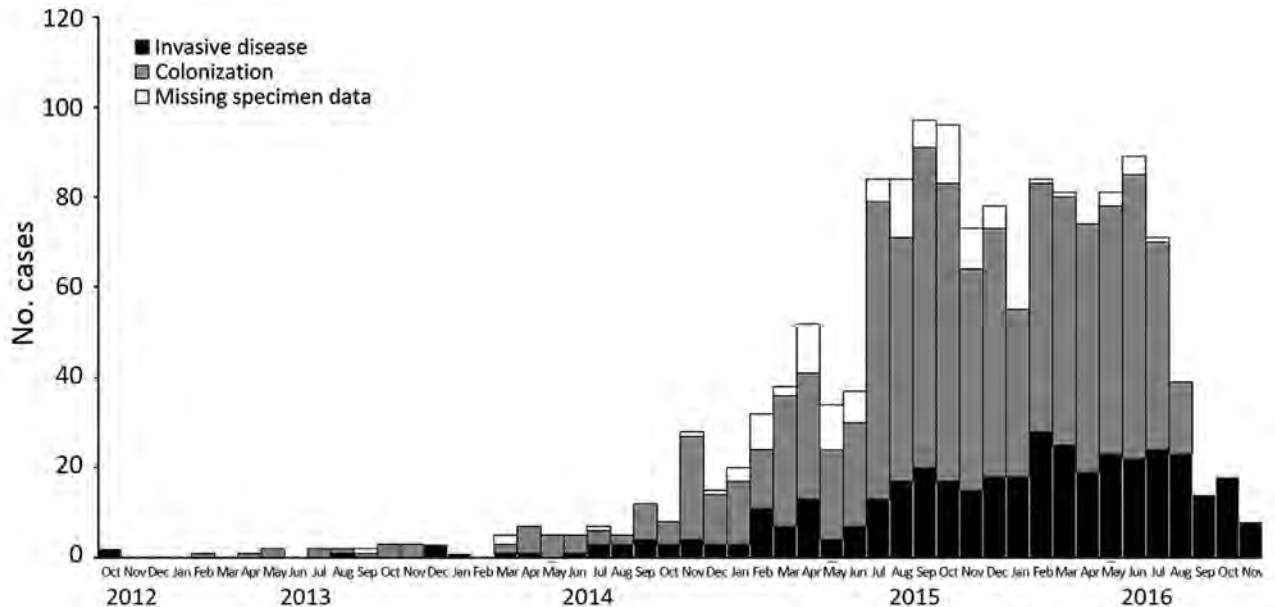
Figure 2. Distribution of cases of *Candida auris* by type of infection and date of specimen collection, South Africa, 2012–2016. n = 1,306.

of flight mass spectrometry or internal transcribed spacer, and D1/D2 sequencing (*9*).

Our study provides a national picture of the emergence of *C. auris* in public and private hospitals. However, the surveillance was limited in several respects. We may have underestimated the number of cases in the public sector because NHLS laboratories did not routinely identify isolates from nonsterile sites to species level; even so, the geographic distribution of cases in the private sector is likely to be accurate. The 4 large private pathology practices that contributed data to the study have a combined national coverage of the private health sector. In addition, we have observed a similar geographic distribution of cases of *C. auris* candidemia detected through our national active population-based surveillance (*6*). We believe that we have observed a real increase in cases over time; this finding is particularly true for private laboratories where *Candida* was routinely identified to species level even from nonsterile sites across the surveillance period. However, some laboratories may have changed their species-level identification practices in response to the emergence of *C. auris*. We included *C. haemulonii* in the case definition because many laboratories used the Vitek 2 YST system without a software update at the time of surveillance, but we did not include yeasts for which other diagnostic platforms can mistake *C. auris*. In addition, cases were diagnosed at some but not all facilities on the basis of clinicians submitting appropriate specimens for fungal culture or of IPC practitioners performing active screening for colonization. We extracted routine laboratory data, often with missing data elements, from several sources and applied a specific surveillance case definition. Deduplication of data to patient

level may have been flawed because unique identifiers are not universally used in the healthcare system.

In conclusion, we report a large increase in cases of *C. auris* invasive disease and colonization since the first isolation of this yeast in South Africa in 2009. The increase is mostly attributable to cases in private hospitals in Gauteng Province.

Conflict of interest: Over the last 36 months, N.P.G. has received a speaker honorarium from Astellas (2015) and a travel grant to a conference from MSD (Pty) Ltd. (2015). No other conflicts are declared.

About the Author

Dr. Govender is head of the Centre for Healthcare-Associated Infections, Antimicrobial Resistance, and Mycoses at the National Institute for Communicable Diseases, Johannesburg, South Africa. He is a medical doctor with a specialist qualification in clinical microbiology and training in medical mycology and epidemiology. His primary research interest is the prevention and control of invasive mycoses in resource-limited settings.

References

1. Magobo RE, Corcoran C, Seetharam S, Govender NP. *Candida auris*–associated candidemia, South Africa. Emerg Infect Dis. 2014;20:1250–1. http://dx.doi.org/10.3201/eid2007.131765
2. Jeffery-Smith A, Taori SK, Schelenz S, Jeffery K, Johnson EM, Borman A, et al.; Candida auris Incident Management Team. *Candida auris*: a review of the literature. Clin Microbiol Rev. 2017;31:e00029-17. http://dx.doi.org/10.1128/CMR.00029-17
3. Escandón P, Chow NA, Caceres DH, Gade L, Berkow EL, Armstrong P, et al. Molecular epidemiology of *Candida auris* in Colombia reveals a highly related, countrywide colonization with regional patterns in amphotericin B resistance. Clin Infect Dis. 2018. http://dx.doi.org/10.1093/cid/ciy411

4. Sherry L, Ramage G, Kean R, Borman A, Johnson EM, Richardson MD, et al. Biofilm-forming capability of highly virulent, multidrug-resistant *Candida auris*. Emerg Infect Dis. 2017;23:328–31. http://dx.doi.org/10.3201/eid2302.161320

5. Ku TSN, Walraven CJ, Lee SA. *Candida auris*: disinfectants and implications for infection control. Front Microbiol. 2018;9:726. http://dx.doi.org/10.3389/fmicb.2018.00726

6. van Schalkwyk E, Shuping L, Ismail H, Thomas J, Govender NP. Independent risk factors associated with *Candida auris* candidaemia in South Africa—an analysis of national surveillance data, 2016–2017. In: Oral Presentation Abstracts of the 7th Conference of the Federation of Infectious Disease Societies of Southern Africa (FIDSSA); Cape Town, South Africa; 2017 Nov 9–11; Abstract ID8382. S Afr J Infect Dis. 2017 Suppl.

7. Lockhart SR, Etienne KA, Vallabhaneni S, Farooqi J, Chowdhary A, Govender NP, et al. Simultaneous emergence of multidrug-resistant *Candida auris* on 3 continents confirmed by whole-genome sequencing and epidemiological analyses. Clin Infect Dis. 2017;64:134–40. http://dx.doi.org/10.1093/cid/ciw691

8. Chowdhary A, Sharma C, Meis JF. *Candida auris*: a rapidly emerging cause of hospital-acquired multidrug-resistant fungal infections globally. PLoS Pathog. 2017;13:e1006290. http://dx.doi.org/10.1371/journal.ppat.1006290

9. Mizusawa M, Miller H, Green R, Lee R, Durante M, Perkins R, et al. Can multidrug-resistant *Candida auris* be reliably identified in clinical microbiology laboratories? J Clin Microbiol. 2017;55:638–40. http://dx.doi.org/10.1128/JCM.02202-16

10. White TJ, Bruns T, Lee S, Taylor J. Amplification and direct sequencing of fungal ribosomal RNA genes for phylogenetics. In: Innis MA, Gelfand,H, Sninsky JJ, White TJ, editors. PCR protocols: a guide to methods and application. London: Academic Press; 1990. p. 315–322.

11. National Institute for Communicable Diseases. Interim guidance for management of *Candida auris* infections in South African hospitals. 2016 Dec [cited 2018 Jul 17] http://www.nicd.ac.za/index.php/candida-auris/

12. Govender NP, Patel J, Magobo RE, Naicker S, Wadula J, Whitelaw A, et al.; TRAC-South Africa group. Emergence of azole-resistant *Candida parapsilosis* causing bloodstream infection: results from laboratory-based sentinel surveillance in South Africa. J Antimicrob Chemother. 2016;71:1994–2004. http://dx.doi.org/10.1093/jac/dkw091

13. Chowdhary A, Prakash A, Sharma C, Kordalewska M, Kumar A, Sarma S, et al. A multicentre study of antifungal susceptibility patterns among 350 *Candida auris* isolates (2009–17) in India: role of the ERG11 and FKS1 genes in azole and echinocandin resistance. J Antimicrob Chemother. 2018;73:891–9. http://dx.doi.org/10.1093/jac/dkx480

14. Centers for Disease Control and Prevention. Tracking *Candida auris*. 2018 Jun 22 [cited 2018 Jul 17]. https://www.cdc.gov/fungal/candida-auris/tracking-c-auris.html

15. Belkin A, Gazit Z, Keller N, Ben-Ami R, Wieder-Finesod A, Novikov A, et al. *Candida auris* infection leading to nosocomial transmission, Israel, 2017. Emerg Infect Dis. 2018;24:801–4. http://dx.doi.org/10.3201/eid2404.171715

16. Welsh RM, Bentz ML, Shams A, Houston H, Lyons A, Rose LJ, et al. Survival, persistence, and isolation of the emerging multidrug-resistant pathogenic yeast *Candida auris* on a plastic health care surface. J Clin Microbiol. 2017;55:2996–3005. http://dx.doi.org/10.1128/JCM.00921-17

Address for correspondence: Nelesh P. Govender, National Institute for Communicable Diseases, Centre for Healthcare-Associated Infections, Antimicrobial Resistance and Mycoses, Private Bag X4, Sandringham, 2132, South Africa; email: neleshg@nicd.ac.za

Rickettsia rickettsii Co-feeding Transmission among *Amblyomma aureolatum* Ticks

Jonas Moraes-Filho, Francisco B. Costa, Monize Gerardi, Herbert S. Soares, Marcelo B. Labruna

Amblyomma aureolatum ticks are vectors of *Rickettsia rickettsii*, the etiologic agent of Rocky Mountain spotted fever in Brazil. Maintenance of *R. rickettsii* in nature depends on by horizontal transmission along tick generations. Although such transmission is known to occur when uninfected and infected ticks feed simultaneously on susceptible animals (co-feeding systemic transmission), we investigated co-feeding nonsystemic transmission, which was based on *R. rickettsii*–infected and –uninfected *A. aureolatum* ticks feeding simultaneously on guinea pigs immune to *R. rickettsii*. Our acquisition and transmission infestations demonstrated that horizontal transmission of *R. rickettsii* by co-feeding ticks on immune hosts with no systemic infection did not occur when uninfected larvae fed distantly from infected nymphs but did occur in a few cases when uninfected larvae fed side-by-side with infected nymphs, suggesting that they shared the same feeding site. The co-feeding nonsystemic transmission type might have no epidemiologic importance for Rocky Mountain spotted fever.

T he bacterium *Rickettsia rickettsii* is the etiologic agent of Rocky Mountain spotted fever or Brazilian spotted fever (*1*). In Brazil, where Brazilian spotted fever fatality rates are >50% (*2*), *R. rickettsii* is transmitted to humans by 2 tick species, *Amblyomma aureolatum* and *A. sculptum* (*3*). Although *R. rickettsii* is transovarially transmitted in ticks, the vertical transmission is not sufficient to guarantee maintenance of this bacterium in the tick population because of low rates of transovarial transmission (*A. sculptum*) (*4*) or because of a higher mortality rate for infected ticks (*A. aureolatum*) (*5*). In either case, the creation of new cohorts of infected ticks by horizontal transmission along tick generations is required for the successful establishment of *R. rickettsii* infection in the tick population (*5*).

Since the classical works of Ricketts (*6*) and subsequent rickettsiologists (*7–9*), horizontal transmission of

Author affiliations: Universidade Santo Amaro, São Paulo, Brazil
(J. Moraes-Filho); University of São Paulo, São Paulo
(J. Moraes-Filho, F.B. Costa, M. Gerardi, H.S. Soares, M.B.
Labruna); Universidade Estadual do Maranhão, São Luís, Brazil
(F.B. Costa).

R. rickettsii has been believed to depend chiefly on the simultaneous feeding of uninfected and infected immature ticks on susceptible animals, also called amplifying hosts (*3,10*). Once infested by an *R. rickettsii*–infected tick, the host develops a systemic infection (rickettsemia) lasting ≈1–3 weeks, during which time uninfected ticks acquire rickettsial infection upon feeding (*7–9*). After this period, the host develops an immune response that precludes new rickettsemia, even when infested again by *R. rickettsii*–infected ticks (*7–9*). Based on these premises, it has been proposed that each individual amplifying host will generate only 1 rickettsemia of 1–3 weeks in its lifespan; thereafter, the host becomes immune to *R. rickettsii* infection (*3,8,11*).

Niebylski et al. (*10*) reported that transmission between co-feeding ticks and by transovarial transmission might further enhance rickettsial infection rates in ticks. In this case, co-feeding refers to the simultaneous feeding of uninfected and infected immature ticks on susceptible host animals (amplifying hosts developing rickettsemia), as reported previously (*6–9*). In the late 1980 and the 1990s, the term co-feeding was introduced for nonsystemic transmission of tickborne viruses in vertebrate hosts (*12–14*). Since then, use of the term co-feeding has apparently generated confusion. Indeed, co-feeding means that ≥2 ticks are feeding simultaneously on the same individual host. Co-feeding ticks can result in 2 main types of horizontal transmission of pathogens: 1) systemic transmission, (e.g., *R. rickettsii*) (*10*); and 2) nonsystemic transmission, (e.g., tickborne encephalitis virus) (*13,14*). Because the co-feeding systemic transmission type is well known for *R. rickettsii* in ticks, we evaluated the occurrence of the co-feeding nonsystemic transmission type in an *A. aureolatum–R. rickettsii*–guinea pig model.

Materials and Methods

Tick Colony and *R. rickettsii* Infection

During 2012, we established a laboratory colony of *A. aureolatum* ticks in the laboratory from engorged females free of rickettsial infection collected on dogs in São Bernardo do Campo in the São Paulo metropolitan area of Brazil, as described (*15*). We divided this colony into 2 cohorts; 1

was experimentally infected by *R. rickettsii*, and the other remained uninfected. The infected cohort was created by allowing larvae to feed on rickettsemic guinea pigs that were intraperitoneally inoculated with the Taiaçu strain of *R. rickettsii*, as described elsewhere (*5,15*). Molecular analysis (detection of rickettsial DNA in postmolting ticks) and feeding on guinea pigs (successful transmission of rickettsia) showed that 100% of the ticks from this cohort were infected by *R. rickettsii* (*15*). For this study, we used nymphs from the infected cohort for rickettsia-donor feeding (for transmission of *R. rickettsii* to guinea pigs) and larvae from the uninfected cohort for acquisition feeding. The Ethical Committee in Animal Research of the Faculty of Veterinary Medicine of the University of São Paulo approved this study.

Acquisition Infestation 1: Susceptible Guinea Pigs

Each of 6 tick-naive (with no previous tick infestation) adult male guinea pigs (guinea pigs 1–6), >5 mo old, weighing >500 g, seronegative for *R. rickettsii* 1 day before tick infestation, had 2 cotton sleeves (5-cm diameter feeding chamber) glued to its shaved dorsum, as described (*16*). The minimum distance between the 2 chambers was 3 cm. On day 0, one chamber received 50 *R. rickettsii*–infected nymphs (IN); on day 3, each of the 2 chambers received 200–300 uninfected larvae (UL). Therefore, in each of the 6 guinea pigs, UL fed with IN inside 1 chamber with the chance to share the same feeding site (Figure). This condition was possible because *A. aureolatum* nymphs take 5–9 days to complete engorgement on guinea pigs (*17*). In the second chamber, UL fed physically separated from IN. All
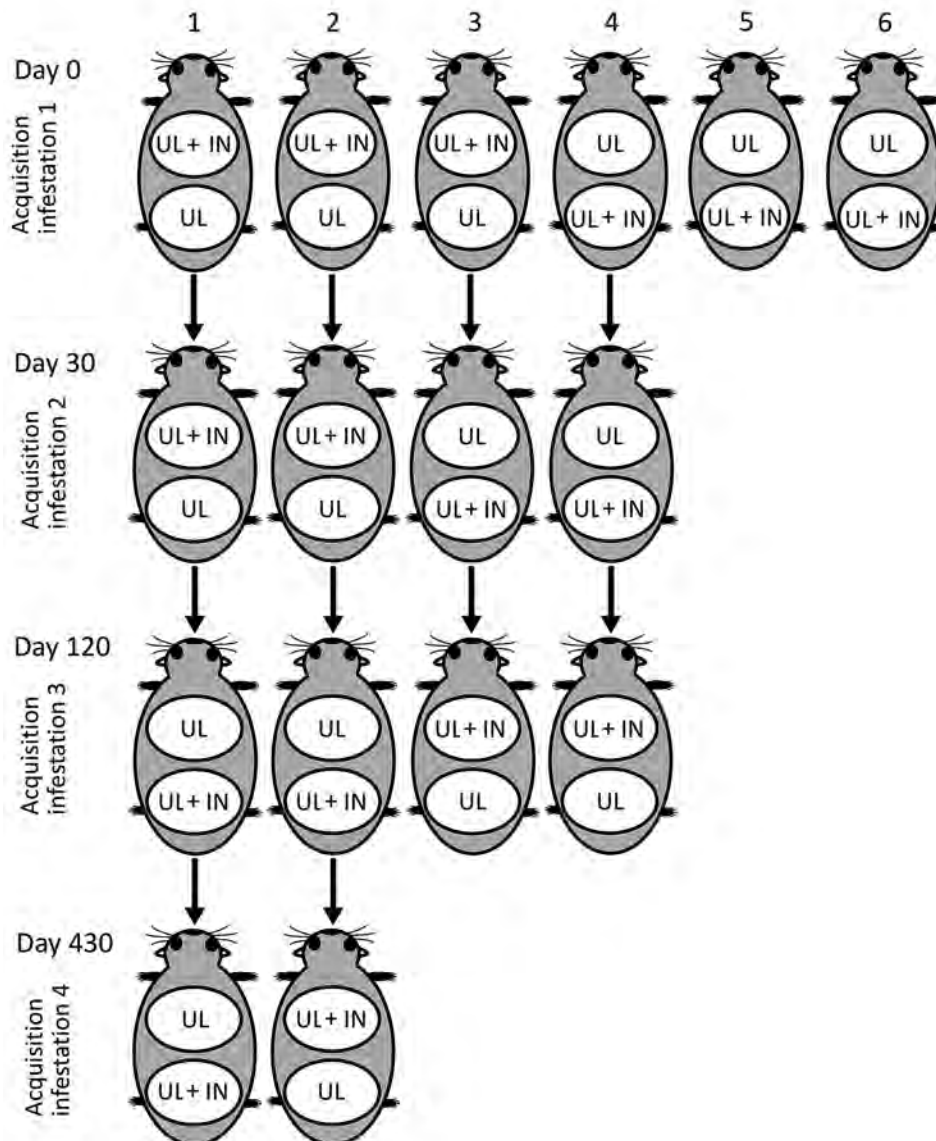
Figure. Experimental procedures to evaluate co-feeding transmission of *Rickettsia rickettsii* among *Amblyomma aureolatum* ticks on 6 guinea pigs (as numbered) subjected to up to 4 consecutive infestations at 0, 30, 120, and 430 days postinfestation, Brazil. Each guinea pig in each acquisition infestation had 2 cotton sleeves (feeding chambers) glued to its shaved back; the 2 chambers each received 200–300 UL, whereas only 1 chamber received 50 *R. rickettsii* IN. White oval indicates feeding chamber. IN, infected nymph; UL, uninfected larvae.

infested animals had their temperature rectally measured daily from the day of infestation (day 0) to 21 days postinfestation (dpi). Guinea pigs were considered febrile if rectal temperature reached >39.5°C. To prevent deaths of these animals, they were treated with a single intramuscular dose of doxycycline (20 mg/kg) at the second febrile day. All animals were tested for seroconversion to *R. rickettsii* antigens at 21 dpi by immunofluorescence assay, as described (*18*). Animals were considered seronegative if their serum IgG was not reactive at the 1:64 dilution. If serum was reactive at the 1:64 dilution, it was titrated to determine endpoint titers to *R. rickettsii*. Each day we recovered naturally detached engorged larvae and nymphs from the feeding chambers and immediately placed them in an incubator (23°C, 95% relative humidity) for molting. From the resultant molted nymphs and adult ticks, a random sample was submitted to DNA extraction by the guanidine isothiocyanate-phenol technique (*19*) 10–20 days after molting and tested by a Taqman real-time PCR targeting the rickettsial *gltA* gene, as described (*20*), to determine the proportion of ticks that contained rickettsial DNA. The sensitivity of this PCR was determined to be 1 DNA copy of *R. rickettsii* (*20*).

Acquisition Infestations 2, 3, and 4: Immune Guinea Pigs

We used 4 guinea pigs from acquisition infestation 1 (guinea pigs 1–4) for acquisition infestations 2 and 3, conducted 30 and 120 days, respectively, after acquisition infestation 1. We used guinea pigs 1 and 2 in acquisition infestation 4, conducted 330 days after acquisition infestation 1. In all cases, each animal had 2 feeding chambers, which received *R. rickettsii* IN, UL, or both, as described for acquisition infestation 1 (Figure). We collected a blood sample on the infestation day to determine the endpoint titer to *R. rickettsii* when guinea pigs received the *R. rickettsii*–IN. Measurements of rectal temperature, recovery of engorged ticks, and molecular tests of ticks were performed as described for acquisition infestation 1.

Transmission Infestations

Unfed nymphs derived from engorged larvae in acquisition infestations 1–4 were used to infest 29 naive adult guinea pigs (guinea pigs 11–39), >3 mo old, weighing >300 g. We considered horizontal transmission of *R. rickettsii* as successful only if these nymphs transmitted rickettsia to these guinea pigs. For this purpose, each guinea pig was prepared with a single feeding chamber that received 20 unfed nymphs derived from engorged larvae from a single feeding chamber in each of the acquisition infestations. This procedure evaluated rickettsial transmission by nymphs that had fed as larvae in the same chamber with IN and by nymphs that had fed as larvae in a chamber physically separated from IN. Procedures for rectal temperature

and seroconversion were as described previously. No febrile guinea pig was treated with doxycycline in these transmission infestations; therefore, if infested guinea pigs died before the 21 dpi, a spleen fragment was submitted to DNA extraction by using the DNeasy Blood and Tissue Kit (QIAGEN, Chatsworth, CA, USA) and tested by the same PCR protocol referenced earlier. Naturally detached engorged nymphs were allowed to molt to adults and then tested by real-time PCR as described for acquisition ticks.

Results

Acquisition Infestation 1

All 6 guinea pigs (nos. 1–6) manifested fever, starting at 5–9 dpi. Larval infestation was done 3 days after the nymphal infestation; therefore, the larval feeding period (4–7 days) overlapped with nymphal feeding (5–9 days) and with febrile periods of the 6 guinea pigs. On the second day of fever, each guinea pig was treated with doxycycline, which resolved fever in 48 h, when most of the larvae had already completed feeding. Blood samples collected at 21 dpi showed seroconversion to *R. rickettsii* (endpoint titers 8,192–65,536). From the engorged larvae and nymphs collected from guinea pigs 1–6, unfed nymphs and adults, respectively, were tested by PCR after molting (Table 1). In all cases, 100% of the ticks contained rickettsial DNA, regardless of the feeding chamber (Table 1). This result demonstrated that *A. aureolatum* larvae acquired rickettsial DNA by feeding either separated from IN (feeding chamber UL) or by feeding together with IN within the same chamber (feeding chamber UL + IN).

Acquisition Infestation 2

This infestation was performed on guinea pigs 1–4, at 30 days after acquisition infestation 1, when their endpoint titers to *R. rickettsii* were 32,768–65,536. None of the 4 guinea pigs manifested fever (Table 2). Unfed nymphs and adults that molted from engorged larvae and nymphs, respectively, were tested by PCR. All adult ticks (derived from *R. rickettsii*–IN) contained rickettsial DNA. None of the unfed nymphs derived from the feeding chamber UL (UL feeding physically separated from IN) contained rickettsia. Similarly, for 2 guinea pigs (nos. 1, 2), none of the unfed nymphs derived from engorged larvae that fed in feeding chamber UL + IN (UL feeding together with IN) contained rickettsia; in contrast, for guinea pigs 3 and 4, 17.7%–33.3% of the unfed nymphs derived from feeding chamber UL + IN contained rickettsial DNA. This result demonstrated that *A. aureolatum* larvae did not acquire rickettsial DNA by feeding separated from IN (feeding chamber UL). When feeding together with IN within the same chamber (feeding chamber UL + IN), for guinea pigs 3 and 4, a minority of *A. aureolatum* larvae acquired

Table 1. *Rickettsia rickettsii* acquisition infestation 1 with *Amblyomma aureolatum* ticks on 6 guinea pigs, Brazil*

Guinea pig	Fever onset, dpi (maximum temperature, °C)	IFA endpoint titer at 21 dpi†	Feeding chamber‡	PCR on ticks after molting, no. infected/no. tested (% infected)	
				Unfed nymphs	Unfed adults
1	6 (40.3)	65,536	UL + IN	10/10 (100)	10/10 (100)
			UL	10/10 (100)	
2	8 (40.0)	65,536	UL + IN	9/9 (100)	10/10 (100)
			UL	10/10 (100)	
3	8 (40.5)	8,192	UL + IN	15/15 (100)	5/5 (100)
			UL	15/15 (100)	
4	5 (40.7)	65,536	UL	15/15 (100)	
			UL + IN	15/15 (100)	8/8 (100)
5	9 (40.0)	16,384	UL	15/15 (100)	
			UL + IN	15/15 (100)	8/8 (100)
6	7 (40.4)	16,384	UL	15/15 (100)	
			UL + IN	15/15 (100)	6/6 (100)

*Each guinea pig was infested on day 0 with *R. rickettsii* IN and on day 3 with UL. Recovered engorged larvae and nymphs were allowed to molt to nymphs and adult ticks, respectively, which were tested by real-time PCR for presence of rickettsial DNA. dpi, days postinfestation; IFA, immunofluorescence assay; IN, infected nymphs; UL, uninfected larvae.
†Blood was collected at 21 dpi and tested by IFA with *R. rickettsii* antigens.
‡Tick infestations were performed on 2 feeding chambers glued to the shaved back of each guinea pig, 1 chamber receiving IN and UL, the other receiving only UL (Figure).

rickettsial DNA, whereas for guinea pigs 1 and 2, *A. aureolatum* larvae did not acquire rickettsial DNA.

Acquisition Infestation 3

This infestation was performed on guinea pigs 1–4 at 120 and 90 days after acquisition infestations 1 and 2, respectively, when their endpoint titers to *R. rickettsii* were 4,096–16,384. None of the 4 animals manifested fever (Table 3). Unfed nymphs and adults that molted from engorged larvae and nymphs, respectively, were tested by PCR. All adult ticks (derived from *R. rickettsii*–IN) contained rickettsial DNA. In guinea pigs 1 and 2, none of the unfed nymphs derived from both feeding chambers (UL or UL + IN) contained rickettsial DNA. For guinea pigs 3 and 4, 10%–28.6% of the unfed nymphs derived from feeding chamber UL + IN contained rickettsial DNA, as did 12.0%–16.7% of the unfed nymphs derived from feeding chamber UL (Table 3). This result demonstrated that, for 2 animals, *A. aureolatum* larvae did not acquire rickettsial DNA by feeding either separated from IN (feeding chamber UL) or together with IN (feeding chamber UL + IN). In 2 other animals, a minority of *A. aureolatum* larvae acquired rickettsial DNA by feeding either separated from IN (feeding chamber UL) or together with IN (feeding chamber UL + IN).

Acquisition Infestation 4

This infestation was performed on guinea pigs 1 and 2 at 430, 400, and 310 days after acquisition infestations 1, 2, and 3, respectively, when their endpoint titers to *R. rickettsii* were 512–4,096. Neither animal manifested fever (Table 4). Unfed nymphs and adults that molted from engorged larvae and nymphs, respectively, were tested by PCR. All adult ticks (derived from *R. rickettsii*–IN) contained rickettsial DNA. No engorged larvae were recovered from guinea pig 1; therefore, there was no molted nymph to be tested. In guinea pig 2, 8.4% of the unfed nymphs derived from feeding chamber UL + IN contained rickettsial DNA, as did 12.5% of the unfed nymphs derived from feeding chamber UL (Table 4).

Table 2. *Rickettsia rickettsii* acquisition infestation 2 with *Amblyomma aureolatum* ticks on 4 guinea pigs 30 days after acquisition infestation 1, Brazil*

Guinea pig	Temperature range, °C	IFA endpoint titer at day 0†	Feeding chamber‡	PCR on ticks after molting, no. infected/no. tested (% infected)	
				Unfed nymphs	Unfed adults
1	No fever to 38.8	32,768	UL + IN	0/10 (0)	2/2 (100)
			UL	0/10 (0)	
2	No fever to 38.4	32,768	UL + IN	0/10 (0)	3/3 (100)
			UL	0/10 (0)	
3	No fever to 39.1	32,768	UL	0/30 (0)	
			UL + IN	10/30 (33)	3/3 (100)
4	No fever to 39.2	65,536	UL	0/30 (0)	
			UL + IN	5/30 (17)	3/3 (100)

*Each guinea pig was infested on day 0 with *R. rickettsii* IN and on day 3 with UL. Recovered engorged larvae and nymphs were allowed to molt to nymphs and adult ticks, respectively, which were tested by real-time PCR for presence of rickettsial DNA. dpi, days postinfestation; IFA, immunofluorescence assay; IN, infected nymphs; UL, uninfected larvae.
†Blood was collected at day 0 (30 days after acquisition infestation 1) and tested by IFA with *R. rickettsii* antigens.
‡Tick infestations were performed on 2 feeding chambers glued to the shaved back of each guinea pig, 1 chamber receiving IN and UL, the other receiving only UL (Figure).

Table 3. *Rickettsia rickettsii* acquisition infestation 3 with *Amblyomma aureolatum* ticks on 4 guinea pigs 120 days after acquisition infestation 1, Brazil*

Guinea pig	Temperature range, °C	IFA endpoint titer†	Feeding chamber‡	PCR on ticks after molting, no. infected/no. tested (% infected)	
				Unfed nymphs	Unfed adults
1	No fever to 38.9	16,384	UL	0/13 (0)	
			UL + IN	0/13 (0)	5/5 (100)
2	No fever to 39.2	8,192	UL	0/13 (0)	
			UL + IN	0/13 (0)	7/7 (100)
3	No fever to 38.9	4,096	UL + IN	2/7 (29)	8/8 (100)
			UL	3/25 (12)	
4	No fever to 38.5	4,096	UL + IN	3/30 (10)	4/4 (100)
			UL	5/30 (17)	

*Each guinea pig was infested on day 0 with *R. rickettsii* IN and on day 3 with UL. Recovered engorged larvae and nymphs were allowed to molt to nymphs and adult ticks, respectively, which were tested by real-time PCR for presence of rickettsial DNA. dpi, days postinfestation; IFA, immunofluorescence assay; IN, infected nymphs; UL, uninfected larvae.
†Blood was collected at day 0 (120 and 90 days after acquisition infestations 1 and 2, respectively) and tested by IFA with *R. rickettsii* antigens.
‡Tick infestations were performed on 2 feeding chambers glued to the shaved back of each guinea pig; 1 chamber receiving IN and UL, the other receiving only UL (Figure).

Transmission Infestations

Nymphs from acquisition infestation 1, which fed as larvae on febrile guinea pigs, were used to infest 7 guinea pigs (nos. 11–17). In all animals, fever developed that started 6–7 dpi. Two animals died during the febrile period, and their spleens contained rickettsial DNA. The remaining 5 guinea pigs seroconverted for *R. rickettsii* with endpoint titers of 65,536. Engorged nymphs recovered from these guinea pigs molted to adults, all of which contained rickettsial DNA (Table 5).

Nymphs from acquisition infestation 2, which fed as larvae on immune guinea pigs, were used to infest 12 guinea pigs (nos. 18–29). In every case in which the nymphs derived from engorged larvae that had fed alone in feeding chamber UL, no rickettsial transmission occurred (nos. 18–23). When nymphs derived from engorged larvae that had fed with *R. rickettsii* IN within the same chamber (UL + IN), absence of rickettsial transmission was demonstrated in 4 guinea pigs (nos. 24, 25, 28, 29), whereas rickettsial transmission was demonstrated by fever and seroconversion in 2 guinea pigs (nos. 26, 27). PCR on ticks demonstrated no rickettsial DNA in adult ticks that molted from engorged nymphs recovered from guinea pigs 18–25 and 28–29, which did not develop fever or serocont. On the other hand, rickettsial DNA was

detected in most (80.0%–91.7%) of adult ticks that molted from engorged nymphs fed on guinea pigs 26 and 27, in which rickettsiosis developed.

We used nymphs from acquisition infestation 3, which fed as larvae on immune guinea pigs, to infest 8 guinea pigs (nos. 30–37). In every case where the nymphs derived from engorged larvae that had fed alone in feeding chamber UL, no rickettsial transmission occurred (guinea pigs 30–33). When nymphs derived from engorged larvae that had fed with *R. rickettsii* IN within the same chamber (UL + IN), absence of rickettsial transmission was demonstrated in 3 guinea pigs (nos. 34, 35, 37), whereas rickettsial transmission was demonstrated by fever and seroconversion in only guinea pig 36. PCR on ticks demonstrated no rickettsial DNA in adult ticks that molted from engorged nymphs recovered from guinea pigs 30–35 and 37. Conversely, we detected rickettsial DNA in 100% of adult ticks that molted from engorged nymphs fed on guinea pig 36, in which rickettsiosis developed.

Nymphs from acquisition infestation 4, which fed as larvae on a single immune guinea pig, were used to infest 2 guinea pigs (nos. 38, 39). When nymphs derived from engorged larvae that had fed alone in feeding chamber UL, no rickettsial transmission occurred. When nymphs derived from engorged larvae that had fed with *R. rickettsii*

Table 4. *Rickettsia rickettsii* acquisition infestation 4 with *Amblyomma aureolatum* ticks on 2 guinea pigs 430 days after acquisition infestation 1, Brazil*

Guinea pig	Temperature range, °C	IFA endpoint titer†	Feeding chambers‡	PCR on ticks after molting, no. infected/no. tested (%)	
				Unfed nymphs	Unfed adults
1	No fever to 38.7	4,096	UL	ND	
			UL + IN	ND	2/2 (100)
2	No fever to 38.7	512	UL	2/16 (13)	
			UL + IN	1/12 (8)	5/5 (100)

*Each guinea pig was infested on day 0 with *R. rickettsii* IN and on day 3 with UL. Recovered engorged larvae and nymphs were allowed to molt to nymphs and adult ticks, respectively, which were tested by real-time PCR for presence of rickettsial DNA. dpi, days postinfestation; IFA, immunofluorescence assay; IN, infected nymphs; ND, not done because very few engorged larvae were recovered from the animal; UL, uninfected larvae.
†Blood was collected at day 0 (430, 400, and 310 days after acquisition infestations 1, 2, and 3, respectively) and tested by IFA with *R. rickettsii* antigens.
‡Tick infestations were performed on 2 feeding chambers glued to the shaved back of each guinea pig, 1 chamber receiving IN and UL, the other receiving only UL (Figure).

Table 5. Transmission infestations on 29 naive guinea pigs infested with *Amblyomma aureolatum* nymphs derived from larvae that had co-fed with *Rickettsia rickettsii*–infected nymphs on 6 guinea pigs during acquisition infestations, Brazil*

	Origin of nymphs		Transmission infestation					PCR on unfed adult ticks after molting from engorged nymphs, no. infected ticks/no. tested ticks (% infection)
AI	Guinea pig†	Feeding chamber†	Guinea pig	Fever onset, dpi	Maximum temperature, °C	Died	IFA endpoint titer‡	
1	3	UL	11	6	39.6	No	65,536	2/2 (100)
	4	UL	12	7	40.7	Yes§	ND	8/8 (100)
	5	UL	13	7	40.4	No	65,536	7/7 (100)
	6	UL	14	7	40.7	No	65,536	14/14 (100)
	3	UL + IN	15	6	40.9	No	65,536	6/6 (100)
	4	UL + IN	16	6	40.3	Yes§	ND	6/6 (100)
	5	UL + IN	17	7	40.6	No	65,536	5/5 (100)
2	1	UL	18	No fever–38.6		No	<64	0/10 (0)
	2	UL	19	No fever–39.1		No	<64	0/10 (0)
	3	UL	20	No fever–39.1		No	<64	0/15 (0)
	3	UL	21	No fever–38.7		No	<64	0/12 (0)
	4	UL	22	No fever–38.8		No	<64	0/8 (0)
	4	UL	23	No fever–39.4		No	<64	0/17 (0)
	1	UL + IN	24	No fever–38.8		No	<64	0/10 (0)
	2	UL + IN	25	No fever–39.4		No	<64	0/10 (0)
	3	UL + IN	26	8–40.6		No	16,384	11/12 (92)
	3	UL + IN	27	13–40.2		No	65,536	8/10 (80)
	4	UL + IN	28	No fever–38.8		No	<64	0/10 (0)
	4	UL + IN	29	No fever–39.4		No	<64	0/10 (0)
3	1	UL	30	No fever–39.3		No	<64	0/5 (0)
	2	UL	31	No fever–39.2		No	<64	0/5 (0)
	3	UL	32	No fever–39.4		No	<64	0/10 (0)
	4	UL	33	No fever–39.1		No	<64	0/11 (0)
	1	UL + IN	34	No fever–39.0		No	<64	0/5 (0)
	2	UL + IN	35	No fever–39.0		No	<64	0/8 (0)
	3	UL + IN	36	6–40.9		No	32,768	7/7 (100)
	4	UL + IN	37	No fever–38.9		No	<64	0/7 (0)
4	2	UL	38	No fever–38.8		No	<64	0/10 (0)
	2	UL + IN	39	10–40.1		No	32,768	10/10 (100)

*AI, acquisition infestation (see Figure 1 and Tables 1–4); dpi, days postinfestation; IN, infected nymphs; ND, not done; UL, uninfected larvae.
†See Figure and Tables 1–4.
‡Blood was collected at 21 days dpi and tested by IFA with *R. rickettsii* antigens.
§This guinea pig died during the febrile period; its spleen was shown by real-time PCR to contain rickettsial DNA.

IN within the same chamber (UL + IN), rickettsial transmission was demonstrated by fever and seroconversion in guinea pig 39. PCR on ticks demonstrated no rickettsial DNA in adult ticks that molted from engorged nymphs recovered from guinea pig 38. Contrastingly, rickettsial DNA was detected in 100% of adult ticks that molted from engorged nymphs fed on guinea pig 39, in which rickettsiosis developed.

In summary, in all cases of rickettsial transmission by nymphs derived from engorged larvae that had fed on immune guinea pigs, the acquisition feeding was from the feeding chamber UL + IN, in which UL had fed with IN (guinea pigs 26, 27, 36, 39) (Table 5). In contrast, in the other 7 guinea pigs (nos. 24, 25, 28, 29, 34, 35, 37), which were infested with nymphs from acquisition feeding in chamber UL + IN, no rickettsial transmission occurred. We observed no rickettsial transmission in the 11 guinea pigs (nos. 18–23, 30–33, 38) that were infested by nymphs derived from engorged larvae that had fed physically separated from IN in feeding chamber UL on immune guinea pigs, even though a few of these nymphs contained rickettsial DNA after molting (Table 3, guinea pigs 3 and 4; Table 4, guinea pig 2).

We tested random samples of 5 real-time PCR–positive nymphs and adults from acquisition/transmission infestations by conventional PCR targeting a 532-bp fragment of the rickettsial *ompA* gene (*21*). PCR products were DNA sequenced and showed to be 100% identical to an *ompA* partial sequence of *R. rickettsii* from GenBank (accession no. KU321853).

Discussion

Since the classical experiments of Ricketts (*6*), guinea pigs have been adopted as the animal model for *R. rickettsii* infection in the laboratory. In susceptible guinea pigs, fever typically develops a few days after infestation by *R. rickettsii*–infected ticks (*7,15,22,23*). This febrile period coincides with rickettsemia, as demonstrated by blood passages and rickettsial titration in guinea pig blood (*6,7,22–24*). During acquisition infestation 1 on susceptible guinea pigs 1–6, fever developed in all animals 5–9 dpi with *R. rickettsii*–IN. Because these febrile guinea pigs served as hosts for *A. aureolatum*–UL, we assume that these larvae fed on rickettsemic hosts. This condition explains the 100% PCR positivity for rickettsial DNA on nymphs that molted from these larvae, regardless of the feeding chamber (UL or UL

+ IN). This PCR positivity was confirmed by the transmission infestation with the molted nymphs, which in all cases transmitted *R. rickettsii* to susceptible guinea pigs. These results demonstrate horizontal transmission of *R. rickettsii* by co-feeding ticks on hosts with systemic *R. rickettsii* infection, which has been well known since Ricketts (*6*).

Guinea pigs from acquisition infestation 1 were exposed again to *R. rickettsii* IN during acquisition infestations 2–4, when fever did not develop in any animals. Based on their anti–*R. rickettsii* IgG titers at the infestation day, coupled with data reported in several previous studies (i.e., a previously infected animal will not develop a second rickettsemia [*7–9,22,23*]), we assume these animals were immune to *R. rickettsii* and did not develop rickettsemia during acquisition infestations 2–4. This statement was corroborated by the fact that none of the nymphs derived from larvae that fed alone (feeding chamber UL) transmitted *R. rickettsii* to susceptible guinea pigs (Table 5). These results demonstrate that horizontal transmission of *R. rickettsii* by co-feeding ticks on hosts with no systemic infection did not occur when UL fed distantly from IN.

When UL fed with *R. rickettsii* IN within the same chamber on immune guinea pigs (acquisition infestations 2–4), in most cases, nymphs that emerged from the engorged larvae were not able to transmit *R. rickettsii* to susceptible guinea pigs. However, in a few cases (guinea pigs 26, 27, 36, 39), rickettsial transmission occurred (fever, seroconversion). These results indicate horizontal transmission of *R. rickettsii* by co-feeding ticks on hosts with nonsystemic infection. We tested only infected donor nymphs with acquisition larvae. Further studies should evaluate the reverse approach—infected donor larvae with acquisition nymphs.

Overall, the transmission infestations were concordant with the PCR results on unfed nymphs before infestation; in every successful transmission of *R. rickettsii* to guinea pigs, specimens of the nymphal batch contained rickettsial DNA, as did the adults that molted from these nymphs. However, in 4 cases, the nymphal batch contained rickettsial DNA, but the nymphs did not transmit *R. rickettsii*; guinea pigs 28, 29, 32, and 33 received nymphs from batches in which 12%–16.7% of nymphs (derived from feeding chamber UL or UL + IN) contained rickettsial DNA, but none of the guinea pigs became infected by *R. rickettsii* (Table 5). These results highlight the weakness of PCR results alone when adopted to evaluate nonsystemic transmission of *R. rickettsii* among co-feeding ticks. Two previous studies proposed nonsystemic transmission of *R. conorii* between *Rhipicephalus sanguineus* ticks upon feeding on immune hosts (*25,26*); however, these studies relied solely on DNA detection in ticks after molting, and PCR results of postmolting ticks were not confirmed by transmission infestations. Our study convincingly demonstrates nonsystemic transmission of rickettsia by exposing postmolting-acquisition ticks to feed on susceptible hosts.

We created an artificial condition in which 200 acquisition larvae were limited to feed on a small area of the host skin (5 cm diameter) together with 50 *R. rickettsii* IN. This condition is unlikely to occur under natural conditions, where much lower number of larvae and nymphs are usually found feeding simultaneously on a small area of the skin. One reasonable explanation for nonsystemic transmission under such conditions, even though it occurred in only a few cases, was that acquisition ticks shared the same feeding site with IN on the host skin; therefore, they could have exchanged salivary secretions containing *R. rickettsii* of nymphal origin. This assumption is corroborated by the fact that all cases of nonsystemic transmission were from UL + IN feeding chambers. Taking into account that *R. rickettsii* infection rates in tick populations under natural conditions are typically very low (0.05%–1%) (*7,9,27–30*) and the low likelihood of ticks sharing the same feeding site, the importance of our results for the ecology of *R. rickettsii* could be insignificant. For example, although the systemic transmission tends to generate a great number of additional infected ticks (those feeding on every part of the host body during the few weeks of rickettsemia), the nonsystemic transmission might generate only 1 additional tick specimen, the one that, by chance, had fed side-by-side with the infected tick. The role of nonsystemic transmission to the ecology of *R. rickettsii* and other spotted fever group rickettsiae needs to be quantified in further studies.

Acknowledgments

About the Author

Dr. Moraes-Filho is a professor of animal parasitic diseases at Santo Amaro University, São Paulo, Brazil. His primary research interest is the epidemiology of ticks and tickborne diseases.

References

1. Parola P, Paddock CD, Socolovschi C, Labruna MB, Mediannikov O, Kernif T, et al. Update on tick-borne rickettsioses around the world: a geographic approach. Clin Microbiol Rev. 2013;26:657–702. http://dx.doi.org/10.1128/CMR.00032-13
2. de Oliveira SV, Guimarães JN, Reckziegel GC, Neves BM, Araújo-Vilges KM, Fonseca LX, et al. An update on the epidemiological situation of spotted fever in Brazil. J Venom Anim Toxins Incl Trop Dis. 2016;22:22.
3. Labruna MB. Ecology of rickettsia in South America. Ann N Y Acad Sci. 2009;1166:156–66. http://dx.doi.org/10.1111/j.1749-6632.2009.04516.x
4. Soares JF, Soares HS, Barbieri AM, Labruna MB. Experimental infection of the tick *Amblyomma cajennense*, Cayenne tick, with

Rickettsia rickettsii, the agent of Rocky Mountain spotted fever. Med Vet Entomol. 2012;26:139–51. http://dx.doi.org/10.1111/j.1365-2915.2011.00982.x

5. Labruna MB, Ogrzewalska M, Soares JF, Martins TF, Soares HS, Moraes-Filho J, et al. Experimental infection of *Amblyomma aureolatum* ticks with *Rickettsia rickettsii*. Emerg Infect Dis. 2011;17:829–34. http://dx.doi.org/10.3201/eid1705.101524

6. Ricketts HT. Some aspects of Rocky Mountain spotted fever as shown by recent investigations. Med Rec. 1909;76:843–55.

7. Price WH. The epidemiology of Rocky Mountain spotted fever. II. Studies on the biological survival mechanism of *Rickettsia rickettsii*. Am J Hyg. 1954;60:292–319.

8. Philip CB. Some epidemiological considerations in Rocky Mountain spotted fever. Public Health Rep. 1959;74:595–600. http://dx.doi.org/10.2307/4590519

9. Burgdorfer W. Ecological and epidemiological considerations of Rocky Mountain spotted fever and scrub typhus. In: Walker DH, editor. Biology of rickettsial diseases. Vol. 1. Boca Raton (FL): CRC Inc.; 1988. p. 33–50.

10. Niebylski ML, Peacock MG, Schwan TG. Lethal effect of *Rickettsia rickettsii* on its tick vector (*Dermacentor andersoni*). Appl Environ Microbiol. 1999;65:773–8.

11. Labruna MB. Brazilian spotted fever: the role of capybaras. In: Moreira JR, Ferraz KMPMB, Herrera EA, Macdonald DW, editors. Capybara: biology, use and conservation of an exceptional neotropical species. New York: Springer Science + Business Media, 2013. p. 371–383.

12. Jones LD, Davies CR, Steele GM, Nuttall PA. A novel mode of arbovirus transmission involving a nonviremic host. Science. 1987;237:775–7. http://dx.doi.org/10.1126/science.3616608

13. Labuda M, Jones LD, Williams T, Danielova V, Nuttall PA. Efficient transmission of tick-borne encephalitis virus between cofeeding ticks. J Med Entomol. 1993;30:295–9. http://dx.doi.org/10.1093/jmedent/30.1.295

14. Labuda M, Danielova V, Jones LD, Nuttall PA. Amplification of tick-borne encephalitis virus infection during co-feeding of ticks. Med Vet Entomol. 1993;7:339–42. http://dx.doi.org/10.1111/j.1365-2915.1993.tb00702.x

15. Saraiva DG, Soares HS, Soares JF, Labruna MB. Feeding period required by *Amblyomma aureolatum* ticks for transmission of *Rickettsia rickettsii* to vertebrate hosts. Emerg Infect Dis. 2014;20:1504–10. http://dx.doi.org/10.3201/eid2009.140189

16. Labruna MB, Ogrzewalska M, Martins TF, Pinter A, Horta MC. Comparative susceptibility of larval stages of *Amblyomma aureolatum*, *Amblyomma cajennense*, and *Rhipicephalus sanguineus* to infection by *Rickettsia rickettsii*. J Med Entomol. 2008;45:1156–9. http://dx.doi.org/10.1093/jmedent/45.6.1156

17. Pinter A, Dias RA, Gennari SM, Labruna MB. Study of the seasonal dynamics, life cycle, and host specificity of *Amblyomma aureolatum* (Acari: Ixodidae). J Med Entomol. 2004;41:324–32. http://dx.doi.org/10.1603/0022-2585-41.3.324

18. Horta MC, Moraes-Filho J, Casagrande RA, Saito TB, Rosa SC, Ogrzewalska M, et al. Experimental infection of opossums *Didelphis aurita* by *Rickettsia rickettsii* and evaluation of the transmission of the infection to ticks *Amblyomma cajennense*. Vector Borne Zoonotic Dis. 2009;9:109–18. http://dx.doi.org/10.1089/vbz.2008.0114

19. Sangioni LA, Horta MC, Vianna MCB, Gennari SM, Soares RM, Galvão MAM, et al. Rickettsial infection in animals and Brazilian spotted fever endemicity. Emerg Infect Dis. 2005;11:265–70. http://dx.doi.org/10.3201/eid1102.040656

20. Labruna MB, Whitworth T, Horta MC, Bouyer DH, McBride JW, Pinter A, et al. *Rickettsia* species infecting *Amblyomma cooperi* ticks from an area in the state of São Paulo, Brazil, where Brazilian spotted fever is endemic. J Clin Microbiol. 2004;42:90–8. http://dx.doi.org/10.1128/JCM.42.1.90-98.2004

21. Regnery RL, Spruill CL, Plikaytis BD. Genotypic identification of rickettsiae and estimation of intraspecies sequence divergence for portions of two rickettsial genes. J Bacteriol. 1991;173:1576–89. http://dx.doi.org/10.1128/jb.173.5.1576-1589.1991

22. Parker R, Philip CB, Jellinson WL. Rocky Mountain spotted fever. Potentialities of tick transmission in relation to geographic occurrence in the United States. Am J Trop Med. 1933;13:341–79.

23. Magalhães O. Contribuição ao conhecimento das doenças do grupo tifo exantematico. Rio de Janeiro: Instituto Oswaldo Cruz; 1952.

24. Burgdorfer W, Friedhoff KT, Lancaster JL Jr. Natural history of tick-borne spotted fever in the USA. Susceptibility of small mammals to virulent *Rickettsia rickettsii*. Bull World Health Organ. 1966;35:149–53.

25. Levin ML, Zemtsova GE, Montgomery M, Killmaster LF. Effects of homologous and heterologous immunization on the reservoir competence of domestic dogs for *Rickettsia conorii* (israelensis). Ticks Tick Borne Dis. 2014;5:33–40. http://dx.doi.org/10.1016/j.ttbdis.2013.07.010

26. Zemtsova G, Killmaster LF, Mumcuoglu KY, Levin ML. Co-feeding as a route for transmission of *Rickettsia conorii israelensis* between *Rhipicephalus sanguineus* ticks. Exp Appl Acarol. 2010;52:383–92. http://dx.doi.org/10.1007/s10493-010-9375-7

27. Pinter A, Labruna MB. Isolation of *Rickettsia rickettsii* and *Rickettsia bellii* in cell culture from the tick *Amblyomma aureolatum* in Brazil. Ann N Y Acad Sci. 2006;1078:523–9. http://dx.doi.org/10.1196/annals.1374.103

28. Guedes E, Leite RC, Pacheco RC, Silveira I, Labruna MB. Rickettsia species infecting *Amblyomma* ticks from an area endemic for Brazilian spotted fever in Brazil. Rev Bras Parasitol Vet. 2011;20:308–11. http://dx.doi.org/10.1590/S1984-29612011000400009

29. Krawczak FS, Nieri-Bastos FA, Nunes FP, Soares JF, Moraes-Filho J, Labruna MB. Rickettsial infection in *Amblyomma cajennense* ticks and capybaras (*Hydrochoerus hydrochaeris*) in a Brazilian spotted fever–endemic area. Parasit Vectors. 2014;7:7. http://dx.doi.org/10.1186/1756-3305-7-7

30. Labruna MB, Krawczak FS, Gerardi M, Binder LC, Barbieri ARM, Paz GF, et al. Isolation of *Rickettsia rickettsii* from the tick *Amblyomma sculptum* from a Brazilian spotted fever–endemic area in the Pampulha Lake region, southeastern Brazil. Vet Parasitol Reg Stud Rep. 2017;8:82–5.

Address for correspondence: Marcelo B. Labruna, University of São Paulo, Preventive Veterinary Medicine, Av. Prof. Orlando Marques de Paiva 87 Cidade Universitaria, São Paulo 05508-000 Brazil; email: labruna@usp.br

Stakeholder Insights from Zika Virus Infections in Houston, Texas, USA, 2016–2017

Stephanie R. Morain, Catherine S. Eppes, Joslyn W. Fisher, Courtenay R. Bruce,[1] Martha Rac, Kjersti M. Aagaard, Rebecca Lunstroth, Savitri Fedson, Pallavi Dinesh, Jean L. Raphael

Responding to Zika virus infections in Houston, Texas, USA, presented numerous challenges across the health system. As the nation's fourth-largest city, in a subtropical region with high travel volume to Latin America and the Caribbean, Houston was an ideal location for studying experiences encountered by clinicians and public health officials as they responded to the Zika virus crisis. To identify the challenges encountered in the response and to explore strategies to improve future responses to emerging infectious diseases, we interviewed 38 key stakeholders who were clinical, scientific, operational, and public health leaders. From the responses, we identified 4 key challenges: testing, travel screening, patient demographics and immigration status, and insufficient collaboration (between public health officials and clinicians and among clinical providers). We also identified 5 strategic areas as potential solutions: improved electronic health record support, specialty centers and referral systems, standardized forms, centralized testing databases, and joint academic/public health task forces.

In February 2016, the World Health Organization (WHO) declared the cluster of cases of microcephaly and other neurologic abnormalities associated with Zika virus a public health emergency of international concern. Since 2015, this virus has infected >1 million persons in 70 countries (1). From 2015 through December 2017 in the United States and its territories, >42,000 laboratory-confirmed symptomatic cases were reported and ≈7,000 pregnant women had laboratory evidence of possible Zika virus infection (2,3).

Responding to Zika virus presented numerous challenges across the health system. Zika virus research before 2015 was scarce, leaving clinicians and public health policy makers with little guidance regarding the virus's natural history, rate of perinatal transmission, or mechanisms or rate by which infections triggered microcephaly and other severe congenital abnormalities. Furthermore, diagnostic tools were limited because of Zika virus cross-reactivity with other flaviviruses on serologic assays, complicating individual diagnoses and population-based serosurveillance (4).

To develop guidelines to support the clinical and public health response, the Centers for Disease Control and Prevention (CDC) mobilized rapidly. Nevertheless, considerable work was needed by those on the ground to translate CDC guidelines and other emerging research into actionable policies at the institutional level.

The challenges encountered by clinicians and public health officials when responding to the emerging Zika virus crisis in Houston, Texas, USA, from January 2016 through June 2017 were ideal for a case study. As the nation's fourth most populous city and with >10 million annual international travelers, Houston is a global gateway to Latin America and the Caribbean, putting it at high risk for travel-associated cases (5). Furthermore, the city's subtropical bayou setting enhances the threat of locally acquired transmission from Aedes aegypti and Ae. albopictus mosquitoes (6). During 2015–2017, a total of 365 Zika virus cases, including at least 7 transmitted by local mosquitoes, were reported in Texas (7). In a 7-month period, 105 pregnant patients were referred to a specialty clinic for potential Zika virus exposure; 75 met testing criteria and 8 ultimately had positive test results, a screen-positive rate of 11% (8).

To explore the clinical and public health responses to Zika virus in Houston, we interviewed expert stakeholders. We report the key challenges they encountered and propose strategies to inform the response to Zika virus and future emerging infectious diseases.

Methods

We conducted semistructured interviews of 38 clinical, scientific, and public health experts in Houston and current or former Texas public health officials (Table 1). Almost half (45%) worked in the fields of obstetrics or pediatrics, and

Author affiliations: Baylor College of Medicine, Houston, Texas, USA (S.R. Morain, C.S. Eppes, J.W. Fisher, C.R. Bruce, M. Rac, K.M. Aagaard, S. Fedson, P. Dinesh, J.L. Raphael); McGovern Medical School at the University of Texas Health Science Center, Houston (R. Lunstroth)

[1]Current affiliation: Houston Methodist Hospital, Houston, Texas, USA.

Primary role	No. respondents
Pediatrics/neonatology	9
Obstetrics–gynecology or maternal–fetal medicine	8
Public health	8
Pathology	6
Infectious disease	3
Operations/leadership	2
Nursing	1
Genetic counseling	1
Total	38

the majority of clinicians were affiliated with an academic medical center. The interview guide elicited participants' perceived challenges related to Zika virus infection prevention, testing, and clinical management, as well as strategies for addressing those challenges. During April–June 2017, a researcher with doctoral training in qualitative methods (S.R.M.) conducted the interviews. When possible, interviews were conducted in person (n = 24); the others were conducted via telephone. All interviews were audiorecorded, transcribed, and reviewed for accuracy. We analyzed transcripts by using MAXQDA (https://www.maxqda.com) and used qualitative coding to identify key themes related to challenges and strategies in the Zika virus response.

Challenges

From stakeholders' discussions of the challenges encountered in responding to Zika virus infection, 4 primary themes emerged. These themes were testing, travel screening, patient demographics and immigration status, and collaboration (between public health entities and clinicians and among clinical providers) (Table 2).

Testing

The most commonly described challenges were associated with Zika virus testing. Every clinician interviewed described such challenges. Five testing issues emerged.

First, clinicians described logistics burdens associated with collecting and submitting samples to public health departments, characterizing the paperwork and approval processes as "redundant," "very time-consuming," and "a significant barrier to care." One case described by an obstetrician exemplifies these challenges. To order serologic testing, the obstetrician had to complete hospital send-out laboratory forms and 3 forms from the Houston Health Department (HHD) and telephone HHD for approval. When the test results returned positive, the clinical team sent a plaque-reduction neutralization test (PRNT) sample to CDC to rule out cross-reactivity with other flaviviruses (9). While awaiting PRNT results, the patient elected amniocentesis, which required completion of 5 more forms and separate HHD approval. At the time she gave birth, the PRNT results were still pending, so the clinical team submitted placental

samples for testing, which required completion of 4 new forms and involvement of the state health department.

Second, clinicians expressed concerns regarding the clinical effects of delayed receipt of test results. These delays were generally longest early in the response, before testing was available via in-house or commercial laboratories and as public health departments faced extensive delays in federal funding to support testing. The delays were particularly challenging given Zika virus's potential effects on fetal development and the relatively short duration of pregnancy. Test results could influence decisions about clinical management; the risks and benefits of amniocentesis or other testing; and reproductive decision-making, including pregnancy termination. As one maternal–fetal medicine specialist summarized, "It's very difficult to base your management decisions on a test that took 6 to 8 weeks in pregnancy."

The third challenge was the complexity and limitations of existing tests, including cross-reactivity with other flaviviruses and the contemporary general understanding of a limited period for IgM detection, which complicated determination of exposure and risks to pregnancy. It was believed that although IgM is expressed as early as several days after exposure, it typically wanes within 3 months, creating challenges for patients with a long duration of exposure or case testing delays of several months. These limitations frustrated efforts to identify true positive exposures and presented challenges for patient education. To quote a maternal–fetal medicine specialist, "The testing is not very specific… it doesn't necessarily eliminate your risk of having Zika… that has been difficult to get our patients to understand. Because most of our patients think that if a test is negative, then the risk is eliminated."

Fourth, several respondents noted the effects of commercially developed tests. According to respondents, commercial tests generally improved result turnaround times, partially alleviating the demand on scarce public health department resources. However, they also introduced new cost pressures, particularly for public institutions, compared with free services available through public health laboratories. Commercial testing also introduced challenges for public health systems because these results often lacked necessary demographic and epidemiologic information to support downstream case investigations of positive test results by local health departments.

Fifth, respondents described poor mechanisms for sharing data between laboratories and providers, including insufficient or delayed electronic health record (EHR) integration for ordering and reporting test results. Clinicians reported resorting to "clunky" workarounds, such as receiving a facsimile from the health department that then had to be scanned into the medical record. Providers expressed concern that such systems could lead to insufficient follow-up, particularly for care of neonates. For example, a pediatrician cited the challenges of exchanging and recording testing

Table 2. Challenges expressed by key stakeholders with regard to Zika virus infections in Houston, Texas, USA, 2016–2017*

Challenge	Quotation
Testing	
Logistical burdens with collecting and submitting samples	"I was filling out a form for the city. I was filling out another form for the state, and another for CDC. All to just be able to submit the samples for testing… it took me about 15–20 minutes just to fill out the paperwork [per patient]. And a lot of it was redundant."—infectious disease specialist
Delays in receiving laboratory results	"… for a lot of women, [test results are] going to make no difference at all because they are going to continue their pregnancy... but, for other women, it may completely change their decision-making…. So that turnaround time matters, absolutely."—maternal–fetal medicine specialist
Complexity and limitations of available Zika virus tests	"The testing is not very specific. It doesn't necessarily eliminate your risk of having Zika, so there's lots of limitations even with a negative test."—academic pediatrician
Influence of commercial testing	"Frankly, the commercial labs–they're a blessing and not so much a blessing at the same time… when PCR specimens are done in a commercial lab and they're positive… we may have a patient name and that's it. Maybe their age, maybe their address, maybe not. And so we don't have all of the demographic information and epidemiologic information that we'd like to have to do a full case investigation."—state official
Poor mechanisms for exchanging laboratory data	"We get [Zika test results from the health department] through the fax… and we'll have medical records scan it in and then I sent that to the provider who is seeing the patient. It's a little clunky, but that's the only way we can do it because of the mode that we're getting it through the fax."—community obstetrician
Travel screening	
Insufficient clinician initiation	"We would love it if our safety net providers… were doing a similar type of Zika screening for all patient visits, not just OB visits, 'cause you're kind of behind the ball if you wait 'til the person's already pregnant and has been exposed."—public health physician
Inaccurate referral information	"So I think particularly for the immigrant population here in Harris County, there is also concerns that, 'why are they asking those questions, do they want to know where I've been and what I've done?' So I think there is also the concern for people who are here illegally perhaps that they don't want to divulge their travel history."—maternal–fetal medicine specialist
Insufficiently precise information	"… pathology would receive a blood sample on a mom who had been to Florida. She said yes to Florida… but based on the form that pathology got, it doesn't say the city that she visited. Before they will send it, they have to verify that it was Miami. I call the mom, well, she went to Jacksonville. She didn't go to Miami. That kind of stuff is very time intensive for somebody to follow up on."—genetic counselor
Patient demographic and immigration status	
Transient and low socioeconomic level population	"… A lot of these patients are very underprivileged and have very low resources, living in charity homes, living in homeless shelters…. How do we provide resources for these patients that have almost no resources to begin with? ... that's a big issue that I'm not really sure how to fully tackle. I think it's a very large issue"—academic pediatrician
Language barriers	"… 100% of our moms were Hispanic and low income. I can't remember a single one of them that spoke English either. And so there's a dynamic of we're trying to have interviews with them in a language that a number of our epidemiologists don't speak and try to find translators to convey whatever we're trying to ask, but then there's the dynamic of these patients with their own providers… there's a loss of information there just on the basis of translation."—public health physician
Undocumented immigration status	"… we're definitely hearing from some people… parents who are not here legally—even if their kids are here legally—are afraid to access medical care for fear of deportation."—community pediatrician
Collaboration among public health clinicians	
Confusion as to appropriate Zika virus "point person" within public health system	"We [academic medical centers] are the laboratories that are actually going to see those patients come in with [an infectious disease] … when you have these brand-new, emergent infections… that line of communication is not well-established. Who's in charge of that at public health? We don't always know."—academic pathologist
Poor communication of testing results to patients	"'They [the public health epidemiologists] say things like, 'You don't have anything to worry about, your IgM is negative.' What they don't know is that this patient's been persistently viremic… and we were very concerned and in fact that patient had an affected fetus… and so then we have to call the Health Department and say, 'Yeah, they have a positive PCR.'"—maternal–fetal medicine specialist
Collaboration among clinicians	
Poor communication between obstetrics and pediatric teams	"… the joke always goes as pediatricians, we knew where babies came from but we didn't know how they got there.... I don't think there's a highly reliable system across the state that ensures that OB providers are giving appropriate information to the [pediatric] team."—public health official
Questions of case "ownership"	"Follow-up for our babies was a big [issue] … who was actually going to do the follow-up? ... They've passed or they've failed their hearing test, so now where do we send them? ... it was just a big black hole."—academic pediatrician

*CDC, Centers for Disease Control and Prevention; OB, obstetrics; Pedi, pediatrics.

data as the reason why one infant in her practice was not evaluated for congenital Zika syndrome until 4 months of age—months beyond the CDC recommendations for evaluation and management of possible congenital infection (*10*).

Travel Screening

We identified 3 themes associated with travel screenings to identify patients with potential Zika virus exposure. First, specialty referral centers reported receiving inaccurate travel histories from patients or referring clinicians. In some circumstances, respondents cited the inaccuracies as probably stemming from patient concerns over divulging travel history because of their immigration status. One obstetrician offered the example of a patient who had become pregnant in Central America and subsequently traveled to the United States. When entering the United States, the patient's husband was detained as an undocumented immigrant and remained incarcerated throughout her pregnancy. The patient subsequently declined to disclose travel history to healthcare providers in Zika virus–endemic regions during several prenatal visits, ultimately notifying providers only of her travel early in her third trimester. According to another respondent, high levels of Zika virus–related anxiety may have motivated some patients to misrepresent their travel history in an effort to be referred for diagnostic testing.

Second, clinicians suggested that insufficient initiation of travel screening probably resulted in some Zika virus–exposed patients "fall[ing] through the cracks" and not receiving recommended evaluation or testing. Some cited institutional barriers, including lack of development or implementation of travel screenings or restricting travel screening to obstetric visits only instead of expanding to primary care and family medicine.

Third, reported travel information was sometimes insufficient or imprecise. For example, a patient might report visiting "Florida" when there was considerable heterogeneity in risk within the state (e.g., in the summer of 2016, a trip to Miami would trigger testing whereas a trip to Jacksonville would not) (*11*) or might list only the month of travel when the exact dates are necessary for ascertaining the most appropriate testing method.

Patient Demographics and Immigration Status

According to respondents, patient demographics presented challenges for access to care and subsequent follow-up. Many patients undergoing evaluation and subsequent care for Zika virus exposure were from or had close family ties to Zika virus–endemic countries. Several respondents characterized patients as often "transient" and described extensive socioeconomic barriers, including lack of stable housing, transportation, or telephone service—all of which could undermine long-term follow-up and care coordination. As a pediatrician explained, "We have a patient that

gave us their cell phone number, but the cell phone went dead. They don't have family in the country and they live in a shelter, so I'm just not sure how to ensure we have good communication, transportation, follow-up, and shelter." Furthermore, respondents noted that for many patients, proficiency in the English language was limited, which respondents described as potentially exacerbating not only the accuracy of travel screenings but also patient education about Zika virus prevention and clinical management.

Several respondents also described extensive issues related to immigration status and implications for healthcare access. Some patients were reluctant to disclose their travel history for fear of deportation. Respondents also noted that concern about immigration status may have dissuaded some patients from seeking care, either during the prenatal period or for subsequent follow-up infant care. Other clinicians noted that immigration status influenced patient behavior across the health system. For example, public health clinicians described a "marked decline" in women accessing services through the Women, Infants, and Children program, reportedly because of concerns over deportation.

Collaboration

We identified 2 types of collaboration challenges. One was between providers and public health agencies and the other among clinicians involved in patient care.

Provider–Public Health Agency Collaboration

Respondents described challenges with communications between clinicians and public health agencies at the local, state, and federal levels. To develop an action plan, the Houston Office of Surveillance and Public Health Preparedness convened local stakeholders, including city departments, researchers, and industry leaders (*12*). Nevertheless, respondents reported missed opportunities for interdisciplinary communication. For example, some clinicians described uncertainty identifying the Zika virus "point person" or team within health departments who could field questions from clinicians and hospital laboratories about case identification and testing or even which health department had responsibility. Furthermore, submitting laboratory testing for one patient could involve numerous health departments, including separate paperwork, processes, and phone approvals for each department—all of which presented additional time burdens for clinicians and delays for patient diagnosis.

According to one public health respondent, such challenges may reflect misunderstandings associated with allocation of responsibility across different public health partners: "I think there's a fundamental misunderstanding of what the CDC does and doesn't do. They have national experts. They provide resources that they get from Congress. There's a national laboratory, but they don't take over a

response. A response is formulated at the local level… [but] local health departments have varying levels of expertise."

Interclinician Collaboration

Several clinicians described interclinician communication about patient care as the "most frustrating" or "hardest" aspect of the Zika virus response. We identified 2 distinct issues. The first and by far most common problem was insufficient or inefficient communication between obstetric and pediatric care providers, including pediatrician notification of suspected or confirmed maternal Zika virus infections. Specific criticisms related to this process included absence of a centralized database of positive test results, lack of connectivity between EHRs across different health systems, and an inability of pediatricians to access relevant maternal medical records.

Second, several clinicians described insufficient clarity regarding case "ownership." Issues included disagreement over which provider or care team was responsible for tracking and communicating test results to patients and which providers (e.g., general pediatricians vs. specialists) should primarily be responsible for long-term evaluation of Zika virus–exposed infants.

Strategies for Improvement

Improved EHR Support

Respondents identified numerous ways in which technology could streamline testing processes, starting from the initial stage of screening patients, progressing to collecting and submitting samples, and then documenting and sharing results among providers and public health systems. Five specific respondent suggestions for improved EHR support were 1) standardizing screening questions within the patient's EHR to ensure accurate assessment of risk exposure; 2) implementing EHR-based decision support systems to help providers select and order the appropriate test(s); 3) enabling electronic ordering of Zika virus testing through the EHR; 4) prepopulating demographic information within the test form to reduce provider time burden and improve the efficiency of public health case investigations; and 5) integrating the testing laboratory and patient EHR to enable test results to be automatically entered into the patient EHR.

Admittedly, revising an EHR system can be an unwieldy process (13,14). Institutions should anticipate this challenge and develop policies to enable timely integration of hospital EHRs to facilitate clinical care and public health reporting.

Specialty Centers and Referral Systems

The rapid evolution of knowledge and the complexity of Zika virus testing and ongoing patient management provide arguments for specialty centers and referral systems. The education, documentation, and reporting requirements associated with patient care in the context of an evolving infectious disease outbreak are extensive and yet are only one of several goals during a patient–provider encounter. As one maternal fetal medicine specialist explained, "This is a pretty specialized area that's rapidly evolving, and it's probably good to send patients for at least a discussion with folks that really have their fingertips on what did we learn last night at midnight when The New England Journal [of Medicine] was released." Several specialty centers were offered as corollaries, including existing models for perinatal HIV infection, congenital cytomegalovirus infection, or newborn screening for genetic conditions, as well as the designation of 3 tiers of health centers in the 2015 domestic Ebola response (15). For example, Illinois's Perinatal Rapid Testing Implementation Initiative for HIV successfully reduced the number of mother–infant pairs who were discharged with unknown HIV status; the initiative created 4 regional networks, a 24-hour hotline, a surveillance system, and implementation resources including template policies and consent forms (16).

Specialty centers and referral systems offer several advantages for managing Zika virus infection and other emerging infectious diseases, including state of the science laboratory and ultrasonography/magnetic resonance imaging with high precision and efficiency, potential to scale up for pandemics and endemic-disease expansion, capacity for prenatal and postnatal diagnosis and postnatal follow-up, follow-up care, and opportunities for research and testing of potential interventions in an enriched population with a higher likelihood of exposure and infection.

Some patients, particularly undocumented immigrants or other patients of low socioeconomic status, may face financial and transportation barriers with regard to accessing specialty centers, particularly for repeated visits. Additional cost pressures may arise in association with imaging and specialty care, even among insured patients. Additional work is needed to identify strategies to improve access while managing patient and system costs; these strategies include using telemedicine, providing transportation support and cell phones or phone cards to enable follow-up, and implementing corresponding regulatory and payment structures to facilitate these services.

Standardized Forms

Several clinicians suggested standardizing forms across local, state, and federal agencies to reduce time burdens associated with testing. Federal, state, and local public health entities in Texas each had their own Zika virus–specific testing forms, for which much of the required information overlapped. Condensing these forms into a single, generalizable form could reduce work redundancies and form completion errors while increasing testing efficiency.

Ideally, these forms would be online, could translate directly into state databases of testing results, and could be integrated into Zika virus registry reporting information.

State or Regional Testing Databases

Providing patients with timely testing, clinical management, and follow-up requires that clinicians know of suspected or confirmed exposures. However, our interviews suggested that clinicians faced several barriers accessing patients' prior Zika virus testing information at the point of care. Insufficient information about prior testing or exposure was particularly challenging for patients who accessed different providers throughout the course of a pregnancy, such as receiving prenatal care from a federally qualified health center, delivering at a county hospital, and going to a separate Medicaid clinic for their neonatal visits. This situation is not uncommon for patients in the demographic group most affected during Houston's Zika virus experience. For most patients, standard practice for Zika virus testing and reporting of results in Texas occurs through county health departments, according to ZIP code. Such practices are particularly challenging for providers in large medical centers, which regularly draw patients from >1 health department. A potential solution would be to create a centralized state or regional database for Zika virus test results. Centralized databases could enable providers to access timely information about prior exposure and testing history, regardless of where that testing occurred, similar to those that already exist for patients with syphilis or HIV infection.

Joint Academic–Public Health Task Force

As emerging arboviruses become the new normal, emerging infectious diseases will continue to pose complex health challenges for communities (*17*). Prior responses demonstrate the value of infrastructure and capacity building to prepare for the inevitability of future outbreaks (*18*). Although national organizations and their state and local affiliates (e.g., CDC, US Department of Health and Human Services, American Medical Association, American College of Obstetrics and Gynecology, American Academy of Pediatrics, and Infectious Disease Society of America) can provide information, guidelines, and algorithms, operationalizing and implementing these resources in clinical settings requires local engagement and adaptation. As a public health official explained, "The algorithms… make sense from the scientific viewpoint, but they get confusing to individual practitioners. So making it easy for individual practitioners on the front line to be able to know who to call to get advice… mapping out those systems of care at the local level, I think, will be very important."

Two levels of local engagement would support the response to emerging infectious diseases: at the community level and within individual institutions. At the community level, task forces composed of health leadership organizations, academic medical centers, and local public health authorities could facilitate communitywide collaboration, addressing such issues as defining roles and responsibilities across partners, communicating to the public about preparedness and response, enhancing laboratory capacity, and expanding testing and surveillance in high-risk areas. This strategy is consistent with prior guidance regarding the importance of training local professionals willing to collaborate with the government in public health management in enabling effective responses to emerging infectious diseases (*19*). Such collaboration will admittedly be challenging in some circumstances because local institutions may be more accustomed to viewing each other as competitors for clinical, philanthropic, and research resources rather than as collaborative partners. Prior successful multiorganizational collaborative efforts may offer some instructive lessons, including enlisting an existing reputable organization as a convening body (e.g., the Texas Medical Center), involving key stakeholders, and using electronic tools for low-cost dissemination (*20*).

At the institutional level (including hospitals, clinics, and academic health centers), leadership should designate an emerging infectious disease point person or committee with the authority and support to rapidly create an ad hoc task force comprising interdisciplinary members needed to effectively address a public health emergency. Diverse representation will be vital to the success of such committees, including clinical leadership to translate national, state, or local algorithms to clinical management plans for the respective institutional contexts; health information management leaders to modify and implement EHR changes to support the clinical response; laboratory personnel to guide testing processes; and communications experts to disseminate guidance on policy and process throughout the institution.

Limitations

For this project, we purposefully selected clinical, operational, and public health leaders with experience responding to Zika virus infections. Consequently, obstetricians, pediatricians, and infectious disease specialists working in academic medical centers were overrepresented. Their experiences shed insight into features of health system capacity and preparedness to respond to an emerging infectious disease. However, involvement of other stakeholders, particularly patients and primary care providers in nonacademic, rural, and resource-poor settings, probably would have provided additional insights.

The suggestions for improvement reflect issues raised by our respondents and are not exhaustive. Other critical issues merit further attention, including how healthcare

providers can ensure that patients feel safe to access needed health services in the face of contemporary government approaches to immigration enforcement (*21*).

Conclusions

The emergence of Zika virus brought numerous challenges to the health system in Houston. Although the virus itself was relatively new, many of the issues confronted by providers and public health officials in the face of the disease were far from novel. Instead, the issues were often the result of known, predictable, and recurring shortcomings in our healthcare system. The insights of expert stakeholders led us to suggest several strategies for improving the response to Zika virus and other future emerging infectious diseases.

Acknowledgments

About the Author

Dr. Morain is an assistant professor in the Center for Medical Ethics and Health Policy at Baylor College of Medicine in Houston, Texas. Her research interests include ethical and practical challenges encountered during efforts to improve the integration of research and clinical care as well as issues at the interface of ethics, law, and public health policy.

References

1   Pan American Health Organization. Zika cases and congenital syndrome associated with Zika virus reported by countries and territories in the Americas, 2015–2017 cumulative cases [cited 2017 Dec 14]. http://www.paho.org/hq/index.php?option=com_docman&task=doc_view&Itemid=270&gid=42362&lang=en

2. Center for Disease Control and Prevention. Pregnant women with any laboratory evidence of possible Zika virus infection, 2015–2017 [cited 2017 Dec 14]. https://www.cdc.gov/zika/reporting/pregwomen-uscases.html

3. Center for Disease Control and Prevention. Cumulative Zika virus disease case counts in the United States, 2015–2017 [cited 2017 Dec 14]. https://www.cdc.gov/zika/reporting/case-counts.html

4. Boeuf P, Drummer HE, Richards JS, Scoullar MJL, Beeson JG. The global threat of Zika virus to pregnancy: epidemiology, clinical perspectives, mechanisms, and impact. BMC Med. 2016;14:112. http://dx.doi.org/10.1186/s12916-016-0660-0

5. Houston Airport System. Media kit fact sheet [cited 2017 Dec 14]. http://www.fly2houston.com/newsroom/media-kit/fact-sheets/

6. Kraemer MU, Sinka ME, Duda KA, Mylne AQ, Shearer FM, Barker CM, et al. The global distribution of the arbovirus vectors *Aedes aegypti* and *Ae. albopictus*. eLife. 2015;4:e08347. http://dx.doi.org/10.7554/eLife.08347

7. Texas Department of State Health Services. Don't give Zika a biting chance [cited 2017 Dec 14]. http://www.texaszika.org

8. Rac M, Eppes C, Dempster C, Ballas J, Davidson C, Aagaard K. Screening for Zika virus in a high-risk non-endemic urban population: patient characteristics and testing outcomes. Obstet Gynecol. 2017; 129:35s. http://dx.doi.org/10.1097/01.AOG.0000514332.47783.0f

9. Eppes C, Rac M, Dunn J, Versalovic J, Murray KO, Suter MA, et al. Testing for Zika virus infection in pregnancy: key concepts to deal with an emerging epidemic. Am J Obstet Gynecol. 2017;216:209–25. http://dx.doi.org/10.1016/j.ajog.2017.01.020

10. Russell K, Oliver SE, Lewis L, Barfield WD, Cragan J, Meaney-Delman D, et al. Update: interim guidance for the evaluation and management of infants with possible congenital Zika virus infection—United States, August 2016. MMWR Morb Mortal Wkly Rep. 2016;65:870–8. http://dx.doi.org/10.15585/mmwr.mm6533e2

11. Centers for Diease Control and Prevention. CDC updates guidance for pregnant women and women and men of reproductive age for Zika virus infection related to the ongoing investigation of local mosquito-borne Zika virus transmission in Miami-Dade County, Florida [cited 2017 Dec 14]. https://emergency.cdc.gov/han/han00398.asp

12. Arafat R, Arnold R, Persse D. Preparing for Zika virus in Houston: a comprehensive, city-wide approach. Int J Infect Dis. 2016;53S:72.

13. Ash JS, Berg M, Coiera E. Some unintended consequences of information technology in health care: the nature of patient care information system-related errors. J Am Med Inform Assoc. 2004;11:104–12. http://dx.doi.org/10.1197/jamia.M1471

14. Boonstra A, Broekhuis M. Barriers to the acceptance of electronic medical records by physicians from systematic review to taxonomy and interventions. BMC Health Serv Res. 2010;10:231. http://dx.doi.org/10.1186/1472-6963-10-231

15. Van Beneden CA, Pietz H, Kirkcaldy RD, Koonin LM, Uyeki TM, Oster AM, et al. Early identification and prevention of the spread of Ebola—United States. MMWR Morb Mortal Wkly Rep. 2016;65(Suppl 3):75–84.

16. Wong AE, Garcia PM, Olszewski Y, Statton A, Bryant Borders A, Grobman WA, et al. Perinatal HIV testing and diagnosis in Illinois after implementation of the Perinatal Rapid Testing Initiative. Am J Obstet Gynecol. 2012;207:401.e1–6. http://dx.doi.org/10.1016/j.ajog.2012.08.006

17. Hotez PJ, Murray KO. Dengue, West Nile virus, chikungunya, Zika—and now Mayaro? PLoS Negl Trop Dis. 2017;11:e0005462. http://dx.doi.org/10.1371/journal.pntd.0005462

18. Paules CI, Eisinger RW, Marston HD, Fauci AS. What recent history has taught us about responding to emerging infectious disease threats. Ann Intern Med. 2017;167:805–11. http://dx.doi.org/10.7326/M17-2496

19. Broome CV. Effective global response to emerging infectious diseases. Emerg Infect Dis. 1998;4:358–9. http://dx.doi.org/10.3201/eid0403.980303

20. Fisher JW, Peek KE. Collaborating for change: creating a women's health network. Women's Health Issues. 2009;19:3–7. http://dx.doi.org/10.1016/j.whi.2008.10.003

21. Saadi A, Ahmed S, Katz MH. Making a case for sanctuary hospitals. JAMA. 2017;318:2079–80. http://dx.doi.org/10.1001/jama.2017.15714

Address for correspondence: Stephanie R. Morain, Baylor College of Medicine, Center for Medical Ethics and Health Policy, One Baylor Plaza, Ste 310D, Houston, TX 77030, USA; email: stephanie.morain@bcm.edu

Hantavirus Pulmonary Syndrome—The 25th Anniversary of the Four Corners Outbreak

Charles J. Van Hook

During the spring of 1993, a mysterious respiratory disease struck the Four Corners region of the southwestern United States. Persons who became ill were generally young and previously healthy before succumbing to an acute febrile illness that began with simple influenza-like symptoms and often culminated in death by pulmonary edema and cardiovascular collapse. With astonishing speed and efficiency, a collaborative team of federal, state, and local healthcare workers, including clinicians, epidemiologists, and laboratory scientists, identified a newly discovered species of hantavirus as the causative agent of the outbreak. In the ensuing 25 years, the epidemiology, virology, pathophysiology, clinical course, and treatment of hantavirus pulmonary syndrome have been the focus of ongoing research. Because of its rarity, and because of the need for early acute intervention in the face of precipitous decline, recognition of the unique laboratory profile of hantavirus pulmonary syndrome in the setting of a predisposing exposure history is of paramount importance.

On the morning of May 14, 1993, a 19-year-old Native American man was traveling by car through the Four Corners region of New Mexico, USA—the area where New Mexico, Arizona, Colorado, and Utah meet—when he became so severely short of breath that his alarmed accompanying family members pulled into a nearby service station to call for help. By all measures, the young man, a competitive marathon runner of local renown, had been in previous good health. A few days earlier, he had visited an outpatient clinic because of fever and myalgia, was treated symptomatically, and was well enough early on the morning of May 14 to embark on a trip from his home in Crownpoint, New Mexico, to Gallup, New Mexico. However, by the time the responding ambulance crew arrived, he had collapsed because of respiratory failure. He was taken to the emergency department at the Gallup Indian Medical Center, where he was found to have florid pulmonary edema, and where, despite maximal resuscitative efforts, he died in the emergency department.

The emergency department medical staff was understandably bewildered as to why an extremely fit adolescent athlete would so swiftly die from acute pulmonary edema. In New Mexico, any unexplained, suspicious, or otherwise irregular death is, by law, reportable to the New Mexico Office of the Medical Investigator. The officer on duty that day in Gallup was a young investigator named Richard Malone.

After arriving at the hospital and hearing the clinical narrative, Malone was startled by the resemblance of this death to another death that he had investigated a few weeks earlier at the same facility. At that time, he had been called after a young woman, also a Navajo tribal member, had died from acute pulmonary edema without any clinical clues pointing to a distinct etiology. Malone had referred that case for a postmortem examination to Patricia McFeeley, a University of New Mexico pathologist who worked in conjunction with the office of the medical examiner. McFeeley had reported that the young woman had died from pulmonary edema that was evident by gross and microscopic examinations. The heart of this patient was structurally normal, and results of serologic and microbiologic tests were nonrevealing.

The pathologist was admittedly puzzled by the case and had discussed her uneasiness with Malone. McFeeley was again at work in Albuquerque on the morning of May 14, and when Malone called and shared his thoughts on the similarity of the 2 cases, she readily agreed to perform an autopsy on the deceased person. With that, Malone made his way toward the emergency department waiting room to approach the family of the young man about obtaining permission to transport the body to the state laboratory in Albuquerque. Mr. Malone expected that he would have to gently persuade the family to agree, because the Navajo people are generally resistant to any action that could be perceived as disturbing the newly dead. When he met the gathered family, he was shocked by their shared story.

The patient had been en route to Gallup from his home in the small Navajo reservation village of Crownpoint that morning to attend a funeral, which was about to begin at a mortuary literally across the street from the

Indian Medical Center. The planned funeral was that of his fiancée, the 21-year-old mother of his infant child. The young woman, who was also an active runner, had died only days earlier at an outlying rural reservation clinic. She had also complained only of antecedent fever and myalgia, and the decline in her health had been so precipitous at the remote clinic that there had been inadequate time to transport her to a fully staffed facility. Because Crownpoint is located on the Navajo reservation and governed by tribal rather than state law, the clinic there was not required to adhere to reporting requirements of New Mexico. Consequently, Malone's office had no record of her death or of the surrounding circumstances. Malone recognized the relevance of this small cluster of cases, and after quickly updating McFeeley by telephone, he convinced the family of the young woman to allow her remains to be examined in Albuquerque. Malone invoked the health of their surviving infant child as a deciding factor in convincing reluctant family members to allow the state to proceed with their autopsies.

After ensuring that both bodies had been secured for transport, Malone sought out Bruce Tempest, the physician who served as the medical director for the Gallup Indian Medical Center. While he listened to Malone's report, Tempest remembered that he had been involved in at least 2 recent informal consultations with other physicians who had cared for young, previously healthy tribal members who had died in a dramatic fashion from a mysterious respiratory illness. Both men agreed that immediate further action was mandated. They decided that Malone would scour the records of the state coroner for information, and that Tempest would survey his clinical colleagues in the Four Corners area for similar cases.

The postmortem examinations of the 2 new case-patients showed only unexplained, severe pulmonary edema. Malone and Tempest quickly uncovered several new suspicious cases from the preceding few months, and on May 17, 1993, the New Mexico Department of Health was notified of their concerns. The state officials crafted a letter that was sent to clinicians in the 4-state area of Arizona, Colorado, New Mexico, and Utah. The communication offered a brief description of the cases to date and asked that any similar cases be reported immediately to them. The mailing was effective in identifying several other potential cases.

Unfortunately, soon thereafter, when the lay press reported that an unexplained illness was killing young tribal members throughout the Four Corners region, a near panic of the general populace ensued. Navajo and Hopi people were shunned, disinvited from regional athletic events, and made to feel unwelcome in public places. Politicians were pressured to act. On May 28, the Friday afternoon of Memorial Day weekend, New Mexico state health officials contacted the Centers for Disease Control and Prevention (CDC), described their predicament, and asked for expert assistance.

Within hours of the call for help, a team of investigators assembled and mobilized. Jay Butler, an experienced epidemiologist in the Epidemic Intelligence Service at CDC, was designated as the leader. Two young Epidemic Intelligence Service officers (Ronald Moolenar and Jeffrey Duchin) assisted him. Less than 24 hours after the group had been organized, they arrived at the Albuquerque airport and were shuttled to the campus of the University of New Mexico, where they were joined by members of the University of New Mexico medical faculty, Indian Health Service physicians, and various other state and federal health officials.

The first order of business was case definition, and the health officials agreed to evaluate any patient from the area who, going forward from January 1, 1993, had demonstrated imaging evidence of unexplained bilateral infiltrates with associated hypoxemia. The team would also evaluate any death that had occurred with unexplained pulmonary edema. More than 30 suspected cases, with varying degrees of available clinical information, were presented to the group. The assembly then evolved into a brainstorming session, where participants were invited to offer their thoughts about potential etiologies of the outbreak. Various ideas were put forth, ranging from the exotic to the mundane. Plague, tularemia, anthrax, and multiple other potential diseases were dismissed as possibilities because of a lack of any corroborating evidence.

By the end of the long weekend, the consensus was that the outbreak was the result of 1 of 3 possible causes. The first consideration was that of a new, aggressive, and previously unrecognized type of viral influenza. The second was that an environmental toxin was the causative agent, which was certainly plausible in an agricultural area with a less than optimal regulatory climate and a history of military weapons testing. The third listed possibility was the most fascinating: that a previously unrecognized pathogen was the cause of the epidemic (1).

On Tuesday, June 1, fifteen members of the CDC team began an on-site, meticulous, review of medical records. They also procured tissue specimens from suspected cases, which were flown to CDC headquarters in Atlanta, Georgia, for immediate analysis. Epidemiologists interviewed patient and control families and performed detailed inspections of their homes and workplaces.

By Friday, June 4, scientists of the Special Pathogens Branch at CDC had tested extracted IgM from 9 patients with a panel of 25 different virus stock samples from the laboratory at CDC. Antibody from all 9 patients showed cross-reactivity with each of 3 different hantavirus species and with none of the other 22 viruses. Hantaviruses were known to be the causative agents of a family of diseases

of varying severity, collectively known as hemorrhagic fever with renal syndrome (HFRS), which affect patients in the Northern Hemisphere from Scandinavia to the Korean Peninsula. The 3 hantavirus samples initially tested were Hantaan virus, the cause of Korean hemorrhagic fever; Seoul virus, the causative agent of a form of HFRS common in Asia; and Puumala virus, the cause of a relatively mild form of HFRS in northern Europe. Shortly thereafter, the same samples were found to cross-react with Prospect Hill virus, which was known to infect voles in Maryland but had never been isolated from human tissue or associated with human disease (*2*).

Several members of the investigating team had extensive international infectious disease experience and knowledge of the epidemiology and clinical course of HFRS. The illness was known to be caused by different types of hantavirus and to be transmitted to humans by inhalation of virus shed in rodent droppings. The syndrome is characterized by an enormous change in vascular endothelial permeability, predominantly in the kidney, with the loss of massive amounts of intravascular fluid into the renal extravascular parenchyma and retroperitoneal space. The degree of intravascular fluid depletion is so severe that hemoconcentration occurs, and patients often have pronounced increases in hemoglobin concentrations and hematocrit values.

The clinicians of the investigation team had noted high levels of hemoconcentration in several of the potential cases and, in light of the CDC findings, they suspected that they were now dealing with a new hantavirus disease. This conclusion was a substantial leap of thought for several reasons. At the time, in the Western Hemisphere, hantaviruses were recognized as infecting only rodents, and no case of human disease had been described. In addition, the study group patients had little evidence of renal involvement; the predominant target organ was the lung in all cases. Undeterred by these discrepancies, some group members postulated, in a profoundly prescient fashion, that the outbreak was caused by an as-yet-unrecognized hantavirus that targeted the pulmonary capillary endothelium.

Acting upon the new information, CDC dispatched a rodent trapping team to New Mexico. Over the ensuing week, ≈1,700 rodents were captured at patient and control sites. The most commonly secured rodent was *Peromyscus maniculatus*, the deer mouse (*3*).

Concurrently, the Special Pathogens Branch in Atlanta worked feverishly to uncover the new hantavirus. On June 10, using reverse transcription PCR technology, these scientists were able to obtain a sequence from the medium segment of the RNA strand of the suspected virus. The Viral Pathology Laboratory also identified hantaviral antigens in endothelium of the pulmonary capillary bed and other tissues (*4*). Less than 1 week later, on June

16, the same team identified an identical virus basepair sequence, as well as a prevalence of hantavirus antibody, from *Peromyscus maniculatus* mouse specimens trapped on site (*5*). The virus and its rodent reservoir had been definitively identified less than 3 weeks after CDC had assembled its task force.

The new virus proved difficult to culture, and it was not until November 1993 that teams from the CDC and the US Army Medical Research Institute of Infectious Diseases (Fort Detrick, MD, USA) were able to culture the virus. Their initial recommendation was to name the pathogen Muerto Canyon virus, after an involved area on the Navajo Reservation. The Navajo people reacted strongly against any further association with the disease that had led to so much initial prejudice, and tribal elders appealed to officials to reconsider. Ultimately, the new agent was officially named Sin Nombre virus (virus with no name).

While the bench scientists were successfully identifying the pathogen, epidemiologists and clinicians were clarifying the clinical course of the newly recognized syndrome. Eighteen patients were found to have had either serologic or PCR evidence of infection. These patients were mostly young adults, with a noticeable sparing of the extremes of life. Physical examinations were remarkable for fever, tachypnea, tachycardia, and hypotension. Severe pulmonary edema was nearly ubiquitous, and the mortality rate in the initial outbreak exceeded 75%. A distinct laboratory pattern was prominent, characterized by hypoxemia, leukocytosis with the presence of peripheral immunoblasts, hemoconcentration with a marked increase in hemoglobin and hematocrit, thrombocytopenia, and increased prothrombin and partial thromboplastin times. The predominant chest radiograph finding was bilateral parenchymal infiltrates. An unusual hemodynamic profile was also observed. Patients in whom pulmonary artery catheters had been placed showed a severe reduction in cardiac output and a marked increase in systemic vascular resistance, in association with normal or low pulmonary capillary wedge pressures, consistent with cardiogenic shock and noncardiogenic pulmonary edema. Histopathologic examination of the lungs of patients who died showed moderate lymphoid interstitial infiltration with severe alveolar edema (*4*).

The remarkable work of the Hantavirus Study Group, describing the newly defined hantavirus pulmonary syndrome (HPS), was published in the April 7, 1994, edition of the New England Journal of Medicine (*6*). A glowing editorial reviewing the team effort appeared in the same issue.

A burning question for the scientific community remained. Why did the outbreak occur in the Four Corners Region, and why did it happen in the spring of 1993? Biologists from the University of New Mexico happened to be studying the deer mouse population in that region at that time. They found that the mouse population in 1993

was 10-fold greater than it had been during the preceding spring. Working with a team of environmental scientists, those biologists demonstrated that, because of the increased moisture of an El Niño winter, there was a relative abundance of springtime vegetation in the Four Corners region that provided shelter and food for regional fauna. The resultant explosive growth of the rodent population was followed by increased human exposure to the deer mouse vector (7).

HPS Today

In the ensuing 25 years, the epidemiology, virology, pathophysiology, clinical course, and treatment for HPS have been the focus of ongoing research. The Sin Nombre virus is a single-stranded, 3-segmented RNA virus of the family *Hantaviridae*. It is the cause of chronic, seemingly innocuous, and persistent infections in the host rodent. Like all hantaviruses, the Sin Nombre virus is principally associated with only 1 rodent species, in this case, the common deer mouse. Other rare hantavirus species in North America have been associated with variants of HPS, and they are also associated predominantly with 1 rodent species.

The disease remains extremely uncommon: <800 HPS cases have been reported in the United States during the past 25 years (8). There is a western states predominance of this disease, and almost all cases are caused by exposure at home or in the workplace (9). The temporal and spatial distribution of cases reflect fluctuations in the population of the rodent host as the virus is transmitted to humans by inhalation of aerosolized particles shed in rodent excreta. Human-to-human spread has never been reported in North America.

The virus has a remarkable predilection for pulmonary capillary endothelial cells and a complex and still poorly understood pathogenesis. Infection by inhalation is followed by an incubation period of 1–5 weeks. A 3–6-day prodromal period then occurs, during which patients first exhibit fever, with respiratory symptoms notably absent. The development of a cough signals the onset of the fulminant cardiopulmonary phase, which is characterized by severe capillary leak, extraordinary pulmonary edema, and myocardial depression, and lasts for up to 1 week. The current mortality rate during the cardiopulmonary phase is ≈40%. Survivors mobilize third-space fluid during the diuretic-recovery phase, which may last up to 2 weeks (10).

Most of the damage during the cardiopulmonary phase of HPS is directly related to cell-mediated immunity gone awry. During the incubation phase, there is a ubiquitous deposition of the virus within the pulmonary endothelium, with no associated changes in either the structural integrity or permeability of the microenvironment (4). During the relatively brief prodromal phase, circulating immunoblasts appear and humoral antibody is produced. It is during the

cardiopulmonary phase that well-differentiated T cells appear on site and participate in the release of soluble mediators (among which tumor necrosis factor-α is prominent); massive changes in pulmonary capillary endothelial cell permeability result (11). Fluid loss into the alveolar and pleural spaces is so voluminous that the heart becomes preload deprived and cardiac output decreases. The same soluble mediators are in part responsible for depression of myocardial contractility that often leads to frank cardiovascular collapse (12).

A distinctive hematologic laboratory profile offers clues to the diagnosis of HPS. Researchers at the University of New Mexico have triaged patients with prodromal symptoms and a consistent exposure history by examining the peripheral blood smear for the presence of 5 factors: thrombocytopenia, hemoconcentration, a granulocytic left shift, the absence of toxic change, and the presence of >10% immunoblasts. If 4 of the 5 factors are present, there is ≈a 90% sensitivity and specificity for the disease (13). Definitive diagnosis of hantavirus infection relies on serologic testing for IgM and IgG, which is highly sensitive and specific, but because of travel times to laboratories performing the assay, it takes >72 hours in most cases to provide results.

Treatment of HPS is challenging. Because of the severity of endothelial leakage, fluid resuscitation can lead to worsening pulmonary edema. Because patients are maximally vasoconstricted, vasopressors are of little benefit. Inotropes, particularly dobutamine, are often used but have no demonstrated value. Steroids have been used, again with no proven benefit (14). Patients in the cardiopulmonary phase have a failing heart and failing lungs. Extracorporeal membrane oxygenation (ECMO) offers a supporting bridge to the diuretic-recovery phase. The University of New Mexico has pioneered the use of ECMO for HPS. Early efforts there to use ECMO were plagued by technical difficulty because health of HPS patients has a tendency to decline so rapidly that clinicians were often left attempting to obtain arterial and venous ECMO access for patients in full cardiac arrest (15). Physicians at the University of New Mexico have now developed a strategy of preemptively placing femoral arterial and venous access catheters in suspected case-patients at the time of hospital arrival, so that ECMO can be initiated at the earliest sign of decompensation. This strategy has resulted in an impressive 80% survival rate in patients despite overt cardiopulmonary collapse. Mortality rates in that subset of patients had previously exceeded 90% (16).

HPS was discovered and defined by the collaborative efforts of federal, state, and local investigators during the spring of 1993. The rapidity of the successful investigation was the result of the presence of competent persons at all levels and to the early actions of the New Mexico Office of

Medical Investigation. HPS is a disease of healthy young persons who have a history of rodent exposure, usually at home or at work. A laboratory examination that demonstrates hemoconcentration, or the presence of immunoblasts on a peripheral blood smear, should raise immediate clinical suspicion. Severe capillary leak with massive pulmonary edema is the hallmark finding of HPS. Frederick Koster, an infectious disease physician in New Mexico who was part of the original Four Corners investigation, has described HPS-associated pulmonary edema as "a disease manifestation without parallel in clinical medicine" (*17*). Suspected case-patients should always be referred to an ECMO-capable center without delay because health decline is precipitous, and ECMO may be lifesaving.

About the Author

Dr. Van Hook is a pulmonologist and critical care specialist in the Department of Pulmonary and Critical Care, Longmont United Hospital, Longmont, CO. His research interests include respiratory infections and the effect of outpatient opioid use in critical illness.

References

1. Sternberg S. Tracking a mysterious killer virus in the southwest. The Washington Post. 1994 Jul 14 [cited 2018 Apr 13]. https://www.washingtonpost.com/archive/lifestyle/wellness/1994/06/14/tracking-a-mysterious-killer-virus-in-the-southwest/5e074ccd-7d88-41c0-9dc4-c0edcc1cd16e/?utm_term=.19320abc19ce
2. Ksiazek TG, Peters CJ, Rollin PE, Zaki S, Nichol S, Spiropoulou C, et al. Identification of a new North American hantavirus that causes acute pulmonary insufficiency. Am J Trop Med Hyg. 1995; 52:117–23. http://dx.doi.org/10.4269/ajtmh.1995.52.117
3. Childs JE, Ksiazek TG, Spiropoulou CF, Krebs JW, Morzunov S, Maupin GO, et al. Serologic and genetic identification of *Peromyscus maniculatus* as the primary rodent reservoir for a new hantavirus in the southwestern United States. J Infect Dis. 1994;169:1271–80. http://dx.doi.org/10.1093/infdis/169.6.1271
4. Zaki SR, Greer PW, Coffield LM, Goldsmith CS, Nolte KB, Foucar K, et al. Hantavirus pulmonary syndrome: pathogenesis of an emerging infectious disease. Am J Pathol. 1995;146:552–79.
5. Nichol ST, Spiropoulou CF, Morzunov S, Rollin PE, Ksiazek TG, Feldmann H, et al. Genetic identification of a hantavirus associated with an outbreak of acute respiratory illness. Science. 1993;262:914–7. http://dx.doi.org/10.1126/science.8235615
6. Duchin JS, Koster FT, Peters CJ, Simpson GL, Tempest B, Zaki SR, et al.; The Hantavirus Study Group. Hantavirus pulmonary syndrome: a clinical description of 17 patients with a newly recognized disease. N Engl J Med. 1994;330:949–55. http://dx.doi.org/10.1056/NEJM199404073301401
7. Yates TL, Mills JN, Parmenter CA, Ksiazek TG, Parmenter RR, Vande Castle JR, et al. The ecology and evolutionary history of an emergent disease: hantavirus pulmonary syndrome. Bioscience. 2002; 52:989–98. http://dx.doi.org/10.1641/0006-3568(2002)052[0989:TEAEHO]2.0.CO;2
8. de St Maurice A, Ervin E, Schumacher M, Yaglom H, VinHatton E, Melman S, et al. Exposure characteristics of hantavirus pulmonary syndrome patients, United States, 1993–2015. Emerg Infect Dis. 2017;23:733–9. http://dx.doi.org/10.3201/eid2305.161770
9. MacNeil A, Ksiazek TG, Rollin PE. Hantavirus pulmonary syndrome, United States, 1993–2009. Emerg Infect Dis. 2011; 17:1195–201. http://dx.doi.org/10.3201/eid1707.101306
10. Simpson SQ, Spikes L, Patel S, Faruqi I. Hantavirus pulmonary syndrome. Infect Dis Clin North Am. 2010;24:159–73. http://dx.doi.org/10.1016/j.idc.2009.10.011
11. Terajima M, Ennis FA. T cells and pathogenesis of hantavirus cardiopulmonary syndrome and hemorrhagic fever with renal syndrome. Viruses. 2011;3:1059–73. http://dx.doi.org/10.3390/v3071059
12. Saggioro FP, Rossi MA, Duarte MI, Martin CC, Alves VA, Moreli ML, et al. Hantavirus infection induces a typical myocarditis that may be responsible for myocardial depression and shock in hantavirus pulmonary syndrome. J Infect Dis. 2007;195: 1541–9. http://dx.doi.org/10.1086/513874
13. Dvorscak L, Czuchlewski DR. Successful triage of suspected hantavirus cardiopulmonary syndrome by peripheral blood smear review: a decade of experience in an endemic region. Am J Clin Pathol. 2014;142:196–201. http://dx.doi.org/10.1309/AJCPNFVWG46NUHED
14. Vial PA, Valdivieso F, Ferres M, Riquelme R, Rioseco ML, Calvo M, et al.; Hantavirus Study Group in Chile. High-dose intravenous methylprednisolone for hantavirus cardiopulmonary syndrome in Chile: a double-blind, randomized controlled clinical trial. Clin Infect Dis. 2013;57:943–51. http://dx.doi.org/10.1093/cid/cit394
15. Dietl CA, Wernly JA, Pett SB, Yassin SF, Sterling JP, Dragan R, et al. Extracorporeal membrane oxygenation support improves survival of patients with severe hantavirus cardiopulmonary syndrome. J Thorac Cardiovasc Surg. 2008;135:579–84. http://dx.doi.org/10.1016/j.jtcvs.2007.11.020
16. Wernly JA, Dietl CA, Tabe CE, Pett SB, Crandall C, Milligan K, et al. Extracorporeal membrane oxygenation support improves survival of patients with hantavirus cardiopulmonary syndrome refractory to medical treatment. Eur J Cardiothorac Surg. 2011; 40:1334–40. http://dx.doi.org/10.1016/j.ejcts.2011.01.089
17. Koster F, Mackow E. Pathogenesis of hantavirus pulmonary syndrome. Future Virol. 2011;7:41–51. http://dx.doi.org/10.2217/fvl.11.138

Address for correspondence: Charles J. Van Hook, Pulmonary and Critical Care, Longmont United Hospital, 2030 Mountain View Ave, Ste 540, Longmont, CO 80502-1659, USA; email: cvhmd7@gmail.com

Human Babesiosis, Yucatán State, Mexico, 2015

**Gaspar Peniche-Lara, Lucero Balmaceda,
Carlos Perez-Osorio, Claudia Munoz-Zanzi**

In 2015, we detected clinical cases of babesiosis caused by *Babesia microti* in Yucatán State, Mexico. Cases occurred in 4 children from a small town who became ill during the same month. Diagnosis was confirmed using conventional PCR followed by sequencing of the DNA fragment obtained.

Protozoa from the genus *Babesia*, specifically *B. microti* and *B. divergens*, can infect humans (*1*). Symptoms of infection include fever (38°C–40°C), malaise, chills, myalgia, and fatigue. In some cases, nausea, emesis, night sweats, weight loss, anemia, and hematuria are reported. Hepatomegaly and splenomegaly also can be present (*1*). Transmission occurs mainly when infected ticks of the *Ixodes* genus feed on humans; however, blood transfusions have been reported as another route.

In Mexico, the only report of human babesiosis is that of isolation of *Babesia* spp. from a blood sample from an asymptomatic human in 1976 (*2*). In Yucatán State, human cases of dengue fever and rickettsiosis are frequent and usually share similar symptoms to babesiosis, which is difficult to diagnose (*3,4*). We describe 4 patients with confirmed babesiosis caused by *B. microti* in Yucatán, Mexico.

Case Reports

All 4 patients were from a small municipality in eastern Yucatán and had disease onset during July 2015. All patients lived in close proximity but in different households. After dengue fever was excluded at the local rural health center, blood samples were sent to the Parasitic and Infectious Diseases Laboratory at the Medicine Faculty of the University Autonomous (Yucatán, Mexico) for rickettsiosis diagnosis. Molecular test and immunofluorescence indirect assay for *Rickettsia* infection were negative in all samples. Independent from clinical management, we conducted additional testing on stored samples, and on the basis of the common history of risk factors, ticks, and

Author affiliations: Universidad Autónoma de Yucatán, Yucatán, Mexico (G. Peniche-Lara, L. Balmaceda, C. Perez-Osorio); University of Minnesota, Minneapolis, Minnesota, USA (C. Munoz-Zanzi)

rodent presence, we suspected babesiosis. Deidentified medical record information was limited about history, clinical presentation, and treatment.

Patient 1 was a 13-year-old boy who was seen at the health service center with signs and symptoms that included fever (39°C), myalgia, fatigue, and arthralgia that started 3 days before his clinic visit. His mother indicated he had frequent contact with vegetation because of work in agricultural activities and close contact with dogs, cats, birds, and cows and noted that ticks parasitized domestic animals and rodents surrounding the house.

Patient 2 was a 12-year-old girl who had a history of fever (38°C) during the previous 3 days that was unresponsive to medication, myalgia, fatigue, nonsevere arthralgia, drowsiness, and paleness. On the day of her clinic visit, myalgia was severe. Fever was initially treated at home with medicinal plants and later with paracetamol (500 mg/6 h). She lived with her parents and performed housework that included close contact with dogs and goats.

Patient 3 was a 14-year old male student with 14 days of symptoms that included fever (38°C), myalgia, arthralgia, and headache. Four days after symptom onset, he went to a private clinic and began treatment with amoxicillin and ambroxol but did not recover. On day 14, fever and other symptoms persisted, in addition to weight loss and drowsiness. He mentioned observing ticks feeding on backyard dogs and having close contact with vegetation while gardening at school.

Patient 4 was an 8-year-old girl with 3 days of fever (39°C), headache, drowsiness, and exanthema in the upper extremities. During physical examination, 2 ticks were found attached to her, 1 on the right groin area and 1 on the scalp. Ticks were not available for laboratory analysis. Her mother stated close contact with dogs in the house and presence of rodents.

For all blood samples, DNA was purified using Quick-gDNA MiniPrep (Zymo Research, Irvine, CA, USA). We used conventional PCR to amplify a 474-bp gene fragment from 18S rRNA of *Babesia* species (*5*). Amplified products were cloned and sequenced (GenBank accession no. MH048838). The amplified products were 100% homologus to *B. microti* from several isolates from Asia (GenBank accession nos. KF410826.1, LC005763.1, LC005772.1). Proper laboratory quality control measures included negative (sterile water as a sample) and positive (*B. microti*

DNA sample) controls. We used separate areas and personnel for DNA extraction, quantitative PCR, and PCR reaction setup.

Because of the mild-to-moderate infection, all patents were treated with chloroquine. All progressed well during the treatment, and they completely recovered.

Conclusions

Our findings document the occurrence of human babesiosis confirmed by molecular methods in Yucatán. Babesiosis is a widespread vectorborne disease transmitted by tick bites, which has similar clinical presentation to infectious diseases that are endemic to Yucatán, such as dengue and rickettsiosis. Increased awareness is needed among health providers about inclusion of babesiosis in the differential diagnosis of undefined febrile illness and to develop guidelines for timely diagnosis in adults and children. Furthermore, studies are required to evaluate the adaptation of *B. microti* to hosts and vectors to which it is endemic, characterize its clinical manifestations, and estimate the real prevalence and incidence of *Babesia* infection in the population of Mexico.

About the Author

Dr. Peniche-Lara works at Facultad de Medicina, Universidad Autonoma de Yucatán, Mexico. His primary research interests include the epidemiology of pathogens transmitted by ticks in southeastern Mexico.

References

1. Rożej-Bielicka W, Stypułkowska-Misiurewicz H, Gołąb E. Human babesiosis. Przegl Epidemiol. 2015;69:489–94, 605–8.
2. Osornio M, Vega C, Ristic M, Robles C, Ibarra S. Isolation of *Babesia* spp. from asymptomatic human beings. Vet Parasitol. 1976;2:10.
3. Dantés HG, Farfán-Ale JA, Sarti E. Epidemiological trends of dengue disease in Mexico (2000–2011): a systematic literature search and analysis. PLoS Negl Trop Dis. 2014;8:e3158. http://dx.doi.org/10.1371/journal.pntd.0003158
4. Labruna MB, Mattar VS, Nava S, Bermúdez S, Venzal JM, Dolz G, et al. Rickettsioses in Latin America, Caribbean, Spain and Portugal. Revista MVZ Córdoba. 2011;16:23. http://dx.doi.org/10.21897/rmvz.282
5. Casati S, Sager H, Gern L, Piffaretti JC. Presence of potentially pathogenic *Babesia* sp. for human in *Ixodes ricinus* in Switzerland. Ann Agric Environ Med. 2006;13:65–70.

Address for correspondence: Gaspar Peniche Lara, Laboratorio de Enfermedades Infecciosas y Parasitarias I, Facultad de Medicina, Universidad Autónoma de Yucatán, Mexico, Avenida Itzaes Num 498 Entre 59 y 59A, Centro, Mérida, Yucatán CP 97000, Mexico; email gaspar.peniche@correo.uady.mx

Detection and Characterization of Human Pegivirus 2, Vietnam

Nguyen To Anh, Nguyen Thi Thu Hong,
Le Nguyen Truc Nhu, Tran Tan Thanh,
Catherine Anscombe, Le Ngoc Chau,
Tran Thi Thanh Thanh, Chuen-Yen Lau,
Direk Limmathurotsakul, Nguyen Van
Vinh Chau, H. Rogier van Doorn, Xutao Deng,
Motiur Rahman, Eric Delwart, Thuy Le,
Guy Thwaites, Le Van Tan, for the Southeast Asia
Infectious Disease Clinical Research Network[1]

We report human pegivirus 2 (HPgV-2) infection in Vietnam. We detected HPgV-2 in some patients with hepatitis C virus/HIV co-infection but not in patients with HIV or hepatitis A, B, or C virus infection, nor in healthy controls. HPgV-2 strains in Vietnam are phylogenetically related to global strains.

Human pegivirus 2 (HPgV-2), also known as human hepegivirus 1, is a recently discovered bloodborne flavivirus (*1*,*2*). Existing evidence suggests that HPgV-2 is more frequently detected in patients with hepatitis C virus (HCV) infection, particularly HCV and HIV co-infection, although detection rates vary between studies and patient groups. In the United States, HPgV-2 was detected in 1.2% (12/983) of patients with active HCV infections (*1*), whereas in China, the reported detection rates of HPgV-2 RNA were 0.29% (7/2440) among HCV monoinfected patients and from 3% (8/270) to 5.7% (4/70) among HCV/HIV co-infected patients (*3*,*4*). HPgV-2 RNA was detected in 10.9% (17/156) of injection drug users in the United States, and there was a strong association between HPgV-2 and other infections such as HCV and SEN virus D (*5*).

Author affiliations: Oxford University, Ho Chi Minh City, Vietnam (N.T. Anh, N.T.T. Hong, L.N.T. Nhu, T.T. Thanh, C. Anscombe, L.N. Chau, T.T.T. Thanh, H.R. van Doorn, M. Rahman, T. Le, G. Thwaites, L.V. Tan); University of Oxford, Oxford, UK (C. Anscombe, D. Limmathurotsakul, H.R. van Doorn, G. Thwaites); National Institutes of Health, Bethesda, Maryland, USA (C.-Y. Lau); Mahidol Oxford Tropical Research Unit, Bangkok, Thailand (D. Limmathurotsakul); Hospital for Tropical Diseases, Ho Chi Minh City, Vietnam (N.V.V. Chau); Blood Systems Research Institute, San Francisco, California, USA (X. Deng, E. Delwart); University of California, San Francisco (X. Deng, E. Delwart)

DOI: https://doi.org/10.3201/eid2411.180668

Given the high burden of HCV and HIV infections worldwide and the potential clinical significance of HPgV-2, we investigated the geographic distribution and genetic diversity of this virus to help prioritize the development and implementation of appropriate intervention strategies. The studies were approved by the corresponding institutional review boards of the local hospitals in Vietnam where patients were enrolled and the Oxford Tropical Research Ethics Committee. We obtained written informed consent from each participant or from the participant's parent or legal guardian.

The Study

Patient information and clinical samples were derived from a multilocation observational study designed to evaluate the causes of community-acquired infection in Southeast Asia (*6*). We included all 493 samples (384 plasma, 92 pooled nasal and throat swabs, 10 stool, and 7 cerebrospinal fluid [CSF]) from 386 patients in Vietnam with community-acquired infection of unknown origin after extensive diagnostic workup for viral metagenomic analysis (*7*).

Analysis of metagenomic data revealed that, in 1 plasma sample, of 98,344 obtained reads, 5,342 reads were of HCV sequences, 430 of HIV sequences, and 273 of HPgV-2 sequences; we confirmed all reads by corresponding virus-specific reverse transcription PCR (RT-PCR). HPgV-2 sequence screening and HPgV-2 RT-PCR testing did not detect HPgV-2 in any of the remaining samples of the patients included in metagenomic analysis.

To explore the prevalence of HPgV-2 in HCV-infected patients in Vietnam, we used a reference-based mapping strategy to screen for HPgV-2 sequences in additional viral metagenomic datasets (Table 1). We detected HPgV-2 sequences in 5/79 HIV/HCV co-infected patients who participated in a trial evaluating the hepatic safety of raltegravir/efavirenz-based therapies in antiretroviral-naive HIV-infected subjects co-infected with HCV. We did not detect HPgV-2 sequences in 394 HCV-infected patients with clinically diagnosed hepatitis who participated in molecular epidemiologic studies of hepatitis viruses (Table 1).

We subsequently confirmed the result of this reference-mapping approach by HPgV-2 multiplex RT-PCR (*8*) testing of the extracted RNA from original samples. We

[1]Members of the Southeast Asia Infectious Disease Clinical Research Network are listed at the end of this article.

Table 1. Samples and viral metagenomic datasets used in screening for HPgV-2 and screening results, Vietnam*

Infection	No. persons	Screening approach	No. positive for HPgV-2	Enrollment period	Setting
Hepatitis C virus and HIV co-infection	79	HPgV-2–specific PCR and reference-based mapping of obtained viral metagenomics data	5	2010–2013	Hospital for Tropical Diseases, Ho Chi Minh City
HIV monoinfection	78	HPgV-2–specific PCR	0	2010–2013	Hospital for Tropical Diseases, Ho Chi Minh City
None (healthy volunteers)	80	HPgV-2–specific PCR	0	2010–2013	Hospital for Tropical Diseases, Ho Chi Minh City
Hepatitis A virus	71	HPgV-2–specific PCR	0	2012–2014	Hospital for Tropical Diseases, Ho Chi Minh City
Hepatitis B virus	103	HPgV-2–specific PCR	0	2012–2016	Hospital for Tropical Diseases, Ho Chi Minh City; Dong Thap General Hospital, Dong Thap; Khanh Hoa Provincial Hospital, Nha Trang; Dac Lac Provincial Hospital, Dac Lac; Hue National Hospital, Hue
Hepatitis C virus†	394	Reference-based mapping of obtained viral metagenomics data	0	2012–2016	Hospital for Tropical Diseases, Ho Chi Minh City; Dong Thap General Hospital, Dong Thap; Khanh Hoa Provincial Hospital, Nha Trang; Dac Lac Provincial Hospital, Dac Lac; Hue National Hospital, Hue

*HPgV-2, human pegivirus.
†Whole-genome sequences of hepatitis C virus were obtained using a viral metagenomics approach (7). The resulting metagenomics datasets were then subjected to a reference-based mapping approach to search for the presence of HPgV-2 sequences.

conducted multiplex RT-PCR screening for HPgV-2 RNA in plasma samples of matched controls (78 HIV-infected patients and 80 healthy volunteers) of the 79 HCV/HIV co-infected patients; we found no evidence of HPgV-2 (Table 1). In addition, we did not detect HPgV-2 RNA in any plasma samples from patients with HAV (n = 71) and HBV (n = 103) infection (Table 1).

HPgV-2 RNA was detectable for ≤18 months in 3/5 patients with HCV/HIV co-infection (Table 2). We did not detect HPgV-2 RNA in the available follow-up serum sample collected 14 days after enrollment from the patient with community-acquired infection (Table 2).

All 5 HCV/HIV co-infected patients had CD4 counts >200 cells/μL at baseline and at 6-, 12-, and 18-month follow-up (Table 2), but none received specific anti-HCV drugs, which was attributed to drug unavailability or unaffordability during the study period. During follow-up, hepatitis and splenic abnormalities were detected in 4/5 patients, which were likely attributable to HCV infection (Table 2). The patient with community-acquired infection was recorded as surviving to 28 days of follow-up (Table 2).

Using deep sequencing and a combination of overlapping PCRs and Sanger sequencing of PCR amplicons (primer sequences available upon request), we obtained 5 nearly complete genomes (coverage of >92%) and another partial genome (coverage of ≈69.1%). Pairwise comparison of HPgV-2 coding regions obtained in this study and previously reported HPgV-2 sequences showed overall sequence identities at the nucleotide level of ≥94.6% and at the amino acid level of ≥95.3% (data not shown).

Phylogenetic analyses revealed a tight cluster between viruses from Vietnam and global strains (Figure). We submitted the HPgV-2 sequences we generated to GenBank (accession nos. MH194408–13).

Of the 5 HPgV-2 genome sequences we recovered, we generated 2 by deep sequencing. The results were above the proposed sequencing-depth threshold of ≥5 for sequences generated by next-generation sequencing (9) and sufficient for intrahost diversity investigation. One sequence we generated had mean coverage of 2,049 (range 12–9,912), with a total of 26 (10 [38%] nonsynonymous) positions carrying minor variations detected in the corresponding dataset (data not shown). For the other sequence, mean coverage was 32,531 (range 13–138,383), with a total of 37 (13 [35%] nonsynonymous) positions carrying minor variations in its dataset (data not shown).

Conclusions

We report the detection and genetic characterization of HPgV-2 in Vietnam and describe the observed demographic and clinical characteristics of patients with HPgV-2 infection. Together with reports from China, Iran, and the United States (1–4,8,10), our findings further emphasize the strong association between HPgV-2 and HCV, especially HCV/HIV co-infection. The absence of HPgV-2 in 394 HCV-infected patients may have been attributed to the small sample size and the fact that the reported prevalence of HIV among HCV-infected patients was ≤6.5% (11,12). Of note, HPgV-2 was detected in only 0.29% of HCV-monoinfected patients in China.

Table 2. Demographic and clinical features of 6 men with human pegivirus infection, Vietnam*

Pt no.	Pt age, y	Time point, mo	HCV RNA+	HPgV-2 RNA+	Total bilirubin, μmol/L	Direct bilirubin, μmol/L	AST, UI/L	ALT, UI/L	CD4 count, cells/μL	HIV RNA, × 10³ copies/μL	AFP, mg/mL	FibroScan result, kPa	Symptoms
1	29	NA	NA	NA	NA	NA	NA	NA	NA	NA	NA	NA	NA
2	47	0	Y	Y	9.8	0.7	30	24	331	120	1.7	11.8	
		6	Y	Y	4.7	1.6	81	83	518	0.07	2.3	NA	
		12	Y	Y	6.9	3.4	55	61	364	0.04	2.6	11.8	Hepatitis
		18	Y	Y	4.8	2.8	37	40	428	UND	2.14	6.1	Hepatomegaly
3	32	0	Y	Y	4.7	3.4	39	10	288	0.198	0.999	6.5	
		6	Y	Y	12.8	4.7	50	19	510	0.04	1.68	NA	
		12	Y	Y	9.5	5.3	63	25	622	UND	1.88	6.2	Liver fibrosis, hepatomegaly
		18	Y	Y	7.6	3.8	42	23	622	UND	1.53	7.2	Hepatitis
4	35	0	Y	Y	7.8	4.9	67	55	290	61.1	2.96	6.4	
		6	Y	Y	10.7	6.3	77	80	411	UND	3.1	NA	
		12	Y	Y	8.8	3.9	76	72	337	UND	4	8.5	Homogeneous hepatomegaly
		18	Y	Y	13	6.3	108	129	455	UND	4.1	8.1	Splenomegaly, liver fibrosis
5	34	0	Y	Y	4.3	2.8	33	43	291	70.2	3.67	6.1	
		6	N	Y	6.5	2.1	35	43	287	UND	3.83	NA	
		12	N	N	5.4	2.6	33	40	484	UND	4.48	4.5	
		18	N	N	6.6	2.6	73	85	546	UND	3.9	3	
6	31	0	Y	Y	4.5	2.4	52.2	36.5	295	96.8	12.7	22.8	
		6	Y	Y	17.1	12.9	64	62	579	UND	16.74	NA	
		12	Y	N	12.3	4.3	114	121	711	UND	46.3	26.3	Mild liver fibrosis, mild splenomegaly
		18	Y	N	10.6	4.9	82	89	816	UND	61.01	NA	Hepatomegaly, splenomegaly

*Age is patient's age at diagnosis; time point is the month at which follow-up visit was conducted; 0 was the baseline examination. ALT, alanine aminotransferase; AS, aspartate aminotransferase; NA, not available; Pt, patient; UND, undetectable.
†Patient 1 belongs to the community-acquired infection cohort.

Previous reports showed that HPgV-2 viremia can be transient or persistent. Likewise, in our study, HPgV-2 RNA became undetectable after 14 days in a HCV/HIV co-infected patient with community-acquired infection of unknown origin, but remained detectable in other HCV/HIV co-infected patients through up to 18 months of follow-up.

The pathogenic potential of HPgV-2 remains unknown. Its role in HCV/HIV co-infection and response to treatment warrants further research, given its low detection rates in blood donors in the United States and China (1,3) and its absence in healthy persons (this study) but close association with HCV/HIV co-infection.

In the era of sequence-based virus discovery, a key question is whether the detected genome represents live virus or a non–replication competent genome. Addressing this question would require recovery of virus in cell culture. However, our detection of minor variations across 2 HPgV-2 genomes suggests that viral replication had occurred in the infected patients. Phylogenetically, the close relatedness between HPgV-2 strains from Vietnam and global strains suggests HPgV-2 has a wide geographic distribution.

Our study has some limitations. First, we only retrospectively tested available archived samples without formal sample size estimation, which may have explained the absence of HPgV-2 in the remaining 394 HCV patients. Second, we did not employ a serologic assay to screen for HPgV-2

antibodies in patients' plasma. Third, we used only multiplex PCR with primers based on a limited number of available HPgV-2 sequences. Therefore, we may have missed genetically diverse HPgV-2 strains, and we may have underestimated the prevalence of HPgV-2 infections in Vietnam.

Our findings contribute expanded data about geographic distribution, demographics, and genetic diversity of HPgV-2. Because HCV and HIV infections are global public health issues, the extent to which HPgV-2 interacts with HCV and HIV in co-infected patients and the possible clinical consequences warrant further research.
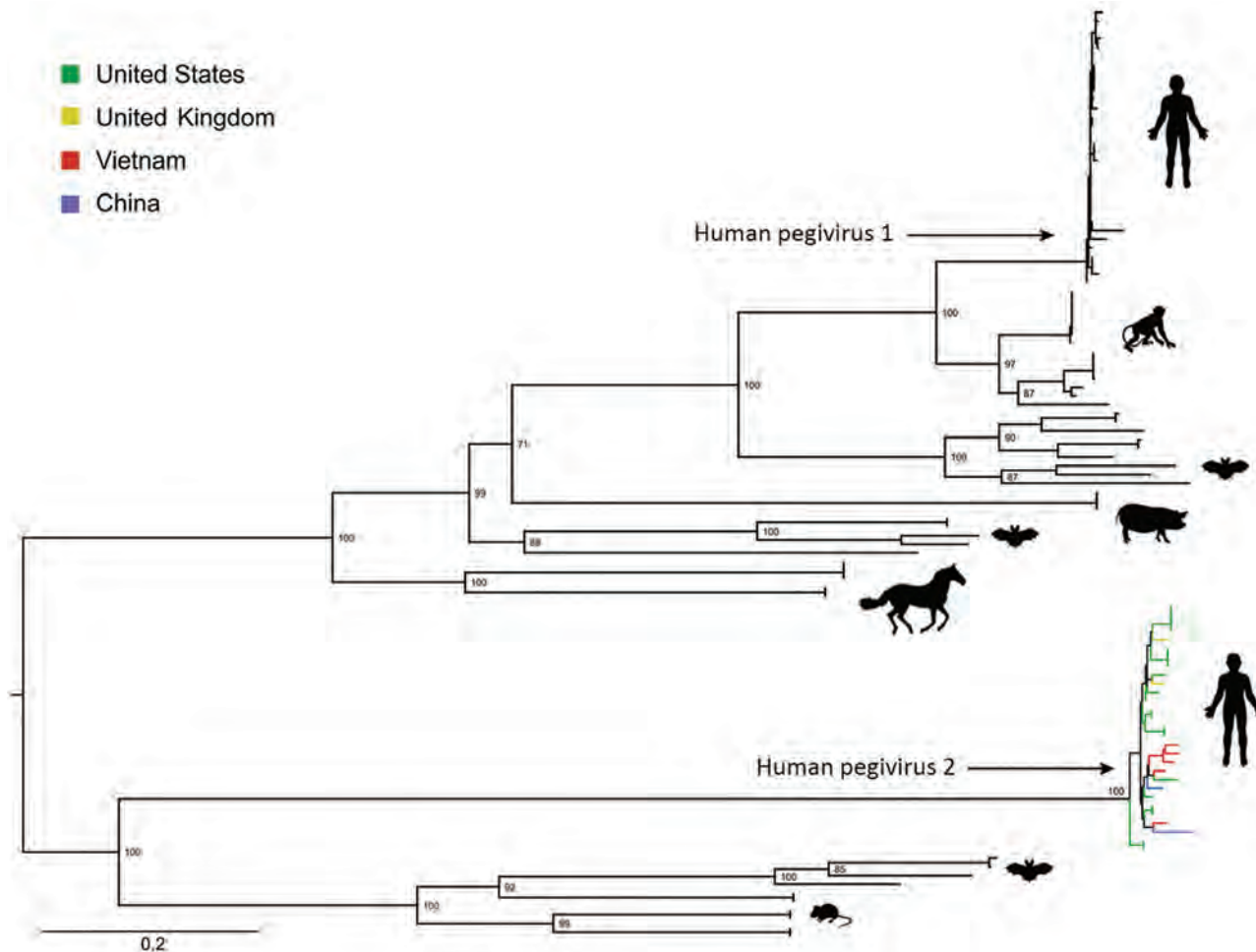
Figure. Maximum-likelihood phylogenetic tree of amino acid sequences of coding sequences of human pegivirus 2 strains from Vietnam compared with global strains and other pegiviruses. We used the general matrix with empirical amino acid frequencies, a gamma distribution of 4 rates, and invariant sites, as suggested by IQ TREE (http://www.iqtree.org), to reconstruct the phylogenetic trees. We assessed support for individual nodes using a bootstrap procedure of 10,000 replicates. Scale bar indicates amino acid substitutions per site.

Medicine Research Unit, Bangkok); Achara Laongnualpanich (Chiang Rai Prachanukroh Hospital, Chiang Rai, Thailand); Prapit Teparrakkul and Pramot Srisamang (Sappasithiprasong Hospital, Ubon Ratchathani, Thailand); Claire Ling (Shoklo Malaria Research Unit, Mae Sot, Thailand); Phan Huu Phuc and Le Thanh Hai (National Hospital of Pediatrics, Hanoi, Vietnam); Nguyen Van Kinh (National Hospital of Tropical Diseases, Hanoi); Bui Duc Phu (Hue Central Hospital, Hue, Vietnam); Nguyen Thanh Hung and Tang Chi Thuong (Children's Hospital 1, Ho Chi Minh City, Vietnam); Ha Manh Tuan (Children's Hospital 2, Ho Chi Minh City); Lam Minh Yen and Nguyen Van Vinh Chau (Hospital for Tropical Diseases, Ho Chi Minh City); Guy Thwaites, Heiman Wertheim, Le Van Tan, Motiur Rahman, and H. Rogier van Doorn (Oxford University Clinical Research Unit, Ho Chi Minh City); and Chuen-Yen Lau (National Institute of Allergy and Infectious Diseases, National Institutes of Health, Bethesda, Maryland, USA).

About the Author

Ms. Nguyen is a PhD student in life science at Open University, Milton Keynes, United Kingdom. Her research interests are virus discovery and evolution of emerging pathogens such as enteroviruses.

References

1. Berg MG, Lee D, Coller K, Frankel M, Aronsohn A, Cheng K, et al. Discovery of a novel human pegivirus in blood associated with hepatitis C virus co-infection. PLoS Pathog. 2015; 11:e1005325. http://dx.doi.org/10.1371/journal.ppat.1005325
2. Kapoor A, Kumar A, Simmonds P, Bhuva N, Singh Chauhan L, Lee B, et al. Virome analysis of transfusion recipients reveals a novel human virus that shares genomic features with hepaciviruses and pegiviruses. MBio. 2015;6:e01466–15. http://dx.doi.org/10.1128/mBio.01466-15
3. Wang H, Wan Z, Xu R, Guan Y, Zhu N, Li J, et al. A novel human pegivirus, HPgV-2 (HHpgV-1), is tightly associated with hepatitis C virus (HCV) infection and HCV/human immunodeficiency virus type 1 coinfection. Clin Infect Dis. 2018;66:29–35. http://dx.doi.org/10.1093/cid/cix748
4. Wang H, Wan Z, Sun Q, Zhu N, Li T, Ren X, et al. Second human pegivirus in hepatitis C virus-infected and hepatitis C virus/HIV-1 co-infected persons who injected drugs, China. Emerg Infect Dis. 2018;24:908–11.
5. Kandathil AJ, Breitwieser FP, Sachithanandham J, Robinson M, Mehta SH, Timp W, et al. Presence of human hepegivirus-1 in a cohort of people who inject drugs. Ann Intern Med. 2017;167:1–7. http://dx.doi.org/10.7326/M17-0085
6. Southeast Asia Infectious Disease Clinical Research Network. Causes and outcomes of sepsis in southeast Asia: a multinational multicentre cross-sectional study. Lancet Glob Health. 2017; 5:e157–67. http://dx.doi.org/10.1016/S2214-109X(17)30007-4
7. Nguyen AT, Tran TT, Hoang VMT, Nghiem NM, Le NNT, Le TTM, et al. Development and evaluation of a non-ribosomal random PCR and next-generation sequencing based assay for detection and sequencing of hand, foot, and mouth disease pathogens. Virol J. 2016;13:125. http://dx.doi.org/10.1186/s12985-016-0580-9
8. Frankel M, Forberg K, Coller KE, Berg MG, Hackett J Jr, Cloherty G, et al. Development of a high-throughput multiplexed real time RT-PCR assay for detection of human pegivirus 1 and 2. J Virol Methods. 2017;241:34–40. http://dx.doi.org/10.1016/j.jviromet.2016.12.013
9. Ladner JT, Beitzel B, Chain PS, Davenport MG, Donaldson EF, Frieman M, et al.; Threat Characterization Consortium. Standards for sequencing viral genomes in the era of high-throughput sequencing.. VIROME: a standard operating procedure for analysis of viral metagenome sequences. MBio. 2014;5:e01360–14.
10. Bijvand Y, Aghasadeghi MR, Sakhaee F, Pakzad P, Vaziri F, Saraji AA, et al. First detection of human hepegivirus-1 (HHpgV-1) in Iranian patients with hemophilia. Sci Rep. 2018;8:5036. http://dx.doi.org/10.1038/s41598-018-23490-4
11. Barclay ST, Cooke GS, Holtham E, Gauthier A, Schwarzbard J, Atanasov P, et al. A new paradigm evaluating cost per cure of HCV infection in the UK. Hepatol Med Policy. 2016;1:2. https://doi.org/10.1186/s41124-016-0002-z
12. Ireland G, Delpech V, Kirwan P, Croxford S, Lattimore S, Sabin C, et al. Prevalence of diagnosed HIV infection among persons with hepatitis C virus infection: England, 2008–2014. HIV Med. 2018 Jul 26 [Epub ahead of print].
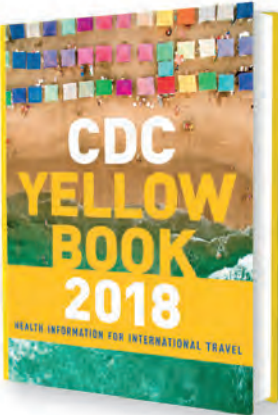
Address for correspondence: To Anh Nguyen or Le Van Tan, Oxford University Clinical Research Unit, Ho Chi Minh City, Vietnam; email: anhnt@oucru.org or tanlv@oucru.org

African Histoplasmosis in HIV-Negative Patients, Kimpese, Democratic Republic of the Congo

Nestor Pakasa, Asaf Biber, Samuel Nsiangana,
Désiré Imposo, Ernest Sumaili, Hypolite Muhindo,
Maria J. Buitrago, Iris Barshack, Eli Schwartz

We describe a case series of histoplasmosis caused by *Histoplasma capsulatum* var. *duboisii* during July 2011–January 2014 in Kimpese, Democratic Republic of the Congo. Cases were confirmed by histopathology, immunohistochemistry, and reverse transcription PCR. All patients were HIV negative. Putative sources for the pathogen were cellarbats and guano fertilizer exploitation.

Infection with the fungus *Histoplasma capsulatum* var. *duboisii*, also known as African histoplasmosis, was described by Dubois et al. in 1952 (*1*). In total, <300 cases have been reported in the literature in Africa, mostly in sporadic forms (*2,3*).

Although the classical histoplasmosis, caused by *H. capsulatum* var. *capsulatum*, involves mainly the lungs, African histoplasmosis commonly involves the skin, followed by the bones. It tends to occur more frequently in patients infected with HIV. The pathogenesis of classical histoplasmosis, inhaling spores from bats' and birds' soil or guano, is well established, but the pathogenesis of African histoplasmosis remains unclear (*2*).

In the past, few reported cases of African histoplasmosis have been described from the Democratic Republic of the Congo; all were sporadic (*3–6*). We describe an unusual case series of African histoplasmosis in HIV-negative patients in Kimpese, Democratic Republic of the Congo.

The Study

All tissue samples diagnosed from histopathology as African histoplasmosis in routine biopsies at Institut Médical Evangélique Kimpese (Kimpese) during 2011–2016

Author affiliations: University of Kinshasa Hospital, Kinshasa, Democratic Republic of the Congo (N. Pakasa, E. Sumaili, H. Muhindo); Chaim Sheba Medical Center, Ramat Gan, Israel (A. Biber, I. Barshack, E. Schwartz); Institut Médical Evangélique, Kimpese, Democratic Republic of the Congo (S. Nsiangana, D. Imposo); University of Antwerp, Antwerp, Belgium (H. Muhindo); Instituto de Salud Carlos III, Madrid, Spain (M.J. Buitrago)

were included in the study. Most patients were female; median age was 20.5 years, and 42% percent were school-age children (Table). All but 3 were residents of Kimpese. Most of the infections occurred during July 2011–October 2012 (n = 32; 88.9%); case rates then sharply declined in 2013 (n = 3; 8.3%), subsiding to zero after January 2014 (Table). Four patients who were available for interviews reported living in houses that were heavily infested with cellar bats; these persons frequently collected guano from cellars to fertilize gardens, although their official occupation was not agricultural.

Laboratory findings, mainly from blood and feces, were nonspecific, apart from an increased erythrocyte sedimentation rate in most patients, a feature not diagnostic per se in the tropics. HIV test results were negative for all patients.

A total of 36 consecutive routine biopsies yielded diagnoses of *H. duboisii*. Seven specimens were from skin, 7 from bones, 5 from lymph nodes, and 8 of crumbly necrotic material. The rest of the specimens were labeled tumor or tumefaction related to clinical preoperative diagnosis.

Biopsy samples were fixed in 10% formalin and processed in the local laboratory using standard techniques of hematoxylin and eosin (HE) staining for light microscopy. Because special staining for fungi is unavailable in Kimpese, paraffin blocks were sent to Sheba Medical Center (Ramat Gan, Israel), where control HE, periodic acid Schiff (PAS), and Grocott methenamine-silver (GMS) staining were performed. Paraffin blocks were also brought to the Institut Pasteur Paris (Paris, France) for immunohistochemistry (IHC) to confirm the identity of the fungus using a noncommercial monoclonal antibody that detects both *H. capsulatum* and *H. duboisii*, distinguishable by their respective sizes (1–5 μm vs. 7–15 μm in diameter). The fungus phenotype was finally validated as *H. capsulatum* var. *duboisii* by the referral center le Centre National de Référence des Mycoses Invasives et Antifongiques in Paris. In addition, molecular analyses were performed at the Mycology Reference Laboratory, Centro Nacional de Microbiología, Instituto de Salud Carlos III (Majadahonda–Madrid, Spain), using a multiplex in-house specific real-time reverse transcription PCR (RT-PCR), as described previously (*7*).

In all tested samples, many intracellular or extracellular microorganisms were conspicuous on HE sections

Table. Characteristics of patients with African histoplasmosis, Democratic Republic of the Congo, July 2011–January 2014

Characteristics	Value*
Sex	
M	13 (36.1)
F	23 (63.9)
Year of diagnosis	
2011	13 (36.1)
2012	19 (52.8)
2013	3 (8.3)
2014	1 (2.8)
Age, y, median (interquartile range)	20.5 (10.5–39.0)
3–16	15 (41.7)
17–49	15 (41.7)
≥50	6 (16.6)
*Values are no. (%) except as indicated.	

(Figure, panel A). In most cases, organisms were seen in the cytoplasm of multiple multinucleated Langhans-type giant cells, often dividing by explosive budding (Figure, panel A) and frequently demonstrating explosive giant asteroid bodies (Figure, panel B), at times undergoing degeneration. The fungus was easily identified on PAS (Figure, panel C) and GMS (Figure, panel D).

Twelve samples from different patients underwent further IHC staining, which revealed a membranous staining of large 7–15-μm yeasts. RT-PCR assays performed in paraffin-embedded tissue samples from 3 patients were all positive for *H. capsulatum*. The technique was unable to differentiate between *H. capsulatum* var. *capsulatum* and var. *duboisii*, because the specific probe was designed to detect both. The average fungal burden detected was 7.6 fg DNA/μL.

Conclusions

This histology-based study identified a novel focus of *H. duboisii* in the Democratic Republic of the Congo in the city of Kimpese and its vicinity. Over a period of ≈2 years, 36 cases were routinely detected in a single pathology laboratory in this area; all patients were HIV negative.

The putative source of infection appears to be cellar bats, *Chaerephon pumilus*, and guano fertilizer overexploitation. African histoplasmosis has previously been reported to be isolated from the intestinal contents of bats belonging to the species *Nycteris hispida* and *Tadarida pumila* from a cave in rural Nigeria and from soil mixed with bat guano (*8*).

The subsiding of new cases could be related to the incidental cessation of the use of bat guano along with the reintroduction of chemical fertilizers. This change was unrelated to any knowledge about the infection risk of guano and may be reversed when the guano accumulates again to sizable amounts.

This case series featured a high incidence of infection in women and girls and in young children, including toddlers and school-age children. Six patients were 3–7 years of age, an age when children are more tied to their mothers, sit on the ground, and may be in contact with contaminated soil. Although HIV tests were negative, other innate or acquired immunosuppression was not ruled out.

During the first year of our case series, more cases were initially labeled as lymphoproliferative disorders
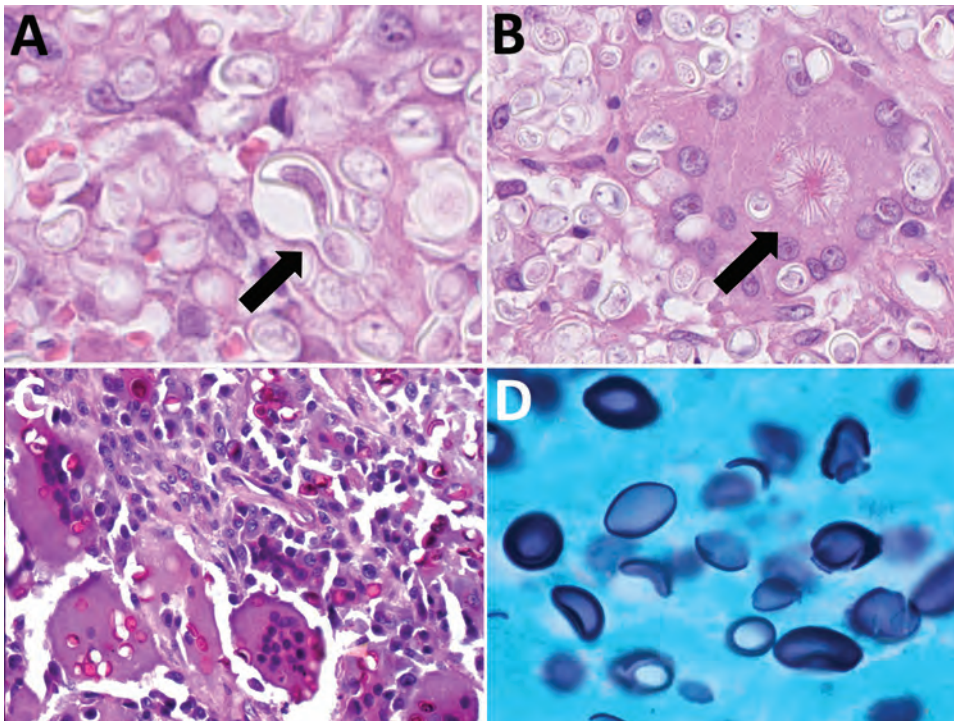

Figure. Pathologic findings from patients infected with African histoplasmosis, Democratic Republic of the Congo, July 2011–January 2014. A) Yeast explosive budding (arrow) (hematoxylin and eosin [HE] staining; original magnification ×160); B) asteroid bodies (arrow) (HE staining; original magnification ×160); C) yeasts in Langhans cells (periodic acid Schiff staining; original magnification ×160); D) lemon-shaped appearance (Grocott methenamine-silver staining; original magnification ×80).

or extrapulmonary tuberculosis, whereas in subsequent years, cases were initially suspected to be histoplasmosis infections. Therefore, it is reasonable to assume that, in endemic areas, where histopathological diagnosis or advanced microbiology labs are not widely accessible, the disease may be underdiagnosed; therefore, the prevalence of African histoplasmosis may be underestimated.

The diagnosis of African histoplasmosis is made mainly by histopathology, which shows granulomatous inflammation and giant cells containing numerous large yeast cells 10–15 µm in diameter, which are thick-walled and divided by narrow budding. The fungus is easily visible by GMS, Gridley, or PAS staining (*4*). IHC staining, which was performed on 12 specimens, is not specific for African histoplasmosis but to *H. capsulatum*; therefore, it may play a role in more accurate and faster diagnosis and enable exclusion of other fungal infections.

In our series, 3 samples were tested by RT-PCR and results were positive in all 3 for *H. capsulatum* diagnosis. Newer PCR protocols have been developed and may provide rapid and species-specific diagnosis (*9*).

Our histopathologic observation has some limitations. IHC and the RT-PCR primers that were used are unable to differentiate between *H. capsulatum* var. *capsulatum* and var. *duboisii*, yet they confirmed the histoplasmosis diagnosis, and IHC together with the large size of the yeast make it specific for *H. duboisii*. Soil and the bat guano from the infected areas have not yet been tested for *H. capsulatum* var. *duboisii*. Among the strengths of this study is that this unusual case series is unique in its extent and clustering of cases. In addition, the available data add novel epidemiologic and diagnostic information to the current knowledge about this neglected disease.

Further investigation should be conducted to understand the reservoir of the pathogen, the types of daily activities that might pose risk factors for acquiring the disease, and the mode of transmission and progression of the disease. Because diagnosis, especially in these rural areas, is challenging, seroepidemiologic surveys are needed to establish the extent of this infection.

About the Author

Dr. Pakasa is a professor of pathology and histology at the University of Kinshasa, Democratic Republic of the Congo, and head of the division of nephropathology and uropathology in the department of pathology. His research interests include tropical infectious nephropathology, including podocytopathies, HIV and APOL-1 associated kidney diseases, and the pathology of neglected tropical diseases, including schistosomiasis and African histoplasmosis.

References

1. Dubois A, Janssens PG, Brutsaert P, Vanbreuseghem R. A case of African histoplasmosis; with a mycological note on *Histoplasma duboisii* n. sp. [in French]. Ann Soc Belg Med Trop. 1952;32:569–84.
2. Gugnani HC. Histoplasmosis in Africa: a review. Indian J Chest Dis Allied Sci. 2000;42:271–7.
3. Loulergue P, Bastides F, Baudouin V, Chandenier J, Mariani-Kurkdjian P, Dupont B, et al. Literature review and case histories of *Histoplasma capsulatum* var. *duboisii* infections in HIV-infected patients. Emerg Infect Dis. 2007;13:1647–52. http://dx.doi.org/10.3201/eid1311.070665
4. Tsiodras S, Drogari-Apiranthitou M, Pilichos K, Leventakos K, Kelesidis T, Buitrago MJ, et al. An unusual cutaneous tumor:African histoplasmosis following mudbaths: case report and review. Am J Trop Med Hyg. 2012;86:261–3. http://dx.doi.org/10.4269/ajtmh.2012.11-0557
5. Therby A, Polotzanu O, Khau D, Monnier S, Greder Belan A, Eloy O. *Aspergillus* galactomannan assay for the management of histoplasmosis due to *Histoplasma capsulatum* var. *duboisii* in HIV-infected patients: education from a clinical case [in French]. J Mycol Med. 2014;24:166–70. http://dx.doi.org/10.1016/j.mycmed.2014.01.002
6. Chandenier J, Goma D, Moyen G, Samba-Lefèbvre MC, Nzingoula S, Obengui, et al. African histoplasmosis due to *Histoplasma capsulatum* var. *duboisii*: relationship with AIDS in recent Congolese cases [in French]. Sante. 1995;5:227–34.
7. Gago S, Esteban C, Valero C, Zaragoza O, Puig de la Bellacasa J, Buitrago MJ. A multiplex real-time PCR assay for identification of *Pneumocystis jirovecii*, *Histoplasma capsulatum*, and *Cryptococcus neoformans/Cryptococcus gattii* in samples from AIDS patients with opportunistic pneumonia. J Clin Microbiol. 2014;52:1168–76. http://dx.doi.org/10.1128/JCM.02895-13
8. Gugnani HC, Muotoe-Okafor FA, Kaufman L, Dupont B. A natural focus of *Histoplasma capsulatum* var. *duboisii* is a bat cave. Mycopathologia. 1994;127:151–7. http://dx.doi.org/10.1007/BF01102915
9. Pellaton C, Cavassini M, Jaton-Ogay K, Carron PN, Christen-Zaech S, Calandra T, et al. *Histoplasma capsulatum* var. *duboisii* infection in a patient with AIDS: rapid diagnosis using polymerase chain reaction-sequencing. Diagn Microbiol Infect Dis. 2009;64:85–9. http://dx.doi.org/10.1016/j.diagmicrobio.2009.01.001

Address for correspondence: Asaf Biber, The Chaim Sheba Medical Center, The Center for Geographic Medicine and Tropical Diseases, Tel Hashomer–Ramat-Gan 52621, Israel; email: asafbib@gmail.com

Mitigation of Influenza B Epidemic with School Closures, Hong Kong, 2018

**Sheikh Taslim Ali, Benjamin J. Cowling,
Eric H.Y. Lau, Vicky J. Fang, Gabriel M. Leung**

In winter 2018, schools in Hong Kong were closed 1 week before the scheduled Chinese New Year holiday to mitigate an influenza B virus epidemic. The intervention occurred after the epidemic peak and reduced overall incidence by ≈4.2%. School-based vaccination programs should be implemented to more effectively reduce influenza illnesses.

Hong Kong, China, located on the coast south of Guangdong Province, has a subtropical climate and a population of 7.3 million. In Hong Kong, influenza epidemics occur during winter every year and sometimes during other seasons (*1*). One of the interventions that has been used by Hong Kong health authorities to control influenza epidemics is school closures; this intervention was previously applied in 2008 (*2*) and 2009 (*3*). During winter 2017–18, an epidemic of influenza B, Yamagata lineage, occurred in Hong Kong. The local media focused on this epidemic for 3 reasons. First, the occurrence of severe influenza cases in Hong Kong (*4*) attracted public concern. Second, the number of school outbreaks reported to the Centre for Health Protection in Hong Kong far exceeded the number reported in previous years (*4*). Third, a severe epidemic of influenza A(H3N2) was ongoing in the United States (*5*), which further increased local concern about influenza in general.

On February 7, 2018, the Hong Kong government announced that all 1,600 kindergartens, primary schools, and special needs schools in Hong Kong would close the following day, 1 week before the Chinese New Year school holiday, which in most schools was scheduled for February 15–23. Thus, in total, schools were closed for 2.5 weeks. We reviewed surveillance data on influenza and influenza-like illness (ILI) activity in Hong Kong to infer the effect of school closures on community transmission.

The Study

As in previous studies, we used ILI surveillance data to indicate the incidence of influenza virus infections in the community (*1,6,7*). The Centre for Health Protection tracks a sentinel network of private doctors and reports the rates

of outpatient consultations for ILI per 1,000 patient consultations every week (*4*), and the Public Health Laboratory Services branch reports the proportion of respiratory specimens testing positive for influenza virus by type and subtype every week (*8*). We multiplied the weekly ILI rates by the weekly influenza B virus detection rates to obtain a proxy (hereafter ILI+ proxy) measure of the number of cases of influenza B virus infection each week (Figure, panel A). We have previously shown that this ILI+ proxy provides an estimate that correlates linearly with the incidence of hospitalizations for influenza A(H1N1)pdm09 in Hong Kong (*6*); some have argued that this metric is a better linear correlate of the incidence of influenza illness than ILI rates alone or laboratory detection rates alone (*9*).

We calculated the ILI+ proxy for influenza B to infer the rate of person-to-person transmission of influenza B virus throughout the epidemic. We used the methods proposed by Cauchemez et al. (*10*) to estimate transmissibility by the effective reproduction number, R_t, which represents the average number of secondary infections that result from a primary case of infection at time t (online Technical Appendix, https://wwwnc.cdc.gov/EID/article/24/11/18-0612-Techapp1.pdf). When R_t exceeds 1, the epidemic is capable of spreading. We used flexible cubic splines to model the weekly influenza B ILI+ proxy values and interpolate daily ILI+ proxy values. We then estimated daily R_t values from the daily influenza B ILI+ proxy values (*7*). We considered the serial interval distribution as the Weibull distribution, with a mean of 3.2 days and SD of 1.3 days (*11*). The estimated R_t was 1.03 (95% CI 0.73–1.34) before the start of the school closure and 0.87 (95% CI 0.54–1.21) during the closure week, corresponding to a 16% (95% CI 10%–26%) reduction in transmissibility (Figure, panel B).

We then simulated the ILI+ proxy for influenza B under the counterfactual scenario of no school closures during February 8–14. Because R_t is affected by the depletion of the susceptible population (h_t, cumulative ILI+ proxy for influenza B at time t) and school closure (C_t, indicator variable at time t), we first fitted a multivariable log-linear regression model for R_t with h_t and C_t as explanatory variables (online Technical Appendix). Using these estimated coefficients in a regression model, we then constructed the transmission rate (β_t, function of initial transmission rate β_0 and C_t) for a susceptible-exposed-infected-recovered compartmental model to simulate incidence over time. To
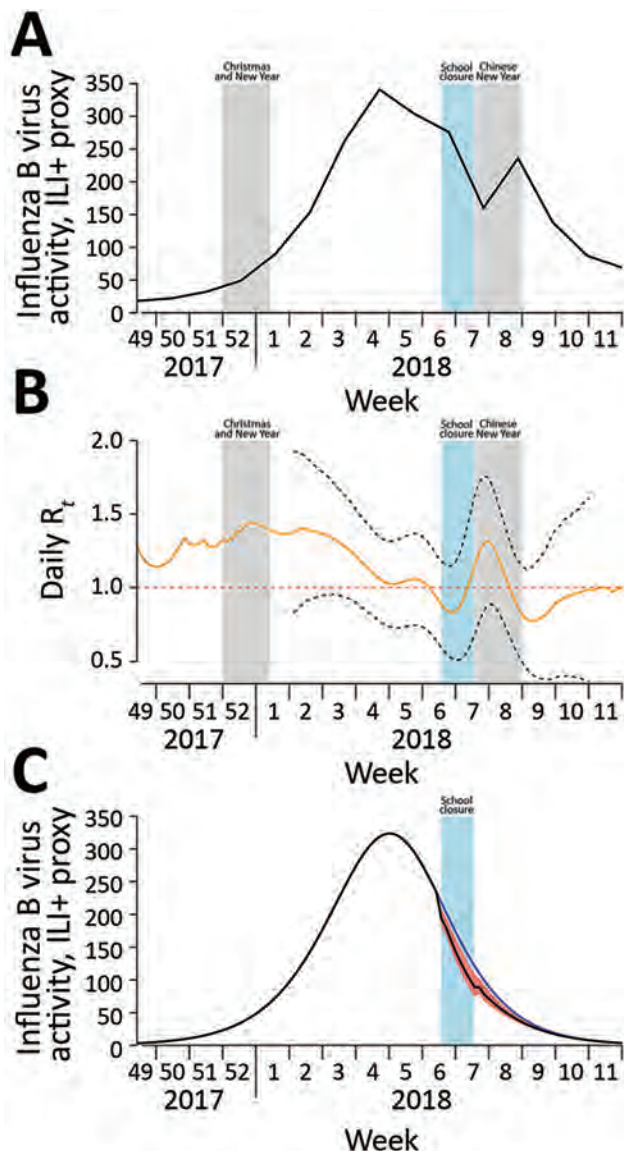
Figure. Influenza B virus activity, by epidemiologic week, Hong Kong, December 2017–March 2018. A) Incidence of influenza B virus measured by using the ILI+ proxy for influenza B, which is calculated by multiplying the weekly rate of ILI per 1,000 consultations by the weekly proportion of respiratory specimens submitted to the Public Health Laboratory Services (Hong Kong) that tested positive for influenza B virus (online Technical Appendix Table 2, https://wwwnc.cdc.gov/EID/article/24/11/18-0612-Techapp1.pdf). Shaded bars show school closure dates. B) Daily real-time estimate of transmissibility (R_t) of influenza B virus. Black dashed lines indicate pointwise 95% CIs; red dashed line indicates transmission threshold. Shaded bars show school closure dates. C) Simulated incidence of influenza B virus with and without implementation of school closure (shaded bar) in Hong Kong during February 8–14, 2018. Blue line indicates the number of cases occurring during the hypothetical scenario of no school closure; black line indicates the number occurring with school closure, which reduced transmissibility by 16%. The difference between these 2 lines represents the 4.2% reduction in incidence of infections; red shading indicates 95% CI. ILI, influenza-like illness; R_t, effective reproduction number at time t.

simulate incidence under no school closure, we set C_t to 0 for the period February 8–14 (online Technical Appendix).

Under the simulated epidemic with no school closures, the cumulative incidence for the entire epidemic was 0.527 (95% CI 0.472–0.574); the incidence was reduced to 0.505 (95% CI 0.494–0.519) when simulated with closures (Figure, panel C). This difference in proportions corresponds to a 4.2% (95% CI 1.5%–6.7%) reduction in infections from school closures. In sensitivity analyses, in which different levels of preexisting immunity (0.1%–30%) in the population were assumed, the estimated reduction in infections ranged from 3.3% (95% CI 1.2%–5.1%) for high (30%) preexisting immunity to 4.1% (95% CI 1.5%–6.7%) for low (0.1%) preexisting immunity. We also simulated the effect of school closures occurring 1 or 2 weeks earlier and estimated that infections would have been reduced by 8.6% if schools closed 1 week earlier (lasting for 2 weeks) and 13.5% if schools closed 2 weeks earlier (lasting for 3 weeks) (online Technical Appendix).

Conclusions

In early 2018, schools were closed an extra week before a holiday in Hong Kong to mitigate an influenza epidemic. Closure after the epidemic peak had a small effect on transmission; we estimated a 4.2% reduction in overall incidence of infections. By the end of the 2017–18 winter season, ≈400 laboratory-confirmed influenza deaths had occurred among the local population of 7.2 million, lower than the rate in the contemporaneous influenza A(H3N2) epidemic in the United States but still a rate of moderate-to-high impact. A reduction in incidence of infections by 4.2% might have reduced hospitalizations and deaths by a similar percentage, with the caveat that hospitalizations and deaths would probably not have been equally distributed among age groups because most infections occur in children and most deaths in older adults.

The school closures were announced <24 hours before they began. We presume that the school closures were disruptive to parents' schedules, potentially forcing some parents to stay home from work, and that many children stayed home during closures (*12*). The 16% reduction in transmission we estimated was lower than that estimated for the school closures that occurred in Hong Kong during June–July 2009 (25% reduction) (*3*). In 2009, the goal was to delay community transmission and spread out disease activity peak; thus, intervention before the peak was essential. In our study, R_t appeared to increase (Figure, panel B) during the Chinese New Year, probably because of increased social interactions during holiday gatherings.

We assumed that the ILI+ proxy for influenza B was linearly correlated with the incidence of infections (*1,6,7*). This correlation could have been affected by changes in healthcare seeking behavior that might have resulted from

private clinic closure, which occurred for a few days during the Chinese New Year holiday. This decreased healthcare access might have shifted the estimated reduction of influenza infections upward.

Influenza vaccination is considered the best preventive measure against influenza. However, >10 years after introduction of the influenza vaccination subsidy scheme for children, influenza vaccination coverage is still low in Hong Kong: ≈10% overall and ≈15% in children for the 2016–17 and 2017–18 winter seasons (*13*). To further increase influenza vaccination coverage in children, a school-based vaccination program should be implemented for the upcoming 2018–19 winter season.

Acknowledgments

About the Author

Dr. Ali works as a postdoctoral fellow at the World Health Organization Collaborating Centre for Infectious Disease Epidemiology and Control, School of Public Health, The University of Hong Kong in Hong Kong, China. His research interests include mathematical and statistical epidemiology, modeling of infectious diseases, and containment and mitigation policies.

References

1. Wu P, Presanis AM, Bond HS, Lau EHY, Fang VJ, Cowling BJ. A joint analysis of influenza-associated hospitalizations and mortality in Hong Kong, 1998–2013. Sci Rep. 2017;7:929. http://dx.doi.org/10.1038/s41598-017-01021-x
2. Cowling BJ, Lau EH, Lam CL, Cheng CK, Kovar J, Chan KH, et al. Effects of school closures, 2008 winter influenza season, Hong Kong. Emerg Infect Dis. 2008;14:1660–2. http://dx.doi.org/10.3201/eid1410.080646
3. Wu JT, Cowling BJ, Lau EH, Ip DKM, Ho LM, Tsang T, et al. School closure and mitigation of pandemic (H1N1) 2009, Hong Kong. Emerg Infect Dis. 2010;16:538–41. http://dx.doi.org/10.3201/eid1603.091216
4. Centre for Health Protection. Local situation of influenza activity (as of Feb 7, 2018). Flu Express. 2018;15:1–8.
5. Budd AP, Wentworth DE, Blanton L, Elal AIA, Alabi N, Barnes J, et al. Update: influenza activity—United States, October 1, 2017–February 3, 2018. MMWR Morb Mortal Wkly Rep. 2018;67: 169–79. http://dx.doi.org/10.15585/mmwr.mm6706a1
6. Wong JY, Wu P, Nishiura H, Goldstein E, Lau EH, Yang L, et al. Infection fatality risk of the pandemic A(H1N1)2009 virus in Hong Kong. Am J Epidemiol. 2013;177:834–40. http://dx.doi.org/10.1093/aje/kws314
7. Ali ST, Wu P, Cauchemez S, He D, Fang VJ, Cowling BJ, et al. Ambient ozone and influenza transmissibility in Hong Kong. Eur Respir J. 2018;51:1800369. http://dx.doi.org/10.1183/13993003.00369-2018
8. Centre for Health Protection. Influenza virus subtyping in 2018. 2018 [cited 2018 Apr 4]. https://www.chp.gov.hk/en/statistics/data/10/641/643/6781.html
9. Goldstein E, Cobey S, Takahashi S, Miller JC, Lipsitch M. Predicting the epidemic sizes of influenza A/H1N1, A/H3N2, and B: a statistical method. PLoS Med. 2011;8:e1001051. http://dx.doi.org/10.1371/journal.pmed.1001051
10. Cauchemez S, Boëlle PY, Thomas G, Valleron AJ. Estimating in real time the efficacy of measures to control emerging communicable diseases. Am J Epidemiol. 2006;164:591–7. http://dx.doi.org/10.1093/aje/kwj274
11. Cowling BJ, Chan KH, Fang VJ, Lau LLH, So HC, Fung ROP, et al. Comparative epidemiology of pandemic and seasonal influenza A in households. N Engl J Med. 2010;362:2175–84. http://dx.doi.org/10.1056/NEJMoa0911530
12. Cauchemez S, Ferguson NM, Wachtel C, Tegnell A, Saour G, Duncan B, et al. Closure of schools during an influenza pandemic. Lancet Infect Dis. 2009;9:473–81. http://dx.doi.org/10.1016/S1473-3099(09)70176-8
13. Chiu SS, Kwan MYW, Feng S, Wong JSC, Leung CW, Chan ELY, et al. Interim estimate of influenza vaccine effectiveness in hospitalised children, Hong Kong, 2017/18. Euro Surveill. 2018;23. http://dx.doi.org/10.2807/1560-7917.ES.2018.23.8.18-00062

Address for correspondence: Benjamin J. Cowling, School of Public Health, Li Ka Shing Faculty of Medicine, The University of Hong Kong, 7 Sassoon Rd, Pokfulam, Hong Kong, China; email: bcowling@hku.hk

World Health Organization Early Warning, Alert and Response System in the Rohingya Crisis, Bangladesh, 2017–2018

Basel Karo, Christopher Haskew, Ali S. Khan, Jonathan A. Polonsky, Md Khadimul Anam Mazhar, Nilesh Buddha

The Early Warning, Alert and Response System (EWARS) is a web-based system and mobile application for outbreak detection and response in emergency settings. EWARS provided timely information on epidemic-potential diseases among ≥700,000 Rohingya refugees across settlements. EWARS helped in targeting new measles vaccination campaigns and investigating suspected outbreaks of acute jaundice syndrome.

The international humanitarian system faces unprecedented challenges with the number of persons displaced by natural disasters and escalating conflicts at its highest in decades (*1*). Understanding the needs of crisis-affected persons and orchestrating rapid response play decisive factors in the effectiveness of humanitarian aid. Innovative technology and products can enhance the provision and quality of humanitarian assistance to contend with these growing challenges (*2,3*).

Since August 2017, violence in Myanmar's Rakhine State has driven hundreds of thousands of Rohingya persons across the border into refugee settlements in Cox's Bazar, Bangladesh (*4,5*). The poor environmental conditions and extremely high population density coupled with a preexisting lack of health services have left the Rohingya community vulnerable to communicable diseases and outbreaks. As a part of a massive response, the World Health Organization (WHO), in partnership with the Bangladesh Ministry of Health and Family Welfare (MoHFW), has implemented an Early Warning, Alert and Response System (EWARS) across the Rohingya settlements. EWARS is a web-based system and mobile application designed to

Author affiliations: Public Health England, London, UK (B. Karo); European Centre for Disease Prevention and Control EPIET European Programme for Intervention Epidemiology Training, Stockholm, Sweden (B. Karo); World Health Organization, Geneva, Switzerland (C. Haskew, J.A. Polonsky); University of Nebraska Medical Center, Omaha, Nebraska, USA (A.S. Khan); World Health Organization, Cox's Bazar, Bangladesh (M.K.A. Mazhar); World Health Organization Regional Office for South-East Asia, New Delhi, India (N. Buddha)

enhance disease surveillance and outbreak detection in emergency settings (*6,7*). EWARS includes an analytic and alert module that signals outbreak at early stages and incorporates a risk assessment framework and matrix. EWARS can be deployed easily; it comes with all the equipment needed to establish surveillance and response activities, including 60 mobile phones, tablets, a local server, and a solar generator and solar chargers (Figure 1). A single kit costs approximately US $15,000 and can support surveillance in up to 60 fixed or mobile clinics serving ≈500,000 persons. WHO developed EWARS in 2015 and has deployed it in humanitarian crises, disease outbreaks, and natural disasters in South Sudan, Chad, Nigeria, Fiji, and Yemen (*6,8,9*).

In December 2017, WHO sent 2 "EWARS in box" kits (Figure 1, panel A) to the WHO office in Cox's Bazar. Over 2 weeks, the WHO team organized 2 workshops and a series of field visits, in which the staff of 151 health facilities run by 23 humanitarian organizations were enrolled and trained as reporting sites for EWARS across the refugee settlements, serving ≥700,000 Rohingya refugees. However, the team continued supportive supervision visits for EWARS upon request, particularly when a new partner or health facility started operating in the camp. WHO supported facilities operating in remote field settings without reliable Internet or electricity by providing mobile phones, a local server, and solar chargers.

The case management team, composed of staff from WHO, MoHFW, and humanitarian organizations, defined the reportable diseases and their alert thresholds on the basis of burden and epidemic potential. The diseases included were acute watery diarrhea, bloody diarrhea, acute respiratory infection, measles/rubella, acute flaccid paralysis, suspected meningitis, acute jaundice syndrome, suspected hemorrhagic fever, neonatal tetanus, adult tetanus, malaria, unexplained fever, and severe malnutrition. Identified diseases were encoded in EWARS as a weekly report of new cases aggregated by site, age, and sex. By the first week of January 2018, humanitarian organizations submitted data by the EWARS mobile application, and the data were immediately available in the EWARS web application for analysis. The WHO team reviewed
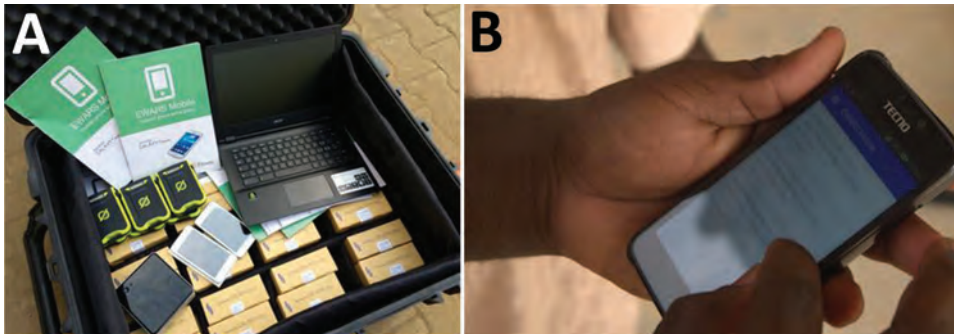
Figure 1. Examples of the World Health Organization EWARS supplies used for public health surveillance of Rohingya refugee populations in Bangladesh, 2017–2018. A) EWARS in a box. B) EWARS mobile application. EWARS, Early Warning, Alert and Response System.

and managed all alerts triggered by EWARS on a weekly basis, following the workflow: alert verification, risk assessment, risk characterization, and outcome (discard, monitor, or respond). On average, there were ≈100 alerts per week; most were discarded as false alerts because of data entry mistakes or because they did not meet the case definition or no cluster was identified. EWARS generated automated weekly bulletins that included reporting
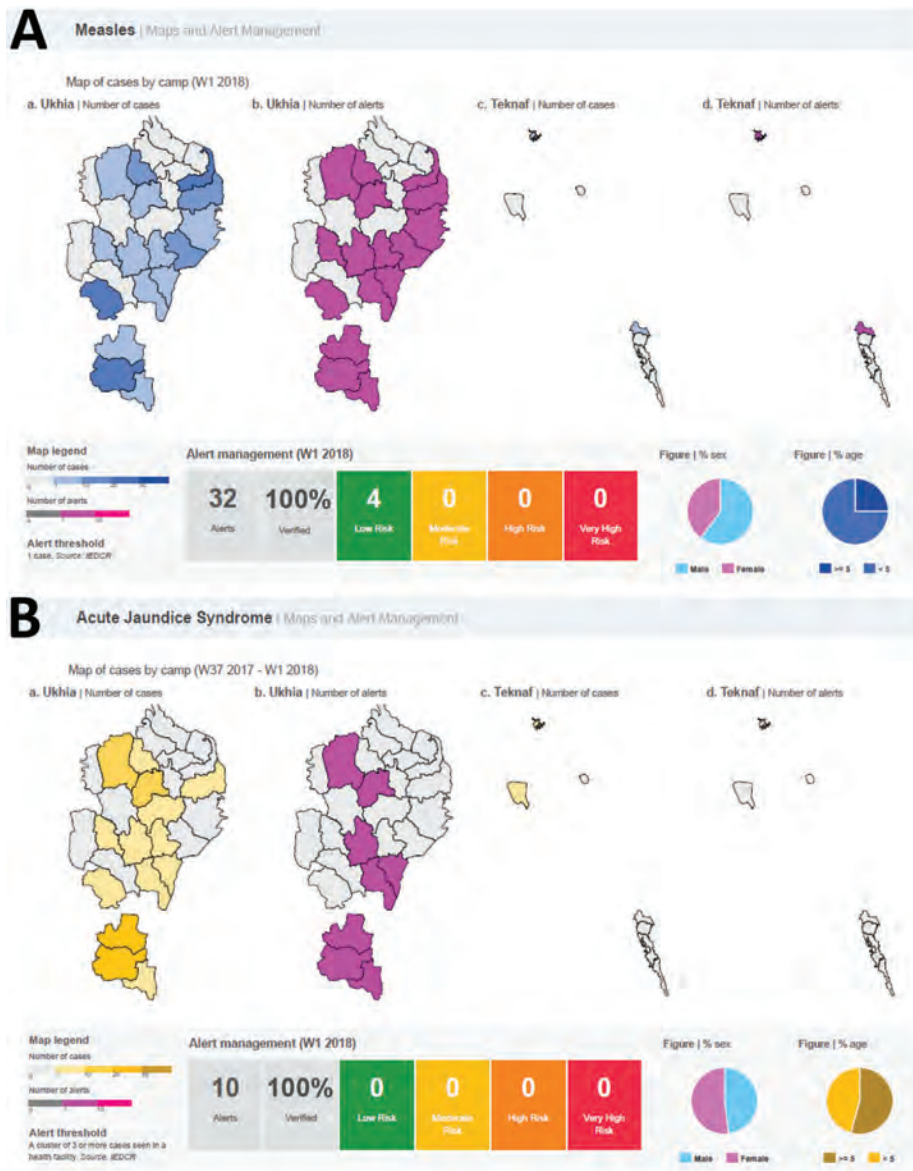

Figure 2. Screenshots of maps and alerts generated by the World Health Organization Early Warning, Alert and Response System during week 1, January 2018, in Rohingya refugee settlements in Cox's Bazar, Bangladesh. A) Measles; B) acute jaundice syndrome.

performance, trend and location of reported diseases, and summary of alerts triggered. The weekly bulletins were disseminated among partners and posted on WHO and MoHFW websites.

Information obtained by the weekly bulletins played an important role in driving public health action. For example, mapping alerts related to measles in EWARS and identifying the affected age groups helped in targeting new vaccination campaigns (Figure 2, panel A). In addition, alerts triggered by EWARS detected clusters of acute jaundice syndrome cases (Figure 2, panel B). Within 1 week, all health facilities were informed of the clusters (with age and site of the case-patients) and a team from the Bangladeshi Institute of Epidemiology, Disease Control and Research (IEDCR) was sent to the field to verify the cluster and collect samples for testing and identifying the etiology of the outbreak. This practice resulted in prompt detection of an outbreak of hepatitis A and the early initiation of appropriate intervention.

EWARS was also used for daily monitoring of a diphtheria outbreak (reporting form, contact tracing form, treatment centers bed counts, and diphtheria antitoxin use). Previously, these forms were submitted daily as spreadsheets; the submitted case reports were noteworthy for being incomplete and with inconsistent variable names and data. Despite challenges in connectivity and data sharing, these new real-time records permitted a more accurate assessment of final outcomes for cases and postdischarge complications. EWARS also enabled the treatment centers to update incomplete data provided during the height of the outbreak from abstracting paper medical records.

A key limitation of the application itself was the lack of availability of mobile networks in some areas of the Rohingya settlements, which was a challenge for partners when trying to edit and update case-based records during the diphtheria outbreak. Although the mobile application can be used offline, the need for case-based records to be regularly edited made a laptop more convenient for this activity. A key lesson learned, therefore, was the need to have a fully offline version of the EWARS application with the capability for installation and use on laptop computers without any Internet connection, before being synchronized with a central server when connection allows.

EWARS is a successful example of innovative technology in humanitarian response with a positive impact for its users and crisis-affected communities. It provides a functional and simple digital surveillance system that can be easily deployed ("EWARS in a box") and rapidly implemented in an emergency setting for timely detection of and response to new outbreaks. It has succeeded in disease monitoring, detecting outbreaks, and driving public health action among the Rohingya refugee population in Cox's Bazar.

About the Author

Dr. Karo is a fellow in the European Programme for Intervention Epidemiology Training (EPIET) based at Field Service, Public Health England. With research interests in tuberculosis, Dr. Karo serves as a technical consultant for World Health Organization Global TB Programme.

References

1. United Nations High Commission on Refugees (UNHCR). Global trends—forced displacement in 2017 [cited 2018 Sep 5]. http://www.unhcr.org/globaltrends2017
2. United Nations Office for the Coordination of Humanitarian Affairs (OCHA). Humanitarian innovation: the state of the art. 2014 [cited 2018 Sep 5]. https://www.rsc.ox.ac.uk/publications/humanitarian-innovation-the-state-of-the-art
3. Haskew C, Spiegel P, Tomczyk B, Cornier N, Hering H. A standardized health information system for refugee settings: rationale, challenges and the way forward. Bull World Health Organ. 2010;88:792–4. http://dx.doi.org/10.2471/BLT.09.074096
4. International Organization for Migration (IOM)—Inter Sector Coordination Group (ISCG). Situation report: Rohingya refugee crisis, Cox's Bazar. 2018 Feb 25 [cited 2018 Sep 5]. https://www.humanitarianresponse.info/en/operations/bangladesh/document/situation-update-rohingya-crisis-coxs-bazar-25-february-2018
5. The Lancet. Our responsibility to protect the Rohingya. Lancet. 2018. 23;390:2740. https://doi.org/10.1016/S0140-6736(17)33356-1
6. World Health Organization. EWARS: a simple, robust system to detect disease outbreaks. 2016 [cited 2018 Sep 5]. http://www.who.int/emergencies/kits/ewars/en/
7. Global EWARS. The Early Warning, Alert and Response System (EWARS): disease surveillance, alert, and response in emergencies [cited 2018 Sep 5]. http://ewars-project.org
8. World Health Organization. Using mobile technology for post-disaster enhanced surveillance in Fiji. 2016 [cited 2018 Sep 5]. http://www.wpro.who.int/southpacific/mediacentre/releases/2016/mobiletech_surveillance/en/
9. World Health Organization. WHO launches new early warning system in a box to help 500,000 people for only $USD 15,000. 2015 Dec 14 [cited 2018 Sep 5]. https://www.afro.who.int/news/who-launches-new-early-warning-system-box-help-500-000-people-only-usd-15-000

Address for correspondence: Basel Karo, Field Epidemiology Service, London, Public Health England, Zone C, Fl 3 Skipton House, 80 London Rd, London SE1 6LH, UK; email: Basel.karo@phe.gov.uk

Rickettsia japonica Infections in Humans, Zhejiang Province, China, 2015

Qunying Lu, Jianping Yu, Liqun Yu,
Yanjun Zhang, Yitao Chen,
Meiai Lin, Xiaofei Fang

We investigated 16 Japanese spotted fever cases that occurred in southeastern China during September–October 2015. Patients had fever, rash, eschar, and lymphadenopathy. We confirmed 9 diagnoses and obtained 2 isolates with high identity to *Rickettsia japonica* strain YH. *R. japonica* infection should be considered for febrile patients in China.

Rickettsia japonica is a member of the spotted fever group rickettsiae (SFGR) that causes tickborne Japanese spotted fever (JSF). First reported in Japan's Tokushima Prefecture in 1984 (*1,2*), JSF has been recognized in multiple countries of Asia, including Japan, South Korea, the Philippines, and Thailand (*3–5*). In China, 4 species of SFGR have been reported to cause human infection: *R. heilongjiangensis*, *R. sibirica* subspecies *sibirica* BJ-90, *Candidatus* R. tarasevichiae, and *R. raoultii* (*6*). In this report, we investigated the causative agent of 16 JSF cases that occurred in southeastern China in late 2015.

The Study

The ethics committee of the Zhejiang Province Center for Disease Control and Prevention, Hangzhou, China, approved this research. During September–October 2015, a total of 16 febrile patients were hospitalized at Linan First People's Hospital (Linan, China). All these patients lived in the Xitianmu Mountain area of Linan in Zhejiang Province. Besides fever (38.8°C–40.3°C), clinical signs of disease in these patients included rashes on the trunk and limbs (15/16) and an eschar (11/16) (Table). In those with eschar, lymphadenopathy was found at the site of the draining lymph node (6/11). Five patients had rash and no eschar. Laboratory results revealed that all patients' leukocyte levels were within reference ranges, but a high percentage of neutrophils (12/16 patients) and minor hepatic transaminase elevation (11/16 patients) were also observed. All 16 patients were treated with doxycycline

or azithromycin and were cured, and no patient experienced severe illness.

With patient consent, we collected acute-phase (n = 16) and convalescent-phase (n = 14) whole blood specimens and sent them to Zhejiang Province Center for Disease Control and Prevention for laboratory confirmation of *Rickettsia* infection. We extracted DNA from acute-phase blood specimens by using the DNeasy Blood & Tissue Kit (QIAGEN, Hilden, Germany). We used nested PCR to amplify the partial *groEL* genes of SFGR, typhus group rickettsiae, and *Orientia tsutsugamushi* bacteria (online Technical Appendix, https://wwwnc.cdc.gov/EID/article/24/11/17-0044-Techapp1.pdf). The targeted fragments (217 bp) were present in the blood specimens from 9 patients (Table). We sequenced these fragments and analyzed them using BLAST (http://www.ncbi.nlm.nih.gov/BLAST), and all had 100% identity to *R. japonica* YH prototype strain (GenBank accession no. NC016050) (*7,8*). All specimens were negative for typhus group rickettsiae and *O. tsutsugamushi* rickettsia DNA by PCR.

We also inoculated 200 μL of acute-phase blood specimens onto HL60 and DH82 cells in 25-mL flasks and cultured at 37°C. Cytopathic effect was not observed with inoculated HL60 cells, but inoculated DH82 cells exfoliated completely by 4 weeks of culture. We also performed indirect immunofluorescence assays (IFAs) every 2 days to access SFGR growth (online Technical Appendix). Two of the inoculated cultures exhibited bright fluorescent apple-green, rod-shaped particles (Table) after 3 weeks of culture, confirming SFGR infection for 2 patients. We then extracted DNA from the 2 SFGR-positive cultures (LA4/2015 and LA16/2015) and amplified and sequenced a 2,493-bp fragment containing the full-length sequences of SFGR *groES* and *groEL* (GenBank accession nos. KY073364–5) and a 609-bp fragment containing the partial rickettsial *ompA* gene sequence (GenBank accession nos. KY347792–3; online Technical Appendix Table). These sequences were found to be 100% identical to the corresponding sequences of *R. japonica* YH.

We used IFAs with bacterial substrate antigens *R. japonica* (HL-60 cells infected with LA4/2015) and *R. rickettsii* (FOCUS Diagnostics Inc., Cyprus, CA, USA) to test patients for specific antibodies, and in all 16 patient serum samples, we detected SFGR IgG. All paired serum samples (n = 14) showed a >4-fold increase in titer against SFGR (Table). The 2 patients we did not receive

Table. Clinical data of febrile patients with Japanese spotted fever diagnoses, Linan, China, 2015*

Patient no.	Age, y/sex	Tick bite	Rash	Eschar	Lymphadenopathy	Days after onset		PCR,†	IFA titer‡		Isolation
						AP	CP	AP	AP	CP	
1	53/M	Not known	Yes	No	No	6	42	–	<64	4,096	–
2	62/M	Not known	Yes	Yes	No	5	58	+	<64	2,048	–
3	52/M	Yes	Yes	Yes	Yes	5	74	+	64	4,096	–
4	79/F	Not known	Yes	No	No	4	60	+	128	9,192	+
5	67/F	No	Yes	No	No	6	75	+	512	4,096	–
6	62/F	Yes	Yes	Yes	No	7	70	–	<64	1,024	–
7	53/F	Yes	No	Yes	No	7	57	–	64	1,024	–
8	63/F	Yes	Yes	Yes	Yes	10	67	–	<64	4,096	–
9	57/M	Yes	Yes	Yes	No	2	45	+	64	9,192	–
10	51/F	Yes	Yes	Yes	Yes	6	§	+	64	§	–
11	53/M	Yes	Yes	Yes	No	3	§	+	<64	§	–
12	45/F	Yes	Yes	Yes	Yes	5	70	+	<64	4,096	–
13	33/F	Yes	Yes	Yes	Yes	6	42	–	64	2,048	–
14	30/F	Not known	Yes	No	No	4	46	–	128	2,048	–
15	36/F	Not known	Yes	No	No	5	54	–	<64	2,048	–
16	67/F	Yes	Yes	Yes	Yes	0	60	+	<64	9,192	+

*AP, acute phase; CP, convalescent phase; IFA, indirect immunofluorescence assay; +, positive test result; –, negative test result.
†PCR amplifying 217-bp sequence of *Rickettsia japonica groEL* gene.
‡Detection of IgG against spotted fever group rickettsiae.
§Convalescent-phase serum samples not obtained.

convalescent-phase serum specimens from were positive for *R. japonica* by PCR.

All serum specimens were negative for *O. tsutsugamushi* IgG. Some convalescent-phase serum specimens had low-titer reactions to *R. typhi* bacterial antigen.

Conclusions

The 4 SFGR species *R. japonica*, *R. heilongjiangensis*, *R. rhipicephali*, and *R. massiliae* have been identified in *Haemaphysalis longicornis* and *Rhipicephalus haemaphysaloides* ticks in Zhejiang Province (*9–11*), indicating a potential for these species to infect humans in China. In our research, we determined the etiologic agent of 16 JSF cases and isolated 2 *R. japonica* rickettsiae. The prototype strain *R. japonica* YH was isolated in Japan in 1985 (*1*). After ≈30 years, only a few *R. japonica* isolates have been isolated from patients in China: 2 from our research and 1 from Li et al. (*12*). Our findings indicate that the full-length *groES* and *groEL* genes and the partial *ompA* gene sequences were 100% identical to *R. japonica* YH, suggesting that the *R. japonica* genome has been relatively conserved. Nine patients had clinically confirmed JSF, displaying fever, rash, eschar, and lymphadenopathy; these signs and symptoms were similar to those seen in JSF patients in Japan (*13*).

Of the vectorborne rickettsial diseases in China, human scrub typhus and murine typhus frequently occur in Zhejiang Province, and spotted fever group rickettsiosis probably occurs but has gone relatively unnoticed. Because the clinical symptoms of spotted fever and scrub typhus are similar, some SFGR infections have likely been diagnosed as scrub typhus. We found that the blood specimens of 7 febrile patients were negative for the targeted PCR fragments but showed a >4-fold increase in antibody titer to SFGR.

Although these results suggest SFGR infection, we cannot conclude these 7 patients were infected with *R. japonica*.

In summary, *R. japonica* infections occur in Zhejiang Province, China. These infections are likely more broadly distributed throughout the mainland areas than had been previously realized. Improvements in JSF clinical diagnosis and human epidemiologic surveillance are urgently needed in China.
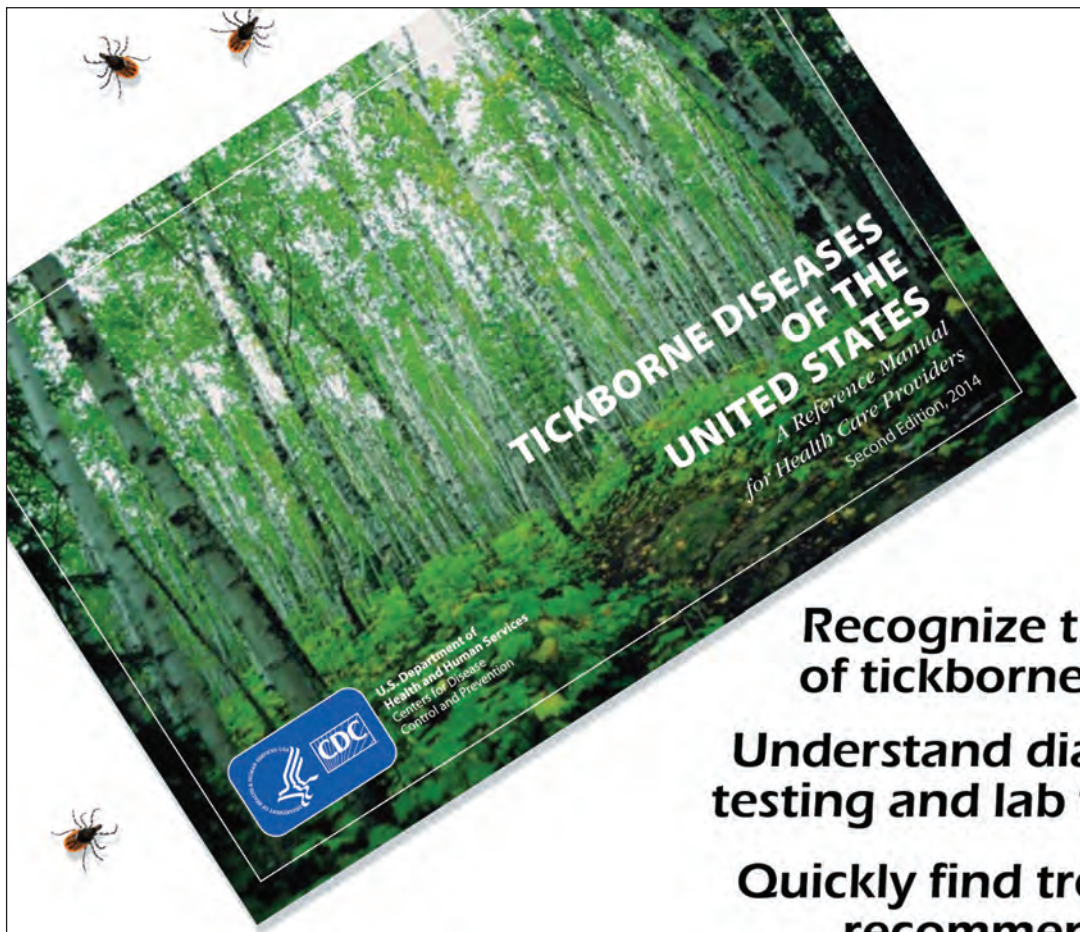
About the Author

Dr. Lu is a principal investigator at the Zhejiang Province Center for Disease Control and Prevention, Hangzhou, China. Her research interests include microbiology, epidemiology, and the ecology of tickborne diseases.

References

1. Uchida T, Uchiyama T, Kumano K, Walker DH. *Rickettsia japonica* sp. nov., the etiological agent of spotted fever group rickettsiosis in Japan. Int J Syst Bacteriol. 1992;42:303–5. http://dx.doi.org/10.1099/00207713-42-2-303
2. Mahara F. Three Weil-Felix reaction OX2 positive cases with skin eruptions and high fever [in Japanese]. J Anan Med Assoc. 1984;68:4–7.
3. Camer GA, Alejandria M, Amor M, Satoh H, Muramatsu Y, Ueno H, et al. Detection of antibodies against spotted fever group *Rickettsia* (SFGR), typhus group *Rickettsia* (TGR), and *Coxiella burnetii* in human febrile patients in the Philippines. Jpn J Infect Dis. 2003;56:26–8. PubMed
4. Chung MH, Lee SH, Kim MJ, Lee JH, Kim ES, Lee JS, et al. Japanese spotted fever, South Korea. Emerg Infect Dis. 2006;12:1122–4. http://dx.doi.org/10.3201/eid1207.051372

5. Gaywee J, Sunyakumthorn P, Rodkvamtook W, Ruang-areerate T, Mason CJ, Sirisopana N. Human infection with *Rickettsia* sp. related to *R. japonica*, Thailand. Emerg Infect Dis. 2007;13:657–9. http://dx.doi.org/10.3201/eid1304.060585

6. Fang LQ, Liu K, Li XL, Liang S, Yang Y, Yao HW, et al. Emerging tick-borne infections in mainland China: an increasing public health threat. Lancet Infect Dis. 2015;15:1467–79. http://dx.doi.org/10.1016/S1473-3099(15)00177-2

7. Dong X, El Karkouri K, Robert C, Raoult D, Fournier PE. Genomic analysis of *Rickettsia japonica* strain YHT. J Bacteriol. 2012;194:6992. http://dx.doi.org/10.1128/JB.01928-12

8. Matsutani M, Ogawa M, Takaoka N, Hanaoka N, Toh H, Yamashita A, et al. Complete genomic DNA sequence of the East Asian spotted fever disease agent *Rickettsia japonica*. PLoS One. 2013;8:e71861. http://dx.doi.org/10.1371/journal.pone.0071861

9. Sun J, Lin J, Gong Z, Chang Y, Ye X, Gu S, et al. Detection of spotted fever group rickettsiae in ticks from Zhejiang Province, China. Exp Appl Acarol. 2015;65:403–11. http://dx.doi.org/10.1007/s10493-015-9880-9

10. Meng Z, Jiang LP, Lu QY, Cheng SY, Ye JL, Zhan L. Detection of co-infection with Lyme spirochetes and spotted fever group rickettsiae in a group of *Haemaphysalis longicornis* [in Chinese]. Zhonghua Liu Xing Bing Xue Za Zhi. 2008;29:1217–20.

11. Cheng SY, Zheng SQ, Meng Z, Ye XD, Jiang LP, Wang ZQ, et al. Analysis of DNA sequences of spotted fever group *Rickettsia* detected from ticks in Zhejiang Province [in Chinese]. Dis Surveil. 2010;25:466–8.

12. Li J, Hu W, Wu T, Li HB, Hu W, Sun Y, et al. Japanese spotted fever endemic in East China, 2013. Emerg Infect Dis. 2018 Nov [cited 2018 Aug 27]. https://doi.org/10.3201/eid2411.170264

13. Mahara F. Japanese spotted fever: report of 31 cases and review of the literature. Emerg Infect Dis. 1997;3:105–11. http://dx.doi.org/10.3201/eid0302.970203

Address for correspondence: Qunying Lu, Zhejiang Province Center for Disease Control and Prevention, No. 3399 Binsheng Rd, Hangzhou, 310052 China; email: lqycdc@163.com

Emergence of *Neisseria meningitidis* Serogroup W, Central African Republic, 2015–2016

Thierry Frank, Eva Hong, Jean-Robert Mbecko, Jean-Pierre Lombart, Muhamed-Kheir Taha,[1] Pierre-Alain Rubbo[1]

We analyzed data from the 2015 and 2016 meningitis epidemic seasons in Central African Republic as part of the national disease surveillance. Of 80 tested specimens, 66 belonged to meningococcal serogroup W. Further analysis found that 97.7% of 44 isolates belonged to the hyperinvasive clonal complex sequence type 11.

Central African Republic (CAR) is localized in the meningitis belt that spans from Senegal to Ethiopia in sub-Saharan Africa. The country experiences meningitis epidemics every year. Eight health districts (Nana Mambéré, Ouham Pendé, Ouham, Nana Gribizi, Bamingui Bangoran, Vakaga, Haute-Kotto, and Ouaka) are at particularly high risk of meningitis outbreaks during the dry season, November–March (Figure 1). During this period, epidemiologic surveillance is reinforced by the health ministry with the help of the World Health Organization (WHO), Institut Pasteur de Bangui (IPB; Bangui, CAR), and nongovernmental organizations, depending on the geographic zone.

The gram-negative bacterium *Neisseria meningitidis* remains the leading cause of meningitis epidemics in Africa. Because of political troubles in the past years and missing reliable information available from the provinces, few epidemiologic and biologic data are available in CAR. Two previous reports, published by IPB in 2006 and 2008, had focused only on cases in Bangui (*1,2*). Data showed that, among proven bacterial disease, *Streptococcus pneumoniae* was the most common organism responsible for meningitis, resulting in a 47% death rate (29/62 cases). *N. meningitidis*, especially serogroup A (NmA), was also responsible for menigitis in Bangui to a lesser extent (*1,2*).

Historically, NmA of sequence types (STs) 5 and 7 was predominant in sub–Saharan Africa; serogroups W (ST11), C, and X (ST181) caused smaller numbers of cases. After introduction of massive vaccination campaigns, serogroup A incidence has massively decreased, and meningococcal strains causing disease shifted toward non-A serogroups (*3*). In particular,

Author affiliations: Institut Pasteur, Bangui, Central African Republic (T. Frank, J.-R. Mbecko, J.-P. Lombart, P.-A. Rubbo); Institut Pasteur, Paris, France (E. Hong, M.-K. Taha)

after the 1996–1997 epidemic in Africa that killed nearly 250,000 persons, the introduction of the MenAfriVac vaccine in 2010 contributed to dramatically reduced NmA cases in 26 countries of the meningitis belt by targeting roughly 65 million persons 1–29 years of age (WHO, http://www.who.int/immunization/newsroom/menafrivac_20121114/en/). Consequently, serogroup replacement has been noted. For example, in 2015, an epidemic with a novel strain of serogroup C was recorded in Niger and Nigeria for the first time since 1975 (WHO, http://www.who.int/wer/2015/wer9047.pdf?ua=1).

Hyperinvasive *N. meningitidis* serogroup W (NmW) cases belonging to the clonal complex ST11 (NmW/cc11) have been reported worldwide since the Hajj 2000–linked outbreak (*3–6*). Moreover, NmW/cc11 cases have been reported in the African meningitis belt at least since the late 1990s (*7*). Epidemics caused by these isolates were reported in 2001 and declined thereafter, but NmW/cc11 seems to have reemerged since 2010 (*8*). The genetic relationships between these NmW/cc11 isolates have been recently resolved using whole-genome sequencing, and 2 major NmW/cc11 lineages were described—the Anglo-French Hajj and South American/UK strains—in addition to several local NmW/cc11 isolates (*5*). We aimed to explore the genetic relationships of the 2015 and 2016 isolates from CAR with this reported population structure of NmW/cc11.

The Study

This study was a collaborative work led by IPB. In 2015 and 2016, CAR experienced annual national meningitis epidemics. All cases confirmed positive for meningococcal meningitis in IPB were from 7 districts in Ouham Prefecture: Batangafo, Besse, Lady, Kambakota, Ouogo, Bongonon, and Kabo.

Each suspected patient meeting the recommended WHO case definition for meningitis (sudden onset of fever >38.5°C rectal or >38.0°C axillary and 1 of the following signs: neck stiffness, altered consciousness, or other meningeal sign) underwent a lumbar puncture and received antimicrobial drug therapy. In some cases, when available, a latex agglutination test (Pastorex; Bio-Rad, Hercules, CA, USA) was done on cerebrospinal fluid (CSF) samples before an aliquot and a clinical case report form for each patient were transported to IPB. We analyzed each sample according to procedures routinely used in IPB for diagnosis and

---

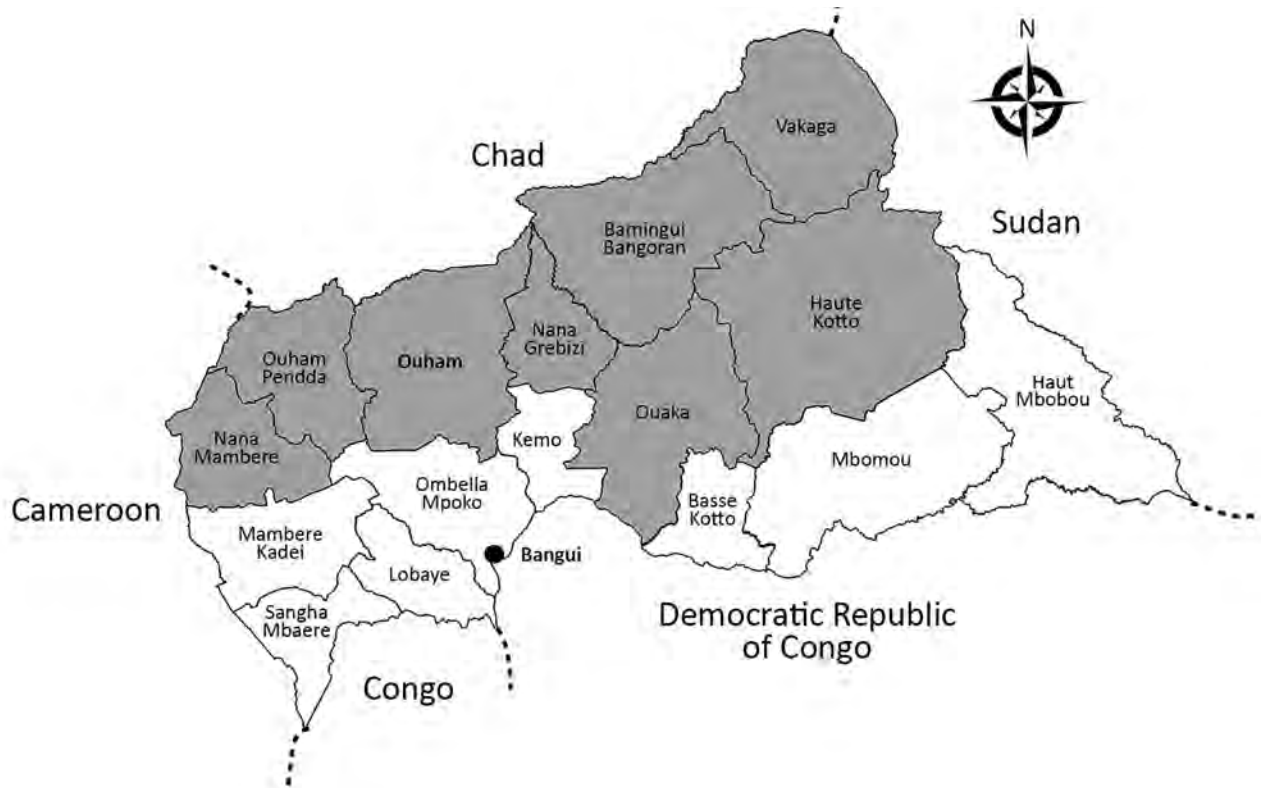[1]These authors contributed equally to this article.

Figure 1. Health districts in Central African Republic. Gray regions correspond to those in the meningitis belt with higher risk for meningitis outbreaks each year. The names of Bangui Prefecture, where the main laboratory (Institut Pasteur) is located, and Ouham Prefecture, where all the 2015 and 2016 meningitis cases occurred, are in bold.

monitoring of meningitis, according to WHO methodology (http://www.who.int/csr/resources/publications/meningitis/WHO_CDS_CSR_EDC_99_7_EN/en/). In brief, laboratory methodology used for NmW identification included Gram stain procedure, primary culture of CSF or transisolate inoculated medium onto blood agar plate and chocolate agar, and PCR testing. If CSF was visibly cloudy when received, we also performed latex agglutination (Pastorex) in the laboratory. NmW was considered as the causative agent when identified by culture, PCR, or both.

We performed molecular identification and genogroup determination using multiplex PCR (*9,10*) and multilocus sequence typing (MLST) using the methodology of the PubMLST *Neisseria* database (http://pubmlst.org/neisseria) on CSF samples (n = 44) using a single round of PCR. We subjected a proportion of cultured isolates (n = 28) to whole-genome sequencing using Illumina NextSeq 500 (Illumina, San Diego, CA, USA) and assembled them as described previously (*11*). We compared genomes using the PubMLST Genome Comparator tool on the basis of core genome (*12*). We visualized phylogenetic trees using SplitsTree4 version 4.13.1 (http://www.splitstree.org).

In 2015 and 2016, a total of 276 suspected cases of meningitis were reported in CAR (Table). Among these

276 patients, 13 died in 2015 and 12 in 2016. Of the 80 CSF samples received at IPB for biologic investigations, 52 bacteriologic cultures and 66 PCR tests were positive for NmW. All samples that were positive in culture were also positive in PCR. All 66 positive PCR tests identified serogroup W, confirming the presence of such epidemic strains in central Africa. We also found 5 PCR tests positive for

Table. Details of suspected and confirmed meningitis cases caused by *Neisseria meningitidis* during the 2015 and 2016 outbreaks in Central African Republic*

Data	2015	2016
Demographics		
Suspected cases, no.	120	156
CSF samples tested, no. (%)	20 (17)	60 (39)
Median age (IQR), mo	60 (36–162)	66 (21–186)
Sex ratio, M/F	11/9	36/24
Clinical data, no. (%)		
Fever	ND†	58 (97)
Weakness/asthenia	ND†	51 (85)
Neck stiffness	ND†	47 (78)
Deaths	13 (11)	12 (8)
Laboratory results, no. (% samples received)		
Positive NmW culture	11 (55)	41 (68)
Positive NmW PCR	20 (100)	46 (77)

*CSF, cerebrospinal fluid; IQR, interquartile range; ND, not determined; NmW, *N. meningitidis* serogroup W.
†Clinical information is missing for suspected cases during the 2015 epidemics.

Figure 2. Core genome multilocus sequence typing (MLST) neighbor-net phylogenetic network for the temporal distribution of *Neisseria meningitidis* serogroup W clonal complex sequence type cc11 isolates from CAR (n = 28) and reference isolates. The tree was built with neighbor-net SplitsTree graphs generated by SplitsTree4 version 4.13.1 (http://www.splitstree.org). The lineages Anglo-French-Hajj and South American/UK are indicated; other indicates 13 isolates retrieved from or based on the work of Lucidarme et al. (*5*). The isolates from CAR are also indicated by gray circles for the isolates of 2015 (n = 4 corresponding to on the PubMLST *Neisseria* database [http://pubmlst.org/Neisseria], 41187–41191) and by black circles for the isolates of 2016 (n = 24 corresponding to the PubMLST database, 44004–44027). The 30 isolates from the PubMLST database are as follows: 2290 (Saudi Arabia 2000); 19957 (United Kingdom 2000); 27087 (Burkina Faso 2002); 21588, 29326, 29337, 29370, 29371, 29382, 29384, 29401, 29406, 29422 (South Africa 2004–2005); 29775, 29928, 29929 (United Kingdom 2000); 30065, 30066, 30067 (Turkey 2005–2006); 30074 (Algeria 1999); 30075, 30079, 30107 (Senegal 2000–2001); and 31164, 31165, 42409, 42758, 42767, 42769, 50815 (France 2000–2016). CAR, Central African Republic.
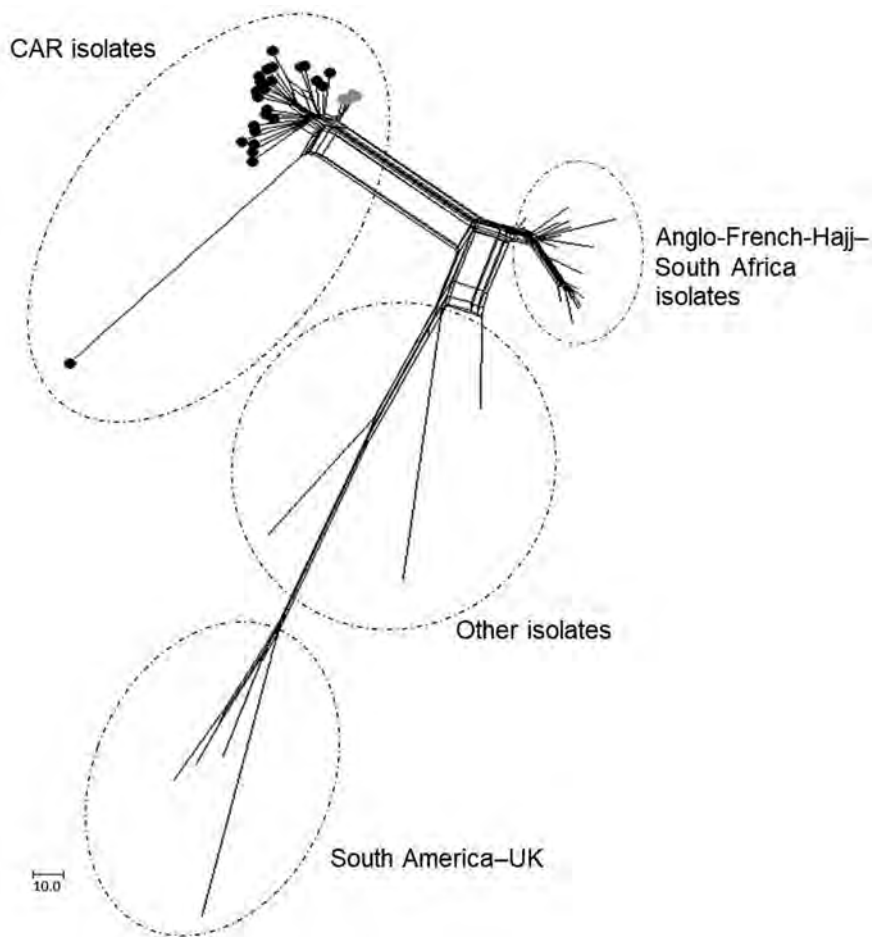
Streptococcus pneumoniae, as well as 9 negative results for both culture and PCR assays on the CSF samples. The most common signs and symptoms among the confirmed NmW case-patients were fever (97%), weakness (85%), and neck stiffness (78%).

From the 66 confirmed NmW cases, 44 CSF samples were sent to the WHO collaborating reference center for meningitis located in Institut Pasteur, Paris, for diagnostic confirmation and genetic analyses. Additionally, 28 isolates underwent genome sequence analysis for evaluating the genetic relationships of NmW strains identified in CAR to others during epidemics elsewhere. Phylogeny results clearly indicated that all the CAR isolates that underwent next-generation sequencing (4 in 2015 and 24 in 2016) were genetically linked. These isolates grouped together in a genetic cluster separated from other NmW/cc11 strains previously described, including the Anglo-French Hajj branch and the South American/UK branch, and from other local strains found in Africa (Figure 2).

Compared with data obtained in Bangui in the past years, which highlighted NmA as the main etiology of meningitis cases, our data show that the strains isolated during epidemic seasons in the north of CAR in 2015 and 2016 were all NmW. In addition, most of the characterized cases (43/44) belonged to the ST11 complex and had the antigenic formula NmW:P1.5,2:F1–1:cc11. The other case isolated in 2016 (1/44) belonged to the ST175 complex, a nonhyperinvasive clonal complex that should promote immune exploration, as such isolates have been reported more frequently among patients with complement deficiencies (*13*).

Conclusions

The number of meningitis cases reported during the 2015 and 2016 epidemic seasons was the most documented in CAR since 2008. We described the presence of a specific endemic NmW strain that appears to be circulating in sub–Saharan Africa, including in CAR. Foci correspond to endemic local strains, which confirms the hypothesis

of the multifocal emergence of specific NmW/cc11 strains (*5,14,15*).

Although CAR experiences epidemics of meningitis each year, the weaknesses of the national health system contribute to a delay in management of suspected cases. The emergence or reemergence of epidemic NmW strains in CAR requires persistent public health surveillance and increased capacity of epidemic detection and prevention, as well as revised vaccination policy.

About the Author

Dr. Frank is a senior medical microbiologist in the Laboratory for Biomedical Analysis of the Institut Pasteur, Bangui, Central African Republic. His primary research interests include surveillance of bacterial diseases such as meningitis in Africa, as well as antimicrobial drug resistance.

References

1. Békondi C, Bernede C, Passone N, Minssart P, Kamalo C, Mbolidi D, et al. Primary and opportunistic pathogens associated with meningitis in adults in Bangui, Central African Republic, in relation to human immunodeficiency virus serostatus. Int J Infect Dis. 2006;10:387–95. http://dx.doi.org/10.1016/j.ijid.2005.07.004
2. Bercion R, Bobossi-Serengbe G, Gody JC, Beyam EN, Manirakiza A, Le Faou A. Acute bacterial meningitis at the "Complexe Pédiatrique" of Bangui, Central African Republic. J Trop Pediatr. 2008;54:125–8. http://dx.doi.org/10.1093/tropej/fmm075
3. Mustapha MM, Marsh JW, Harrison LH. Global epidemiology of capsular group W meningococcal disease (1970–2015): Multifocal emergence and persistence of hypervirulent sequence type (ST)-11 clonal complex. Vaccine. 2016;34:1515–23. http://dx.doi.org/10.1016/j.vaccine.2016.02.014
4. Ladhani SN, Beebeejaun K, Lucidarme J, Campbell H, Gray S, Kaczmarski E, et al. Increase in endemic *Neisseria meningitidis* capsular group W sequence type 11 complex associated with severe invasive disease in England and Wales. Clin Infect Dis. 2015;60:578–85. http://dx.doi.org/10.1093/cid/ciu881
5. Lucidarme J, Hill DM, Bratcher HB, Gray SJ, du Plessis M, Tsang RS, et al. Genomic resolution of an aggressive, widespread, diverse and expanding meningococcal serogroup B, C and W lineage. J Infect. 2015;71:544–52. http://dx.doi.org/10.1016/j.jinf.2015.07.007
6. Zhou H, Liu W, Xu L, Deng L, Deng Q, Zhuo J, et al. Spread of *Neisseria meningitidis* serogroup W clone, China. Emerg Infect Dis. 2013;19:1496–9. http://dx.doi.org/10.3201/eid1909.130160
7. Kwara A, Adegbola RA, Corrah PT, Weber M, Achtman M, Morelli G, et al. Meningitis caused by a serogroup W135 clone of the ET-37 complex of Neisseria meningitidis in West Africa. Trop Med Int Health. 1998;3:742–6. http://dx.doi.org/10.1046/j.1365-3156.1998.00300.x
8. Collard JM, Maman Z, Yacouba H, Djibo S, Nicolas P, Jusot JF, et al. Increase in *Neisseria meningitidis* serogroup W135, Niger, 2010. Emerg Infect Dis. 2010;16:1496–8. http://dx.doi.org/10.3201/eid1609.100510
9. Fraisier C, Stor R, Tenebray B, Sanson Y, Nicolas P. Use of a new single multiplex PCR-based assay for direct simultaneous characterization of six *Neisseria meningitidis* serogroups. J Clin Microbiol. 2009;47:2662–6. http://dx.doi.org/10.1128/JCM.02415-08
10. Bronska E, Kalmusova J, Dzupova O, Maresova V, Kriz P, Benes J. Dynamics of PCR-based diagnosis in patients with invasive meningococcal disease. Clin Microbiol Infect. 2006; 12:137–41. http://dx.doi.org/10.1111/j.1469-0691.2005.01327.x
11. Taha MK, Claus H, Lappann M, Veyrier FJ, Otto A, Becher D, et al. Evolutionary events associated with an outbreak of meningococcal disease in men who have sex with men. PLoS One. 2016;11:e0154047. http://dx.doi.org/10.1371/journal.pone.0154047
12. Jolley KA, Maiden MC. BIGSdb: Scalable analysis of bacterial genome variation at the population level. BMC Bioinformatics. 2010;11:595. http://dx.doi.org/10.1186/1471-2105-11-595
13. Rosain J, Hong E, Fieschi C, Martins PV, El Sissy C, Deghmane AE, et al. Strains responsible for invasive meningococcal disease in patients with terminal complement pathway deficiencies. J Infect Dis. 2017;215:1331–8. http://dx.doi.org/10.1093/infdis/jix143
14. Hossain MJ, Roca A, Mackenzie GA, Jasseh M, Hossain MI, Muhammad S, et al. Serogroup W135 meningococcal disease, The Gambia, 2012. Emerg Infect Dis. 2013;19:1507–15. http://dx.doi.org/10.3201/eid1909.130077
15. Cibrelus L, Medah I, Koussoubé D, Yélbeogo D, Fernandez K, Lingani C, et al. Serogroup W meningitis outbreak at the subdistrict level, Burkina Faso, 2012. Emerg Infect Dis. 2015;21:2063–6. http://dx.doi.org/10.3201/eid2111.150304

Address for correspondence: Pierre-Alain Rubbo, Institut Pasteur de Bangui, BP 923, Avenue de l'Indépendance, Bangui, Central African Republic; email: pierre-alain.rubbo@pasteur.fr

Fatal Case of Diphtheria and Risk for Reemergence, Singapore

Yingqi Lai, Parthasarathy Purnima, Marc Ho, Michelle Ang, Rama N. Deepak, Ka Lip Chew, Shawn Vasoo, Dimatatac F. Capulong, Vernon Lee

We report a fatal autochthonous diphtheria case in a migrant worker in Singapore. This case highlights the risk for individual cases in undervaccinated subpopulations, despite high vaccination coverage in the general population. Prompt implementation of public health measures and maintaining immunization coverage are critical to prevent reemergence of diphtheria.

Diphtheria is an acute respiratory disease caused by infection with *Corynebacterium diphtheriae*. Case-fatality rates for respiratory diphtheria reached 50% in epidemics in the 1880s and remain ≈5%–10% even after use of antitoxin. Virulence is mediated by production of toxin by the *tox* gene of β-corynebacteriophage (1).

Global incidence of diphtheria decreased by >90% during 1980–2016 after initiation of the World Health Organization Expanded Programme on Immunization in 1974 (2). This decrease was also reflected by the shifting age distribution from children to adolescents and adults (3). Although the World Health Organization South-East Asia Region was estimated to contain 55%–99% of all reported diphtheria cases during 2011–2015, diphtheria cases have been reported in industrialized countries (2,4–7).

Singapore is a densely populated (8,000 persons/km^2) city-state in Southeast Asia and a trade and travel hub. It last had an autochthonous case of toxigenic *C. diphtheriae* in 1992. This low incidence has been achieved by ensuring high population immunity through mandatory vaccination since 1962. A primary course of diphtheria, tetanus, and acellular pertussis vaccine is given to infants at 3, 4, and 5 months of age; booster vaccines are given at 18 months and 10–11 years of age. Immunization coverage for 2-year-olds has been >95% for the past 14 years (8).

On August 3, 2017, the Ministry of Health Singapore was notified of a diphtheria case in a person who had no recent travel overseas or known contact with an infected person. We describe the public health measures implemented to prevent further spread, and discuss risks for diphtheria reemergence in countries with high vaccination coverage, particularly those with insufficiently vaccinated subpopulations.

The Study

A 23-year-old man from Bangladesh who had been a construction worker in Singapore for the previous 10 months had fever, sore throat, and neck pain develop on July 30, 2017. He visited a primary care clinic on July 31 and was given symptomatic treatment.

His symptoms worsened, and he came to an emergency department because of odynophagia and hemoptysis on August 1. He was hypoxic and needed ventilation through a tracheostomy. Throat examination and subsequent intraoperative findings showed extensive soft palate edema obscuring the uvula and tonsils; purulent secretions obstructing the airway; and pseudomembranous mucosa over bilateral, necrotic-looking tonsils, the base of the tongue, and the larynx. Computed tomography showed extensive soft tissue edema causing near-complete airway narrowing from the choana to supraglottis and multiple enlarged cervical lymph nodes.

We made a clinical diagnosis of respiratory diphtheria. The patient was isolated immediately and given diphtheria antitoxin and intravenous erythromycin. However, his condition deteriorated rapidly, and he died of respiratory obstruction 48 hours after admission.

We obtained a laboratory diagnosis through parallel culture of tonsillar and pharyngeal tissue on trypticase soy agar containing 5% sheep blood, chocolate agar, and Mac-Conkey agar. All cultures were incubated at 37°C in an atmosphere of 5% CO_2 in a primary laboratory. Culture of laryngeal and nasal discharge was performed in the referral laboratory on Tinsdale Columbia CNA agar (Becton Dickinson, Sparks, MD, USA) containing 5% sheep blood and sheep blood agar. Bacterial colonies grew in all cultures; gram-positive rods were identified as *C. diphtheriae* by using the API Coryne System (BioMérieux, Marcy l'Etoile, France) and Bruker MALDI Biotyper (Bruker Daltonics, Bremen, Germany). We detected toxin A and B subunits of the *C. diphtheriae* toxin (*tox*) gene in the tonsil isolate by using an adapted PCR (9).

The patient isolate (OTH-17-20) was confirmed as toxigenic *C. diphtheriae* biovar mitis. In silico multilocus

sequence typing (MLST) showed that OTH-17-20 belonged to sequence type (ST) 50, which was unrelated to the STs of nontoxigenic isolates obtained from public hospitals in Singapore during 2013–2017 (BioProject PRJNA445775) (Figure 1). When we compared OTH-17-20 with 4 other available ST50 genomes in GenBank by core-genome, single-nucleotide polymorphism analysis, we found that this isolate was more related to the cluster of 3 ST50 genomes from India than to 1 isolate from Germany (Figure 2; online Technical Appendix, https://wwwnc.cdc.gov/EID/article/24/11/18-0198-Techapp1.pdf).

Movement of the patient was confined to his dormitory room and worksite. Because the moribund patient could not communicate, we conducted interviews with his colleagues, employer, and dormitory roommates to ascertain possible exposure(s). These interviews included identifying close contacts, who were defined as persons with similar proximity and duration of exposure as household contacts who were directly exposed to large-particle droplets or secretions from the patient (11).

Adopting a precautionary approach, we identified 3 groups of contacts. The first group was 11 persons who lived in the same dormitory room. The second group was 37 colleagues who worked together or shared transportation to the workplace. The third group was 72 healthcare workers who provided direct care to the patient without adequate personal protective equipment.
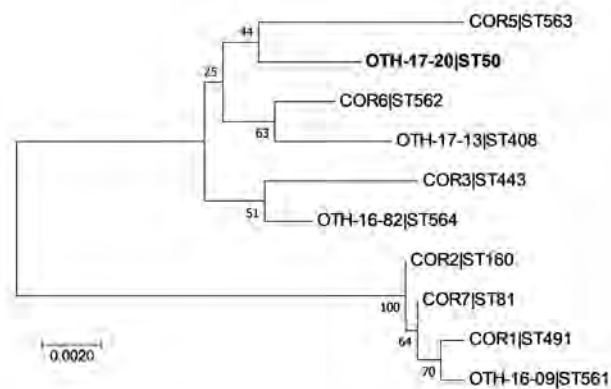

Figure 1. Phylogenetic analysis of *Corynebacterium diphtheriae* isolate from a 23-year-old man who died from diphtheria (OTH-17-20; bold) and 9 other isolates collected from hospitals in Singapore during 2013–2017. The tree was constructed by using 7 concatenated housekeeping gene sequences corresponding to the *C. diphtheriae* multilocus sequence typing scheme (https://pubmlst.org/cdiphtheriae/). Sequences were extracted from whole-genome sequences of each isolate. Concatenated sequences were aligned by using ClustalW (http://www.clustal.org/). Phylogeny was inferred by using the maximum-likelihood method, neighbor-joining algorithm based on the Jukes-Cantor model, and MEGA7 software (10). There were 2,544 positions in the final dataset. Numbers next to branches show bootstrap values calculated by using 1,000 reiterations. Scale bar indicates nucleotide substitutions per site. ST, sequence type.

Among the second group, 3 persons had sore throats develop; they were immediately placed in isolation in the hospital. Nasopharyngeal and throat swab specimens obtained from these 3 patients before they received antimicrobial drugs were negative for *C. diphtheriae*. All 3 patients recovered without complications.

Dormitory and workplace contacts were of various nationalities (age range 22–39 years). All contacts were given 7 days of oral erythromycin or clarithromycin and a diphtheria toxoid booster vaccination if they had not received this vaccination in the previous 5 years or if vaccination history was unknown. Most dormitory and workplace contacts could not recall their vaccination history or did not have vaccination records.

To determine possible sources of exposure or onward transmission, we obtained nasopharyngeal and throat swab specimens before administration of antimicrobial drugs on August 4 from dormitory and workplace contacts for concurrent culture on selective media and testing by PCR. All swab specimens were negative for *C. diphtheriae*, and no secondary cases were detected at the end of 2 incubation periods.

Conclusions

We report potential reemergence of locally transmitted toxigenic diphtheria in Singapore. As with cases in other industrialized countries, investigations could not identify a source of infection (4,7). Asymptomatic carriers remained a possibility because studies have reported bacterial carriage in vaccinated persons and nontoxigenic strains that underwent phage conversion (5,6,12–15). Because the patient had an unknown vaccination history, missing childhood vaccinations might have put him at risk for infection.

Such risks from severe vaccine-preventable diseases are present because of movement of unvaccinated or inadequately vaccinated persons. For migrants, these risks are compounded by population density and working conditions. Singapore hosts workers from countries such as India, Bangladesh, and Myanmar, to which diphtheria is endemic (2). Although these countries have now achieved high immunization coverage, levels were much lower decades ago when current migrant workers were children. In Bangladesh, where the patient originated from, 97% of infants received a primary course of diphtheria vaccine in 2016, compared with 84% in 1994 when the patient was an infant (2). Seroprotection has been shown to wane over time after a primary infant series (1). Therefore, booster doses during adolescence and adulthood are needed to maintain immunity.

This fatal case is a reminder that unvaccinated persons among specific subpopulations remain vulnerable to severe vaccine-preventable diseases, such as diphtheria. Clinicians and public health practitioners should remember that primary prevention through up-to-date vaccinations are necessary not only for children but also for adults who
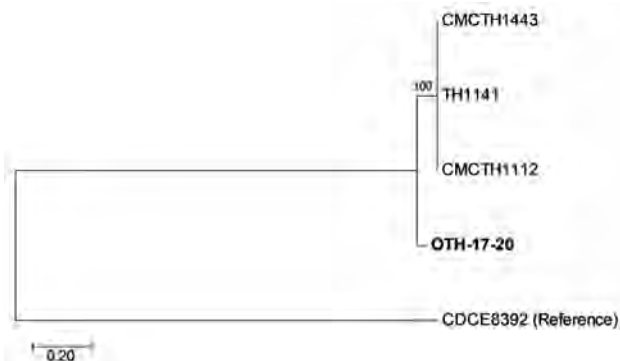
Figure 2. Core-genome single-nucleotide polymorphism (SNP) phylogeny of *Corynebacterium diphtheriae* isolate from a 23-year-old man who died from diphtheria (OTH-17-20; bold) and 4 publicly available ST50 genomes (TH1141, GenBank accession no. GCA_001723455.1; CMCTH1443, accession no. GCA_001981275.1; CMCTH1112, accession no. GCA_001981275.1; and CDCE8392, accession no. GCA_000255215.1) of isolates collected from hospitals in Singapore during 2013–2017. Phylogeny was deduced by alignment with Parsnp (http://harvest.readthedocs.io/en/latest/content/parsnp.html), a rapid core-genome multialignment tool for genome assemblies. Extracted SNPs were concatenated, and phylogeny was inferred as described in Figure 1. There were 26,785 positions in the final dataset. Numbers next to branches show bootstrap values calculated by using 1,000 reiterations. Scale bar indicates nucleotide substitutions per site. ST, sequence type.

do not have appropriate coverage. In this regard, Singapore implemented the National Adult Immunization Schedule in 2017 to increase vaccination uptake.

Similar to other diseases with widespread childhood vaccine coverage, diphtheria has been mostly forgotten among healthcare professionals in industrialized countries. Clinical suspicion and diagnosis of this case was instrumental for rapid implementation of control measures. Clinicians, microbiologists, and public health specialists should be reminded of the risk for reemerging diphtheria.

About the Author

Ms Lai is an epidemiologist at the Communicable Diseases Division, Ministry of Health, Singapore. Her research interests include vaccine-preventable diseases and antimicrobial drug resistance.

References

1. Tiwari TS, Wharton M. Diphtheria toxoid. In: Plotkin SA, Orenstein WA, Offit P, editors. Plotkin's vaccines. 7th ed. Philadelphia: Elsevier; 2017. p. 261–75.
2. World Health Organization. Immunization, vaccines and biologicals: data, statistics and graphs [cited 2018 Apr 9]. http://www.who.int/immunization/monitoring_surveillance/data/en/
3. Clarke KE. Review of the epidemiology of diphtheria, 2000–2016 [cited 2018 Apr 9]. http://www.who.int/immunization/sage/meetings/2017/april/1_Final_report_Clarke_april3.pdf?ua=1
4. Berger A, Meinel DM, Schaffer A, Ziegler R, Pitteroff J, Konrad R, et al. A case of pharyngeal diphtheria in Germany, June 2015. Infection. 2016;44:673–5. http://dx.doi.org/10.1007/s15010-016-0882-2
5. Rasmussen I, Wallace S, Mengshoel AT, Høiby EA, Brandtzæg P. Diphtheria outbreak in Norway: lessons learned. Scand J Infect Dis. 2011;43:986–9. http://dx.doi.org/10.3109/00365548.2011.600326
6. European Centre for Disease Prevention and Control. A case of diphtheria in Spain, June 15, 2015 [cited 2018 Aug 15]. https://ecdc.europa.eu/sites/portal/files/media/en/publications/Publications/diphtheria-spain-rapid-risk-assessment-june-2015.pdf
7. Perkins S, Cordery R, Nixon G, Abrahams A, Andrews J, White J, et al. Investigations and control measures following a non-travel-associated case of toxigenic *Cornyebacterium diphtheriae*, London, United Kingdom, December 2009–January 2010. Euro Surveill. 2010;15:pii: 19544.
8. Ministry of Health Singapore. Communicable diseases surveillance in Singapore 2016 [cited 2018 Apr 9]. https://www.moh.gov.sg/content/dam/moh_web/Publications/Reports/2017/Full%20Version.pdf
9. Nakao H, Pruckler JM, Mazurova IK, Narvskaia OV, Glushkevich T, Marijevski VF, et al. Heterogeneity of diphtheria toxin gene, *tox*, and its regulatory element, *dtxR*, in *Corynebacterium diphtheriae* strains causing epidemic diphtheria in Russia and Ukraine. J Clin Microbiol. 1996;34:1711–6.
10. Kumar S, Stecher G, Tamura K. MEGA7: Molecular Evolutionary Genetics Analysis version 7.0 for bigger datasets. Mol Biol Evol. 2016;33:1870–4. http://dx.doi.org/10.1093/molbev/msw054
11. Diphtheria Guidelines Working Group, Public Health England. Public health control and management of diphtheria (in England and Wales), 2015 guidelines [cited 2018 Aug 15]. https://www.gov.uk/government/publications/diphtheria-public-health-control-and-management-in-england-and-wales
12. Lumio J, Suomalainen P, Olander RM, Saxén H, Salo E. Fatal case of diphtheria in an unvaccinated infant in Finland. Pediatr Infect Dis J. 2003;22:844–6. http://dx.doi.org/10.1097/01.inf.0000083906.24285.23
13. Farizo KM, Strebel PM, Chen RT, Kimbler A, Cleary TJ, Cochi SL. Fatal respiratory disease due to *Corynebacterium diphtheriae*: case report and review of guidelines for management, investigation, and control. Clin Infect Dis. 1993;16:59–68. http://dx.doi.org/10.1093/clinids/16.1.59
14. Bowler IC, Mandal BK, Schlecht B, Riordan T. Diphtheria: the continuing hazard. Arch Dis Child. 1988;63:194–5. http://dx.doi.org/10.1136/adc.63.2.194
15. Simmons LE, Abbott JD, Macaulay ME, Jones AE, Ironside AG, Mandal BK, et al. Diphtheria carriers in Manchester: simultaneous infection with toxigenic and non-toxigenic mitis strains. Lancet. 1980;1:304–5. http://dx.doi.org/10.1016/S0140-6736(80)90793-X

Address for correspondence: Yingqi Lai, College of Medicine Building, Ministry of Health, 16 College Rd, Singapore 169854; email: lai_yingqi@moh.gov.sg

Ehrlichia Infections, North Carolina, USA, 2016

**Ross M. Boyce, Alan M. Sanfilippo,
John M. Boulos, Meghan Cleinmark,
John Schmitz, Steve Meshnick**

Nearly two thirds of persons suspected of having tickborne illness in central North Carolina, USA, were not tested for *Ehrlichia*. Failure to test may have resulted in a missed diagnosis for ≈13% of these persons, who were therefore substantially less likely to receive antimicrobial treatment and to have follow-up testing performed.

Incidence of spotted fever group *Rickettsia* (SFGR), which include the causative agent of Rocky Mountain spotted fever (RMSF), is high in North Carolina, USA (*1*). Entomologic studies, however, suggest that the principal vector in this state is the lone star tick (*Amblyomma americanum*), which is a major vector for *Ehrlichia chaffeensis* and *E. ewingii* (*2,3*). The clinical spectrum of *Ehrlichia* infection, which causes nonspecific signs and symptoms including fever, headache, and malaise, resembles that of RMSF (*4,5*). Therefore, we examined clinical practice patterns associated with the evaluation and treatment of patients suspected of having tickborne illness to determine if *Ehrlichia* infection causes underrecognized tickborne illness in North Carolina.

The Study

We performed a retrospective chart review of all patients who had undergone serologic testing for tickborne illness at University of North Carolina hospitals and associated clinics during June 8–September 8, 2016. We abstracted demographic information, test results, and treatment plans for patients with signs and symptoms consistent with acute infection (i.e., fever, headache, myalgia) or recent tick exposure. Patients were excluded if testing had been ordered for chronic symptoms, including fatigue or neurocognitive deficits. Testing for *Borrelia burgdorferi* (Lyme disease) was performed by chemiluminescent immunoassay (Diasorin, Inc., Stillwater, MN, USA). Indirect immunofluorescence antibody (IFA) testing for SFGR was performed by using *R. rickettsia*–coated slides and a polyvalent conjugate, whereas testing for *Ehrlichia* was performed by using an IgG-based IFA (both from Biocell Diagnostics Inc, Baltimore, MD, USA). If testing for *Ehrlichia* was not ordered

at the time of the initial healthcare visit, this testing was performed on stored serum (retrospective testing). Given potential cross-reactivity, we also tested retrospective samples for *Anaplasma phagocytophilum*. A positive test was defined as a positive IFA result with a subsequent IgG titer of ≥80 for SFGR and ≥64 for *Ehrlichia*.

We compared characteristics of the cohort by using the Student *t*-test for continuous variables and the Pearson χ^2 test for categorical variables. We fit univariable Poisson regression models to examine associations between doxycycline prescriptions and test results. The study was approved by the University of North Carolina institutional review board.

We screened 226 records, from which 194 patients were included in the analysis (Table). The most common reason for patient exclusion was having been tested in response to longstanding symptoms (Figure). Tick exposure was documented for 61 (61.6%) of 99 encounters, although many providers did not record exposure history. The most commonly reported signs and symptoms were fever (38.1%), headache (27.8%), and myalgia (21.7%). The median duration of symptoms for those reporting an illness was 6 days (interquartile range 3–14 days).

Most (91.8%) patients were seen in ambulatory clinics and emergency departments. Overall, most patients were tested for SFGR (154, 79.4%) and Lyme disease (128, 66.0%), but testing for *Ehrlichia* was ordered for only 70 (36.1%) patients.

A total of 154 patients were initially tested for SFGR and results for 37 (24.0%) were positive; 70 patients were initially tested for *Ehrlichia* and results for 9 (12.9%) were positive. Only 1 Lyme disease test result was positive. Of the 124 patients who did not initially have *Ehrlichia* testing performed, retrospective testing results were *Ehrlichia* positive for 25 (20.2%); none were positive for *Anaplasma*. Among those with a positive retrospective test result for whom results of a complete blood count or transaminase levels were available, 2 (12.5%) of 16 had concurrent thrombocytopenia and 1 (10.0%) of 10 had elevated transaminase levels. Convalescent-phase serologic testing results were obtained for 24 (12.5%) patients, among whom there was only 1 occurrence of a 4-fold titer increase in a patient with positive *Ehrlichia* titers. Convalescent-phase serologic testing was more frequently ordered for patients for whom acute-phase serologic results for SFGR, *Ehrlichia*, or both were positive (19/24, 79.2%).

Table. Patient characteristics stratified by provider-ordered *Ehrlichia* testing, North Carolina, 2016*

Characteristic	Tested for *Ehrlichia*, no. (%), n = 70†	Not tested for *Ehrlichia*, no. (%), n = 124†	p value
Sex			
M	39 (55.7)	64 (52.0)	0.48
F	31 (44.2)	60 (48.0)	
Setting			0.09
Outpatient clinic	42 (63.4)	57 (48.3)	
Emergency department	16 (24.2)	47 (39.8)	
Inpatient	8 (12.1)	14 (11.9)	
Provider medical specialty			**0.001**
Emergency medicine	13 (18.8)	43 (34.7)	
Family medicine	16 (23.2)	20 (16.1)	
Infectious diseases	9 (13.0)	2 (1.6)	
Internal medicine	15 (21.7)	18 (14.5)	
Other	16 (23.2)	41 (33.1)	
Reported signs and symptoms			
Fever	27 (38.6)	47 (37.9)	0.93
Headache	22 (31.4)	32 (25.8)	0.40
Myalgia	11 (15.7)	31 (25.0)	0.13
Rash	12 (17.1)	27 (21.8)	0.44
Tick exposure‡	28 (41.2)	33 (27.7)	**0.05**
Testing			
SFGR	62 (88.6)	92 (74.2)	**0.02**
Lyme disease	48 (68.6)	80 (64.5)	0.57
Positive test result			
Ehrlichia	9 (12.9)	25 (20.2)	0.20
SFGR	15 (24.2)	22 (23.9)	0.97
Lyme disease	0 (0.0)	1 (1.3)	0.44
Doxycycline prescribed	27 (39.7)	67 (55.8)	**0.03**
Convalescent-phase serology performed	15 (21.7)	10 (8.1)	**0.007**

*Boldface indicates significance at p<0.05. IQR, interquartile range; SFGR, spotted fever group *Rickettsia*.
†Among those tested for *Ehrlichia*, median (IQR) age was 53.5 (33–67) y, and among those not tested for *Ehrlichia*, median (IQR) age was 46 (30–61.5) y (p = 0.48). Among those tested for *Ehrlichia*, duration of symptoms was 6.5 (3–14) d, and among those not tested for *Ehrlichia*, duration was 5.5 (3–14) d (p = 0.59). Numbers and percentages vary because some data were not available.
‡Unable to determine exposure status for 24 (35.3%) of 68 patients tested for *Ehrlichia* and 64 (53.8%) of 119 patients not tested for *Ehrlichia*.

Doxycycline was prescribed for half of all patients for whom treatment was known (94/188, 50.0%). Patients for whom acute SFGR serologic results were positive were more likely than those whose results were negative to receive doxycycline (odds ratio [OR] 7.52, 95% CI 2.73–20.8; p<0.001), but this finding was not true with regard to patients with positive versus negative results for *Ehrlichia*. Of note, doxycycline was prescribed less frequently for patients with a positive retrospective *Ehrlichia* test result (30.4%) than for those with a positive provider-ordered test (77.8%) (OR 0.13, 95% CI 0.02–0.78; p = 0.03). Similarly, convalescent-phase serologic testing was performed less often for patients with a positive retrospective test result (16.0%) than for those with a positive provider-ordered test result (55.6%) (OR 0.15, 95% CI 0.03–0.85; p = 0.03).

Our results demonstrate that *Ehrlichia* accounted for a large proportion of reactive antibodies among a cohort of patients suspected of having tickborne illness in central North Carolina. These findings provide strong, albeit circumstantial, evidence that *Ehrlichia* infection is as prevalent as SFGR infection. Yet, providers ordered *Ehrlichia* testing much less frequently than SFGR or even Lyme disease testing, despite the low incidence of Lyme disease in the state. This disparity may be attributable to unfamiliarity with local vector epidemiology and to the greater attention given to RMSF and Lyme disease by the general population.

Our results show that testing strategies had a clear effect on patient care. Despite the recommendation that doxycycline be empirically given to patients suspected of having RMSF, our findings show that providers were significantly more likely to prescribe doxycycline when the acute-phase serologic test results were reactive (*6*). By extension, because providers were ordering testing for *Ehrlichia* less frequently, patients who were ultimately found to have positive retrospective serologic results were not identified during routine evaluation and thus were less likely to receive antimicrobial therapy.

Our study has several limitations, the most relevant of which is the reliance on single time point serologic testing for most patients. The absence of convalescent-phase serologic testing adversely affects our ability to discriminate acute infection from prior exposure. The presence of thrombocytopenia or elevated transaminase levels suggests that at least a portion of patients found to have reactive antibodies by retrospective testing had acute infections, but testing for these laboratory abnormalities was not performed for all patients. Thus, we may have misclassified some prior exposures as acute infections and some acute infections as noninfections.
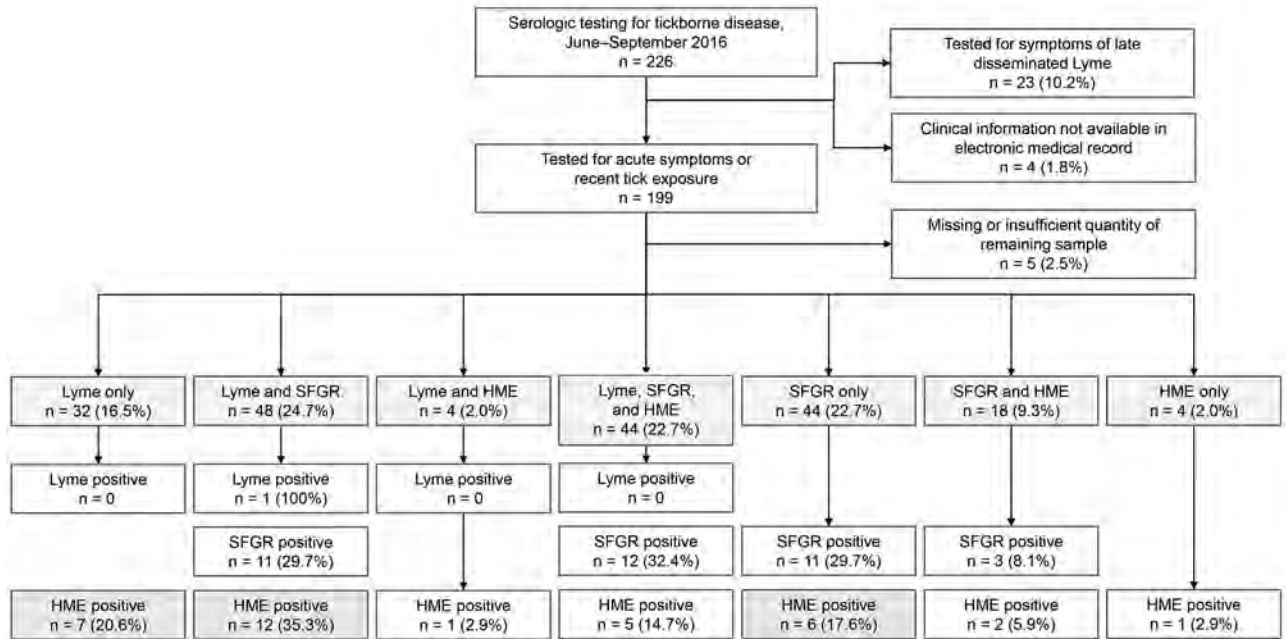
Figure. Summary of cohort selection and initial diagnostic testing results (light gray boxes) for 226 patients who had undergone serologic testing for tickborne illness, North Carolina, USA, in 2016. Results of retrospective testing for *Ehrlichia* are shown in dark gray boxes. HME, human monocytic ehrlichiosis; Lyme, Lyme disease; SFGR, spotted fever group rickettsiosis.

Further complicating the picture is the issue of cross-reactivity, especially between members of SFGR, such as *Rickettsia rickettsii* and *R. parkeri*, and potentially with the newly classified *R. amblyommatis* (7), which is also transmitted by lone star ticks. The use of PCR for the diagnosis of *Ehrlichia* infection could have overcome issues related to *E. ewingii* cross-reactivity but was not routinely ordered and could not be performed on stored serum. We did, however, perform IFA testing for *A. phagocytphilum* on retrospective samples to ensure no cross-reactivity with *Ehrlichia*.

Our sampling strategy probably did not capture all suspected cases in the specified period. Patients with a compelling history and clinical signs and symptoms may have empirically received doxycycline without testing. This practice could have biased our sample such that the patients most likely to have acute infection were treated empirically, whereas testing was only performed only for those with less typical presentations.

Conclusions

Our results demonstrate that, when considering tickborne illnesses, providers in North Carolina consider ehrlichiosis less frequently than RMSF and Lyme disease, despite the relatively high seroprevalence of antibodies reactive against *Ehrlichia* spp. in our cohort. Statewide education efforts targeting primary care offices and emergency departments are needed to improve provider awareness of

and approaches to this potentially severe disease. Given the wide and growing distribution of lone star ticks, these findings are probably generalizable to much of the mid-Atlantic United States (8).

About the Author

Dr. Boyce is a clinical instructor in the Division of Infectious Diseases at the University of North Carolina. His primary research interest is the spatial and clinical epidemiology of vectorborne diseases, including malaria in rural sub-Saharan Africa and tickborne illnesses in North Carolina.

References

1. Centers for Disease Control and Prevention. National Notifiable Diseases Surveillance System, 2016 annual tables of infectious disease data. Atlanta: The Centers; 2017.
2. Lee S, Kakumanu ML, Ponnusamy L, Vaughn M, Funkhouser S, Thornton H, et al. Prevalence of Rickettsiales in ticks removed from the skin of outdoor workers in North Carolina. Parasit Vectors. 2014;7:607. http://dx.doi.org/10.1186/s13071-014-0607-2
3. Apperson CS, Engber B, Nicholson WL, Mead DG, Engel J, Yabsley MJ, et al. Tick-borne diseases in North Carolina: is

"*Rickettsia amblyommii*" a possible cause of rickettsiosis reported as Rocky Mountain spotted fever? Vector Borne Zoonotic Dis. 2008;8:597–606. http://dx.doi.org/10.1089/vbz.2007.0271

4. Eng TR, Harkess JR, Fishbein DB, Dawson JE, Greene CN, Redus MA, et al. Epidemiologic, clinical, and laboratory findings of human ehrlichiosis in the United States, 1988. JAMA. 1990; 264:2251–8. http://dx.doi.org/10.1001/jama.1990.03450170099030

5. Dumler JS, Madigan JE, Pusterla N, Bakken JS. Ehrlichioses in humans: epidemiology, clinical presentation, diagnosis, and treatment. Clin Infect Dis. 2007;45(Suppl 1):S45–51. http://dx.doi.org/10.1086/518146

6. Biggs HM, Behravesh CB, Bradley KK, Dahlgren FS, Drexler NA, Dumler JS, et al. Diagnosis and management of tickborne rickettsial diseases: Rocky Mountain spotted fever and other spotted fever group rickettsioses, ehrlichioses, and anaplasmosis—United States. MMWR Recomm Rep. 2016;65:1–44. http://dx.doi.org/10.15585/mmwr.rr6502a1

7. Karpathy SE, Slater KS, Goldsmith CS, Nicholson WL, Paddock CD. *Rickettsia amblyommatis* sp. nov., a spotted fever group *Rickettsia* associated with multiple species of *Amblyomma* ticks in North, Central and South America. Int J Syst Evol Microbiol. 2016;66:5236–43. http://dx.doi.org/10.1099/ijsem.0.001502

8. Dahlgren FS, Paddock CD, Springer YP, Eisen RJ, Behravesh CB. Expanding range of *Amblyomma americanum* and simultaneous changes in the epidemiology of spotted fever group rickettsiosis in the United States. Am J Trop Med Hyg. 2016;94:35–42. http://dx.doi.org/10.4269/ajtmh.15-0580

Address for correspondence: Ross M. Boyce, University of North Carolina at Chapel Hill, Division of Infectious Diseases, 130 Mason Farm Rd, Chapel Hill, NC 27599, USA; email: ross.boyce@unchealth.unc.edu
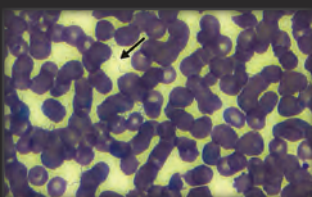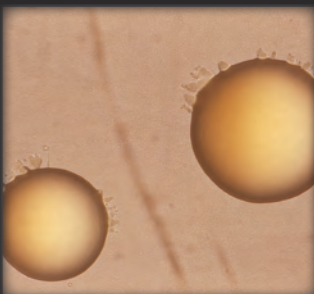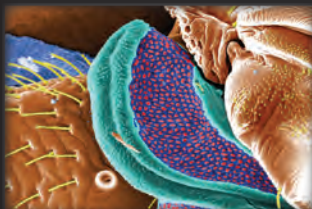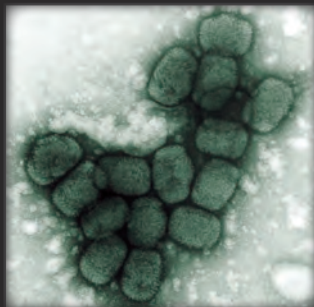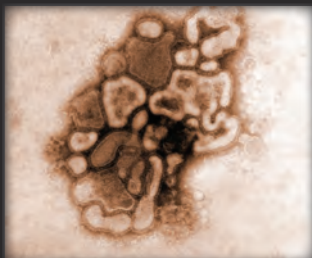
Burkholderia thailandensis Isolated from Infected Wound, Arkansas, USA

Jay E. Gee, Mindy G. Elrod,
Christopher A. Gulvik, Dirk T. Haselow,
Catherine Waters, Lindy Liu, Alex R. Hoffmaster

The bacterium *Burkholderia thailandensis*, a member of the *Burkholderia pseudomallei* complex, is generally considered nonpathogenic; however, on rare occasions, *B. thailandensis* infections have been reported. We describe a clinical isolate of *B. thailandensis*, BtAR2017, recovered from a patient with an infected wound in Arkansas, USA, in 2017.

*B*urkholderia thailandensis is a member of the *Burkholderia pseudomallei* complex and is generally considered nonpathogenic (*1*). *B. pseudomallei* causes the disease melioidosis and can be fatal even when properly treated (*1–3*). *B. thailandensis* was first discovered in Thailand and was differentiated from *B. pseudomallei* phenotypically by its ability to assimilate arabinose (*3*). *B. thailandensis*, like *B. pseudomallei*, naturally occurs in the environment (e.g., in moist soils) and is associated with tropical or subtropical climates (*3,4*). Environmental isolates of *B. thailandensis* have been predominantly recovered in Southeast Asia, with sporadic reports in other regions such as in Australia, which is considered the ancestral origin for *B. pseudomallei* based on analysis of genomic single-nucleotide polymorphisms (SNPs) (*4–6*).

The phenotypic similarities are substantial among members of the *B. pseudomallei* complex, other *Burkholderia* species, and other bacteria such as *Pseudomonas* spp. Laboratory personnel unfamiliar with *B. pseudomallei* often have difficulty identifying it using microbiologic methods commonly available in clinical settings. Automated biochemical systems might also misidentify *B. pseudomallei* because of an insufficient number of reference strains in their databases. Incorrect identification can delay appropriate antimicrobial therapy (*1,4,7*).

Although rare, *B. thailandensis* infections in humans have been reported. The first case reported in the literature occurred in or before 1999 in Thailand in a 16-year-old

boy who suffered compound fractures in a motorcycle accident (*8*). The second case occurred in 1997 in a 76-year-old man in Louisiana, USA, who had a pleural wound; this case resulted in recovery of isolate H0587 (also known as CDC2721121). Further details on the wound and whether it was acquired locally or whether the patient had a travel history to areas endemic for *B. thailandensis* are not available. The third case occurred in 2003 in a previously healthy 2-year-old boy in Texas, USA, who aspirated water from a ditch after a car accident; this case resulted in recovery of isolate TXDOH (also known as CDC3015869) (*9*). The fourth case occurred in 2011 in a 42-year-old man in Malaysia who had a foot abscess with ankle swelling and skin cellulitis (*10*). The fifth report was a fatal case that occurred in 2013 in a 67-year-old man who was treated at a hospital in Chongqing, China (*11*); however, subsequent correspondence suggested that the species had been identified incorrectly and was most likely *B. pseudomallei* (*12*).

In April 2017, a 29-year-old woman with diabetes in Arkansas, USA, crashed into a large metal trash bin while driving an all-terrain vehicle, resulting in an open bone forearm fracture. Treatment of the wound included installation of a metal plate. Approximately 3 months later, the patient returned to the hospital because of a 2-week history of swelling of her forearm. An isolate was recovered from pure culture graded 1+ (trace growth) from a deep operative tissue specimen from the forearm wound. Initial antimicrobial treatment consisted of piperacillin/tazobactam, vancomycin, and cefazolin. Testing of the isolate using the Microscan Walkaway automated biochemical system (Beckman Coulter, Atlanta, GA, USA) by the hospital laboratory identified *B. pseudomallei*. Based on this result, the Arkansas Department of Health (DoH) contacted the Centers for Disease Control and Prevention (CDC) about a suspected case of melioidosis. After the hospital transferred the isolate to the Arkansas DoH, *B. pseudomallei* was ruled out by using biochemical and PCR testing. The isolate was presumptively identified as *B. thailandensis* by using the Bruker MALDI Biotyper mass spectrometer (Bruker Daltonics, Billerica, MA, USA). Arkansas DoH forwarded the isolate, designated BtAR2017, to CDC for confirmation and further characterization. The patient was discharged with 6 weeks of intravenous ceftazidime treatment. She last saw her healthcare provider in December 2017 and was reported completely healed.

The Study

Biochemical testing, including arabinose assimilation, identified isolate BtAR2017 as *B. thailandensis*. We extracted DNA from the isolate for next-generation sequencing (online Technical Appendix, https://wwwnc.cdc.gov/EID/article/24/11/18-0821-Techapp1.pdf). We analyzed the genome of BtAR2017 for multilocus sequence typing (MLST), which yielded sequence type (ST) 101. ST101 was previously identified in *B. thailandensis* isolates TXDOH and H0587 (*9*). Although MLST is commonly used to subtype members of the *B. pseudomallei* complex, it has only a moderate level of resolution and, because of recombination, might not reflect actual levels of relatedness (*5,13*).

For high-resolution analysis, we compared the genome of BtAR2017 with a reference panel of publicly available *B. thailandensis* genomes (Table). A dendrogram based on the SNP analysis indicates that BtAR2017 clusters with H0587 and TXDOH (Figure). Also within the BtAR2017 cluster is E555, an environmental isolate recovered in Cambodia in 2005, and strain 2.1, which metadata in the National Center for Biotechnology Information entry indicate was recovered in June 2017 from soil in Vietnam (*14*). This cluster appears as an outlier subgroup compared with other examples of *B. thailandensis,* including E264^T (type strain). MLST indicates that E555 is ST696, which is a single-locus variant of ST101. Comparison of the genome sequences indicates >4,700 core SNPs between BtAR2017 and E555, compared with >32,700 SNPs between BtAR2017 and E264^T. BtAR2017 has >2,200 SNPs compared with H0587 but >5,900 SNPs compared with TXDOH.

Sim et al. (*14*) previously noted this outlier subgroup and postulated that its members, including E555, might be more virulent than typical examples of *B. thailandensis*. However, their studies challenging BALB/c mice and the nematode *Caenorhabditis elegans* with E555 did not reveal any significant difference in virulence compared with E264^T (*14*). Another study by Deshazer using TXDOH and H0587 to challenge mice and hamsters indicated that in these models TXDOH also had a similar level of virulence as E264^T, whereas H0587 was avirulent (*15*). E555 is known to have features such as a *B. pseudomallei*–like capsular polysaccharide (*14*). We tested BtAR2017 for *B. pseudomallei* capsular polysaccharide, but results were negative.

We analyzed average nucleotide identity (ANI) and determined that the genome for BtAR2017 has 98.99% identity with that of E264^T, which is above the 95% threshold commonly used for distinguishing species. The BtAR2017 genome also had an ANI of 99.75% compared with TXDOH but only 92.7% compared with K96243, a representative *B. pseudomallei* strain used in lieu of the species type strain. Although BtAR2017 is in the outlier subgroup resolved by genomic SNP analysis, these ANI results suggest that BtAR2017 and other members of the subgroup are *B. thailandensis* and not a novel species.

Conclusions

The recovery of the clinical isolates suggests that *B. thailandensis* might be endemic to the continental United States

Table. Reference *Burkholderia* spp. genomes used for characterization of *Burkholderia thailandensis* isolated from an infected wound, Arkansas, USA, 2017*

Isolate	Other identifiers	Origin	Source	ST†	GenBank accession nos.	ANI	SNP
82172	34; 2002721621	France	Horse (foal)	73	NZ_LNNG00000000		X
Bt4	49639	Australia	Environmental	699	NZ_ABBH00000000		X
E1		Papua New Guinea	Environmental	669	NZ_LOXF00000000		X
E254		Thailand	Environmental	345	NZ_CP004381.1; NZ_CP004382.1		X
E264	ATCC 700388	Thailand	Environmental	80	CP008785.1; CP008786.1	X	X
E444		Thailand	Environmental	79	NZ_CP004117.1; NZ_CP004118.1		X
E555		Cambodia	Environmental	696	NZ_AECN00000000		X
H0587	BtCDC2721121; 2002721121	USA (Louisiana)	Human	101	NZ_CP013409.1; NZ_CP013410.1		X
K96243		Thailand	Human	10	NC_006350.1; NC_006351.1	X	
MSMB59	MSMB0059	Australia	Environmental	699	NZ_CP004385.1; NZ_CP004386.1		X
MSMB60	MSMB0060	Australia	Environmental	699	NZ_LOXG00000000		X
Phuket 4W-1		Thailand	Environmental	80	NZ_AQQJ01000000		X
Strain 2.1		Vietnam	Environmental	696	PHRD00000000		X
TXDOH	CDC3015869; 2003015869	USA (Texas)	Human	101	NZ_CP013360.1; NZ_CP013361.1	X	X
USAMRU Malaysia no. 20	Malaysia #20; 2002721744	Malaysia	Unknown	80	NZ_CP004383.1; NZ_CP004384.1		X

*X indicates inclusion in analysis. ANI, average nucleotide identity; SNP, single nucleotide polymorphism; ST, sequence type.
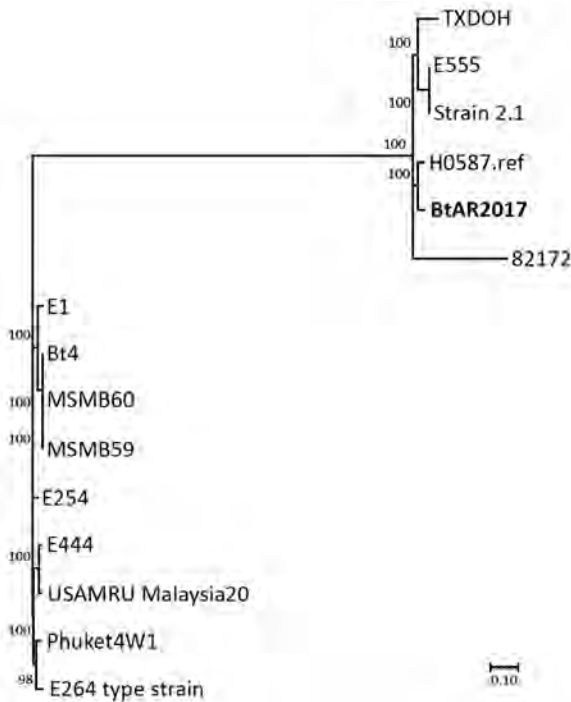†By multilocus sequence typing.

Figure. Dendrogram used for characterization of *Burkholderia thailandensis* isolate (bold) from an infected wound, Arkansas, USA, 2017; compared with reference isolates. Generated in MEGA 7.0 software (http://www.megasoftware.net) from results of maximum-parsimony phylogenetic analysis of core single-nucleotide polymorphisms from available *B. thailandensis* genomes (conducted by using Parsnp, a component of the Harvest 1.3 software suite [https://github.com/marbl/harvest]). Scale bar indicates number of substitutions per SNP.

and capable of causing opportunistic infections associated with traumatic injuries. Because of the limited number of reports, this bacterium's geographic range in North America is unknown. Two of the 3 clinical isolates recovered in the United States are now well documented and were acquired in the southern states of Texas and Arkansas, possibly reflecting the affinity for warm climates associated with most members of the *B. pseudomallei* complex (the exception being *B. mallei*, which is host-adapted to equids and does not persist in the environment). These 3 clinical isolates also are members of the outlier subgroup on the dendrogram (Figure), which suggests a genetic bottleneck or discrete seeding event for the United States, assuming the Louisiana case was acquired locally. Further study of *B. thailandensis* will improve our knowledge of its geographic range and ability to cause infections.

About the Author

Dr. Gee is a research biologist in the Bacterial Special Pathogens Branch, Division of High-Consequence Pathogens and Pathology, National Center for Emerging and Zoonotic Infectious Diseases, Centers for Disease Control and Prevention. His primary research interest is molecular epidemiology of members of the *B. pseudomallei* complex and other emerging bacterial pathogens.

References

1. Tuanyok A, Mayo M, Scholz H, Hall CM, Allender CJ, Kaestli M, et al. *Burkholderia humptydooensis* sp. nov., a new species related to *Burkholderia thailandensis* and the fifth member of the *Burkholderia pseudomallei* complex. Appl Environ Microbiol. 2017;83:e02802-16. http://dx.doi.org/10.1128/AEM.02802-16
2. Wiersinga WJ, Virk HS, Torres AG, Currie BJ, Peacock SJ, Dance DAB, et al. Melioidosis. Nat Rev Dis Primers. 2018;4:17107. http://dx.doi.org/10.1038/nrdp.2017.107
3. Brett PJ, DeShazer D, Woods DE. *Burkholderia thailandensis* sp. nov., a *Burkholderia pseudomallei*–like species. Int J Syst Bacteriol. 1998;48:317–20. http://dx.doi.org/10.1099/00207713-48-1-317
4. Levy A, Merritt AJ, Aravena-Roman M, Hodge MM, Inglis TJ. Expanded range of *Burkholderia* species in Australia. Am J Trop Med Hyg. 2008;78:599–604.
5. Pearson T, Giffard P, Beckstrom-Sternberg S, Auerbach R, Hornstra H, Tuanyok A, et al. Phylogeographic reconstruction of a bacterial species with high levels of lateral gene transfer. BMC Biol. 2009;7:78. http://dx.doi.org/10.1186/1741-7007-7-78
6. Ginther JL, Mayo M, Warrington SD, Kaestli M, Mullins T, Wagner DM, et al. Identification of *Burkholderia pseudomallei* near-neighbor species in the Northern Territory of Australia. PLoS Negl Trop Dis. 2015;9:e0003892. http://dx.doi.org/10.1371/journal.pntd.0003892
7. Hoffmaster AR, AuCoin D, Baccam P, Baggett HC, Baird R, Bhengsri S, et al. Melioidosis diagnostic workshop, 2013. Emerg Infect Dis. 2015;21.
8. Lertpatanasuwan N, Sermsri K, Petkaseam A, Trakulsomboon S, Thamlikitkul V, Suputtamongkol Y. Arabinose-positive *Burkholderia pseudomallei* infection in humans: case report. Clin Infect Dis. 1999;28:927–8. http://dx.doi.org/10.1086/517253
9. Glass MB, Gee JE, Steigerwalt AG, Cavuoti D, Barton T, Hardy RD, et al. Pneumonia and septicemia caused by *Burkholderia thailandensis* in the United States. J Clin Microbiol. 2006;44:4601–4. http://dx.doi.org/10.1128/JCM.01585-06
10. Zueter AM, Abumarzouq M, Yusof MI, Wan Ismail WF, Harun A. Osteoarticular and soft-tissue melioidosis in Malaysia: clinical characteristics and molecular typing of the causative agent. J Infect Dev Ctries. 2017;11:28–33. http://dx.doi.org/10.3855/jidc.7612
11. Chang K, Luo J, Xu H, Li M, Zhang F, Li J, et al. Human infection with *Burkholderia thailandensis*, China, 2013. Emerg Infect Dis. 2017;23:1416–8. http://dx.doi.org/10.3201/eid2308.170048
12. Dance DAB, Sarovich D, Price EP, Limmathurotsakul D, Currie BJ. Human Infection with *Burkholderia thailandensis*, China, 2013. Emerg Infect Dis. 2018;24:953–4. http://dx.doi.org/10.3201/eid2405.180238

13. Gee JE, Gulvik CA, Elrod MG, Batra D, Rowe LA, Sheth M, et al. Phylogeography of *Burkholderia pseudomallei* isolates, Western Hemisphere. Emerg Infect Dis. 2017;23:1133–8. http://dx.doi.org/10.3201/eid2307.161978

14. Sim BM, Chantratita N, Ooi WF, Nandi T, Tewhey R, Wuthiekanun V, et al. Genomic acquisition of a capsular polysaccharide virulence cluster by non-pathogenic *Burkholderia* isolates. Genome Biol. 2010;11:R89. http://dx.doi.org/10.1186/gb-2010-11-8-r89

15. DeShazer D. Virulence of clinical and environmental isolates of *Burkholderia oklahomensis* and *Burkholderia thailandensis* in hamsters and mice. FEMS Microbiol Lett. 2007;277:64–9. http://dx.doi.org/10.1111/j.1574-6968.2007.00946.x

Address for correspondence: Jay E. Gee, Centers for Disease Control and Prevention, 1600 Clifton Rd NE, Mailstop G34, Atlanta, GA 30329-4027, USA; email: xzg4@cdc.gov
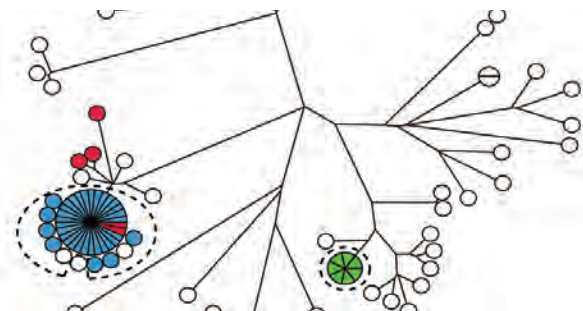
October 2017: **Bacterial Infections**

EMERGING INFECTIOUS DISEASES

Timing the Origin of *Cryptococcus gattii* sensu stricto, Southeastern United States

**Shawn R. Lockhart, Chandler C. Roe,
David M. Engelthaler**

We conducted molecular clock analysis of whole-genome sequences from a set of autochthonous isolates of *Cryptococcus gattii* sensu stricto from the southeastern United States. Our analysis indicates that *C. gattii* arrived in the southeastern United States approximately 9,000–19,000 years ago, long before its arrival in the Pacific Northwest.

The *Cryptococcus gattii* species complex consists of ≥4 major subtypes (VGI–VGIV), which are now considered to be different species (*1*). *C. gattii* species complex is often described as native to tropical and subtropical regions, but recent reports have shown that it is more cosmopolitan than previously thought (*2*). In North America, the emergence of *C. deuterogattii* (VGII) in the Pacific Northwest of Canada and the United States generated a great deal of interest in the study of *C. gattii* species complex in this area (*3*). Although this emergence was the impetus for the study of *C. gattii* species complex in the United States, this pathogen has actually been known and documented in the United States for multiple decades, especially in southern California (*4*). Despite its occurrence in the Pacific Southwest, the emergence in the Pacific Northwest is thought to be quite recent. Recent work using Bayesian evolutionary analysis by sampling trees generated using BEAST software showed that the emergence of *C. deuterogattii* in the Pacific Northwest was a recent event, occurring within the last 60–100 years (*5*).

Historical reports have described the presence of *C. gattii* species complex in the southeastern United States, where documented clinical cases are rare. However, these cases are often unacknowledged by literature reviews because they occurred when *C. gattii* could only be detected as a unique serotype of *C. neoformans*, before it became known as a separate species (*6*). Although published reports have been rare, recent *C. gattii* cases have been reported in the southeastern United States (*7–9*). We recently described the population structure of 10 *C. gattii* sensu stricto (VGI) patient isolates from the southeastern United States (*6*). Here we describe

Author affiliations: Centers for Disease Control and Prevention, Atlanta, Georgia, USA (S.R. Lockhart); Northern Arizona University, Flagstaff, Arizona, USA (C.C. Roe); Translational Genomics Research Institute, Flagstaff (D.M. Engelthaler)

selecting 8 of those same isolates and using BEAST software (http://beast.community) to predict the timing of the emergence of *C. gattii* in the southeastern United States.

The Study

We identified single-nucleotide polymorphisms (SNPs) and conducted phylogenetic analyses as previously described (*10*). We identified 43,731 total SNPs among 8 isolates, based on a genome quality breadth of 16,991,136 bases. The maximum-likelihood tree (Figure) had a consistency index of 1.0, and all branching bootstrap values equaled 100 for 100 replicates. Because all isolates in the southeastern United States group contain only the α mating type and the phylogenies have a perfect consistency index (i.e., demonstrating no homoplasy), we assume a clonal expansion for this population (i.e., lack of multiple mating types limits opportunity for recombination), although cryptic recombination cannot be ruled out. We therefore applied the clonal mutation rate obtained from the prior Bayesian molecular clock analysis (using BEAST software [*10*]) of the Pacific Northwest *C. gattii* species complex, specifically for VGIIa and VGIIc (1.59×10^{-8} SNPs/base/y). We determined the best-fitting clock and demographic model combination by implementing path and stepping stone sampling marginal-likelihood estimators as described previously (*5*). We implemented a general time-reversible nucleotide substitution model and an uncorrelated log-normal molecular clock with a Bayesian skyline model across 4 chains with 3 billion iterations and achieved across- and within-chain convergence.

Employing these previously described methods with a log-normal Bayesian skyline model on the genomes from the 8 isolates from the southeastern United States, BEAST provided an estimated range of time to most recent common ancestor (tMRCA) of approximately 9,000–19,000 years. A general recombining population mutation rate for *Cryptococcus* was previously estimated at 2.0×10^{-9} (*11*), which is an order of magnitude slower than the estimated clonal rate; therefore, applying this rate provides for a tMRCA that is nearly an order of magnitude greater (77,000–148,000 years).

Conclusions

The clonal mutation rate appears to be more appropriate than the general mutation rate for recombining populations for estimating tMRCA, showing that the timing of *C. gattii* emergence and subsequent divergence in the southeastern United States is clearly much older than the Pacific
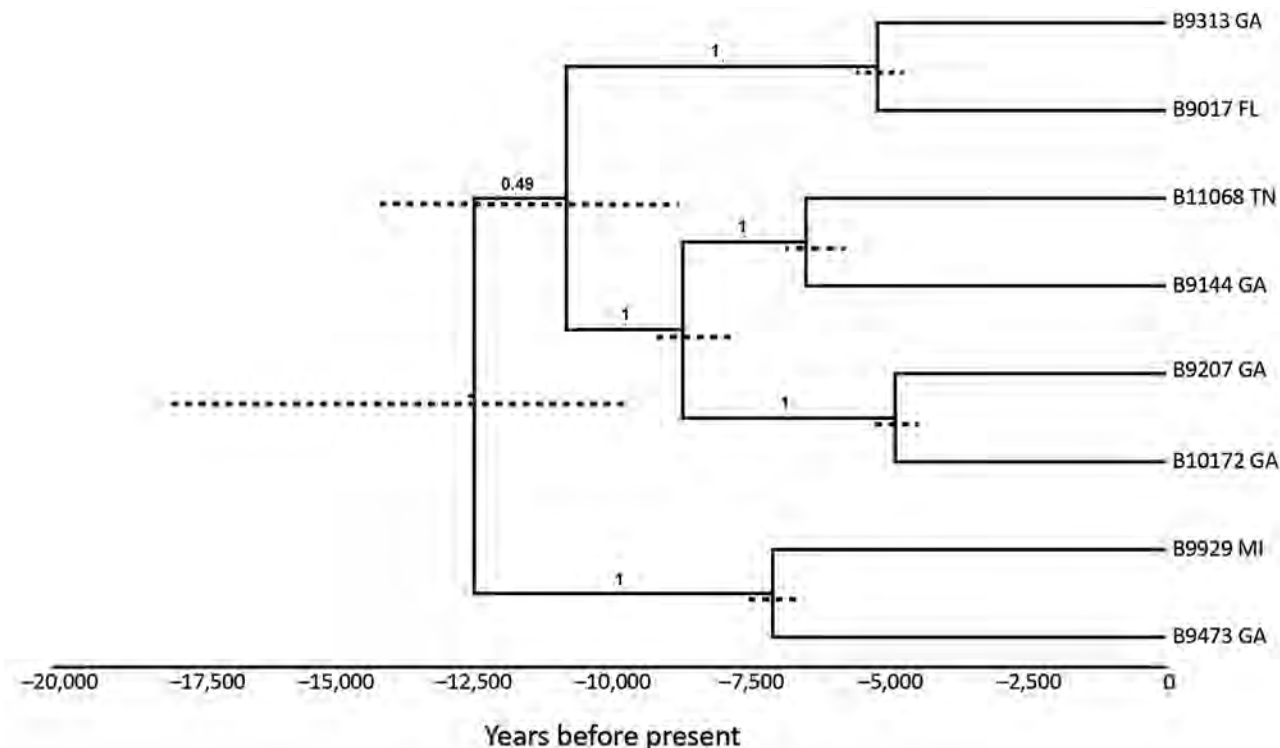
Figure. Bayesian phylogenetic analyses of 8 isolates of *Cryptococcus gattii* sensu stricto from the southeastern United States. We used BEAST 1.8.4 software (http://beast.community) to produce calibrated phylogenies with the mean estimates of time to most recent common ancestor. The tips of the branches correspond to the year of sampling. Dotted node bars are shown for each node and indicate 95% CIs for the timing estimate. The timeline represents years before the present day.

Northwest emergence. The sharp contrast in the time of arrival compared with *C. deuterogattii* in the Pacific Northwest is considerable. Although *C. gattii* has apparently been in the southeastern United States for thousands more years than *C. deuterogattii* has been in the Pacific Northwest, the number of cases detected in the southeastern United States is far fewer. Infections in the South are probably not regularly missed, given that *C. gattii* in the southeastern United States causes primarily a devastating meningitis or meningoencephalitis (*6,9*). Questions of whether subacute cases might be going undetected, whether the distribution of the fungus in the environment might be lower, or whether the niche is not readily accessible by humans remain unanswered. We clearly know less about the *Cryptococcus* species that has been in the United States for thousands of years (*C. gattii* sensu stricto) than we know about the one that has only recently arrived (*C. deuterogattii*).

The Pacific Northwest emergence has been hypothesized to be related to the opening of the Panama Canal, enabling more shipping from eastern ports of South America to the West Coast of North America (*5*). The estimated timing of emergence of *C. gattii* in the southeastern United States occurred long before industrial shipping. Although humans might have populated the southeastern United States by the time of the dispersal, most of the human movement was north to south rather than the reverse (*12*). This relatively recent emergence during the Pleistocene epoch is different from what has been hypothesized for other endemic mycoses, a much older fungal species dispersal resulting from mass migration of animal populations between continents (*13*). The idea of recent emergence also departs sharply from what has been hypothesized as a speciation attributable to prehistoric land movements, as has been proposed for larger *Cryptococcus* species separations (*14*). *C. gattii* sensu stricto has been found in and likely originates from South American locales (*15*). Besides anthropogenic means, possible dispersal mechanisms out of South America might have included animal, bird, or insect species migration or even ocean detritus brought by Caribbean currents or hurricanes. However, given the lack of population structure, dispersal probably occurred through a discrete event or through limited events from the same originating population. No matter the mechanism of arrival, *C. gattii* has been hiding, mostly undetected, in the southeastern United States for millennia.

About the Author

Dr. Lockhart is director of the Fungal Reference Laboratory, Mycotic Diseases Branch, Division of Foodborne, Waterborne, and Environmental Diseases, National Center for Emerging and

Zoonotic Infectious Diseases, Centers for Disease Control and Prevention. His research interests include antifungal resistance and fungal population structure.

References

1. Hagen F, Khayhan K, Theelen B, Kolecka A, Polacheck I, Sionov E, et al. Recognition of seven species in the *Cryptococcus gattii/Cryptococcus neoformans* species complex. Fungal Genet Biol. 2015;78:16–48. http://dx.doi.org/10.1016/j.fgb.2015.02.009
2. Springer DJ, Phadke S, Billmyre B, Heitman J. *Cryptococcus gattii*, no longer an accidental pathogen? Curr Fungal Infect Rep. 2012;6:245–56. http://dx.doi.org/10.1007/s12281-012-0111-0
3. Fraser JA, Subaran RL, Nichols CB, Heitman J. Recapitulation of the sexual cycle of the primary fungal pathogen *Cryptococcus neoformans* var. *gattii*: implications for an outbreak on Vancouver Island, Canada. Eukaryot Cell. 2003;2:1036–45. http://dx.doi.org/10.1128/EC.2.5.1036-1045.2003
4. Bennett JE, Kwon-Chung KJ, Howard DH. Epidemiologic differences among serotypes of *Cryptococcus neoformans*. Am J Epidemiol. 1977;105:582–6. http://dx.doi.org/10.1093/oxfordjournals.aje.a112423
5. Roe CC, Bowers J, Oltean H, DeBess E, Dufresne PJ, McBurney S, et al. Dating the *Cryptococcus gattii* dispersal to the North American Pacific Northwest. mSphere. 2018;3:e00499–17.
6. Lockhart SR, Roe CC, Engelthaler DM. Whole-genome analysis of *Cryptococcus gattii*, southeastern United States. Emerg Infect Dis. 2016;22:1098–101. http://dx.doi.org/10.3201/eid2206.151455
7. Sellers B, Hall P, Cine-Gowdie S, Hays AL, Patel K, Lockhart SR, et al. *Cryptococcus gattii*: an emerging fungal pathogen in the southeastern United States. Am J Med Sci. 2012;343:510–1. http://dx.doi.org/10.1097/MAJ.0b013e3182464bc7
8. Kunadharaju R, Choe U, Harris JR, Lockhart SR, Greene JN. *Cryptococcus gattii*, Florida, USA, 2011. Emerg Infect Dis. 2013;19:519–21. http://dx.doi.org/10.3201/eid1903.121399
9. Franco-Paredes C, Womack T, Bohlmeyer T, Sellers B, Hays A, Patel K, et al. Management of *Cryptococcus gattii* meningoencephalitis. Lancet Infect Dis. 2015;15:348–55. http://dx.doi.org/10.1016/S1473-3099(14)70945-4
10. Drummond AJ, Suchard MA, Xie D, Rambaut A. Bayesian phylogenetics with BEAUti and the BEAST 1.7. Mol Biol Evol. 2012;29:1969–73. http://dx.doi.org/10.1093/molbev/mss075
11. Sharpton TJ, Neafsey DE, Galagan JE, Taylor JW. Mechanisms of intron gain and loss in *Cryptococcus*. Genome Biol. 2008;9:R24. http://dx.doi.org/10.1186/gb-2008-9-1-r24
12. Fisher MC, Koenig GL, White TJ, San-Blas G, Negroni R, Alvarez IG, et al. Biogeographic range expansion into South America by *Coccidioides immitis* mirrors New World patterns of human migration. Proc Natl Acad Sci U S A. 2001;98:4558–62. http://dx.doi.org/10.1073/pnas.071406098
13. Engelthaler DM, Roe CC, Hepp CM, Teixeira M, Driebe EM, Schupp JM, et al. Local population structure and patterns of Western Hemisphere dispersal for *Coccidioides* spp., the fungal cause of valley fever. MBio. 2016;7:e00550–16. http://dx.doi.org/10.1128/mBio.00550-16
14. Casadevall A, Freij JB, Hann-Soden C, Taylor J. Continental drift and speciation of the *Cryptococcus neoformans* and *Cryptococcus gattii* species complexes. mSphere. 2017;2:e00103–17.
15. Hagen F, Ceresini PC, Polacheck I, Ma H, van Nieuwerburgh F, Gabaldón T, et al. Ancient dispersal of the human fungal pathogen *Cryptococcus gattii* from the Amazon rainforest. PLoS One. 2013;8:e71148. http://dx.doi.org/10.1371/journal.pone.0071148

Address for correspondence: Shawn R. Lockhart, Centers for Disease Control and Prevention, 1600 Clifton Rd NE, Mailstop G-11, Atlanta, GA 30329-4027, USA; email: gyi2@cdc.gov

February 2017: Fungal Infections

- Delivering on Antimicrobial Resistance Agenda Not Possible without Improving Fungal Diagnostic Capabilities
- Changing Epidemiology of Human Brucellosis, China, 1955–2014
- Multidrug-Resistant *Candida haemulonii* and *C. auris*, Tel Aviv, Israel
- Detection of Multiple Parallel Transmission Outbreak of *Streptococcus suis* Human Infection by Use of Genome Epidemiology, China, 2005
- Correlation of West Nile Virus Incidence in Donated Blood with West Nile Neuroinvasive Disease Rates, United States, 2010–2012
- Highly Pathogenic Influenza A(H5Nx) Viruses with Altered H5 Receptor-Binding Specificity
- Livestock Susceptibility to Infection with Middle East Respiratory Syndrome Coronavirus

- Swine Influenza Virus (H1N2) Characterization and Transmission in Ferrets, Chile
- Spread and Evolution of Respiratory Syncytial Virus A, Genotype ON1, Coastal Kenya 2010–2015
- Genetic Diversity and New Lineages of Dengue Virus Serotypes 3 and 4 in Returning Travelers, Germany, 2006–2015
- Changing Epidemiology of Hepatitis A and Hepatitis E Viruses in China, 1990–2014
- Fatal Infection with Murray Valley Encephalitis Virus Imported from Australia to Canada, 2011
- Oral Transmission of L-Type Bovine Spongiform Encephalopathy Agent among Cattle

https://wwwnc.cdc.gov/eid/articles/issue/23/2/table-of-contents

EMERGING INFECTIOUS DISEASES

Hospitalizations for Influenza-Associated Severe Acute Respiratory Infection, Beijing, China, 2014–2016

Yi Zhang, David J. Muscatello, Quanyi Wang,
Peng Yang, Yang Pan, Da Huo, Zhongcheng Liu,
Xiaojuan Zhao, Yaqing Tang, Chao Li,
Abrar A. Chughtai, C. Raina MacIntyre

We analyzed surveillance data for 2 sentinel hospitals to estimate the influenza-associated severe acute respiratory infection hospitalization rate in Beijing, China. The rate was 39 and 37 per 100,000 persons during the 2014–15 and 2015–16 influenza seasons, respectively. Rates were highest for children <5 years of age.

Influenza virus circulates worldwide, causing substantial rates of illness and death (*1*). In recent years, better estimates of influenza have been possible in low- and middle-income countries because of the development of surveillance systems (*2,3*).

Beijing is located in northern China in a temperate climate zone. Previous studies used surveillance to estimate the incidence of seasonal influenza infections in Beijing (*4*). However, hospitalizations associated with influenza have not been evaluated. We aimed to estimate the influenza-associated severe acute respiratory infection (SARI) hospitalization using the methods recommended by the World Health Organization (*5*).

The Study

We introduced screening of inpatients for SARI at 2 sentinel hospitals in Beijing during October 2014–September 2016. Throat swabs were collected from all SARI patients with their verbal consent. To explore the characteristics

Author affiliations: University of New South Wales, Sydney, New South Wales, Australia (Y. Zhang, D.J. Muscatello, A.A. Chughtai, C.R. MacIntyre); Beijing Municipal Centre for Disease Prevention and Control, Dongcheng District, Beijing, China (Y. Zhang, Q. Wang, P. Yang, Y. Pan, D. Huo); Beijing Research Center for Preventive Medicine, Beijing (Y. Zhang, Q. Wang, P. Yang, Y. Pan, D. Huo); Chang Ping Centre for Disease Prevention and Control, Changping District, Beijing (Z. Liu, Y. Tang); Huai Rou Centre for Disease Prevention and Control, Huairou District, Beijing (X. Zhao, C. Li); Arizona State University, Phoenix, Arizona, USA (C.R. MacIntyre)

of severe influenza infections, we investigated the demographic characteristics and clinical courses of SARI patients (online Technical Appendix, https://wwwnc.cdc.gov/EID/article/24/12/17-1410-Techapp1.pdf).

We estimated the rate of influenza-associated SARI hospitalizations using WHO-recommended methods (*5*). First, we defined the catchment area of the 2 hospitals. We acquired home address (village or town) of all inpatients hospitalized in 2015 from the hospital discharge registry. Villages and towns from which most (≥80%) SARI patients came were defined as the catchment area. We restricted the number of SARI and hospitalized patients to patients residing in the catchment area. Second, we estimated the number of laboratory-confirmed influenza cases among SARI patients residing in the catchment area, adjusting pro rata for the proportion of SARI patients from whom specimens were obtained and tested by age group. Third, we estimated the catchment population size by 5 age groups (<5 years, 5–14 years, 15–24 years, 25–59 years, and ≥60 years). Catchment populations were obtained from local population statistics (*6,7*). Next, we obtained the age group–specific annual number of patients with physician-diagnosed pneumonia served by each of the hospitals in the catchment area by examining hospital discharge registers. We adjusted catchment population size pro rata for the proportion of pneumonia patients served by the sentinel site. The rate of influenza-associated SARI hospitalization was estimated as follows: ([number of laboratory-confirmed influenza SARI patients in catchment area ÷ proportion swabbed] ÷ [population size of catchment area × proportion of pneumonia patients served by the sentinel site]) × 100,000.

During the study period, 14,523 persons were hospitalized in the 2 sentinel hospitals, including 4,097 SARI patients. Eight towns were identified as catchment areas of the 2 hospitals (Figures 1, 2). Of the 4,097 SARI patients, 3,899 (95.2%) resided in catchment areas and were enrolled. Swabs were collected from 3,130 (80.3%) SARI patients. Of these, 520 tested positive for influenza, resulting in a laboratory-confirmed influenza-positive proportion of 16.6%. Adjusting pro rata, the number of laboratory-confirmed influenza infections was 648 of 3,899 total SARI patients. The 2 hospitals served 93.2% of pneumonia patients in their

Figure 1. Geographic distribution of sentinel hospitals and catchment areas for surveillance of severe acute respiratory infection, Beijing, China, 2014–2016. CP, Chang Ping; CY, Chao Yang; DC, Dong Cheng; DX, Da Xing; FS, Fang Shan; FT, Feng Tai; HD, Hai Dian; HR, Huai Rou; MTG, Men Tou Gong; MY, Mi Yun; PG, Ping Gu; SJS, Shi Jing Shan; SY, Shun Yi; TZ, Tong Zhou; XC, Xi Cheng; YQ, Yan Qing.

catchment areas. Adjusting pro rata for this proportion provides a total catchment population of 842,895. Overall, the influenza-confirmed SARI hospitalization rate was 39 (95% CI 35–44) per 100,000 population during the 2014–15 influenza season and 37 (95% CI 33–41) per 100,000 population during the 2015–16 influenza season. The influenza A–

Figure 2. Number of total (N = 3130) and influenza-confirmed (n = 520) SARI patients from 2 sentinel hospitals combined, Beijing, China, week 40, 2014–week 39, 2016. SARI, sudden acute respiratory infection.

Table 1. Rates of influenza-associated severe acute respiratory infection hospitalizations, Beijing, China

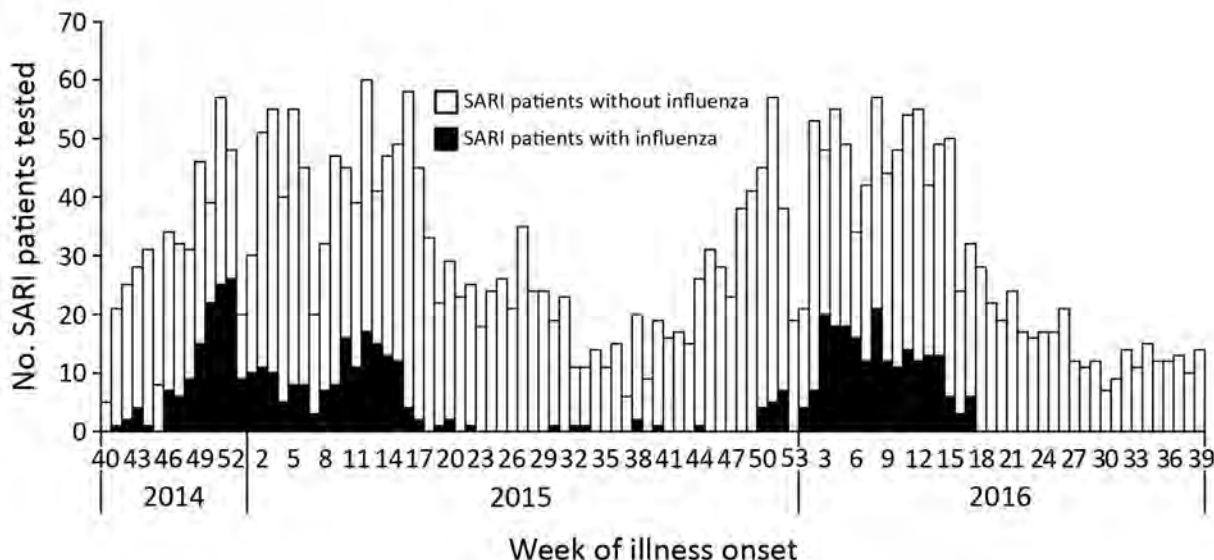|	Cases/100,000 population (95% CI).					
	2014–15 influenza season			2015–16 influenza season		
Age group, y	Influenza A	Influenza B	All influenza	Influenza A	Influenza B	All influenza
<5	223 (176–278)	109 (77–149)	335 (277–401)	286 (233–348)	243 (194–301)	529 (456–611)
5–14	58 (41–80)	61 (43–84)	119 (94–150)	26 (15–42)	72 (53–97)	98 (75–126)
15–24	2 (1–5)	0 (0–3)	2 (1–6)	0	0	0
25–59	5 (3–8)	4 (3–7)	10 (7–13)	3 (2–6)	1 (0–3)	4 (3–7)
≥60	69 (52–88)	38 (26–53)	105 (85–129)	56 (41–74)	10 (5–20)	66 (50–86)
Overall	24 (21–28)	15 (13–18)	39 (35–44)	21 (18–24)	16 (14–19)	37 (33–41)

confirmed SARI hospitalization rate was 24 (95% CI 21–28) per 100,000 population during the 2014–15 influenza season and 21 (95% CI 18–24) per 100,000 population during the 2015–16 influenza season; the influenza B–confirmed SARI hospitalization rate was 15 (95% CI 13–18) per 100,000 population during the 2014–15 influenza season and 16 (95% CI 14–19) per 100,000 population during the 2015–16 influenza season. In both seasons, the rate of influenza-associated SARI was highest for children <5 years of age: 335 (95% CI 277–401) hospitalizations per 100,000 population in the 2014–15 season and 529 (95%

CI 456–611) hospitalizations per 100,000 population in the 2015–16 season. The rate was lowest in the 25–59-year age group: 2 (95% CI 1–6) hospitalizations per 100,000 population in the 2014–15 season and <1 hospitalization per 100,000 population in the 2015–16 season (Tables 1, 2; online Technical Appendix).

Conclusions

In Beijing, influenza accounted for 16.6% of SARI in the 2 years studied; the hospitalization rate for all ages was 38–39 per 100,000 persons. This finding was much lower than

Table 2. Outcomes of SARI patients with and without laboratory-confirmed influenza, Beijing, China, week 40, 2014–week 39, 2016*

Characteristic	All SARI patients, n = 2,212	SARI patients without confirmed influenza, n = 1,759	SARI patients with confirmed influenza, n = 453	p value†
Sex				
M	1,298 (58.7)	1,030 (58.6)	268 (59.2)	0.816
F	914 (41.3)	729 (41.4)	185 (40.8)	
Age group, y				
0–4	973 (44.0)	778 (44.2)	195 (43.1)	<0.001
5–14	368 (16.6)	260 (14.8)	108 (23.8)	
15–24	40 (1.8)	35 (2.0)	5 (1.1)	
25–59	284 (12.8)	235 (13.4)	49 (10.8)	
≥60	547 (24.7)	451 (25.6)	96 (21.2)	
Underlying medical condition				
≥1‡	548 (24.8)	450 (25.6)	98 (21.6)	0.083
Pulmonary diseases§	224 (10.1)	175 (10.0)	49 (10.8)	0.585
Cardiovascular diseases	380 (17.2)	321 (18.3)	59 (13.0)	0.009
Metabolic diseases¶	71 (3.2)	61 (3.5)	10 (2.2)	0.175
Renal dysfunction	22 (1.0)	19 (1.1)	3 (0.7)	0.424
Hepatic dysfunction	10 (0.5)	10 (0.6)	0 (0.0)	0.108
Tumor	31 (1.4)	27 (1.5)	4 (0.9)	0.292
Immune system diseases	1 (0.1)	1 (0.1)	0 (0.0)	0.612
Received influenza vaccine within 1 y	121 (5.5)	90 (5.1)	31 (6.8)	0.15
Treatment				
Antiviral drugs	30 (1.4)	14 (0.8)	16 (3.5)	<0.001
Antibacterial drugs	2,171 (98.2)	1,722 (97.9)	449 (99.1)	0.086
Corticosteroids	214 (9.7)	154 (8.8)	60 (13.3)	0.004
Oxygen therapy	589 (26.6)	492 (28.0)	97 (21.4)	0.005
Mechanical ventilation	12 (0.5)	8 (0.5)	4 (0.9)	0.428
Complication	510 (23.1)	415 (23.6)	95 (21.0)	0.237
Pneumonia	389 (17.6)	321 (18.3)	68 (15.0)	0.106
Median length of hospital stay, d (IQR)	8.8 (8.6–9.0)	9.0 (8.7–9.3)	8.0 (7.5–8.4)	<0.001
Admission to ICU	28 (1.3)	20 (1.1)	8 (1.8)	0.286
Died	9 (0.4)	8 (0.5)	1 (0.2)	0.485

*Values are no. (%) unless otherwise indicated. The weeks range from 2014 Sep 29 through 2016 Oct 2. ICU, intensive care unit; IQR, interquartile range; SARI, severe acute respiratory infection.
†Calculated by χ^2 test.
‡Defined as any inpatient stays with admission diagnosis in any of the following diseases, symptoms, or signs: pulmonary disease, cardiovascular disease, chronic metabolic disease, renal dysfunction, hepatic diseases, or tumor.
§Asthma, chronic obstructive pulmonary disease, emphysema, chronic bronchitis.
¶Diabetes, dyslipidemia.

that reported for Jingzhou, a city in central China, in which estimates ranged from 115 to 142 per 100,000 population in the 2010–12 influenza season (*8*). Although a similar method was used in these 2 studies, they had several differences. First, they estimated the hospitalization rate among different influenza seasons with different influenza activity and circulating strains. Second, the influenza circulation patterns differed (*9*); Beijing had 1 winter peak, whereas Jingzhou had an additional peak in summer. Moreover, the SARI definition used differed between the studies, with a lower fever threshold of ≥37.3°C in their study. As in other studies of age-specific influenza-associated SARI or hospitalization from other regions (*3,10,11*), we observed the most severe influenza disease in young children (<5 years). This finding underscores a need to consider influenza vaccination programs directed toward young children.

Although influenza B is often considered less severe than influenza A (*12*), 40.7% of influenza-confirmed SARI patients were influenza B–positive in this study, suggesting influenza B makes up an important component of overall influenza severity. Among the outpatient influenza infections in Beijing, 42.4% were influenza B during our study period, similar to the proportion in SARI patients (41.5%). These results suggest that influenza B is equally as responsible for mild and severe respiratory infections as influenza A.

Our study has some limitations. First, the results have limited generalizability because estimation was based on only 2 hospitals. However, 5 of the other sentinel hospitals are in the business district and serve populations of numerous districts and non-Beijing residents, making the catchment population difficult to estimate. We excluded the remaining 3 suburban sentinel hospitals because they did not have pediatric wards enrolled in SARI surveillance or the quality of their surveillance database was uncertain. Second, 19.7% of SARI patients in our study were not swabbed. We assumed the proportion of influenza-positive among them was the same as among swabbed SARI patients. However, according to clinician descriptions, most of these patients were children <5 years of age. Because the proportion of influenza-positive patients is higher among young children, we might have underestimated overall influenza-associated SARI. Third, because older adults often have complicated illness and not typical SARI symptoms, SARI might be underestimated among the older adult population. Fourth, surveillance covers only respiratory disease–related wards, but SARI patients might be hospitalized in other wards because of influenza complications (*13,14*), which might have led to underestimation of influenza. Finally, patients with influenza complications requiring admission might have had a relatively long delay from symptom onset to hospitalization, leading to possible false-negative laboratory results, thereby underestimating influenza.

Overall, most SARI patients in this study had influenza A, but the percentage with influenza B was also substantial. The findings of this study expanded knowledge about the impact of severe influenza and challenge the view that influenza B is a mild infection. These findings can be used to inform local policies on influenza prevention and control.

About the Author

Ms. Zhang, a PhD candidate in epidemiology in the University of New South Wales, works in the Beijing Municipal Center for Disease Prevention and Control. Her research interests focus on influenza vaccine effectiveness assessment, influenza burden estimation, and risk assessment of influenza and other respiratory infectious diseases.

References

1. World Health Organization. WHO global epidemiological surveillance standards for influenza. Jan 2014 [cited 2017 Aug 12]. http://www.who.int/influenza/resources/documents/WHO_Epidemiological_Influenza_Surveillance_Standards_2014.pdf?ua=1
2. Emukule GO, Khagayi S, McMorrow ML, Ochola R, Otieno N, Widdowson MA, et al. The burden of influenza and RSV among inpatients and outpatients in rural western Kenya, 2009–2012. PLoS One. 2014;9:e105543. http://dx.doi.org/10.1371/journal.pone.0105543
3. Nukiwa N, Burmaa A, Kamigaki T, Darmaa B, Od J, Od I, et al. Evaluating influenza disease burden during the 2008–2009 and 2009–2010 influenza seasons in Mongolia. Western Pac Surveill Response J. 2011;2:16–22. http://dx.doi.org/10.5365/wpsar.2010.1.1.004
4. Wang X, Wu S, Yang P, Li H, Chu Y, Tang Y, et al. Using a community based survey of healthcare seeking behavior to estimate the actual magnitude of influenza among adults in Beijing during 2013–2014 season. BMC Infect Dis. 2017;17:120. http://dx.doi.org/10.1186/s12879-017-2217-z
5. World Health Organization. A manual for estimating disease | burden associated with seasonal influenza [cited 2017 Aug 12]. http://www.who.int/iris/handle/10665/178801
6. Huairou Bureau of Statistics. Statistical yearbook of Huairou (2015) [cited 2018 May 31]. https://wenku.baidu.com/view/8deb29e4ed630b1c59eeb5cc.html

7. Changping Bureau of Statistics. Statistical yearbook of Changping (2016) [cited 2018 May 31]. http://www.bjchp.gov.cn/tjj/tabid/621/InfoID/397815/frtid/5909/Default.aspx

8. Yu H, Huang J, Huai Y, Guan X, Klena J, Liu S, et al. The substantial hospitalization burden of influenza in central China: surveillance for severe, acute respiratory infection, and influenza viruses, 2010–2012. Influenza Other Respi Viruses. 2014;8:53–65. http://dx.doi.org/10.1111/irv.12205

9. Yu H, Alonso WJ, Feng L, Tan Y, Shu Y, Yang W, et al. Characterization of regional influenza seasonality patterns in China and implications for vaccination strategies: spatio-temporal modeling of surveillance data. PLoS Med. 2013;10:e1001552. http://dx.doi.org/10.1371/journal.pmed.1001552

10. Sheu SM, Tsai CF, Yang HY, Pai HW, Chen SC. Comparison of age-specific hospitalization during pandemic and seasonal influenza periods from 2009 to 2012 in Taiwan: a nationwide population-based study. BMC Infect Dis. 2016;16:88. http://dx.doi.org/10.1186/s12879-016-1438-x

11. Fuller JA, Summers A, Katz MA, Lindblade KA, Njuguna H, Arvelo W, et al. Estimation of the national disease burden of influenza-associated severe acute respiratory illness in Kenya and Guatemala: a novel methodology. PLoS One. 2013;8:e56882. http://dx.doi.org/10.1371/journal.pone.0056882

12. Kim YH, Kim HS, Cho SH, Seo SH. Influenza B virus causes milder pathogenesis and weaker inflammatory responses in ferrets than influenza A virus. Viral Immunol. 2009;22:423–30. http://dx.doi.org/10.1089/vim.2009.0045

13. Ang LW, Yap J, Lee V, Chng WQ, Jaufeerally FR, Lam CSP, et al. Influenza-associated hospitalizations for cardiovascular diseases in the tropics. Am J Epidemiol. 2017;186:202–9. http://dx.doi.org/10.1093/aje/kwx001

14. Sellers SA, Hagan RS, Hayden FG, Fischer WA II. The hidden burden of influenza: a review of the extra-pulmonary complications of influenza infection. Influenza Other Respi Viruses. 2017; 11:372–93. http://dx.doi.org/10.1111/irv.12470

Address for correspondence: Quanyi Wang, Beijing Municipal Center for Disease Prevention and Control (CDC), Institute for Infectious Disease and Endemic Disease Control, No. 16 He Ping Li Middle St, Dong Cheng District, Beijing 100013, China; email: bjcdcxm@126.com

Severe Fever with Thrombocytopenia Syndrome Virus Infection, South Korea, 2010

Young Ree Kim,[1] Yeojun Yun,[1] Seung Geon Bae, Dahee Park, Suhyun Kim, Jae Myun Lee, Nam-Hyuk Cho, Yang Soo Kim, Keun Hwa Lee

Author affiliations: Jeju National University College of Medicine, Jeju, South Korea (Y.R. Kim, S.G. Bae, D. Park, S. Kim, K.H. Lee); Ewha Womans University, Seoul, South Korea (Y. Yun); Yonsei University College of Medicine, Seoul (J.M. Lee); Seoul National University College of Medicine, Seoul (N.-H. Cho); University of Ulsan College of Medicine, Seoul (Y.S. Kim).

Severe fever with thrombocytopenia syndrome (SFTS) was reported in China in 2009 and in South Korea in 2012. We found retrospective evidence of SFTS virus infection in South Korea in 2010, suggesting that infections in South Korea occurred before previously reported and were more concurrent with those in China.

Severe fever with thrombocytopenia syndrome virus (SFTSV) is a tickborne virus (genus *Phlebovirus*, family *Phenuiviridae*) that can cause hemorrhagic fever (*1,2*). Severe fever with thrombocytopenia syndrome (SFTS) was confirmed in China in 2009 (*2*) and then retrospectively reported in South Korea in 2012 and in western Japan in 2013 (*3,4*). Most SFTSV infections occur through bites from *Haemaphysalis longicornis* ticks, although transmission can also occur through close contact with an infected patient (*5–7*). We provide retrospective evidence of SFTSV infections in South Korea from 2010, confirming that infections in South Korea occurred earlier than previously reported and were more concurrent with the first reported infections in China.

For this study, we used stored serum samples from 58 patients who had high erythrocyte sedimentation rates (ESRs) and were admitted to Jeju National University Hospital in Jeju, South Korea, during July 2010; SFTS was not a criterion for selection. Jeju is a high-prevalence region for SFTS, and July is the month with the highest SFTS prevalence in South Korea. The major clinical signs and symptoms of SFTS are an acute and high fever, thrombocytopenia, leukopenia, elevated serum hepatic enzyme levels, gastrointestinal symptoms, and multiorgan failure, with a death rate of 12%–30%. However, atypical signs and symptoms of SFTS have been identified, and asymptomatic infections among humans have been reported in South Korea (*3,6,8*).

For molecular diagnosis of SFTSV, we extracted RNA from serum by using the QIAamp Viral RNA Mini Kit (QIAGEN, Hilden, Germany). We performed real-time reverse transcription PCR (RT-PCR) to amplify the partial small (S) segment of the viral RNA from the stored serum and confirm SFTSV infection (*9*). We sequenced real-time RT-PCR products using the BigDye Terminator Cycle Sequencing kit (Perkin Elmer Applied Biosystems, Warrington, UK). We conducted phylogenetic analysis of partial S segment sequences using MEGA6 (*10*) and constructed phylogenetic trees using the maximum-likelihood method (Figure).

Our results showed 2 positive results from the stored serum of 2 patients. Neither patient reported history of travel to other endemic countries, such as China or Japan.

Patient Jeju 01-South Korea-07-2010 (no. 430), a 77-year-old man, had diabetes and hypertension for 45 years. The patient had received a diagnosis of end-stage renal disease 7 years before admission and was on hemodialysis; he experienced an episode of gout 5 years before admission. The patient came to the hospital's orthopedic outpatient clinic reporting that he had pain, swelling, and febrile sensation of the right lateral malleolus area for several days. He had undergone orthopedic surgery with debridement for a wound of the right lateral malleolus area caused by an electric plate burn 1.5 years earlier. He was retired, lived in Jeju, and was admitted to the hospital for emergency orthopedic surgery. Physical examination recorded body temperature of 37.2°C, blood pressure 140/60 mm Hg, heart rate 78/min, and respiratory rate 20 breaths/min. Initial laboratory data revealed slight thrombocytopenia (199,000 platelets/mm^3), and absolute neutrophil count (ANC) was 7,374. Alkaline phosphatase (ALP), aspartate aminotransferase (AST), and alanine aminotransferase (ALT) levels were within reference ranges; however, ESR (112 mm/h), blood urea nitrogen (24.8 mg/dL), and creatinine (4.8 mg/dL) were elevated.

Patient Jeju 02-South Korea-07-2010 (no. 468), a 76-year-old woman, visited the hospital's orthopedic outpatient clinic reporting pain in both knees for 10 years. She was a housewife, lived in Jeju, and had received temporary symptom treatment from local clinics. She was admitted to the hospital for total knee replacement arthroplasty. Her only underlying disease was diabetes. Physical examination recorded body temperature of 36.8°C, blood pressure 120/60 mm Hg, heart rate 68/min, and respiratory rate 20 breaths/minute. Initial laboratory test results were within reference ranges except for urine glucose (4+); platelet count was 620,000/mm^3, ANC was 2,065, and ALP, AST, and ALT levels were within reference ranges. Her ESR level was elevated, at 74 mm/h.

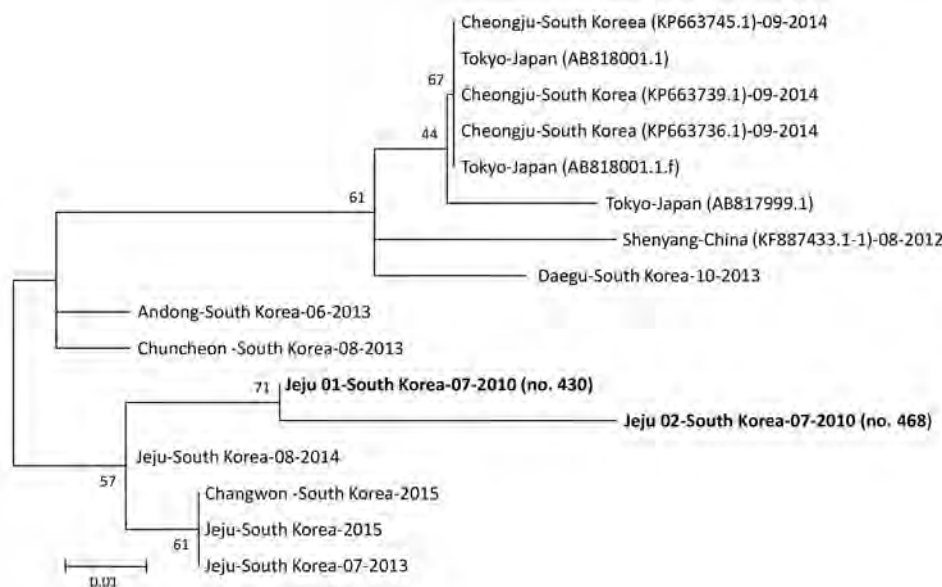[1]These authors contributed equally to this article.

Figure. Phylogenetic tree constructed based on partial small segment sequences of severe fever with thrombocytopenia syndrome virus identified in stored serum samples collected in 2010 from 2 patients in South Korea (bold) compared with reference viruses. We constructed the tree using the maximum-likelihood method with MEGA 6 (*10*). The partial small sequence data for the viruses identified in China, South Korea, and Japan were obtained from GenBank (accession numbers in parentheses). Scale bar indicates nucleotide substitutions per site.

SFTSV was reported in South Korea in 2012 (*3*). In this study, we retrospectively confirmed 2 SFTSV infections in South Korea in 2010 by amplification of the partial S segment of the viral RNA from stored serum of patients with a high ESR. Atypical signs and symptoms of SFTS among patients and asymptomatic infections have previously been reported in South Korea (*3,6,8*). In this study, we found that the signs and symptoms of SFTS were distinct from the major clinical signs and symptoms of SFTS, and the knee pain was coincidence. However, a case study showed that 1 SFTS patient had a crusted erythematous ulcer on the lateral side of the left knee, accompanied with left inguinal lymphadenopathy.

In conclusion, we suggest that SFTSV infections in South Korea have occurred during a period similar to the period reported for China, where SFTSV was found in 2009. In addition, the signs and symptoms of SFTS may be atypical. Therefore, further clinical, epidemiologic, and laboratory research is needed to better understand the transmission dynamics of SFTSV and prevent additional SFTSV infections in other populations.

About the Authors

Dr. Kim is a professor at the Department of Laboratory Medicine, Jeju National University College of Medicine, Jeju, South Korea. Dr. Yun is a research professor at Ewha Medical Research Institute, Ewha Womans University, Seoul, South Korea. Their primary research interest is clinical microbiology.

References

1. International Committee on Taxonomy of Viruses (ICTV). Taxonomy. 2017 [cited 2017 May 3]. https://talk.ictvonline.org/taxonomy
2. Yu XJ, Liang MF, Zhang SY, Liu Y, Li JD, Sun YL, et al. Fever with thrombocytopenia associated with a novel bunyavirus in China. N Engl J Med. 2011;364:1523–32. http://dx.doi.org/10.1056/NEJMoa1010095
3. Kim KH, Yi J, Kim G, Choi SJ, Jun KI, Kim NH, et al. Severe fever with thrombocytopenia syndrome, South Korea, 2012. Emerg Infect Dis. 2013;19:1892–4. http://dx.doi.org/10.3201/eid1911.130792
4. Takahashi T, Maeda K, Suzuki T, Ishido A, Shigeoka T, Tominaga T, et al. The first identification and retrospective study of severe fever with thrombocytopenia syndrome in Japan. J Infect Dis. 2014;209:816–27. http://dx.doi.org/10.1093/infdis/jit603
5. Liu Q, He B, Huang SY, Wei F, Zhu XQ. Severe fever with thrombocytopenia syndrome, an emerging tick-borne zoonosis. Lancet Infect Dis. 2014;14:763–72. http://dx.doi.org/10.1016/S1473-3099(14)70718-2
6. Yoo JR, Heo ST, Park D, Kim H, Fukuma A, Fukushi S, et al. Family cluster analysis of severe fever with thrombocytopenia syndrome virus infection in Korea. Am J Trop Med Hyg. 2016;95:1351–7. http://dx.doi.org/10.4269/ajtmh.16-0527
7. Bao CJ, Guo XL, Qi X, Hu JL, Zhou MH, Varma JK, et al. A family cluster of infections by a newly recognized bunyavirus in eastern China, 2007: further evidence of person-to-person transmission. Clin Infect Dis. 2011;53:1208–14. http://dx.doi.org/10.1093/cid/cir732
8. Wi YM, Woo HI, Park D, Lee KH, Kang C-I, Chung DR, et al. Severe fever with thrombocytopenia syndrome in patients suspected of having scrub typhus. Emerg Infect Dis. 2016;22:1992–5. http://dx.doi.org/10.3201/eid2211.160597
9. Zhang YZ, He YW, Dai YA, Xiong Y, Zheng H, Zhou DJ, et al. Hemorrhagic fever caused by a novel bunyavirus in China:

pathogenesis and correlates of fatal outcome. Clin Infect Dis. 2012;54:527–33. http://dx.doi.org/10.1093/cid/cir804

10. Tamura K, Stecher G, Peterson D, Filipski A, Kumar S. MEGA6: Molecular Evolutionary Genetics Analysis version 6.0. Mol Biol Evol. 2013;30:2725–9. http://dx.doi.org/10.1093/molbev/mst197

Address for correspondence: Keun Hwa Lee, Department of Microbiology and Immunology, Jeju National University College of Medicine, 15, Aran 13-gil, Jeju 63241, South Korea; email: yomust7@jejunu.ac.kr

Spotted Fever Group Rickettsiae in Inner Mongolia, China, 2015–2016

Gaowa, Wulantuya, Xuhong Yin, Shengchun Guo, Chunlian Ding, Minzhi Cao, Hiroki Kawabata, Kozue Sato, Shuji Ando, Hiromi Fujita, Fumihiko Kawamori, Hongru Su, Masahiko Shimada, Yuko Shimamura, Shuichi Masuda, Norio Ohashi

Author affiliations: College of Hetao, Bayan Nur City, Inner Mongolia, China (Gaowa, Wulantuya, X. Yin, S. Guo, C. Ding); Bayan Nur Centers for Disease Control and Prevention, Bayan Nur City (M. Cao); National Institute of Infectious Diseases, Shinjuku-ku, Tokyo, Japan (H. Kawabata, K. Sato, S. Ando); Mahara Institute of Medical Acarology, Anan City, Tokushima, Japan (H. Fujita); University of Shizuoka, Shizuoka City, Japan (F. Kawamori, H. Su, M. Shimada, Y. Shimamura, S. Masuda, N. Ohashi)

We found *Rickettsia raoultii* infection in 6/261 brucellosis-negative patients with fever of unknown origin in brucellosis-endemic Inner Mongolia, China. We further identified *Hyalomma asiaticum* ticks associated with *R. raoultii*, *H. marginatum* ticks associated with *R. aeschlimannii*, and *Dermacentor nuttalli* ticks associated with both rickettsiae species in the autonomous region.

Spotted fever group rickettsiae (SFGR) are vector-borne pathogens. In China, 5 SFGR genotypes have been identified as causative agents of human rickettsiosis: *R. heilongjiangensis*, *R. sibirica* subsp. *sibirica* BJ-90, *Candidatus* Rickettsia tarasevichiae, *R. raoultii*, and *Rickettsia* sp. XY99 (*1–4*).

Brucellosis, a zoonotic disease, is highly endemic to Inner Mongolia, China, and is increasing in workers in agriculture or animal husbandry (*5*). However, some agriculture workers with brucellosis-like symptoms, including general malaise and fever, were seronegative for *Brucella* spp. We suspected that fever of unknown origin among brucellosis-seronegative patients might be caused by tickborne pathogens. We identified 6 cases of human *R. raoultii* infections in brucellosis-seronegative patients in western Inner Mongolia, and we investigated exposure to ticks infected with SFGR.

During 2015–2016, we obtained 261 blood samples from brucellosis-seronegative patients with fever of unknown origin in Bayan Nur Centers for Disease Control and Prevention (Bayan Nur City, Inner Mongolia, China). The review board of the Department of Medicine at College of Hetao (Bayan Nur City) approved the study. We extracted DNA from each blood sample using the DNeasy Mini Kit (QIAGEN, Hilden, Germany) and conducted PCR targeting SFGR *gltA* (*6*). The PCR primers used, gltA-Fc (5′-CGAACTTACCGCTATTAGAATG-3′) and gltA-Rc (5′-CTTTAAGAGCGATAGCTTCAAG-3′), were described previously (*4*). We designed the primers 16S rDNA R-2F (5′-GAAGATTCTCTTTCGGTTTCGC-3′), 16S rDNA R-2R (5′-GTCTTGCTTCCCTCTGTAAAC-3′), rompA-Fb (5′-GGTGCGAATATAGACCCTGA-3′), and rompA-Ra (5′-TTAGCTTCAGAGCCTGACCA-3′) for this study and deposited the sequences obtained of *gltA*, *ompA*, and 16S rDNA into GenBank (accession nos. MH267733–47). We used genomic DNA extracted from L929 cells infected with *Rickettsia* sp. LON-13 (*gltA*: AB516964) as a positive control.

We detected *gltA* amplicons from 6/261 (2.3%) blood samples (Table). All 6 patients had strong malaise and mild fever of 36.8°C –37.3°C but no rash. Five of these patients also had arthralgia and vomiting.

Sequence and phylogenetic analysis showed that the sequences of 6 nearly full-length (1.1 kb) *gltA* amplicons with were identical to each other and to *R. raoultii gltA* (GenBank accession no. DQ365803). We further analyzed *ompA* and 16S rDNA in *gltA*-positive samples. All 6 samples were PCR positive for both genes; 552-bp sequences of the amplicons were identical to sequences of *R. raoultii ompA* (GenBank accession no. AH015610), and 389-bp sequences of the amplicons were identical to sequences of *R. raoultii* 16S rDNA (GenBank accession no. EU036982). PCR results were negative for the genes *Anaplasma phagocytophilum p44/msp2*, *Ehrlichia chaffeensis p28/omp-1*, and *Borrelia* spp. *flaB*. An indirect immunofluorescence assay showed that IgM and IgG titers against *R. japonica* were 40–80 for IgM in 3 patients and 160 for IgG in 2 patients.

Table. PCR survey of SFGR infections in patients and ticks, Inner Mongolia, China, 2015–2016*

Patient type or tick species	No. tested	Rickettsia raoultii	R. aeschlimannii	Total
		No. (%) gltA positive for SFGR		
Brucellosis-seronegative patients	261	6 (2.3)	0	6 (2.3)
Ticks				
Hyalomma asiaticum	766	118 (15.4)	0	118 (15.4)
Hyalomma marginatum	198	0	160 (80.8)	160 (80.8)
Dermacentor nuttalli	1,418	830 (58.5)	158 (11.1)	988 (69.7)†
Rhipicephalus turanicus	76	0	0	0
Total ticks	2,458	948 (38.6)	318 (12.9)	1,266 (51.5)

*SFGR, spotted fever group rickettsiae.
†We did not detect dual infection with *R. raoultii* and *R. aeschlimannii* in *D. nuttalli* ticks in this study.

To assess patients' risk of infection with SFGR by tick exposure, we collected 2,458 ticks morphologically identified as *Hyalomma marginatum* (n = 198), *H. asiaticum* (n = 766), *Dermacentor nuttalli* (n = 1,418), and *Rhipicephalus turanicus* (n = 76) from livestock and pet animals including sheep, cattle, camels, and dogs in western Inner Mongolia during 2015–2016 (online Technical Appendix Figure 1, https://wwwnc.cdc.gov/EID/article/24/11/16-2094-Techapp1.pdf). We collected unattached ticks within animal hair, but not attached ticks. We prepared DNA extracted from salivary glands of each tick and conducted PCR screening by rickettsial *gltA* detection as described. We detected *gltA* in 1,266 (51.5%) of the total 2,458 ticks.

We classified the amplicons into 2 groups by restriction fragment–length polymorphism using *Alu*I and *Rsa*I, and we sequenced 25–45 representative amplicons in each group. On the basis of this analysis, we found that the sequences from the 2 groups were either identical to that of *R. raoultii* (GenBank accession no. DQ365803) or to that of *R. aeschlimannii* (GenBank accession no. HM050276) (Table; online Technical Appendix Figure 2). We detected *R. raoultii* DNA in *H. asiaticum* (118/766, 15.4%) and *D. nuttalli* (830/1,418, 58.5%) ticks and *R. aeschlimannii* DNA from *H. marginatum* (160/198, 80.8%) and *D. nuttalli* (158/1,418, 11.1%) ticks. We did not detect rickettsial DNA in *R. turanicus* ticks (0/76, 0%).

Recently, human cases of *R. raoultii* infection have been reported in China, including northeastern Inner Mongolia (1,4). Potential vectors for *R. raoultii* are *Dermacentor* spp. ticks in Europe, Turkey, and northern Asia and *Haemaphysalis* spp. and *Amblyomma* sp. ticks in southern Asia (7,8). Other studies have identified *Hyalomma* spp., *Rhipicephalus* spp., and *Amblyomma* sp. ticks as potential vectors for *R. aeschlimannii* (7,8); human cases of *R. aeschlimannii* infection have been reported in Italy and Morocco (7,9). We detected *R. raoultii* in *H. asiaticum* as well as *D. nuttalli* ticks, but in Mongolia, *R. raoultii* has been detected only in *D. nuttalli* ticks, and not *H. asiaticum* ticks (10). We identified *D. nuttalli* ticks as another potential vector for *R. aeschlimannii*. Our work contributes to the knowledge of the epidemiology, clinical characteristics, and known tick vectors associated with *R. raoultii* and *R. aeschlimannii*.

About the Author

Dr. Gaowa is an associate professor in Inner Mongolia Key Laboratory of Tick-Borne Zoonosis, Department of Medicine, College of Hetao, Bayan Nur, Inner Mongolia, China. Her primary research interests are molecular biology, ecology, and epidemiology of zoonotic parasites, especially tickborne pathogens.

References

1. Jia N, Zheng YC, Ma L, Huo QB, Ni XB, Jiang BG, et al. Human infections with *Rickettsia raoultii*, China. Emerg Infect Dis. 2014;20:866–8. http://dx.doi.org/10.3201/eid2005.130995
2. Fang LQ, Liu K, Li XL, Liang S, Yang Y, Yao HW, et al. Emerging tick-borne infections in mainland China: an increasing public health threat. Lancet Infect Dis. 2015;15:1467–79. http://dx.doi.org/10.1016/S1473-3099(15)00177-2
3. Li H, Cui XM, Cui N, Yang ZD, Hu JG, Fan YD, et al. Human infection with novel spotted fever group *Rickettsia* genotype, China, 2015. Emerg Infect Dis. 2016;22:2153–6. http://dx.doi.org/10.3201/eid2212.160962
4. Li H, Zhang PH, Huang Y, Du J, Cui N, Yang ZD, et al. Isolation and identification of *Rickettsia raoultii* in human cases: a surveillance study in 3 medical centers in China. Clin Infect Dis. 2018;66:1109–15. http://dx.doi.org/10.1093/cid/cix917
5. Li MT, Sun GQ, Zhang WY, Jin Z. Model-based evaluation of strategies to control brucellosis in China. Int J Environ Res Public Health. 2017;14:295. http://dx.doi.org/10.3390/ijerph14030295
6. Gaowa, Ohashi N, Aochi M, Wuritu D, Wu, Yoshikawa Y, et al. Rickettsiae in ticks, Japan, 2007–2011. Emerg Infect Dis. 2013;19:338–40. http://dx.doi.org/10.3201/eid1902.120856
7. Parola P, Paddock CD, Socolovschi C, Labruna MB, Mediannikov O, Kernif T, et al. Update on tick-borne rickettsioses around the world: a geographic approach. Clin

Microbiol Rev. 2013;26:657–702. 1 http://dx.doi.org/10.1128/CMR.00032-13

8. Karasartova D, Gureser AS, Gokce T, Celebi B, Yapar D, Keskin A, et al. Bacterial and protozoal pathogens found in ticks collected from humans in Corum province of Turkey. PLoS Negl Trop Dis. 2018;12:e0006395. http://dx.doi.org/10.1371/journal.pntd.0006395

9. Tosoni A, Mirijello A, Ciervo A, Mancini F, Rezza G, Damiano F, et al.; Internal Medicine Sepsis Study Group. Human *Rickettsia aeschlimannii* infection: first case with acute hepatitis and review of the literature. Eur Rev Med Pharmacol Sci. 2016;20:2630–3.

10. Boldbaatar B, Jiang RR, von Fricken ME, Lkhagvatseren S, Nymadawa P, Baigalmaa B, et al. Distribution and molecular characteristics of rickettsiae found in ticks across Central Mongolia. Parasit Vectors. 2017;10:61. http://dx.doi.org/10.1186/s13071-017-1981-3

Japanese Spotted Fever in Eastern China, 2013

Jiabin Li,[1] Wen Hu,[1] Ting Wu, Hong-Bin Li, Wanfu Hu, Yong Sun, Zhen Chen, Yonglin Shi, Jia Zong, Adams Latif, Linding Wang, Li Yu, Xue-Jie Yu, Bo-Yu Liu, Yan Liu

Author affiliations: The First Affiliated Hospital of Anhui Medical University, Hefei, China (J. Li, T. Wu, H.-B. Li); The First Affiliated Hospital of the University of Science and Technology of China, Hefei (Wen Hu); Anhui Center for Disease Control and Prevention, Hefei (Wanfu Hu, Y. Sun, Y. Shi); Anhui Medical University, Hefei (Z. Chen, J. Zong, A. Latif, L. Wang, L. Yu, B.-Y. Liu, Y. Liu); Wuhan University School of Health Sciences, Wuhan, China (X.-J. Yu)

DOI: https://doi.org/10.3201/eid2411.170264

We isolated *Rickettsia japonica* from a febrile patient in Lu'an City, China, in 2013. Subsequently, we found an *R. japonica* seroprevalence of 54.8% (494/902) in the rural population of Anhui Province and an *R. japonica* prevalence in *Haemaphysalis longicornis* ticks of 0.5% (5/935). *R. japonica* and its tick vector exist in China.

[1]These authors contributed equally to this article.

Spotted fever group rickettsiae are tickborne, obligatory intracellular, gram-negative bacteria with a worldwide distribution. However, the distribution of each species of spotted fever group rickettsiae is limited to geographic areas by their specific tick vectors. Japanese spotted fever is a severe rickettsiosis caused by *Rickettsia japonica* bacterium (*1,2*), which has been present in Japan since 1984 and isolated from patients in other countries of Asia (e.g., South Korea, the Philippines, and Thailand) over the past decade (*3,4*). In this study, we present information on an *R. japonica* isolate acquired from a febrile patient and *R. japonica* seroprevalence in Anhui Province in eastern China.

On August 7, 2013, a 61-year-old man from Shucheng County, Lu'an City, China, in the Dabie Mountain area of Anhui Province (online Technical Appendix Figure 1, https://wwwnc.cdc.gov/EID/article/24/11/17-0264-Techapp1.pdf) with fever and headache for 1 week was admitted into Shucheng County People's Hospital. The patient reported several tick bites 10 days before the onset of his illness. At admission, the patient was conscious and had fever (39.0°C); he did not have jaundice, and no bleeding was found on his skin or mucosal membranes. A papular rash with papules 0.1–0.5 cm in diameter was noted all over his body (online Technical Appendix Figure 2). Blood cell counts showed the patient had leukocytosis (10.34×10^9 cells/L), increased neutrophils (87.5%), and a platelet count within reference range (130×10^9/L). Blood chemistry testing revealed a urea nitrogen concentration of 9.12 mmol/L (reference range 2.9–8.2 mmol/L), creatinine of 0.758 mg/dL (67 μmol/L, reference range 53–106 μmol/L), C-reactive protein of 77.5 nmol/L (reference range 0.76–28.5 nmol/L), and an erythrocyte sedimentation rate of 22 mm/h (reference range 0–20 mm/h). A urine test showed a procalcitonin concentration of 0.806 ng/mL (reference range $\leq$0.15 ng/mL) and an interleukin 6 concentration of 52 pg/mL (reference range $\leq$1.8 pg/mL). The patient had rough lung breath sounds, and computed tomography showed inflammatory infiltrates in the middle right lung and lower left lung lobe, bullae on the upper left lung lobe, and emphysematous changes. The patient was suspected to have a rickettsial infection and was given minocycline and meropenem on the day of his admission. Two days later, on August 9, 2013, the patient's fever subsided (36.2°C), and he was discharged.

A blood sample taken from the patient 1 day after admission was inoculated onto THP-1 and Vero E6 cells; after 10 days, cytopathic effect was visible by light microscopy with only the THP-1 cells. Diff-Quick (Thermo Fisher Scientific, Kalamazoo, MI, USA)–stained smears of THP-1 cells showed *Rickettsia*-like bacilli in the cytoplasm. Electron microscopy showed the bacilli localized to the cytoplasm and nucleus and had the typical ultrastructure of *Rickettsia* bacteria. This species was highly pleomorphic

but mainly had dimensions 0.2 μm × 0.5–1 μm (online Technical Appendix Figure 3).

We amplified and sequenced the 17-kDa protein gene, 16S rRNA gene, *ompA*, *ompB*, and gene D of *R. japonica* (GenBank accession nos. KY364904, KY484160, KY484162, KY484163, and KY488633; online Technical Appendix Table). These gene sequences were 99.8%–100% homologous with the corresponding gene of an *R. japonica* isolate (GenBank accession no. AP017602.1).

Hard-body tick species *Haemaphysalis longicornis*, *H. flava*, and *Dermacentor taiwanensis* (*5,6*) have been reported as *R. japonica* transmission vectors. We acquired questing *H. longicornis* ticks in Shandong Province, China, in 2013 and found them positive for the *R. japonica* 17-kDa protein and 16S rRNA genes by PCR (online Technical Appendix). The percentage of *H. longicornis* ticks infected with *R. japonica* rickettsia in Shandong Province was 0.5% (5/975). The *H. longicornis* tick, which is prevalent in East China and feeds on domestic animals and small mammals, might be a major vector of *R. japonica* rickettsia in China

(*7,8*). Phylogenic analysis of the 16S rRNA (Figure, panel A) and 17-kDa protein (Figure, panel B) genes indicated that the rickettsial isolates from the patient and *H. longicornis* tick were identical to *R. japonica* isolates and in the same clade with *R. heilongjiangensis*.

Examination by indirect immunofluorescence assay showed that the patient's acute (1:80 dilution) and convalescent (1:1,280 dilution) serum samples reacted to isolated antigen of *R. japonica* bacterium. During 2013, we collected serum samples from 902 healthy persons living in rural areas of Anhui Province (online Technical Appendix Figure 1) and tested them with the same assay. We found 54.8% (494/902) of serum samples positive for *R. japonica*–specific antibodies.

In summary, we detected *R. japonica* bacteria in a patient and an *H. longicornis* tick and demonstrated high *R. japonica* seroprevalence among the rural population of Anhui Province. In agreement with Lu et al.'s work in 2015 (*9*), our findings suggest that *R. japonica* might be more prevalent in China than previously thought. Physicians in
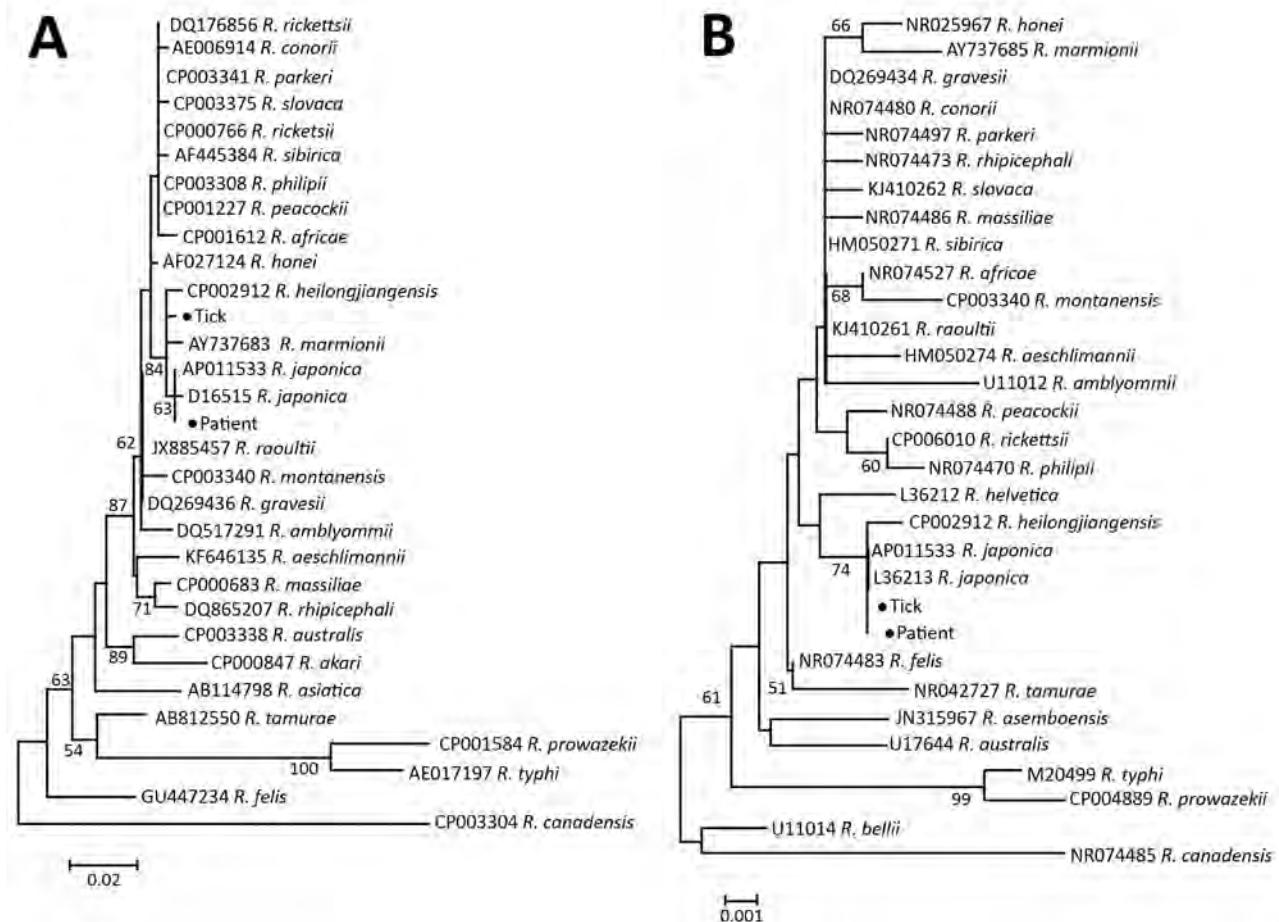
Figure. Phylogenetic analysis of *Rickettsia* isolate from patient with Japanese spotted fever in Anhui Province and isolate from *Haemaphysalis longicornis* tick in Shandong Province, China, 2013 (black dots), compared with reference isolates. Unrooted neighbor-joining trees of 16S rRNA gene (A) and 17-kDa protein gene (B) were constructed by using MEGA 5.2 (https://www.megasoftware.net/) and 1,000 bootstrap replications. Scale bars represent substitutions per nucleotide.

China need to become aware of *R. japonica* disease presentation, so they can administer the appropriate treatment to patients with suspected *R. japonica* infections.

About the Authors

Dr. Li is a research coordinator at The First Affiliated Hospital of Anhui Medical University, Hefei, China. His research interests are pathogenic mechanisms of tickborne infectious diseases, including severe fever with thrombocytopenia syndrome, human granulocytic anaplasmosis, and spotted fever group rickettsioses. Dr. Wen Hu is an electron microscope technician at The First Affiliated Hospital of the University of Science and Technology of China, Hefei, China. His research interest is pathogen structure.

References

1. Uchida T, Yu XJ, Uchiyama T, Walker DH. Identification of a unique spotted fever group rickettsia from humans in Japan. J Infect Dis. 1989;159:1122–6. http://dx.doi.org/10.1093/infdis/159.6.1122
2. Mahara F. Japanese spotted fever: report of 31 cases and review of the literature. Emerg Infect Dis. 1997;3:105–11. http://dx.doi.org/10.3201/eid0302.970203
3. Chung MH, Lee SH, Kim MJ, Lee JH, Kim ES, Lee JS, et al. Japanese spotted fever, South Korea. Emerg Infect Dis. 2006; 12:1122–4. http://dx.doi.org/10.3201/eid1207.051372
4. Gaywee J, Sunyakumthorn P, Rodkvamtook W, Ruang-areerate T, Mason CJ, Sirisopana N. Human infection with *Rickettsia* sp. related to *R. japonica*, Thailand. Emerg Infect Dis. 2007;13:657–9. http://dx.doi.org/10.3201/eid1304.060585
5. Uchida T, Yan Y, Kitaoka S. Detection of *Rickettsia japonica* in *Haemaphysalis longicornis* ticks by restriction fragment length polymorphism of PCR product. J Clin Microbiol. 1995;33:824–8.
6. Ishikura M, Fujita H, Ando S, Matsuura K, Watanabe M. Phylogenetic analysis of spotted fever group rickettsiae isolated from ticks in Japan. Microbiol Immunol. 2002;46:241–7. http://dx.doi.org/10.1111/j.1348-0421.2002.tb02692.x
7. Luo LM, Zhao L, Wen HL, Zhang ZT, Liu JW, Fang LZ, et al. *Haemaphysalis longicornis* ticks as reservoir and vector of severe fever with thrombocytopenia syndrome virus in China. Emerg Infect Dis. 2015;21:1770–6. http://dx.doi.org/10.3201/eid2110.150126
8. Tenquist J, Charleston W. A revision of the annotated checklist of ectoparasites of terrestrial mammals in New Zealand. J R Soc N Z. 2001;31:481–542. http://dx.doi.org/10.1080/03014223.2001.9517666
9. Lu Q, Yu J, Yu L, Zhang Y, Chen Y, Lin M, et al. *Rickettsia japonica* infections in humans, Zhejiang Province, China, 2015. Emerg Infect Dis. 2018 Nov [*date cited*]. https://doi.org/10.3201/eid2411.170044

Address for correspondence: Yan Liu, Anhui Medical University, School of Basic Medical Sciences, Anhui, 230032, China; email: yliu16888@163.com; Bo-Yu Liu; email: centian2004@163.com

Burkholderia lata Infections from Intrinsically Contaminated Chlorhexidine Mouthwash, Australia, 2016

Lex E.X. Leong, Diana Lagana, Glen P. Carter, Qinning Wang, Kija Smith, Tim P. Stinear, David Shaw, Vitali Sintchenko, Steven L. Wesselingh, Ivan Bastian, Geraint B. Rogers

Author affiliations: South Australian Health and Medical Research Institute, Adelaide, South Australia, Australia (L.E.X. Leong, S.L. Wesselingh, G.B. Rogers); Flinders University, Bedford Park, South Australia, Australia (L.E.X. Leong, G.B. Rogers); Royal Adelaide Hospital, Adelaide (D. Lagana, D. Shaw); University of Melbourne, Melbourne, Victoria, Australia (G.P. Carter, T.P. Stinear); The University of Sydney, Westmead, New South Wales, Australia (Q. Wang, V. Sintchenko); SA Pathology, Adelaide (K. Smith, I. Bastian)

Burkholderia lata was isolated from 8 intensive care patients at 2 tertiary hospitals in Australia. Whole-genome sequencing demonstrated that clinical and environmental isolates originated from a batch of contaminated commercial chlorhexidine mouthwash. Genomic analysis identified efflux pump–encoding genes as potential facilitators of bacterial persistence within this biocide.

Burkholderia contaminans and *B. lata* together form group K of the *B. cepacia* complex (Bcc). These predominantly environmental species are a major cause of pharmaceutical contamination and have been linked to multiple instances of associated opportunistic infection (*1*). Although both species are capable of causing serious infections in humans (*2*,*3*), only *B. contaminans* has been associated with infection outbreaks (*3*,*4*). We report a healthcare-associated *B. lata* infection outbreak occurring in intensive care units (ICUs) in 2 tertiary hospitals in Australia.

During May–June 2016, bacterial contamination of chlorhexidine mouthwash (0.2% mg/mL) was associated with an interjurisdictional outbreak in New South Wales and South Australia. Bcc isolates were obtained from blood and tracheal aspirates from 6 ICU patients in hospital A (South Australia) (sample information and isolation protocols detailed in the online Technical Appendix, https://wwwnc.cdc.gov/EID/article/24/11/17-1929-Techapp1.pdf). An investigation by the hospital's infection and prevention control team noted discoloration of a commercial chlorhexidine mouthwash. Bcc isolates were cultured from

all 5 tested bottles from the discolored batch but not from 11 bottles tested from 4 other batches. Isolates were further obtained from the surfaces of hand basins in 3 separate ICU rooms, where bottles of mouthwash from the contaminated batch were in use. Separately, a Bcc isolate was obtained from the sputum of an ICU patient in hospital B (New South Wales), where the same batch of mouthwash was in use. After a nationwide recall of the contaminated mouthwash batch, no further cases were reported.

The genomes of 15 Bcc isolates from the 2 hospitals were sequenced (online Technical Appendix). A closed genome of isolate A05 was generated as a reference, consisting of 3 circular chromosomes of 3.93, 3.71, and 1.15 Mbp (National Center for Biotechnology Information BioProject accession no. PRJNA419071).

Genome analysis identified an Australasian sublineage of B. lata as the cause of the outbreak. Specifically, all isolates were sequence type 103 (ST103), which sits within a subclade of B. lata isolates from Australia and New Zealand (online Technical Appendix Figure 1). Two isolates from hand basins (A07 and A08) and 1 from a hospital bench (A10) were of unknown sequence type.

Single-nucleotide polymorphism (SNP)–based phylogenetic analysis identified the outbreak strain as a distinct clonal lineage (0–1 SNPs) within the group K clade (Figure), separated from other members of the group by a minimum of 167,662 SNPs. SNP variation within the clonal sublineage ranged from 0 to 2 SNPs across isolates from contaminated mouthwash bottles and patients. A single SNP distinguished isolates from patient 4 in room 21 (A04)

and the hand basin in the same room (A08) (collected 2 days apart). Three of the taxa isolated from the hospital environment (A07, A08, and A10) had substantial SNP variations compared with contaminated mouthwash and patient isolates (an average of 191,893 SNPs for A07, 655 SNPs for A08, and 1,408 SNPs for A10).

Differences of 0–1 SNPs between isolates from mouthwash in the 2 hospitals, including from unopened bottles, strongly suggests contamination during the manufacturing process. After several previous incidents of contamination of cosmetic, toiletry, and pharmaceutical products by members of Bcc, the US Food and Drug Administration commented that these bacteria very likely are introduced into the manufacturing processes through contaminated water (https://www.fda.gov/Drugs/DrugSafety/ucm559508.htm). Direct patient-to-patient transmission of B. lata would appear unlikely in this instance, given the use of individual ICU rooms with nonshared facilities and incomplete overlap in periods of care.

Chlorhexidine mouthwash is perhaps a surprising source of B. lata infection, given its potent biocidal properties. However, Bcc species have been isolated previously from 0.02% chlorhexidine gluconate (in irrigation apparatuses used for vaginal douching) and from 0.05% preparations (used for storage of suction catheters) (5). The ability of B. lata to remain viable in chlorhexidine appears to be a result of a combination of efflux pump activity, biofilm formation, and cell wall impermeability (1,6,7). These mechanisms probably also contribute to the common inefficacy of combination antibiotic therapy
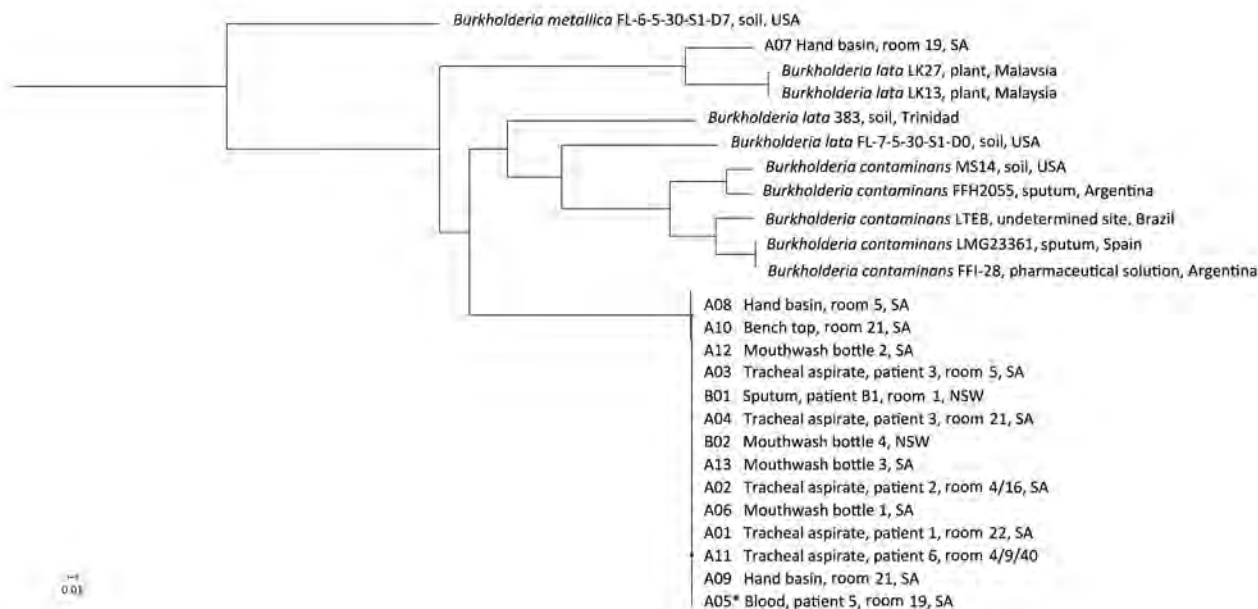
Figure. Phylogenetic analysis of isolates implicated in an outbreak *Burkholderia lata* infection from intrinsically contaminated chlorhexidine mouthwash, Australia, 2016. The maximum-likelihood tree is constructed from core genome single-nucleotide polymorphism alignments (N = 512,480) of the outbreak genomes, bootstrapped 1,000 times, and archival genomes from *B. cepacia* complex group K, relative to the reference genome *B. lata* A05 (identified by an asterisk). *B. metallica* was included as a comparator.

in the treatment of associated infections (8). Prolonged exposure to microbiocides, including chlorhexidine, has been shown to result in a stable increase in the expression of antibiotic-resistance mechanisms (1,6), and elevated chlorhexidine resistance has been reported in multidrug-resistant strains of *B. cenocepacia* from cystic fibrosis patients (9). Three resistance-nodulation-division (RND) efflux pump genes (RND3, RND4, and RND9) have been shown to be essential for chlorhexidine tolerance in *B. cenocepacia* (9). Examination of the complete genome of *B. lata* isolate A05 revealed the presence of RND3, RND4, and RND9 in each strain (≥94% sequence identity) (online Technical Appendix Figure 2).

B. contaminans is the cause of widespread pharmaceutical product contamination, and infection outbreaks by this species are well-documented (3,10). Our findings suggest that the other member of Bcc group K, *B. lata*, also represents an important opportunistic pathogen of relevance to infection control, particularly given its intrinsic biocide tolerance.

About the Author
Dr. Leong is a research scientist at the South Australian Health and Medical Research Institute. His research interests include pathogen genomic epidemiology and infection outbreaks.

References
1. Rushton L, Sass A, Baldwin A, Dowson CG, Donoghue D, Mahenthiralingam E. Key role for efflux in the preservative susceptibility and adaptive resistance of *Burkholderia cepacia* complex bacteria. Antimicrob Agents Chemother. 2013;57: 2972–80. http://dx.doi.org/10.1128/AAC.00140-13
2. Pope CE, Short P, Carter PE. Species distribution of *Burkholderia cepacia* complex isolates in cystic fibrosis and non-cystic fibrosis patients in New Zealand. J Cyst Fibros. 2010;9:442–6. http://dx.doi.org/10.1016/j.jcf.2010.08.011
3. Medina-Pascual MJ, Valdezate S, Carrasco G, Villalón P, Garrido N, Saéz-Nieto JA. Increase in isolation of *Burkholderia contaminans* from Spanish patients with cystic fibrosis. Clin Microbiol Infect. 2015;21:150–6. http://dx.doi.org/10.1016/j.cmi.2014.07.014
4. Martina P, Bettiol M, Vescina C, Montanaro P, Mannino MC, Prieto CI, et al. Genetic diversity of *Burkholderia contaminans* isolates from cystic fibrosis patients in Argentina. J Clin Microbiol. 2013;51:339–44. http://dx.doi.org/10.1128/JCM.02500-12
5. Oie S, Kamiya A. Microbial contamination of antiseptics and disinfectants. Am J Infect Control. 1996;24:389–95. http://dx.doi.org/10.1016/S0196-6553(96)90027-9
6. Knapp L, Rushton L, Stapleton H, Sass A, Stewart S, Amezquita A, et al. The effect of cationic microbicide exposure against *Burkholderia cepacia* complex (Bcc); the use of *Burkholderia lata* strain 383 as a model bacterium. J Appl Microbiol. 2013;115: 1117–26. http://dx.doi.org/10.1111/jam.12320
7. Drevinek P, Holden MT, Ge Z, Jones AM, Ketchell I, Gill RT, et al. Gene expression changes linked to antimicrobial resistance, oxidative stress, iron depletion and retained motility are observed when *Burkholderia cenocepacia* grows in cystic fibrosis sputum. BMC Infect Dis. 2008;8:121. http://dx.doi.org/10.1186/1471-2334-8-121
8. George AM, Jones PM, Middleton PG. Cystic fibrosis infections: treatment strategies and prospects. FEMS Microbiol Lett. 2009; 300:153–64. http://dx.doi.org/10.1111/j.1574-6968.2009.01704.x
9. Coenye T, Van Acker H, Peeters E, Sass A, Buroni S, Riccardi G, et al. Molecular mechanisms of chlorhexidine tolerance in *Burkholderia cenocepacia* biofilms. Antimicrob Agents Chemother. 2011;55:1912–9. http://dx.doi.org/10.1128/AAC.01571-10
10. Martin M, Christiansen B, Caspari G, Hogardt M, von Thomsen AJ, Ott E, et al. Hospital-wide outbreak of *Burkholderia contaminans* caused by prefabricated moist washcloths. J Hosp Infect. 2011; 77:267–70. http://dx.doi.org/10.1016/j.jhin.2010.10.004

Address for correspondence: Lex Leong, South Australian Health and Medical Research Institute, North Terrace, Adelaide, South Australia 5000, Australia; email: lex.leong@sahmri.com

Estimating Latent Tuberculosis Infection Using Interferon-γ Release Assay, Japan

Tomoyasu Nishimura, Masaki Ota, Masaaki Mori, Naoki Hasegawa, Hiroshi Kawabe, Seiya Kato

Author affiliations: Keio University, Tokyo, Japan (T. Nishimura, M. Mori, H. Kawabe); Research Institute of Tuberculosis—Japan Anti-Tuberculosis Association, Tokyo (M. Ota, S. Kato); Keio University School of Medicine, Tokyo (N. Hasegawa)

We estimated the latent tuberculosis infection (LTBI) rate for foreign-born students at Keio University, Tokyo, Japan, using an interferon-γ release assay. The LTBI rate for students from countries with estimated tuberculosis incidence >100 cases/100,000 persons was high (10.0%). Universities should screen for LTBI in students from countries with high tuberculosis incidence.

The proportion of foreign-born tuberculosis (TB) patients among all TB patients in Japan is increasing, particularly for those 20–29 years of age (57.7% in 2016) (1). The Tokyo metropolitan government revealed a foreign-born student–related TB outbreak at a Japanese language school in 2016 (2). TB outbreaks involving foreign-born students create concerns that TB infection from such students, particularly those from countries with a high incidence of TB, might spread to the population of Japan.

In Japan, university students, including foreign-born students, undergo TB screening with chest radiograph; however, a chest radiograph cannot detect LTBI; it detects only pulmonary TB. Because immigrants may develop TB after entry (3), screening with chest radiograph might be ineffective; therefore, screening for LTBI may be necessary to prevent TB outbreaks. However, only a few surveys of TB infection among foreign-born persons have been conducted in Japan (4). We conducted a survey of LTBI among foreign-born students by using an interferon-γ release assay (IGRA).

Keio University has 6 campuses in the greater Tokyo area comprising ≈33,000 students, of whom ≈1,600 are foreign-born from 74 countries. During September 2016–September 2017, we recruited foreign-born students ≥20 years of age studying at Keio University who had no history of mycobacterial diseases or HIV infection. After obtaining informed consent, we collected whole blood specimens for the T-SPOT.TB test (Oxford Immunotec Ltd., Abington, UK), an IGRA available in Japan. All participants were screened for pulmonary TB with chest radiograph. We interviewed participants using a structured questionnaire on identification and demographic information, the date of first arrival in Japan, and history of TB. We derived country-specific estimated TB incidence rates from the World Health Organization website (5). Statistical results were computed by using R software (The R Foundation, Vienna, Austria). This study was conducted in compliance with the Declaration of Helsinki and approved by the institutional ethics review committee for human research of the Keio University School of Medicine and Hospital (no. 20160080).

We enrolled 177 participants 20–42 years of age (median 23 years), of whom 98 (55.1%) were female (Table). Participants were from China (55 students), Indonesia (24 students), France (19 students), Germany (9 students), and Thailand (8 students); the remaining participants were from 28 different countries, including 50 from countries with estimated TB incidence rates >100 cases/100,000 persons. We excluded data for 1 participant with an indeterminate IGRA result. A total of 117 (66.1%) students participated in this study within 1 month after arriving in Japan.

Overall, 8 (4.5% [95% CI 2.0%–8.7%]) students tested positive on IGRA (2 each from China and Thailand and 1 each from Ghana, Indonesia, South Korea, and the Philippines). The rate of the positive IGRA result for students from countries with an estimated TB incidence rate of >100 cases/100,000 persons was 10.0% (95% CI 3.3%–21.9%) and relative risk was 4.2 (95% CI 1.1–17.1), whereas the rate for students from countries with an estimated TB incidence rate of <100 cases/100,000 persons was 2.4% (95% CI 0.49%–6.7%). Even IGRA positivity of students 20–29 years of age from countries with estimated TB incidence rates of >100 cases/100,000 persons was 9.4% (95% CI 2.0%–25.0%). Chest radiograph found no students with pulmonary TB. We recommended that all IGRA-positive students receive LTBI treatment and close follow-up to detect the development of TB as early as possible.

The overall rate of LTBI among foreign-born students at Keio University was 4.5%. This rate was significantly higher for these students than for Keio University students from Japan assessed during 2009–2013 (0.73% [95% CI 0.39%–1.2%]; T. Nishimura et al., unpub. data). Our findings are consistent with those of previous studies. Ogiwara et al. showed that 7.8% of study participants tested positive for LTBI using the QuantiFERON-TB Gold test on 384 foreign-born students, of whom 363 were from countries with high TB incidence rates (4).

Table. Characteristics and IGRA results of participants in a study of latent TB infection, Japan, 2016–2017*

Characteristic	IGRA positive, no. (%, 95% CI), n = 8	IGRA negative, no., n = 169	p value†
Sex			
F	5 (5.1, 1.7–11.5)	93	0.733
M	3 (3.8, 0.79–10.7)	76	
Age, y			
20–29	6 (3.9, 1.4–8.3)	148	0.278
≥30	2 (8.7, 1.1–28.0)	21	
TB incidence rate in country of origin			
<100 cases/100,000 population	3 (2.4, 0.49–6.7)	124	0.042‡
>100 cases/100,000 population	5 (10.0, 3.3–21.8)	45	
Time living in Japan, y			
<1	5 (3.4, 1.1–7.9)	140	0.158
≥1	3 (9.4, 2.0–25.0)	29	

*IGRA, interferon-γ release assay; TB, tuberculosis.
†Differences between positive and negative groups were tested using Fisher exact test.
‡p<0.05.

Our study had a few strengths and limitations. The number of study participants was large enough for us to stratify the participants by estimated TB incidence rates for their countries of origin. One limitation was that the participation rate was small. Just ≈11% of foreign-born students at Keio University participated; therefore, the results obtained might not be representative of LTBI in all foreign-born students.

In conclusion, we found that estimated LTBI rates for foreign-born students in Japan from countries with high TB incidence rates were higher than those for students from countries with low TB incidence rates and for students from Japan. Based on our findings, we recommend that universities screen for LTBI using IGRAs in students from countries with high TB incidence rates (i.e., >100 cases/100,000 persons).

About the Author
Dr. Nishimura is a physician working as an assistant professor at Keio University. His primary research interest is mycobacterial diseases.

References
1. Kekkaku Yobo kai (Japan Anti-Tuberculosis Association). Kekkaku no toukei 2017 (Statistics of TB 2017) [in Japanese]. Tokyo: Kekkaku Yobo kai (Japan Anti-Tuberculosis Association); 2017.
2. The Japan Times. Tokyo reveals rare outbreak of tuberculosis, plays down ongoing risk [cited 2017 Nov 23]. https://www.japantimes.co.jp/news/2016/05/18/national/tokyo-reveals-rare-outbreak-of-tuberculosis-plays-down-ongoing-risk/
3. Public Health England. Non-UK born TB cases. In: Tuberculosis in England. 2015 Report (presenting data to end of 2014) version 1.1 [cited 2017 Nov 20]. https://www.gov.uk/government/uploads/system/uploads/attachment_data/file/564649/TB_annual_report_2015.pdf
4. Ogiwara T, Kimura T, Tokue Y, Watanabe R, Nara M, Obuchi T, et al. Tuberculosis screening using a T-cell interferon-γ release assay in Japanese medical students and non-Japanese international students. Tohoku J Exp Med. 2013;230:87–91. http://dx.doi.org/10.1620/tjem.230.87
5. World Health Organization. Tuberculosis country profiles [cited 2017 Nov 21]. http://who.int/tb/country/data/profiles/en/

Address for correspondence: Tomoyasu Nishimura, Health Center, Keio University, 35 Shinanomachi, Shinjuku-ku, Tokyo 160-8582, Japan; email: tnishimura@keio.jp

Effect of Inactivated Poliovirus Vaccine Campaigns, Pakistan, 2014–2017

Nicholas C. Grassly, Mufti Zubair Wadood, Rana M. Safdar, Abdirahman Sheikh Mahamud, Roland W. Sutter

Author affiliations: Imperial College London, London, United Kingdom (N.C. Grassly); World Health Organization, Geneva, Switzerland (M.Z. Wadood, R.W. Sutter); Ministry of National Health Services, Islamabad, Pakistan (R.M. Safdar); World Health Organization, Islamabad (A.S. Mahamud)

Pakistan began using inactivated poliovirus vaccine alongside oral vaccine in mass campaigns to accelerate eradication of wild-type poliovirus in 2014. Using case-based and environmental surveillance data for January 2014–October 2017, we found that these campaigns reduced wild-type poliovirus detection more than campaigns that used only oral vaccine.

Routine immunization with ≥1 dose of inactivated poliovirus vaccine (IPV) in all countries using oral poliovirus vaccine (OPV) was recommended by the World Health Organization (WHO) in November 2012, before the global withdrawal of the serotype 2 component from OPV (1). IPV has also been used since 2014 in mass campaigns to help interrupt wild poliovirus transmission and stop serotype 2 vaccine-derived poliovirus (VDPV2) outbreaks. The IPV supply was severely constrained during 2016–2017; only 2 manufacturers supply the United Nations Children's Fund, and their failure to produce the expected bulk product has meant that only about half the awarded quantities were supplied (2). As a result of these unplanned reductions in IPV supply, countries have delayed the introduction of IPV to routine immunization or faced stockouts, and mass campaigns with IPV in response to VDPV2 are no longer recommended by WHO (3). Nonetheless, where possible, IPV continues to be used in mass campaigns for outbreak response; for example, Pakistan, Afghanistan, Nigeria, and Syria all used IPV in mass campaigns in 2017.

Given that IPV supply constraints are likely to continue until at least the end of 2018, it is crucial that available IPV be optimally allocated between routine immunization and mass campaigns. We recently published estimates of the impact of OPV mass campaigns with and without the inclusion of IPV in Nigeria and Pakistan during January 2014–April 2016 (4). These estimates demonstrated

a reduction in the incidence of poliomyelitis and detection of poliovirus in the environment after campaigns that used IPV in Nigeria but not in Pakistan, where statistical power was limited. We have now updated these estimates in Pakistan for January 2014–October 2017, thereby including a longer period of surveillance and additional campaigns during a period when wild-type 1 poliovirus has been circulating (online Technical Appendix, https://wwwnc.cdc.gov/EID/article/24/11/18-0050-Techapp1.pdf). We find evidence of an impact of campaigns that used IPV alongside OPV (bivalent, trivalent, or monovalent) on the incidence of poliomyelitis caused by wild-type poliovirus (incidence rate ratio [IRR] for 90 days after compared with before the campaign, IRR 0.62, 90% bootstrap CI 0.23–1.14), and a significant impact on the detection of this virus in environmental samples (prevalence ratio [PR] 0.63, 90% CI 0.47–0.81) (Figure; online Technical Appendix Table). The effect of campaigns using only bivalent OPV was less than the effect of campaigns that included IPV (IRR for poliomyelitis 0.79 [90% CI 0.64–0.98] and PR for environmental detection 0.92 [90% CI 0.83–1.00] for the 90 days after compared with before the campaign); this difference was statistically significant for detection of poliovirus in the environment (bootstrap p values 0.239 comparing the IRRs and 0.005 comparing the PRs for campaigns with and without IPV). We did not update estimates for Nigeria because only 2 campaigns using IPV occurred during April 2016–October 2017, in areas with very limited VDPV2 detection.

Several caveats relate to this analysis, reflecting its observational nature, reliance on routinely collected data, and lack of randomization. Campaigns that included IPV may have been implemented with different standards and, potentially, greater coverage, although data supporting this assertion have not been presented. It is often assumed that campaigns including IPV would have lower coverage because IPV must be administered by trained healthcare staff from fixed points rather than in house-to-house campaigns (5). Furthermore, these findings may not apply to more recent serotype-2 vaccine-derived poliovirus outbreaks, which have occurred in countries without recent use of a serotype-2–containing oral vaccine, thereby limiting boosting of mucosal immunity by IPV to older cohorts.

In conclusion, these updated estimates from Pakistan provide support for including IPV in mass campaigns with OPV to reduce poliovirus transmission, in agreement with results from Nigeria. Intradermal administration of a 1/5 fractional dose may allow dose sparing during these campaigns while maintaining comparable immunogenicity (6). These findings are informing discussions about the role of IPV in stopping the last remaining chains of wild-type 1 poliovirus transmission, responding to VDPV2 outbreaks, and protecting children who have not received vaccine containing serotype 2.
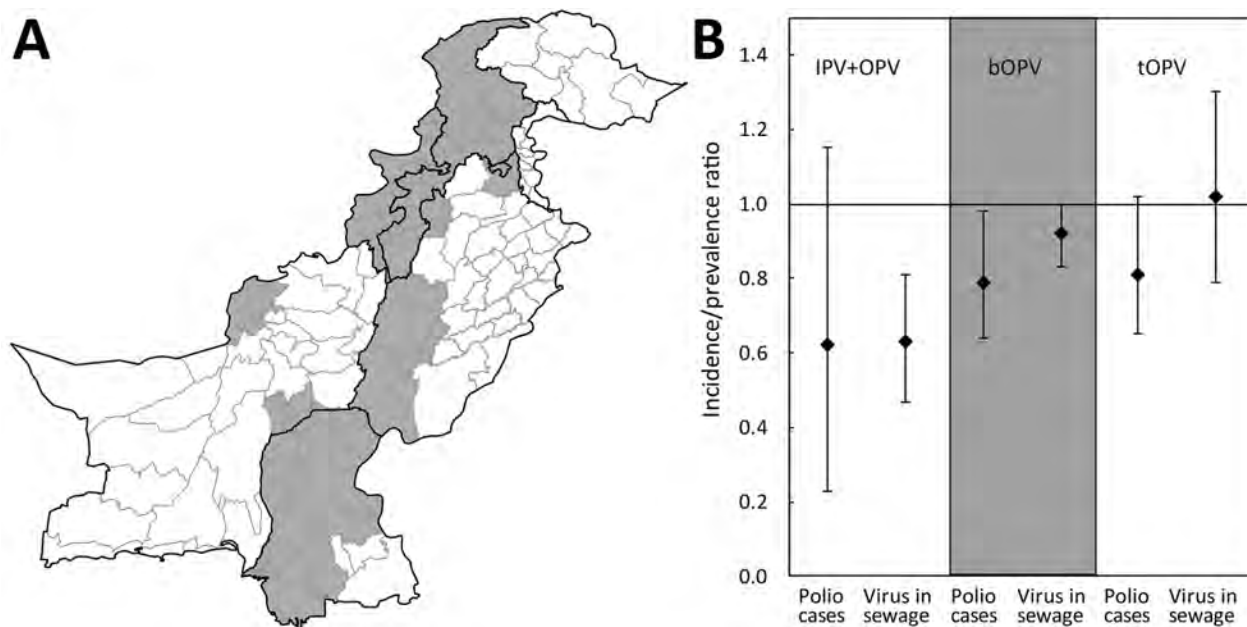
Figure. Location and impact of mass campaigns in Pakistan during January 2014–October 2017 that have included inactivated poliovirus vaccine (IPV) alongside oral vaccine. A) Gray shading indicates districts in Pakistan that conducted campaigns with IPV during January 2014–October 2017. B) The incidence rate ratio (IRR) for poliomyelitis and the prevalence ratio (PR) for poliovirus detection in environmental samples (sewage) during 90 days after compared with 90 days before mass vaccination campaigns with different vaccines. The mean estimates (diamonds) are shown with 90% bootstrap CIs (error bars). Detailed methods and results are given in the online Technical Appendix (https://wwwnc.cdc.gov/EID/article/24/11/18-0050-Techapp1.pdf). bOPV, bivalent oral poliovirus vaccine; IPV, inactivated poliovirus vaccine; tOPV, trivalent oral poliovirus vaccine.

Acknowledgments

About the Author

Dr. Grassly is a professor of vaccine epidemiology in the department of infectious disease epidemiology at Imperial College London, London, UK. His primary research interests are the epidemiology of enteric viruses and immune response to infection and vaccination.

References

1. World Health Organization. Meeting of the Strategic Advisory Group of Experts on Immunization, November 2012—conclusions and recommendations. Wkly Epidemiol Rec. 2013;88:1–16.
2. Lewis I, Ottosen A, Rubin J, Blanc DC, Zipursky S, Wootton E. A supply and demand management perspective on the accelerated global introductions of inactivated poliovirus vaccine in a constrained supply market. J Infect Dis. 2017;216(suppl 1):S33–9. http://dx.doi.org/10.1093/infdis/jiw550
3. Global Polio Eradication Initiative. Standard operating procedures: responding to a poliovirus event or outbreak. V2.3 01; 2017 [cited 2017 May 7]. http://www.polioeradication.org
4. Shirreff G, Wadood MZ, Vaz RG, Sutter RW, Grassly NC. Estimated effect of inactivated poliovirus vaccine campaigns, Nigeria and Pakistan, January 2014–April 2016. Emerg Infect Dis. 2017;23:258–63. http://dx.doi.org/10.3201/eid2302.161210
5. Pervaiz A, Mbaeyi C, Baig MA, Burman A, Ahmed JA, Akter S, et al. Fractional-dose inactivated poliovirus vaccine campaign—Sindh Province, Pakistan, 2016. MMWR Morb Mortal Wkly Rep. 2017;66:1295–9. http://dx.doi.org/10.15585/mmwr.mm6647a4
6. Okayasu H, Sein C, Chang Blanc D, Gonzalez AR, Zehrung D, Jarrahian C, et al. Intradermal administration of fractional doses of inactivated poliovirus vaccine: a dose-sparing option for polio immunization. J Infect Dis. 2017;216(suppl 1):S161–7. http://dx.doi.org/10.1093/infdis/jix038

Address for correspondence: Nicholas C. Grassly, Imperial College London, Department of Infectious Disease Epidemiology, Norfolk Place, W2 1PG, UK; email: n.grassly@imperial.ac.uk

Enterovirus D68 Surveillance, St. Louis, Missouri, USA, 2016

Mythili Srinivasan, Angela Niesen, Gregory A. Storch

Author affiliations: Washington University, St. Louis, Missouri, USA (M. Srinivasan, G. Storch); St. Louis Children's Hospital, St. Louis (A. Niesen)

A fall 2016 outbreak of enterovirus D68 infection in St. Louis, Missouri, USA, had less effect than a fall 2014 outbreak on hospital census, intensive care unit census, and hospitalization for a diagnosis of respiratory illness. Without ongoing surveillance and specific testing, these cases might have been missed.

The largest known outbreak of enterovirus D68 (EV-D68) occurred in the United States in 2014 (*1*). Severe respiratory illnesses increased in fall of 2014, corresponding to a period when EV-D68 was present in the community, at St. Louis Children's Hospital (St. Louis, Missouri, USA) and elsewhere in the United States (*1,2*). Multiple reports suggested that the predominant virus was from clade B1, although some viruses from clades B2 were also detected (*3–5*). During 2015, there were few reports of EV-D68 circulating in the United States (*6*); however, in 2016, EV-D68 reappeared in multiple US locations (New York, Colorado); virus sequences suggested that the predominant virus was from clade B3 (*4,7*). We also documented EV-D68 activity in St. Louis in 2016. Sequencing of viruses from 2 patients tested in the St. Louis Children's Hospital virology laboratory revealed clade B3 with 99% identity to the clade B3 virus from New York (*8*). Our goal with this study was to determine if the 2016 outbreak had caused an increase in hospital census or increase in patients admitted with respiratory diagnosis, as was seen during the 2014 outbreak.

During August 7, 2016, through December 16, 2016, we used a previously described EV-D68–specific PCR to test 5%–10% of enterovirus/rhinovirus–positive samples submitted each week to the St. Louis Children's Hospital diagnostic virology laboratory. The samples had been obtained from patients seen at the hospital's emergency department or clinics or admitted to the inpatient units and had been routinely tested by a FilmArray Respiratory Panel (BioFire, Salt Lake City, UT, USA) (*9*). Samples were selected by laboratory staff without regard to patient characteristics and were deidentified before EV-D68 testing. We obtained inpatient and intensive care unit (ICU) census data for all patients (not limited to those with a

respiratory diagnosis) and discharge diagnoses for hospitalized patients from the hospital's Health Information Management System, an administrative database, for 2013–2016.

Discharge diagnoses were categorized as respiratory or nonrespiratory. A respiratory diagnosis was defined as any principal diagnosis referring to disease processes of the respiratory tract (e.g., asthma exacerbation, bronchiolitis, respiratory distress, respiratory failure, pneumonia). We used the Pearson χ^2 test of independence to compare the frequency distribution of patients with a respiratory diagnosis in 2014 and 2016 with frequency of those in 2013 and 2015 combined. All analyses were done with SAS/STAT software version 9.4 for Windows (SAS Institute, Cary, NC, USA). The Washington University Institutional Review Board determined that this project did not meet the definition of human subject research and, as such, was not subject to institutional review board review.

During August 7–November 5, 2016, we tested a total of 4,190 samples by using the viral respiratory panel; 1,058 (25%) were positive for rhinovirus/enterovirus. Further testing of 179 samples positive for rhinovirus/enterovirus revealed that 19 (11%) were positive for EV-D68 (online Technical Appendix Figure, panel A, https://wwwnc.cdc.gov/EID/article/24/11/18-0397-Techapp1.pdf). During November 6–26, 2016, we tested 47 rhinovirus/enterovirus–positive samples, and 4/47 (9%) were positive for EV-D68. During November 27–December 10, 2016, we tested 33 rhinovirus/enterovirus–positive samples, and none were positive for EV-D68. We did not include EV-D68 testing data from November 6–December 10, 2016, in the online Technical Appendix Figure because of the difficulty in obtaining discharge diagnosis data (changes in registration systems affected data collection during that period).

In contrast to the experience in 2014, overall inpatient or ICU census did not increase during this outbreak except for a 1–2 week period in October (online Technical Appendix Figure, panels B–D). During August 7–November 5, 2014, the number and percentage of patients hospitalized with a respiratory diagnosis increased significantly (852/5,894, 14%) compared with the corresponding periods in 2013 and 2015 combined (1,156/10,958, 11%; p<0.0001). This increase in patients hospitalized with respiratory diagnoses in 2014 overlapped with the increase in EV-D68 activity in our hospital. In 2014, we tested 572 rhinovirus/enterovirus–positive specimens from August 3, 2104–October 31, 2014, and 159 (28%) were positive for EV-D68 (*2*). In contrast, the number and percentage of patients admitted with a respiratory diagnosis during August 7–November 5, 2016, decreased significantly (483/5,304, 9%) compared with the corresponding periods in 2013 and 2015 combined (p = 0.004).

The overall effects of the 2016 outbreak seem to have been less than those of the 2014 outbreak. The epidemiologic data from our hospital, which has a broad catchment area in the central United States, confirm that the period of EV-D68 activity in 2016 had less effect on hospital census, ICU census, and hospitalization for respiratory diagnosis than that in 2014. Although the measured parameters are relatively crude, we found no changes in data collection procedures that explain the observed differences, suggesting that the differences are the result of lower levels of EV-D68 circulation in the population in 2016. Our study suggests that surveillance using specific testing is needed to detect EV-D68 activity, which would have been missed if we had monitored only for increases in patients with respiratory diagnoses or hospital census.

Acknowledgments

About the Author
Dr. Srinivasan is a pediatric hospitalist at St. Louis Children's Hospital. Her research interest is the effects of EV-D68 in hospitalized children.

References
1. Midgley CM, Watson JT, Nix WA, Curns AT, Rogers SL, Brown BA, et al.; EV-D68 Working Group. Severe respiratory illness associated with a nationwide outbreak of enterovirus D68 in the USA (2014): a descriptive epidemiological investigation. Lancet Respir Med. 2015;3:879–87. http://dx.doi.org/10.1016/S2213-2600(15)00335-5
2. Orvedahl A, Padhye A, Barton K, O'Bryan K, Baty J, Gruchala N, et al. Clinical characterization of children presenting to the hospital with enterovirus D68 infection during the 2014 outbreak in St. Louis. Pediatr Infect Dis J. 2016;35:481–7. http://dx.doi.org/10.1097/INF.0000000000001060
3. Huang W, Wang G, Zhuge J, Nolan SM, Dimitrova N, Fallon JT. Whole-genome sequence analysis reveals the enterovirus D68 isolates during the United States 2014 outbreak mainly belong to a novel clade. Sci Rep. 2015;5:15223. http://dx.doi.org/10.1038/srep15223
4. Wang G, Zhuge J, Huang W, Nolan SM, Gilrane VL, Yin C, et al. Enterovirus D68 subclade B3 strain circulating and causing an outbreak in the United States in 2016. Sci Rep. 2017;7:1242. http://dx.doi.org/10.1038/s41598-017-01349-4
5. Wylie KM, Wylie TN, Orvedahl A, Buller RS, Herter BN, Magrini V, et al. Genome sequence of enterovirus D68 from St. Louis, Missouri, USA. Emerg Infect Dis. 2015;21:184–6. http://dx.doi.org/10.3201/eid2101.141605
6. Abedi GR, Watson JT, Nix WA, Oberste MS, Gerber SI. Enterovirus and parechovirus surveillance—United States, 2014–2016. MMWR Morb Mortal Wkly Rep. 2018;67:515–8. http://dx.doi.org/10.15585/mmwr.mm6718a2
7. Messacar K, Robinson CC, Pretty K, Yuan J, Dominguez SR. Surveillance for enterovirus D68 in Colorado children reveals continued circulation. J Clin Virol. 2017;92:39–41.
8. Wylie KM, Wylie TN, Storch GA. Genome sequence of enterovirus D68 from St. Louis, Missouri, USA, 2016. Genome

Announc. 2017;5:e01630-16. http://dx.doi.org/10.1128/genomeA.01630-16

9. Wylie TN, Wylie KM, Buller RS, Cannella M, Storch GA. Development and evaluation of an enterovirus D68 real-time reverse transcriptase polymerase chain reaction (RT-PCR) assay. J Clin Microbiol. 2015;53:2641–7. http://dx.doi.org/10.1128/JCM.00923-15

Address for correspondence: Mythili Srinivasan, Washington University School of Medicine, St. Louis Children's Hospital, Department of Pediatrics, One Children's Place, NWT 9113, St. Louis, MO 63110, USA; email: srinivasan_m@kids.wustl.edu

Adenovirus-Associated Influenza-Like Illness among College Students, Pennsylvania, USA

Holly M. Biggs, Xiaoyan Lu, Lisa Dettinger, Senthilkumar Sakthivel, John T. Watson, Sameh W. Boktor

Author affiliations: Centers for Disease Control and Prevention, Atlanta, Georgia, USA (H.M. Biggs, X. Lu, J.T. Watson); Pennsylvania Department of Health, Harrisburg, Pennsylvania, USA (L. Dettinger, S. Boktor); Batelle, Atlanta (S. Sakthivel)

Among students with influenza-like illness at a Pennsylvania college student health center during 2016–2017, 44 (15%) of 288 with respiratory specimens tested positive for human adenovirus (HAdV). HAdV-3, -7, and -4 predominated, and types clustered temporally. HAdV infection should be considered among college students with acute respiratory illness.

Human adenoviruses (HAdVs) cause a range of clinical manifestations, most commonly acute respiratory illness (ARI), gastroenteritis, and conjunctivitis. Seven HAdV species (A–G) and >80 types are known to cause human infection, and certain HAdV types are associated with particular tissue tropisms and clinical syndromes (1). Outbreaks of HAdV infection occur in a variety of settings, including schools, long-term care facilities, military recruit training facilities, and the civilian community (2–4). The substantial impact of HAdV ARI among US military recruits drove development of the first live oral vaccine for HAdV types 4 and 7 for military use. After vaccine introduction in 1971, and again after reintroduction in 2011, dramatic declines were documented in respiratory illness among recruits (5). Currently, the HAdV vaccine for types 4 and 7 is licensed in the United States for use in military personnel 17–50 years of age and is administered routinely at all US basic military training sites (5). However, despite some similarities between military recruits and civilian college students, including age and sharing of residences, little is known about the contribution of HAdV to respiratory illness in college students.

The Pennsylvania Department of Health (PDH) conducts surveillance for influenza-like illness (ILI), defined as fever (temperature ≥100°F [≥37.8°C]) plus cough or sore throat without a known cause other than influenza, at participating outpatient healthcare facilities throughout the state. Basic demographic information is recorded, and from a convenience sample of cases, a nasopharyngeal swab specimen is collected. These specimens are tested by the PDH Bureau of Laboratories using Centers for Disease Control and Prevention (CDC) real-time reverse transcription PCR for influenza A and B, HAdV, respiratory syncytial virus, human metapneumovirus, rhinovirus, and parainfluenza virus types 1–3.

We describe HAdV types associated with ILI among students who sought care at a student health center (SHC) on a large college campus during August 28, 2016–August 26, 2017. Specimens identified as HAdV-positive among students with ILI at the SHC were sent to CDC to determine HAdV species and type. Molecular typing was performed by PCR and sequencing of the hexon hypervariable regions 1–6 (6).

During the study period, 1,149 ILI cases were reported from the SHC; for 288 (25%), a nasopharyngeal swab specimen was tested for respiratory viruses (Figure, panel A). Of these, 44 (15%) specimens were positive for HAdV. Three HAdV species and 4 HAdV types were detected: HAdV-3 and HAdV-7 of species HAdV-B in 21 (48%) and 16 (36%), respectively; HAdV-4 of species HAdV-E in 5 (11%); and HAdV-1 of species HAdV-C in 2 (5%). The median age of HAdV-positive students was 19 years (range 18–27 years), and 31 (70%) were male. Among HAdV-positive specimens, rhinovirus was co-detected in 4 and parainfluenza virus type 2 in 1.

HAdV-3 was identified during September–December; no additional HAdV-3 was identified after the 4-week winter break. HAdV-7 and -4 were first detected in December, before winter break, then throughout the spring; HAdV-7 was the most commonly detected type during this period (Figure, panel B).
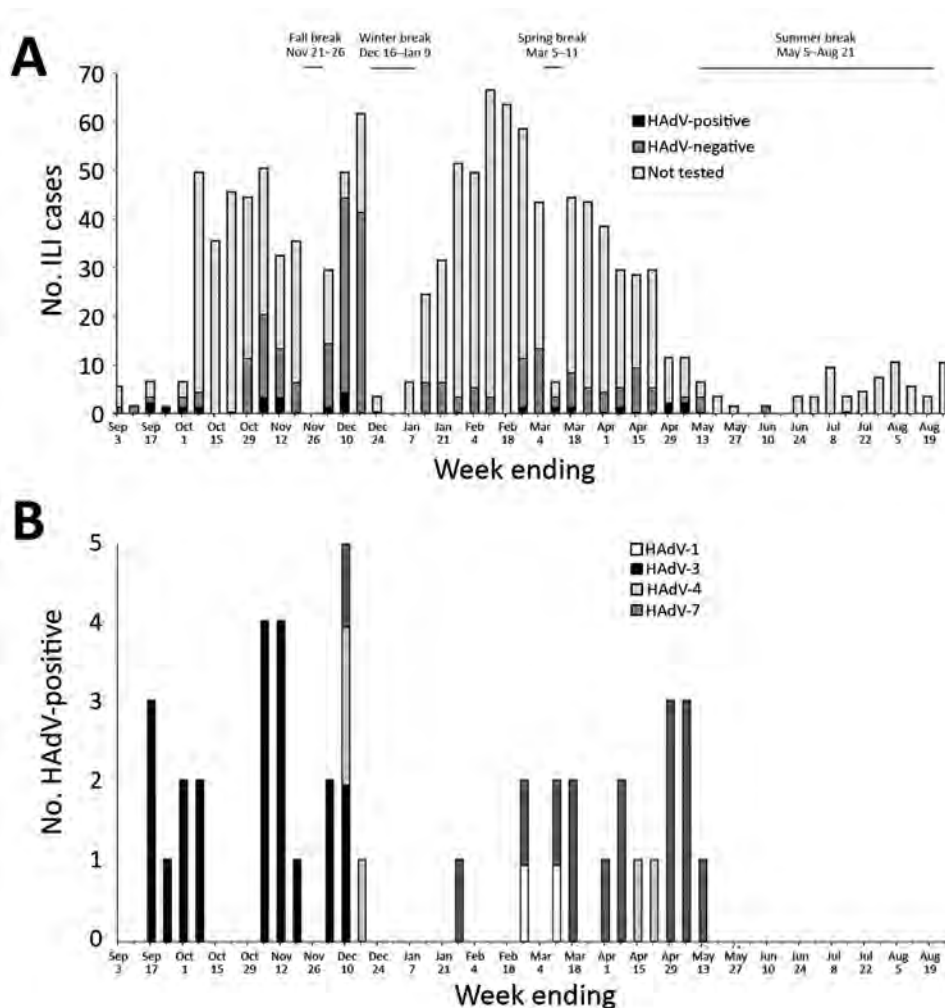
Figure. Adenovirus-associated ILI among students at a state college, Pennsylvania, USA, August 28, 2016–August 26, 2017. A) ILI cases from the student health center (SHC) and weekly number of human adenovirus (HAdV)–positive, –negative, and not tested cases. B) HAdV types identified from the SHC. HAdV detections were aggregated by epidemiologic week based on specimen collection date. Fall semester 2016 began August 22, 2016; spring semester 2017 ended May 5, 2017; fall semester 2017 began August 21, 2017. ILI, influenza-like illness.

The HAdV types detected from the SHC are recognized causes of ARI. HAdV-3 was the most commonly reported HAdV type in the United States during 2003–2013 (7). HAdV-4 and -7 are increasingly recognized as causes of respiratory illness in the community and other nonmilitary populations (7–9); HAdV-7, in particular, has been associated with severe respiratory illness in adults. A male predominance was observed among HAdV-positive students at the SHC; this finding has been previously described, but its significance is unknown (2,4).

HAdVs circulate throughout the year without a discernable seasonality, although some reports describe a winter and spring predominance of respiratory outbreaks (1). The temporal clustering of types that we observed might reflect transmission dynamics within the college population rather than viral seasonal patterns per se; however, additional surveillance may help further define circulation patterns of HAdV types (8). In a comparable report from New York, during the 2014–15 influenza season, ≈8% of samples tested from students with ILI at 1 college were

positive for HAdV; HAdV-14 and -4 were most frequently detected (10).

Our findings are subject to several limitations. Specimens tested for respiratory viruses represent a convenience sample of ILI cases, and the proportion sampled varied by week. We report findings from surveillance at a single college SHC; phylogenetic analysis of hexon sequences was not conducted, preventing comparisons between the detected virus strains and those reported to circulate in military or other civilian communities.

Although recruits at basic military training are recognized to be at risk for infection with HAdV, less is known about the risk for HAdV in nonmilitary congregate settings. We detected HAdV in a substantial proportion of ILI cases among a convenience sample of young adults at an SHC surveillance site at a large university during the 2016–17 academic year. Understanding the effects of HAdV respiratory illness on college campuses, including severity, missed class time, and occurrence of outbreaks, would be useful in assessing potential control measures in these settings.

Acknowledgments

About the Author

Dr. Biggs is a medical epidemiologist with the Division of Viral Diseases, National Center for Immunization and Respiratory Diseases, CDC. Her interests include respiratory virus surveillance and outbreak response.

References

1. Lion T. Adenovirus infections in immunocompetent and immunocompromised patients. Clin Microbiol Rev. 2014;27: 441–62. PubMed http://dx.doi.org/10.1128/CMR.00116-13
2. Centers for Disease Control and Prevention. Civilian outbreak of adenovirus acute respiratory disease—South Dakota, 1997. MMWR Morb Mortal Wkly Rep. 1998;47:567–70.
3. Kandel R, Srinivasan A, D'Agata EM, Lu X, Erdman D, Jhung M. Outbreak of adenovirus type 4 infection in a long-term care facility for the elderly. Infect Control Hosp Epidemiol. 2010;31:755–7. PubMed http://dx.doi.org/10.1086/653612
4. Lewis PF, Schmidt MA, Lu X, Erdman DD, Campbell M, Thomas A, et al. A community-based outbreak of severe respiratory illness caused by human adenovirus serotype 14. J Infect Dis. 2009;199:1427–34. PubMed http://dx.doi.org/10.1086/598521
5. Radin JM, Hawksworth AW, Blair PJ, Faix DJ, Raman R, Russell KL, et al. Dramatic decline of respiratory illness among US military recruits after the renewed use of adenovirus vaccines. Clin Infect Dis. 2014;59:962–8. PubMed http://dx.doi.org/10.1093/cid/ciu507
6. Lu X, Erdman DD. Molecular typing of human adenoviruses by PCR and sequencing of a partial region of the hexon gene. Arch Virol. 2006;151:1587–602. PubMed http://dx.doi.org/10.1007/s00705-005-0722-7
7. Binder AM, Biggs HM, Haynes AK, Chommanard C, Lu X, Erdman DD, et al. Human adenovirus surveillance—United States, 2003–2016. MMWR Morb Mortal Wkly Rep. 2017;66:1039–42. PubMed http://dx.doi.org/10.15585/mmwr.mm6639a2
8. Scott MK, Chommanard C, Lu X, Appelgate D, Grenz L, Schneider E, et al. Human adenovirus associated with severe respiratory infection, Oregon, USA, 2013–2014. Emerg Infect Dis. 2016;22:1044–51. PubMed http://dx.doi.org/10.3201/eid2206.151898
9. Kajon AE, Lamson DM, Bair CR, Lu X, Landry ML, Menegus M, et al. Adenovirus type 4 respiratory infections among civilian adults, northeastern United States, 2011–2015. Emerg Infect Dis. 2018;24:201–9. PubMed http://dx.doi.org/10.3201/eid2402.171407
10. Lamson DM, Kajon A, Shudt M, Girouard G, St George K. Detection and genetic characterization of adenovirus type 14 strain in students with influenza-like illness, New York, USA, 2014–2015. Emerg Infect Dis. 2017;23:1194–7. http://dx.doi.org/10.3201/eid2307.161730

Address for correspondence: Holly M. Biggs, Centers for Disease Control and Prevention, 1600 Clifton Rd NE, Mailstop A34, Atlanta, GA 30329-4027, USA; email: hbiggs@cdc.gov

Investigating the Role of Easter Island in Migration of Zika Virus from South Pacific to Americas

Edson Delatorre, Jorge Fernández, Gonzalo Bello

Author affiliations: Instituto Oswaldo Cruz/Fiocruz, Rio de Janeiro, Brazil (E. Delatorre, G. Bello); Public Health Institute of Chile, Santiago, Chile (J. Fernández)

The role of Easter Island in the dissemination of Zika virus from the Pacific islands into the Americas remains unclear. We analyzed new Zika virus sequences from Eastern Island and found that Zika virus was independently disseminated from French Polynesia into the Americas and Easter Island at around the same time.

Zika virus is a mosquitoborne flavivirus associated with several recent outbreaks in human populations in the Pacific region and the Americas. Phylogeographic studies indicate that Zika virus strains circulating in South Pacific islands and Latin America comprise a single lineage (ZIKV$_{SP-AM}$) that arose because of sequential single viral disseminations from Southeast Asia into French Polynesia and from the South Pacific into Latin America (1–5). However, whether the ancestral Zika virus strain introduced into the Americas arose directly from French Polynesia or from another South Pacific island is unclear.

In early 2014, a Zika virus outbreak occurred in Easter Island (6), months before the first identification of Zika virus in Brazil (7). Easter Island is located at the southeastern edge of the Polynesian Triangle, roughly equidistant from French Polynesia and the South America mainland. Geographic position and intense touristic activity make Easter Island a potential staging post in the spread of Zika virus from French Polynesia to continental America. This hypothesis was suggested previously (4), but the study used a limited sequence dataset. We tested this hypothesis by using a more comprehensive dataset of Zika virus sequences from the South Pacific.

Blood samples from suspected Zika virus–infected human patients who visited the emergency unit of Hanga Roa Hospital on Easter Island during January–May 2014 were sent to the Public Health Institute of Chile for characterization, according to Ministry of Health of Chile guidelines for surveillance of transmissible diseases. The complete E and partial NS5 genes of 7 Zika virus strains were obtained as previously described (6). The concatenated fragments were aligned with Zika virus Asian genotype sequences available in GenBank and used for spatiotemporal viral diffusion

reconstruction (online Technical Appendix, https://wwwnc.cdc.gov/EID/article/24/11/18-0586-Techapp1.pdf).

The overall timescale of the phylogenetic tree estimated for Zika virus Asian genotype strains was fully consistent with previous reports (*1–5*; online Technical Appendix Table 2). Asymmetric (online Technical Appendix Figure 1) and symmetric (online Technical Appendix Figure 2) phylogeographic models placed the most recent common ancestor of the Asian genotype epidemic strains in Southeast Asia (posterior state probability [PSP] $\geq$0.96) at 1999 (Bayesian credible interval [BCI] 1996–2002) and support 2 independent disseminations from Southeast Asia into the Pacific region—the first in Micronesia around 2007, with no further spread, and the second originating the $ZIKV_{SP-AM}$ lineage that fueled epidemics during 2013–2016 in the South Pacific and the Americas.

The origin of the $ZIKV_{SP-AM}$ lineage was traced to French Polynesia (PSP $\geq$0.98) at 2013.3 (BCI 2012.9–2013.6). This lineage exhibits strong geographic subdivision; several highly supported island-specific monophyletic subclades nested among basal strains from French Polynesia (*5*), besides the $ZIKV_{AM}$ subclade (online Technical Appendix Figures 1, 2). We found 2 major clades within the $ZIKV_{SP-AM}$; clade I (posterior probability [PP] 0.97) contains strains from French Polynesia, the Americas, New Caledonia, and Vanuatu, whereas clade II (PP $\geq$0.94) encloses strains from Easter Island and the Cook Islands. Zika virus strains from Fiji, American Samoa, Samoa, Tonga, and the Solomon Islands branched together in a large but not well-supported (PP $\leq$0.57) monophyletic group.

French Polynesia was the most probable source location of the Zika virus clade I strains introduced into the Americas (PSP 1), Vanuatu (PSP 1), and New Caledonia (PSP $\geq$0.98), as well as of the clade II strain introduced into Easter Island (PSP $\geq$0.77), refuting the hypothesis of introduction of Zika virus into the Americas through Easter Island. The source location of the clade II strain of the Cook Islands was traced to French Polynesia (PSP >0.34) or Easter Island (PSP $\geq$0.37). Our analyses indicate that Zika virus was introduced into Easter Island, New Caledonia, the Cook Islands, and the Americas at around the same time (BCI 2013.6–2014.8), supporting a much longer period of undetected Zika virus transmission in the Americas ($\approx$15 months) (*7,8*) than in those South Pacific islands (<1 month) (*8*). Zika virus also spread from French Polynesia into Samoa, Fiji, Tonga, and American Samoa from late 2015 to early 2016, probably following a stepping-stone process (online Technical Appendix Figures 1, 2). Migratory routes between those islands, however, were difficult to resolve (inconsistency between phylogeographic models) or do not fully agree with epidemiologic data (e.g. the dissemination from Tonga to Fiji) (*8*).

Our results indicate that French Polynesia was the main hub of dissemination of the $ZIKV_{SP-AM}$ lineage and seeded independent outbreaks in several South Pacific islands (including Easter Island) and the Americas from late 2013 to mid-2014, coinciding with a peak in the number of suspected Zika cases in French Polynesia. The long period of cryptic circulation of Zika virus in the Americas, the early detection of Zika virus in the Caribbean in December 2014 (*4*), and the reported dissemination of dengue (*9*) and chikungunya (*10*) viruses from French Caribbean territories into French Polynesia during 2013–2014 support the hypothesis that Zika virus might have been introduced to and circulated in the Caribbean region for several months before its detection in Brazil in 2015. Human movement between overseas French territories might create an epidemiologic link for arboviral transmissions between the South Pacific and the Caribbean region.

About the Author

Dr. Delatorre is a postdoctoral fellow at the AIDS and Molecular Immunology Laboratory, Oswaldo Cruz Institute, Oswaldo Cruz Foundation, Brazil. His research interests include the evolution and phylodynamics of viruses, including Zika virus.

References

1. Faria NR, Azevedo RDSDS, Kraemer MUG, Souza R, Cunha MS, Hill SC, et al. Zika virus in the Americas: early epidemiological and genetic findings. Science. 2016;352:345–9. http://dx.doi.org/10.1126/science.aaf5036
2. Faria NR, Quick J, Claro IM, Thézé J, de Jesus JG, Giovanetti M, et al. Establishment and cryptic transmission of Zika virus in Brazil and the Americas. Nature. 2017;546:406–10. http://dx.doi.org/10.1038/nature22401
3. Metsky HC, Matranga CB, Wohl S, Schaffner SF, Freije CA, Winnicki SM, et al. Zika virus evolution and spread in the Americas. Nature. 2017;546:411–5. http://dx.doi.org/10.1038/nature22402
4. Lednicky J, Beau De Rochars VM, El Badry M, Loeb J, Telisma T, Chavannes S, et al. Zika virus outbreak in Haiti in 2014: molecular and clinical data. PLoS Negl Trop Dis. 2016;10:e0004687.
5. Dupont-Rouzeyrol M, Diancourt L, Calvez E, Vandenbogaert M, O'Connor O, Teissier A, et al. Zika virus evolution on the edges of the Pacific Ocean. Emerg Microbes Infect. 2017;6:e111.
6. Tognarelli J, Ulloa S, Villagra E, Lagos J, Aguayo C, Fasce R, et al. A report on the outbreak of Zika virus on Easter Island, South Pacific, 2014. Arch Virol. 2016;161:665–8. http://dx.doi.org/10.1007/s00705-015-2695-5
7. Campos GS, Bandeira AC, Sardi SI. Zika virus outbreak, Bahia, Brazil. Emerg Infect Dis. 2015;21:1885–6. http://dx.doi.org/10.3201/eid2110.150847
8. Petersen LR, Jamieson DJ, Powers AM, Honein MA. Zika virus. N Engl J Med. 2016;374:1552–63. http://dx.doi.org/10.1056/NEJMra1602113

9. Cao-Lormeau V-M, Roche C, Musso D, Mallet H-P, Dalipanda T, Dofai A, et al. Dengue virus type 3, South Pacific Islands, 2013. Emerg Infect Dis. 2014;20:1034–6. http://dx.doi.org/10.3201/eid2006.131413

10. Aubry M, Teissier A, Roche C, Richard V, Yan AS, Zisou K, et al. Chikungunya outbreak, French Polynesia, 2014. Emerg Infect Dis. 2015;21:724–6. http://dx.doi.org/10.3201/eid2104.141741

Address for correspondence: Edson Delatorre, Laboratório de AIDS & Imunologia Molecular, Instituto Oswaldo Cruz - FIOCRUZ. Av. Brasil 4365, Manguinhos, 21040-360, Rio de Janeiro, RJ, Brazil; email: delatorre.ioc@gmail.com or edsonod@ioc.fiocruz.br

Novel Multidrug-Resistant *Cronobacter sakazakii* Causing Meningitis in Neonate, China, 2015

Haiyan Zeng,[1] Tao Lei,[1] Wenjing He,[1] Jumei Zhang, Bingshao Liang, Chengsi Li, Na Ling, Yu Ding, Shi Wu, Juan Wang, Qingping Wu

Author affiliations: Guangdong Institute of Microbiology, Guangzhou, China (H. Zeng, T. Lei, W. He, J. Zhang, C. Li, N. Ling, S. Wu, Q. Wu); Guangzhou Women and Children's Medical Center, Guangzhou (B. Liang); Jinan University, Guangzhou (Y. Ding); South China Agricultural University, Guangzhou (J. Wang)

We report a case of meningitis in a neonate in China, which was caused by a novel multidrug-resistant *Cronobacter sakazakii* strain, sequence type 256, capsular profile K1:CA1. We identified genetic factors associated with bacterial pathogenicity and antimicrobial drug resistance in the genome and plasmids. Enhanced surveillance of this organism is warranted.

*C*ronobacter sakazakii* is a foodborne pathogen associated with outbreaks of life-threatening necrotizing enterocolitis, meningitis, and sepsis in neonates and infants. Although the incidence of *C. sakazakii* infection is low, fatality rates range from 40% to 80% (*1*). Infections are usually limited to specific sequence types (STs) and complex clonal complexes (*2–4*). *C. sakazakii* ST4 is

predominantly associated with meningitis in neonates; *C. sakazakii* ST12, with necrotizing enterocolitis in neonates (*2*,*3*). *C. sakazakii* is usually resistant to cephalothin and penicillin but is more sensitive to antimicrobial drugs than are other members of the family *Enterobacteriaceae*. Few reports describe drug-resistance patterns in *C. sakazakii* isolates (*4–6*). We report 1 multidrug-resistant (MDR) *C. sakazakii* ST256 strain that caused meningitis in a neonate in China.

On September 29, 2015, a 26-day-old boy, who was born after 38 weeks' gestation and had abdominal distention, fever, and jaundice, was hospitalized in a children's hospital in Guangzhou, China. He was fed breast milk; however, it could not be determined whether he had been exclusively breast-fed or whether the breast milk had been expressed by use of a pump. His cerebrospinal fluid contained numerous leukocytes, and his cerebrum contained abscesses. After a series of symptomatic treatments, including initial intravenous ceftazidime followed by meropenem, his clinical signs gradually improved. However, when discharged from the hospital after 3 weeks, his mental and physical development were remarkably impaired.

Cronobacter, isolated from brain abscess fluid, was identified by using an automated VITEK 2 Compact system (bioMérieux, Marcy l'Etoile, France). An isolate, GZcsf-1, was determined to be *C. sakazakii* ST256 with serotype O1. The *Cronobacter* PubMLST (https://pubmlst.org/cronobacter/) contains 2 ST256 isolates: MOD1-Ls15 g, isolated from the alimentary canal of the green bottle fly, *Lucilia sericata*, in the United States; and 2061 (no source information), detected in France. This ST had not been reported to cause meningitis in neonates. Susceptibility to 15 antimicrobials was tested by using the broth dilution method; MICs are shown in the online Technical Appendix (https://wwwnc.cdc.gov/EID/article/24/11/18-0718-Techapp1.pdf). GZcsf-1 was resistant to 8 antimicrobials: ampicillin, cefazolin, ceftriaxone, aztreonam, gentamicin, tetracycline, chloramphenicol, and trimethoprim/sulfamethoxazole.

The Beijing Genomics Institute performed genomic and plasmid DNA sequencing by using the PacBio RS II (Pacific Biosciences, Menlo Park, CA, USA) and HiSeq (Illumina, San Diego, CA, USA) platforms. The annotations were performed as previously described (*7*). *C. sakazakii* GZcsf-1 had 1 circular chromosome, 4.43 Mb long, containing 56.87% GC and 2 plasmids (denoted pGW1, 340,723 bp, 57.2% GC; pGW2, 135,306 bp, 54.0% GC) (GenBank accession nos. CP028974–6). On the basis of the characteristics of K antigen and colanic acid biosynthesis encoding genes in GZcsf-1, we determined its capsular profile to be K1:CA1, which differs from the capsular profile K2:CA2, proposed to be strongly associated with *C. sakazakii* isolated from neonates with severe infection (*3*). The subtype I-E
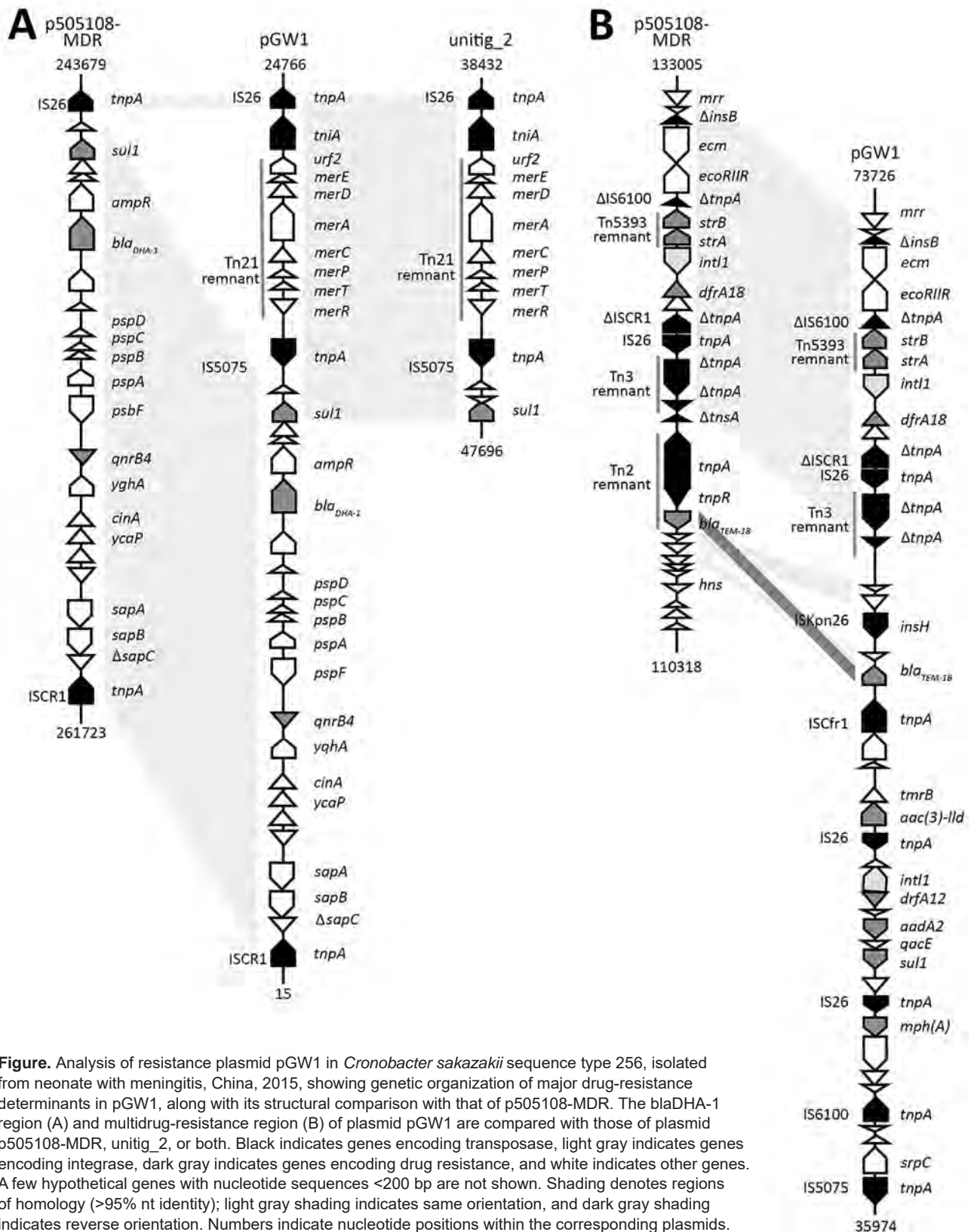

Figure. Analysis of resistance plasmid pGW1 in *Cronobacter sakazakii* sequence type 256, isolated from neonate with meningitis, China, 2015, showing genetic organization of major drug-resistance determinants in pGW1, along with its structural comparison with that of p505108-MDR. The blaDHA-1 region (A) and multidrug-resistance region (B) of plasmid pGW1 are compared with those of plasmid p505108-MDR, unitig_2, or both. Black indicates genes encoding transposase, light gray indicates genes encoding integrase, dark gray indicates genes encoding drug resistance, and white indicates other genes. A few hypothetical genes with nucleotide sequences <200 bp are not shown. Shading denotes regions of homology (>95% nt identity); light gray shading indicates same orientation, and dark gray shading indicates reverse orientation. Numbers indicate nucleotide positions within the corresponding plasmids.

CRISPR-Cas system and CRISPR1 to CRISPR3 arrays were detected (*7*).

We identified mobile elements and different types of secretion systems by using VRprofile (http://202.120.12.134/STEP/STEP_VR.html) (online Technical Appendix). Although virulence genes in *C. sakazakii* have not yet been clarified, T4SS, T6SS, and prophages may contribute to the pathogenicity of GZcsf-1. More importantly, full-plasmid comparison by blastn (http://blast.ncbi.nlm.nih.gov/Blast.cgi) revealed pGW2 to be closely related to IncFIB-type plasmid pESA3, which has been widely identified as a virulence plasmid in pathogenic strains of *C. sakazakii* (*8*).

We identified drug-resistance genes by using ResFinder 2.1 (https://cge.cbs.dtu.dk/services/ResFinder-2.1/). Except for 2 drug-resistance genes in the genome, 19 were integrated in pGW1, indicating that the MDR phenotype of *C. sakazakii* GZcsf-1 resulted from plasmid-mediated resistance (online Technical Appendix). By performing plasmid multilocus sequence typing (https://pubmlst.org/bigsdb?db=pubmlst_plasmid_seqdef&page=sequenceQuery), we determined that pGW1 is IncHI2-ST1 and is mainly found in other countries (*9*). Full-plasmid comparison revealed that pGW1 is closely related to p505108-MDR (*5*).

The drug-resistance gene bla_{DHA-1}, encoding an AmpC β-lactamase and conferring cephalosporin resistance, was found in pGW1 (Figure, panel A). According to a previous report, this gene is associated with ISCR1 (*10*). The difference between the 2 plasmids pGW1and p505108-MDR was in the insertion of a 7-kb fragment, associated with mercury resistance, between *sul1* and IS26 in pGW1 (Figure, panel A). This fragment was also detected in plasmid unitig_2, implying that there might be a transposition or homologous recombination. Of 19 drug-resistance genes, 9 (47.4%) were integrated in the MDR region of pGW1 (Figure, panel B). The fragment from Tn3 remnant to *mrr* gene in pGW1 was identical to that in p505108-MDR. Compared with the Tn2 remnant in p505108-MDR, only bla_{TEM-1B} in reverse orientation was conserved in pGW1. We found 5 new drug-resistance genes in pGW1—*mph(A)*, *sul1*, *aadA2*, *dfrA12*, and *aac(3)-IId*—adjacent to IS26, IS5075, and ISCfr1, constituting new accessory modules. Mobilization of these accessory resistance modules into plasmid backbones may be promoted by transposition and homologous recombination.

This study provides a new insight into *C. sakazakii* pathovars and raises concern that plasmid-mediated MDR *C. sakazakii* maybe a threat to infant health. Enhanced surveillance of antimicrobial drug–resistant *Cronobacter* is warranted.

About the Author

Dr. Zeng is an assistant professor at Guangdong Institute of Microbiology, Guangzhou, Guangdong Province, China. Her research is focused on adaptive evolution, drug resistance, and pathogenesis of *Cronobacter*.

References

1. Bowen AB, Braden CR. Invasive *Enterobacter sakazakii* disease in infants. Emerg Infect Dis. 2006;12:1185–9. http://dx.doi.org/10.3201/eid1208.051509
2. Baldwin A, Loughlin M, Caubilla-Barron J, Kucerova E, Manning G, Dowson C, et al. Multilocus sequence typing of *Cronobacter sakazakii* and *Cronobacter malonaticus* reveals stable clonal structures with clinical significance which do not correlate with biotypes. BMC Microbiol. 2009;9:223. http://dx.doi.org/10.1186/1471-2180-9-223
3. Ogrodzki P, Forsythe SJ. DNA-sequence based typing of the *Cronobacter* genus using MLST, CRISPR-*cas* array and capsular profiling. Front Microbiol. 2017;8:1875. http://dx.doi.org/10.3389/fmicb.2017.01875
4. Cui JH, Yu B, Xiang Y, Zhang Z, Zhang T, Zeng YC, et al. Two cases of multi-antibiotic resistant *Cronobacter* spp. infections of infants in China. Biomed Environ Sci. 2017;30:601–5.
5. Shi L, Liang Q, Zhan Z, Feng J, Zhao Y, Chen Y, et al. Co-occurrence of 3 different resistance plasmids in a multi-drug resistant *Cronobacter sakazakii* isolate causing neonatal infections. Virulence. 2018;9:110–20. http://dx.doi.org/10.1080/21505594.2017.1356537
6. Liu BT, Song FJ, Zou M, Hao ZH, Shan H. Emergence of colistin resistance gene *mcr-1* in *Cronobacter sakazakii* producing NDM-9 and *Escherichia coli* from the same animal. Antimicrob Agents Chemother. 2017;61:e01444-16.
7. Zeng H, Zhang J, Li C, Xie T, Ling N, Wu Q, et al. The driving force of prophages and CRISPR-Cas system in the evolution of *Cronobacter sakazakii*. Sci Rep. 2017;7:40206. http://dx.doi.org/10.1038/srep40206
8. Joseph S, Desai P, Ji Y, Cummings CA, Shih R, Degoricija L, et al. Comparative analysis of genome sequences covering the seven *Cronobacter* species. PLoS One. 2012;7:e49455. http://dx.doi.org/10.1371/journal.pone.0049455
9. Haenni M, Saras E, Ponsin C, Dahmen S, Petitjean M, Hocquet D, et al. High prevalence of international ESBL CTX-M-15-producing *Enterobacter cloacae* ST114 clone in animals. J Antimicrob Chemother. 2016;71:1497–500. http://dx.doi.org/10.1093/jac/dkw006
10. Guo Q, Spychala CN, McElheny CL, Doi Y. Comparative analysis of an IncR plasmid carrying *armA, blaDHA-1* and *qnrB4* from *Klebsiella pneumoniae* ST37 isolates. J Antimicrob Chemother. 2016;71:882–6. http://dx.doi.org/10.1093/jac/dkv444

Address for correspondence: Qingping Wu, Guangdong Institute of Microbiology, State Key Laboratory of Applied Microbiology Southern China, Guangdong Provincial Key Laboratory of Microbiology Culture Collection and Application, Guangdong Open Laboratory of Applied Microbiology, Xianlie Zhong Rd 100, Guangzhou 510070, Guangdong Province, China; email: wuqp203@163.com

etymologia

Ronnie Henry

Cronobacter sakazakii [kro'no-bak"tər sak'ə-zak"ee-ī]

The first documented isolation of what would become known as *Cronobacter sakazakii* was from a can of dried milk in 1950, although these organisms have likely existed for millions of years. In 1980, John J. Farmer III, proposed the name *Enterobacter sakazakii* for what had been known as "yellow-pigmented *E. cloacae*," in honor of Japanese bacteriologist Riichi Sakazaki. Over the next decades, *E. sakazakii* was implicated in scores of cases of meningitis and sepsis among infants, frequently in association with powdered infant formula. In 2007, the genus *Cronobacter* was created to accommodate the biogroups of *E. sakazakii*, with *C. sakazakii* as the type species. The genus was named for Cronos, the Titan of Greek myth, who devoured his children as they were born.
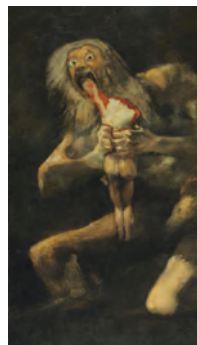
Francisco Goya (1746–1828), *Saturn Devouring His Son*, 1819–1823, oil mural transferred to canvas, via Wikimedia Commons.

Sources

1. Farmer JJ III. My 40-year history with *Cronobacter/Enterobacter sakazakii*—lessons learned, myths debunked, and recommendations. Front Pediatr. 2015;3:84. http://dx.doi.org/10.3389/fped.2015.00084
2. Farmer JJ, Asbury MA, Hickman FW, Brenner DJ. The *Enterobacteriaceae* Study Group. *Enterobacter sakazakii*: a new species of "Enterobacteriaceae" isolated from clinical specimens. Int J Syst Evol Microbiol. 1980;30:569–84.
3. Iversen C, Mullane N, McCardell B, Tall BD, Lehner A, Fanning S, et al. *Cronobacter* gen. nov., a new genus to accommodate the biogroups of *Enterobacter sakazakii*, and proposal of *Cronobacter sakazakii* gen. nov., comb. nov., *Cronobacter malonaticus* sp. nov., *Cronobacter turicensis* sp. nov., *Cronobacter muytjensii* sp. nov., *Cronobacter dublinensis* sp. nov., *Cronobacter genomospecies* 1, and of three subspecies, *Cronobacter dublinensis* subsp. *dublinensis* subsp. nov., *Cronobacter dublinensis* subsp. *lausannensis* subsp. nov. and *Cronobacter dublinensis* subsp. *lactaridi* subsp. nov. Int J Syst Evol Microbiol. 2008;58:1442–7. http://dx.doi.org/10.1099/ijs.0.65577-0

Address for correspondence: Ronnie Henry, Centers for Disease Control and Prevention, 1600 Clifton Rd NE, Mailstop E28, Atlanta, GA 30329-4027, USA; email: boq3@cdc.gov

No *Plasmodium falciparum* Chloroquine Resistance Transporter and Artemisinin Resistance Mutations, Haiti

Jeanne P. Vincent, Kanako Komaki-Yasuda, Alexandre V. Existe, Jacques Boncy, Shigeyuki Kano

Author affiliations: National Center for Global Health and Medicine, Tokyo, Japan (J.P. Vincent, K. Komaki-Yasuda, S. Kano); University of Tsukuba, Tsukuba, Japan (J.P. Vincent, S. Kano); Laboratoire National de Santé Publique, Port-au-Prince, Haiti (A.V. Existe, J. Boncy)

We obtained 78 human blood samples from areas in Haiti with high transmission of malaria and found no drug resistance–associated mutations in *Plasmodium falciparum* chloroquine resistance transporter and Kelch 13 genes. We recommend maintaining chloroquine as the first-line drug for malaria in Haiti. Artemisinin-based therapy can be used as alternative therapy.

Haiti is a unique country in the Americas because malaria is caused there mainly by *Plasmodium falciparum*. Despite chloroquine being used for treatment of malaria since 1955, *P. falciparum* is generally still susceptible to this drug (*1*). Thus, chloroquine, plus a single dose of the gametocytocidal drug primaquine, is still the first-line treatment for uncomplicated malaria in Haiti, as indicated by the ministry of health. This regimen began to be challenged 9 years ago after a study reported chloroquine-resistant

haplotypes in Haiti (2). Since that time, other studies have reported no or few chloroquinine-resistance haplotypes (3–6), but an in vivo study reported a decrease in susceptibility to this drug (7).

Artemisinin, has been used only sporadically in Haiti, but it was recently implemented by health authorities to be the second-line antimalarial drug. We evaluated 2 drug resistance markers, the *P. falciparum* chloroquine resistance transporter (*pfcrt*) gene and the artemisinin resistance gene Kelch 13 (*k13*), in malaria parasites in Haiti to determine prevalences and provide information and recommendations for clinical practice to support malaria elimination efforts.

We conducted an epidemiologic survey during the summer of 2017. The study protocol was reviewed and approved by the Ethics Committee of the National Center for Global Health and Medicine (reference no. NCGM-G-002260–00) in Japan and the National Bioethics Committee (reference no. 1617–48) in Haiti.

We recruited febrile patients at 3 public hospitals in 3 departments in southern Haiti. We tested these patients by using a rapid diagnostic test (SD Bioline Malaria Ag Pf/Pan; Standard Diagnostics, Inc., Suwon, South Korea) at the point of care. These patients were a subsample of 556 patients from which we selected 144 patients with blood samples positive for *P. falciparum* DNA by the loop-mediated isothermal amplification method (Loopamp MALARIA Pan/Pf Detection Kit; Eiken Chemical Co., Tokyo, Japan). These 144 patients were potentially eligible for genotyping analysis.

We confirmed 80 positive samples from these patients by using a nested PCR specific for the 18S rRNA gene for analysis of *pfcrt* and *k13* genes. Conditions for this nested PCR were as reported (8). We performed the second PCR with only *P. falciparum*–specific primers. We amplified the *k13* gene by using a modified method of Ménard et al. (9) and newly designed primers specific for the *pfcrt* gene (Table). For *pfcrt* or *k13* genes, secondary PCR products were sequenced directly.

We analyzed samples from 78 patients for *k13* and samples from all 80 patients for *pfcrt*. The 80 patients had a mean age of 26.97 years (range 1–70 years): 13 were from Grand'Anse Department, 24 from Nippes Department, and 43 from Sud Department. Of these samples, 71 were also positive for the Pf-specific HRP2 band of the rapid diagnostic test but only 52 for the *Plasmodium*-universal LDH band. Microscopy results identified only 40 of these patients as being positive for malaria.

All samples analyzed had the wild-type amino acid sequence CVMNK at positions 72–76 of *pfcrt*. Resistant haplotypes of *pfcrt* were first reported in Haiti in 5 of 79 analyzed samples from Artibonite Department (2). Others studies have reported chloroquine-resistant haplotypes in 2 travelers returning from Haiti (3), 2/901 persons with possible mixed infections (chloroquine resistant and chloroquine sensitive) (4), and 1/108 cases analyzed in which microsatellite genotyping showed that the chloroquine-resistant haplotype detected was distinct from those of parasites circulating in Haiti (5). Analysis of parasite population structure in 2 of these studies (4,5) could not eliminate the possibility that these cases might be exogenous infections. In addition, Elbadry et al. did not report any chloroquine-resistant haplotypes in Haiti (6).

None of the 78 samples we tested had any resistance-associated polymorphisms in *k13*. Five (6.41%) samples had a synonymous mutation at nt position 1359 (bp position T1359A, codon position G453). This mutation was previously reported in only 1/82 samples in a study in Haiti (10). These findings are not an indication of artemisinin resistance because artemisinin-based combination therapy is rarely used in Haiti. However, these results are useful for following the evolution of resistance to this drug in Haiti.

In this study, we analyzed patients from areas of Haiti that have high rates of malaria transmission and found no drug resistance–associated mutations for the *pfcrt* and *k13* genes. Despite the limitation of a small sample size and consideration of findings of previous studies and our recent findings, we can assert that drug-resistant haplotypes are not currently circulating in Haiti.

Affordable and widely available, chloroquine is still the treatment of choice for uncomplicated *Plasmodium* spp. malaria in Haiti. Artemisinin-based combination therapy can be used as an alternative treatment for persons who cannot be given chloroquine. Although post-

Table. Primers used for nested PCRs to detect *Plasmodium falciparum* chloroquine resistance transporter and artemisin gene resistance mutations, Haiti*

Target	Primer sequences, 5′→3′	Primer annealing positions
pfcrt, primary PCR	F: ATGGCTCACGTTTAGGTGGAGGT	92–114
	R: CGGATGTTACAAAACTATAGTTACCA	258–283
pfcrt, secondary PCR	F: GTCTTGGTAAATGTGCTCATGTGT	119–142
	R: CTATAGTTACCAATTTTGTTTAAAGTTCT	241–269
k13, primary PCR	F: GAAGCCTTGTTGAAAGAAGCA	1276–1296
	R: CCAAGCTGCCATTCATTTGT	2107–2126
k13, secondary PCR	F: GCCTTGTTGAAAGAAGCAGAA	1279–1299
	R: GTGGCAGCTCCAAAATTCAT	2011–2030

*Secondary PCR products were directly sequenced by using the BigDye Terminator version 3.1 Cycle Sequencing Kit and analyzed with a 3130xl Genetic Analyzer (both from Thermo Fisher Scientific Inc., Waltham, MA, USA). F, forward; *k13*, Kelch 13; *pfcrt*, *P. falciparum* chloroquine resistance transporter; R, reverse.

treatment follow-up visits with blood testing of malaria patients can be challenging in Haiti, healthcare professionals should strive to implement these goals. Implementation would enable continuous in vivo monitoring of drug susceptibility of parasites and provide real-time data to public health authorities to formulate evidence-based policy.

About the Author

Dr. Vincent is a doctoral candidate in the Department of Tropical Medicine and Malaria of the Research Institute National Center for Global Health and Medicine, Tokyo, Japan. Her research interests include *Plasmodium* biology, malaria diagnosis, field studies for controlling malaria, and other public health issues.

References

1. von Fricken ME, Weppelmann TA, Hosford JD, Existe A, Okech BA. Malaria treatment policies and drug efficacy in Haiti from 1955–2012. J Pharm Policy Pract. 2013;6:10. http://dx.doi.org/10.1186/2052-3211-6-10
2. Londono BL, Eisele TP, Keating J, Bennett A, Chattopadhyay C, Heyliger G, et al. Chloroquine-resistant haplotype *Plasmodium falciparum* parasites, Haiti. Emerg Infect Dis. 2009;15:735–40. http://dx.doi.org/10.3201/eid1505.081063
3. Gharbi M, Pillai DR, Lau R, Hubert V, Khairnar K, Existe A, et al.; French National Reference Center for Imported Malaria Study. Chloroquine-resistant malaria in travelers returning from Haiti after 2010 earthquake. Emerg Infect Dis. 2012;18:1346–9. http://dx.doi.org/10.3201/eid1808.111779
4. Charles M, Das S, Daniels R, Kirkman L, Delva GG, Destine R, et al. *Plasmodium falciparum* K76T *pfcrt* gene mutations and parasite population structure, Haiti, 2006–2009. Emerg Infect Dis. 2016;22:786–93. http://dx.doi.org/10.3201/eid2205.150359
5. Morton LC, Huber C, Okoth SA, Griffing S, Lucchi N, Ljolje D, et al. *Plasmodium falciparum* drug-resistant haplotypes and population structure in postearthquake Haiti, 2010. Am J Trop Med Hyg. 2016;95:811–6. http://dx.doi.org/10.4269/ajtmh.16-0214
6. Elbadry MA, Existe A, Victor YS, Memnon G, Fukuda M, Dame JB, et al. Survey of *Plasmodium falciparum* multidrug resistance-1 and chloroquine resistance transporter alleles in Haiti. Malar J. 2013;12:426. http://dx.doi.org/10.1186/1475-2875-12-426
7. Raccurt CP, Brasseur P, Cicéron M, Parke DM, Zervos MJ, Boncy J. In vivo study of *Plasmodium falciparum* chloroquine susceptibility in three departments of Haiti. Malar J. 2017;16:313. http://dx.doi.org/10.1186/s12936-017-1961-2
8. Komaki-Yasuda K, Vincent JP, Nakatsu M, Kato Y, Ohmagari N, Kano S. A novel PCR-based system for the detection of four species of human malaria parasites and *Plasmodium knowlesi*. PLoS One. 2018;13:e0191886. http://dx.doi.org/10.1371/journal.pone.0191886
9. Ménard D, Khim N, Beghain J, Adegnika AA, Shafiul-Alam M, Amodu O, et al.; KARMA Consortium. A worldwide map of *Plasmodium falciparum* K13-propeller polymorphisms. N Engl J Med. 2016;374:2453–64. http://dx.doi.org/10.1056/NEJMoa1513137
10. Carter TE, Boulter A, Existe A, Romain JR, St Victor JY, Mulligan CJ, et al. Artemisinin resistance–associated polymorphisms at the K13-propeller locus are absent in *Plasmodium falciparum* isolates from Haiti. Am J Trop Med Hyg. 2015;92:552–4. http://dx.doi.org/10.4269/ajtmh.14-0664

Address for correspondence: Shigeyuki Kano, Department of Tropical Medicine and Malaria, Research Institute, National Center for Global Health and Medicine, 1-21-1 Toyama, Shinjuku, Tokyo 162-8655, Japan; email: kano@ri.ncgm.go.jp

Racial/Ethnic Disparities in Antimicrobial Drug Use, United States, 2014–2015

Scott W. Olesen, Yonatan H. Grad

Author affiliations: Harvard T.H. Chan School of Public Health, Boston, Massachusetts, USA (S.W. Olesen, Y.H. Grad); Brigham and Women's Hospital, Boston (Y.H. Grad)

Using a US nationwide survey, we measured disparities in antimicrobial drug acquisition by race/ethnicity for 2014–2015. White persons reported twice as many antimicrobial drug prescription fills per capita as persons of other race/ethnicities. Characterizing antimicrobial drug use by demographic might improve antimicrobial drug stewardship and help address antimicrobial drug resistance.

Antimicrobial drug use varies by sex, age, and geography (*1*), and antimicrobial drug prescribing practice for specific medical conditions and age cohorts varies by patients' race/ethnicity (*2–4*). Many studies on the role of patient race/ethnicity in antimicrobial drug prescribing practice focus on acute respiratory illnesses because antimicrobial drugs are often inappropriately prescribed for these conditions. The subjective diagnostic criteria for respiratory illnesses might result in race/ethnicity influencing prescribing practice more for these illnesses than for other illnesses (*4*). Despite our increasing knowledge of the role of patient race/ethnicity in drug prescribing practice for specific

conditions, how or whether these specific effects translate into overall antimicrobial drug use by race/ethnicity remains unclear. In this report, we address this gap in knowledge by describing the extent of racial/ethnic disparities in overall antimicrobial drug prescription fill rates in the United States.

We used the nationwide Medical Expenditure Panel Survey (MEPS) to acquire data about race/ethnicity and outpatient antimicrobial drug use for 2014–2015, the latest years with data available. MEPS contains data on members of a nationally representative sample of households (5,6). A person's race/ethnicity is reported by the respondent and imputed in <0.1% of cases. Information about race and Hispanic ethnicity are collected in separate questions. Data regarding prescriptions filled at outpatient pharmacies are collected from the respondent and, if the respondent approves, verified with the filling pharmacy. Data are afterward cross-referenced and cleaned by survey preparers (5).

We used 2 exposure variables. The first was a categorical race/ethnicity variable with 5 values: Hispanic, non-Hispanic white only, non-Hispanic black only, non-Hispanic Asian only, and non-Hispanic other or multiple race. The second exposure variable was dichotomous and indicated whether white was the race or 1 of the races of the respondent. This exposure variable included all persons from the non-Hispanic white category, some from the Hispanic category, and some from the other or multiple race category. The main outcome was reported outpatient antimicrobial drug prescription fills per 1,000 persons per year stratified by major antimicrobial drug class (penicillins, macrolides, quinolones, sulfonamides, other). The complex survey design was accounted for when computing rates and CIs with survey package version 3.32 in R version 3.4.1 (online Technical Appendix, https://wwwnc.cdc.gov/EID/article/24/11/18-0762-Techapp1.pdf).

The reported annual outpatient prescription fill rate for all antimicrobial drugs was 373 (95% CI 358–388) fills/1,000 persons. This rate varied by race/ethnicity; non-Hispanic whites reported the highest rate, followed by persons of other or multiple race/ethnicity, Hispanics, non-Hispanic blacks, and non-Hispanic Asians (Figure, panel A). White persons reported 2.0 (95% CI 1.9–2.2)–fold more fills per capita than nonwhite persons (Figure, panel B). The reported fill rate disparity was similar for macrolides (2.0 [95% CI 1.8–2.4]–fold higher), sulfonamides (2.2 [95% CI 1.8–2.7]–fold higher), and quinolones (2.3 [95% CI 1.9–2.8]–fold higher) but smaller for penicillins (64% [95% CI 48%–82%] higher).

We found a large disparity in antimicrobial drug fill rates by race/ethnicity: white persons reported making twice as many antimicrobial drug prescription fills as persons who were not white. Disparities were apparent for each major antimicrobial drug class, rather than different drug classes being used more predominantly by persons of particular race/ethnicities.

This study is subject to several limitations. First, the survey is not a perfect measure of antimicrobial drug use. Survey respondents report medications they remember filling, subjecting results to systematic differences in respondents' abilities to recall medications (6). Survey preparers then obtain information about those medications from the pharmacies the respondents visited, which themselves might have systematic differences in completeness of records (5). Also, respondents might not have complete information about other household members' antimicrobial drug use or might choose not to disclose all antimicrobial drug use. Second, nonprescription antimicrobial drug use might be higher among minority groups (7), perhaps mitigating the observed disparity. Last, the survey measures reported antimicrobial drug fills and not actual use (8); the fill rates we report are substantially lower than those measured by others using sales data (1) or other national surveys (9).

Whether differences in antimicrobial drug use and race/ethnicity lead to disparities in antimicrobial drug resistance is unclear. We expect that disparities in use, regardless of their cause, will lead to disparities in the proportions of carried bacteria that are antimicrobial drug–resistant. Absolute rates of antimicrobial drug–resistant
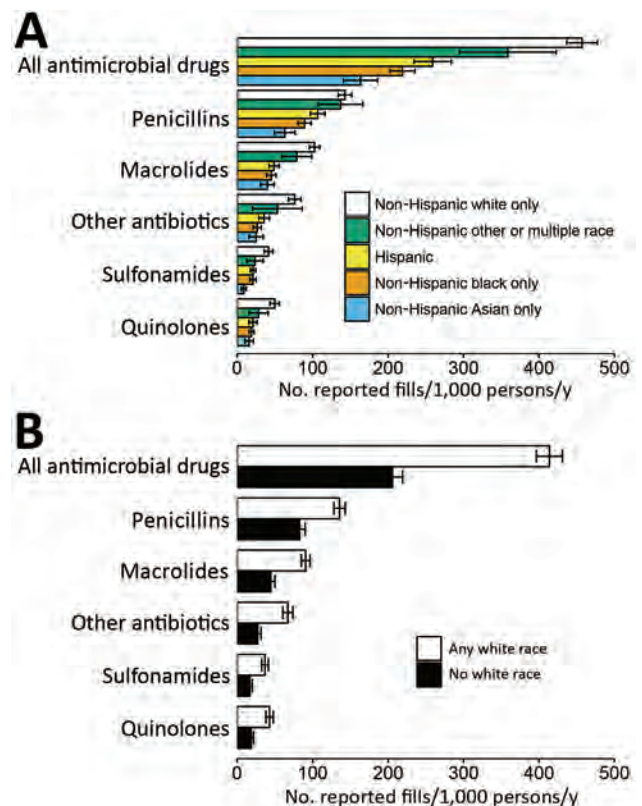

Figure. Annual antimicrobial drug use reported by Medical Expenditure Panel Survey respondents, by race/ethnicity, United States, 2014–2015. Error bars indicate 95% CIs. A) Drug use by race/ethnicity category. B) Drug use among persons who reported white as their race or 1 of their races and among those who did not.

infections, however, might follow different patterns (*10*). For example, higher macrolide use among white persons might lead to macrolide resistance in a greater proportion of *Streptococcus pneumoniae* bacteria carried by whites, but if white persons have fewer *S. pneumoniae* infections, then they would incur a lower absolute rate of macrolide-resistant *S. pneumoniae* infections. Further studies comparing antimicrobial drug use, antimicrobial drug resistance, and disease prevalence by race/ethnicity will be critical for addressing this question and improving antimicrobial drug stewardship.

About the Author

Dr. Olesen is a postdoctoral fellow at the Harvard T.H. Chan School of Public Health, Boston, Massachusetts, USA. His research interests include antimicrobial drug use and resistance. Dr. Grad is the Melvin J. and Geraldine L. Glimcher Assistant Professor of Immunology and Infectious Diseases at the Harvard T.H. Chan School of Public Health. His research interests include antimicrobial drug use and resistance and the evolution and spread of pathogens.

References

1. Hicks LA, Bartoces MG, Roberts RM, Suda KJ, Hunkler RJ, Taylor TH Jr, et al. US outpatient antibiotic prescribing variation according to geography, patient population, and provider specialty in 2011. Clin Infect Dis. 2015;60:1308–16.
2. Goyal MK, Johnson TJ, Chamberlain JM, Casper TC, Simmons T, Alessandrini EA, et al.; Pediatric Care Applied Research Network. Racial and ethnic differences in antibiotic use for viral illness in emergency departments. Pediatrics. 2017;140:e20170203. http://dx.doi.org/10.1542/peds.2017-0203
3. Steinman MA, Landefeld CS, Gonzales R. Predictors of broad-spectrum antibiotic prescribing for acute respiratory tract infections in adult primary care. JAMA. 2003;289:719–25. http://dx.doi.org/10.1001/jama.289.6.719
4. Gerber JS, Prasad PA, Localio AR, Fiks AG, Grundmeier RW, Bell LM, et al. Racial differences in antibiotic prescribing by primary care pediatricians. Pediatrics. 2013;131:677–84. http://dx.doi.org/10.1542/peds.2012-2500
5. Hill SC, Roemer M, Stagnitti MN. Methodology report #29. Outpatient prescription drugs: data collection and editing in the 2011 medical expenditure panel survey. 2014 Mar [cited 2018 May 7]. https://meps.ahrq.gov/data_files/publications/mr29/mr29.shtml
6. Hill SC, Zuvekas SH, Zodet MW. Implications of the accuracy of MEPS prescription drug data for health services research. Inquiry. 2011;48:242–59. http://dx.doi.org/10.5034/inquiryjrnl_48.03.04
7. Zoorob R, Grigoryan L, Nash S, Trautner BW. Nonprescription antimicrobial use in a primary care population in the United States. Antimicrob Agents Chemother. 2016;60:5527–32. http://dx.doi.org/10.1128/AAC.00528-16
8. Tamblyn R, Eguale T, Huang A, Winslade N, Doran P. The incidence and determinants of primary nonadherence with prescribed medication in primary care: a cohort study. Ann Intern Med. 2014;160:441–50. http://dx.doi.org/10.7326/M13-1705
9. Fleming-Dutra KE, Hersh AL, Shapiro DJ, Bartoces M, Enns EA, File TM Jr, et al. Prevalence of inappropriate antibiotic prescriptions among US ambulatory care visits, 2010–2011. JAMA. 2016;315:1864–73. http://dx.doi.org/10.1001/jama.2016.4151
10. Kanjilal S, Sater MRA, Thayer M, Lagoudas GK, Kim S, Blainey PC, et al. Trends in antibiotic susceptibility in *Staphylococcus aureus* in Boston, Massachusetts, from 2000 to 2014. J Clin Microbiol. 2017;56:e01160-17. http://dx.doi.org/10.1128/JCM.01160-17

Congenital Zika Virus Infection with Normal Neurodevelopmental Outcome, Brazil

Alessandra Lemos de Carvalho, Carlos Brites, Tânia Barreto Taguchi, Suely Fernandes Pinho, Gúbio Campos, Rita Lucena

Author affiliations: SARAH Network of Rehabilitation Hospitals, Salvador, Brazil (A.L. de Carvalho, T.B. Taguchi, S.F. Pinho); Federal University of Bahia, Salvador (C. Brites, G. Campos, R. Lucena)

We describe a case of a 20-month-old girl with probable congenital Zika virus infection and normal neurodevelopment, despite microcephaly and abnormal neuroimaging. This case raises questions about early prognostic markers and draws attention to the need for investigation in suspected Zika cases, even if the child's early neurodevelopment is normal.

Zika virus is a mosquitoborne RNA virus (genus *Flavivirus*, family Flaviviridae) that was first isolated in 1947 from monkeys in the Zika Forest in Uganda (*1*). In November 2015, there was an outbreak of congenital microcephaly in the northeast states of Brazil (*2*). Further confirmation of this syndrome's relationship with Zika virus infection during pregnancy was then possible (*3*). Congenital Zika syndrome has been recognized as a new clinical entity (*4,5*). Most published case series focus on the picture of severely affected infants (*6,7*). We describe a case of a child with probable congenital Zika virus infection whose neurodevelopment was normal, despite

microcephaly and abnormal neuroimaging. The mother provided written informed consent for this report.

The patient, a girl, was born at 36 weeks, 4 days' gestation; Apgar scores were 8 at first minute and 9 at fifth minute. There was no family history of microcephaly, and the parents were phenotypically normal. The pregnancy occurred during Brazil's Zika virus epidemic and the mother lived in Bahia, the state where the virus was first detected and one of the most affected areas. She was 27 years of age, in her third pregnancy, and had a history of rash at 12 weeks' gestation, followed by fever, headache, arthralgia, and conjunctivitis. She recovered after 1 week, without a specific diagnosis. At 24 weeks' gestation, a routine ultrasound exam detected microcephaly in the fetus. Testing for HIV, human T-lymphotropic virus, cytomegalovirus, toxoplasmosis, rubella, syphilis, and hepatitis B and C in the mother yielded negative results. She had no further complications except for high blood pressure detected 3 days before delivery, the discovery of which led to an elective cesarean section.

At birth, the infant's weight was 2,496 g (–0.6 SD), length was 45 cm (–1.1 SD), and head circumference was 29.5 cm (–2.4 SD) (8). She had no neonatal complications and was breast-fed without difficulty. Test results were negative for chikungunya, dengue, rubella, toxoplasmosis, cytomegalovirus, parvovirus B19, and herpes virus I and II. However, serum testing (EuroImmun, Lubeck, Germany) showed positive results for Zika virus IgM. Results of biochemical analysis of cerebrospinal fluid, abdominal ultrasound, and neonatal metabolic screening were all normal, as were ophthalmologic and auditory evaluations. Transfontanellar ultrasound showed focal calcification in basal ganglia that was more pronounced in the right hemisphere. Results of cerebral computed tomography conducted during the neonatal period showed mild craniofacial disproportion, slightly decreased brain volume, and small calcifications in the right nucleocapsular area and around the left thalamus.

In January 2016, at 6 months of age, the patient entered a neurorehabilitation program, during which she reached normal achievement of developmental milestones. Further investigation included a videoelectroencephalogram and auditory and visual evoked potentials; results were all normal. We diagnosed probable congenital Zika virus infection, considering the gestational history, congenital microcephaly, positive serologic test results, and neuroradiological findings, which were mild but consistent with Zika virus infection. A follow-up cerebral scan performed at 7 months of age showed mild calcifications at the right lenticular nucleus and posterior arm of the left internal capsule (Figure).

The patient started to walk independently at 13 months of age, and her gait pattern did not show any abnormality. We performed a follow-up assessment at 20 months of age. Neurologic examination was normal, except for microcephaly (head circumference 42.5 cm, –3 SD) (9). Weight was within reference range (8.7 kg, between –1 and –2 SD), but length was below reference values (74 cm, between –2 and –3 SD). The child was otherwise healthy. We performed developmental evaluation using Bayley-III Scales of Infant Development (10). All composite scores were within average classification (online Technical Appendix, https://wwwnc.cdc.gov/EID/article/24/11/18-0883-Techapp1.pdf).

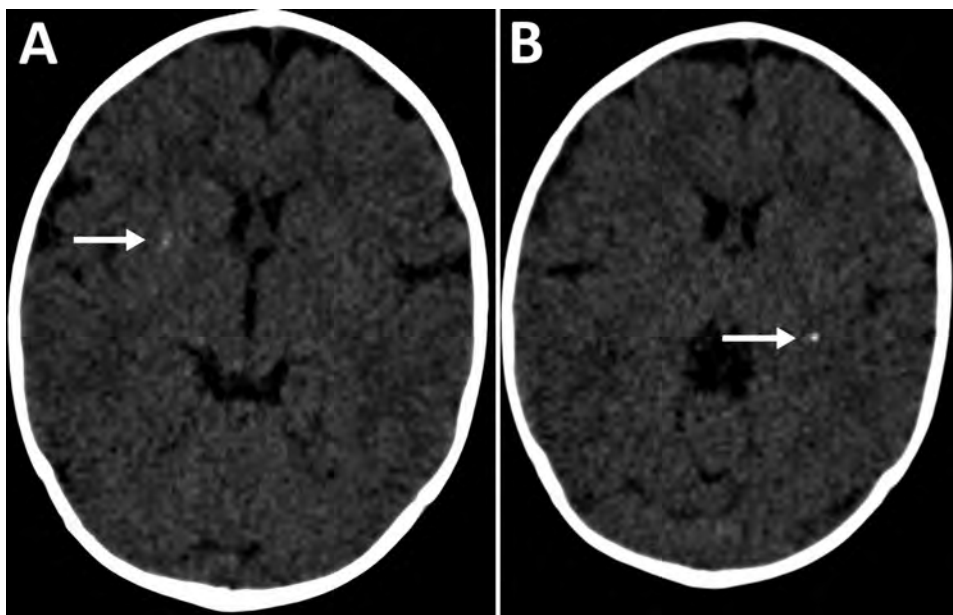Neurodevelopment is a dynamic process that depends on the interaction between neurobiological and

Figure. Cerebral computed tomography images of infant with probable congenital Zika virus infection at 7 months of age, Brazil. A) Mild calcification at the right lenticular nucleus (arrow); B) calcifications at the posterior arm of the left internal capsule (arrow).

environmental factors. Children initially developing within the expected range for their age group may experience a slowdown as demands of neurodevelopment become more extensive. We cannot make inferences about long-term prognosis from the patient's condition at 20 months of age. Developmental evolution should be determined prospectively, using the same instrument so that results can be compared over time.

This report has 2 main limitations. First, molecular confirmation of Zika virus infection in the mother or the child was not possible. Second, we did not perform PCR or culture for cytomegalovirus. Nevertheless, the child's Zika virus IgM was positive in the neonatal period, and her mother's clinical symptoms suggested Zika virus infection during pregnancy, which occurred during the Zika virus epidemic in Brazil, in one of the most affected areas.

This case may indicate a broader spectrum in congenital Zika syndrome, raising questions about early prognostic markers. Our findings draw attention to the need for detailed evaluation even for typically developing children with possible congenital Zika virus infection who receive medical attention later.

Acknowledgment

About the Author

Dr. Carvalho is a pediatrician at the Child Rehabilitation Center of SARAH Network of Rehabilitation Hospitals, Salvador Unit. She is currently a master's degree student at the Postgraduate Program in Medicine and Health, Federal University of Bahia, Bahia, Brazil. Her primary clinical practice and research interests are in cerebral palsy and congenital Zika virus infection.

References

1. Dick GWA, Kitchen SF, Haddow AJ. Zika virus. I. Isolations and serological specificity. Trans R Soc Trop Med Hyg. 1952;46: 509–20. http://dx.doi.org/10.1016/0035-9203(52)90042-4
2. Pan American Health Organization; World Health Organization. Epidemiological update: Neurological syndrome, congenital anomalies, and Zika virus infection. 2016 Jan 17 [cited 2018 Sep 19]. https://www.paho.org/hq/dmdocuments/2016/2016-jan-17-cha-epi-update-zika-virus.pdf
3. de Araújo TVB, Ximenes RAA, Miranda-Filho DB, Souza WV, Montarroyos UR, de Melo APL, et al. Association between microcephaly, Zika virus infection, and other risk factors in Brazil: final report of a case-control study. Lancet Infect Dis. 2018;18:328–36.
4. del Campo M, Feitosa IML, Ribeiro EM, Horovitz DDG, Pessoa ALS, França GVA, et al.; Zika Embryopathy Task Force-Brazilian Society of Medical Genetics ZETF-SBGM. The phenotypic spectrum of congenital Zika syndrome. Am J Med Genet A. 2017;173:841–57. http://dx.doi.org/10.1002/ajmg.a.38170
5. Moore CA, Staples JE, Dobyns WB, Pessoa A, Ventura CV, Fonseca EB, et al. Characterizing the pattern of anomalies in congenital Zika syndrome for pediatric clinicians. JAMA Pediatr. 2017;171:288–95. http://dx.doi.org/10.1001/jamapediatrics.2016.3982
6. Schuler-Faccini L, Ribeiro EM, Feitosa IML, Horovitz DDG, Cavalcanti DP, Pessoa A, et al.; Brazilian Medical Genetics Society–Zika Embryopathy Task Force. Possible association between Zika virus infection and microcephaly—Brazil, 2015. MMWR Morb Mortal Wkly Rep. 2016;65:59–62. http://dx.doi.org/10.15585/mmwr.mm6503e2
7. Moura da Silva AA, Ganz JSS, Sousa PD, Doriqui MJR, Ribeiro MRC, Branco MD, et al. Early growth and neurologic outcomes of infants with probable congenital Zika virus syndrome. Emerg Infect Dis. 2016;22:1953–6. http://dx.doi.org/10.3201/eid2211.160956
8. Villar J, Cheikh Ismail L, Victora CG, Ohuma EO, Bertino E, Altman DG, et al. International standards for newborn weight, length, and head circumference by gestational age and sex: the newborn cross-sectional study of the INTERGROWTH-21st Project. Lancet. 2014;384:857–68. https://doi.org/10.1016/S0140-6736(14)60932-6
9. World Health Organization Multicentre Growth Reference Study Group. WHO child growth standards: length/height-for-age, weight-for-age, weight-for-length, weight-for-height, and body mass index-for-age: methods and development. Geneva: The Organization; 2006 [cited 2018 Aug 14]. http://www.who.int/childgrowth/standards/technical_report/en
10. Bayley N. Bayley scales of infant and toddler development. 3rd ed. San Antonio (TX, USA); Psychological Corp.; 2005.

Address for correspondence: Alessandra Lemos de Carvalho, SARAH Salvador Hospital, Av Tancredo Neves, 2782, Caminho das Árvores, Salvador, BA 41820-900, Brazil; email: alessandracarvalhoped@gmail.com

Molecular Characterization of African Swine Fever Virus, China, 2018

Shengqiang Ge,[1] Jinming Li,[1] Xiaoxu Fan,[1] Fuxiao Liu,[1] Lin Li,[1] Qinghua Wang, Weijie Ren, Jingyue Bao, Chunju Liu, Hua Wang, Yutian Liu, Yongqiang Zhang, Tiangang Xu, Xiaodong Wu, Zhiliang Wang

Author affiliation: China Animal Health and Epidemiology Center, Qingdao, China

On August 3, 2018, an outbreak of African swine fever in pigs was reported in China. We subjected a virus from an African swine fever–positive pig sample to phylogenetic analysis. This analysis showed that the causative strain belonged to the p72 genotype II and CD2v serogroup 8.

African swine fever (ASF) is a disease that is reportable to the World Health Organisation for Animal Health. This disease causes high fever, hemorrhages, ataxia, and severe depression in domestic pigs and has mortality rates approaching 100%. Its causative agent is African swine fever virus (ASFV; family *Asfarviridae*, genus *Asfivirus*), a large, enveloped, double-stranded DNA virus (*1*). ASF was first described in Kenya in 1921, and was introduced into the Republic of Georgia in 2007, after which it spread into other countries in eastern Europe, including Russia (2007), Ukraine (2012), Belarus (2013), Lithuania (2014), Estonia (2014), Poland (2014), Latvia (2014), Romania (2017), the Czech Republic (2017), and Hungary (2018).

During July 1–August 1, 2018, a total of 47 of 383 pigs died on a farm in the Shenbei District of Shenyang, Liaoning Province, China. Postmortem analysis performed by local veterinarians showed an ASF-typical lesion in pig spleens that were extremely swollen and severely necrotic. Other pathologic changes included hemorrhages in tonsils and lungs, marbled lesions in mandibular and mesenteric lymph nodes, and diffuse hemorrhages in a large part of gastric serosa.

We collected samples from 2 dead pigs and 6 live pigs on this farm and sent these samples to our Biosafety Level 3 laboratory for confirmation of ASFV infection. We performed a real-time PCR for ASFV as recommended by the World Health Organisation for Animal Health protocol. Results confirmed ASFV infections in China (*2*).

After confirmation of ASFV infection by our laboratory, we used nucleic acid extracts from an ASFV-infected sample for conventional PCR amplification with 3 pairs of primers. We amplified 3 gene fragments: a partial gene fragment of the B646L gene encoding the p72 capsid protein (*3*), a fragment of the EP402R gene encoding the CD2v protein (*4*), and a tandem repeat sequence (TRS) located between the I73R and I329L genes (*5*).

We subjected 3 amplified products to nucleotide sequencing and deposited the resulting sequences in GenBank (accession nos. MH722357, MH735142, and MH735144). We used the p72 fragment sequence for phylogenetic analysis of the genotype, and the CD2v fragment sequence for phylogenetic analysis of the serogroup (*6*). We constructed 2 phylogenetic trees by using MEGA 5.0 software (https://www.megasoftware.net/). These trees showed that the causative strain (China 2018/1) in this study belonged to p72 genotype II (Figure, panel A) and to CD2v serogroup 8 (Figure, panel B).

Genotype identification of ASFV often depends on partial p72 gene characterization (*3*). During ASF outbreaks, this genotyping approach can be used to identify possible origins of viruses and differentiate them from closely related strains (*7*). In this study, we classified China 2018/1 as genotype II (Figure, panel A), the sequences we obtained had extremely high homology with those of other genotype II strains, therefore suggesting the origin of China 2018/1 from a homogenotypic strain.

In addition to conventional genetic typing, serologic typing is another method for classifying ASFVs on the basis of hemadsorption inhibition (HAI). Eight ASFV serogroups have been identified (*6*). Moreover, HAI typing places ASFV into discrete serogroups not necessarily resolved by the p72-based genetic typing. For example, serogroup 1, 2, and 4 strains can be simultaneously classified as having the P72 genotype I (*7*). In this study, we found that China 2018/1 belonged to serogroup 8 as determined by phylogenetic analysis, suggesting the same HAI characteristics as those for other strains in the homoserogroup (Figure, panel B).

We compared Georgia 2007/1, which is representative of genotype II, with China 2018/1. China 2018/1 had a 10-bp additional fragment (5′-GGAATATATA-3′) that was inserted into the TRS between the I73R and I329L genes and was identical to those of the Bel13/Grodno, Ukr12/Zapo, Lt14/1490, Lt14/1482, Pol14/Sz, and Pol14/Krus strains (*5*).

ASF causes devastating socioeconomic consequences in the global pig industry, especially for countries with large-scale pig production and pork consumption. After the confirmation of ASF outbreak in China in August 2018, we characterized the causative strain, China 2018/1, by phylogenetic comparison with previous strains. We classified this new strain as having the p72 genotype II and 100% p72 sequence identity with several strains from eastern Europe and Africa, such as Bel13/Grodno, Voronezh 2016, Mal 2011/01, and ZIM/2015/01.
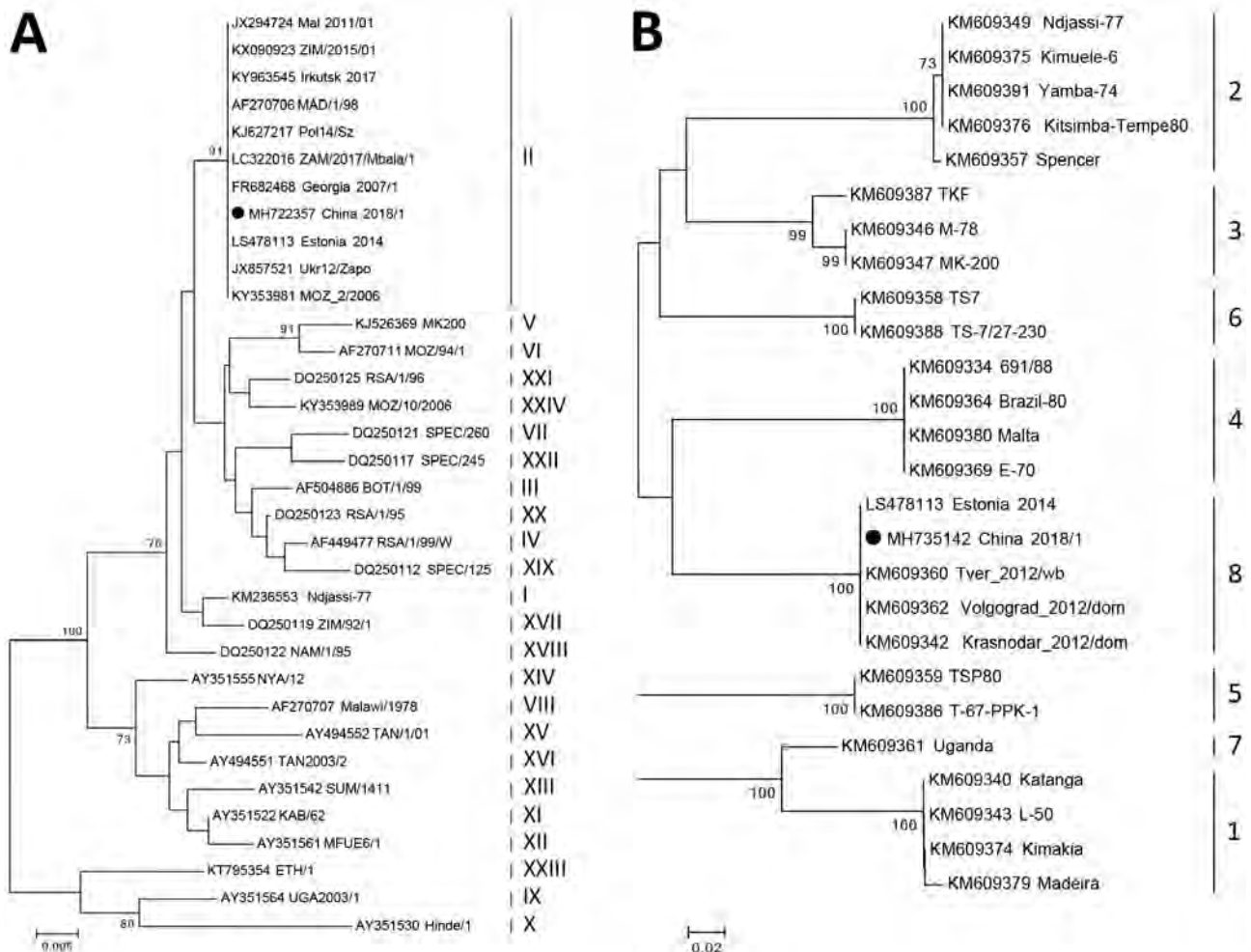
Figure. Phylogenetic analysis of a causative virus strain (China 2018/1) of an African swine fever outbreak, China, 2018. A) p72 genotype; B) CD2v serogroup. The neighbor-joining method and Kimura 2-parameter model were used for construction of phylogenetic trees in MEGA 5.0 software (https://www.megasoftware.net/). Numbers along branches indicate bootstrap values >70% (1,000 replicates). Black circles indicate causative virus from this study. Roman numerals to the right in panel A indicate p72 genotypes. Numbers to the right in panel B indicate CD2v serogroups. GenBank accession numbers are provided for all sequences. Scale bars indicate nucleotide substitutions per site.

On the basis of serologic typing, we found that China 2018/1 belonged to the CD2v serogroup 8. In addition, this strain had a 10-bp additional fragment (5'-GGAATATATA-3') in its TRS when compared with others in the homogenotype.

Because ASFV is a large DNA virus with a stable genome, it is hardly unexpected that the sequence of China 2018/1 had extremely high homology with sequences in genotype II over a wide geographic area. However, it remains to be elucidated from where China 2018/1 was introduced into China.

About the Author

Dr. Ge is a virologist at the National Research Center for Exotic Animal Diseases, Animal Health and Epidemiology Center, Qingdao, China. His primary research interest is prevention and control of exotic animal diseases.

References

1. Alonso C, Borca M, Dixon L, Revilla Y, Rodriguez F, Escribano JM; ICTV Report Consortium. ICTV virus taxonomy profile: Asfarviridae. J Gen Virol. 2018;99:613–4. http://dx.doi.org/10.1099/jgv.0.001049
2. Wang Q, Ren W, Bao J, Ge S, Li J, Li L, et al. The first outbreak of African swine fever was confirmed in China [in Chinese]. Journal of China Animal Health Inspection. 2018;35:1–5.
3. Bastos AD, Penrith ML, Crucière C, Edrich JL, Hutchings G, |Roger F, et al. Genotyping field strains of African swine fever virus by partial p72 gene characterisation. Arch Virol. 2003;148:693–706. http://dx.doi.org/10.1007/s00705-002-0946-8
4. Sanna G, Dei Giudici S, Bacciu D, Angioi PP, Giammarioli M, De Mia GM, et al. Improved strategy for molecular characterization of African swine fever viruses from Sardinia, based on analysis of p30, CD2V and I73R/I329L variable regions. Transbound Emerg Dis. 2017;64:1280–6. http://dx.doi.org/10.1111/tbed.12504
5. Gallardo C, Fernández-Pinero J, Pelayo V, Gazaev I, Markowska-Daniel I, Pridotkas G, et al. Genetic variation among African swine fever genotype II viruses, eastern and central Europe. Emerg Infect Dis. 2014;20:1544–7. http://dx.doi.org/10.3201/eid2009.140554
6. Malogolovkin A, Burmakina G, Tulman ER, Delhon G, Diel DG, Salnikov N, et al. African swine fever virus CD2v and C-type lectin gene loci mediate serological specificity. J Gen Virol. 2015;96:866–73. http://dx.doi.org/10.1099/jgv.0.000024
7. Malogolovkin A, Burmakina G, Titov I, Sereda A, Gogin A, Baryshnikova E, et al. Comparative analysis of African swine fever virus genotypes and serogroups. Emerg Infect Dis. 2015;21:312–5. http://dx.doi.org/10.3201/eid2102.140649

Address for correspondence: Xiaodong Wu or Zhiliang Wang, National Research Center for Exotic Animal Diseases, China Animal Health and Epidemiology Center, 369 Nanjing Rd, Qingdao, Shandong 266032, China; emails: wuxiaodong@cahec.cn or wangzhiliang@cahec.cn

LETTERS

Familial Transmission of *emm12* Group A *Streptococcus*

Rachel Mearkle, Sooria Balasegaram, Shiranee Sriskandan, Vicki Chalker, Theresa Lamagni

Author affiliations: Public Health England, Chilton, UK (R. Mearkle); Public Health England, London, UK (S. Balasegaram, V. Chalker, T. Lamagni); Imperial College, London, UK (S. Sriskandan)

To the Editor: We read with interest the recent research letter by Duployez et al. describing a cluster of invasive group A *Streptococcus* (iGAS) infections in a cohabiting couple in their 60s (*1*). The report illustrates the increased risk of infection for persons living in a household with someone with iGAS infection. We write to draw readers' attention to our recent study, which adds to the body of evidence on the risk of household transmission of iGAS (*2*).

Population-based studies from Australia, Canada, the United Kingdom, and the United States, based on 13 household clusters, assessed the risk of transmitting iGAS infection through household contact (*3*). We identified an additional 24 household clusters in England using addresses captured through national surveillance in 2009 and 2011–2013. For all 12 clusters in which *emm* typing was performed on both patients, results were the same for both. All secondary cases occurred within 1 month of the index case (median 2 days). Among contacts, the 30-day incidence rate was 4,520/100,000 person-years, 1,940 times higher than the background incidence (2.34/100,000 person-years). Spouses and partners ≥75 years of age (6 pairs) were at particularly high risk for developing infection; incidence was estimated at 15,000 (95% CI 5,510–32,650)/100,000 person-years, 1,650 times higher than the background risk in this age group (9.09/100,000, 95% CI 5,510–32,650). These data resulted in an estimated number needed to treat of 82 (46–417).

Duployez's article also highlights differences between countries in policies for antimicrobial chemoprophylaxis. National guidance for public health management of community iGAS infection is being revised in the United Kingdom; oral penicillin V is currently recommended as the first choice for chemoprophylaxis (*4*). However, questions remain about the efficacy of chemoprophylaxis and the practicalities of timely administration to benefit others in a household, given that 38% of pairs were co-primary cases or had only 1 day between initial and subsequent infections.

References

1. Duployez C, Vachée A, Robineau O, Giraud F, Deny A, Senneville E, et al. Familial transmission of *emm12* group A *Streptococcus*. Emerg Infect Dis. 2017;23:1745–6. http://dx.doi.org/10.3201/eid2310.170343

2. Mearkle R, Saavedra-Campos M, Lamagni T, Usdin M, Coelho J, Chalker V, et al. Household transmission of invasive group A *Streptococcus* infections in England: a population-based study, 2009, 2011 to 2013. Euro Surveill. 2017;22:30532. http://dx.doi.org/10.2807/1560-7917.ES.2017.22.19.30532

3. Lamagni TL, Oliver I, Stuart JM. Global assessment of invasive group A *Streptococcus* infection risk in household contacts. Clin Infect Dis. 2015;60:166–7.

4. Health Protection Agency, Group A Streptococcus Working Group. Interim UK guidelines for management of close community contacts of invasive group A streptococcal disease. Commun Dis Public Health. 2004;7:354–61.

Address for correspondence: Rachel Mearkle, Public Health England South East, Thames Valley Health Protection Team, Chilton, Oxfordshire, OX11 0RE, UK; email: Rachel.Mearkle@phe.gov.uk

Acquired Resistance to Antituberculosis Drugs

Htin Lin Aung, Wint Wint Nyunt, Yang Fong, Bruce Russell, Gregory M. Cook, Si Thu Aung

Author affiliations: University of Otago, Dunedin, New Zealand (H.L. Aung, B. Russell, G.M. Cook); Ministry of Health and Sports, Yangon, Myanmar (W.W. Nyunt); Massey University, Palmerston North, New Zealand (Y. Fong); Ministry of Health and Sports, Naypyitaw, Myanmar (S.T. Aung)

To the Editor: We read with great interest the article by Loutet et al. on acquired resistance to antituberculosis drugs in low-burden settings, such as England, Wales, and Northern Ireland (*1*), and support their assertion that detecting acquired resistance should be a priority in high-burden settings. This objective is particularly urgent in Myanmar, where tuberculosis (TB) is highly endemic (*2*) and drug-resistant TB is present through both acquired drug resistance and direct transmission. Unfortunately, the overwhelming number of TB cases precluded routine phenotypic drug susceptibility testing (DST) of first- or second-line drugs, so we began using whole-genome sequencing (WGS), which enabled us to more rapidly diagnose drug-resistant TB (*3*). Here, we briefly describe 2 cases of acquired antituberculosis drug resistance detected by WGS.

Patient A, diagnosed with rifampin-susceptible TB by Xpert (Cepheid Inc., Sunnyvale, CA, USA), received a treatment regimen containing first-line drugs but failed to achieve smear conversion at the 3-month follow-up. WGS indicated that the isolate was resistant to isoniazid, streptomycin, and rifampin. WGS and phenotypic DST of the isolate at baseline revealed it was resistant to isoniazid and streptomycin. Isolates from before and after treatment differed by 2 single-nucleotide polymorphisms, suggesting that rifampin resistance was acquired during therapy (*4*). Patient B was diagnosed with rifampin-resistant TB and reported that he had started multidrug-resistant (MDR) TB treatment 6 months earlier but failed to continue the treatment. WGS and phenotypic DST showed the case had been MDR TB (resistant to isoniazid, rifampin, and streptomycin, but sensitive to amikacin) at baseline but had become pre–extensively drug resistant (amikacin resistance was acquired during treatment).

Loutet et al. showed that WGS provides an effective way to evaluate TB drug resistance in low-endemicity settings (*5*). We believe WGS is even more vital to help direct MDR TB treatment in high-burden settings, to halt the continued spread of TB.

References

1. Loutet MG, Davidson JA, Brown T, Dedicoat M, Thomas HL, Lalor MK. Acquired resistance to antituberculosis drugs in England, Wales, and Northern Ireland, 2000–2015. Emerg Infect Dis. 2018;24:524–33. http://dx.doi.org/10.3201/eid2403.171362

2. World Health Organization (WHO). Global tuberculosis report 2017. Geneva: WHO; 2017 [cited 8 Mar 2018]. http://www.who.int/tb/publications/global_report/en/

3. Aung HL, Nyunt WW, Fong Y, Cook GM, Aung ST. First 2 extensively drug-resistant tuberculosis cases from Myanmar treated with bedaquiline. Clin Infect Dis. 2017;65:531–2. http://dx.doi.org/10.1093/cid/cix365

4. Eldholm V, Norheim G, von der Lippe B, Kinander W, Dahle UR, Caugant DA, et al. Evolution of extensively drug-resistant *Mycobacterium tuberculosis* from a susceptible ancestor in a single patient. Genome Biol. 2014;15:490. http://dx.doi.org/10.1186/s13059-014-0490-3

5. Walker TM, Cruz ALG, Peto TE, Smith EG, Esmail H, Crook DW. Tuberculosis is changing. Lancet Infect Dis. 2017;17:359–61. http://dx.doi.org/10.1016/S1473-3099(17)30123-8

Address for correspondence: Htin Lin Aung, Sir Charles Hercus Health Research Fellow, Department of Microbiology and Immunology, School of Biomedical Sciences, University of Otago, PO Box 56, Dunedin, New Zealand; email: htin.aung@otago.ac.nz

The Politics of Vaccination: A Global History

Nothing happens in a vacuum, including public health interventions, which do have unintended consequences; whether those consequences are positive or negative may depend on the eye of the beholder. The Politics of Vaccination: A Global History, edited by Christine Holmberg, Stuart Blume, and Paul Greenough, describes the political and cultural contexts of vaccination efforts throughout history. The book examines the tensions existing between national independence and global interdependence, top-down program implementation and grassroots development, and individual rights and the common good. Each chapter tells the story of a specific vaccination program, and although time and place differ, when taken together, they highlight the push-and-pull that exists between individuals, nations, and multinational agencies in this context.

The book is divided into three sections. The first demonstrates how national identity is shaped by the way the nation's people respond to vaccine campaigns and interventions, especially when initiated by an outside agency. The second section traces the rise and fall over time of national vaccine production and the eventual transition to and reliance on multinational agencies to meet national needs, other than in outlier countries like Brazil and Japan. These accounts leave the reader unsure of how reliable these agencies will remain for individual countries in the future. The third section studies the pitfalls of the top-down approach in surveillance and prevention campaigns and underlines the difficulty of balancing individual rights with obligations to protect the public.

These three sections are outlined in an introduction by the editors, which lays out a map for the reader to follow throughout the book. The commentary in the afterward, by asserting that the top-down approach of vaccine campaigns initiated by outside global leaders in developing nations results in significant collateral damage and ignores the national priorities, finalizes the tone for the book as a whole.

Readers, regardless of their stances on the issues raised, will be challenged to think about the different lenses through which individuals or nations might see vaccine campaigns, and even public health interventions in general. Medical historians and anthropologists will appreciate the book's perspectives on past experiences, which will be thought-provoking to public health practitioners and global health activists as well. Readers will enjoy the rich detail and historical references in each chapter and be intrigued by the character studies of textbook global health heroes, such as Dr. Alexander Langmuir and Dr. William Foege. The expert information can help public health practitioners consider in advance the effects, including potential unintended consequences, that large-scale interventions may have on a population. And, although the book may challenge those looking for a more straightforward account of the history of vaccination, most readers will find topics of interest within the various time periods and countries described. The Politics of Vaccination: A Global History, through its fresh and sometimes provocative perspective on global public health, reminds readers of the importance of political and cultural context when practicing disease surveillance and prevention.

Laura E. Power

Author affiliation: University of Michigan, Ann Arbor, Michigan, USA

Address for correspondence: Laura E. Power, University of Michigan School of Public Health, 1415 Washington Heights M5224, Ann Arbor, MI 48109, USA; email: lejohns@umich.edu

Ernst Liebenauer (1884–1970), *In Entrenchment, World War I* **(c. 1915).** Watercolor, pencil, and gouache on paper, 5.6 in x 4 in/14.2 cm x 10.1 cm. Digital image from private collection, Atlanta, Georgia, USA.

Trench Conflict with Combatants and Infectious Disease

Terence Chorba

Acentury ago, the world was ensnared in the Great War, 1914–1918, now known as the First World War. During that war, an estimated 9 million combatants and as many as 7 million civilians died, and it brought to an end the German, Russian, Austro-Hungarian, and Ottoman Empires. Infectious diseases played a prominent role in that war, resulting in more casualties than did war-inflicted wounds. With several decades of knowledge about bacterial organisms, armies had implemented sanitation measures such as latrines and water purification methods to control diarrheal

Author affiliation: Centers for Disease Control and Prevention, Atlanta, Georgia, USA

and dysenteric diseases. Vaccine successes had been documented for smallpox and typhoid. However, louse-borne typhus killed 2–3 million soldiers and civilians on the Eastern Front, and the war's end in November 1918 was hastened by an influenza pandemic that had begun in January 1918 and eventually claimed the lives of an estimated 50 million.

Because of the huge numbers of casualties, control of media was important for maintaining positive public opinion and support for the war efforts; all combatant countries developed central censorship and propaganda offices. The United States entered the war in April 1917, fully two-and-a-half years into the conflict, and created its own Committee on Public Information and its own Censorship Board. For the Austro-Hungarian forces, the central censorship

and propaganda institution was the War Press Office, or *Kriegspressequartier*, which eventually included more than 750 writers, journalists, photographers, and filmmakers, and some 150 visual artists. Painters and photographers worked in the field of combat, many as military officers, and sketched quick impressions, which they could later render more elaborate or refined, when they were away from the dangers of the front. Among these many painters was a young artist, Ernst Liebenauer (1884–1970), who had studied under reknowned realist Christian Griepenkerl at the *Wiener Akademie der Bildenden Künste* (Viennese Academy of Fine Arts) and later at the *Spezialschule für Historienmalerei* (Special School for Historical Painting) under another well-known Austrian portrait and landscape painter, Franz Rumpler. During the war, Liebenauer focused on military subjects, but after the war, he became a painter of landscapes, still life, portraits, and mythical scenes. He was best known as an illustrator of children's books and fairy tales, including versions of Daniel Defoe's *Robinson Crusoe* and the works of the Brothers Grimm.

On this month's cover, Liebenauer's impressionist watercolor sketch, *In Entrenchment, World War I*, presents an almost pristine, impressionist picture of the Austro-German trenches. The 5-year conflict was fought at sea and on land, but the principal battlefields emerged where opposing sides constructed elaborate lines of fortified trenches that meandered for two thousand miles on the Western Front, from the North Sea to the border of Switzerland with France. Between the opposing trenches was a "no man's land" of barbed wire and mines. Liebenauer's sketch portrays no carnage, no deprivation, no disorder. A long-coated military officer calmly supervises four soldiers, clad in orderly uniforms under a bright and colorful sky, as they fire rifles across no man's land. What may be random, penciled sketch lines may also be intended to resemble the pervasive barbed wire of the trenches, and the blue, shadowed trough in parallel with the step up to the trench wall may be intended to convey an image of pooled water or snow. The overall mood is relatively tranquil. The sketch is inspirational, consistent with the desires of the *Kriegspressequartier*, featuring the bravery of the soldiers at the front, and devoid of the horrors of the conflict or the ubiquitous filth of the trenches.

There are conflicting theories as to the site of origin of the H1N1 strain of the influenza virus that swept across the world, infecting perhaps 500 million; but the spread of the epidemic was amplified by forced congregate settings, mass migrations, intercontinental traffic, and abject living conditions. Spain did not enter the conflict and was less engaged in requiring censorship or promoting propaganda. Consequently, the 1918 pandemic became known as "Spanish flu," as its burden was reported more quickly and more extensively in the Spanish press.

In addition to trench warfare itself, World War I gave us trench-warfare disease terms: trench foot (or immersion foot, a noninfectious, nonfreezing, damp exposure injury that often led to gangrene, often necessitating amputations), and trench mouth (acute necrotizing ulcerative gingivitis, a painful, fast-moving, noncontagious infection by mostly anaerobic bacteria, particularly *Fusobacterium, Prevotella intermedia,* and spirochete species). It also gave us the term trench fever*,* the sudden onset of undulating fever, headache, and dizziness, caused by *Bartonella quintana* infection, for which the principal vector is the human body louse. Infection with *B. quintana* also causes endocarditis, chronic bacteremia, bacillary angiomatosis, and anomalous development of blood-filled cavities in the liver (peliosis hepatis).

The centenary of the end of the Great War this month reminds us of the wealth of antimicrobials and vaccines that the last century has brought. Unfortunately, with increasing antimicrobial drug resistance, we are also burdened with fear of a return to a setting in which we have few defenses against the most common of infectious disease foes.

References

1. Aichelburg W. Das Kriegspressequartier – KPQ (The War Office) [cited 2018 Sep 7]. http://www.wladimir-aichelburg.at/kuenstlerhaus/mitglieder/kriegspressequartier/
2. Anstead GM. The centenary of the discovery of trench fever, an emerging infectious disease of World War 1. Lancet Infect Dis. 2016;16:e164–72. http://dx.doi.org/10.1016/S1473-3099(16)30003-2
3. Cornwall M. The undermining of Austria-Hungary: the battle for hearts and minds. London: St. Martin's Press; 2000. p. 16–39.
4. Foucault C, Brouqui P, Raoult D. *Bartonella quintana* characteristics and clinical management. Emerg Infect Dis. 2006;12:217–23. http://dx.doi.org/10.3201/eid1202.050874
5. Haller JS Jr. Trench foot—a study in military-medical responsiveness in the Great War, 1914–1918. West J Med. 1990;152:729–33.
6. Lang N, Soskolne WA, Greenstein G, Cochran D, Corbet E, Meng HX, et al. Consensus report: necrotizing periodontal diseases. Annals of Periodontology. 1999;4:78. http://dx.doi.org/10.1902/annals.1999.4.1.78
7. Tschanz DW. Typhus fever and the destruction of the Grand Army. Command. 1991;11:22–5.
8. Wever PC, van Bergen L. Death from 1918 pandemic influenza during the First World War: a perspective from personal and anecdotal evidence. Influenza Other Respir Viruses. 2014;8:538–46. http://dx.doi.org/10.1111/irv.12267

Address for correspondence: Terence Chorba, Centers for Disease Control and Prevention, 1600 Clifton Rd NE, Mailstop US12-4, Atlanta, GA 30329-4027; email: tlc2@cdc.gov

EMERGING INFECTIOUS DISEASES®

Upcoming Issue

- Autochthonous Human Case of Seoul Virus Infection, the Netherlands

- Outbreak of HIV Infection Linked to Nosocomial Transmission, China, 2016–2017

- Reemergence of St. Louis Encephalitis Virus in the Americas

- Substance Use and Adherence to HIV Preexposure Prophylaxis for Men who Have Sex with Men

- Crimean-Congo Hemorrhagic Fever Virus, Mongolia, 2013–2014

- Prevalence of Avian Influenza A H5 and H9 Viruses in Live Bird Markets, Bangladesh

- Spatial Analysis of Wildlife Tuberculosis Based on a Serologic Survey Using Dried Blood Spots, Portugal

- Novel Type of Chronic Wasting Disease Detected in European Moose (*Alces alces*), Norway

- Survey of Ebola Viruses in Frugivorous and Insectivorous Bats in Guinea, Cameroon, and the Democratic Republic of the Congo, 2015–2017

- Rat Lungworm Infection in Rodents, New Orleans, Louisiana, USA, 2015–2017

- Genomic Characterization of β-Glucuronidase–Positive *Escherichia coli* O157:H7 Producing Stx2a

- Isolation of *Burkholderia pseudomallei* from a Pet Green Iguana, Belgium

- *Candidatus Cryptoplasma* Associated with Green Lizards and *Ixodes ricinus* Ticks, Slovakia

- Excess Mortality and Causes Associated with Chikungunya, Puerto Rico, 2014–2015

- In-Host Adaptation of *Salmonella* Dublin during Prosthetic Hip Joint Infection

- Using PCR-Based Sequencing to Diagnose *Haycocknema perplexum* Infection in Human Myositis Case, Australia

- Conservation of Wild White Rhinoceroses Threatened by Bovine Tuberculosis, South Africa, 2016–2017

- Locally Acquired Leptospirosis in Expedition Racer, Manitoba, Canada

- Chuzan Virus in Yaks, Qinghai-Tibetan Plateau, China

- *Mycoplasma ovipneumoniae* in Wildlife Species beyond Subfamily *Caprinae*

Complete list of articles in the December issue at
http://www.cdc.gov/eid/upcoming.htm

Upcoming Infectious Disease Activities

November 9–12, 2018
ProMED
International Society
for Infectious Diseases
7th International Meeting on
Emerging Diseases and Surveillance
Vienna, Austria
http://imed.isid.org/index.shtml2019

March 4–7, 2019
Conference on Retroviruses and
Opportunistic Infections
Seattle, WA, USA
http://www.croiconference.org/

April 13–16, 2019
European Congress of Clinical
Microbiology and Infectious Diseases
29th Annual Congress
Amsterdam, Netherlands
http://www.eccmid.org/

April 16–18, 2019
International Conference on
One Health Antimicrobial Resistance
Amsterdam, Netherlands
https://www.escmid.org/
ICOHAR2019/

May 5–9, 2019
ASM Clinical Virology Symposium
Savannah, GA, USA
https://10times.com/clinical-
virology-symposium
June 20–24, 2019

June 20–24, 2019
ASM Microbe 2019
San Francisco, CA, USA
https://www.asm.org/index.php/
asm-microbe-2019

Announcements
**Email announcements to EID
Editor (eideditor@cdc.gov).
Include the event's date, location,
sponsoring organization, and a
website. Some events may appear
only on EID's website, depending
on their dates.**

Earning CME Credit

To obtain credit, you should first read the journal article. After reading the article, you should be able to answer the following, related, multiple-choice questions. To complete the questions (with a minimum 75% passing score) and earn continuing medical education (CME) credit, please go to http://www.medscape.org/journal/eid. Credit cannot be obtained for tests completed on paper, although you may use the worksheet below to keep a record of your answers.

You must be a registered user on http://www.medscape.org. If you are not registered on http://www.medscape.org, please click on the "Register" link on the right hand side of the website.

Only one answer is correct for each question. Once you successfully answer all post-test questions, you will be able to view and/or print your certificate. For questions regarding this activity, contact the accredited provider, CME@medscape.net. For technical assistance, contact CME@medscape.net. American Medical Association's Physician's Recognition Award (AMA PRA) credits are accepted in the US as evidence of participation in CME activities. For further information on this award, please go to https://www.ama-assn.org. The AMA has determined that physicians not licensed in the US who participate in this CME activity are eligible for AMA PRA Category 1 Credits™. Through agreements that the AMA has made with agencies in some countries, AMA PRA credit may be acceptable as evidence of participation in CME activities. If you are not licensed in the US, please complete the questions online, print the AMA PRA CME credit certificate, and present it to your national medical association for review

Article Title

Rickettsia typhi as Cause of Fatal Encephalitic Typhus in Hospitalized Patients, Hamburg, Germany, 1940–1944

CME Questions

1. You are advising a medical facility for a refugee camp regarding a potential typhus outbreak. According to the histopathological study by Rauch and colleagues, which of the following statements about molecular and other findings related to pathogens identified in archived 73-year-old tissue blocks from 7 patients diagnosed with typhus during World War II is correct?

A. Conventional polymerase chain reaction (PCR) testing identified *Rickettsia prowazekii* in 2 samples
B. Using a specific nested quantitative polymerase chain reaction (qPCR) allowed successful amplification of *Rickettsia typhi* DNA in 2 samples
C. Conventional light microscopy identified *Rickettsia* in 3 Giemsa-stained brain sections
D. The study proved louse-borne epidemic *R. prowazekii* was responsible for all 7 typhus cases

2. According to the study by Rauch and colleagues, which of the following statements about immunohistochemical and histopathological findings in archived 73-year-old tissue blocks from patients diagnosed with typhus during World War II is correct?

A. Brain lesions in *R. typhi*–positive but not in *R. typhi*–negative brain tissue showed perivascular B cell accumulation

B. Nodular cell accumulations of cluster of differentiation (CD)4+ and CD8+ T cells, CD68+ microglia and macrophages, and rarely neutrophils occurred around blood vessels
C. Typhus nodules were most prominent in the cerebellum
D. Histopathology and immunohistochemistry were significantly different in nodules positive for *R. typhi* and those negative for *R. typhi*

3. According to the histopathological study by Rauch and colleagues, which of the following statements about clinical and public health implications of findings from archived 73-year-old tissue blocks from patients diagnosed with typhus during World War II is correct?

A. These fatal typhus cases were exclusively louse-borne
B. Cases of typhus during times of war, displacement of people, poverty, and overcrowding are usually attributed to fleaborne endemic *R. typhi*
C. More cases of typhus should undergo molecular testing for the presence of either rickettsial pathogen
D. *R. prowazekii* uses rats as natural reservoirs

Earning CME Credit

To obtain credit, you should first read the journal article. After reading the article, you should be able to answer the following, related, multiple-choice questions. To complete the questions (with a minimum 75% passing score) and earn continuing medical education (CME) credit, please go to http://www.medscape.org/journal/eid. Credit cannot be obtained for tests completed on paper, although you may use the worksheet below to keep a record of your answers.

You must be a registered user on http://www.medscape.org. If you are not registered on http://www.medscape.org, please click on the "Register" link on the right hand side of the website.

Only one answer is correct for each question. Once you successfully answer all post-test questions, you will be able to view and/or print your certificate. For questions regarding this activity, contact the accredited provider, CME@medscape.net. For technical assistance, contact CME@medscape.net. American Medical Association's Physician's Recognition Award (AMA PRA) credits are accepted in the US as evidence of participation in CME activities. For further information on this award, please go to https://www.ama-assn.org. The AMA has determined that physicians not licensed in the US who participate in this CME activity are eligible for AMA PRA Category 1 Credits™. Through agreements that the AMA has made with agencies in some countries, AMA PRA credit may be acceptable as evidence of participation in CME activities. If you are not licensed in the US, please complete the questions online, print the AMA PRA CME credit certificate, and present it to your national medical association for review

Article Title
Cryptococcus gattii Complex Infections in HIV-Infected Patients, Southeastern United States

CME Questions

1. Your patient is a 34-year-old HIV-positive man from southwestern Georgia who has headaches, neurological symptoms, and lumbar puncture findings consistent with cryptococcal meningitis. On the basis of the case series report by Bruner and colleagues, which one of the following statements about the epidemiology of *Cryptococcus gattii* complex infections is correct?

A.   Historically, most *C. gattii* cases were identified in patients living in the central United States
B.   Recent data suggest longer duration of endemicity in the southeastern United States, specifically caused by *C. gattii* VGI-SE clade
C.   Before the present case series, the only cases of *C. gattii* in patients with HIV/AIDS were from the Pacific Northwest
D.   *C. gattii* was first documented as an emerging pathogen in the United States in 1999, during an outbreak in California

2. According to the case series report by Bruner and colleagues, which one of the following statements about the clinical features of *C. gattii* complex infections is correct?

A.   The 3 patients in this case series had recently traveled to the Pacific Northwest

B.   CD4+ T-cell counts were normal in 2 of the 3 patients
C.   Similar to *Cryptococcus neoformans*, *C. gattii* is acquired through inhalation, which can progress to pneumonia and central nervous system disease by bloodstream dissemination
D.   *C. gattii* is less virulent and has less severe neurological manifestations than *C. neoformans*

3. On the basis of the case series report by Bruner and colleagues, which one of the following statements about clinical implications of *C. gattii* complex infections is correct?

A.   Increased awareness of the detection of *C. gattii* complex in HIV-infected patients in the southeastern United States is essential to improve diagnosis, treatment, and patient outcomes
B.   Distinguishing *C. neoformans* from *C. gattii* complex infections does not change clinical management
C.   Dexamethasone use is contraindicated in *C. gattii* complex meningitis
D.   Fluconazole monotherapy is the standard of care for antifungal therapy in *C. gattii* complex infection

Summary of Authors' Instructions

Authors' Instructions. For a complete list of EID's manuscript guidelines, see the author resource page: http://wwwnc.cdc.gov/eid/page/author-resource-center.

Manuscript Submission. To submit a manuscript, access Manuscript Central from the Emerging Infectious Diseases web page (www.cdc.gov/eid). Include a cover letter indicating the proposed category of the article (e.g., Research, Dispatch), verifying the word and reference counts, and confirming that the final manuscript has been seen and approved by all authors. Complete provided Authors Checklist.

Manuscript Preparation. For word processing, use MS Word. Set the document to show continuous line numbers. List the following information in this order: title page, article summary line, keywords, abstract, text, acknowledgments, biographical sketch, references, tables, and figure legends. Appendix materials and figures should be in separate files.

Title Page. Give complete information about each author (i.e., full name, graduate degree(s), affiliation, and the name of the institution in which the work was done). Clearly identify the corresponding author and provide that author's mailing address (include phone number, fax number, and email address). Include separate word counts for abstract and text.

Keywords. Use terms as listed in the National Library of Medicine Medical Subject Headings index (www.ncbi.nlm.nih.gov/mesh).

Text. Double-space everything, including the title page, abstract, references, tables, and figure legends. Indent paragraphs; leave no extra space between paragraphs. After a period, leave only one space before beginning the next sentence. Use 12-point Times New Roman font and format with ragged right margins (left align). Italicize (rather than underline) scientific names when needed.

Biographical Sketch. Include a short biographical sketch of the first author—both authors if only two. Include affiliations and the author's primary research interests.

References. Follow Uniform Requirements (www.icmje.org/index.html). Do not use endnotes for references. Place reference numbers in parentheses, not superscripts. Number citations in order of appearance (including in text, figures, and tables). Cite personal communications, unpublished data, and manuscripts in preparation or submitted for publication in parentheses in text. Consult List of Journals Indexed in Index Medicus for accepted journal abbreviations; if a journal is not listed, spell out the journal title. List the first six authors followed by "et al." Do not cite references in the abstract.

Tables. Provide tables within the manuscript file, not as separate files. Use the MS Word table tool, no columns, tabs, spaces, or other programs. Footnote any use of boldface. Tables should be no wider than 17 cm. Condense or divide larger tables. Extensive tables may be made available online only.

Figures. Submit editable figures as separate files (e.g., Microsoft Excel, PowerPoint). Photographs should be submitted as high-resolution (600 dpi) .tif or .jpg files. Do not embed figures in the manuscript file. Use Arial 10 pt. or 12 pt. font for lettering so that figures, symbols, lettering, and numbering can remain legible when reduced to print size. Place figure keys within the figure. Figure legends should be placed at the end of the manuscript file.

Videos. Submit as AVI, MOV, MPG, MPEG, or WMV. Videos should not exceed 5 minutes and should include an audio description and complete captioning. If audio is not available, provide a description of the action in the video as a separate Word file. Published or copyrighted material (e.g., music) is discouraged and must be accompanied by written release. If video is part of a manuscript, files must be uploaded with manuscript submission. When uploading, choose "Video" file. Include a brief video legend in the manuscript file.

Types of Articles

Perspectives. Articles should not exceed 3,500 words and 50 references. Use of subheadings in the main body of the text is recommended. Photographs and illustrations are encouraged. Provide a short abstract (150 words), 1-sentence summary, and biographical sketch. Articles should provide insightful analysis and commentary about new and reemerging infectious diseases and related issues. Perspectives may address factors known to influence the emergence of diseases, including microbial adaptation and change, human demographics and behavior, technology and industry, economic development and land use, international travel and commerce, and the breakdown of public health measures.

Synopses. Articles should not exceed 3,500 words in the main body of the text or include more than 50 references. Use of subheadings in the main body of the text is recommended. Photographs and illustrations are encouraged. Provide a short abstract (not to exceed 150 words), a 1-line summary of the conclusions, and a brief biographical sketch of first author or of both authors if only 2 authors. This section comprises case series papers and concise reviews of infectious diseases or closely related topics. Preference is given to reviews of new and emerging diseases; however, timely updates of other diseases or topics are also welcome. If detailed methods are included, a separate section on experimental procedures should immediately follow the body of the text.

Research. Articles should not exceed 3,500 words and 50 references. Use of subheadings in the main body of the text is recommended. Photographs and illustrations are encouraged. Provide a short abstract (150 words), 1-sentence summary, and biographical sketch. Report laboratory and epidemiologic results within a public health perspective. Explain the value of the research in public health terms and place the findings in a larger perspective (i.e., "Here is what we found, and here is what the findings mean").

Policy and Historical Reviews. Articles should not exceed 3,500 words and 50 references. Use of subheadings in the main body of the text is recommended. Photographs and illustrations are encouraged. Provide a short abstract (150 words), 1-sentence summary, and biographical sketch. Articles in this section include public health policy or historical reports that are based on research and analysis of emerging disease issues.

Dispatches. Articles should be no more than 1,200 words and need not be divided into sections. If subheadings are used, they should be general, e.g., "The Study" and "Conclusions." Provide a brief abstract (50 words); references (not to exceed 15); figures or illustrations (not to exceed 2); tables (not to exceed 2); and biographical sketch. Dispatches are updates on infectious disease trends and research that include descriptions of new methods for detecting, characterizing, or subtyping new or reemerging pathogens. Developments in antimicrobial drugs, vaccines, or infectious disease prevention or elimination programs are appropriate. Case reports are also welcome.

Research Letters Reporting Cases, Outbreaks, or Original Research. EID publishes letters that report cases, outbreaks, or original research as Research Letters. Authors should provide a short abstract (50-word maximum), references (not to exceed 10), and a short biographical sketch. These letters should not exceed 800 words in the main body of the text and may include either 1 figure or 1 table. Do not divide Research Letters into sections.

Letters Commenting on Articles. Letters commenting on articles should contain a maximum of 300 words and 5 references; they are more likely to be published if submitted within 4 weeks of the original article's publication.

Commentaries. Thoughtful discussions (500–1,000 words) of current topics. Commentaries may contain references (not to exceed 15) but no abstract, figures, or tables. Include biographical sketch.

Another Dimension. Thoughtful essays, short stories, or poems on philosophical issues related to science, medical practice, and human health. Topics may include science and the human condition, the unanticipated side of epidemic investigations, or how people perceive and cope with infection and illness. This section is intended to evoke compassion for human suffering and to expand the science reader's literary scope. Manuscripts are selected for publication as much for their content (the experiences they describe) as for their literary merit. Include biographical sketch.

Books, Other Media. Reviews (250–500 words) of new books or other media on emerging disease issues are welcome. Title, author(s), publisher, number of pages, and other pertinent details should be included.

Conference Summaries. Summaries of emerging infectious disease conference activities (500–1,000 words) are published online only. They should be submitted no later than 6 months after the conference and focus on content rather than process. Provide illustrations, references, and links to full reports of conference activities.

Online Reports. Reports on consensus group meetings, workshops, and other activities in which suggestions for diagnostic, treatment, or reporting methods related to infectious disease topics are formulated may be published online only. These should not exceed 3,500 words and should be authored by the group. We do not publish official guidelines or policy recommendations.

Photo Quiz. The photo quiz (1,200 words) highlights a person who made notable contributions to public health and medicine. Provide a photo of the subject, a brief clue to the person's identity, and five possible answers, followed by an essay describing the person's life and his or her significance to public health, science, and infectious disease.

Etymologia. Etymologia (100 words, 5 references). We welcome thoroughly researched derivations of emerging disease terms. Historical and other context could be included.

Announcements. We welcome brief announcements of timely events of interest to our readers. Announcements may be posted online only, depending on the event date. Email to eideditor@cdc.gov.

Ernst Liebenauer (1884–1970), *In Entrenchment, World War I* (c. 1915). Watercolor, pencil, and gouache on paper, 5.6 in x 4 in/14.2 cm x 10.1 cm. Digital image from private collection, Atlanta, Georgia, USA.